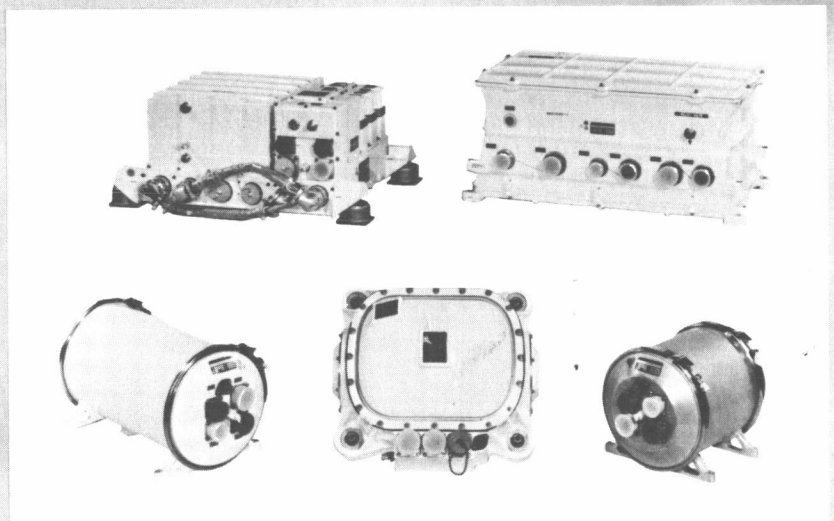


CENTAUR IN RETROSPECT

A TECHNICAL SURVEY OF THE CENTAUR
INERTIAL GUIDANCE SYSTEM EVOLUTION
FROM 1959 TO 1967



GPO PRICE \$ _____

CFSTI PRICE(S) \$ _____

Hard copy (HC) 3.00

Microfiche (MF) 65

ff 653 July 65

NASA ELECTRONICS RESEARCH CENTER

NAS 12-587

N68-19164

(ACCESSION NUMBER)

(THRU)

781
(PAGES)

(CODE)

CR-86040
(NASA CR OR TMX OR AD NUMBER)

21
(CATEGORY)

FACILITY FORM 602

Honeywell

AEROSPACE DIVISION
ST. PETERSBURG, FLORIDA



NASA No. CR-
Honeywell R-ED 27290

CENTAUR IN RETROSPECT:

A Technical Survey of the Centaur

Inertial Guidance System Evolution

from 1959 to 1967

January, 1968

Prepared under Contract No. NAS 12-587

by

HONEYWELL INCORPORATED

Aerospace Division

St. Petersburg, Florida

for

Electronics Research Center

NATIONAL AERONAUTICS AND SPACE ADMINISTRATION

PREFACE

This report was prepared in accordance with the statement of work for NASA/ERC, contract NAS 12-587, by the Aerospace Division of Honeywell Inc., St. Petersburg, Florida.

The work performed under this contract was carried out to provide the NASA Space Vehicle Design Criteria Program with source material to support the future preparation of Design Criteria Monographs.

In performing this design survey, Honeywell has paid particular attention to Design Criteria Program objectives and the role which these Surveys are intended to fulfill. Special emphasis has been given to the desired Technical Content which NASA-ERC defined to Honeywell in the Statement of Work for the NAS 12-587 Contract.

Technical objectivity has been the keynote of this design survey. It discusses the accomplishments and problems, the successes and failures, which occurred throughout the evolution and application of the Centaur IGS. The discussion includes the definition of the design requirements, alternatives and trade-offs which lead to design decisions, the decisions which were made, new concepts and major design changes which evolved, and finally, the application of "20-20 hindsight" to "how we would do it over again".

One of the challenges of the Centaur IGS Design Survey effort has been to compress the significant technical points into a document which won't overwhelm its readers with the sheer bulk of it. To read it, one should be able to carry it! Volumes of technical data have been studied by the Centaur Program Engineers who prepared this report. They have sifted and condensed, summarized, analyzed and interpreted, and the result is this document, entitled "Centaur in Retrospect; A Technical Survey of the Centaur Inertial Guidance System Evolution from 1959 to 1967".

To aid the reader in studying this report, which has been organized in accordance with the Outline provided in the Statement of Work, the authors suggest the following approach:

1. Read Section 1 first, to become acquainted with the IGS and IMG hardware, the major phases of the IGS Program, the Centaur mission requirements and results, and the major technical accomplishments.
2. Then proceed to Section 6, where the Guidance System Engineering Topics are presented, to gain further insight into the overall system, its characteristics, functions, mechanization, problems, and solutions.
3. With the background of Sections 1 and 6, the reader should then be able to study the remaining four Sections in any sequence, according to his own dictates or interests.

To assist the reader further in using this report, the authors have provided the following aids:

1. Cross referencing between related topics is used liberally throughout the text.
2. A lengthy List of Abbreviations and definitions of symbols has been included, following the List of Illustrations, to help the reader interpret terminology "short-cuts" and the many "-isms" which are bound to appear on a technical program, which has spanned eight years and several major advances in the state of the art of its engineering disciplines.
3. Each Section, Topic, and Sub-Topic has been identified by a standard Honeywell numbering sequence. Although not in full accordance with "Contractor Report Exhibit", ERC HB 2230.1, this approach has been found to be most useful in a document of this size, especially where there is a need to move back and forth from one topic to another.

4. Last, in the organization of each Topic, an attempt has been made to follow the NASA recommended organization of report material, with the following major breakdown -- Summary, Introduction, Main Body of Text, Conclusions. Therefore, for the reader whose time is very limited, but who wants to get the "gist" of this report, the authors suggest reading the introductory and concluding sub-topics for each major Topic of interest. The major points are included therein.

The terms IGS and IMG are used extensively in this report. The reader is encouraged to make a mental note of the distinction between them. The IGS is the present Inertial Guidance System (including the IMU, Computer, and GSE), which was developed and produced in the 1959-1967 period. The IMG is the new subsystem (IMU plus Test Set), which is being developed for use in 1971 and beyond.

R-ED 27290

ACKNOWLEDGEMENTS

This report was prepared by the Honeywell Guidance and Navigation Department Staff at the Aerospace Division, St. Petersburg, Florida. Overall Honeywell program direction was provided by P. V. Yingst (Centaur Program Manager), W. H. Isely (Centaur Technical Director), and W. L. McNabb who acted as Technical Staff Consultant. Detailed technical direction was provided by M. J. Hadfield (Systems Project Engineer), assisted by A. E. Roberts and H. H. Dubendorff, who also authored several topics. Authors of other topics were members of the Centaur Engineering and Product Assurance Staffs. The authors were W. R. Barnes, R. L. Boothroyd, R. P. Climo, W. W. Kroepel, R. F. Malzahn, F. W. Morse, K. H. Nichols, P. C. Odell, R. L. Prather, R. M. Rasmussen, J. S. Rice, L. W. Silas, N. H. Voissem, and A. H. Walker. They were supported in data gathering and assembly of the document by F. A. Calhoun, G. R. Homer, and R. L. Willms. Typing and typing coordination of the manuscript was performed by Miss Louise Lomelo. Technical Publication Coordinator for the final document was W. L. Moore.

In addition to those mentioned above, the authors are grateful to Messrs. James Patterson and William Monzel of NASA-LeRC; A. F. Fleisher, D. M. Fair, R. P. Gannon, and C. A. Nichols of Honeywell for their suggestions during the study period and their technical review of the final report manuscript.

Mr. Frank Carroll and Mr. Lee Bystock of the NASA-ERC Design Criteria office provided program direction to Honeywell. Mr. James Patterson represented NASA-LeRC in all technical matters and provided important Centaur program insight related to this survey. Dr. Arthur Lipton and Mr. Robert Wedan of NASA-ERC provided technical support for this effort.

R-ED 27290

TABLE OF CONTENTS

<u>Subject</u>	<u>Page</u>
Preface	iii
Acknowledgements	vii
List of Illustrations	xiii
List of Tables	xxi
Definition of Abbreviations and Symbols	xxiii

SECTION 1 - INTRODUCTION

1.1	Introduction to The Chronology of The Centaur IGS Program	1.1-1
1.2	Design Survey Results - Conclusions and Recommendations	1.2-1
1.3	Description of IGS	1.3-1
1.4	Description of Centaur IMG	1.4-1
1.5	Mission Requirements and Their Evolution	1.5-1
1.6	Program Accomplishments	1.6-1

SECTION 2 - INERTIAL MEASURING UNIT

2.1	Introduction To The IMU and IMG	2.1-1
2.2	Platform Gyros	2.2-1
2.3	Platform Accelerometers	2.3-1
2.4	Platform Resolvers	2.4-1
2.5	Platform Torque Motors	2.5-1
2.6	Platform Slip Rings	2.6-1
2.7	Platform Gyro and Accelerometer Preamplifiers	2.7-1
2.8	Platform Temperature Control Amplifiers	2.8-1
2.9	Platform Mechanical Design	2.9-1
2.10	Platform Thermal Environment and Control	2.10-1
2.11	Platform Electronics Gimbal Stabilization Electronics	2.11-1

TABLE OF CONTENTS (Continued)

<u>Subject</u>	<u>Page</u>
2.12 Platform Electronics Resolver Electronics	2.12-1
2.13 Signal Conditioners	2.13-1
2.14 Platform Electronics and Signal Conditioner Unit Packaging Design	2.14-1
2.15 Pulse Rebalance Accelerometer Loop Electronics	2.15-1
2.16 Coupler Precision Timing Functions	2.16-1
2.17 Gyro Torquing Electronics	2.17-1
2.18 Coupler Excitation for Platform Sensors	2.18-1
2.19 Coupler Unit Packaging Design	2.19-1

SECTION 3 - COMPUTER EQUIPMENT

3.1 Introduction and Computer Development Summary	3.1-1
3.2 Computer Memory	3.2-1
3.3 Computer Input/Output Unit	3.3-1
3.4 Input/Output Functional Characteristics	3.4-1
3.5 Software Design and Control	3.5-1
3.6 Computer Packaging Design	3.6-1

SECTION 4 - ACTIVATION AND VEHICLE INTERFACE

4.1 Introduction	4.1-1
4.2 IGS/IMG - Autopilot Interface	4.2-1
4.3 Primary Power Interface	4.3-1
4.4 Telemetry Interface	4.4-1
4.5 Electromagnetic Compatibility	4.5-1
4.6 Structural Interface	4.6-1

TABLE OF CONTENTS (Continued)

<u>Subject</u>	<u>Page</u>
SECTION 5 - CONTROL AND DISPLAY (SYSTEM AND COMPUTER GSE)	
5.1 Introduction	5.1-1
5.2 Systems GSE	5.2-1
5.3 Computer Test Equipment	5.3-1
5.4 Optical Alignment Control Group	5.4-1
SECTION 6 - GUIDANCE AND CONTROL SYSTEM	
6.1 Introduction	6.1-1
6.2 Error Budgeting, Analysis and Model Synthesis	6.2-1
6.3 Major IGS Control Loops	6.3-1
6.4 Velocity Measurement Loops	6.4-1
6.5 Platform Stabilization Loops	6.5-1
6.6 Platform Coarse Align Loops	6.6-1
6.7 Steering Signal Coordinate Transformation	6.7-1
6.8 Automatic Self-Leveling	6.8-1
6.9 Final Azimuth Alignment	6.9-1
6.10 Active Temperature Control Loops	6.10-1
6.11 Gyro Torquing Mechanization	6.11-1
6.12 Present MGS & GSE Mode Control	6.12-1
6.13 System Power Requirements and Distribution	6.13-1
6.14 IGS Electrical Interface and Grounding	6.14-1
6.15 IGS Mechanical Design	6.15-1
6.16 System Operational Requirements and Techniques	6.16-1
6.17 IGS Testing	6.17-1
6.18 Design - Reliability Approach	6.18-1
6.19 Specifications and Standards	6.19-1

R-ED 27290

LIST OF ILLUSTRATIONS

<u>Figure</u>	<u>Title</u>	<u>Page</u>
1. 1-1	Scientific Passenger Pod Installed on Missile 25E	1. 1-2
1. 1-2	Centaur Surveyor Launches	1. 1-6
1. 1-3	Launch of Atlas/Centaur 10	1. 1-8
1. 3-1	Centaur Inertial Guidance System Installation	1. 3-3
1. 3-2	Guidance Installed in Vehicle	1. 3-4
1. 3-3	Centaur Missile Guidance System	1. 3-5
1. 3-4	Centaur Auxiliary Signal Conditioner	1. 3-8
1. 4-1	Centaur Improved IMG	1. 4-2
1. 4-2	IMG Test	1. 4-4
2. 2-1	GG49 Miniature Integrating Gyro	2. 2-3
2. 2-2	Gyro Drift Vibration Test	2. 2-10
2. 2-3	Basic Band and Mean Band Vibration Test Sequence	2. 2-10
2. 2-4	Gyro Stability S/N G-8 BB Platform G-14 (Typical)	2. 2-23
2. 2-5	Gyro Stability S/N I-25 Platform G-5 (Best Case)	2. 2-25
2. 3-1	DGG116 Accelerometer	2. 3-3
2. 3-2	Accelerometer Vibration	2. 3-9
2. 3-3	Accelerometer Float Positions	2. 3-14
2. 3-4	Non-ported Versus Ported Configuration	2. 3-16
2. 3-5A	DGGJ1 Hinged Pendulum Accelerometer	2. 3-22
2. 3-5B	DGG177B9 Hinged Pendulum Accelerometer	2. 3-23
2. 3-6	Heater Sensor Configurations	2. 3-25
2. 3-7	Simplified Accelerometer Seal Diagram	2. 3-27
2. 4-1	Centaur Resolver	2. 4-3
2. 4-2	Centaur Resolver Chain	2. 4-5
2. 4-3	Resolver Tuning Network	2. 4-6
2. 6-1	Slip-ring Capsule	2. 6-2
2. 6-2	Cross Section through Rings and Brushes of Centaur Slip Ring	2. 6-3
2. 6-3	Slip Ring Molded Brush Block	2. 6-5
2. 6-4	Cross Section through Rings and Brushes of Gemini Slip Ring	2. 6-9
2. 7-1	Accelerometer and Gyro Preamplifier	2. 7-2
2. 7-2	Gyro Preamplifier (IMG)	2. 7-6
2. 7-3	Accelerometer Preamplifier (IMG-PRE) (First Stage on Inertial Block)	2. 7-7

LIST OF ILLUSTRATIONS (Continued)

<u>Figure</u>	<u>Title</u>	<u>Page</u>
2.8-1	Temperature Control Amplifier Schematic	2.8-3
2.8-2	TCA Modification (Addition of R_F)	2.8-9
2.8-3	Centaur IMG Temperature Control Amplifier Loop	2.8-12
2.9-1	Random Vibration Input Versus Power Spectral Density	2.9-4
2.9-2	Simplified Math Vibration Model of Centaur Platform (Y Axis)	2.9-8
2.9-3	Gimbal Configuration	2.9-9
2.10-1	Platform Heat Balance	2.10-12
2.10-2	Platform Thermal Resistance Network	2.10-15
2.10-3	Comparison of Platform Surface Temperature Profiles; Cyclic Equivalent Solar Input	2.10-17
2.10-4	Centaur Platform Thermal Model Schematic of 27-Mode	2.10-21 2.10-22
2.11-1	Gimbal 1, 2, 3 GCA Block Diagram	2.11-2
2.11-2	400 Hz Modulator	2.11-4
2.11-3	Diode Clipping Circuit	2.11-5
2.11-4	-3B Stabilization Electronics Design	2.11-6
2.11-5	-3 Rate Network (Before)	2.11-8
2.11-6	-3 Limiting Rate Network (After)	2.11-8
2.11-7	Gimbal Control Electronics	2.11-9
2.13-1	Flow Diagram of Three Phases of Signal Conditioners	2.13-3
2.14-1	Signal Conditioner	2.14-3
2.15-1	Velocity Loop Functional Interface	2.15-2
2.15-2	Velocity Loop Analog Section	2.15-4
2.15-3	Digital Section Block Diagram	2.15-6
2.15-4	Accelerometer Pulse Rebalance Current Bridge Logic Diagram	2.15-8
2.15-5	Accelerometer Pulse	2.15-9
2.15-6	Bridge Gate Switching Diagram	2.15-10
2.15-7	Bridge Gate Switching Diagram	2.15-10
2.15-8	Bridge Gate Switching Diagram	2.15-11
2.15-9	Bridge Gate Switching Diagram	2.15-11
2.15-10	Bridge Gate Switching Diagram	2.15-12
2.15-11	Bridge Gate Switching Diagram	2.15-12
2.15-12	Bridge Gate Switching Diagram	2.15-13
2.15-13	Bridge Gate Switching Diagram	2.15-13
2.15-14	Bridge Gate Switching Diagram	2.15-14
2.15-15	DC Amplifier Block Diagram	2.15-16

LIST OF ILLUSTRATIONS (Continued)

<u>Figure</u>	<u>Title</u>	<u>Page</u>
2.16-2	Timing Diagram for Precision Timing Generator	2.16-25
2.17-1a	Gyro Pattern Field Supply	2.17-2
2.17-1b	Gyro Control Field Circuitry	2.17-2
2.17-2	IMG Gyro Torquing Mechanization	2.17-6
2.18-1	Precision Frequency and Timing Block Diagram	2.18-2
3.2-1	Typical Flip-Flop Schematic Diagram	3.2-3
3.2-2	Typical Emitter-Follower Schematic Diagram	3.2-6
3.2-3	Write Amplifier Schematic Diagram	3.2-9
3.2-4	Main Memory Schematic Diagram	3.2-11
3.2-5	Memory Drum Tracks	3.2-15
3.2-6	Clock Amplifier Schematic Diagram	3.2-17
3.3-1	Navigation Computer Functional Diagram	3.3-3
4.5-1	CS-EMC-1 Test Methods as Applied to the System Interface	4.5-7
4.5-2	Conducted Power Interface	4.5-8
4.5-3	Conducted Signal Interface	4.5-9
4.6-1	Random Noise Power Spectral Density Specification	4.6-2
4.6-2	Centaur Jettisonable Insulation System	4.6-3
5.2-1	Original Configuration of Laboratory Rack Assembly DUG8057A1	5.2-2
5.2-2	Flow Diagram of Complete Laboratory Checkout Station	5.2-3
5.2-3	Original Configuration of Trailer Rack Assembly DUG8063A1	5.2-5
5.2-4	Flow Diagram of Complete Trailer Checkout Station	5.2-6
5.2-5	Configuration of Original Launch Control GSE	5.2-7
5.2-6	Flow Diagram of Complete Launch Site Checkout Equipment	5.2-8
5.2-7	Flow Diagram of Complete Set of Maintenance Equipment	5.2-9
5.2-8	Configuration of Launch Control GSE after Panel Rearrangement	5.2-12
5.2-9	Remote Load and Read Test Set	5.2-16
5.2-10	Optical Alignment Control Group	5.2-18
5.2-11	Bays 2 and 3 of Blockhouse Equipment, after Interim Configuration	5.2-21
5.2-12	Guidance Launch Control Equipment Group Final Configuration, GSE 6	5.2-23

LIST OF ILLUSTRATIONS (Continued)

<u>Figure</u>	<u>Title</u>	<u>Page</u>
2.15-16	Accelerometer Rebalance Logic and Level Discriminator Block Diagram	2.15-18
2.15-17	Control Logic and Current Bridge Block Diagram	2.15-20
2.15-18	Master Gate Block Diagram	2.15-21
2.15-19	14.4 KC Demodulator Driver	2.15-23
2.15-20	Precision Voltage Supply and Accelerometer Rebalance Current Supplies	2.15-24
2.15-21	-3 Centaur Velocity Loop	2.15-29
2.15-22	Integrated Rate Loop Block Diagram	2.15-30
2.15-23	Gain From Signal Generator to Logic Input	2.15-32
2.15-24	"Pure Rate" Derivation at Zero G Input	2.15-34
2.15-25	Linear Analogy of Integrated Rate Loop	2.15-35
2.15-26	1.8 kHz Isolated Power Supply Block Diagram	2.15-49
2.15-27	Accelerometer Signal Generator Excitation	2.15-55
2.15-28	Temperature Control Amplifier, Electrical Schematic	2.15-58
2.15-29	Carrier Amplifier Schematic	2.15-60
2.15-30	14.4 kHz Demodulator Driver	2.15-63
2.15-31	Test Circuit	2.15-66
2.15-32	Analog Accelerometer Loop	2.15-71
2.15-33	SEU Logic and Gating	2.15-72
2.15-34	One Hundred Percent Duty Cycle Loop	2.15-73
2.15-35	Pulse Rebalance Electronics Block Diagram	2.15-78
2.16-1	Precision Timing Generator Block Diagram and Timing Pulses	2.16-2
2.16-2	Precision Timing Generator Block Diagram	2.16-6
2.16-3	Timing, Frequency Divider and Clock Pulse Generator	2.16-7
2.16-4	Velocity Loop Timing Pulses	2.16-8
2.16-5	Precision Timing Generator	2.16-10
2.16-6	Basic Oscillator Types	2.16-13
2.16-7	Crystal Controlled Oscillator	2.16-16
2.16-8	Crystal Controlled Oscillator Redrawn	2.16-17
2.16-9	Required Precision Frequencies	2.16-18
2.16-10	Proposed Countdown Mechanization	2.16-19
2.16-11	Precision Timing Generator - Frequency Division (Sheet 1 of 2)	2.16-21
2.16-11	Precision Timing Generator - Frequency Division (Sheet 2 of 2)	2.16-23

LIST OF ILLUSTRATIONS (Continued)

<u>Figure</u>	<u>Title</u>	<u>Page</u>
5.2-13	Guidance Launch Control Equipment Group Final Configuration, GSE 7	5.2-24
5.2-14	Guidance Launch Control Equipment Group New Guild, GSE 15	5.2-25
5.2-15	Vehicle Guidance Simulator	5.2-28
5.2-16	MGS Preflight Control Panel	5.2-30
5.2-17	Guidance Control Panel	5.2-31
5.2-18	Computer Controlled Launch Set Interface	5.2-36
5.2-19	Typical Mode Switch Assembly	5.2-42
5.2-20	Typical Mode Switch Wafer	5.2-42
5.2-21	Illustration of Wiper Contacts across Insertion Slot	5.2-44
5.2-22	Typical Langevin Switch	5.2-45
5.2-23	Revised Resolver Drive Motor Circuit	5.2-50
5.4-1	Block Diagram, OACG	5.4-4
6.2-1	IGS Error Source Control (Preflight and Flight)	6.2-3
6.2-2	Prediction of Hardware Capability Improvement Made in 1962	6.2-4
6.2-3	Error Model Construction Diagram	6.2-7
6.2-4	Calculated FOM's from Acceptance Data Accumulative by System for Each Phase of Program with Actual Flight MCR's Superimposed	6.2-9
6.4-1	Evolution to Bang Bang Rebalance Technique	6.4-3
6.4-2	Pulse on Demand Loop	6.4-4
6.4-3	Integrated Rate Loop Block Diagram	6.4-5
6.4-4	Coupler Operational Block Diagram	6.4-7
6.4-5	Accelerometer Bias and Scale Factor Correction Coefficients	6.4-9
6.5-1	Functional Diagram of Inertial Platform Stabilization Loops	6.5-4
6.5-2	Fourth Gimbal Phasing and Cage Circuits	6.5-5
6.5-3	A Method for Coarse Alignment Loop Mechanization	6.5-9
6.5-4	GCE Block Diagram	6.5-15
6.6-1	Simplified Coarse Alignment Loop	6.6-3
6.6-2	Typical Resolver Coarse Align Loop	6.6-4
6.6-3	Platform Gimbal Spin Inhibit Printed Board - Block Diagram	6.6-6
6.6-4	Platform Gimbal Spin Inhibit Schematic	6.6-7
6.6-5	Gimbal Spin Inhibit Block Diagram	6.6-9
6.6-6	Gimbal Spin Inhibit Schematic	6.6-10
6.6-7	GTE Block Diagram	6.6-12
6.7-1	Coordinate Transformation	6.7-2

LIST OF ILLUSTRATIONS (Continued)

<u>Figure</u>	<u>Title</u>	<u>Page</u>
6.7-2	Coordinate Transformation about Angles α_1 and α_2	6.7-3
6.7-3	Resolver Chain Schematic and Signal Flow Graph	6.7-5
6.7-4	Coordinate Transformation of U into X	6.7-7
6.7-5	Function of the Coordinate Transformation Resolver Chain	6.7-8
6.8-1	Level Loop Diagram	6.8-2
6.9-1	Self-Leveling Gyrocompassing Loop, Simplified Block Diagram	6.9-3
6.9-2	Alignment of Inertial Components in Launch Configuration	6.9-4
6.9-3	Azimuth Alignment Control System, Block Diagram	6.9-7
6.9-4	Launch Complex Site Layout	6.9-8
6.9-5	Autotheodolite	6.9-11
6.9-6	Optical Alignment Control Loop	6.9-15
6.10-1	Platform Case Temperature during Flight	6.10-2
6.10-2	Inertial Platform Steady State Power As A Function of Case Temperature	6.10-3
6.10-3	Thermal Lag Time Between Heater and Sensor TCA Controlling at 6 Watts	6.10-5
6.10-4	Temperature Control Amplifier Operational Curve	6.10-6
6.11-1	Computer Gyro Torquing	6.11-2
6.11-2	Optical Gyro Torquing Loop	6.11-4
6.13-1	Power Distribution Block Diagram	6.13-2
6.13-2	400 Hertz, Phase A Present Centaur MGS Power Characteristics	6.13-4
6.13-3	400 Hertz, Phase B Present Centaur MGS Power Characteristics	6.13-5
6.13-4	400 Hertz, Phase C Present Centaur MGS Power Characteristics	6.13-6
6.13-5	Present Centaur MGS Power Characteristics 28 VDC	6.13-7
6.13-6	DC Prime Power Distribution	6.13-10
6.13-7	AC Prime Power Distribution	6.13-11
6.13-8	IMG Power Control	6.13-18
6.13-9	IMG Power Sequencing Relays	6.13-19
6.13-10	SEU Functional Block Diagram	6.13-20
6.13-11	DC Power Supply Mechanization Preliminary	6.13-21
6.13-12	Power Supply Block Diagram - Alternate A	6.13-23
6.13-13	Power Supply Block Diagram - Alternate B	6.13-24
6.13-14	Power Supply Block Diagram - Alternate C	6.13-26

LIST OF ILLUSTRATIONS (Continued)

<u>Figure</u>	<u>Title</u>	<u>Page</u>
6.14-1	Computer to RL&R Signal Communication Link (Sheet 1 of 2)	6.14-5
6.14-1	Computer to RL&R Signal Communication Link (Sheet 2 of 2)	6.14-6
6.14-2	Computer Radio Noise Filter Schematic	6.14-10
6.14-3	Resolver Common Interconnection from Platform to ARU (Sheet 1 of 2)	6.14-12
6.14-3	Resolver Common Interconnection from Platform to ARU (Sheet 2 of 2)	6.14-13
6.14-4	Delta V Compatibility and An Associated Ground Loop	6.14-15
6.16-1	Acceptance Test Schedule and Parameter Shift Nomenclature	6.16-3
6.16-2	Acceptance Test Schedule with Calibration- Recalibration Philosophy	6.16-6
6.17-1	Platform Detail Test Flow (Rev A)	6.17-13
6.17-2	Platform Electronics Detail Test Flow	6.17-15
6.17-3	PRE Detailed Test Flow	6.17-17
6.17-4	Signal Conditioner Detailed Test Flow	6.17-19
6.17-5	System Confidence and SAT Test (Rev A)	6.17-21
6.17-6	-1 MGS Post Shipment Testing (1959-1962)	6.17-27
6.17-7	-3 MGS Post Shipment Testing (1961-1965)	6.17-28
6.17-8	Present Day Phase II PIP Post Shipment Testing (1965-1967)	6.17-30
6.18-1	Centaur Reliability Growth Curve	6.18-14

LIST OF TABLES

<u>Table</u>	<u>Title</u>	<u>Page</u>
2.2-I	Summary Of Gyro Problems and Corrective Action	2.2-2
2.2-II	Gyro Comparison At Time Of Selection Of MSDF Gyro	2.2-5
2.2-III	Short Term Requirements	2.2-8
2.2-IV	Long Term Requirements	2.2-8
2.2-V	Vibration Requirements	2.2-9
2.3-I	116A Accelerometer Requirements	2.3-4
2.3-II	DGG177 Performance Requirements	2.3-6
2.3-III	Storage Schedule	2.3-8
2.9-I	Vibration Test Data	2.9-10
2.10-I	Control Heater Power Comparison Between Centaur -1 and -3 Configuration	2.10-6
2.13-I	Selected Signals For Conditioning	2.13-2
2.15-I	14.4 kHz Amplifier Worst Case Analysis Results	2.15-52
2.15-II	Power Converter Worst Case Error Analysis Results	2.15-52
2.15-III	Noise Analysis Results (20VDC Line To Load)	2.15-53
2.15-IV	Velocity Loop Error Budget	2.15-80
2.19-I	-3 Coupler Vibration Transmissibilities	2.19-5
3.4-I	Instruction Word Format	3.4-2
3.4-II	Data Word Format	3.4-2
3.4-III	Arithmetic Operations	3.4-4
4.6-I	MGS Unit to Vehicle Mounting	4.6-4
6.2-I	Evolution Of Parameter Shift Requirements (Acceptance Tests)	6.2-5
6.5-I	Comparison Of -3 Centaur Versus Expected IMG Loop Performance	6.5-16
6.13-I	Present MGS Average Power Characteristics	6.13-8
6.13-II	Navigation Computer (GPK-33) Power Characteristics	6.13-9
6.16-I	Align Mode Summary	6.16-5
6.16-II	Compensation Parameters	6.16-8
6.18-I	Configuration Complexity and Reliability	6.18-20

PRECEDING PAGE BLANK NOT FILMED.

R-ED 27290

DEFINITION OF ABBREVIATIONS AND SYMBOLS

In a study of this type, where program and technical terminology has evolved over a period of eight years, the reader encounters many unique abbreviations and symbols. Whenever these are used in the text, the authors have attempted to define the abbreviation or symbol just prior to its use. However, the need may arise for the reader to have a quick reference source. The list which follows is intended to fulfill that need.

List of Abbreviations

A/B	Airborne
AC	Alternating Current
ACCEL	Accelerometer
ACP0	Assembly for Clock Pulse Zero
ACP1	Assembly for Clock Pulse One
A/D	Analog-to-Digital
ADACS	Automatic Data Acquisition and Conversion System
ADLE	Automatic Data Loading Equipment
AGE	Aerospace Ground Equipment
A/P	Autopilot
ARCS	Accelerometer Rebalance Current Supply
ARPA	Advanced Research Projects Agency
ARU	Alignment Reference Unit
ASC	Auxiliary Signal Conditioner
ATS	Applications Technology Satellite
BECO	Booster Engine Cut-Off
B/H	Blockhouse
B/U	Back Up
CAT	Composite Acceptance Test Program
CCC	Computer Control Corporation
CCLS	Computer Controlled Launch Set
CERB	Centaur Equations Review Board
CFTU	Computer Fill and Test Unit
CMTR	Computer
C/N	Computer Navigation
C/O	Check Out

List of Abbreviations (Continued)

CPG	Clock Pulse Generator
CP0, -1, etc.	Clock Pulse Zero, -One, etc.
COUPLER (PRE)	Airborne Pulse Rebalance, Gyro Torquer and Power Supply
CRS	Command Rate Sensitivity
CSTS	Combined System Test Stand
CT	Constant Torque
CVR	Combined Voltage Regulator
D/A	Digital to Analog or Design Assurance
DC	Direct Current
DCAS	Defense Contract Administrative Services
DCU	Digital Computing Unit
DD210	Display System (CCLS)
DELTA V (ΔV)	Incremental Velocity
DET	Design Evaluation Test
DGG49	Also GG49 - Centaur IGS Gyro
DGG116	Also GG116 and 116 - Centaur IGS (Floated Pendulum) Accelerometer
DGG177	Also GG177 and 177 - Centaur IGS (Flexure Pivot) Accelerometer
DPDT	Double Pole, Double Throw (Switch)
DPT	Design Proof Test
DR	Discrepancy Report
DVM	Digital Voltmeter
ECAP	Electronics Circuit Analysis Program
EMC	Electromagnetic Compatibility
ES	Engineering Specification
EST	Earth Spin Test
ES (T)	Engineering Specification (Test)

List of Abbreviations (Continued)

ETI	Elapsed Time Indicator
ETR	Eastern Test Range
FACT	Flight Acceptance Composite Test
FAR	Failure Analysis Report
FGP	Forward Ground Plate
FLRT	Flex Lead Reaction Torque
FOM	Figure of Merit
FTE	Factory Test Equipment
FTS	Factory Test Station
FTU	Fill Test Unit
"G" or "g"	Gravity
GAP	Guidance Autopilot Test
GCA	Gimbal Control Amplifier
GCE	Gimbal Control Electronics
GCP	Guidance Control Panel
GD/A	General Dynamics/Astronautics
GD/C	General Dynamics/Convair
GERB	Guidance Equation Review Board
GFE	Government Furnished Equipment
GFP	Government Furnished Property
GLCEG	Guidance Launch Control Equipment Group
GOAS	Guidance Optical Alignment Shelter
GPFC	Gyro Pattern Field Current
GSE	Ground Support Equipment
GSI	Gimbal Spin Inhibit
GTF	Gyro Transfer Function
Hw	Spin Motor Angular Momentum
Hz	Cycles Per Second

List of Abbreviations (Continued)

IA	Input Axis
IAT	Individual Acceptance Test
IC	Integrated Circuit
ICD	Interface Control Drawing
IGS	Inertial Guidance System
IMG	Inertial Measuring Group
IMU	Inertial Measuring Unit
I/O	Input/Output Unit of Computer
IPS	Isolated Power Supply
IR	Inspection Report (GD/C Equivalent to DR)
IRU	Inertial Reference Unit
KSMD	Kearfott - San Marcos Division
LCM	Limit Cycle Monitor
LCP	Launch Control Panel
LeRC	Lewis Research Center
LOCP	Local Optical Control Panel
LOT	Launch on Time
LR2B	Long Range Autotheodolite
MB	Mean Band
MCO	Main Cut-Off
MCR	Midcourse Correction Requirement
MECO	Main Engine Cut-Off
MGs	Missile Guidance Set (or Subsystems)
MR or mr	Milli-Radian(s)
MRB	Material Review Board
MSDF	Miniature Single Degree of Freedom (Gyro)
MSFC	Marshall Space Flight Center
MTBF	Mean Time Between Failure
MTTFF	Mean Time to First Failure

List of Abbreviations (Continued)

MTU	Marginal Test Unit
MUIA	Mass Unbalance along the Input Axis
MUSA	Mass Unbalance along the Spin Axis
MV or mv	Milli-Volt(s)
NASA	National Aeronautics and Space Administration
NET-1	Network Analysis Program
OA	Output Axis
OACG	Optical Alignment Control Group
OA H	Output Axis Horizontal
OA O	Orbiting Astronomical Observatory
OA V	Output Axis Vertical
O & M	Operation and Maintenance
OSC	Operational Signal Conditioner
PAST	Phase Angle Shift Technique
PC	Power Control
PE	Platform Electronics
P/F	Platform
PI	Power Interlock Panel
PIP	Product Improvement Program
PLC	Pulse Limit Cycle
PRE	Pulse Rebalance Electronics
PSSA	Pulse Shift and Squaring Amplifier
PTG	Precision Timing Generator
PVR	Precision Voltage Reference
RC	Recorder Control Panel
RCC	Recorder-Counter Control Panel
RCRM	Recorder-Counter Relay Matrix
RFI	Radio Frequency Interference

List of Abbreviations (Continued)

RG	Returned Goods
RL&R	Remote Load and Read Equipment
RNF	Radio Noise Filter
ROCP	Remote Optical Control Panel
RTC	Remote Torquing Control
ρ	RHO Angle-Angle Between Two Accelerometer Input Axes
SA	(Gyro) Spin Axis
SAT	Systems Acceptance Test
SC	Signal Conditioner
S/C	Spacecraft
SCATE	Self-Calibration, Alignment, and Testing
SDF	Single Degree of Freedom Gyro
SDS	Scientific Data Systems
SECO	Sustainer Engine Cut-Off
SEU	Systems Electronics Unit
SF	Scale Factor
SG	Signal Generator
SMRT	Spin Motor Reaction Torque
SRA	(Gyro) Spin Reference Axis
STL	Space Technology Laboratories
SVT	Synchronous Vibration Torque
TB-2	Terminal Board #2 in Coupler
TCA	Temperature Control Amplifier
TCL	Technical Coordination Letter
TDF	Two Degree of Freedom Gyro
TDS	Technical Development Specification
T & E	Test and Evaluation
TG	Torque Generator

List of Abbreviations (Continued)

TGRT	Torque Generator Reaction Torque
T/S	Test Set
T/S	Troubleshoot
Ua	U Accelerometer
UAT	Unit Acceptance Test
Ug	U Gyro
UGT	Universal Ground Test Program
URT	Unit Readiness Test
UTP	Unified Test Plan
Va	V Accelerometer
VCO	Vernier Cut-Off
VCP	Vendor Change Proposal
Vdc	Voltage, Direct Current
VECO	Vernier Engine Cut-Off
Vg	V Gyro
VIR	Vendor Information Request
VOM	Volt/Ohm Meter
VRIA	Voltage Reference Isolation Amplifier
Vrms	Voltage, Root Mean Square
VTVM	Vacuum Tube Voltmeter
Wa	W Accelerometer
WCCA	Worst Case Circuit Analysis
Wg	W Gyro

Definition of Symbols

$d1, 2, 3$	- scale factors for the u, v, w accelerometers, respectively
$d4, 5, 6$	- misalignment angles between the u-v, u-w, and v-w accelerometer input axes respectively
$d7, 8, 9$	- bias compensations for the u, v, w accelerometers
$d10, 13, 16$	- g-insensitive drift rate compensations for u, v, w gyros
$d11, 14, 17$	- g-sensitive drift compensation coefficients for mass unbalance along the input axes of the u, v, w gyros (MUIA)
$d12, 15, 18$	- g-sensitive drift rate compensation coefficients for mass unbalance along the spin reference axes of the u, v, w gyros (MUSRA)
$d19$	- misalignment angle between the platform Porro prism and the u accelerometer input axis (in the u-v plane)
g	- acceleration due to gravity (varies with location)
$K_{1, 2, 3}$	- gain constants for closed loop level hold loops
$V_{\sigma u, v, w}$	- sigmator velocity from u, v, w accelerometers
$V_{\sigma A}$	- sigmator velocity from vertical-action accelerometer
$V_{u, v, w}$	- velocity compensated for accelerometer scale factor and bias
V_N, E, A	- compensated velocity transformed into north, east, and azimuth reference coordinates
$V_{EA, ED, E(D+E)}$	- compensated velocity accumulated from east-acting accelerometer during Phases A, D, and D+E
V_{NA}	- compensated velocity accumulated for north-acting accelerometer during Phase A
$\Delta W_{N, E}$	- corrective torquing rates for closed loop level hold

Definition of Symbols (Continued)

$W_{dN, E, AO}$	- gyro drift rate compensation plus Earth rate components
$W_{N, E, A}$	- total torquing rates in north, east, and azimuth reference
$WT_{u, v, w}$	- total torquing rates transformed into u, v, w reference
WDN_j	- drift rate compensation for north-acting gyro computed in mode j
τ_σ	- sigmator time
ϕT	- desired duration of Phase ϕ
$\theta_{N, E}$	- angular rotation about north or east axis which is to be torqued out during Phase B, B^1 , or F
λ	- geodetic latitude
β	- angle of launch from east
Ω	- Earth's rotation rate
μ	- micro

SECTION 1

INTRODUCTION

Topic 1.1

Introduction to The Chronology of The Centaur IGS Program

1.1.1. Introduction to The Chronology of The Centaur Guidance Program. - In response to an RFQ by General Dynamics/Convair (formerly Convair-Astronautics) in January 1959, Honeywell embarked upon a program to supply inertial guidance systems for the Atlas-Centaur space booster. Honeywell submitted a proposal that same month for a full Missile Guidance Set (MGS) and Guidance Ground Support Equipment (GSE) for the Centaur Model 55 vehicle. The combination of MGS and GSE defined the total Inertial Guidance System (IGS).

In July of 1959, a contract was received to design and build nine so-called -1 inertial guidance systems. Each of these systems contained a digital Navigation Computer purchased from Librascope*. Also, three (later amended to eight) sets of GSE were to be delivered under this contract.

After a brief development program, the first MGS was shipped in August of 1960. The initial flight test of an MGS was aboard an Atlas Missile on 2 October 1961. This test was dubbed "piggy-back" because the MGS was a passenger on the Atlas vehicle and MGS operation was open loop (refer to Figure 1.1-1). The next flight (AC-1), in May 1962, saw the MGS installed on the Centaur vehicle, but operating open loop (no steering or cutoff commands) during the powered phases of flight.

In March of 1961, a contract was negotiated for Honeywell to supply eight additional guidance systems. These guidance systems were of an improved design (-3 configuration). The first five of these systems (MGS 10 through 14) were -3A designs, which greatly improved the reliability and capability of the MGS over the -1 design. Toward the end of the -3 build, there were a number of additional reliability improvements in the Coupler, Platform Electronics, and platform mechanical units.

* Later became a part of Kearfott Division, General Precision Equipment, Inc.

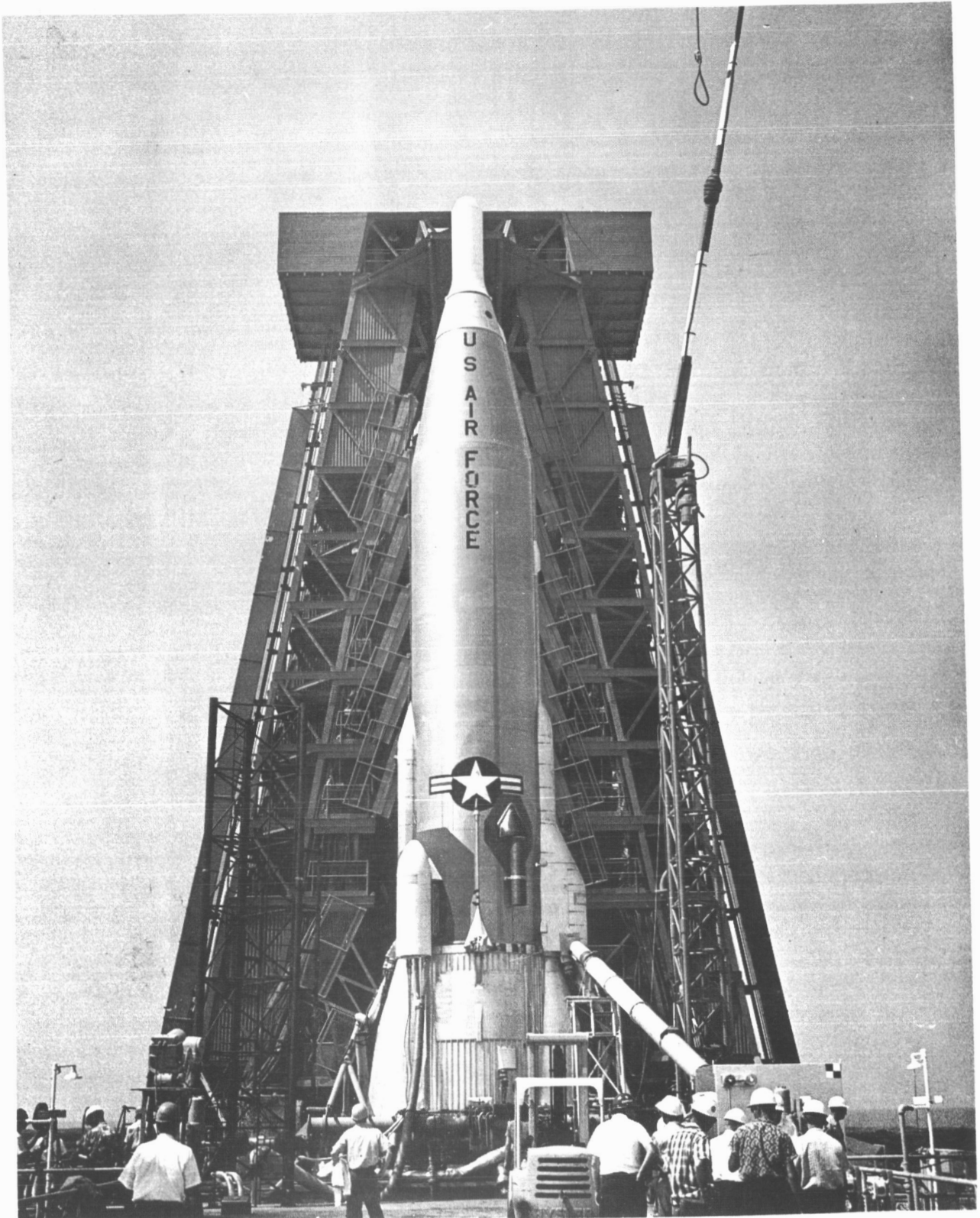


FIGURE 1. 1-1. SCIENTIFIC PASSENGER POD INSTALLED
ON MISSILE 25E

In the first half of 1963, two contracts were awarded for a total of eleven additional systems (MGS 18 through 28) of the late -3 configuration. In November 1963, vehicle AC-2 was flown, with the MGS providing an attitude reference for the vehicle.

The year 1964 was a significant year for the Centaur IGS program. Three additional systems were procured early in the year, followed by initiation of a retrofit contract to make improvements to existing flight hardware. The retrofit program was known as the Phase I Product Improvement Program (PIP). The Phase I PIP changes were originally authorized for an MGS which employed GG116 accelerometers, but because of a subsequent retrofit program to phase in GG177 accelerometers, no MGS of this configuration ever flew.

Also in 1964, Honeywell's responsibilities were changed to those of an associate prime contractor to NASA-LeRC. Honeywell's first contract for management and engineering services began in January 1965. There were two successful test flights, AC-3 and -4, of the Centaur MGS during the year, with the second flight using closed loop guidance for the first time. The AC-3 flight was delayed two days because of an MGS performance anomaly. This was to become the only flight delay, caused by the IGS, throughout the entire flight program.

The GG177 accelerometer-dual fourth gimbal resolver retrofit contract was added to the IGS program in January 1965. This contract provided for refitting all flight platforms with the flexure pivot type, GG177 accelerometer, and a new fourth gimbal resolver to allow steering during the Atlas boost phase. In addition, the Coupler and Platform Electronics units were modified as required to accomplish these tasks. Systems were retrofitted to include both the Phase I PIP and the GG177/DR design changes.

A second round of product improvements was proposed and acceptance of these occurred in June 1965 with the Phase II PIP contract. The improvements brought by this program (along with the GG177 accelerometer retrofit), were the most effective technical steps of the IGS program. A significant number of chronic and persistent technical problems were overcome by these two retrofit programs. Two months later, a study contract was let, by NASA-LeRC, to investigate a complete redesign and mechanization of the Coupler, Platform Electronics, and Signal Conditioner. The main goal of this study was to provide a unit preliminary design capable of 2,000 hours MTBF. The resulting electronics unit was designated the System Electronics Unit (SEU), and was to be a replacement for the Coupler and the six D/A converters in the Navigation Computer. The study was completed, and the report was submitted in March 1966.

By the completion date of the SEU study, experience had been gained with Phase II PIP systems. Although the Couplers in these systems did not approach 2,000 hours MTBF, the performance and reliability was much improved. NASA LeRC evaluated the net benefit of incorporating the SEU into the existing MGS and decided that the effectiveness-to-cost ratio of the SEU was not favorable, particularly since the platform and computer had now become the limiting units, in terms of reliability. As a result an additional IMG study was undertaken in 1966.

In mid-1966, the reliability and operational capability of the MGS was compared to the upcoming, post-Surveyor payload requirements. A decision was made for Honeywell to begin studying an improved Centaur guidance system design. A go-ahead on this study was received in July 1966.

Just prior to the IMG study authorization in 1966, Honeywell was given a follow-on order for six additional systems to support Atlas/Centaur launches of ATS, OAO, and Mariner/Mars payloads. These "ADD-6" systems are currently being built, with the final one scheduled for a March 1968 delivery. In addition, one more MGS has been contracted for and will be delivered in April 1968.

The improved Centaur guidance study resulted in a simplified, two-unit configuration, called the Inertial Measurement Group. Under this system concept, all inertial measurement sensors, loops, and critical electronics are contained in one unit, called the Inertial Reference Unit (IRU). Power supplies are contained in another unit, called the System Electronics Unit (SEU). Following completion of the IMG study, NASA-LeRC authorized Honeywell to proceed with the detailed design and fabrication of one prototype IMG. This authorization occurred in early 1967.

The IMG design effort is well underway and current program plans call for completing the fabrication of an engineering prototype system, and beginning of the Design Evaluation Test program, during 1968.

Table 1.1-I shows the milestones in the Centaur guidance system development. To the right of the table is shown the chronology of cognizant Government agencies, involved in the Program.

TABLE 1.1-I

CENTAUR GUIDANCE DEVELOPMENT MILESTONES

		COGNIZANT AGENCY
	Honeywell proposes miniaturized MGS	ARPA
1959	Honeywell authorized to build nine -1 systems	
	First -1 system shipped	
1960		
	Follow-on contract for eight -3 systems	MSFC (Huntsville)
1961	First test flight	
1962	Follow-on contract for three -3B systems	LeRC
	Follow-on contract for eight -3B systems	
1963	Follow-on contract for three -3B systems	
	Phase I PIP authorized	
1964	Honeywell designated prime contractor for guidance	
	GG177/Dual Resolver Retrofit authorized	
1965	Phase II PIP authorized	
	SEU study authorized	
1966	Follow-on contract for six Phase II PIP systems	
	IMG Study authorized	
1967	IMG engineering prototype approved	

0268-332A

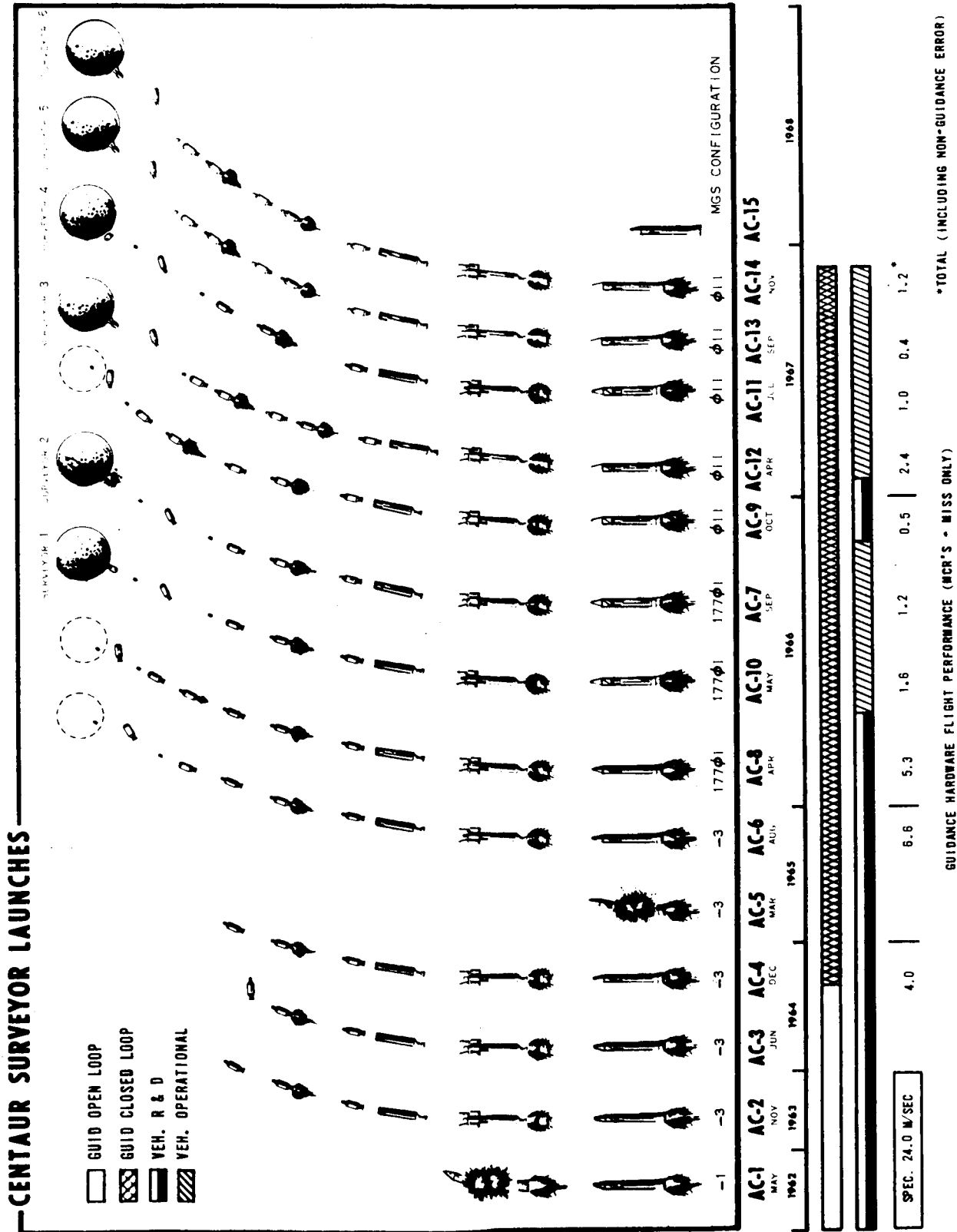


FIGURE 1.1-2. CENTAUR SURVEYOR LAUNCHES

1.1.2. Flight Summary. - The Centaur flight program has been a success. There have been 15 flights of the Centaur guidance system, including the aforementioned Atlas "piggy-back" flight. Figure 1.1-2 shows the Atlas/Centaur launch record with a date-information scale at the bottom. (A detailed account of guidance flight objectives and results is given in Topic 6.17 of this report.) From the guidance aspect of the flight program, there were three phases of development. The first phase involved use of the guidance system in several open loop configurations, for R&D purposes, on AC-1,2, 3. The next phase saw use of the guidance system for control of R&D vehicles. There were five flights of this configuration, with AC-9 being the final R&D vehicle. On 30 May 1966, the first fully operational flight occurred (refer to Figure 1.1-3, Launch of AC-10), and the Surveyor spacecraft was successfully boosted to a lunar transfer orbit and soft-landing. Since becoming operational, the Centaur guidance system has steered six Atlas/Centaur vehicles, which Surveyor spacecraft successfully injected into a lunar trajectory. The lowest horizontal scale in Figure 1.1-2 shows the IGS hardware accuracy attained in these flights, as well as those which were aimed for hypothetical targets (AC-4, AC-6, AC-8, AC-9). The specified maximum Midcourse Correction is 24 meters per second for guidance. Since MGS flight performance has been well within expected limits, an increased level of confidence in guidance accuracy has allowed spacecraft planners to reduce the fuel carried on the spacecraft for the later flights, thus permitting greater flexibility in payload and mission trajectories.

After a final Surveyor launch in early 1968, there will be five more Centaur launches (under present authorizations). Two Applications Technology Satellites (ATS) will be placed in 24-hour Earth orbits, and two Mariner Spacecraft will be aimed for Mars flyby missions. The remaining mission will place an Orbiting Astronomical Observatory (OAO) in a circular, geocentric, 417 nautical mile orbit.

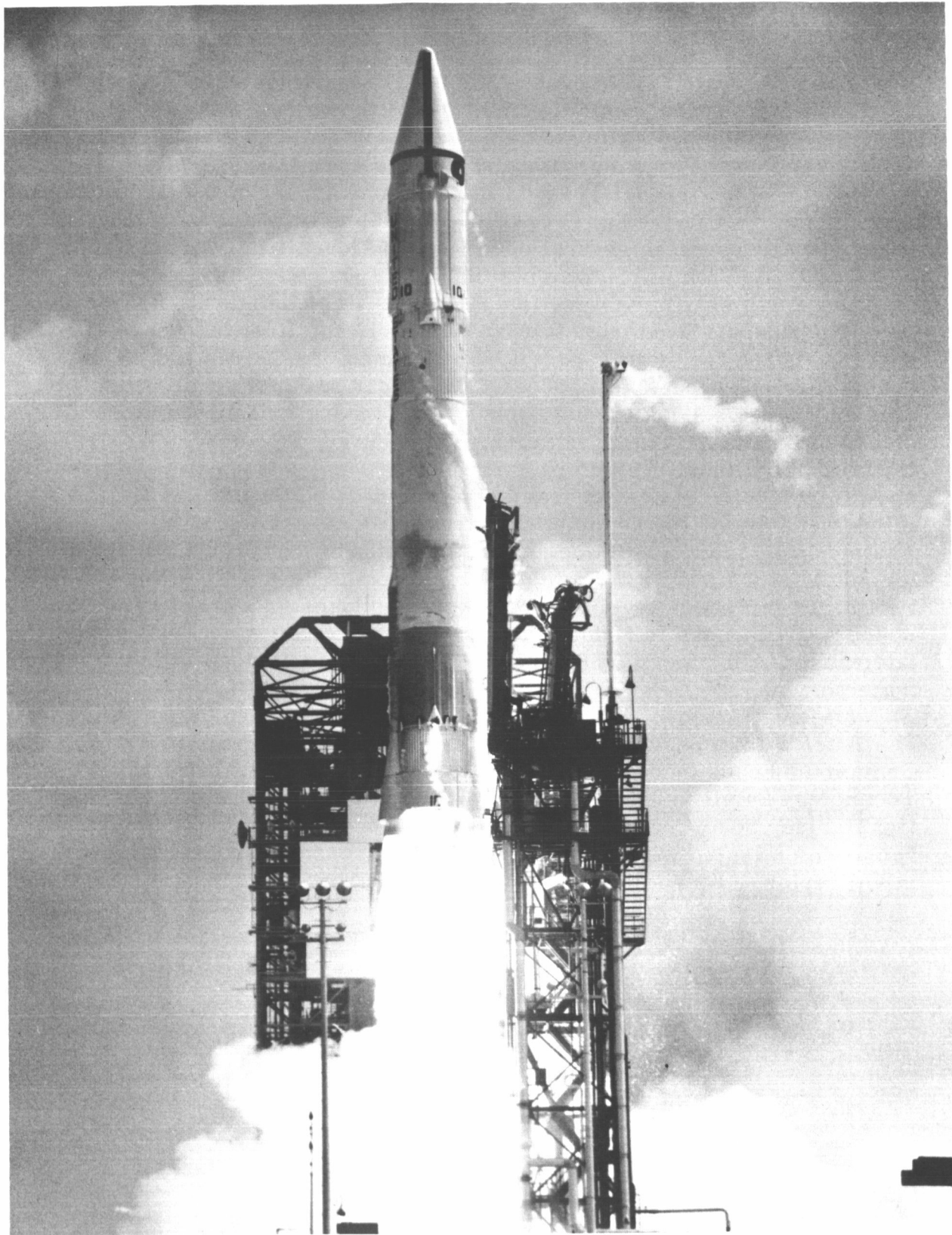


FIGURE 1.1-3. LAUNCH OF ATLAS/CENTAUR 10

Topic 1.2

Design Survey Results -
Conclusions And Recommendations

1.2.1 Summary. - A number of important lessons have been learned throughout the Centaur IGS development program. Some of these evolved from "doing it right the first time", and some significant ones resulted from mistakes or deficiencies in the early program phases. These shortcomings were studied thoroughly, later in the program, and corrective action taken to 1) solve the original problems, and 2) avoid the introduction or recurrence of similar problems. Since the program is now over eight years old and the IGS has been fully operational for almost two years, there has been adequate opportunity to measure the results of the corrective actions.

The Design Survey concentrated upon the IGS program problems and corrective actions, with the result that specific conclusions were drawn and recommendations generated for use on future IGS programs. The conclusions and recommendations are divided into four general categories:

1. Perform early and comprehensive analyses.
2. Establish effective component and design control standards.
3. Perform a thorough ground test and evaluation program.
4. Implement other effective program practices to insure meeting all objectives.

Specific recommendations are outlined for each of these categories in the following paragraphs. While many of these recommendations may seem obvious to the reader, their importance to a low risk program cannot be overemphasized. However, they are often overlooked in the electronics industry, since it is surprisingly easy to sacrifice the use of complete, thorough analyses and testing, as well as effective program controls in the interest of apparent cost and delivery schedule needs (i. e., not enough money and time to do the job right the first time). Centaur experience has shown that had the recommended design disciplines, controls and program practices, which are in use today, been implemented at the beginning, many of the problems encountered during the IGS development period would have been avoided and a lower technical risk maintained throughout the program. Of course, it must be recognized

that some of the disciplines were not even in existence at the beginning of the Centaur program. The reader is also reminded that these recommendations are not intended to be all inclusive; i. e., they do not define the total criteria for an IGS program.

1.2.2 Perform Early and Comprehensive Analyses. - The analysis category can be broken down into:

1. Performance Analysis (error analysis or budgeting and error model synthesis). Both parts of this task, analysis and synthesis, must be done as early as possible in the program to ensure complete control of significant IGS performance parameters. The error model should be updated for any design modifications or new data which are generated during the program (reference Topic 6.2).
2. Control Loop (Servomechanism) Analysis (including both mechanization, or synthesis, and analysis). This too should be performed early in the program. It should include linear and nonlinear servo characteristics. The analyses should be kept abreast of design modifications, and of course, should be considered in developing and evaluating recommended modifications (reference Topics 6.3, 6.4, 6.5, 6.6, 6.8, 6.9, and 6.10).
3. Calibration and Alignment. The basic techniques and calibration equations should be developed with special attention paid to the transient and steady-state characteristics of the gyros and accelerometers. Stability as functions of time, temperature, mechanical disturbances (rotation with open or closed nulling loop, etc.), magnetic fields, and other factors should be considered. Relationships between flight orientations and calibration orientations, relative to "g", can also be significant. Automatic and manual techniques should also be assessed (reference Topics 2.3, 6.6, 6.8, 6.9, and 6.11).
4. Computer Sizing. There is a general tendency to "size" a computer for a specific mission application and inadvertently limit the ability to increase memory capacity, memory access, and basic I/O capacity. For a multipurpose vehicle like Centaur, such restrictions can prove costly. It is possible to mechanize the computer so as to have a reasonably easy way of expanding capacity, or some degree of "excess" capacity may be designed

in, right from the start. Both alternatives should be carefully considered. The computer programming approach can also be established so as to make future expansion more efficient (reference Topics 3.1, 3.2, 3.5).

5. Computer Input/Output Flexibility. This aspect of computer and systems interface design must also be considered from the viewpoint of future mission needs. Although it may not be desirable to carry excess I/O capability, it should be possible to mechanize the I/O such that its functions can be reasonably altered or expanded at a future date (reference Topics 3.3 and 3.4).
6. Structural Analyses (Thermal and Vibration). Early performance of thorough structural analyses is essential to any good mechanical design. However, in the case of an IGS, the ultraprecise performance of electronic and electromechanical components (including gyros and accelerometers) is highly dependent upon the operating environment. Hence it is very important to perform rigorous thermal and vibration analyses, making full use of digital and analog computer simulation techniques. Actual vehicle environment should be established at an early date (reference Topics 2.8, 2.9, 2.10, 2.19, 4.6, and 6.15).
7. System Reliability. A system reliability budget and a reliability model, with the attendant analysis, are just as important to assuring reliability objectives as the error budget and error models, discussed above, are to the performance success of an IGS. The reliability analysis should start with the preliminary design, be updated to reflect design changes, and be used as a tool in developing and evaluating these changes (reference Topic 6.18).
8. Worst-Case Circuit Design. The use of worst-case circuit analysis (WCCA) techniques - including design centering, computer aided DC and AC techniques, and marginal power, temperature and electrical noise conditions - is invaluable to insuring a good electronics design. It must be recognized that WCCA is no panacea, however, and there may be cases where the desired worst-case performance margin is not physically realizable. If the same circuit design is used, rather than some alternate one, at least the designer will know where his margin is and how much is available. Thus, a compromise "safety factor" can be developed; this is especially important to digital circuitry

wherein it is possible to operate "right on the brink" of circuit malfunction without realizing it. One small variant, such as an ambient temperature change, can then unexpectedly cause a malfunction. With a thorough WCCA available, operating too close to the margin would be avoided (reference Topics 2.11, 2.15, 3.1, and 6.18).

9. Electronics Parts Stressing. Calculation of expected parts stressing due to electrical circuit parameters and ambient environment is a necessary part of developing a reliable and consistent electronics design. These calculations should be performed for the worst-case conditions to insure an adequate safety margin. The results of these analyses form an important part of the overall reliability model (reference Topics 2.8, 2.15, 3.1 and 6.18).
10. Operational Constraints. How a system will be used must be thought out well in advance and the operational constraints applied to the hardware design. This includes the interface of the IGS with other vehicle systems, ground test equipment and vehicle operating environment. The impact of long term stability requirements on gyros and accelerometers is an especially important factor. Launch preparation time and facilities must also be considered in this analysis. The hardware maintenance considerations must also be analyzed early in the program (reference Topic 6.16).

1.2.3 Component and Design Control Standards. - Program technical standards must be established and used in at least the following areas:

1. Subcontractor/Vendor Selection and Technical Management. All facets of a potential vendor's ability to perform must be considered. The technical quality of his design, his process and quality control standards, his willingness to work with the IGS Contractor in solving problems, are all important, as is his financial ability to perform. His technical competence in the component design areas and his ability to understand the application problems are important factors. This lesson was "drilled home" on the Centaur IGS program, especially in the areas of inertial components, resolvers, slip rings, torque motors, and the computer (reference Topics 2.2, 2.3, 2.4, 2.5, 2.6 and 3.1). Where program volume and funding permit, competitive dual sources can be used effectively. The standards

and means by which the IGS Contractor will exercise technical management must also be established with each subcontractor and vendor. These standards should be such that control of parts, processes, design changes, and the other important disciplines discussed herein, are applied consistently to all procurements.

2. Component Selection and Screening. Reliance upon vendor and Government specifications for electrical components can be misleading. Some high-reliability parts may be qualified with a particular application in mind, which may be at variance with the IGS design or program requirements. Special attention must be given to insuring that all needed parameters are properly considered and specified. Screening tests by the vendor, or by the Contractor, should be carefully considered (reference Topics 3.1, 6.18 and 6.19).
3. Component Derating. A conservative and consistent derating policy must be developed early and applied to all elements of the electronics design. This factor is very important to a reliable design and is closely akin to the worst-case circuit analysis and reliability models discussed above (reference Topics 6.18 and 6.19).
4. Worst-Case Electronic Design. The value of worst-case circuit analysis has already been covered. The major point here is that use of these techniques must be standardized and applied to all units of the IGS and its test equipment in order to assure well-balanced and reliable hardware designs (reference Topic 6.18).
5. Mechanical Design Criteria. Derating or "safety margin" criteria are important to mechanical designs, just as they are to electronic parameters. The usual practice on past IGS programs was to inconsistently apply mechanical design safety factors. The result inevitably was underdesign in some units and overdesign in other units of the same guidance system. This approach was both inefficient and dangerous. The proper approach would be to establish consistent and conservative criteria for all parts of the IGS vehicleborne equipment. Design criteria for test equipment must be tailored to its function, with special attention given to the use of precision fixturing and optical alignment techniques (reference Topics 2.9, 2.19, 3.6, 4.6, 5.4, and 6.15).

6. EMC and Interface Control. An IGS is often thought of as a "low frequency" system and EMC considerations de-emphasized. This practice usually leads to problems, especially because of the high degree of precision performance expected of the electronic circuits, which may utilize relatively high frequency signal content, particularly in digital circuits. A standardized design approach to susceptibility, radiated and conducted noise emission, plus optimized grounding and shielding, will pay off handsomely in a well-balanced and high-performance IGS-- one which is capable of working with other vehicle and ground test systems, without affecting or being affected by them (reference Topics 2.15, 4.2, 4.3, 4.4, 4.5, 6.13 and 6.14).
7. Signal Monitoring. Early definition of the signal monitoring philosophy, including the protection of monitored circuits, is a must. A good guideline to use is to get the necessary functional or performance data from the IGS in as well isolated a manner as possible. An excellent tool for doing this is the IGS computer which can obtain the necessary data in a closed, protected system, and prepare it for transmission via the computer telemetry channel. Definition and integration of this concept into the basic IGS hardware design can avoid many problems - especially during the evaluation, production, and flight test phases of the program. It also provides much more flexibility in application of the IGS to other vehicles or other launch sites (reference Topic 2.13).
8. Test Monitoring and Control. Early development of the overall IGS testing philosophy provides a base from which to define detailed hardware design constraints. Again, consistency and thoroughness are especially important. The depth (component or subassembly up to the system level) and breadth (from engineering evaluation to production process/acceptance and field operation) of testing should be spelled out. The expected degree of operator skills, training levels, and other human factors must be considered. Wherever possible, the common use of test equipment for subassembly, assembly, and unit and system level testing should be considered. Engineering evaluation testing should be a complementary adjunct to the analysis work, not a substitute for it (reference Topic 6.17).

9. Producibility Considerations. Standards should be developed early in the program to insure that the final hardware design is one which can be produced economically (in relation to the overall program cost and schedule). The relationship between producibility and reliability must not be overlooked. The plans for detailed review of hardware designs by production engineers should be established early in the program.

1.2.4 Thorough Ground Test and Evaluation Program. - As was just mentioned, the early development of an overall IGS testing approach is of paramount importance. Particular attention should be directed to a development of a thorough ground test and evaluation program. The performance of such a program in conjunction with a rigorous analytical effort can provide the early detection of design deficiencies and hence lessen the impact of their corrective actions. On the other hand, it can also provide additional confidence in those aspects of a system design which are meeting their performance and reliability criteria. The ground test and evaluation program can be thought of in eight different categories:

1. Gyros and Accelerometers. It is important that the gyros and accelerometers be tested as early as possible in the program. Their performance should be measured, not only in the laboratory environment, but also in as close a simulation as can be obtained of the actual system and vehicle environments. Failure to do this can result in costly modifications to the components themselves or to the inertial platform and electronics circuits later in the program (reference Topics 2.2 and 2.3).
2. Breadboards and Prototypes. Breadboards of electronic circuits should be developed as soon as the initial paper design is well along. Breadboard and prototype testing should be used to confirm the results of a worst-case design. The testing should not replace the worst-case analytical work, although there may be exceptions where testing is needed in order to complete the definition of (unspecified) parameters in the paper design. In those cases where it is not possible to achieve the desired worst-case safety margin, the breadboard and prototype testing can be used to measure and confirm actual hardware safety margins (reference Topics 6.17 and 6.18).
3. Component and Subassemblies. The rotary components such as platform resolvers, torque motors and slip rings should be tested as early as possible. This applies particularly to the early production models of these components. The same holds true for

the early production models of the electrical subassemblies within the IGS. In this way, any variances in performance or reliability, which are a function of the production build processes, can be determined and corrected through modification where necessary (reference Topics 2.4, 2.5, 2.6 and 2.15).

4. Laboratory Test Bed Units and Systems. The need for test bed hardware at the unit and system level early in the program, and then on a continuing basis, cannot be overstated. These tools are essential to the Design and Evaluation engineers in determining if the paper design is "going together properly". It is also invaluable in duplicating and solving field problems, in a controlled environment. Failure to provide a test bed capability in the early -1 Centaur days proved to be a costly mistake (reference Topic 6.17).
5. Performance Testing (Static and Dynamic). Performance tests should be conducted as soon as possible on hardware which is typical of the Production configuration. The performance tests should include the characteristics in a static or laboratory environment. They should also include dynamic testing, such as that involving the use of a precision centrifuge to test accelerometers and their rebalance loops. Performance of precision centrifuge testing, four years into the Centaur IGS program, proved to be a major factor in replacing the GG116 accelerometer with the GG177 model (reference Topics 2.3, 6.4 and 6.17).
6. Environmental Testing. The early performance of a full range of environmental tests is also important to the IGS design effort. Particular emphasis should be placed on the exposure to vibration, thermal and EMC environments for these are the ones which usually have the most significant effect on performance accuracy and reliability of an IGS. Environmental testing must be performed up to the design limits, but it may also be desirable to perform these tests at levels in excess of the design limits to help confirm the degree of safety factor in the design (reference Topic 6.17).
7. Reliability Demonstration Testing. The reliability of a Production or Production prototype model of the IGS can be determined in two ways. The reliability demonstration tests can be performed separately, or they may be included in the overall evaluation test program and made part of the performance and environmental

testing. The latter approach was taken on the Centaur IGS program and was found to be quite effective. However, the preferred alternative will depend upon individual program reliability requirements and cost factors (reference Topics 6.17 and 6.18).

8. Sled Testing. The early performance of sled testing can be helpful in determining the ability of the IGS hardware to withstand the combined environments similar to those which will be experienced in the vehicle. Most of the usual environmental tests covered above can be performed singly, but sled testing provides the opportunity to obtain an exposure to the composite of several environments. Sled testing was used on the Centaur IGS program and helped build confidence in the mechanical integrity as well as the high "g" functional capability of the overall system (reference Topic 6.17).

1.2.5 Effective Program Practices. - The program practices which may be invoked to insure the successful accomplishment of all program objectives are many fold. However, in the following paragraphs, nine particular practices which were important to the Centaur IGS program are summarized:

1. Technical Coordination and Representatives. The early incorporation of effective technical coordination is essential to accomplishing a mutual understanding on the part of the Agency and the Contractor of the total IGS requirements and capabilities. To be most effective, this technical coordination should include the assignment of resident representatives of the Agency to the Contractor's facility and vice versa. In addition, there should be frequent informal and formal technical coordination meetings to discuss specific aspects of the design program. The results of these meetings should be documented to help promote a fuller understanding of the topics and action items.
2. Design Reviews. To insure that the IGS Design is "on the way" to accomplishing the design objectives, a complete program of informal and formal design reviews should be established. The informal reviews are conducted by the Contractor Management Personnel with or without agency representation. In addition, a formal series of thorough design reviews should be conducted by agency personnel to insure that the Contractor is meeting the intent of the design objectives as the Agency defined them.

3. Design Documentation and Control. The entire IGS design effort should be adequately documented. This begins with the initial analyses and trade-off studies, and proceeds through the detailed design, test and evaluation. The production build effort should begin with a well-defined set of drawings and specifications, which have been thoroughly reviewed and understood by Production personnel. Proper configuration controls should be implemented and maintained with the production release.
4. Subcontractor and Vendor Control. As stated earlier, specific standards must be established for the selection of subcontractors and vendors. Once these are established, however, there must be consistent and thorough follow-through to insure that the standards are applied to all of the major subcontract and vendor items. This is a case where "the chain is truly only as strong as its weakest link". In other words, it takes only one improperly controlled component to destroy the integrity or reliability of an otherwise good system design.
5. Standardized Testing Approach. The need for a design control standard in the area of overall testing, test monitoring and test controls was mentioned under the Design Control Standards. Once the overall testing philosophy and standards have been established, it then becomes necessary to follow consistent program practices to insure the implementation of the testing philosophy. This is particularly true as the program passes into the Production build phase and field testing activities. An overall test plan, supplemented by detailed test flow charts, should be established to control testing at all sites.
6. Failure Analysis and Corrective Action. Even in the best designed system, from a reliability standpoint, there will be some failures. The early analysis of these failures and diagnosis of their causes is an important element in obtaining reliable flight hardware. A formal failure analysis program with direct and effective action is necessary in order to accomplish the desired flight reliability as early as possible. In addition to the formal failure analysis program, the Contractor should implement a program of discrepancy reporting which includes not only out-of-specification tolerances or component failures during the build process, but also assesses the trend of performance characteristics and includes the taking of positive action before an anomaly develops into a major problem.

7. Traceability of Parts and Assemblies. An important tool in the performance of a formal or informal failure analysis program is the ability to trace individual lots of electronic or electromechanical parts and assemblies. In this way, process variances which may have been introduced at the Vendor's facility, can be isolated and the extent of the impact on completed flight hardware can be adequately assessed. Thus, any repair or modification program can be efficiently tailored to the affected hardware.
8. Maintenance and Repair Philosophy. To be most effective, the maintenance and repair philosophy for flight hardware should be determined at an early point in the program and made as much a part of the design constraints as are, for example, the environmental requirements. The philosophy must then be carried through and applied during the initial field testing program and finally to the operational usage of the IGS equipment.
9. Specialized Technical Support. The Centaur IGS program has demonstrated that effective use can be made of the special design capability possessed by the IGS Contractor to solve not only IGS, but other vehicle-related problems. The use of this technical capability can be applied not only during the initial evaluation and later Production phases, but it can also be used effectively throughout the flight test program and finally the operational flight test activities. In this way, any impact upon guidance hardware due to changing mission requirements and other factors can be assessed at an early point and the necessary trade-offs made to minimize or eliminate potential problems. Also, the results of the flight data analysis activities can be much more meaningful if the data is interpreted by engineers who are intimately familiar with the detailed hardware design and design characteristics. This participation by Contractor personnel should supplement rather than replace the activity performed by Agency personnel and other consulting or service organizations.

Topic 1.3

Description of IGS

1.3.1. Introduction. - The purpose of this topic is merely to introduce the reader to the Centaur IGS and make him familiar with its basic parts. The Centaur Inertial Guidance System (IGS) consists of two parts, the Missile Guidance Set (MGS) and the Ground Support Equipment (GSE).

The MGS performs the following flight functions:

1. Atlas steering augmentation during boost phase.
2. Booster engine cutoff discrete (BECO).
3. Atlas steering during sustainer phase.
4. Sustainer cutoff discrete backup (SECO).
5. Centaur guidance and vehicle steering.
6. Centaur main engine cutoff discrete (MECO).
7. Centaur vernier engine cutoff discrete (VECO).
8. Centaur second burn main engine start.
9. Centaur second burn main engine cutoff.
10. Centaur second burn vernier engine cutoff.
11. Re-orient after spacecraft separation.
12. Attitude stabilization during retro-maneuver.
13. Guidance telemetry signal conditioning.

Within the MGS, are the Inertial Measurement Units (IMU), and the Vehicleborne Computer/Navigation Unit (C/N). This distinction has been made because (1) the Computer is a purchased unit, produced by Kearfott Division of General Precision, Inc., and (2) IMU and Computer functions are basically different--a measurement and a computation function, respectively.

The GSE provides operational and maintenance testing support to the MGS for:

1. Laboratory Operation and calibration.
2. Factory checkout of the MGS on the vehicle.
3. Simulated launch site operation (at the Composite Systems Test Stand - CSTS - in San Diego).
4. Launch site operation and calibration.

Basic MGS Description. - The MGS is comprised of the following units:

<u>Honeywell Part Number</u>	<u>Unit</u>	<u>Designation</u>
DGG8024	1	Inertial Platform
DEG8039	2	Platform Electronics
DDG8015	3	Signal Conditioner
DBG8016	4	Computer Memory-NOTE 1
DDG8014	5	Pulse Rebalance, Gyro Torquer, and Power Supply (Coupler)
DBG8016	6	Computer Input/Output-NOTE 1
DDG8032	8	Auxiliary Signal Conditioner- NOTE 2

NOTE 1: The two units which comprise the computer are physically separate but are actually assembled together on one chassis.

NOTE 2: Unit 8 was only used on R&D flights, as required by telemetry instrumentation assignment.

The units of the MGS, when installed on the Centaur vehicle, are physically mounted on shelves placed on the forward end of the hydrogen tank. (See Figures 1.3-1, 1.3-2.)

The total power consumed by the MGS while in flight is approximately 500 watts

1.3.2. Detailed Unit Descriptions. - The following is a brief description of each MGS unit (Please refer to Figure 1.3-3.)

1. Inertial Platform DGG8024. - In the center of the picture is the Inertial Platform which provides the basic reference frame. The Inertial Platform is a four-gimbal assembly which contains three miniature integrating gyros and three pendulous accelerometers. The platform consists essentially of a case, a gimbal structure, gimbal drive motors which reposition the gimbals, gimbal angle resolvers which provide coordinate transformation and angle pickoff information, and the inertial components with their temperature control assemblies. The platform assembly weighs 30.5 pounds and occupies a volume of 0.88 cubic foot. The platform gimbals are cast of a high damping magnesium alloy which provide lightweight, structural rigidity.

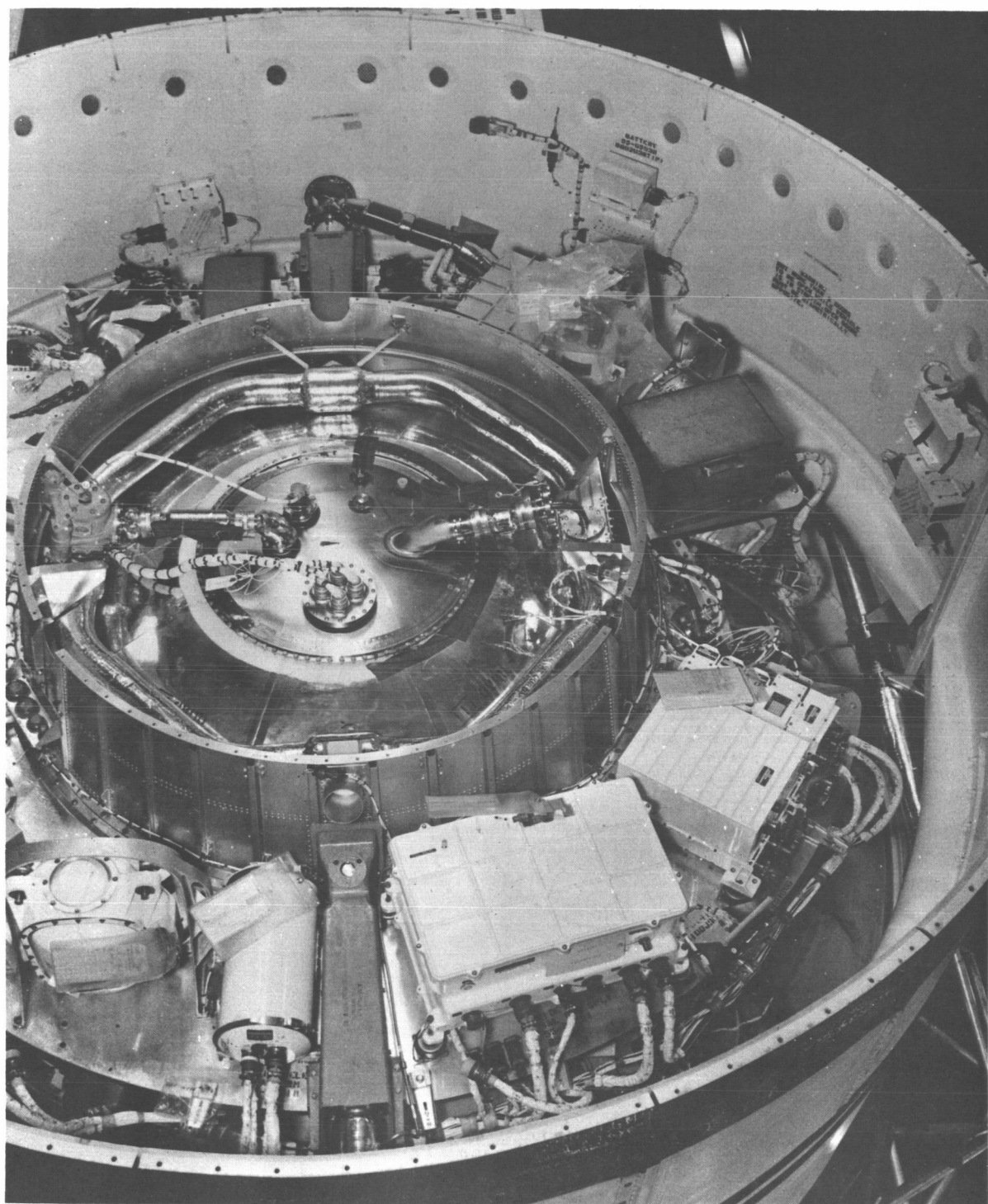


FIGURE 1. 3-1. CENTAUR INERTIAL GUIDANCE
SYSTEM INSTALLATION

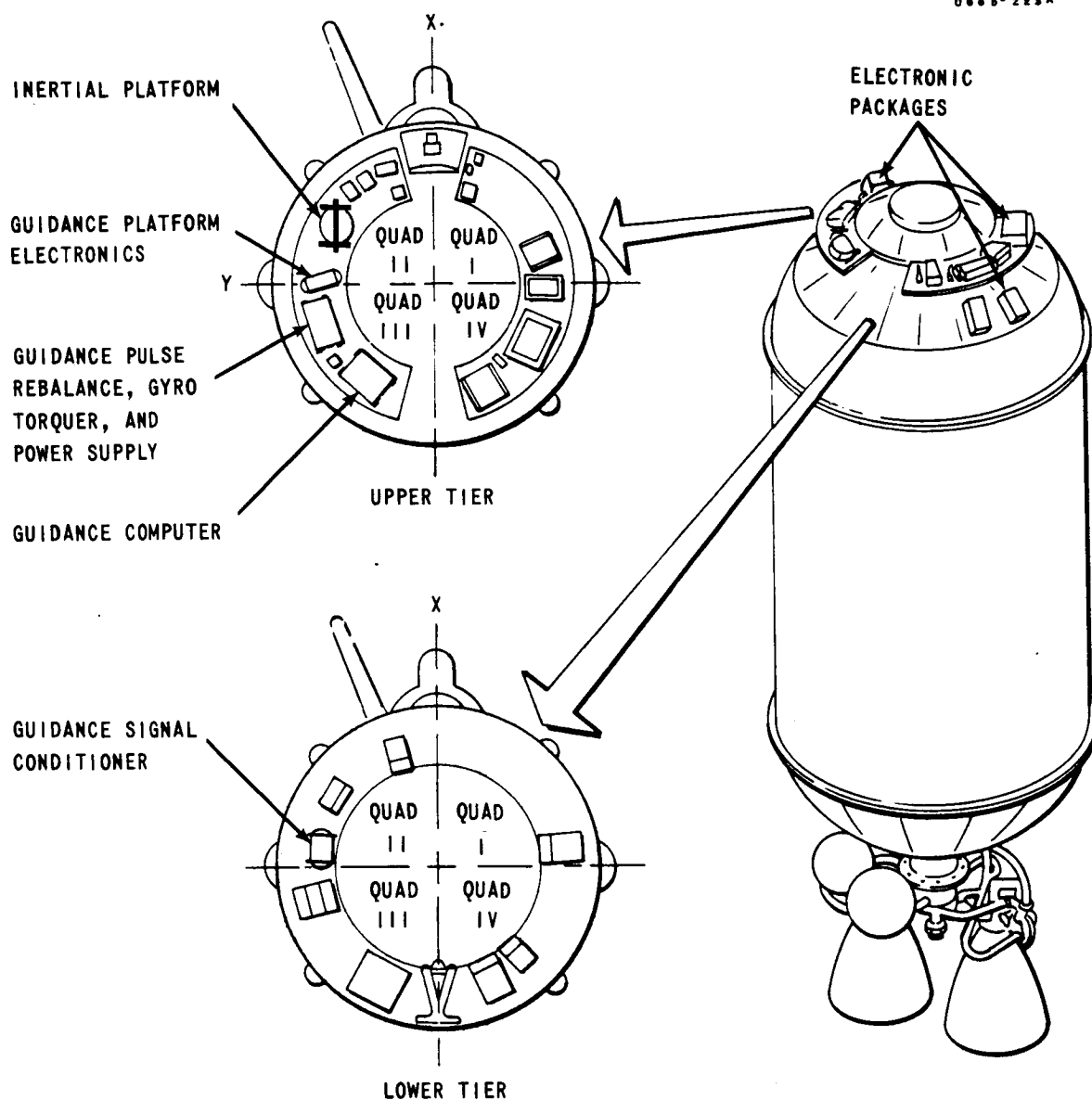


FIGURE 1.3-2. GUIDANCE INSTALLED IN VEHICLE

A6405-94 -01

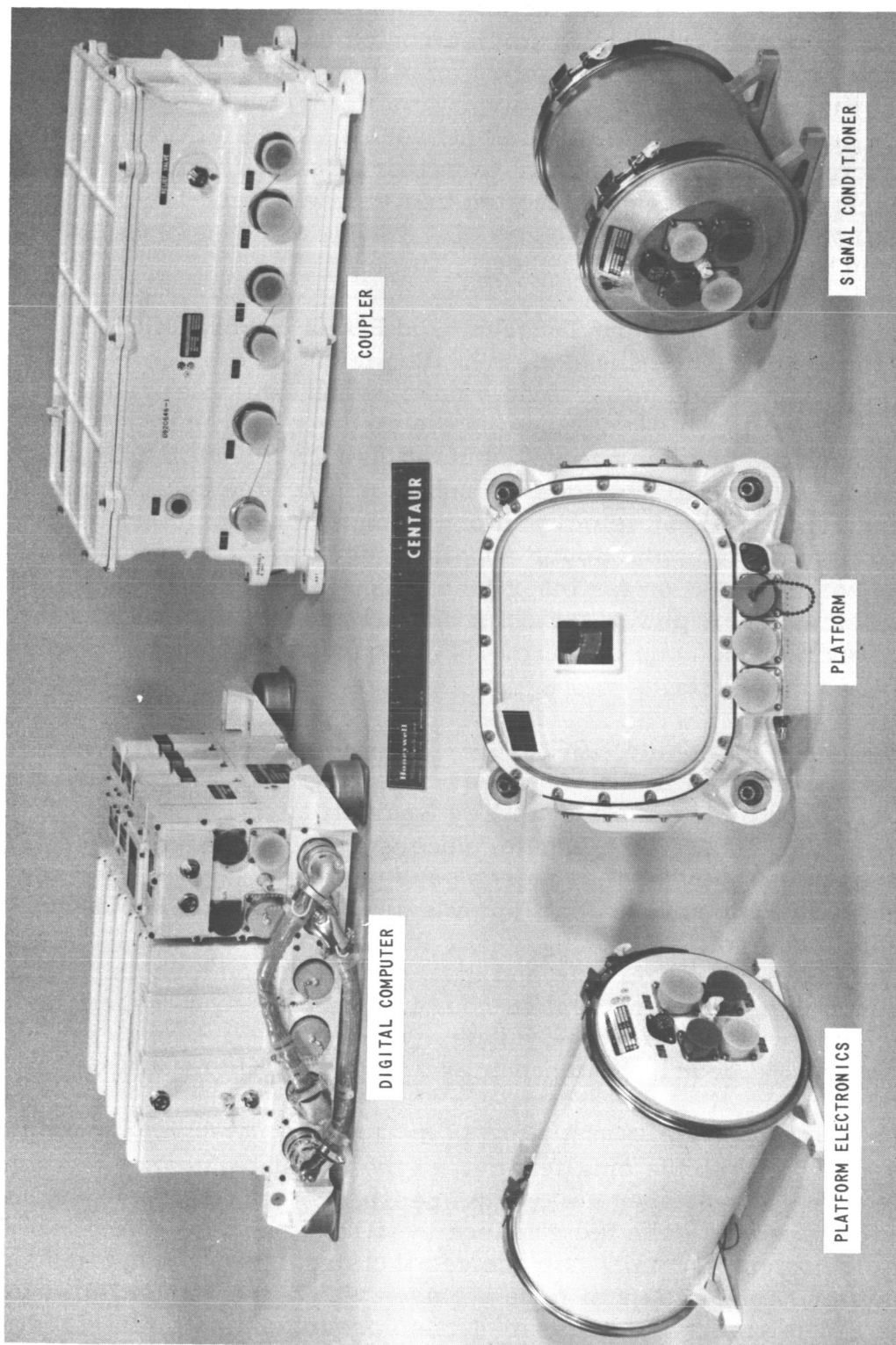


FIGURE 1.3-3. CENTAUR MISSILE GUIDANCE SYSTEM

2. Platform Electronics DEG8039. - In the lower left-hand corner of the picture is the platform electronics unit. This package contains the four gimbal control amplifier assemblies for the stabilization loops, five resolver amplifiers, various switching functions, and their associated networks. The platform electronics package consists of a tubular container designed to achieve light-weight and compact construction that will withstand the required environment. The unit weighs 18.5 pounds and is approximately 17 inches long by 7-1/2 inches in diameter.
3. Pulse Rebalance, Gyro Torquer, and Power Supply DGG8014. - In the upper right-hand corner of the picture is a pulse rebalance, gyro torquer, and power supply unit, which is also called the coupler unit. This unit contains the electronics required to feedback the accelerometer's output through a combined analog and digital loop to provide both rebalancing of the accelerometer pendulum and input velocity information to the computer. This unit also contains the power supplies necessary for gyro torquing and basic excitation for other functions within the missile guidance system. Major power switching functions are also provided by this unit. The coupler weighs 62.5 pounds and occupies a volume of 1.58 cubic feet.
4. Navigation Computer DBG8016.- The digital navigation computer is pictured in the upper left-hand corner of Figure 1.1-3. It has been built for Honeywell by Kearfott Division of General Precision, Inc. The computer receives velocity information from accelerometer rebalance pulses, and performs both inflight and preflight computations. Its outputs are discrete commands for vehicle control, a steering vector in inertial coordinates via self-contained D/A converters, and gyro compensation torquing during ground tests. The navigation computer is a drum storage type machine with approximately 3000, twenty-five bit, word capacity. It weighs 67 pounds, and occupies 1.83 cubic feet of space.
5. Signal Conditioner DDG8015. - In the lower right-hand corner of Figure 1.3-3 is the smallest unit of the missile guidance system, the signal conditioner unit. This package is an electronic device which prepares selected guidance system signals for transmission via the telemetry unit. It receives the signals from other guidance units and converts them to dc voltages which are compatible with the FM telemetry equipment. It also provides a path for direct digital telemetry transmission from the computer unit. The signal conditioner package is very similar to that of the platform electronics and weighs approximately 10 pounds.

6. Auxiliary Signal Conditioner DDG8032. - The 10 pound auxiliary signal conditioner is pictured in Figure 1.3-4. This unit was used to provide an additional nine channels of guidance telemetry for certain R&D flights. The housing assembly is identical in size to the DDG8015 signal conditioner.

1.3.3. Basic -3 GSE Description. - The -3 GSE consists of the following assemblies (it should be noted that any single field site does not have all of these assemblies):

<u>Honeywell Part Number</u>	<u>Designation</u>
DYG8021	Launch Site MGS Checkout Set
DYG8020	Trailer MGS Checkout Set
DYG8019	Laboratory MGS Checkout Set
DUG8043	Maintenance Equipment
DUG8058	Computer Test and Loading Equipment
DUG8205	Remote Load and Read Test Set
DUG8221	System Test Set

A brief description of each GSE assembly follows:

1. Launch Site MGS Checkout Set, DYG 8021. - This GSE set is used for non-automatic checkout of the MGS at the launch site or at the Combined Systems Test Stand (CSTS). The GSE provides computer and IMU mode control, platform coarse alignment, and monitoring capabilities for important MGS signals. The launch site equipment also contains a Launch-On-Time (LOT) Decoder to monitor ETR time signals, decode the time, and transmit a signal to the computer. The computer flight equations are modified by the output signal from the LOT Decoder.

In the past year, this GSE has been replaced by the Computer-Controlled Launch Set (CCLS) for primary prelaunch MGS checkout.

2. Trailer MGS Checkout Set, DYG8020. - The GSE used to perform guidance system checkout in the vehicle contractor's factory can be located in a mobile trailer. The functions performed are similar to those of other GSE, with essentially only the physical configuration changed to accommodate the trailer.
3. Laboratory MGS Checkout Set, DYG8019. - This configuration GSE is located in the guidance laboratories at Honeywell, the vehicle contractor's factory, and at ETR. The control and checkout functions provided by the lab set are quite similar to those provided by the previous two GSE's.



FIGURE 1.3-4. CENTAUR AUXILIARY
SIGNAL CONDITIONER

4. Maintenance Equipment, DUG8043. - The GSE maintenance equipment consists of special purpose extender cables, breakout test point boxes, and some general purpose commercial test equipment. The primary function of this equipment is to provide added versatility of monitoring for fault isolation.
5. Computer Test and Loading Equipment, DUG8058. - This group of equipment may be required for testing a guidance computer individually, or to control and communicate with the computer as a part of the MGS. It consists of four separate parts:
 - a. Fill and Test Unit (FTU), which is used to load the computer memory or test the operation of the computer.
 - b. Tape Reader, which is used with the FTU to verify computer memory drum loading.
 - c. Input/Output Test Set, which is used to simulate computer inputs and outputs to check the computer.
 - d. Card Checker, which is used to individually test computer circuit boards.
6. Remote Load and Read (RL&R) Test Set, DUG8205. - The RL&R is used for communication with the temporary storage of the guidance computer. Using the computer's mode control lines, the RL&R is able to alter the computer's temporary storage as required. Also, certain data may be read from the computer (via its telemetry output line) into the RL&R, when required during MGS ground operation.
7. System Test Set, DUG8221. - This GSE set is similar, functionally, to the previously described MGS checkout sets, except that it is used in the Honeywell Engineering test laboratory for IGS development. Its main differences from other GSE sets are that it is equipped with casters for mobility and bulkhead connectors for easy removal of cables. Modifications of this configuration are used by Honeywell Production for MGS acceptance testing.

More detailed MGS and GSE information will be discussed within the individual topics in Sections 2 through 6 of this report.

Topic 1. 4

Description of Centaur IMG

1. 4. 1. Introduction. - The Centaur Inertial Measurement Group (IMG) consists of two units, the Inertial Reference Unit (IRU) and the System Electronics Unit (SEU). The IMG units perform basically the same flight functions as the present Phase II PIP IMU. There is, however, the added capability of three axis steering within the IMG. The IMG was designed to meet the following goals (relative to the IMU):

1. Increased reliability (1350 hours MTBF versus 225 hours for the MGS).
2. Simplified interface within the major guidance control loops.
3. Reduced weight and power consumption.
4. Lower build and test time.
5. Low technical risk through full application of rigorous design practices.
6. Derived vehicle turning rates from the steering chain data.

1. 4. 2. Detailed Unit Description. - The following is a brief description of each IMG unit (units shown in Figure 1. 4-1).

1. Inertial Reference Unit (IRU). - On the left of the figure is the Inertial Reference Unit, which contains both the inertial reference platform and its related control loops. There are basically two halves to the IRU. The half with the window visible contains the equivalent of the present IGS platform. It contains GG49 gyros, GG177 accelerometers, IGS platform, gimbals, etc. A significant difference is that the gimbal structure is supported by trunnions, which contain "doughnut" type flight vibration isolators. The other (top) half of the IRU contains all control loop electronics subassemblies, grouped by function in an aluminum casting. This half of the IRU is equivalent to portions of the Coupler and PE in the IGS. The IRU weighs approximately 53 pounds, measures 13.2 inches x 14.1 inches x 17.7 inches and occupies approximately 1.9 cubic feet of space. The IRU may be vehicle-mounted in any of several different attitudes.
2. System Electronics Unit (SEU). - The System Electronics, shown on the right-hand half of Figure 1. 4-1, features a large central casting to which are mounted the major components, assemblies,

A6707-76

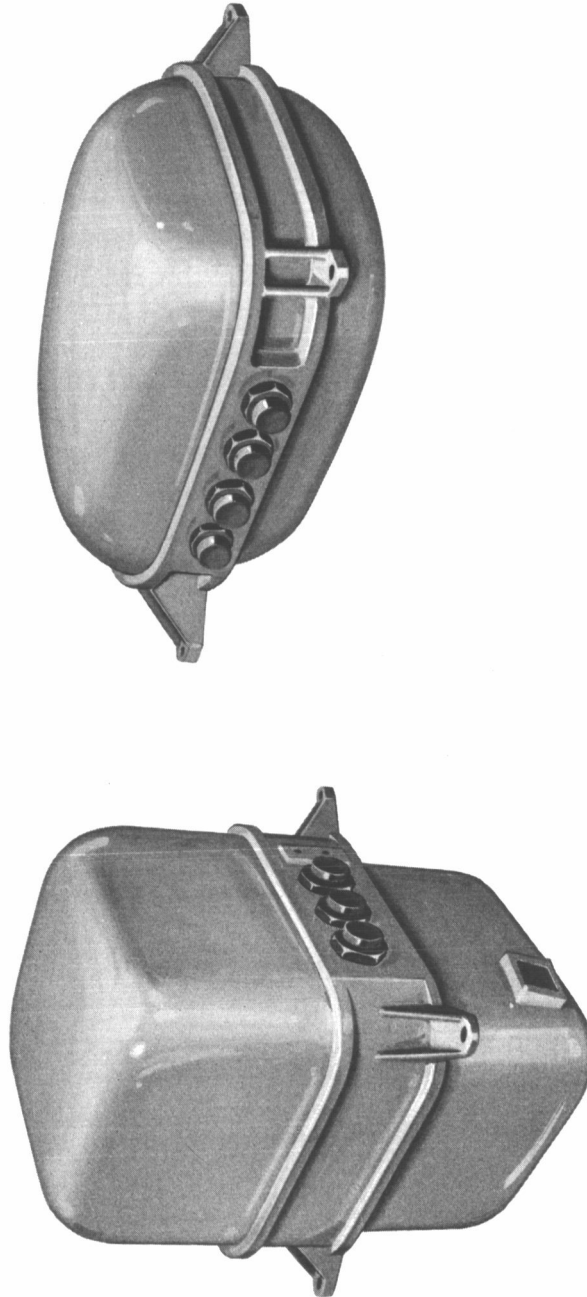


FIGURE 1.4-1. CENTAUR IMPROVED IMG

and connectors. The SEU contains radio and audio noise filters, power supplies, and mode sequencing components. The SEU measures 8 inches X 12 inches X 16.75 inches, occupies a volume of one cubic foot and weighs 27 pounds.

1.4.3. Automatic Ground Equipment (AGE). - Launch site calibration and control of the IMG will be performed by launch site computer-controlled equipment. However, in the Honeywell factory and laboratories, IMG (and unit) testing will be performed by an instrumentation rack, manual test set rack, and a Honeywell DDP-516 commercial computer. Figure 1.4-2 depicts the planned equipment arrangement for a laboratory test of the IMG.

With the use of an external test computer, the test and calibration operations of the IMG will be fully automated. This approach is a further improvement beyond those of the IGS program, where manual and semi-automatic techniques are used.

0967-198AS

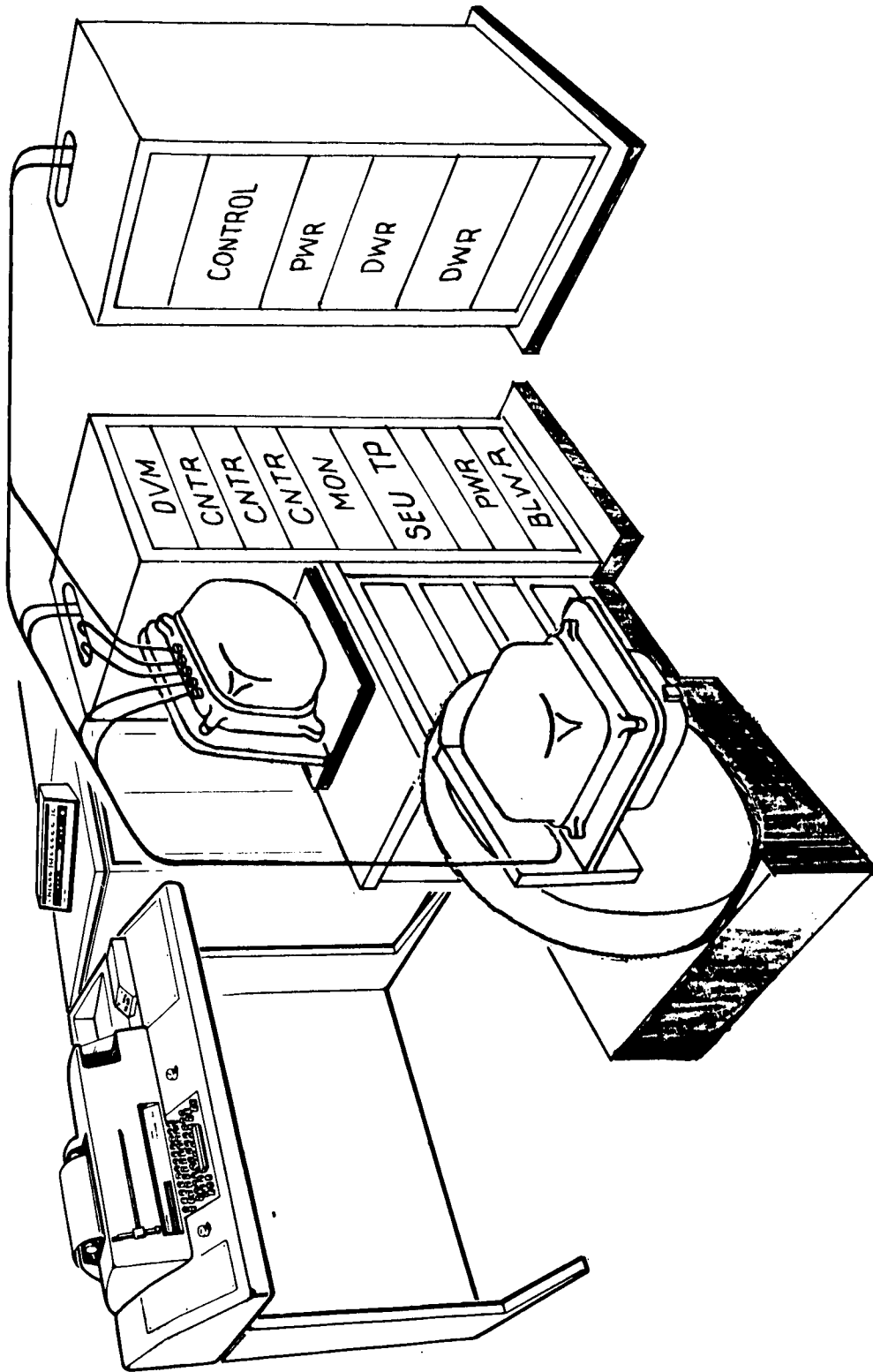


FIGURE 1.4-2. IMG TEST

Topic 1.5

Mission Requirements and Their Evolution

1.5.1. Definition of Requirements. - There are any number of performance criteria which can be used to define the mission requirements of a guidance system. The overall criterion chosen for the Centaur MGS is the magnitude of the correcting velocity impulse, which would have to be applied to the payload to correct for launch vehicle injection errors. For Surveyor and Mariner missions the midcourse correcting velocity impulse is that required to cause the payload to pass through the target point. For the case of the Earth orbits, the post-injection correcting velocity impulse is that required to cause the payload to assume the intended orbit. The correcting velocity impulse is denoted as the Midcourse Correction Requirement (MCR) when arrived at by an algebraic summation of individual errors, or as the "Figure of Merit" (FOM), when it is a statistical combination of errors. It is usually defined for a particular mission and is normally expressed in meters/sec. A low MCR or FOM therefore corresponds to good system performance and may be used as a convenient indication of relative system performance, as well as an absolute measure of any one system.

The major IGS error sources relate primarily to uncertainties in the inertial components, their associated circuitry, and their calibration techniques. Therefore, a valid estimate of performance of the IGS can be made by classifying error sources into equivalent gyro and accelerometer parameters, and combining these parameters.

1.5.2. Evolution of Centaur Mission Requirements. - As originally conceived, the Atlas-Centaur vehicle was a general purpose space booster-- that is, it was intended to fulfill a wide range of missions from a low altitude, near-Earth circular orbit, through the gamut of escape-type missions, such as the Surveyor lunar payload and the Mariner interplanetary payload, and up to a highly precise, synchronous orbit, such as would be used for a 24-hour communication satellite. However, the original mission requirements were based on Earth orbits: (1) a 300 nautical mile orbit and an equatorial 24-hour synchronous orbit for the dash 1 MGS; and, (2) a 110 nautical mile orbit and equatorial 24-hour synchronous orbit for the early dash 3 MGS. The low orbit placed stringent accuracy constraints on accelerometer misalignment angles and gyro MUSA. The

24-hour orbit placed a severe constraint on gyro CT. The total result was a rigid set of performance specification requirements which covered all three missions. Prior to the Phase I PIP design improvements in the hardware, the mission emphasis was shifted to Surveyor escape-type missions. The results of the Surveyor mission emphasis were a relaxation of portions of the performance specifications (down-range and vertical gyro CT and MU terms and cross-range accelerometer loop errors) and an increased emphasis on the down-range accelerometer loop errors and cross-range gyro terms. Thus, the performance specifications were tailored to the general Surveyor mission sensitivities. The Phase I PIP improved the mission-critical error sources. Further IGS accuracy improvement was obtained as a result of the improved calibration procedures, and as a bonus result of the Phase II PIP. Today, the mission emphasis is again expanding to cover the full range of the previously named missions. The MGS accuracy has progressively improved, and it is now considered sufficient to meet all of the potential mission requirements.

Topic 1.6

Program Accomplishments

1.6.1. Summary. - The results of the Centaur IGS development program have been the evolution, qualification, and use of an all-inertial guidance system for boost vehicle applications. Originally, the IGS was marginal in both performance and reliability, but it has since been improved and has become a fully operational system. This was not achieved without problems and set-backs along the way. However, an operational system was obtained and, in the process, a number of important advancements were achieved in the field of inertial guidance. Several, previously untried, design concepts for space vehicle guidance were proven in the total space flight environment. The most significant technical accomplishments resulting from the program are summarized in the following paragraphs of this topic. (Note: There is no correlation between the sequence of the items and their relative significance. Rather, the items are presented in the same sequence in which they appear in later Topics within this report.)

1.6.2. Miniature Gyro. - The single-degree-of-freedom Miniature Inertial Gyro, which is used in the Centaur IGS, has been proven capable of performing the task of accurate space booster guidance. This was accomplished within the complex environment of the platform and vehicle (electrical noise, vibration, magnetic fields, complex thermal environment, etc.). The performance of the present model of the DGG49 gyro, in the platform, approaches the same performance level that it is capable of when operated singly in a benign test environment (reference Topic 2.2 for details).

1.6.3. Accelerometers. - The DGG177 flexure pivot accelerometer has also been proven for the Centaur boost vehicle guidance application. It has solved the accuracy problems which were associated with its predecessor, the DGG116 floated pendulum accelerometer (reference Topic 2.3).

1.6.4. Resolvers and Torque Motors. - The application of pancake type, direct drive torque motors and resolvers has been successful in the Centaur platform. This was a major factor leading to a truly miniature platform. The use of pancake type rotary components not only facilitated platform miniaturization, but also provided added performance capability

by the elimination of gear train backlash. However, consistent performance and reliability can be accomplished only through strong vendor control and attention to process quality control (reference Topics 2.4 and 2.5).

1.6.5. Sliprings. - A relatively trouble-free, miniaturized, 38-circuit slipring assembly has been developed, produced, and found suitable for inertial platform application. This breakthrough occurred after several years of significant slipring problems. The present Centaur slipring design has exhibited a level of reliability, which previously was not thought possible (reference Topic 2.6).

1.6.6. Platform Thermal Environment and Control. - System flight performance results have shown that the gyro and accelerometer environment within the platform can be controlled so that the full performance capability of the inertial elements can be realized even when exposed to the full space vehicle environment. To accomplish this, required the development of sophisticated math models for both thermal and vibration control. Definition of the significant thermal and vibration factors, and their interactions, proved to be invaluable to understanding, predicting, and controlling the internal platform environment. This analytical tool was combined with detailed thermal and vibration mapping of the platform hardware, realistic solar simulation tests, and the development of precise vibration isolators for platform mounting to realize the full performance potential of the inertial instruments (reference Topics 2.9 and 2.10).

1.6.7. Gimbal Stabilization. - The completion of a detailed linear servo analysis of each IGS stabilization loop and the design of a simplified dc servo loop for the IMG application are significant milestones within the Centaur guidance program. The expanded servo analysis, which was performed in 1964-1965, has been helpful in solving subsequent gimbal stabilization loop problems. Although the present IGS loops have met their requirements, the dc servo loop should prove to be more reliable, efficient and economical than the present IGS mechanization (reference Topics 2.11 and 6.5).

1.6.8. Pulse Rebalance Electronics. - The initial development of the accelerometer pulse rebalance electronics loop was an advance in the state of the art of inertial guidance systems. Further refinement, throughout the Centaur program, has resulted in a sophisticated design, possessing good reliability and accuracy well within expected limits. The DGG177 accelerometer and the Centaur PRE mechanization approach the capability of pendulous gyro accelerometers (PGA's) in the area of scale factor stability, and meet or better them in the areas of bias and

axis alignment stability. The PRE mechanization for the IMG further refines and simplifies the pulse rebalance concept, with the expected result being additional gains in reliability and accuracy (reference Topic 2.15).

1.6.9. Navigation Computer Utilization. - Optimum use of the guidance computer was made by utilizing it not only for its necessary flight function, but for preflight operations as well (semiautomatic system calibration). This was accomplished, despite limited computer memory and input/output capability, and the unique programming problems associated with optimizing memory access in a drum computer program (reference Topic 3.5).

1.6.10. Primary Power Interface. - A single 28VDC prime power vehicle interface has been defined for the IMG development. This is an interface simplification over the present AC (115V, 400 Hz, 3-Phase)/DC (28V) interface. The areas of both ground-to-vehicleborne power switchover and electromagnetic interference control, which had been problems during the IGS development, should become greatly simplified (reference Topics 4.3 and 6.13).

1.6.11. MGS/GSE Mode Control. - An advancement within the program has been the implementation of the Computer Control Launch Set (CCLS) which provides automatic mode control of the MGS at the launch complex. This has increased guidance calibration and checkout efficiency during prelaunch operations. This innovation insures strict adherence to detailed operating procedures, thereby eliminating problems of operator error which were not uncommon with the original manual mode control mechanization. The automatic mode control technique is being carried forward into the Centaur IMG development program (reference Topics 5.2 and 6.12).

1.6.12. Computer Test Equipment. - A major advancement within the program was the development of a reliable means to communicate with the memory of the Navigation-Computer over the long landlines at the ETR launch complex. This provided a high degree of flexibility in launch operations and was a significant improvement over the original manual Fill/Test Unit, which had been used at the MGS location on the vehicle. This use of the FTU was somewhat hazardous for launch operations because of its relatively complex manual operating requirements (reference Topic 5.3). The need for automatic techniques, using a ground-based computer, was aptly proven on the IGS program (reference Topics 5.2, 5.3, and 6.12).

1.6.13. Steering and Coordinate Transformation. - The basic IGS two-axis steering approach of transforming a pointing vector from inertial coordinates into vehicle coordinates, by means of a resolver chain, has been extended, via frequency multiplexing to provide three-axis steering with the IMG. Simultaneously, the overall accuracy of coordinate transformation is being improved by the use of active compensation networks, which better simulate the impedance characteristics of the resolvers over the frequency range of interest. The result should be a more accurate and reliable coordinate transformation scheme to support full, guidance controlled, vehicle steering from lift-off for future missions. (reference Topic 6.7.)

1.6.14. Automatic Self-Leveling. - The Centaur Inertial Guidance System has demonstrated the technique of automatic self-leveling, without use of auxiliary leveling devices or electronics. Mechanization of the basic acceleration sensing function of the system to sense and correct for off-level angles, through computer controlled gyro torquing, has proven to be accurate and trouble-free. It will be used for the improved Centaur IMG. (reference Topic 6.8.)

1.6.15. Miniaturization. - The Centaur miniature platform has demonstrated that boost vehicle guidance, within acceptable limits of present day mission accuracy requirements, can be realized from a relatively small inertial package. This inertial platform packaging technique complements present day (microminiaturized) electronics packaging techniques and reduction in total guidance system size, weight, and power consumption can be achieved. However, care must be taken on future designs to insure that the objective of miniaturization does not get out of perspective and force unnecessary constraints upon the overall IGS design, producibility, and reliability. (reference Topic 6.15, also Topics 2.9, 2.10, 2.14 and 2.19.)

1.6.16. The Final Result. - The total effect of these technical accomplishments has been a 3:1 performance improvement and a 4:1 reliability improvement during the IGS evolution. From the original -1 system which, at best, demonstrated only marginal performance and reliability, the Centaur IGS has now developed into a fully operational system which has successfully guided the Atlas-Centaur vehicle for six operational Surveyor flights.

SECTION 2

INERTIAL MEASURING UNIT

Topic 2.1

Introduction To The IMU and IMG

2.1.1. General. - Section 2 provides a technical discussion of the sensor systems, along with related tests, specifications, problems encountered and lessons learned. The presentation of these subjects is divided by unit. This is done because each unit was designed, tested, etc., as a separate entity, even though its functional aspects involve other units. Where the interface is critical, sufficient information will be presented in each unit level topic to permit the reader to "close the loop". In some cases, it will be helpful to refer to the system design topics in Section 6 in order to place an electronics topic in proper perspective. Frequent cross-referencing by Topic Number is provided in this section to aid the reader in this regard.

2.1.2. IMU Functional Description. - The guidance system sensors and support electronics are contained in the units defined as the IMU (refer to Topic 1.3 for a description). The IMU and Navigation computer, together, are defined as the MGS. Within the IMU are the following units:

1. Inertial Platform,
2. Platform Electronics,
3. Coupler,
4. Signal Conditioner.

There are basically three sensor subsystems in the IMU. Inertial sensors are installed on the innermost (first) gimbal of the platform. These sensors provide:

1. Space stabilization under vehicle turning rates by gyroscopic principles.
2. Linear acceleration measurement in Earth-referenced coordinates by single-axis, hinged-pendulum accelerometers.

The platform electronics unit contains the electronics which provide corrective commands to the platform gimbal torque motors, based upon gyro gimbal displacement information. The coupler unit contains the electronics necessary to pulse-rebalance the accelerometer pendulums, and to provide velocity information to the coupler.

The IMU resolver chain function relates vehicle coordinates to the inertial platform coordinates. This function is performed by a resolver chain, composed of the resolvers on the end of each platform gimbal. The input and output amplifiers for the resolver chain are contained in the platform electronics unit.

Secondary power supplies necessary for the performance of these sensing functions are placed in the coupler unit. The coupler also contains the circuits for applying gyro torquing signals from the computer.

2.1.3. IMG Functional Description. - The IMG is the Improved Centaur equivalent to the IMU. Fundamental sensor systems are similar to the IMUs, but the emphasis on the IMG is for increased reliability, lower build and test time, and reduced power and weight requirements.

Topic 2.2

Platform Gyros

2.2.1. Introduction and Summary. - The purpose of this topic is to discuss the evolution of the floated, miniature single degree of freedom (MSDF) gyros used on the Centaur -1 and -3 IGS program. A problem definition-design solution approach will be used throughout with key dates and periods defined. A discussion of the most significant problems and their solutions will be found under the sub-topic headings. A brief summary of gyro problems and corrective design changes is listed in Table 2.2-1. Major gyro problems in the early phases of the program were predominantly performance oriented, including both grossly erratic and marginal drift rate stability, in both acceleration sensitive and acceleration insensitive terms. Catastrophic type failure (opens and shorts) also constituted another problem category.

The first step in a future program to preventing many of the type problems encountered in the past is to define and document carefully the detailed gyro requirements via technical development specifications. In this phase of the program, the systems engineer, platform designer, and gyro designer must work very closely together. To supplement this, timely and periodic design reviews should be initiated at the beginning of each design phase. The gyro characteristics should be completely evaluated, early in the program, by a thorough evaluation test program at the gyro, platform, and system levels. Rigid process, configuration, and test controls should be implemented, once the gyro design is released. With incorporation of and adherence to these aids, the probability of confidently meeting system design requirements for the gyro will be greatly enhanced.

2.2.2. General Background. - The gyro used in the Missile Guidance Set (MGS) on the Centaur Program is classified as a Miniature Inertial Gyro (MIG). The DGG49 gyro that has been used throughout the Centaur Program is a single degree of freedom (SDF) gyro. (Reference Figure 2.2-1.) Design changes to the gyro have been incorporated throughout the program in order to further develop its ultimate growth potential. The DGG49 gyro was selected as the gyro for Centaur in early 1959. Consideration was also given to a different model of the MIG, known as the DGG8001. It differed from the DGG49 principally in that it contained improved pickoff

TABLE 2.2-1

SUMMARY OF GYRO PROBLEMS AND CORRECTIVE ACTION

Gyro Designation	Major Problem Areas	Design Changes at Gyro Level for Corresponding Problem	Design Release Effectivity Date
DGG49D6 -1 Centaur (1959-1961)	1. Large mass shifts. 2. Dualsyn dielectric breakdown. 3. Constant Torque stability and Random Drift.	1. Work in process on balance pan. 2. Dualsyn magnet wire changed from Formvar to Nyleze insulation. 3. Studies in process to isolate cause.	1. Balance pan installed in DGG49D15 for -3 program in late 1962. 2. Formvar to Nyleze in mid-1961. 3. None on -1 program.
DGG49D15 -3 Centaur (1962-1964)	1. Large mass shifts. 2. Dualsyn dielectric breakdown. 3. Constant Torque stability and Random Drift. 4. Changing Gyro Transfer Function with heater power.	1. Balance pan incorporated. 2. Mylar interskin inserts added. 3. Flex lead clips and ABEC-9 bearing plus controlled oil retention retainers. 4. Distributed heater-sensor and changed damping fluid.	1. (See 1 above) 2. Effective in late 1963. 3. Effective late 1962. 4. Effective late 1962.
DGG49D20 -3 Centaur (1964-1965)	1. Drift rate stability with platform gimbal orientation. 2. Constant Torque and Random Drift (OAV)	1. Studies in process to isolate causes. 2. Steps to incorporate small stop angles and new flex leads initiated. NOTE: The DGG49D20 is the same as the DGG49D15 except D20 designates mylar dualsyn.	1. None. 2. Effective in mid-1965.
DGG49D26 -3 Centaur (1965-Present)	1. Drift rate stability with platform gimbal orientation. 2. Constant Torque and Random Drift (OAV).	1. Fine balanced spin motors and detuned platform from 400 Hz mechanical resonance. 2. Reduced stop angle and incorporation of new flex leads. NOTE: The DGG49D26 is the same as the DGG49D20 except for reduced stop angles and new flex leads (thinner and wider).	1. Fine balance spin motor and platform detuned in late 1965. 2. Effective late 1965.

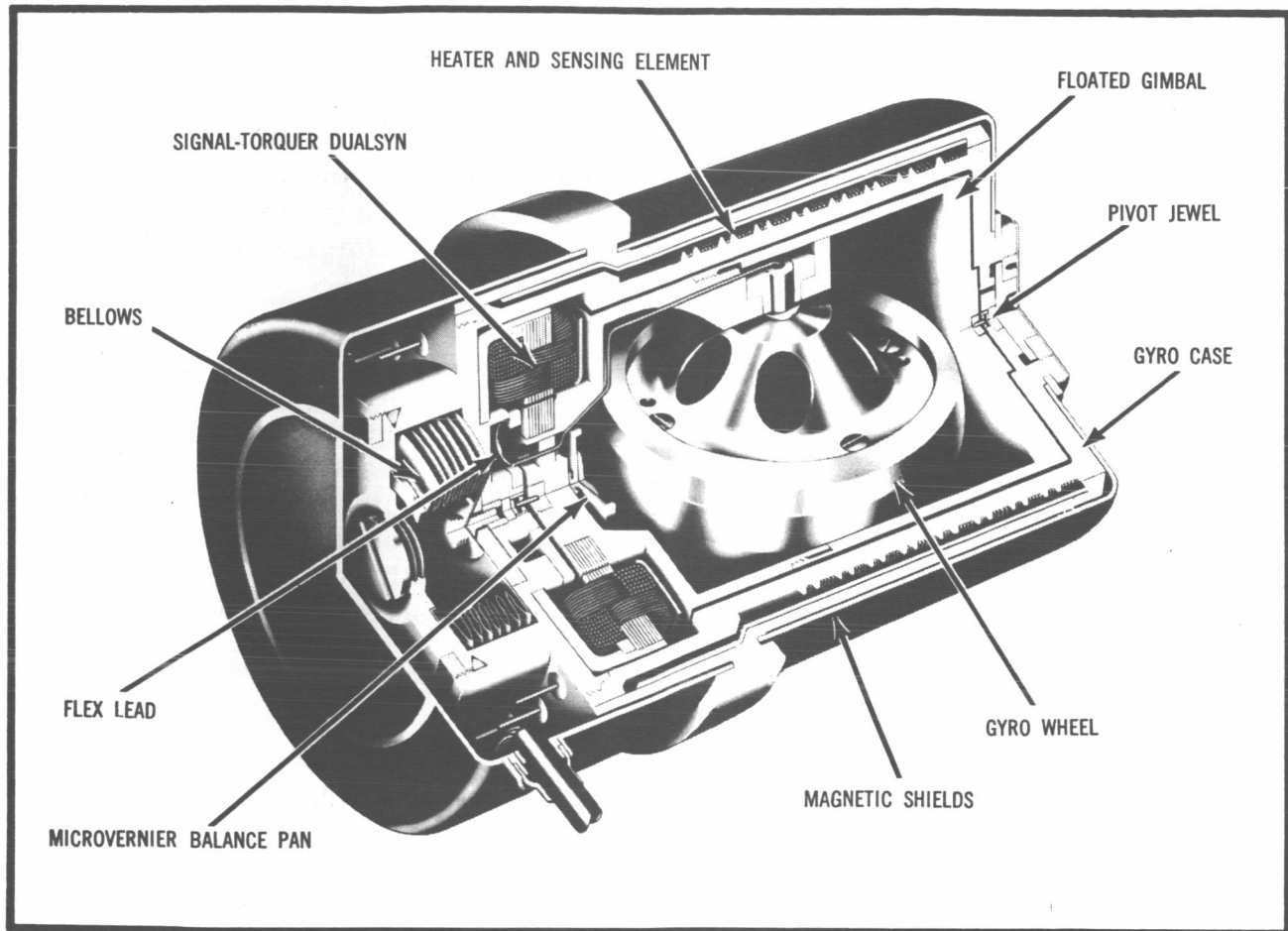


FIGURE 2.2-1. GG49 MINIATURE INTEGRATING GYRO

and torquer assemblies. The DGG8001 was also a SDF gyro. The DGG49 was selected over the 8001 because it presented lower risk, having been in production for several years. The SDF gyro was chosen over the two-degree of freedom (TDF) gyro for this application. Some factors that enter in the tradeoff studies of miniature SDF versus TDF gyros are shown in Table 2.2-II.

2.2.3. Design Characteristics - (DGG49 SDF Gyro). -

1. Spin Motor. - A three-phase hysteresis synchronous motor is used. At 24,000 rpm (synchronous speed), the motor develops an angular momentum of 10^5 gm cm²/sec. Nominal running power is 2-1/2 to 3 watts.
2. Suspension and Damping. - The motor is contained in a floated cylindrical gimbal. Suspension of the gimbal is achieved through the buoyant support, provided by the high density fluid (fluorolube) between the gimbal and case. The gimbal is centered radially and restricted axially within the case by pivots and jewels. The fluid density at operating temperature has about the same density as the float (gimbal). By floating the gimbal, low pivot-jewel friction is realized. This design also possesses an inherent high resistance to shock and vibration.

Gimbal damping results from the action of the viscous shear of the damping fluid in the gimbal-case gap. The damping magnitude is dependent upon the fluid viscosity and the gimbal-case surface geometry.

3. Dualsyn. - The dualsyn is a magnetic pickoff and torquer, physically combined into one subassembly. The signal generator (SG) output is a function of relative gyro gimbal-case angular motion about the gyro output axis. The stator windings are wound on a laminated iron core so the SG functions as a differential transformer, with an output proportional to the angular displacement of the moving iron rotor attached to the gimbal. A phase reversal occurs in the output as the gimbal passes through SG electrical null; therefore, gimbal rotational sense is indicated by the relative phase of the output.

The gyro torque generator (TG) can be used to receive external compensation or command signals for introduction into the gyro, and hence the platform attitude control loop. The DGG49 torquer

TABLE 2.2-II

GYRO COMPARISON AT TIME OF SELECTION OF MSDF GYRO*

Factors Considered	TDF	MSDF
Float	Must be balanced precisely around two axes (center of gravity, center of flotation with center of support). Symmetrical heat flow distribution is essential.	Less difficult to build, precision balancing required only around one axis. Symmetrical heat flow desirable but not as critical as TDF gyro.
Extra Gyro Gimbal	Must be small to avoid paddle damping effects; balanced and floated to avoid disturbing torques and friction.	(None required)
Flex Leads	More required due to two torquers and two pickoffs. Must possess same flexible characteristics in two directions. Higher flex lead reaction torque at zero position.	Fewer required. Flex lead need be flexible in one direction only. Attachment makes possible lower flex lead reaction torque.
Gyros Required	Two	Three
Platform Packaging	Poorer density factor with two gyros.	Better density factor for three-gyro package.
Power		Slightly higher due to third gyro motor power.
Weight	Heavier, but only two required. Total weight of two gyros is approximately 6 to 8 pounds.	Lighter, but three required. Total weight of three gyros is 1.5 pounds.

* Comparison studies were made in 1958 for available gyros compatible with miniature inertial platforms.

utilizes both a pattern field and a control field. Both fields must be excited to produce a torque about the gyro OA. The pattern field is normally excited with a fixed current, whereas the control field is excited with a variable current, proportional to the desired compensation or command rate. The torque produced is a function of the product of the currents in the two windings. The DGG49 gyro has a maximum continuous torquing capability of 7200 deg/hr.

4. Heater - Sensor. - Proper operating temperature is maintained by means of an internal temperature sensing element and heaters operating in conjunction with an external temperature control amplifier (TCA). The heater and sensor are noninductively bifilar wound, in close proximity to each other and to the damping gap. Close thermal coupling (heater-sensor) and efficient heat flow to fluid gap results. The sensor has a nominal sensitivity of +1.5 ohms/°F change in temperature. There are two heaters: (1) a warm-up heater used for fast warm-up, and (2) a control heater distributed over the entire length of the damping gap to provide uniform heat dissipation.

2.2.4. Special Design Feature. - The DGG49 features a Microvernier Balance Pan, a major design advancement in float balancing. The balance pan is a small disc which contains a heater and is partially filled with an eutectic alloy. The heater is used to incrementally melt and shift the eutectic mass to permit precise radial balancing of the gimbal. The balance pan is mounted on the inside of the gimbal, along the output axis. The design of the microvernier balance pan permits new techniques in the actual balancing process without disturbing the hermetic seal and eliminates the need for coarse balance adjustments on the float. In addition to gains achieved during gyro build and calibration processes, this feature permits gyro gimbal rebalancing in the laboratory, whenever necessary, after initial gyro installation in the platform.

2.2.5. Evolution of Requirements. - The early 1961-1963 mission requirements for the MGS were predicated upon placing a spacecraft fired from the Eastern Test Range into a 110-nautical mile orbit. In addition, the guidance set was required to be capable of placing a satellite into an equatorial 24-hour orbit after a coast time of up to 15 hours. (Reference Topic 1.5.)

In 1963, the mission objectives for the MGS were redefined. The new requirement for the guidance set was defined in terms of placing a spacecraft in a lunar trajectory (Surveyor Mission). The reflection of the 24-hour orbit mission requirements into the gyro requirements were as follows:

1. The 24-hour synchronous orbit mission placed emphasis on long-term operating stability requirements for the acceleration insensitive gyro drift term. Stability requirements for the gyro were:
 - a. Acceleration Sensitive: 0.04 deg/hr/g (1-sigma) determined from a 24-hour random drift test.
 - b. Acceleration Insensitive: 0.12 deg/hr (6-sigma band) determined from OA vertical up-down test.

It is to be noted that the V gyro acceleration insensitive term (Vg CT) was calibrated during system level tests with the OA vertical up, and in the final align or launch orientation the OA was vertical down. To control the OA \uparrow to OA \downarrow drift rate changes, a stringent "dumping" test was levied on all flight gyros. This condition remained up to the incorporation of the UGT calibration program, which was implemented in early 1966. With the UGT program, changes were made in calibration orientations such that the V gyro is now calibrated and flown with the OA vertical down. In turn, the U gyro is now calibrated with the OA vertical up and flown with the OA vertical down. This change was predicated upon the relative mission sensitivities for the U gyro and V gyro Constant Torque (CT) the V gyro being the larger. The V gyro CT, calibration induced flight error that resulted from calibrating the term in one attitude and flying in another was thus eliminated.

2. Surveyor mission requirements permitted a slight relaxation in gyro stability requirements. Initial calibration requirements for the system were such that up to 8 consecutive days of system calibrations could be performed without removing the MGS from the vehicle. Calibration accuracy from day-to-day was subject to the removal of all system power, with only forced air convection being used in the guidance compartment to maintain case skin temperatures between +40°F to +120°F. This reflected into the following gyro requirements:
 - a. Eight-day stability requirements for MUSA with following inputs:
 - (1) Seven +40°F cool-downs.
 - (2) Seven spin motor run downs (total excitation removal).

- b. CT, MUIA, and MUSA magnitudes remained less than 2.0 deg/hr with the same inputs as applied in a.(1) and (2), above.

The Surveyor mission requirements were reflected into the gyro test requirements and philosophy in early 1963. The gyro specifications in Tables 2.2-III, 2.2-IV, and 2.2-V resulted.

TABLE 2.2-III

SHORT TERM REQUIREMENTS

<u>Drift Term</u>	<u>Short Term (12-Hr) 6-Sigma (Avg Basic Band)</u>	<u>Comments</u>
CT	0.15 deg/hr	4 Bands each, consisting of (N) data points obtained with (N-1) spin motor run downs.
MUIA	0.20 deg/hr/g	
MUSA	0.35 deg/hr/g	

Long term (7-day) shifts in the arithmetic mean of the gyro drift terms across three cooldown and storage cycles to +70°F were as shown in Table 2.2-IV.

TABLE 2.2-IV

LONG TERM REQUIREMENTS

<u>Drift Term</u>	<u>7-Day, 6-Sigma (Mean Band) of Arithmetic Means</u>	<u>Comments</u>
CT	0.25 deg/hr	Deleted in recent speci- fications. CT and MUIA predicated on possible deletion of launch pad cali- bration and MUSA calibration on pad not planned for.
MUIA	0.25 deg/hr/g	
MUSA	0.50 deg/hr/g	

Table 2.2-V shows the gyro drift shift specification across vibration. The vibration input is shown in Figure 2.2-2 and has been "shaped" to reflect the relative "g" inputs at different frequencies, due to platform isolator and structural transmissibilities.

TABLE 2.2-V
VIBRATION REQUIREMENTS

<u>Drift Term</u>	<u>6-Sigma (Mean Band) Shift Across Vibration</u>	<u>Comments</u>
CT	0.05 deg/hr	(See Figure 2.2-2)
MUIA	0.15 deg/hr/g	
MUSA	0.30 deg/hr/g	

The 7-day test sequence for BB and MB requirements, for +70°F cooldown and storage, was predicated upon the test cycle in Figure 2.2-3.

Interpretation of the specifications, based upon Figure 2.2-3, is as follows:

1. M_1 , M_2 , M_3 , and M_4 represent the arithmetic mean of (N) data points obtained with (N-1) spin motor power interruptions (gyro wheel allowed to run down to zero RPM).
2. BB_1 , BB_2 , BB_3 , and BB_4 represent the maximum spread of the data points used in determining the individual arithmetic means. Basic Bands (BB) are obtained without cooldown, the only disturbance being removal of spin motor excitation.
3. The test portion of each cycle of Figure 2.2-3 consisted of approximately 12 hours, with the remaining time devoted to cooling down to and storing at +70°F. The cooldown rate is by natural means (no fans) such that approximately two hours is required to cooldown to +70°F. The gyro is cooled down and stored in the test fixture to avoid remounting and realignment induced errors in the data.
4. Table 2.2-III, average Basic Band specification, represents the average of the four Basic Bands.

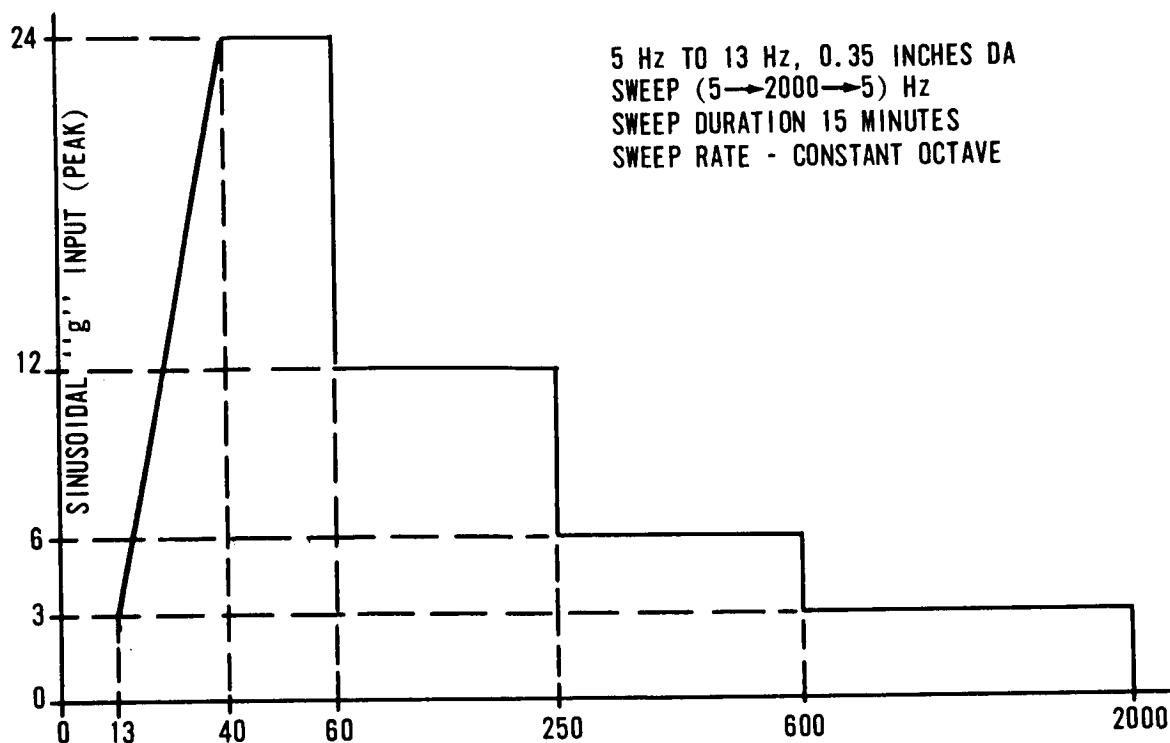


FIGURE 2.2-2. GYRO DRIFT VIBRATION TEST

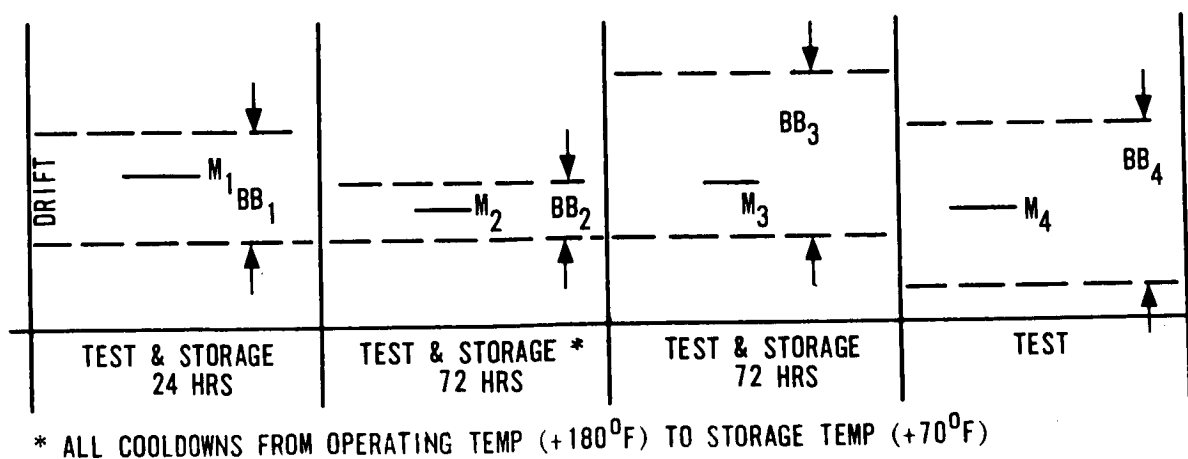


FIGURE 2.2-3. BASIC BAND AND MEAN BAND VIBRATION TEST SEQUENCE

5. Table 2.2-IV, Mean Band specification, represents the maximum spread in any two of the four means. For the case shown in Figure 2.2-3, the Mean Band would be determined from the spread between M_1 and M_4 .
6. Table 2.2-V, Vibration specification, is to be interpreted as explained in (5) above, for cooldown and storage.

The specifications in Tables 2.2-III, 2.2-IV, and 2.2-V have been subject to minor changes throughout the program. In addition, the following performance requirements have been added:

1. 12-hour random drift for CT (0.03 deg/hr) and (CT + MUSA) (0.05 deg/hr), both expressed in terms of maximum spread of 10-minute averaged drift rates.
2. 400 Hz side bands of the 7.2 kHz Signal Generator center frequency held to 100 microvolts (rms) or less.
3. Synchronous Vibration Torque (SVT) held to 1.0 deg/hr/g rms (see later discussion).

To summarize, evolution of gyro performance requirements has generally followed the evolutions of mission requirements and operational concepts. With the aid of well defined mission error sensitivities and system forcing functions, placement of proper emphasis on appropriate drift terms has resulted.

2.2.6. Gyros For Centaur -1 IGS (1959-1962). - In early 1959, the gyro to be used in the Centaur -1 system was defined. This gyro was designated a Miniature Inertial Gyro (MIG) DGG49D6. Three gyros were used to provide a stable element triad in inertial coordinates. This gyro was not without its problems throughout the -1 program. Primary among these were mass shifts and dualsyn shorts. The dualsyn used in the DGG49 gyro is an electromagnetic device, which combines both the functions of a gyro torque generator and signal generator, all encapsulated in one small unit. The dualsyn has a wire wound stator, fixed to the gyro case, and a moving iron rotor, fixed to the gyro gimbal. Four windings, electrically isolated from each other, make up the dualsyn. These windings are the: (1) signal generator (SG) primary, (2) SG secondary, (3) torque generator (TG) pattern field, and (4) TG control field. This brief description of the dualsyn is presented here to aid the reader in understanding its problems, and design solutions, which are discussed in later paragraphs.

As stated above, both mass shifts and dualsyn shorts constituted a major portion of the gyro problems on the -1 program. Other less significant problems at this time were constant torque (CT) stability and random drift stability. Due to the relatively short duration of the -1 program and the premature application of "fixed price" constraints on the D6 gyro, most of the gyro design changes were not implemented until well into the -3 Centaur development program. For this reason, only a brief treatment of the -1 Centaur gyro is given here with greater emphasis being placed on the -3 gyro development.

2.2.7. Gyros For The Centaur -3 IGS (1961-1967). - The -3 program, which began in 1961, initially used the DGG49D15 gyro. This gyro was identical to the -1 program's DGG49D6, except for the separation of the control and warm-up heaters on the gyro case. Early in the -3 program, three different SDF gyros were evaluated to see if significant performance improvement could be realized with another gyro but without causing major interface compatibility problems, using existing platform/MGS hardware. The three gyro types which were evaluated for the -3 program were the DGG8001, the DGG49D15 (both Honeywell gyros) and the M-2516 Kearfott gyro. All three types were miniature, floated, single-degree-of-freedom gyros.

The DGG8001 and M-2516 gyros contained permanent magnet (PM) torquers. Because of the previous problems encountered with the dualsyn on the -1 program, the reliability improvement factor with the PM torquer was of significance. However, there were many other factors which had to be considered. The major factors which were considered in evaluating the three gyros were:

1. Performance capability versus Centaur requirements.
2. Cost.
3. Interface compatibility with existing hardware.
4. Producibility.
5. Growth potential.

An extensive evaluation was performed and data compared between the DGG49D15 and M-2516 performance improvements were not significant. Comparison of the DGG49D15 performance with the DGG8001 also resulted in the same conclusion. When comparing performance capability of the three different type gyros, each had its own strong points. However, when viewed from the cost effectiveness point of view, the DGG49 gyro proved to be the gyro to continue with. This decision was heavily weighted by cost (8001 and 49 gyros were approximately the same in cost whereas

the M-2516 was approximately 40 percent higher). Another prime consideration was the type of torquing used. The DGG8001 and M-2516 permanent magnet torquers were capable of being pulse torqued, a desirable feature but not compatible with the existing computer I/O mechanization. The DGG49 dualsyn did not lend itself readily to pulse torquing of the type then considered, due to excessive cross-coupling between the torque generator and signal generator windings of the dualsyn. On the debit side, however, the permanent magnet torquer gyros had high torquer scale factors (or Command Rate Sensitivities, CRS), on the order of 80 deg/hr/ma, approximately four times that of the DGG49. The high CRS proved to be an undesirable feature at the time since the low torquing rates required inflight, for the Centaur application, would result in very low torquing current levels, well down into the noise range of the then troublesome platform sliprings. (See Topic 2.6.) Therefore, to incorporate the DGG8001 would have required an expensive I/O redesign.

From a thermal and mechanical interface point of view, the DGG8001 and DGG49 gyros were interchangeable. The M-2516, however, required approximately 30 percent more wheel power, thus aggravating an already marginal thermal control problem for the specified platform skin temperature range (reference Topic 2.10). The M-2516 also presented mechanical interface changes that were not considered advisable at the time.

The preceding paragraphs have been included in this report to provide some insight into the factors involved in making a recommended gyro change early in the -3 program. In many instances, previously defined, hardware interface constraints played an important part in the final decisions. To satisfy thermal, electrical and mechanical interface requirements, every factor must be considered, but with the proper emphasis being placed on each factor. Only in this manner can the optimum gyro design be realized for a given system application. Obviously, the best time to do this is early in the system design phase, not when the program is three years "down the road".

2.2.8. DGG49 Dualsyn Problems and Solutions. - Throughout the -1 and -3 Centaur Programs, the individual problems associated with the gyro and application thereof were defined. The two biggest problems, which constituted approximately 70 percent of the -1 gyro failures in the system, were large mass shifts and dualsyn dielectric breakdown. The original dualsyns in the 49D6 were wound with Formvar insulated magnet wire. A design change, from Formvar to Nyleze insulated wire, was incorporated in June of 1961. Factors considered in this decision were uniformity of insulation, dielectric strength, "cold flow" properties and others. Incidence

of dualsyn failures in the 49D6 gyro after incorporation of the Nyleze dualsyns initially indicated the design change was a success. However, a little later in the -3 program, the dualsyn problem once again appeared and became a major cause of gyro failures. Early in 1963, it became evident that the dualsyn dielectric problem was not solved. A rash of failures was evidenced at the component, platform, and system levels. A full investigation was initiated both at the gyro manufacturer (Honeywell Aero-Minneapolis) and at the users (Honeywell Aero-Florida) facility to isolate the cause or causes for these failures.

Since dielectric breakdown in a material is generally the result of a cumulative overstress either mechanical, or electrical, or both, the individual point or points in the build and use cycle where overstressing might be occurring was difficult to isolate. To cover all possibilities, an investigation was made of switching transients at all levels of testing, including component, platform, and system. In using the DGG49 gyro, two sources of current were supplied to the torquer. A fixed DC current was fed to the pattern field (usually supplied for gyro or platform tests by a John Fluke Model 351-A Constant Current Supply in the Test Station). In addition, a current, proportional to drift rate was normally applied to the control field. The later was limited to 2 ma at system level by the Computer I/O torquing potentiometers. The results of the transient investigation revealed that at various levels of testing, voltage spikes of 400 to 500 volts were occurring when switching the pattern field on and off, with the gyro connected. The situation exhibited itself as an inductive load (dualsyn pattern field) being switched on to a constant current supply with no overvoltage protection in the supply. All stations were then modified as needed to incorporate a pattern field "dummy" load and a "make-before-break" switching arrangement. Transient voltage spikes were reduced to 20 volts or less. Similar action was requested of field sites and at the gyro manufacturer. In a review of dielectric testing at the gyro manufacturer, it was observed that with the particular equipment and test procedure used, 900-volt spikes were produced when setting up for a 500-volt dielectric test. This undesirable condition was immediately corrected.

Having isolated these two causes of repeated voltage overstress and implemented corrective action to eliminate them, the problem of how to handle the existing situation (potentially overstressed dualsyns in flight gyros) and not shut down platform and system level production was at hand. It was at this time that the "weak sister", and "Zap test" theory was developed. This theory evolved from a study which indicated that if a dielectric breakdown were to occur, its process could be speeded up by

a series of temperature cycling (to aggravate cold flow) and controlled high voltage exposures. The "weak sisters" would be eliminated during this test cycle, and those dualsyns which survived had a higher probability of continuing to perform satisfactorily. This theory was put into practice at the gyro and platform levels. All flight gyros were subjected to the temperature-voltage cycling at the users facilities. The manufacturer performed the same test cycle on all gyros prior to shipment. Some 30 gyros were subjected to the test cycle at the Aero-Florida facility, with approximately 30 percent failing due to a dielectric breakdown in the dualsyn. This test process, intended only as a temporary means of filtering potential dualsyn failures, accomplished its objective.

Since the "Zap test" was implemented only as an interim safeguard, the pursuit of a permanent design fix was continued. A vendor survey conducted by a Materials, Design, and Production Engineering team evaluated all available magnet wire on the market. Teardown analysis of all dualsyn failures was performed, and the results showed that 95 percent of all the failures involved breakdown between the pattern field and control field windings (interskein breakdown). This study indicated that turn-to-turn breakdown, within a given winding, did not appear to be a problem. Test samples of several types of magnet wire were investigated. One of the basic groundrules was that whatever design solution resulted had to be 100 percent interchangeable with existing delivered hardware. This, by necessity, reduced some design flexibility in arriving at a permanent and optimum fix. After intensive studies and tests, a decision was made to continue with Nyleze insulated magnet wire but with the addition of mylar interskein inserts. This change was incorporated as a mandatory change in late 1963 on all new build and reworked gyros. Through the incorporation of this design change, along with process control and the previously mentioned test station changes, the dualsyn dielectric problem was solved. The mylar interskein inserts were incorporated in DGG49D15 gyros and identified as Series 8. Later a directive was issued to further identify this design change; thus the DGG49D20 designation resulted.

2.2.9. DGG49 Mass Unbalance Problems. - In reviewing the platform gyro failures attributed to large mass shifts, a number of changes resulted. Due to computer limited, maximum in-flight torquing capability, the maximum tolerable mass unbalance for a given gyro axis was held to 2.0 deg/hr/g or less (this changed in later years to 3.0 deg/hr/g). In the process of shipping from the vendor, incoming inspection, and installation in the platform, large mass shifts frequently occurred to magnitudes, which exceeded the compensation capability of the computer. To provide a mass trim capability for the gyro, whether in a platform or at the component level, a microvernier balance pan was incorporated into the DGG49 gyro

design. The balance pan, located in the gyro gimbal, consisted of a small hollow disc, wound with a heater and partially filled with an eutectic alloy. When heater power is applied to the pan and the gyro oriented to a pre-scribed orientation, near zero (0.2 to 0.5 deg/hr/g) mass rebalance can be achieved for both MUIA and MUSA. Prior to incorporation of the balance pan, no means existed to retrim mass shifts after final gyro assembly.

The balance pan did not cure the cause of the mass shift but merely dealt with the effects. Gyro handling, platform assembly processes, and tolerance studies were initiated to define and deal with the possible causes for the mass shifts. Worst case treatment of tolerance buildups indicated possible mechanical interface problems for the gyro in the platform.

One such source of mass shifts was found to exist during component alignment in the platform. Location of the gyro cable exit from the top cover of the gyro was not specified by print to be close enough to the gyro input axis (IA). During alignment of the gyro IA to an orthogonal triad, with worst case conditions, the "snout" would mechanically interfere with one of the terminal boards. If excessive torque was applied at the gyro flange to bring the gyro IA into the prescribed alignment, it resulted in loose dust covers and in many instances, large mass shifts. Process changes and relocation and tolerancing of the gyro "snout" location resulted in minimizing this problem. This change was implemented on the -3 program in early 1964.

Additional dimensional controls specified on the total gyro envelope, plus tightening of tolerances on the platform first gimbal assembly, resulted in sufficient clearance to handle a worst-case build-up of tolerances.

Another cause for mass shifts was identified with the thermal control of the Centaur -1 Platform. (Reference Platform Temperature Control Amplifier, Topic 2.8.) Azimuth block heaters and proportionally (TCA) controlled gyro heaters were used for thermal control. Tests indicated thermal control problems associated with this configuration could result in overheating the gyros. This overheating was caused by thermal overshoot, which in turn was due to thermal lag between the block heater (controlled by the V accelerometer) and the proportional TCA Control (controlled by the individual gyro sensor). Temperature control problems were identified with large gyro mass shifts during gyro teardown and analysis. The teardown analysis indicated discoloration of cements and flexleads, plus ruptured bellows (used to compensate for volumetric expansion) in some instances, all pointing to overheat of the gyros. This problem was

eliminated, for all practical purposes, at the beginning of the -3 Centaur program when the new TCA design was implemented, the block heater was deleted, and the distribution of heat among individual inertial components in the platform was changed.

2.2.10. Platform Gimbal Spin Problems - Damaged Gyros. - During platform and system level testing throughout the -1 and early -3 Centaur build, numerous platform gimbal spins occurred. Excessive rates about the gyro IA caused large mass shifts and in some instances, shearing of the pivots on the gyro gimbal. Correction of this situation was realized with a design change to the ground support equipment. Addition of a gimbal spin inhibit (GSI) circuit was put in all GSE, thus eliminating the possibility of a dangerous spin occurring. The GSI circuit in effect shorted out the input to the gimbal control amplifiers at a predetermined level, deemed safe when platform gimbal rates were reflected back into gyro IA rates. This change to the GSE proved effective in eliminating excessive rates. The change was incorporated into the GSE in early 1965 and made even more effective in 1966.

2.2.11. Other DGG49 Problems. - The preceding paragraphs have dealt with shifts in mass unbalance magnitude, and design changes implemented in the gyro and IMU to reduce the cause and effect of same.

Two other areas which constituted significant problems were acceleration insensitive or constant torque (CT) stability (particularly with cooldown) and OAV random drift. One of the initial mission objectives for the Centaur guidance was known as the 24-hour synchronous orbit mission (for the Advent communications satellite). Operational concepts for this mission reflected into a 24-hour random drift requirement on the gyro. Gyrocompassing also played an important part in the initial phase of the -3 program, thus requiring an East gyro with good CT stability. Both random drift and CT stability requirements constituted a major cause for rejection throughout the -1 program and early in the -3 program. Studies were conducted both at the gyro and platform level to isolate causes and develop corrective action. The gyrocompassing mode of operation was later eliminated in 1964.

Design changes implemented at the gyro level to improve performance in these two areas were as follows:

1. Retainer Controlled Oil Retention. - Historically abrupt drift rate changes, followed by an exponential decay back to the original level or some permanent offset, had been observed. This abrupt change was attributed to excessive oil from the impregnated

retainer being "spun out" to the bearing race, creating a thicker oil film, and in turn a rotor shift. Also occurring with an oil sling would be a minute change in spin motor running power. This theory was proven in tests and new retainers, with controlled oil retention, were implemented into the gyro design in early 1964.

2. Improved Grade Motor Bearings. - Extensive investigation into gyro random drift indicated a direct correlation between random drift and rotor shift. Using capacitor probes to detect axial rotor shifts, correlation between random drift and rotor movement was shown. As a result of these tests, a vendor survey of bearing manufacturers was conducted and a higher quality bearing was procured. The new bearings were phased into the DGG49D15 gyros in early 1964. Results indicated fewer rejects at motor level and gyro level for motor power jags and associated torque changes.

3. Distributed Heaters and Sensor. - The original -1 Centaur gyros (DGG49D6's) and early -3 Centaur gyros, had both the warm-up and control heaters located below the flange on the gyro. In tests performed at the gyro level, it was observed that the gyro transfer function ($GTF = H/C \times K_{SG}$) varied inversely with gyro heater power required to maintain the gyro at operating temperature. This study was prompted by poor correlation of gyro transfer function between two different holding fixtures, one was an unheated fixture and the other a heated fixture (supplying part of the total heat to the gyro). Due to the wide platform ambient skin temperature range over which the gyro had to operate without degraded performance, it became imperative that design improvements be made. Design studies, supported by tests, indicated that a redistribution of the thermal interface resistances was needed. The objective was to obtain optimum balancing of the heater-to-sensor, heater-to-fluid gap, and heater-to-mounting flange conduction paths, as evidenced by variation of GTF with changes in external ambient temperature. Since the mounting flange was the primary path for heat loss, it was shown that more heater-sensor winding was needed in closer proximity to the flange. The distributed heater-sensor configuration was implemented in early 1963 in the DGG49D15 gyros. Heater and sensor windings distributed above and below the mounting flange, along with a damping fluid change, resulted in a GTF which was independent of heater power for all practical purposes, over the full

ambient temperature range of interest. A more uniform flange temperature was also realized, resulting in smaller temperature gradients across the gyro flange (an aid to gyro mass stability).

4. Flex Lead Clips. - In an effort to improve Constant Torque (CT) stability when the gyro is subjected to cooldown, a requirement that applies throughout various levels of operation, an investigation into the area of flex lead reaction torques was pursued. It was observed upon teardown of gyros, which had been temperature cycled to low temperatures, that indications of concentrated stresses and sometimes kinks occurred at the point of flex lead attachment. It was theorized that these concentrated stresses were caused by minute movement of the flex leads during cooldown, when the fluid was going through various states of viscosity. If cooled to the cracking point of the fluid, shear stresses set up in the fluid caused severe stress on the flex leads, resulting in kinks, and in turn permanent damage to the lead. Tests were performed using various configurations of flex leads and means of attachment. The most practical design change in attaching the flex leads was by means of flex lead clips. Through incorporation of the flex lead clip, controlled stress distribution in the flex lead was achieved. This was obtained by controlling the bend radius of the clip and hence the bend radius of the flex lead itself. A design change was made in mid-1964, calling for flex lead clips on all DGG49D15 gyros. Improvement in CT with cooldown resulted, verifying design objectives.
5. Reduced Stop Angles and Modified Flex Leads. - Aided by an invaluable tool, the system error analysis studies, a need for further improvement in CT stability was evident in mid-1964.

The Vg CT error contribution still constituted a major error source at system level. To further improve CT stability, studies, supported by test data indicated a reduction in stop angle for the gyro (gimbal travel about the output axis) and thinner, wider flex leads would be very effective. These changes were compatible with interface hardware, and they could be phased in on a non-interference basis. Early in 1965, this design change was implemented into the -3 Centaur IGS. Improvements up to 4:1 in CT stability and 10:1 in OA vertical random drift were realized after the incorporation of the change.

6. Synchronous Vibration Torque. - With the incorporation of the previously mentioned design changes, along with process control changes, improved performance was realized. One, still "mystic", problem area continued to plague gyro performance after it was installed and operated in a completed platform. This problem was evidenced as drift rate change as a function of platform gimbal orientation. This problem became even more apparent after other performance anomalies were cleared up. In mid-1965, an exhaustive test and analysis program was initiated to isolate the cause for the poor gyro performance with respect to gimbal orientation. With the gyro held fixed in inertial space and platform gimbals moved with respect to each other, major performance degradation occurred. After close evaluation of the data, it was shown that: (1) the data for a given orientation was very repeatable; (2) drift rate changed almost instantaneously with platform gimbal angle change; and (3) certain gimbal angle relationships, with respect to each other, produced a worst case condition of drift rate change. After a thorough review of test results, thermal influence upon the test data was eliminated. It was also shown that when additional magnetic shielding was added, little, if any, influence upon the data resulted. It was at this point that interaction of one gyro upon the performance of another in the platform was suspected. Further testing showed that each gyro was acting as a vibration source in the platform, due to a mechanism known as synchronous vibration torque (SVT). Synchronous vibration torque is a torque produced about the gyro output axis when vibrated along the spin axis at the same frequency as the wheel angular rate.

It was later shown that the platform gimbal structure had a mechanical resonance coincident with the synchronous speed of the gyro spin motor, when the latter was excited with the normal 400 Hz excitation. As gimbals were reoriented with respect to each other, the transmissibility factor would change, resulting in different magnitudes of coupling from one gyro to another and also reflection of a gyro back upon itself.

Action was immediately initiated after identifying the generic problem. During the test at platform level, three gyros were interchanged in the azimuth block. One gyro appeared to exhibit predominantly worse performance. According to the SVT theory, in the gyros which were acting as vibration sources, the magnitude of vibration was a function of spin motor unbalance. The three test gyros were removed from the platform, and special tests, performed at the component level, verified this theory. Immediate action was taken to measure and control the static and dynamic

unbalance of the motors at the component level. At the same time, the platform was detuned from the 400 Hz mechanical resonance by the addition of weights to the second gimbal. Platform gimbal resonance tests were then initiated on flight platforms to measure the separation between the gimbal f_r and 400 Hz. This test utilized an accelerometer pickoff, mounted on the second gimbal to determine the vibration levels. The three gyros were then excited, using a variable frequency spin motor power supply, and the accelerometer pickoff output put on an X-Y plotter. At the frequency of interest (400 Hz), the gimbal angles were changed to produce the highest transmissibility. At this orientation, a frequency sweep was made ± 60 Hz about 400 Hz and the resulting X-Y plot made for vibration level versus frequency. Gimbal weights were then added and the same test repeated. The effect of mechanically detuning the platform was pronounced when comparing the two X-Y plots (before and after weights). As an interim platform fix, design changes were made to incorporate the added gimbal weights.

In effect, through detuning the platform mechanical resonance, gyros with relatively high static and dynamic rotor unbalance, but which were already in platforms, were desensitized. However, changes were also made at the gyro level, on a forward build basis, to specify tighter static and dynamic balancing. Performance tests were also incorporated, both at the gyro and platform level, to assure conformance to these changes. These changes were incorporated into the -3 Centaur program in late 1965 and early 1966. The combination of detuning the platform from 400 Hz resonance, plus addition of fine balanced spin motors, resulted in major CT performance improvements at all levels of platform and system operation.

2.2.12. Gyro Yield and Reliability. - The performance of the GG49D26 gyro, as presently used on Centaur is adequate. However, there have been yield and reliability problems associated with this gyro which have been and are now getting intensive investigation, and corrective action. Corrective actions which have been taken to reduce some of these problems are as follows:

1. Spin motor bearing quality has been improved by instituting spin motor run-in and power-jag testing at the wheel and gimbal level. Maximum power variation limits have been established to assure that the spin motor bearings are running smooth and are free of contamination and excessive oil.

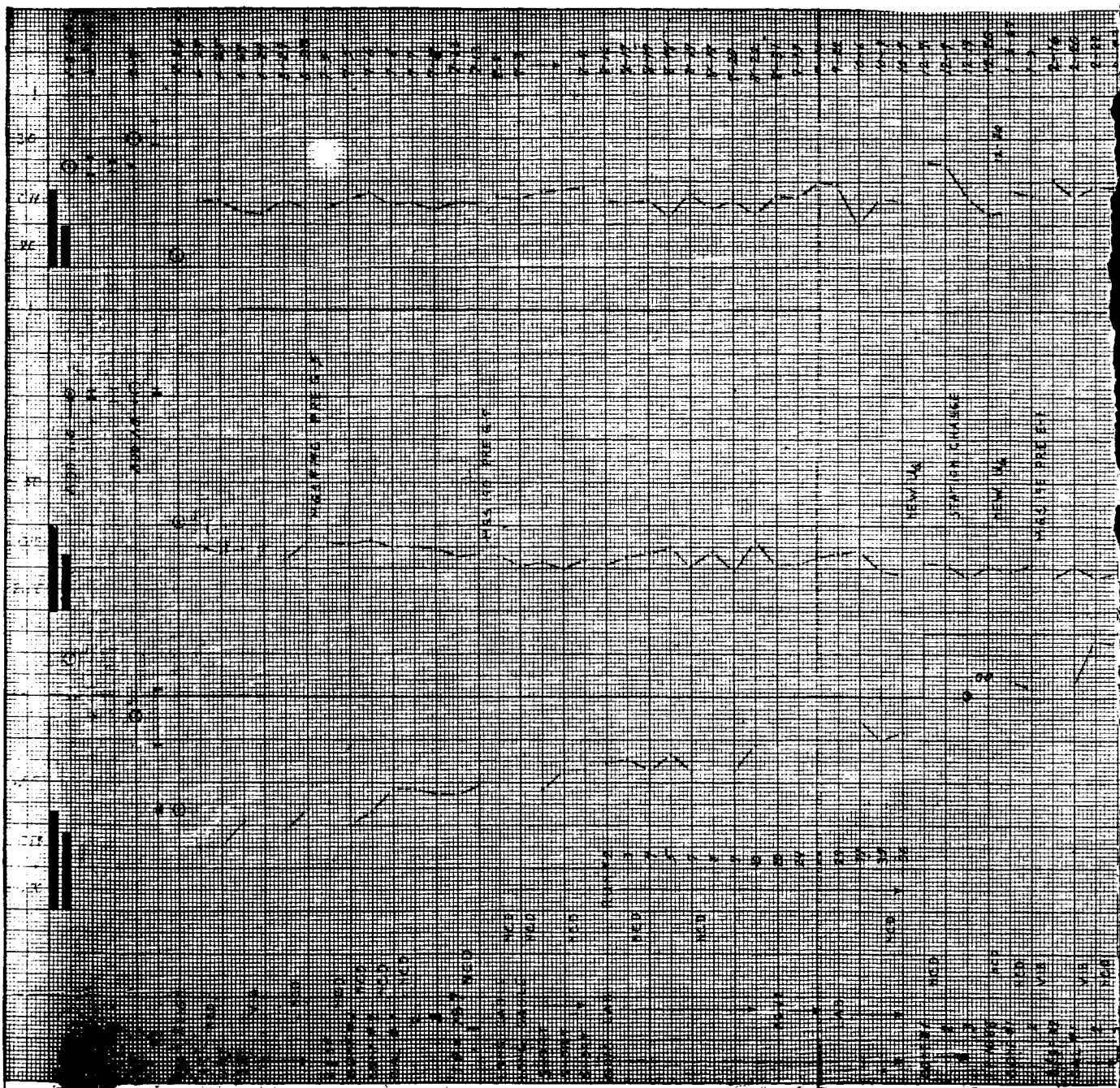
2. Gyro burn-in at the unit level is used to assume that the gyro will operate satisfactorily for a minimum of 150 hours prior to platform installation. This has been very successful in weeding out poor performance gyros, prior to platform installation, thus reducing platform gyro pulls in the platform build stages.
3. Improvements have been made in parts cleaning, deburring, handling (by incorporating parts kitting) and inspection (under a 20 power microscope).
4. In-line processing of the gyros has been examined in detail and changed to place restrictions on the amount of mass balance shift allowable after fine gimbal balance, jewel inspection under an 80 power microscope, and several other changes and improvements made.
5. In-line screening tests have been added to screen out questionable gyros early in the build process.
6. All gyros are now given tumble tests about the output axis and the spin axis prior to installation in the platform.

The above corrective actions have resulted in a significant reduction in number of gyros pulled from platforms and an increase in MTBF.

2.2.13. Conclusions (-3 IGS). - Through the incorporation of the design changes presented in this report, along with continual improvement in test procedures, process controls and better definition and reflection of mission operational concepts into the test requirements, a much improved gyro in terms of performance, reliability, and producibility has resulted. A direct reflection of this improvement is evidenced by system performance during ground testing and flight tests during the last two years (see Figures 2.2-4 and 2.2-5 for typical and "best-case" gyro performance histories).

2.2.14. IMG Gyro. - The performance of the GG49D26, as presently used on Centaur is also adequate for the IMG System. With the corrective action taken on the present D26 gyro, as described in Topic 2.2-12, it is also anticipated that the required MTBF of 13,000 hours will be met with the IMG gyro.

It is recognized, however, that to a certain extent the performance and reliability is attained through intensive screening and testing of each gyro prior to use. This results in a less than desirable yield rate. To



FOLDOUT FRAME

2-2-23

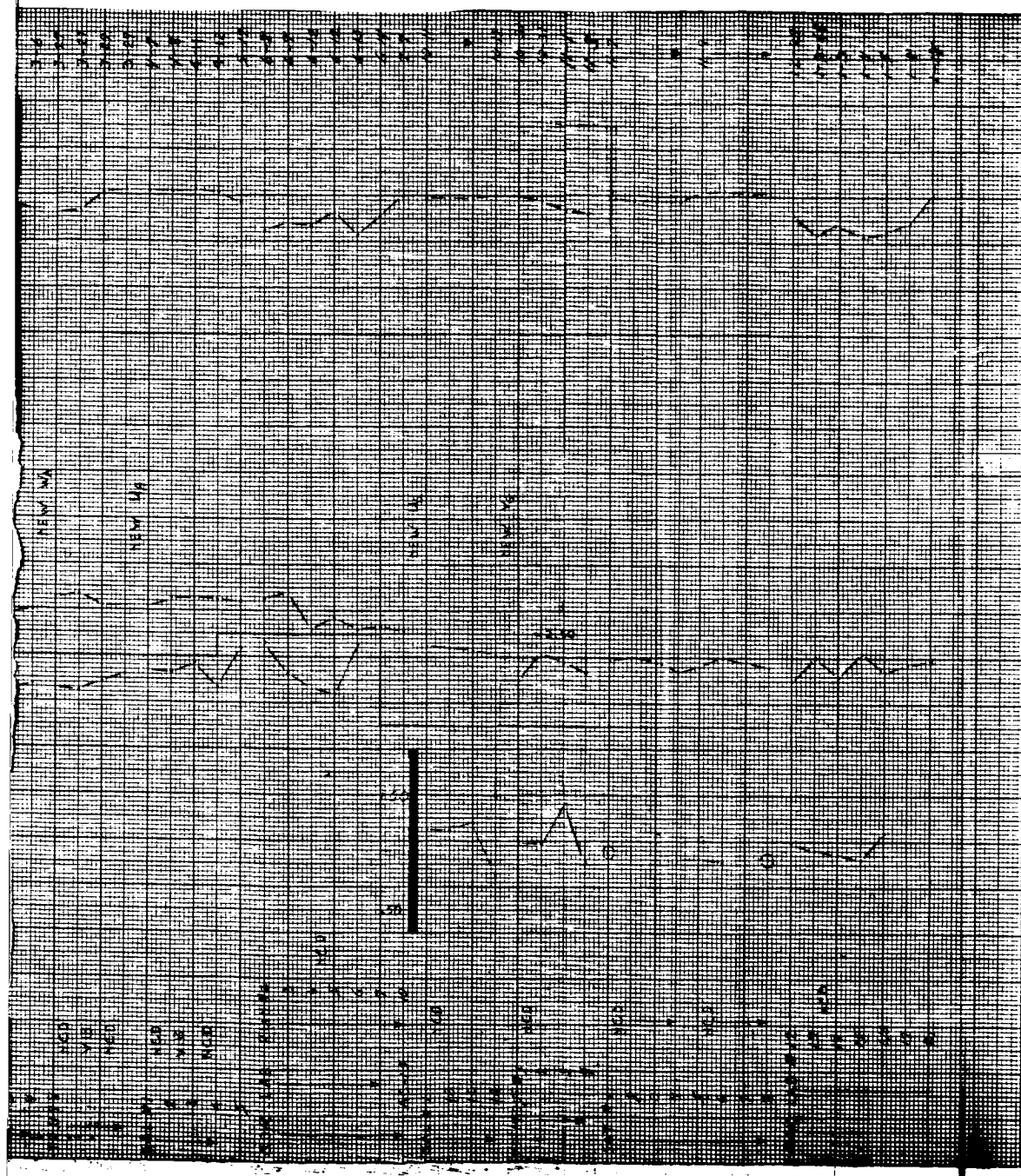
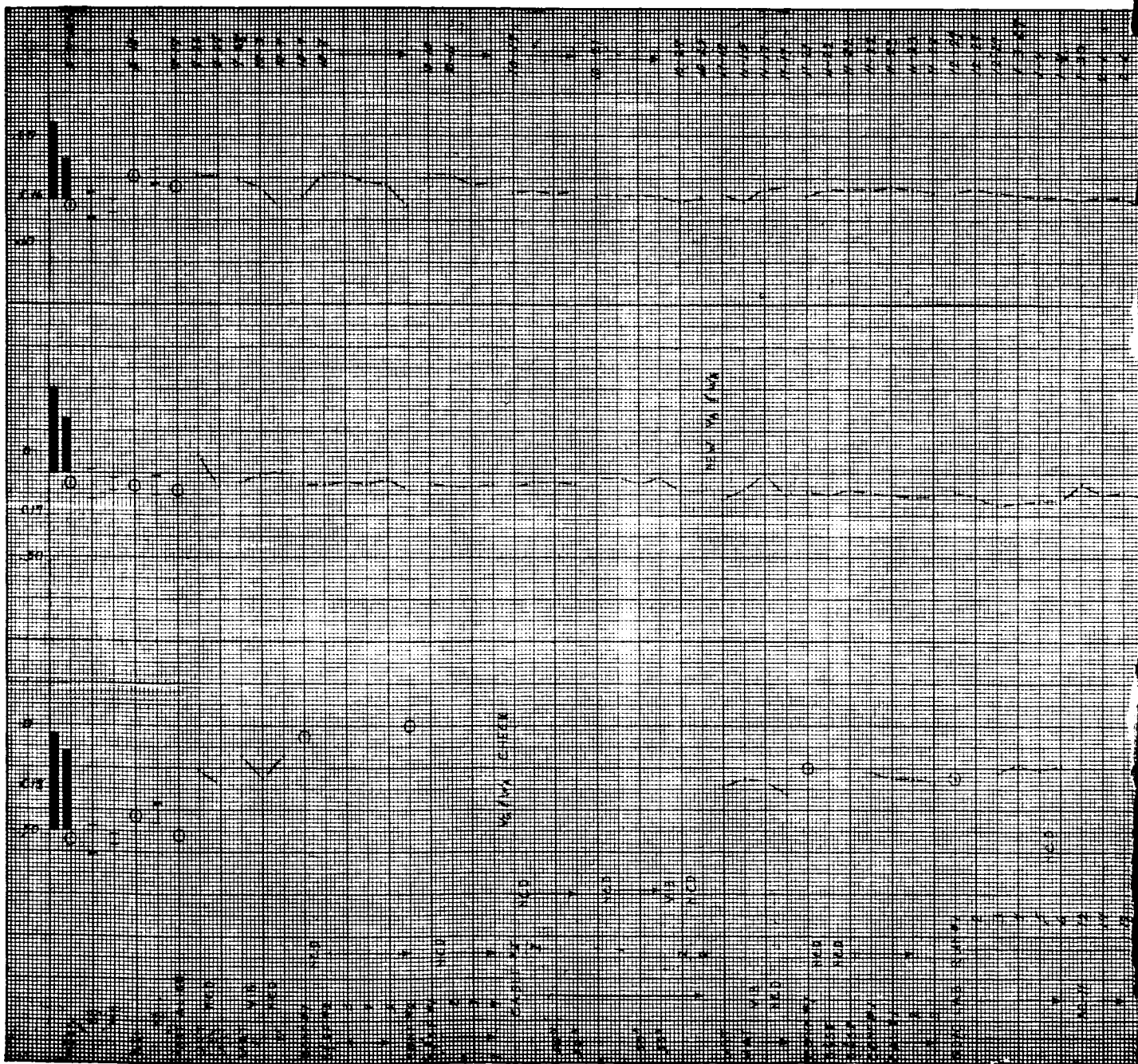


FIGURE 2.2-4. GYRO STABILITY
S/N I-25 TYPICAL PLATFORM G-5

~~2.2-23~~
2.2-24



2-2-25

FOLDOUT FRAME



FIGURE 2.2-5. GYRO STABILITY
S/N G-8 BEST CASE PLATFORM G-14

~~2.2-25~~

2.2-26

this end, a study has been made to determine potential GG49 design improvements to increase the performance margin versus the Centaur IMG system requirements and result in higher yield rates. The preliminary results of the study indicate that the best approach would be to increase the wheel momentum by a factor of two over the present 1×10^5 gm-cm²/second. This would result, of course, in a significant reduction in the drift to gimbal torque ratio, and a corresponding improvement in performance margin. It appears that this change could be accomplished in the present GG49 case envelope. It also appears as if the gyro time constant ($T = I/C$) could remain the same, which would require minimum servo loop changes. Various other changes were considered, such as a 4-pole, 800 cps spin motor and changes in pivot and jewel configuration. However, the predicted improvements with these changes were not as significant.

Topic 2.3

Platform Accelerometers

2.3.1. Introduction and Summary. - In early 1959, the DGG116A2 Accelerometer was selected for use in the -1 Centaur Missile Guidance Set (MGS). The 116A accelerometer is an improved version of the GG56 accelerometer. The GG56 model was designed for analog operation whereas the 116A series was designed for analog or digital operation.

During the -1 Program there were numerous problems directly associated with the accelerometer. Some of the more serious of these were:

1. Pendulum hang up.
2. Poor repeatability at null during analog operation.
3. Large digital dead zone while operating near zero "g" input.
4. Main seal leaks.
5. Leaky gimbal resulting in change in pendulous mass.
6. Thermal Control problems (ref. Topics 2.8 and 2.10).

In late 1961, the -3 Centaur Program began. Except for minor changes, the accelerometer was basically the same as that used on the -1 Program. To identify these changes, the -3 Program accelerometer was designated the DGG116A6. Except for the thermal control problem associated with the 116A2 accelerometer, the same basic problems that prevailed during the -1 Program still persisted with the 116A6 accelerometer.

Plagued by continuing performance problems, attention was directed towards replacing the 116A6 accelerometer in early 1964. Mission sensitivities, for the Centaur two-burn mission, in conjunction with the accelerometer error model, indicated that the mission accuracy requirements could not be met with the 116A6 accelerometer. An extensive evaluation program was run during 1964 on both the 116A6 and the DGG177 accelerometer. As a result, the DGG116 was replaced in early 1965 by the DGG177.

A more detailed discussion of the accelerometer design evolution for each major phase of the program can be found under the major sub-topics of this discussion. The discussion is presented in a problem definition-design solution approach, with key dates and periods pointed out.

Many of the problems encountered in the past might be avoided in future designs by more carefully defining and documenting all accelerometer requirements via technical development specifications.

To further improve the probability of meeting design goals with minimum risk, close technical coordination must be maintained among the accelerometer designer, Platform designer, and Systems Engineer, and Production Engineer. The "our problem" attitude rather than the "your problem" approach must be developed.

To supplement a good design, adequate piece part manufacturing and process controls are necessary. Timely and periodic design reviews must be conducted during each major phase of the Program. Last, but not least, the accelerometers must undergo a very thorough test and evaluation program to insure that all their characteristics are known and acceptable.

2.3.2. General Description DGG116. - The DGG116A is a Miniature Pendulous Accelerometer. The unit provides the function of sensing linear acceleration. In combination with the Pulse Rebalance loops (ref. Topic 2.15) precise velocity information is provided. The DGG116A Accelerometer is similar to the earlier GG56. Improvements incorporated into the 116A series were primarily oriented toward the use of digital torquing. These included torquer improvements to minimize axial displacement torque uncertainties, reduced torquer coil time constant, increased scale factor (higher resolution) and slight reduction in gimbal polar moment of inertial about the output axis. Figure 2.3-1 depicts a DGG116 accelerometer.

2.3.3. Design Characteristics (DGG116). -

2.3.3.1. Gimbal. - The gimbal which contains the pendulous mass, is of the float type. A high density fluid is used to provide damping as well as buoyant support to the gimbal. The gimbal is radially centered in the case via pivot and jewels. The 116A gimbal pendulosity is 1.02 gm-cm.

2.3.3.2. Torquer. - The 116A accelerometer is a permanent magnet (PM) torquer. The torquer characteristics were as follows:

1. Sensitivity: 119 dyne cm/ma
2. Maximum continuous input: 12g
3. Characteristic time (L/R): 20 microseconds

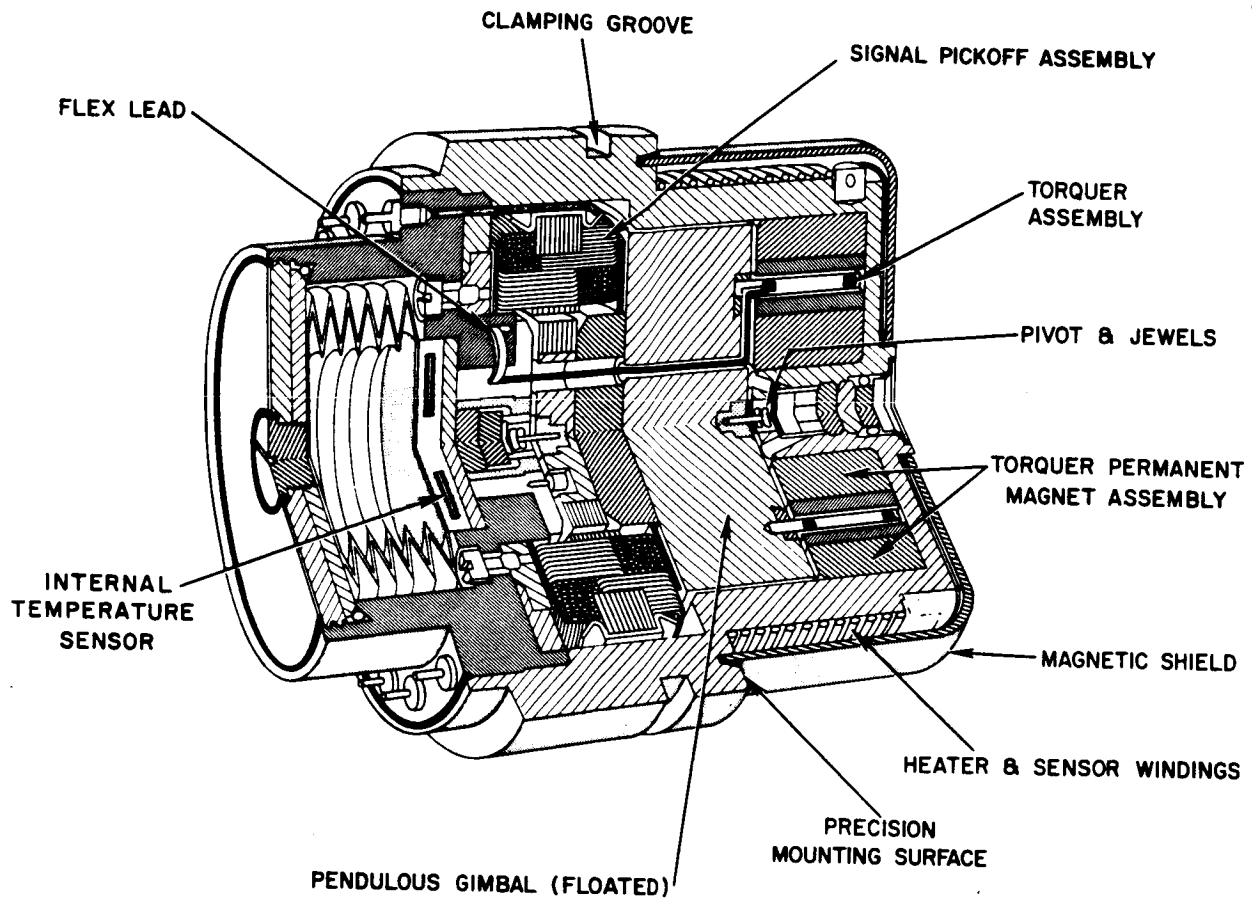


FIGURE 2.3-1. DGG116 ACCELEROMETER

2.3.3.3. Signal Generator (Pickoff). - The signal generator (SG) consisted of two windings, (1) the SG Primary, and (2) SG Secondary. The output of the SG secondary was proportional to the relative gimbal-case angular displacement about the output axis, the nominal sensitivity being mv/mr.

2.3.3.4. Heat Sensor. - Two heaters integrally wound with a temperature sensor, were located below the flange mounting surface. One heater, the warm-up heater, was used for fast warm-up from low ambient temperatures. The control heater, in conjunction with the TCA, provided proportional control at the operating temperature set point. The heaters and sensor were non-inductively wound (Bifilar). The nominal sensitivity of the sensor was +1.5 ohms/°F. The heaters could be excited with ac or dc.

2.3.3.5. Case and Mounting. - The case utilized flange mounting for the mechanical interface with the platform. A mu-metal "dust" cover was utilized to cover that portion of the case below the flange (torquer end).

2.3.3.6. Special Feature. - A special design feature of the 116 accelerometer was the addition of a modulation winding. The purpose of this winding was to induce mechanical dither through electrical means. Through the use of pendulous axis dithering, a reduction in pivot jewel loading resulted, thus producing a lower static threshold and reduced null uncertainty.

2.3.4. Requirements. - Refer to Topic 1.5 for evolution of mission requirements and their reflection upon accelerometer requirements. Table 2.3-I lists the requirements for the 116A accelerometer.

TABLE 2.3-I

116A ACCELEROMETER REQUIREMENTS

Parameter	Magnitude	Stability	Shift (3 σ *)	Comment
Scale Factor	8.4 ma/g	± 200 PPM	300 PPM	*Cool down and vibration
Bias	$\pm 100\mu g$	$\pm 50\mu g$	$150\mu g$	Cool down and vibration
Null Uncertainty	OAH $\pm 50\mu g$ OAV $\pm 100\mu g$			6 σ band 6 σ band

Bias and Scale Factor (SF) stability requirement for the 116 accelerometer was subjected to three vibration exposures at 5.4 g (peak) between 500 and 600 Hz for 30 seconds. In addition, the accelerometer was subjected to three +40°F cold soaks each of two hours duration.

Mission requirements for the Surveyor Program reflected the most stringent requirements upon the down range (U) accelerometer. Both Bias and SF instabilities were large error contributors in the down range velocity measurement. From the supply of acceptable accelerometers, selection of the U accelerometer was therefore made, based upon Bias and SF stability, in order to optimize system performance.

2.3.5. General Description DGG177 Accelerometer. - The DGG177 hinged pendulum accelerometer is a single axis accelerometer, with a moving coil ac signal generator (SG) and a permanent magnet (PM) torquer. The pendulous mass is supported on a pair of hinged pivots, contained in a common plane. Free deflection in one axis is afforded, while high stiffness is exhibited in the other axes. Viscous damping is provided by silicone oil, which fills the entire housing. Fluid density is of little consequence since the device is not floated. Acceleration along the Input Axis (IA) causes pendulum deflection about the hinge axis. The SG output is proportional to pendulum displacement with respect to the core. Depending upon SG primary excitation loading and SG secondary tuning, the SG sensitivity can be varied over a wide range. The units for SG sensitivity are mv/mr.

2.3.6. Design Characteristics (DGG177). - The DGG177 is a single axis hinged pendulum accelerometer. The accelerometer consists of the following basic components.

2.3.6.1. Hinged Pendulum. - The hinged pendulum which makes up the pendulous mass is supported on a pair of flexure pivots. These pivots deflect freely in one direction (input axis) but are highly resistant to displacement in the other. Since the pendulum is not floated, fluid density is not a critical parameter. The pendulous scale factor for the 177 is 2800 dyne cm/g (nominal).

2.3.6.2. Torquer. - A permanent magnet (PM) torquer is utilized in the 177. The torquer characteristics are:

1. Sensitivity: 467 dyne cm/ma
2. Characteristic Time (L/R): 25 microsec (nominal)

2.3.6.3. Signal Generator. - The SG consists of two windings (1) the Primary and (2) the Secondary. The output of the SG secondary is proportional to relative pendulum-case displacement. The SG sensitivity is 36 mv/mr with normal excitation and loading.

2.3.6.4. Heater Sensor. - The DGG177J1 utilizes a wrap around thermal foil heater-sensor. Both a warm-up heater, for fast warm-up, and a control heater which in conjunction with the TCA, provides proportional control. The heaters and sensors are distributed along the case to provide uniform heat dissipation. The nominal sensor sensitivity is $+1.5 \text{ ohm}/^{\circ}\text{F}$. The heaters are capable of being excited with either ac or dc.

2.3.6.5. Case and Mounting. - The case utilizes flange mounting for mechanical interface with the platform. A mu-metal "dust" cover both above and below the flange provides effective shielding from external magnetic fields.

2.3.7. Requirements. - The performance requirements for the DGG177J are as shown in Table 2.3-II.

TABLE 2.3-II

DGG177 PERFORMANCE REQUIREMENTS

Parameter	Magnitude	Stability	Analysis	Comment
Scale Factor	5.7 ma/g	40 PPM		6 hours
		70 PPM	MB	cool down and storage
		50 PPM	MB	vibration
Bias	$\pm 1000 \mu\text{g}$	20 μg		6 hours
		100 μg	MB	cool down and storage
		50 μg	MB	
Null Uncertainty	40 μg			Any orientation
Static Threshold	10 μg			
				MB = Mean Band

Bias and Scale Factor (SF) stability requirements for the DGG177 were subjected to the environmental inputs shown in Table 2.3-III.

One test cycle, shown by the schedule in Table 2.3-III, consisted of a six line test at the four cardinal points (0, 90, 180 and 270 degrees) followed by a cool down from operating temperature and storage at +72°F. M_1 , M_2 , M_3 , and M_4 represents the arithmetic mean of the four test cycles for the particular parameter being determined (bias determined from two zero "g" readings obtained with the pendulum vertical up and vertical down, SF from pendulum horizontal, $\pm 1g$).

Mean Band, as used in Table 2.3-II, is the maximum spread of any two of the four arithmetic means (M_1 through M_4). The arithmetic mean for a given test and storage cycle is determined from a six line test. A line of data consists of one set of data taken at 0, 90, 180 and 270 degrees which corresponds to, two zero "g" inputs and one each $\pm 1g$ input.

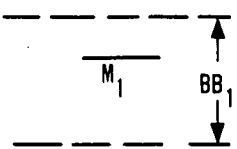
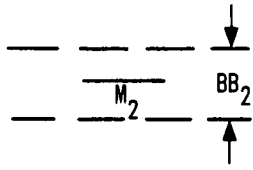
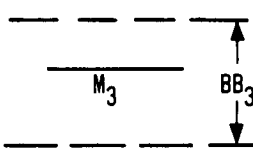
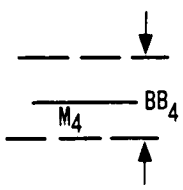
In addition to cool down and storage, the accelerometer is subjected to vibration. The profile shown by Figure 2.3-2 is applicable to the requirements shown in Table 2.3-II.

Throughout the recent IGS development, requirements and test philosophy have been adjusted for the accelerometer, as missions evolved and operational concepts changed. Through proper reflections of mission requirements, including both performance and operational concept, into the component specification, the probability of confidently meeting the end requirements have been enhanced. Whenever new requirements have resulted, several test accelerometers have been tested to insure the design capability to meet the requirements.

2.3.8. Accelerometer Experience on -1 Centaur. - The DGG116A2 accelerometer was specified for the MGS in early 1959. As the Centaur -1 program progressed, problems associated with the accelerometer were encountered. The DGG116 accelerometer evolved from the DGG56 accelerometer in early 1958.

The MGS mechanization specified a digital accelerometer loop for Centaur. Differences in performance of the 116 were immediately observed between digital and analog operation. These differences were noticed early in the -1 program but due to other development problems, specific problem definition and isolation of causes directly associated with

TABLE 2. 3-III. STORAGE SCHEDULE

			
TEST & STORAGE 8 HRS	TEST & STORAGE 8 HRS	TEST & STORAGE 8 HRS	TEST

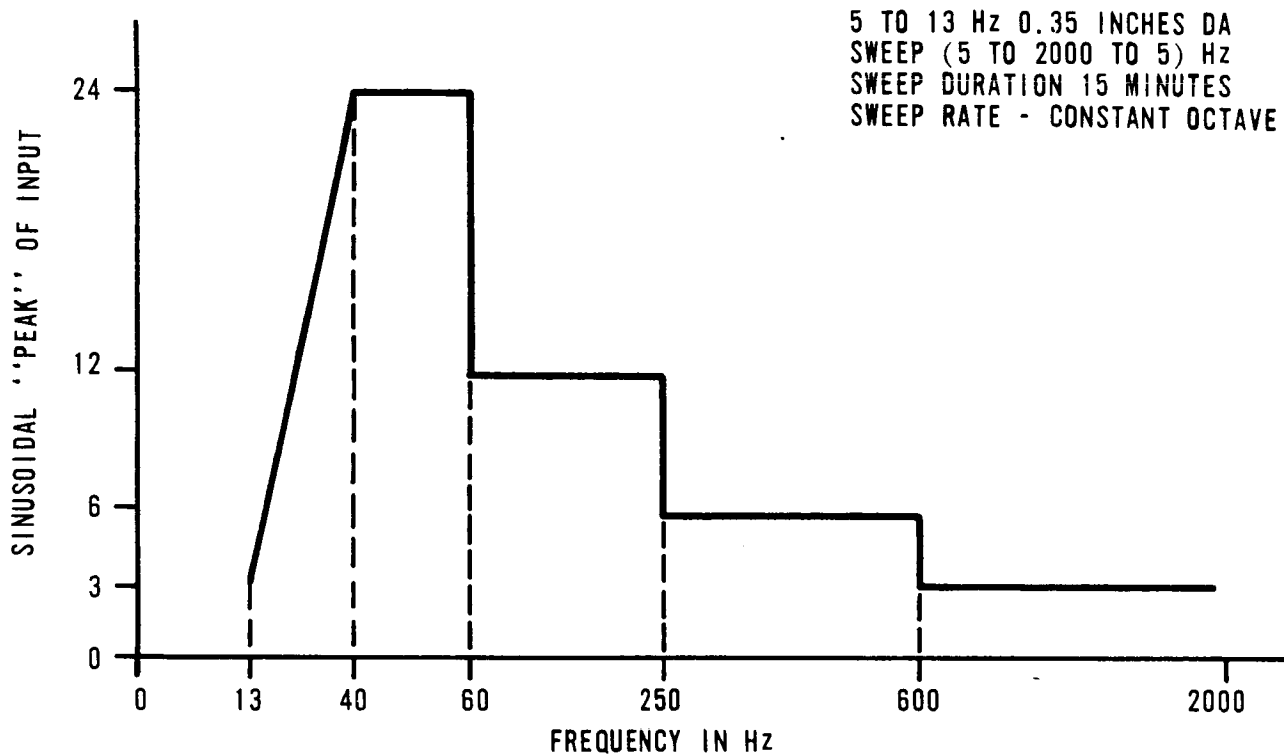


FIGURE 2.3-2. ACCELEROMETER VIBRATION

the accelerometer were not realized until the Centaur -3 program. Performance anomalies noted in the early stages of the -1 program were numerous. The following list contains a few of the more pronounced problems:

1. Null torque difference between analog and digital tests.
2. Null uncertainty.
3. Pendulum hang-up.
4. Leakers (external).
5. Scale Factor Stability.
6. IA alignment shifts.

Performance patterns established by the -1 program provided sufficient evidence to warrant design changes in the accelerometer. These changes were implemented upon entering into the -3 program.

2.3.9. Accelerometer Used on -3 Centaur. - More power was needed in the inertial component heaters in order to maintain thermal control over the specified platform external temperature environment. To accomplish this, the -3 program accelerometer heater resistance values were decreased for both the warmup heater and control heater. The accelerometer was redesignated the DGG116A6. Design differences between the 116A2 and 116A6 were as follows:

<u>Design Parameter</u>	<u>DGG116A2</u>	<u>DGG116A6</u>
Control Heater resistance	160 ohms	110 ohms
Warmup heater resistance	200 ohms	30 ohms
Torquer paddler	NONE	PADDED TO 66 ohms

Beginning with the -3 program, the TCA output was increased from 28 volts dc (-1 design) to 40 volts (ref: Topic 2.8). Incorporation of these two changes helped to reduce the thermal control problem. Among the list of -1 accelerometer problems, null uncertainty was by far the greatest cause for rejection. Both in-house failures, at the component and platform level, as well as vendor component in-line build processes, were caused by this problem. Output axis vertical (OAV) and output axis horizontal (OAH) orientations were specified for null uncertainty. The OAV orientation was the worst orientation insofar as null uncertainty was concerned. Null uncertainty was an important parameter for several reasons. During accelerometer alignment in the platform, the ability to accurately null the accelerometer was essential to an accurate alignment of the input axis. Large values of null uncertainty reflected into a null

torque uncertainty and in turn IA alignment uncertainty. Calibration of critical gyro drift parameters using accelerometer velocity loop (ΔV) information was also adversely affected. Due to the importance of the parameter, studies supplemented by tests were conducted at the component level in an effort to isolate causes within the accelerometer. Among some of the factors observed that affected this term were:

1. Dither current.
2. Operating temperature.
3. Heater power.
4. Damping fluid viscosity.

It may be worthwhile to regress for a moment to explain the purpose of dither. Early in DGG116 development testing it was observed that with the addition of a modulation winding in which ac current was passed, a mechanical (ideally radial) gimbal motion could be produced. This motion, in effect, centered the float in the fluid gap thus tending to unload the pivot-jewel mating, resulting in a much lower threshold accelerometer. Various levels of dither current were used in testing to arrive at an optimum value. Null uncertainty changes with dither current were significant above and below the optimum value. Though many tests were run, good correlation of accelerometer to accelerometer performance or establishment of a good performance pattern could not be obtained. Since the same problem existed at the component build level, the accelerometer manufacturer initiated detailed studies on all failed devices to see if a predominant failure pattern existed. Upon close examination of piece parts it was observed that almost 100 percent of the torn down devices had cracked or shattered thrust jewels. Further teardown studies showed that the torquer thrust jewel was the predominant jewel failure. Detailed piece part dimensional studies further showed poor dimension control on pivots and jewels.

During the investigation to isolate the causes for the poor null uncertainty performance (early 1963) various studies resulted. Aided by the teardown analysis results, a full program was developed to isolate the causes of jewel failures. The objectives of this program were to determine if correlation between jewel failure and null uncertainty existed, and if causes were isolated and correlation determined, what corrective action could be implemented. It was later found that during teardown, the normal process was to drain and flush the fluid then inspect the jewels and pivots. This was performed in two different areas, thus the devices were handled "dry" with little or no fluid support for the gimbal. This potential problem source was corrected along with other

changes which resulted in a drastic reduction in jewel problems, however, little improvement was realized in null uncertainty performance.

To cover all possibilities, other 116 type accelerometers were evaluated and null uncertainty performance compared. From this study it was observed that null uncertainty of the DGG116E accelerometer (a paddle damped accelerometer with approximately one-half the viscous damping) was improved when compared to the 116A devices. From this observation studies were directed toward viscous damping and operating temperature.

Investigative testing was continued, concentrating on OAV null uncertainty. It was observed that with the output axis vertical and directed up, that with sufficient settling time allowed, null uncertainty would settle out to a very repeatable and bounded value. It was further shown that with inversion of the accelerometer with respect to the local gravity vector, large excursions in rebalance current resulted. These large excursions were evidenced for up to 90 minutes (on overflowed devices) at which time the uncertainty in nulling current would settle to a very repeatable bounded value. For Centaur application, settling time of three minutes or less was needed during MGS calibration. Several DGG116A accelerometers were run through this test sequence, all resulting in similar results. Having sufficient data on 116A type devices, the sample test sequence was performed on the paddle damped 116E type accelerometer. When the data was compared on the two devices, results showed that the 116E settling time was approximately five times faster, but once settled, the uncertainty band was essentially the same as for the 116A devices. The theory was developed that true null uncertainty was really that band of uncertainty in the null rebalance current after settling out. It was further hypothesized that the large excursions evidenced immediately upon repositioning the accelerometer output axis to vertical were really changes in null torque. To explain the mechanism thought to be responsible for the long stabilization time once again we must digress momentarily.

As mentioned, earlier stabilization time of up to 90 minutes was required when reorienting from OAH to OAV or OAV up to OAV down. During build process the accelerometer pendulum is balanced (end to end) and floated. Neutral buoyancy (Σ fill fluid buoyant force + all other forces acting on pendulum = 0) for the DGG116A6 occurred at approximately +200°F. For Centaur application, the accelerometers were operated at +180°F, thus the overfloatation terminology. It was thus believed that the pendulum was actually moving, end to end, in the case

as the accelerometer was reoriented with respect to the gravity vector. The long settle time was a direct reflection of this translation. In order to check out this theory an accelerometer was built using conducting end jewels. Since the accelerometer was over floated, the steady state float position would always be toward the gravity vector as shown by Figure 2.3-3.

With the accelerometer stabilized (OAV up), conduction resulted, indicating the pivot and jewels were in contact. The accelerometer was then immediately reoriented to OAV down. The conduction path was immediately broken and some 80 minutes later re-established through the end jewel at the opposite end of the case. This test was very significant, since it established that float motion end-to-end was occurring and that the time required to traverse jewel-to-jewel was coincident with previously observed accelerometer stabilization time. With these two factors established, the exact mechanism producing the torque instability during the transient stabilization period was isolated to a few prime sources. These factors were:

1. Flex lead distortion due to piston action of float.
2. Changing gap distance in magnetic circuits.
3. Fluid piston action in a non-concentric piston-cylinder configuration.
4. End-to-end thermal gradient change.

Returning to the DGG116E paddle damped accelerometer comparison, it was shown that settling time was approximately five times faster than the DGG116A type device. The basic difference in the 116E design was a wider fluid gap and the use of a less viscous fluid. Settling time improvement realized by this device thus indicated that a predominate factor in controlling the stabilization time was the piston action taking place. Accelerometer reorientation, resulted in pendulum movement, thus requiring fluid displacement. The rate of fluid displacement for a given temperature is predominantly controlled by the net unbalance in forces acting on the gimbal, the fluid gap clearance and the fluid viscosity. Since the 116E accelerometer had a less viscous fluid and wider damping gap, faster settling times would be expected. Ideally in a concentric cylinder-piston configuration, net fluid torques would approach zero for the case in study. Local turbulence in the fluid, due to nonconcentricities, actually produce fluid torques on the gimbal during reorientation. This fluid turbulence resulted in erratic performance during float transition. Several factors, attributed to the fluid turbulence, produce erratic torques on the float. Among these are float "cocking" in the case, eccentric cylinder-piston configuration, fluid disturbance by flex leads and dither

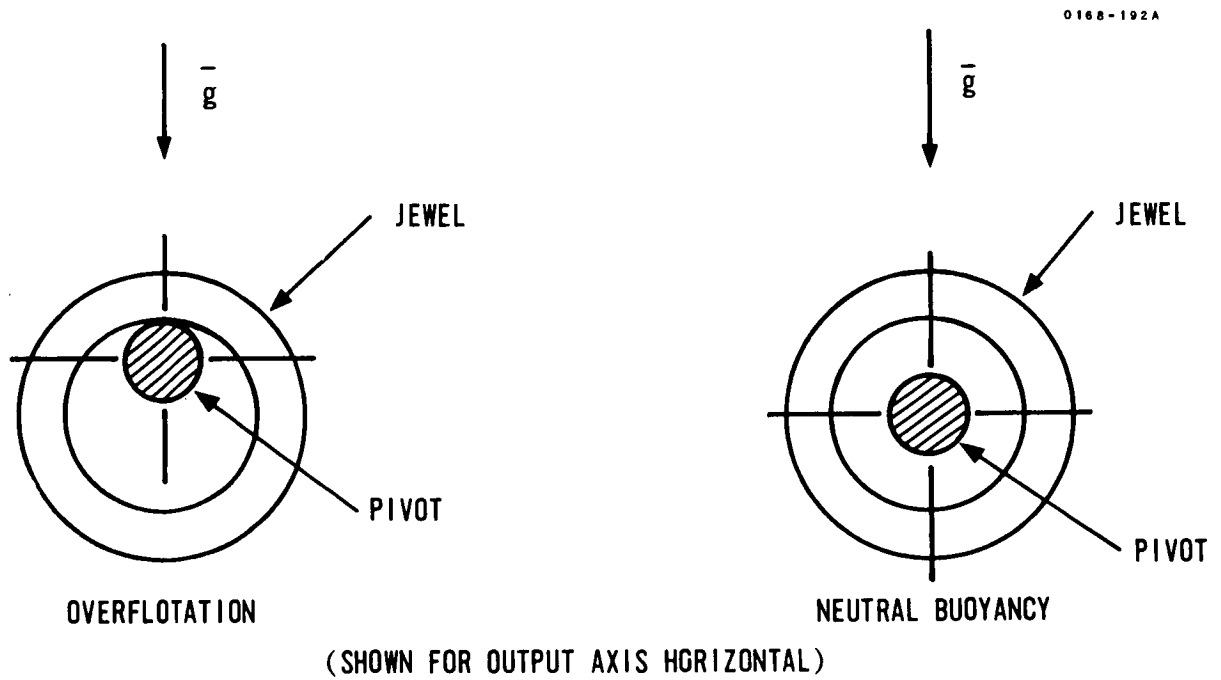


FIGURE 2. 3-3. ACCELEROMETER FLOAT POSITIONS

action. Once factors that contributed to the long stabilization time were isolated, immediate design action was initiated.

In formulating the best approach to take in correcting the problem, basic confinements were imposed upon the design. Among these were:

1. No damping change.
2. No electrical interface change.
3. No mechanical interface change.
4. Thermal compatibility with existing hardware be maintained.
5. No performance degradation with existing environmental requirements.

These restrictions were necessary, since several Centaur -3 platforms were already built and a decision to retrofit these platforms required complete interface compatibility with a modified accelerometer. With these ground rules, design approaches to the problem were quickly reduced to the "ported" or fluid by-pass configuration. Figure 2.3-4 shows the basic difference between the "non-port" and the "ported" configuration. The "ported" case made possible an increase in the fluid flow rate during gimbal axial translation, resulting in reduced stabilization time.

The "ported" DGG116A6 was subjected to a complete design proof program. All results showed that in all areas of performance, the new ported devices were equal to or better than the non-port configuration. The major improvement realized was in stabilization time. The study came to an end in late 1963 and the 116A6 Ported Configuration was released to production in early 1964.

One configuration not previously mentioned that took place during the stabilization - null uncertainty investigation (early 1963) was the neutral buoyant device. The DGG116 accelerometer was neutral buoyant at +200°F (OAH orientation) and used at +180°F for Centaur application. During the phases of the initial null uncertainty investigation it was observed that when the accelerometer fill fluid was changed such that neutral buoyance occurred at the +180°F operating temperature (fluid density changed, fluid viscosity remained the same) null uncertainty performance improvement resulted. The reason for the apparently improved null uncertainty was later shown to be a direct function of the test sequence. Data was taken at each orientation within two minutes after reaching the particular position. With the accelerometer operating as a theoretically neutral buoyant device, (i. e., the actual summation of forces acting on the gimbal $\rightarrow 0$) the small resultant force acting on the gimbal was not sufficient to cause gimbal translation of any appreciable

0168-193A

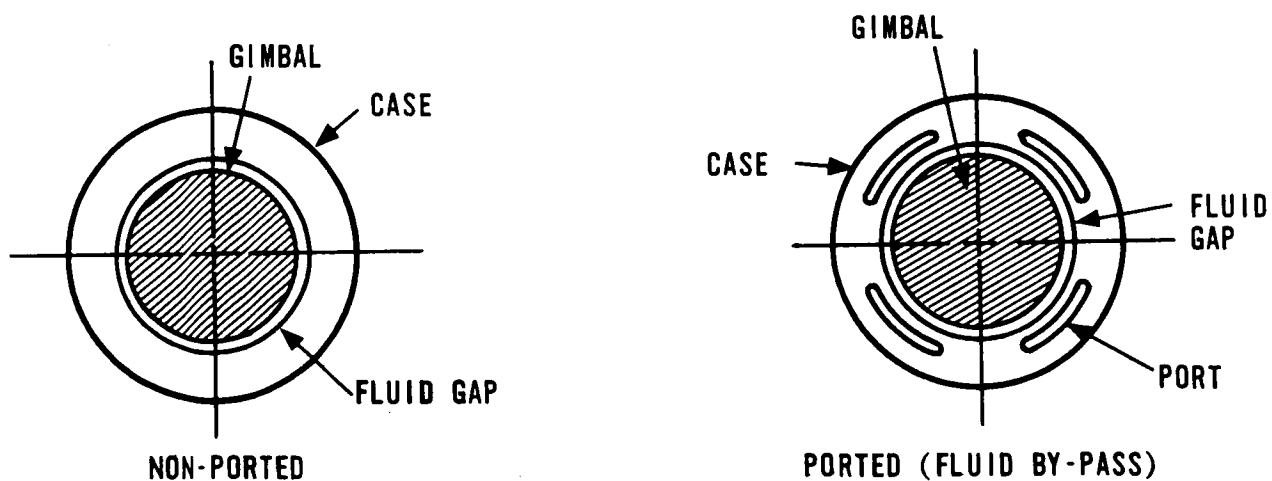


FIGURE 2.3-4. NON-PORTED VERSUS PORTED CONFIGURATION

amount, during the data collection period. As a result a much improved yield in null uncertainty was noted. At this time, a change was made to float the gimbal at the device operating temperature (+180°F). Later tests showed that due to the neutral buoyant condition, continuous float wander resulted, in which the device never reached stable operation. This condition was intolerable from a system point of view, thus the return to the +200°F over-flotation configuration.

2.3.10. Transition Period (DGG116 to DGG177). - As mission performance requirements became better defined and reflected into accelerometer requirements and performance capability of the DGG116 type accelerometer became better established, it became evident that the DGG116 accelerometer could not meet the performance required of the most stringent Surveyor missions.

It was further shown that for the less critical missions the DGG116 would provide only marginal performance. Therefore, while studies were being conducted on the DGG116 to determine if performance improvements could be made, other accelerometers were being surveyed as prospective replacements for the DGG116. Considered in this survey were the Kearfott 2401, the Bell Model III B, the Bell Model VII and Honeywell DGG177; all hinged pendulum accelerometers. Using, as a basic ground rule, minimum change to existing hardware, the results of this survey showed that all four accelerometers could meet the performance requirement for Centaur when tested as analog devices. The two Bell accelerometers and the Kearfott 2401 were designed to be used in analog loop closure (Bell accelerometers designed to be used in analog mode with analog to digital conversion electronics) and did not adapt themselves readily to the pulse rebalance electronics used by Honeywell. The DGG177 was designed to be used with the Centaur-type digital rebalance loops.

Other factors considered in the survey were the relative requirements for interface electronics changes. Mechanical compatibility with existing platforms was another important factor. The Bell accelerometers were electrically damped devices which, along with their incompatibility with current pulse torquing techniques, would have required major changes to Centaur's Coupler Electronics. The Kearfott 2401 would also require major changes in the Honeywell rebalance loop in order to be compatible. Mechanically, the Kearfott 2401 would require a new case in order to conform to flange mounting requirement of existing platforms. The Bell III B was too large for retrofit, and the Bell VII required the addition of a mounting flange and relocation of header pin terminals. The DGG177,

which required the least amount of change to existing pulse rebalance loops required a housing change for mechanical compatibility. Considering all of these factors, the DGG177 design was chosen for further evaluation.

Early in 1963 five prototype DGG177 accelerometers, designated as DGG177B9's, were ordered for evaluation purposes. In early 1964, these accelerometers were subjected to an extensive evaluation program. During this program all known error sensitivities were established. The accelerometers were operated in both analog and digital loops during the program.

Parallel to the DGG177 evaluation program, preparations were completed for Centrifuge tests using the DGG116A6 ported and non-porting accelerometers, at Holloman AFB. Three non-porting and three porting accelerometers were centrifuged in a triple block assembly (i. e., three loop simultaneously closed as in the system). The results of the centrifuge test program, which was completed in mid-1964, showed that the porting accelerometers yielded somewhat better data than the non-porting devices, but the improvement was not significant when compared to the adverse performance common to both type devices. The undesirable characteristics that were common to both the porting and non-porting accelerometers and had not previously been detected were:

1. High non-linear cross axis loading terms.
2. Digital deadzone (loss of velocity information) under high acceleration loading along the output axes.
3. Large bias shifts under compound high-g loading.

During the DGG116 centrifuge tests, the DGG177B9 accelerometers were going through the in-house test and evaluation program. Upon completion of these tests, three of the five DGG177B9's were sent to Holloman AFB and run through the same centrifuge program just completed by the DGG116 accelerometers.

Results of the DGG177 centrifuge tests showed that all of the undesirable performance characteristics that were observed in the DGG116 centrifuge tests were either eliminated or reduced to insignificance in the 177. It was also shown from the digital data, that the accelerometer bias changed with the pulse rebalance limit cycle.

Since pulse limit cycle (PLC) changes with acceleration level, for the type loops used by Centaur, bias changes with limit cycle is classified as an acceleration sensitive error source. At one extreme, zero "g", a

two-pulse limit cycle results with a fundamental frequency of 900 Hz. At the other extreme (maximum "g" loop capability) the fundamental PLC frequency approaches zero. Bias change with frequency was previously noted during the in-house evaluation test program. During a portion of these tests, the accelerometer was operated in an analog loop with different discrete frequencies superposed on the analog rebalance. It was at this time that bias changes as a function of frequency was fully realized as a potential problem area. The effect of frequency change upon bias in the 116 type device was less obvious, due to the masking effect of other large error sources.

Bias change with frequency has been designated torque generator reaction torque (TGRT). The term is not new, nor is it unique, with the DGG177 accelerometer. Any permanent magnet type torquing device exhibits this characteristic to varying degrees. Early in the 177 development, steps were taken to minimize TGRT. At that time, TGRT was thought to be only current sensitive (shown to be a function of torquer current squared). Since the type rebalance loops used by Centaur are in essence a constant current source insofar as what the torquer sees, no real problem was foreseen with TGRT. As a means of reducing the TGRT magnitude as a function of current, improved torquer magnet matching was implemented in the build cycle of Centaur 177 flight devices. Perfectly matched magnets (physically unrealizable) theoretically result in equalized or symmetric solenoidal action (TGRT as a function of current approaches zero), whereas any mismatch is observed as a bias. It was soon observed during the DGG177B9 test program that TGRT also varied as a function of the frequency seen by the torquer.

Torque generator reaction torque results from the interaction of the flux associated with the torque producing current and the flux lines established by the permanent magnet field. An equation of the total rebalance torque is the sum of the two current produced torques or $T = K_T i + K_R i^2$ where K_T is the torquer sensitivity (dyne cm/ma), (i) is the torquing current and K_R the reaction torque coefficient.

For a sinusoidal torquing current of Amplitude A and frequency ω , the torque can be represented as

$$T = K_T A \sin \omega t + K_R (A \sin \omega t)^2$$

$$= K_T A \sin \omega t - K_R \left(\frac{A^2}{2} \cos 2 \omega t \right) + K_R \frac{A^2}{2}$$

The term $K_R \frac{A^2}{2}$ is the TGRT for this sinusoidal input. It represents a dc offset or bias resulting from a symmetrical input. The K_R term is a frequency dependent term. The sign may vary for K_R from accelerometer to accelerometer but will remain of the same sign for a given unit regardless of ac current level. The units placed upon K_R are $\mu g/[ma(rms)]^2$. Studies have been made to determine a means of compensation for TGRT versus frequency. From these studies, supported by test results, it has been shown that over the frequency range, of primary interest, TGRT versus frequency could be reduced to an insignificant value through incorporation of a compensation winding. This winding permitted external compensation. TGRT as an error source was evaluated as not significant, and incorporation of the winding was dropped.

In late 1964, the final report on the DGG177B9 test and evaluation program was released. During this same time, centrifuge results of the DGG116 and DGG177 were compared. In addition, a thorough review was made of the Surveyor two-burn mission requirements. The conclusions were:

1. The present DGG116A6 accelerometer error contribution to the two-burn mission was not tolerable.
2. Performance anomalies observed during centrifuge testing of the DGG116 accelerometer were not tolerable.
3. No firm cause or causes could be arrived at for the large bias shift observed during DGG116 centrifuge tests, therefore, no immediate design change to correct for this anomaly was anticipated.
4. All problems observed with the DGG116 were either eliminated or reduced to insignificance by incorporating the DGG177.
5. Growth potential for the DGG116 type accelerometer design was at a practical end, whereas growth potential for the DGG177 type device was still possible.

2.3.11. DGG177 Retrofit. - Having considered all factors, a fully documented plan to incorporate the DGG177J1 accelerometer on a retrofit basis was presented. Early in 1965, go-ahead was received to retrofit Centaur -3 program platforms with DGG177 accelerometers. Based upon DGG177B9 data and improvements anticipated from changes being incorporated into the Pulse Rebalance Electronics (Coupler) the following predicted improvements were expected (direct ascent):

	<u>GG116 and Present Electronics</u>	<u>GG116 Bypass With Improved Electronics</u>	<u>DGG177 With Improved Electronics</u>
Midcourse * Correction	9.0	7.0	4.9

* Units one sigma (meters/sec)

The DGG177B9, as was previously mentioned, required a change in the housing. The overall length of the accelerometer presented no problem. A worse case tolerance build up did show, however, that a second gimbal swing clearance problem could result due to the height above the flange. This mechanical incompatibility was defined prior to embarking on the B9 evaluation program. Studies were initiated at that time to determine the ultimate design changes which would result in the desired mechanical configuration. The B9 accelerometer was also equipped with self-leads, (i.e., a cable coming out of the top cover), whereas the DGG116 had exposed header pins to which wiring harness in the platform was connected. Prior to the end of the DGG177B9 test program, a final design configuration was arrived at which would result in a direct compatible retrofit into the existing platform design. This configuration was designated as the DGG177J1 accelerometer.

Internally, the DGG177B9 and J1 piece parts were interchangeable. It is seen that basically the J1 is an inverted B9 minus the cable. See Figure 2.3-5A and 2.3-5B.

The differences just described were necessary in order to realize full mechanical interface compatibility with existing IMU design.

During the initial DGG177B9 development phase, a value engineering team was formed. The charter of the team was to look at the DGG177 line of accelerometers and make recommended design and process changes which would result in better or equal performance, ease of producibility and improved reliability. One recommendation resulting from this effort

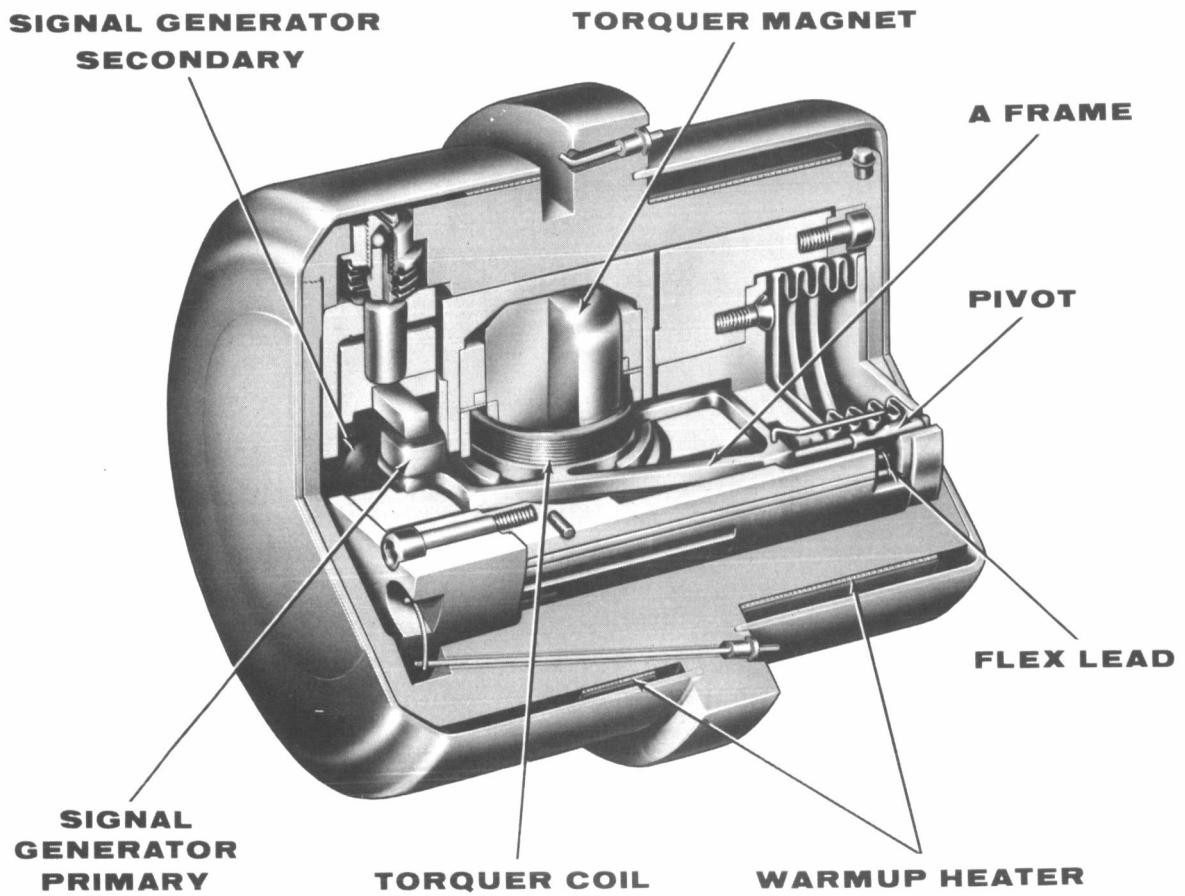


FIGURE 2.3-5A. DGG177J1 HINGED PENDULUM
ACCELEROMETER

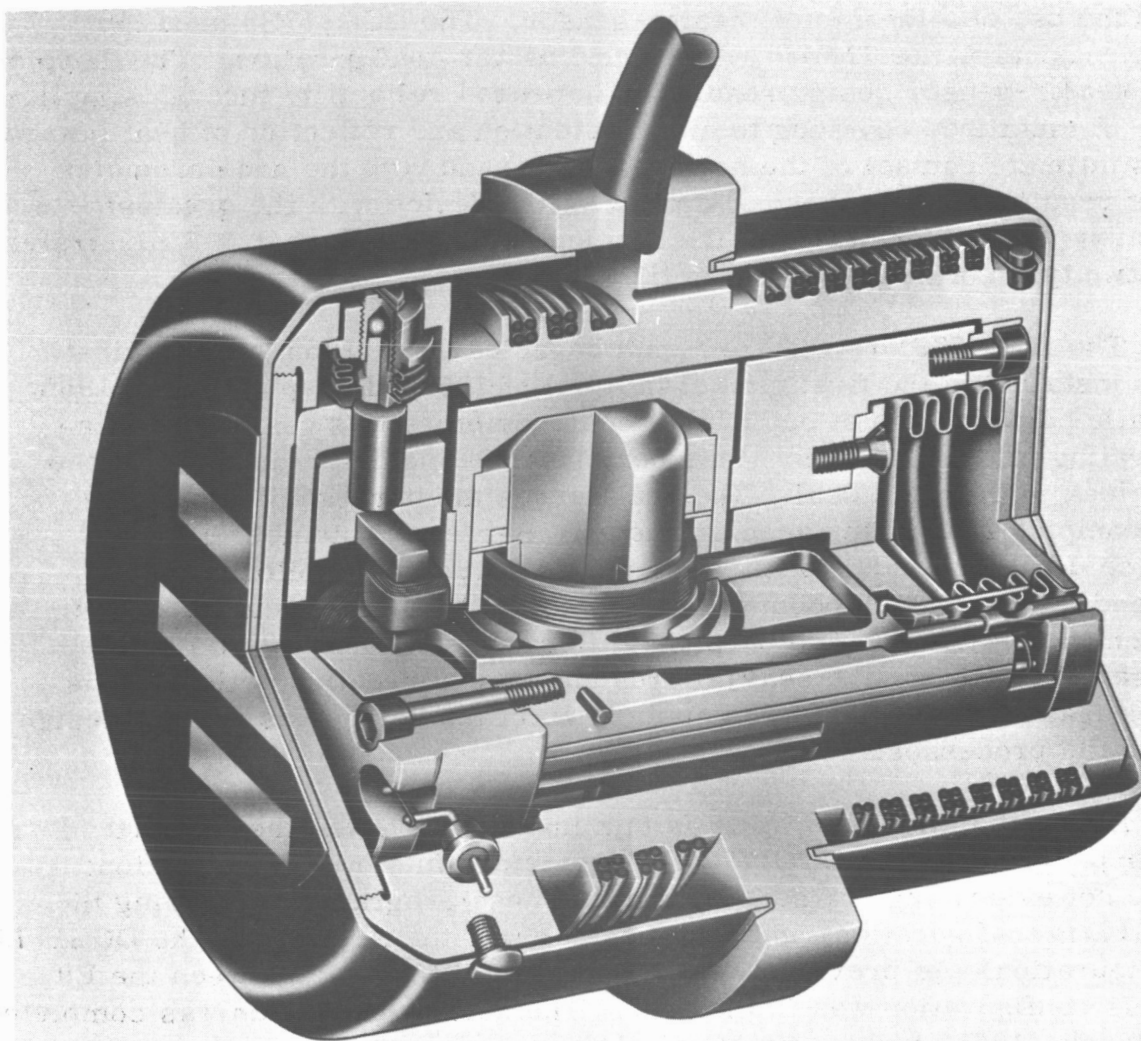


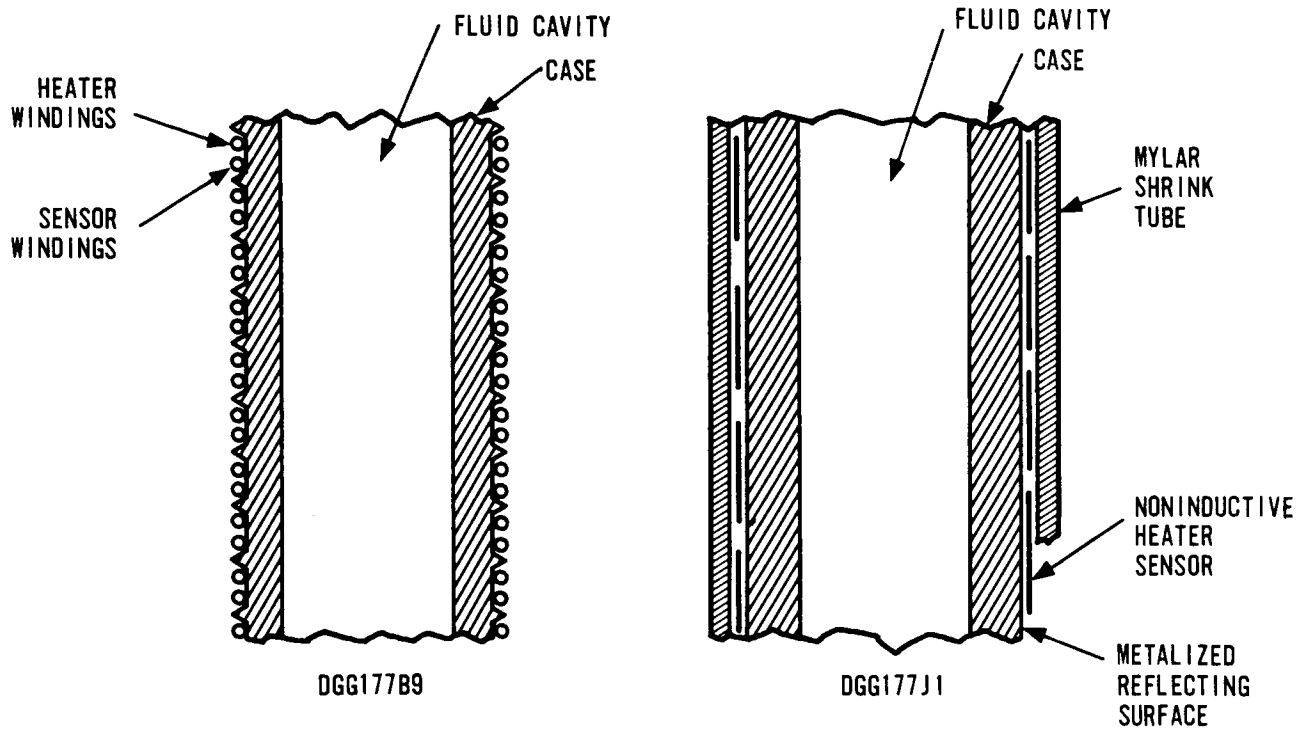
FIGURE 2.3-5B. DGG177B9 HINGED PENDULUM ACCELEROMETER

was the use of a thermofoil heater-sensor. The DGG177B9 used the Conventional Acme Thread Wire wound heater configuration. The thermofoil heater-sensor design results in improved reliability through simplicity. A metalized covering to aid in retention and reflection of heat inward, plus intimate contact of the heater-sensor band with the accelerometer case results in close thermal control of the device with the greatest efficiency heat transfer in to the accelerometer. Figure 2.3-6 illustrates the two types of heater configurations.

The DGG177J1 retrofit program began early in 1965 with the first J1's installed in the first gimbal in April of 1965. In September of 1965, erratic performance of one of the accelerometers was observed while operating in the Platform. This performance anomaly was later traced to a leak in the main seal. The seal serves the purpose of containing the damping fluid in the accelerometer. Between September 1965 and March 1966, five additional seal failures occurred. Following the second failure, which occurred in November 1965, an intensive investigation was initiated. The purpose of this investigation was to find the cause or causes for the seal failures and take corrective action. This investigation covered both the application of the device, as well as design and build processes.

An immediate observation in this investigation was the fact that other programs using DGG177 accelerometers in similar applications were not evidencing any seal failures. These programs were using the DGG177B configuration, whereas Centaur was the first to use the DGG177J configuration. As previously mentioned, the difference between the B9 and J1 configuration was in the case. The seal investigation was completed in March, 1966 at which time a final report was issued.

In analyzing differences in the B9 and J1 case configuration it was noted that the J1 case was structurally stronger. When the thermofoil heater-sensor was implemented in the J1 design, a thicker case wall resulted at the main seal end while the case outside and inside diameter remained relatively unchanged. The J1, being the most advanced DGG177 design at the time was the only accelerometer in the 177 line with the thicker case. As part of the overall investigation a detailed stress analysis was performed. This analysis showed that due to the differential expansion rates of dissimilar materials, undesirable stress loading could result at the seal. The seal loading is a result of differential expansion rates of dissimilar materials. In the DGG177 accelerometer a stainless steel slider bar is used for initial null torque adjustment. The stress analysis showed that the principal source of strain resulted from thermal



SCALE: NONE

FIGURE 2. 3-6. HEATER SENSOR CONFIGURATIONS

contraction and expansion of the aluminum case and cover with respect to stainless steel slider housing at low temperatures. Figure 2.3-7 shows a simplified cross section of this assembly. The stress set up by the slider bar tends to elongate the case at low temperatures. Case elongation produces excessive stress on the seal epoxy-thread. Fracturing of the epoxy permitted the nitrogen helium fill gas used in the platform to enter. Due to the high penetration property of helium, it was possible for helium to enter the fluid cavity through the fractured epoxy seal, before fluid actually appeared on the outside of the fracture. Once the helium entered the fluid cavity, a bubble would form. Depending upon the bubble location, various degrees of erratic performance was evidenced. X-ray techniques were developed and implemented to determine if an accelerometer had developed or was in the process of developing a seal fracture. The X-ray technique merely photographed the bellows which are used for volumetric expansion. In units exhibiting seal problems, the X-rays showed the bellows to be partially collapsed or compressed. By comparing normal bellows travel (X-rays taken with the accelerometer at operating temperature and at room temperature) of known good units, an early indication of impending problems was provided.

To supplement the stress analysis, a dummy accelerometer was built and instrumented with strain gages. Results from this instrument verified the analysis, showing the primary loading on the seal was attributed to the thermal expansion contraction differential of the metals. From this investigation, two possible design changes resulted. The first change considered, was the incorporation of a small spring in the slider bar assembly. The purpose of this spring would be to absorb some of the force produced on the case due to expansion-contraction differences in the housing-case assembly. Tests were performed using the spring loaded slider bar. Concern was primarily centered around null torque stability of the device since the slider bar was the adjustment used to mechanically compensate for null torque. Test results indicated stress relief was obtained when the spring was added; however, further tests were required to evaluate null torque stability. The other possible solution to the seal problem was the incorporation of a redundant seal. The redundant seal served two purposes - (1) isolated the dust cover from the seal head both thermally and mechanically, and (2) would prevent fluid leaks if the seal did crack. Material studies were made and showed that polyurethane was a compatible material for the application. A polyurethane coating on the main seal end was tried on one accelerometer. Forced failure of the main seal was produced on a redundant seal device and no performance degradation was observed. After intensive tests and analysis, the redundant seal approach was recommended as the best

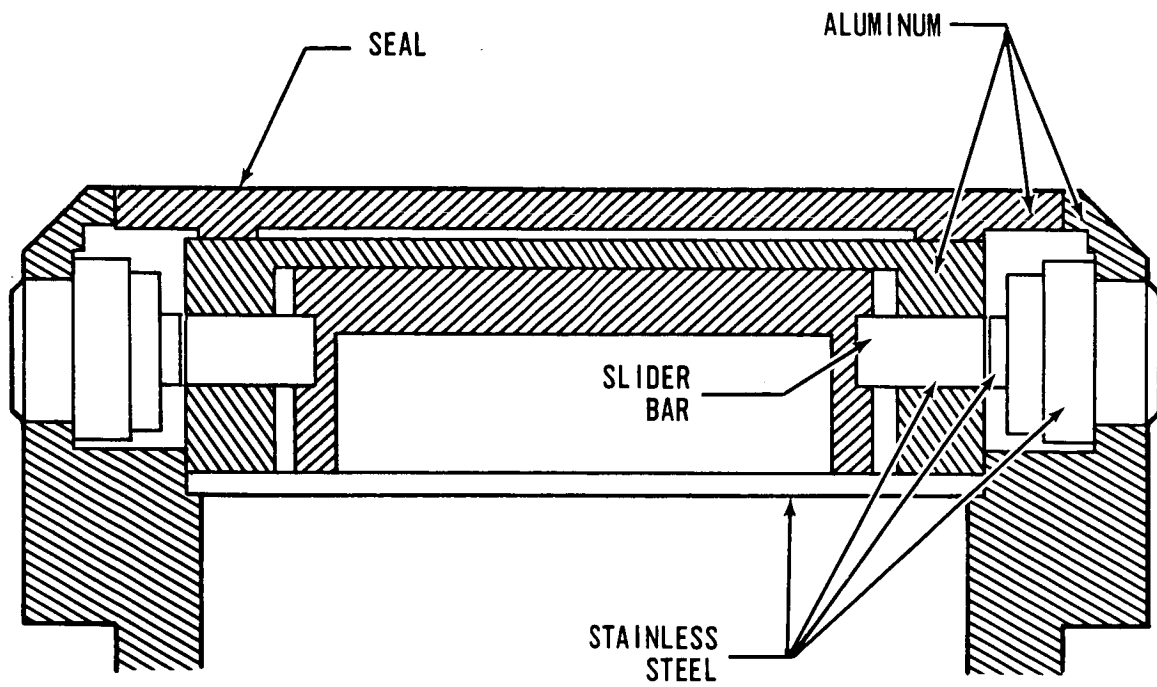


FIGURE 2.3-7. SIMPLIFIED ACCELEROMETER SEAL DIAGRAM

immediate design solution to the main seal problem. All DGG177J1 accelerometers were thus recycled through the polyurethane coating process and redesignated as DGG177J3's. The DGG177J3 seal configuration has proven to be a very satisfactory design. No seal problems have occurred since the redundant seal was added in early 1966. Subsequent design and evaluation resulted in a recommended design change to the slider bar adjust and seal area. Tests showed the spring loaded, slider bar adjust, to be an effective means of reducing the main seal load. An electron beam (EB) welded main seal also proved to be superior to the present thread seal configuration. These design changes along with process changes were recommended in a final report on the DGG177J main seal redesign but have not been approved for use in Centaur devices, since no seal problems are being encountered in the existing devices.

2.3.12. GG177 Reliability Problems. - In addition to the main case seal leak problem discussed in Paragraph 2.3.11, other reliability problems were noted in the GG177 accelerometer. In each case, however, immediate corrective action was applied and the GG177J3 accelerometer has become an extremely reliable device. The problems and corrective action is presented in the following paragraphs.

2.3.12.1. Torque Generator Shorts. - These shorts include those due to torquer bobbin insulation failure, those due to workmanship problems in which the wire was routed too close to the bobbin exit slots, and those due to contamination found in the windings on terminal pin insulation. The corrective action for this problem was extensive. It consisted of:

1. The bobbin insulation was changed to a better material, easier to apply and with a higher dielectric strength.
2. The minimum bobbin insulation thickness was increased and improved inspection methods established to assure the minimum insulation is maintained and that the coating is free of contamination.
3. A design change was made increasing the width of the bobbin exit slots. These changes reduce the possibility of the wire shorting at an exit slot.
4. The magnet wire has been changed from single coated thermister wire to double coated Isonel 200 wire, resulting in improved insulation thickness and fewer number of voids or breaks in the insulation.

5. The magnet wire is periodically tested to assure the wire insulation specifications are met.
6. The coil winding operation has been moved to a clean area to reduce possibilities of contamination and an automatic coil winder is being used.
7. The torquer bobbin dielectric test requirements have been increased from 250 to 500 volts rms.

The above corrective action has resulted in no torque generator short problems in any of the units having the above changes in eighteen months of operating history.

2.3.12.2. Contamination Failures. - These failures consisted primarily of partial hang-ups caused by loose contamination. The corrective action consisted of close examination of all cleaning, assembly, and deburring procedures and instituting corrective action as follows:

1. Piece part and subassembly inspection was improved by adding a kitting operation in which all piece parts and sub-assemblies for a particular device are placed in a kit prior to start of final assembly. The piece parts are then inspected by quality, under a 20 power microscope, and certified clean and free of burrs.
2. Steps were taken to reduce soda contamination, from soda blast processing, by adding acetic acid rinses in the processing.
3. The pendulum and pivot assembly now require an ultrasonic cleaning cycle following pivot lapping to remove traces of lapping compound.
4. A radius has been added to the end cap land area to reduce the possibility of producing burrs during assembly.
5. Steps have been taken to improve parts cleaning by improving the parts cleaning area and parts cleaning facilities.
6. All final assembly operations have been moved from a clean area to a super clean cubicle. No contamination failures have been noted since incorporating this corrective action.

2.3.13. IMG Accelerometers. - The performance of the GG177 accelerometer is judged to be adequate for the improved Centaur System. The corrective action taken to improve the GG177J3 accelerometer has been carried through into the GG177J5 IMG accelerometer, which is of the same design as the GG177J3 except for the heater configuration. With the corrective action, no problem is anticipated in meeting the accelerometer MTBF of 40,000 hours required for the IMG.

A main case seal redesign program was initiated at the same time the redundant seal fix was formulated so that a more positive design solution to the main case seal leak problem would be available for later accelerometers. Several areas were investigated including (1) an "O" ring seal, (2) a spring loaded axial shaft assembly, (3) a shrink fit end cap, (4) an electron beam welded seal. The program included the build and test of several prototype units. The conclusions reached were that the shrink fit end cap in conjunction with the spring loaded slider would give a more than adequate safety factor for the main case seal. This design was available for the GG177J5 IMG accelerometer. However, with the demonstrated success of the redundant seal fix on the J3 devices, the decision was made not to change at this time.

2.3.14. Conclusion. - The original Centaur accelerometer, the DGG116, was a precision sensing device. However, due to its basic design, undesirable performance characteristics were exhibited when evaluated against Surveyor Mission requirements. Primary problems were:

1. Output axis loading effects.
2. Bias and Scale Factor instability.
3. Large digital dead zone.
4. High sensitivity to magnetic fields.

The causes of the problems were not always easily identified. The cause and effect relationship must be established when dealing with design problems such as those encountered with the 116, in order to determine if a design improvement is feasible in the same device. As in the case of the large bias shifts that occurred in the 116 during Centrifuge tests, no real cause was ever isolated for these shifts. Theories were, however, put forth which if proven to be the cause would have resulted in a different type of accelerometer construction such as a hinged pendulum type device being needed.

The systems error analysis proved to be a very useful tool in evaluating the needed performance for any given mission against that performance attainable. It was through use of the error analysis that

predicted shortcomings of the 116, again based upon past performance, was afforded. The DGG177 accelerometer has performed up to expectations since its incorporation into the system, except for several early process reliability problems, which have been corrected.

TGRT changes with Pulse Limit Cycle (PLC) changes is a well-defined error source for any given accelerometer and a significant one for operation in a pulse-rebalance loop. By constraining the PLC (forced 2 PLC at zero "g"), the error has been bounded somewhat. Design changes at the accelerometer level are feasible. Means of compensating for TGRT in the Computer are also feasible. The error as it exists today, however, is deemed insufficient to warrant any design or programming changes.

The GG177 accelerometer, in its current configuration, is suitable for the Centaur IMG. The only modification being incorporated for the IMG device is a heater-sensor change to operate the heaters directly from 28V dc.

Future problems, of the type experienced on Centaur IGS accelerometers, may be reduced through the incorporation of good requirements definition via technical development specifications. Initiation of timely design reviews at all stages of the design cycle and implementation of good process and configuration control will further enhance a successful design. A rigorous analysis and test evaluation program must be performed to insure that all accelerometer characteristics which may affect mission performance are fully known.

Topic 2.4

Platform Resolvers

2.4.1. Summary. - The dual pancake resolvers used in the Centaur Platform have been one of the more critical components during the IGS development. There have been design and build problems involving the resolver itself as well as expanded application of resolvers and the resolver chain during the Centaur Program.

The major problems created by the resolver have been both electrical and mechanical in nature. There have been:

1. Tuning Capacitor Failures.
2. Shielding deficiencies.
3. Tuning problems.
4. Bearing problems.
5. Housing problems.

Areas of expanded application have been:

1. Providing three axis steering capability.
2. Measuring gyro drift with the resolver chain.
3. Measuring vehicle twist on the launch pad with the resolver chain.
4. Design and build of a multiplexed resolver chain for the IMG.

During the Centaur Program much has been learned about the design and application of these rotary components including:

1. Specification requirements.
2. Vendor control (design, configuration and processes).
3. Test procedures.
4. Application in miniature inertial platforms.

The following sections contain discussion of the above topics. The discussion begins with a general description of the resolver and its uses, then follows through with the problem areas encountered, and concludes with what knowledge can be applied to new IGS development programs.

2.4.2. General Description of the Electrical Characteristics. - A resolver is a member of the synchro family. The Centaur Resolver is used in the inertial platform to resolve a voltage vector into its orthogonal components. The resolvers used in the Centaur platform are "pancake" type units, each containing two resolvers, whose electrical characteristics are independent of one another. Each resolver assembly is a "two space phase -- two space assembly" designed to provide two independent angular pickoffs. For purposes of identification, the two halves of each Centaur resolver are designated Resolver "A" and Resolver "B". Each resolver has two identical rotor windings displaced at 90 degree space quadrature. Each stator likewise has two identical windings at 90 degree space quadrature.

Resolver "A" - 400 Hz Unit. - This resolver incorporates a tuning network that produces a stable transformation ratio (TR) of 0.65 ± 0.2 percent and a phase shift of zero degrees, nominal. The tuning network is designed so that frequency changes from 394 to 406 Hz will not cause an angular error greater than ± 14.0 arc-minutes. In order to insure accuracy requirements, the null voltage cannot exceed 50 mv maximum at 20 vrms excitation. The 400 Hz resolver ("A") performs the following functions in the Centaur platform:

1. Provides coarse gimbal alignment and control signals for platform orientation.
2. Provides the steering command coordinate transformation for both Atlas and Centaur vehicles.

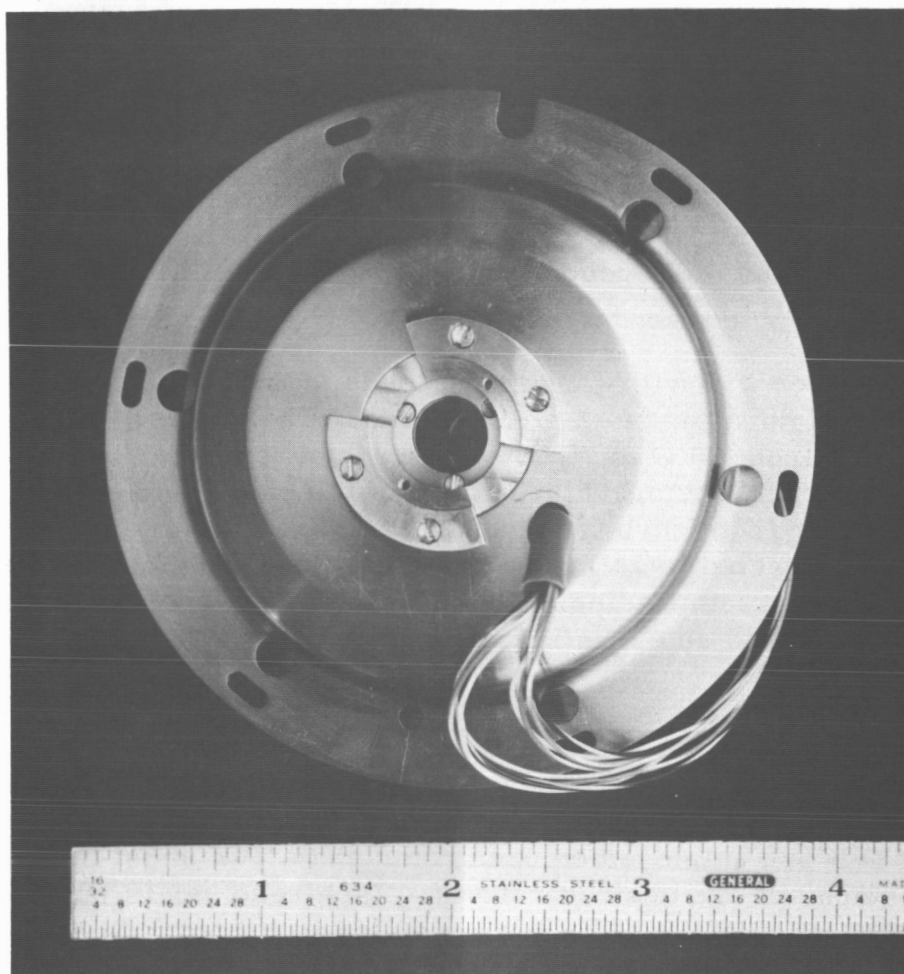
Resolver "B" - 7,200 Hz Unit. - The total null voltage cannot exceed 24 mv at 20 volts (rms) excitation. The angular accuracy cannot exceed ± 14 arc-minutes. The transformation ratio of this unit is not critical and is nominally 0.35 (reference Topic 6.5). The 7,200 Hz unit performs the following functions:

1. Resolves the output signals of the U and V gyros to gimbal 2 and 3 stabilization loops.
2. Provides direction information for fourth gimbal drive.

2.4.3. General Description of the Mechanical Characteristics. - The mechanical dimensions of the Centaur Resolver Assembly (A and B Units) are pictorially shown in Figure 2.4-1. Its maximum weight is 16 ounces. The bearing assembly consists of a duplex pair of ball bearings, suitably

R-ED 27290

A6412-02



A6411-82

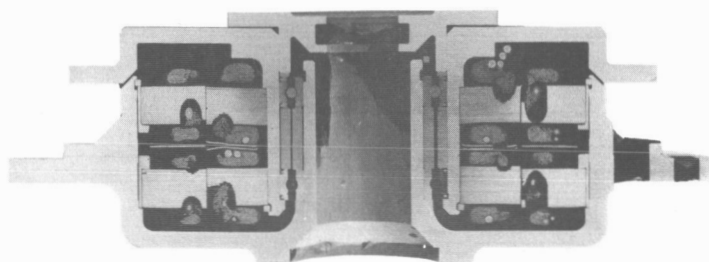


FIGURE 2.4-1. CENTAUR RESOLVER

restrained to withstand external axial loads in either direction. The axial preload is five pounds minimum at a temperature of 150°F. The resolver is so designed that Honeywell can replace bearing assemblies, rather than return the resolver to the Vendor for this repair. The static or breakaway friction is 0.32 oz-in. maximum unloaded. The running friction torque is 0.17 oz-in. maximum, while subjected to a radial load of eight pounds. The resolver operates to specification limits under a sustained axial load of 80 pounds in either direction. It also operates to specification limits under a sustained radial load of 85 pounds.

The resolver will withstand shock loads of $30\text{ g} \pm 3\text{ g}$ in any direction for a maximum duration of 12 milliseconds. The resolver meets specification limits from 20°C to 70°C. The unit will operate, but with degraded performance, over a temperature range of minus 65°C to plus 93°C. The unit will operate from zero to 55,000 feet equivalent atmospheric pressure. Each unit is subjected to an insulation test of 250 vrms between windings and 500 vrms between windings and the case. The resolver has a storage life of two years and an operating life of at least 2,000 hours.

2.4.4. Using The Resolver in the Resolver Chain (Figure 2.4-2). - In performing the resolver chain function, the transformation ratio and phase shift are the critical parameters. Each resolver in the chain must see the same source and load impedance at all input voltage levels. Therefore, the tuning network employed on each rotor and stator must be carefully selected to achieve the desired results. Each resolver is tuned to produce an input impedance of $5K < 0^\circ$ when the stator is loaded with a 5K ohm resistor. The tuning networks are shown in detail in Figure 2.4-3 and are supplied by the Vendor with the resolver.

In addition to the tuning networks, "T-pads" are employed to correct overall chain gain for transformation ratio where the signal paths bypass a resolver. Each T-pad produces a 5K resistive load and the desired transformation ratio of 0.65. (Figure 2.4-2.)

2.4.5. Electrical Problem Areas During the Centaur Development. - The two major electrical problems with Centaur resolvers have been 1) phase shift, and 2) resolver shielding/crosstalk. Each will be discussed in the following paragraphs.

Throughout the history of the Centaur program, resolver chain phase shift has been a continuing problem. The problem manifests itself as an overall gain reduction since the 400 Hz output of the chain is demodulated in the autopilot. The sources of phase shift are discussed below in the sequence that they were encountered and corrected during the development program.

0 166-196A

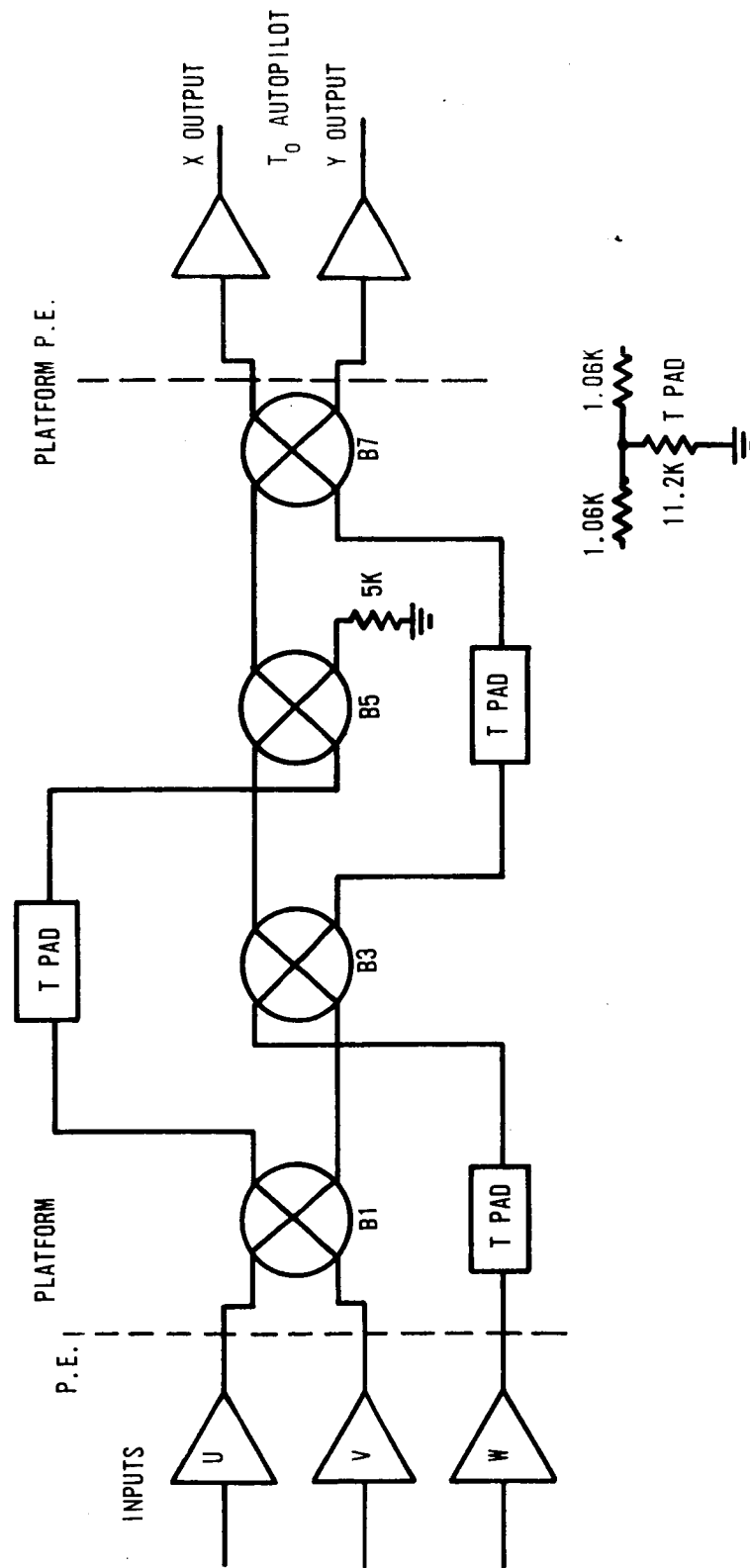
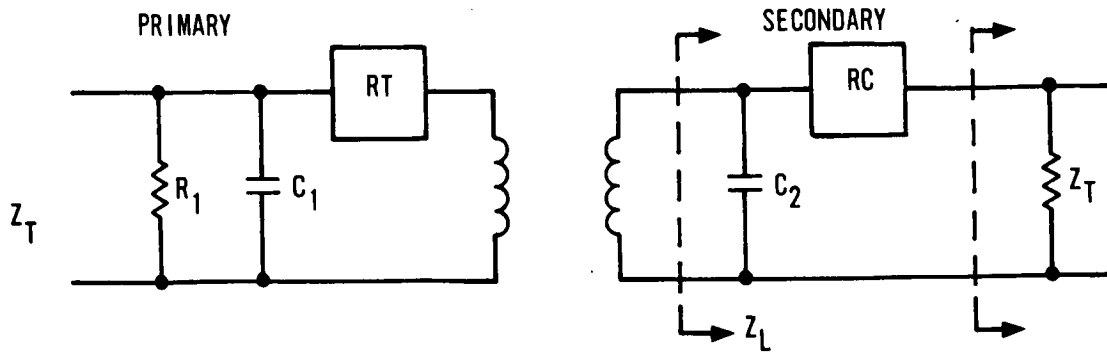


FIGURE 2.4-2. CENTAUR RESOLVER CHAIN



$$Z_T = 5K \pm 75 \Omega$$

$$Z_L = 5.56K \Omega \angle -26^\circ$$

R_1 AND C_1 = PRIMARY TUNING COMPONENTS

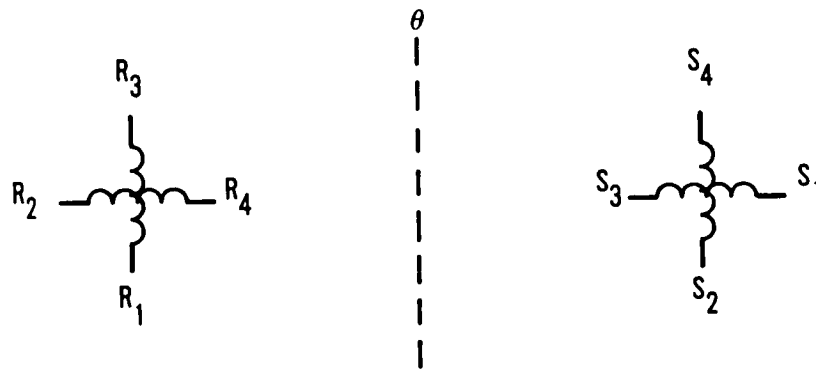
R_T = RESISTOR

R_C = ATTENUATION RESISTOR OR THERMIST-RESISTOR COMBINATION

Z_T = RESISTIVE ITERATIVE IMPEDANCE

Z_L = LOAD IMPEDANCE

C_2 = SECONDARY TUNING COMPONENT



$$E_{S_{4-2}} = K (E_{R_{3-1}} \cos \theta + E_{R_{4-2}} \sin \theta)$$

$$E_{S_{3-1}} = (-E_{R_{4-2}} \cos \theta + E_{R_{3-1}} \sin \theta)$$

WHERE K = TRANSFORMATION RATIO

FIGURE 2.4-3. RESOLVER TUNING NETWORK

Tuning Capacitor Failure. - As mentioned previously and shown in Figure 2.4-3, each rotor and stator uses a capacitor for tuning. There have been numerous capacitor failures resulting in large phase shifts (12 degrees-20 degrees) at the output. Honeywell has directed the resolver vendor on three occasions to change this tuning capacitor.

The first capacitor used (from 1959 to 1963 in -1 and -3 platforms) was a hand rolled foil capacitor that was covered with a silicon rubber material. The failure mode of this capacitor was an open, which usually occurred at the bond between the foil and the lead.

The second capacitor was a plastic encapsulated version of the original. Although the failures were fewer in number, they were still too frequent to be tolerated. The failure mode again was an open in the lead joint. This capacitor was used from 1963 to 1965.

The third capacitor has been in use since 1965. It is a hermetically sealed unit. Again the number of failures has been reduced, but occasionally this capacitor also fails in the open mode.

A study program is again underway to improve the present tuning capacitor.

The alternatives considered throughout the program on the capacitor failures were:

1. Seek a new source for capacitors.
2. Improve existing capacitors.
3. Do away with passive tuning altogether and replace it with an actively tuned resolver chain.

Schedule and cost considerations always necessitated the approach of improving existing components, until the current IMG development, which is now utilizing an actively tuned chain.

2.4.6. DC Current As a Phase Shift Source. - In early 1964, several platforms exhibited resolver chain phase shift in excess of 10 degrees. It was determined that this phase shift varied with the operation of the Temperature Control Amplifiers (TCAs). It was also found that the phase variation was caused primarily by the gyro and accelerometer TCA dc current that was carried by the slip-ring assemblies. Slip rings are used to connect electrical signals and power to the various gimbals of the

Platform (reference Topic 2.6). These slip rings are installed in the axial holes of the resolvers and torque motors. Although the slip rings are not an integral part of the resolvers or torque motors, they can effect resolver performance through electrical or mechanical coupling.

The -3 platform configuration in 1964 was such that the heater return current for all the gyros was carried by slip rings in the resolver end of each gimbal. The return current for the accelerometers was routed through the resolver end of the azimuth gimbal and then through the torque motor end of the remaining gimbals.

Wired in this manner, all four resolvers had, in effect, a turn of wire through their centers. The current through this turn was sufficient to alter the B-H curve of the iron used in the resolver core. This in turn changed its mutual inductance. Because each resolver had been tuned to minimize phase shift, this change in inductance then appeared as a phase shift in the resolver.

Alternatives considered:

1. Change the platform wiring so that all the 48V TCA leads went through the torque motor end of the gimbals.
2. Redesign the TCAs.
3. Change the 48V high side leads.

The problem was corrected by re-routing the 48V dc returns through the same rotary component as the high side 48V dc lines. This, in effect, created an equal and opposing magnetic field and negated any effects upon the B-H curves, and hence phase shift of each resolver. All platforms were retrofitted in 1964 with this change.

2.4.7. Resolver Shielding. - Each resolver is constructed to include a shield between the 7,200 Hz and 400 Hz rotor and stator stacks. Honeywell first noticed that a coupling problem existed in early 1964. The transformation ratio (TR) would change as a function of magnitude of applied voltage. It was later determined that the vendor had made four changes to the resolver to upgrade internal yield, which was low because of out-of-specification resolver null voltages. The four changes were:

1. Changed wire size of rotor and stators from AWG 41 to AWG 42. This permitted easier pressing of the end turns lowering the stress on the core.
2. Lowered the number of turns on rotor and stator.

3. Decreased the rotor to stator air gap from 0.004 to 0.0025.
4. Removed the Mu Metal shield between the rotor stacks.

These four changes were made to lower the null voltage to within the specification limits of 1.5 mv/volt input.

These changes to the resolvers resulted in the following Platform problems:

1. The Resolver Chain failed its accuracy requirement of 60 arc-minutes.
2. A cross coupling problem was created between the 7,200 Hz section and the 400 Hz section. The effect of this problem was to introduce a large noise contribution into the stabilization loops.

Alternatives considered for solution of these problems were:

1. Replace the 27 units affected with new units, having proper shielding.
2. Actively tune the chain to eliminate variable reactive interaction between resolvers.
3. Try to establish a new vendor with a quick delivery capability.
4. Retrofit the existing 27 resolvers with shields.
5. Attempt to use the unshielded resolvers where possible and replace only those in the most critical positions with shielded units.

Cost and schedule considerations resulted in a choice of solution 5 to the above problems. Specifically, each resolver in the chain was manually tuned to the expected input voltage. This was accomplished by knowing the profile vectors and computing what each of the four resolvers would have as input voltages. Knowing the voltage range for each resolver allowed the tuning network to be altered to operate over a limited voltage range. The overall accuracy requirement was also raised from 60 arc-minutes to 120 arc-minutes. Those resolvers which affected overall system performance were replaced. It turned out that only one of the

platform resolvers was a mandatory change item. This was the first gimbal resolver, which resolves the 7,200 Hz U and V gyro stabilization loop signals.

2.4.8. Mechanical Problem Areas. - The main resolver mechanical problem area throughout the Centaur program has been bearings. The original resolver (in the -1 and early -3 Platforms) used a "snap ring" to hold the bearing assembly in place. This snap ring was nothing more than a 3/4 ("C" shaped) ring that snapped into place. A grooved area was machined in the resolver housing to hold this ring. This type of assembly was changed in late 1963 to a capped bearing enclosure. This was necessitated due to high friction levels encountered during platform level testing. The "snap ring" sliding out of its groove was the cause of the high friction levels.

Although the snap rings were a major source of high resolver friction levels, they were not the only source. In July of 1964, Honeywell directed the vendor to study the use of selective fits on the bearings and housings. This was necessary after Honeywell determined that there was no selection performed during assembly and preloading was performed at room temperature. With the tolerances used by the vendor, the assembly was made with either line-to-line, or loose fits. At resolver operating temperature, approximately 160°F, the result was an excessively tight fit between the shaft OD and bearing ID or a loose fit between housing ID and bearing OD. The vendor was requested to incorporate the following changes:

1. Establish new basic dimensions and tolerances for housing shafts and bores.
2. Code housing shafts and bores in 0.0001 inch increments.
3. Require bearing supplier to code bearings in 0.000050 inch increments.
4. Using a selection table supplied by Honeywell, assemble bearings to housings. Heat housings during assembly to prevent interference fits while assembling.
5. Adjust preload at Resolver operating temperature.
6. Inspect the final resolver assembly at operating temperature for geometric tolerances.

Most of these changes were incorporated in mid-1964 with the result being a better resolver in the friction area.

2.4.9. 4th Gimbal Resolver Change. - The fourth gimbal resolver was originally a single 400 Hz resolver that separately performed the caging and the chain functions during the various pre-flight and flight modes of operation. Late in 1964, NASA requested Honeywell to utilize a dual resolver in the fourth gimbal position, in order to use the steering chain during the Atlas boost phase of flight. This change was made to all platforms in the 1965-66 period, as part of the Phase I PIP (GG177) system retrofit program.

2.4.10. Gimbal No. 1 Rotor Tuning Capacitor Removal (1964). - During an investigation of No. 1 platform gimbal loop oscillation problems, it was determined that the resolver input amplifier could break into oscillation. This oscillation was of sufficient amplitude that the shield in first gimbal resolver did not block the oscillating 400 Hz signal from cross-coupling into the 7,200 Hz section.

A short time prior to discovering this problem, the vendor had redesigned the resolver tuning network, raising the rotor shunt capacitor from 0.030 mfd to 0.035 mfd. The amplifier, being only marginally stable before this change, went unstable with the added capacitive load. To eliminate the problem, Honeywell removed the capacitor on the first gimbal resolver rotor tuning network and at the same time changed a feedback resistor in the input amplifier to improve its phase margin. These changes were proven to be effective, and the instability problem has not recurred. This problem again emphasized the need for more effective technical coordination with, and configuration control of, a rotary component vendor.

2.4.11. Need for a Centaur Resolver Second Source. - After the series of problems in late 1964, Honeywell decided that development of a second source for resolvers was a necessary step. At the time this development of a second source was proposed, 158 resolvers had been received at Honeywell with a 61 percent rejection rate. To prepare for dual sourcing, a new specification was written for the RFQ, which was sent to 12 companies. Three of these companies responded to the RFQ. Each of the three companies was surveyed by a Honeywell engineering team to determine the technical and production capabilities, and to discuss, in detail, the requirements of the new resolvers. The companies were found to be competent and capable of meeting the specified requirements. However, the second

source concept was rejected, based on an analysis of economic tradeoffs. Further attention was then focused on improving the single-source's capability, and this source is still in use today on the Centaur Program. In retrospect, many of the early resolver problems (in the 1963 to 1965 period) could have been solved sooner and more effectively with the competitive motivation that results from a good dual-source arrangement.

2. 4. 12. The IMG Alternative Resolver Chain Mechanization (Active Compensation). - In an effort to do away with the use of troublesome compensative networks, other Honeywell projects developed a resolver chain using active compensation. This active compensation technique utilized emitter follower circuits in lieu of the resistor-capacitor tuning components. This concept was used on the X-20 Dyna-Soar project. The IMG will use active, operational type amplifiers between each resolver stage.

There are advantages in using an actively tuned resolver chain. The advantages include:

1. Significantly improved pointing accuracy.
2. Capability for providing three axis steering by frequency multiplexing techniques, made possible through expanded bandwidth in the tuning stages.
3. Capability of providing gain between resolvers to offset the attenuation within resolvers or any other desired value and hence permitting an overall chain gain of unity.
4. Provision of accurate and stable impedance matching, which results in:
 - a. Uniform Transformation ratios.
 - b. Minimum phase shift in each resolver and thence, the overall chain.

2. 4. 13. Expanded Centaur Resolver Applications. - Two new resolver chain applications have been developed on the Centaur Program. These are:

1. Measuring Gyro MUSA terms without the use of optics. There was a definite need to provide the capability of updating all three MUSA terms with the platform installed on the vehicle, where

optics cannot be conveniently used. The Centaur resolver chain was used to provide an accurate (0.016 deg/hr/g, one-sigma) direct readout of these terms. Through the use of predetermined inputs, the chain provides an X and Y output change directly proportional to gyro drift angle.

2. Vehicle Twist Measurements on the launch pad were also made possible using the changes in X and Y resolver chain outputs as a direct readout of vehicle motion. The accuracy of these readouts are within ± 25 arc-seconds. A similar technique, using only the azimuth resolver, has been used to determine vehicle twist during tanking tests. It is being used again, but with full chain operation, to obtain more accurate data in support of an ATS mission study.

2.4.14. Conclusions. - Throughout the development phases of the Centaur Program, problems associated with the platform resolvers were numerous and troublesome. The major problem areas were:

1. Friction levels.
2. Capacitor failures in compensation networks.
3. Resolver tuning problems.

There have been many areas of analysis and test performed on these resolver problems. These areas include:

1. Transformation ratio variations with input voltage change.
2. Phase shift in individual resolver stages and in the overall chain.
3. Input isolation amplifier loading.

These investigations and problem solutions have improved the overall performance and reliability of the present Centaur resolvers. They have also permitted an expanded use of these resolvers for 1) calibration of gyro MUSA terms without the use of optics and 2) the measurement of Atlas-Centaur vehicle twist characteristics during vehicle tanking operations.

The experience gained on Centaur has also pointed out several important lessons, which should be applied to future IGS development programs. These lessons include:

1. Special attention must be given to:
 - a. Specification of resolver requirements.
 - b. Evaluation and selection of vendors.

- c. Review and control of vendor designs, processes, inspection points, and test methods.
 - d. Continuing configuration control once the design, processes, etc., are acceptable.
- 2. Development of a resolver second source or use of standard designs, available from several sources, are worthwhile undertakings on a new program.
- 3. Mechanization of resolver chains, using active compensation techniques, is highly desirable for either two-axis or three-axis coordinate transformation.
- 4. The applications of resolver chains can be expanded on future programs (as has been already done on Centaur and other existing programs) to include gyro drift calibrations, measurement of vehicle perturbations (such as twist), etc.

Topic 2.5

Platform Torque Motors

2.5.1. Summary. - The gimbal torque motors used in the Centaur Platform have been one of the more troublesome components throughout IGS development and production. There have been design and build, as well as maintenance, problems involving the torque motor.

The major problems with the torque motors have been mechanical in nature. There have been:

1. Parallelism Problems, consisting of:
 - a. Bearing Problems.
 - b. Housing Problems.
2. Contamination Problems resulting in high friction due to:
 - a. Basic Design Problems.
 - b. Build Deficiencies.
3. Test Technique Problems in measurement of:
 - a. Friction.
 - b. Sensitivity.

During the Centaur Program much has been learned about the design and application of "pancake type" torque motors including:

1. Specification requirements.
2. Vendor control.
3. Test procedures.

The following paragraphs contain a discussion of the above topics. The discussion begins with a general description of the torque motor, then follows through with the problem area encountered and concludes with what knowledge can be applied to future IGS development.

2.5.2. General Description. - The gimbal torque motors used in the Centaur platform are direct drive, permanent magnet, direct current devices in a "pancake" configuration, which provides optimum performance in minimum space. The direct drive feature has greatly improved servo

performance by eliminating gear tooth friction, backlash, runout, adjustment, and the inertia present in gear driven gimbal systems. In a loop using torque motors of the direct drive design, the static loop gain available to the servo designer is limited only by the basic sensitivity of the gyros. The torque motors are mounted at one end of each platform gimbal axis, with the motor rotor fixed to the inner gimbal and the stator fixed to the outer gimbal or case (for the outer roll or fourth axis). The duplex bearings mounted between the motor rotor and stator provide support for the driven gimbal at one end of the axis. The torque motors which drive the first, second, and third platform gimbals are rated at a nominal output of 15 ounce-inches. The nominal output rating of the torque motor which drives the fourth gimbal is 45 ounce-inches.

2.5.3. Electrical Characteristics. - The electrical characteristics of both sizes of torque motors are identical, except for developed torque and armature resistance, and hence they will be treated as one unit. The armature resistance of the 15 oz-in. unit is 48 ohms (± 12 percent) while the 45 oz-in. unit is 40 ohms (± 12 percent). The armature resistance is measured over continuous rotation of the inner element relative to the outer element. A nominal sensitivity 15 oz-in. unit develops rated torque with the average dc input current not exceeding 540 ma at room temperature, while a nominal sensitivity 45 oz-in. unit develops rated torque at 750 ma under the same conditions. Both sized motors must withstand dielectric testing at 500 volts rms between mounting surfaces and the armature winding. The contact resistance between each of the four brushes and each commutator segment is less than 0.20 ohm, when measured at a current of 15 ± 5 milliamps.

2.5.4. Mechanical Requirements. - The static or breakaway friction torques, with the axis aligned to local vertical within ± 2 degrees, are:

1. 15 oz-in. unit, 0.94 oz-in.
2. 45 oz-in. unit, 1.60 oz-in.

Ripple torque is held to less than ± 6 percent at gimbal servo threshold levels. The running friction for each unit, at 25 rpm, is 0.48 oz-in. maximum, with a radial load of 8 pounds. The ball complement of the individual bearing is 18, with a Rockwell hardness of C-56-64. The motor, when supported by appropriate maintenance and repair programs has a life expectancy of 5 years. The operating life at 15 rpm is 2,000 hours.

2.5.5. Centaur -1 and -3 Comparisons. - The platform torque motors during the -1 phase of the Centaur program used a stainless steel case. The resolver on the other end of the gimbal used an aluminum case. To counter balance the additional weight caused by the stainless steel housing of the torque motors, weights were added to the resolver end of the gimbal. With the advent of the -3 system, the torque motor housings were fabricated from aluminum, thus eliminating the additional weights. In addition the -3 Centaur systems utilized a higher rated torque unit. The torque rating on the first, second, and third gimbal torque motors were raised from 10 oz-in. to 15 oz-in. and the fourth gimbal torque motor from 30 oz-in. to 45 oz-in. The increase in torque resulted in a smoother drive to each of the four gimbals.

2.5.6. Parallelism Problems. - In August 1963, the vendor's production line of torque motors was shut down due to a parallelism problem. The vendor could not meet the mounting flange parallelism requirement of 0.0014 inch (Total Indicator Reading). Honeywell reviewed all the parts drawings, including the housing flanges, the bearing retention caps, the bearing assembly, and the armature assembly. This review resulted in recommended changes for the dimensional control required to insure the axes of rotation of both flanges were perpendicular to the mounting surface. Honeywell also witnessed inspection of all piece parts and determined that there were problem areas in:

1. The bearing outer race retainer cap.
2. The bearing assembly, consisting of two angular contact bearings, with spacers on the inner and outer race.

The solutions to the parallelism problem were:

1. Specify the amount of torquing to the six screws in the retainer cap.
2. Impose new dimensional control of the bearing assembly.
3. Replace the face to face bearings with back to back bearings.
4. Change preload to a nominal of 5 pounds, with a contact angle of 27 degrees.

The parallelism inspection techniques were revised to include adequate height gages to check the critical dimensions of the flanges. The entire unit was checked by rotating one flange with respect to the other flange until the two worst case conditions were achieved. Differential readings taken at these two points yielded the parallelism value.

2.5.7. Contamination Problems. - At several points throughout the Centaur program there have been torque motor contamination problems. Those problems exist today although they no longer occur with the frequency of past years. The causes are twofold in nature:

1. The basic design of the torque motor.
2. The build process.

The design of the torque motor is such that a minute particle of any foreign material in the torque motor can degrade performance. In addition, many external openings in the torque motor case allow the entry of contaminants. The build process includes drilling two holes in the stator flange of the motor for sector switch mounting. In the past, this operation was performed at Honeywell, with the result that some small metal chips remained in the motor. The hole drilling operation is now performed by the vendor, prior to assembly, thus reducing contamination.

In late 1966, after experiencing a series of contaminated units, Honeywell instigated a thorough cleaning process, that is performed at the Honeywell plant. This cleaning process has greatly reduced the overall contamination problem. In addition, the Vendor was appraised of the deficiencies in cleanliness of his build and test areas, and these deficiencies have been corrected.

At this writing, Honeywell is investigating a possible contamination problem caused by the vendor's change in the potting process. The wire wrapping technique and wire wrapping material (tie card) no longer adequately hold the coils of magnet wire within the confines of the potting mold. The result is a void in the winding with flakes of wire wrapping material being present within the torque motor housing. An interim fix, now in process, allows a coating material to be brushed over the affected area. The results of this "fix" are not yet known, but a process review by Honeywell Materials Engineering indicates it will be effective.

2.5.8. Test Technique Problems. - Several problems were encountered due to noncompatibility of test techniques between the Vendor and Honeywell. This was mostly due to insufficient initial communication and poorly

defined requirements in the torque motor procurement specification. Examples are:

1. Motor Sensitivity. - The Vendor measured motor sensitivity (oz-in. /amp) in such a way that the effect of motor friction was cancelled out. The Honeywell technique did not eliminate the effect of friction. The Honeywell Receiving Inspection measurements were consistently lower than those of the Vendor. This resulted in many invalid rejections of good motors by Honeywell. This situation was corrected in late 1966, and the test data are now comparable at the two facilities.
2. Friction Measuring Technique. - The Vendor currently uses a gravity system of measuring motor friction. Honeywell uses a precision "torque watch". Although the results to date have been comparable, this difference could become a problem if motor friction started falling "out-of-spec" at Honeywell receiving inspection. Work is underway to resolve this difference and ensure full compatibility of Honeywell and Vendor data.

2.5.9. Conclusions. - In review, torque motor problems have been numerous throughout the development phases of the Centaur Program. They have been a frequent target of engineering investigation and rework. The major problem areas have been and are:

1. Parallelism.
2. Contamination.
3. Test Techniques.

The basic torque motor performance throughout Centaur guidance development has improved. However future programs could avoid many of Centaur's problems by:

1. Taking special care to obtain definitive specification requirements.
2. Careful evaluation and selection of vendors (preferably with a second source also selected).
3. More control over and communication with the vendors.
4. Closer correlation between Vendor test techniques and customer Acceptance test techniques.

Topic 2.6

Platform Slip Rings

2.6.1. Introduction and Summary. - The miniaturized slip-ring assemblies used in the Centaur platform were one of the most troublesome components during the early phases of IGS development. Redesign and improved assembly techniques, however, have brought slip-ring failure rates down to acceptable levels.

The major problems experienced with slip rings were:

1. Noise
2. Contamination
3. Friction.

During the Centaur Program, much has been learned about the design and application of slip rings including:

1. Specification requirements
2. Testing
3. Vendor monitoring and control.

The following sections contain a discussion of the above topics. The discussion begins with a general description of the slip ring, follows with the problem areas encountered, the corrective action taken, and concludes with what knowledge can be applied to future IGS development.

2.6.2. General Description. - The miniaturized slip rings and wiper capsule assembly shown in Figures 2.6-1 and 2.6-2 permits transmission of electrical signals and power to and from the moving platform gimbals and inertial sensors. The 38 ring, encapsulated assemblies are mounted coaxially with the gimbal torque motors and resolvers at each end of the gimbals. A significant feature of the design is the integral unitized "capsule" construction of the ring and wiper. This feature makes it possible to pre-set and control the wiper contact pressure, of a few grams, during slip-ring assembly operations, rather than at the gimbal assembly level. The wiper blocks consist of two separate units, located around the slip ring in a manner that facilitates inspection of the final capsule assembly.

A6412-01

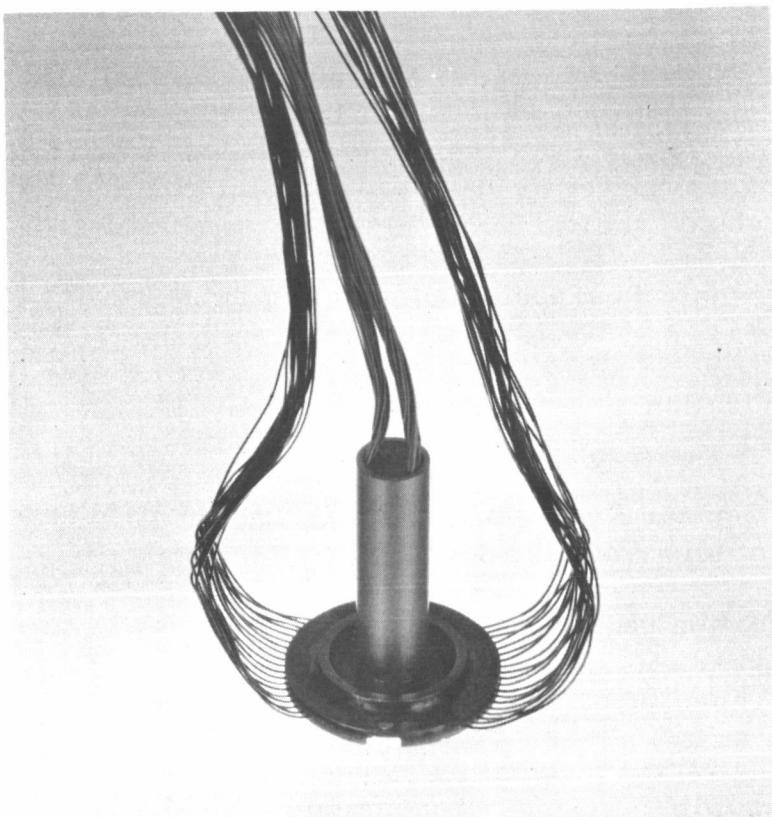


FIGURE 2.6-1. SLIP-RING CAPSULE

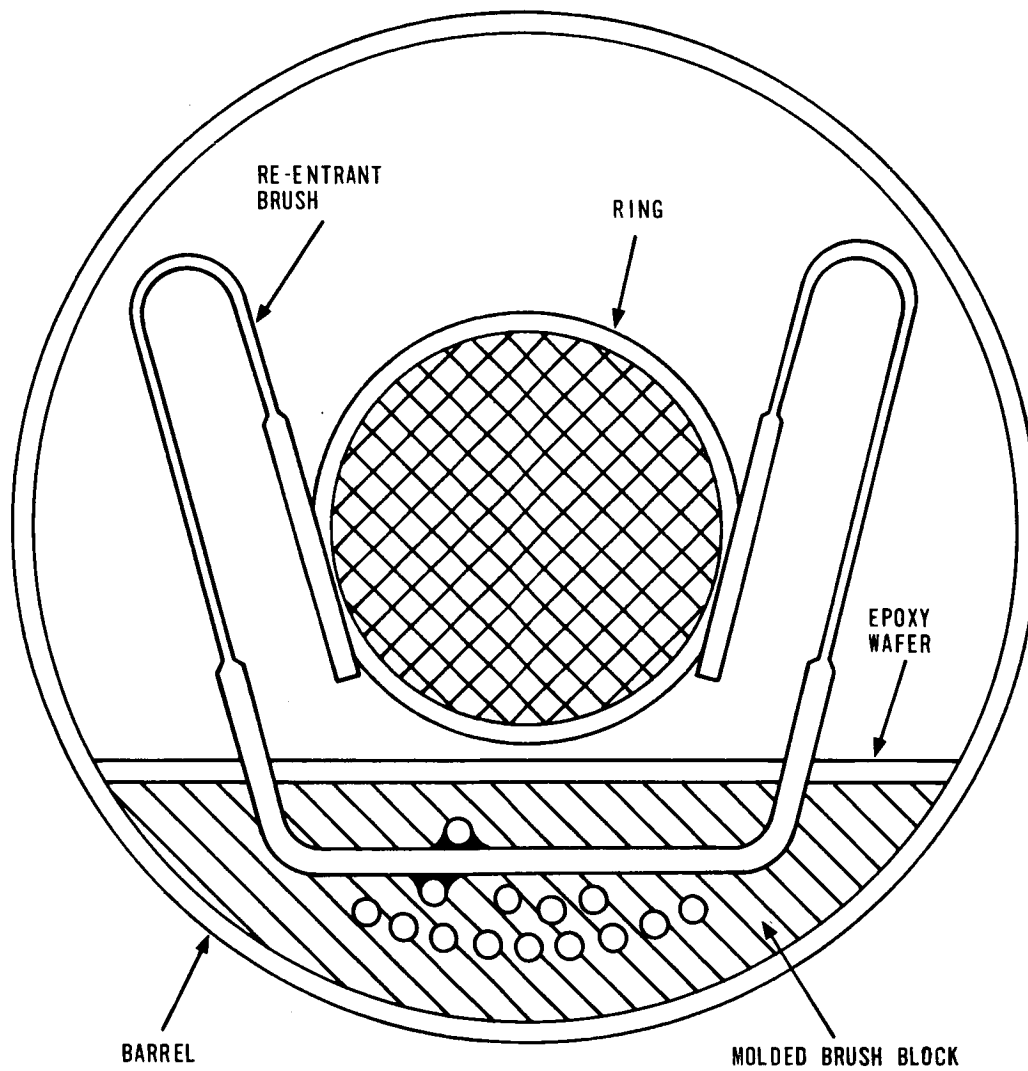


FIGURE 2.6-2. CROSS SECTION THROUGH RINGS AND BRUSHES OF CENTAUR SLIP RING

The slip-ring assembly consists of a rotor and a case. The rotor is supported in the case by very low-friction bearings. The rotor includes modified "V"-groove contact rings and associated electrical leads. The case contains the brushes and electrical leads. Two brushes shown in Figure 2.6-3, with a common lead wire, make contact with each collector ring. The rotor utilizes a flange to allow attachment to the driving member. The rotor leads are encased in this flange and extend radially outward from the center of the hub. The case leads project axially from the end of the case opposite the rotor flange and extend parallel to the rotor axis. Stress relief is provided in the case so that the brush leads can be bent back to within the axial length of the assembly after installation. The rotor and case electrical leads are insulated from each other and the associated housings. The rotor and case incorporates barriers between exposed conductive surfaces to prevent arc-over.

2.6.3. Electrical Requirements. - The basic electrical requirements for the slip-ring assembly are:

1. Contact Resistance Variation. - The maximum contact resistance variation does not exceed 15 milliohms over 360 degrees of rotation.
2. Resistance. - The resistance of each individual slip ring, excluding lead wire, does not exceed 0.125 ohm when measured with a current of one milliamp flowing through the circuit. The variations in resistance when the rotor is rotated through one complete revolution does not vary by more than ± 0.0075 ohm.

2.6.4. Mechanical Requirements. - The mechanical requirements for the slip-ring assembly are:

1. Friction. - The breakaway friction level is 0.42 oz-in. at room temperature.
2. Lubrication. - There are no lubricants permitted on slip-ring contact surfaces.
3. Life. - The operating life of the slip-ring assembly is 5,000 hours without maintenance or repair.
4. Reliability. - The slip-ring assembly has a design goal failure rate of 0.15 percent per 1,000 hours.

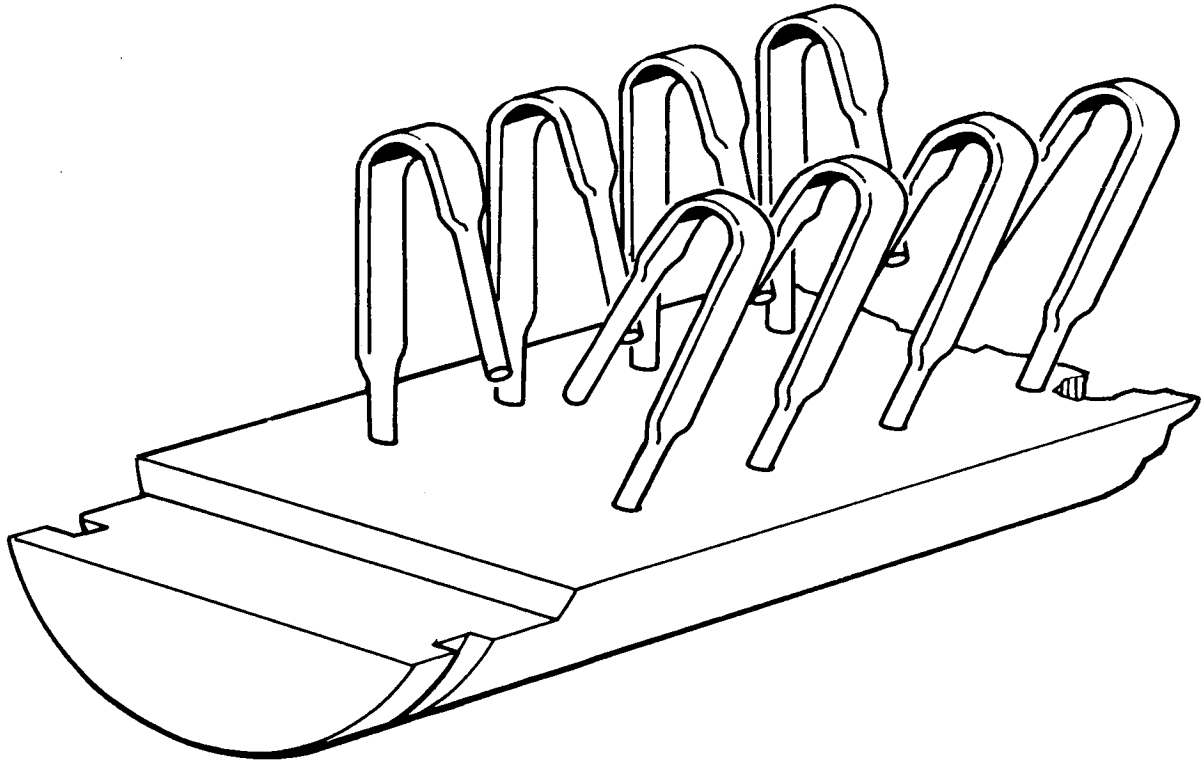


FIGURE 2.6-3. SLIP RING MOLDED BRUSH BLOCK

2.6.5. -1 Centaur Slip-Ring Experience. - The slip rings used in the -1 Centaur platform was a 32 ring assembly. The major problem encountered with this slip ring was contamination. It was found that in the platform, certain materials used in the slip ring reacted with other materials leaving a residue within the slip ring capsule. These materials include:

1. Polyester tape
2. Fungicidal varnish
3. Rubber adhesive
4. Polyurethane potting compound
5. DC-4 grease.

The action taken to eliminate this problem was to replace contaminating materials or change processes that utilized contaminating materials.

The -1 slip ring, containing only 32 rings, left no spares with which to parallel critical circuits for redundancy and improved reliability. With knowledge that the -3 Centaur system was in the offing, no attempt was made to redesign the -1 slip ring to incorporate more circuits.

2.6.6. -3 Centaur Slip-Ring Evolution. - With the advent of the -3 systems, Honeywell attempted to eliminate the problem areas encountered with the -1 slip rings. Changes made were:

1. New specifications that detailed materials, processes, workmanship standards, and test procedures.
2. A 38 ring assembly that allowed paralleling of critical circuits.
3. Qualification of more than one vendor.

There were a total of four vendors used during the -3 Centaur IGS development. They are enumerated Vendors A, B, C, and D. Vendor A was the slip-ring supplier during the -1 program. Each vendor had trouble meeting the -3 slip-ring specification at one time or another. By 1966, all vendors, except Vendor A, were disqualified as slip-ring suppliers because of high failure rates during use of their assemblies. Vendor A, by far, had the lowest slip-ring failure rate and today is the single-source supplier of Centaur slip rings. The problem areas encountered, and the corrective action taken are listed in the following paragraphs.

Noise. - In 1962, all Centaur slip-ring vendors encountered problems meeting the Honeywell imposed noise requirements. It was determined that all four vendors were not testing the slip rings per Honeywell specification requirements. The corrective action items used were:

1. Change the method for mounting the brush blocks.
2. Study the effects of increased temperature to determine if the brushes exhibit a "memory".
3. Reject all units which fail to pass the correct noise requirements.
4. Improve tooling and reduce handling and adjustment techniques.
5. Improve the alignment of the brushes in the groove and maintain the proper brush pressure.
6. Select the best vendor and eliminate the other suppliers.

Contamination. - The contamination problem associated with slip rings was a continuing problem. There were contamination problems from the beginning of the -3 program through 1965. An investigative program, lasting for almost two years, yielded the following results. The initial part of the investigation dealt with determining the cause of increasing resistance of rings in the Platform. Failed rings were disassembled and examined. Contamination was observed and an analysis was attempted unsuccessfully. It was later determined through testing that friction polymer was the most probable culprit. This problem became very acute at Honeywell, with all vendor's rings, and affected other Honeywell projects. This problem was later corrected by:

1. Re-designing lead entry and exit on the brush block assembly to reduce flaking from the lead wire insulation.
2. Additional testing at both unit and Platform levels.
3. Elimination of vendors B, C, and D after allowing them the opportunity to redesign their slip rings; the redesigns were unsuccessful.
4. Concentrating on developing the most promising vendor, including recommendations for process improvements.

In addition, a "Slip-Ring Continuity" test was initiated at the Platform level, in 1964 to:

1. Discover any intermittently open slip rings.
2. Discover any points requiring excessive torque motor breakaway voltage (an indication of possible slip-ring problems).

This test was performed after Platform vibration.

Other major changes to the slip-ring design and test philosophy were:

1. Redesign the slip-ring mounting shims to provide more consistent wiper arm tension on the brushes.
2. Require the vendor to subject all slip-ring capsules to a low level vibration (for one hour), followed by ultrasonic cleaning.
3. Rerouting of high and low numbered rings to allow paralleling of critical circuits.

Friction. - Again throughout the Centaur IGS development stages, high friction levels existed in slip rings. This problem was magnified by side-loading of the slip-ring assembly. Side-loading was corrected by replacing an "O" ring that held the barrel part of the slip ring with a rubber bumper. The rubber bumper allowed the ring to run in its natural path and greatly reduce the side-loading effects. This fix also eliminated any discrete resonant frequencies.

2.6.7. Alternate Slip-Ring Considerations. - In 1965, Honeywell investigated the possible use of the NASA-Gemini "advanced design" slip-ring assembly in Centaur Platforms. This action was initiated because of the higher-than-normal-failure rate experienced with the higher-numbered rings (31-38) of the existing assembly. The NASA slip-ring assembly was reported to have the following advantages over the Centaur slip ring. The advanced ring used a straight cantilevered brush, which is not flattened at any point (see Figure 2.6-4). This gave more consistent brush pressure. The brush block stiffener and end bushings were machined from the same piece of metal, and the stiffener was much heavier than the present one. This resulted in better maintenance of alignment between the brushes and rings. The most significant difference was the process by which the brushes and rings were mated. In the rings, used at this time, the brushes were all

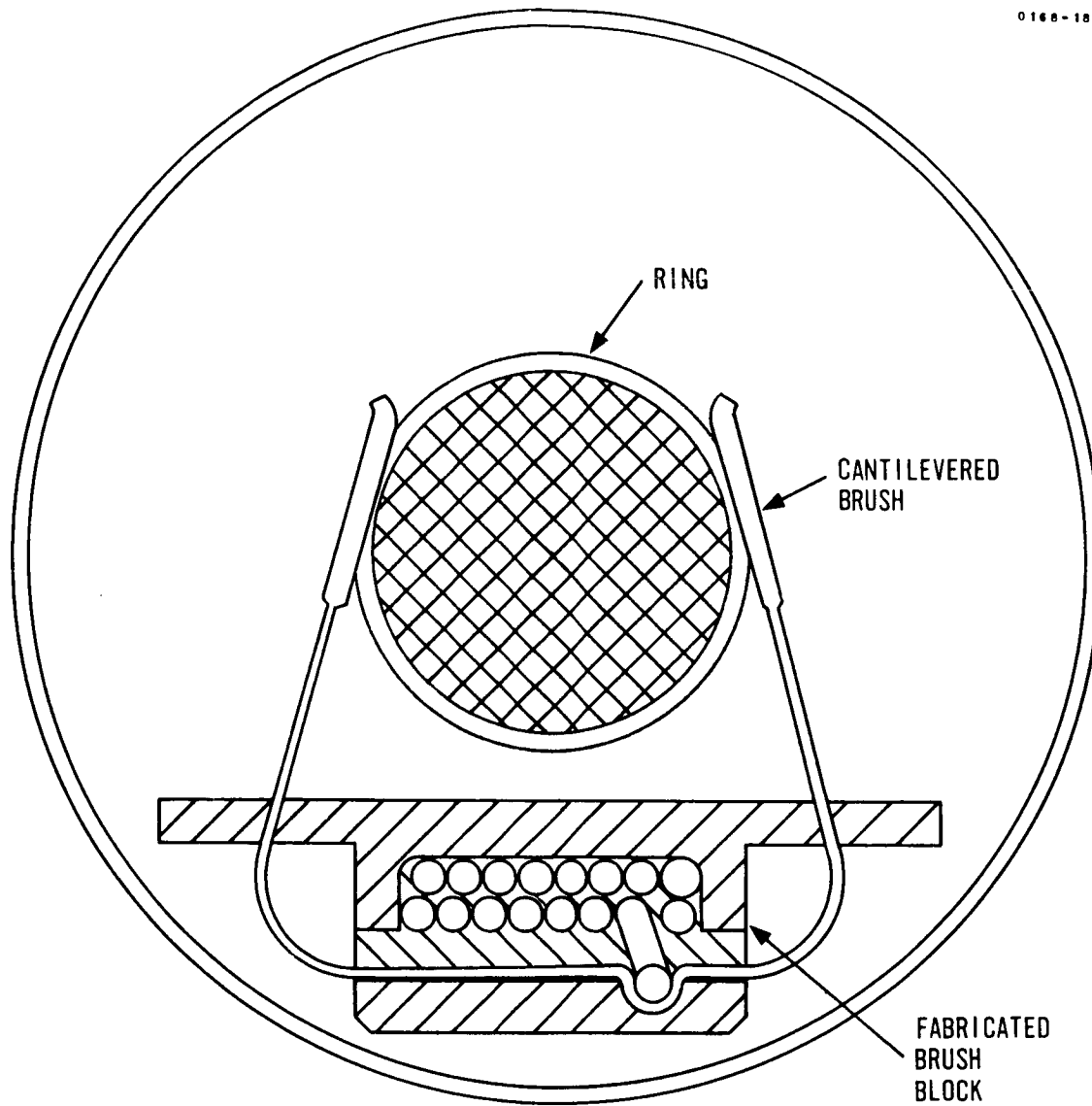


FIGURE 2. 6-4. CROSS SECTION THROUGH RINGS AND BRUSHES
OF GEMINI SLIP RING

mounted into the block and the rings assembled together independently; then, the entire brush assembly was mated to the rings. In the new design, the ring and rotor assembly was mated with the stator assembly before the brushes were assembled to the block. After all brushes were mated in this manner, the block was potted. This technique prevented any side loading on the brushes due to relative misalignments between the brush and ring assemblies.

After extensive investigation by the Centaur platform designers, it was determined that the Centaur slip ring was superior to the NASA-Gemini slip ring for the following reasons:

1. The failure rate of the Centaur slip ring was lower, by a factor of three, than that of the NASA ring used in the Gemini platform.
2. The NASA slip ring experienced difficulties with
 - a. Galling between rings and brushes.
 - b. Intermittent electrical noise between rings and brushes.

Aside from the technical factors, the NASA ring was three times more expensive than the Centaur ring.

2.6.8. IMG Slip-Ring Development. - The -3 Centaur slip-ring assembly failure rate has improved sufficiently to permit the IMG to use the present slip ring without any modifications.

2.6.9. Conclusions. - Throughout the development phases of the Centaur Program, there have been many troublesome problems associated with the slip-ring assembly. The major problem areas were:

1. Noise
2. Contamination
3. Friction
4. Qualification of vendors.

The problems once associated with the -3 Centaur slip-ring assembly have been corrected by the following techniques:

1. A final ultrasonic cleaning
2. A brush block redesign
3. The replacement of the "O" ring with rubber bumper
4. The installation of an improved slip-ring mounting shims
5. The rerouting of approximately 70 percent of the higher and lower numbered slip rings for redundant usage.

6. Improved specifications
7. Vendor careful selection and control
8. Elimination of polymer forming materials from the platform.

Through the analysis, design, and tests performed on slip-ring assemblies, Honeywell has learned the need for:

1. Special attention to specifications, test procedures, vendor processes, and vendor facilities.
2. Active participation in the vendor's design process through design concept, progress and final reviews, plus close periodic and thorough technical coordination.

Topic 2.7

Platform Gyro and Accelerometer Preamplifiers

2.7.1. Summary. - The gyro and accelerometer preamplifiers used in the Centaur platform have exhibited good performance and reliability throughout the IGS development. There have been relatively few problem areas. Areas where problems did occur were primarily concerned with cross-coupled noise, which was solved simply by additional shielding of wires and wire re-routing external to the preamplifier assembly. There were also several output coupling capacitor failures on -1 and early -3 Preamps.

2.7.2. Introduction. - The gyro and accelerometer preamplifier assembly used in the Centaur platform is similar to circuits previously designed for use in platforms built by Honeywell for Fairchild Aircraft and Republic Aviation surveillance drone programs for the Army Signal Corps. The original basic design is still in use in the Centaur platform.

A miniature, transistorized preamplifier is provided for each gyro and accelerometer. The three gyro and three accelerometer preamps are packaged together in one assembly. The triple gyro and accelerometer preamplifier assembly is mounted on the platform first gimbal. The primary purpose of the inertial component preamplifiers is to gain a favorable signal-to-noise ratio of the component 7.2 kHz and 14.4 kHz output signals prior to transmission through the platform slip rings, external connectors and cabling.

2.7.3. Description of Accelerometer Preamplifier. - Each accelerometer preamplifier is a two-stage, transistorized voltage amplifier. The primary supply voltage generated for the preamplifier assembly is +35 volts dc, obtained from the +35 volts dc supply in the coupler. The schematic for the preamplifier assembly is shown in Figure 2.7-1. The 14.4 kHz input to each accelerometer preamplifier is from the accelerometer signal generator secondary. The output of each accelerometer preamplifier feeds into a bandpass amplifier in the coupler. The voltage gain of the circuit is adjusted to 100 volts per volt, ± 5 percent, prior to installation into the platform. The variable resistor R5, which is a part of the negative feedback control circuit, is adjusted so as to provide 3.6 volts/mr, ± 5 percent, loop gain as required for each accelerometer.

0765-317A

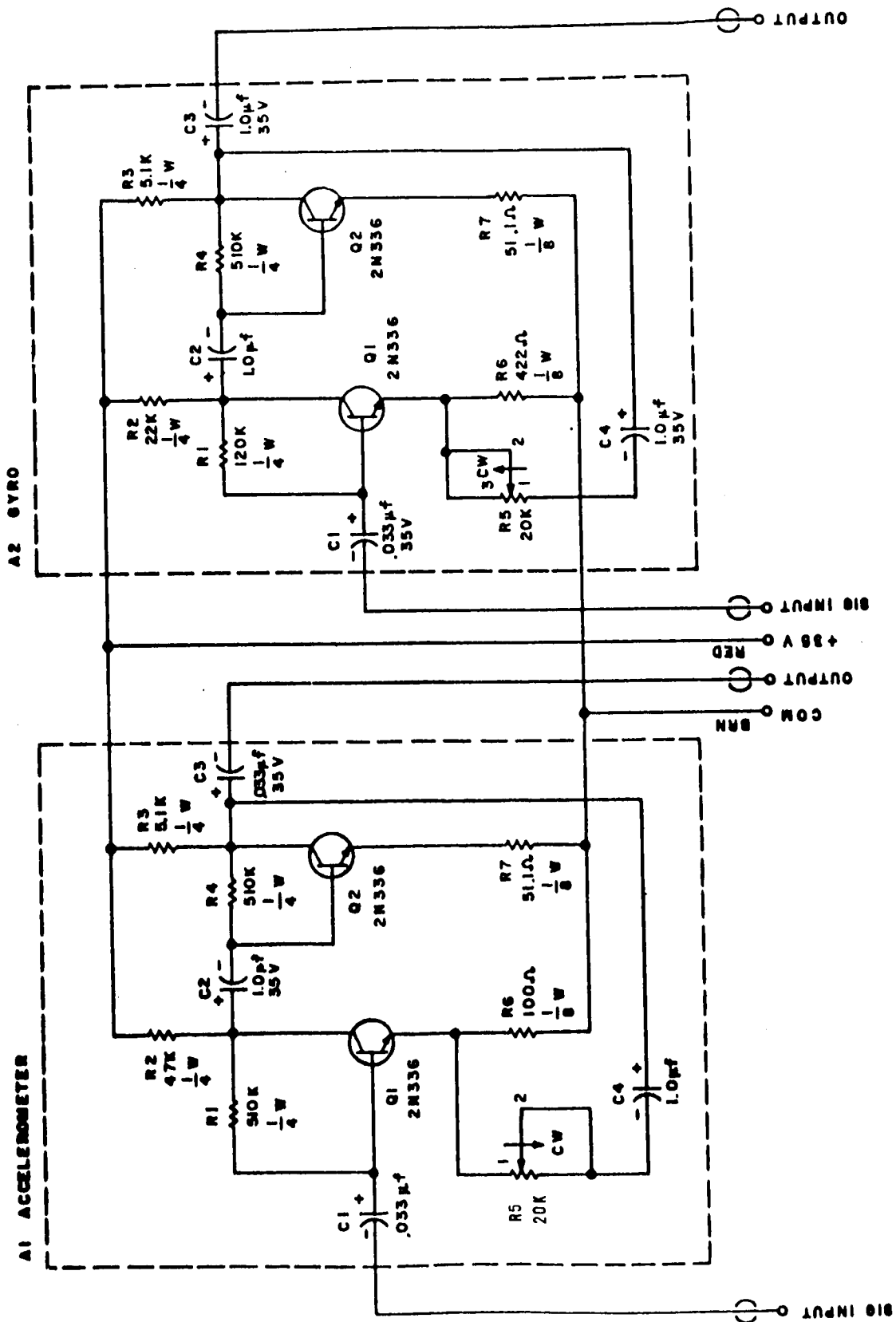


FIGURE 2.7-1. ACCELEROMETER AND GYRO PREAMPLIFIER

2.7.4. Description of Gyro Preamplifier. - Each gyro preamplifier is also a two-stage transistorized voltage amplifier energized by the same +35V Supply. The 7.2 kHz input to each preamp is derived directly from the gyro signal generator secondary. The voltage gain of the preamplifier circuit is adjusted to 30 volts per volt, ± 5 percent, prior to installation in the platform. After installation in the platform, the gain of each gyro preamplifier is readjusted to compensate for gyro transfer function variations. The preamplifier outputs are checked to insure proper torquer/signal generator/preamp phasing. The signal generator secondary of each gyro is wired directly to the gyro preamplifier input. The outputs from two of the preamplifiers, the U and V preamplifiers, feed into the rotor windings of the azimuth or first gimbal resolver. The outputs of the azimuth resolver, the resolver which interchanges the pitch and roll functions, become the V stabilization and U stabilization signals which feed the No. 2 and No. 3 gimbal control amplifiers in the Platform Electronics Unit. The output of the third or W preamplifier feeds directly into the azimuth or gimbal 1 control amplifier in the PE unit. The gain from gyro input to preamplifier output is nominally 4.5 volts per milliradian of gyro gimbal motion. The U and V resolver transformation ratio is 0.35 V/V.

2.7.5. Preamplifier Assembly Problem Areas. - As stated earlier, there have been relatively few problems with the inertial component preamplifiers during the course of the Centaur program. Those areas where problems did occur are discussed in the paragraphs which follow.

Cross Coupling/Noise. - In the early days of the Centaur program (1960-61) problems arose in the preamplifier assembly with noise and cross coupling ("cross talk") with other platform circuits. It was found through test and analysis that the noise and coupling problems could be reduced to an acceptable level by additional shielding and re-routing of wiring. This was done in the early platforms, eliminating the problem.

Output Capacitor Failures. - During the -1 and early -3 Centaur program there were several output capacitor (tantalum) failures. These failures were observed especially in the second and third gimbal stabilization signals. These signals are resolved in the platform. When the capacitors started to leak, the DC voltage would upset the B-H curve of the resolver, and the overall loop gain was affected. To eliminate this problem these capacitors were purchased from a different vendor. The capacitor type was satisfactory for the application, but its use required special attention to good quality control practices by the vendor.

Potentiometer Solder Joint Problem. - In 1964, the preamplifier assembly was modified to alleviate a problem encountered with cracked solder joints, resulting in intermittent operation of the adjusting potentiometer. The preamp adjusting potentiometer was of the type normally used for printed circuit applications; i. e., the leads protruded from the bottom of the potentiometer through to the opposite side of the circuit board where the solder joint was made. The number and arrangement of the board components and the space between boards, when installed, presented a crowded situation such that space was not available for clinching the potentiometer lead wires, prior to soldering. Vibration due to handling and testing caused the joint to crack. The cracked solder joint problem was corrected by replacement of the printed circuit type potentiometer with a potentiometer using flex leads and associated terminals, thereby eliminating the soldering space problem exhibited by the feedthrough leads.

Gimbal Saturation Recovery Time Problem. - In 1965, during unit level test, several platforms containing D20 gyros exceeded the 750 milliseconds, maximum allowable time for the gimbals to recover when switching from "Coarse Align" (open gyro loops) to "Fine Align" (closed loop, gyro stabilized mode). Investigation of the excessive recovery time disclosed that during saturated operation of the gyro preamplifier, coupling capacitor C2 (Figure 2.7-1) retained a negative charge. This negative charge caused an overstressed condition on the base-to-emitter junction of transistor Q2 and resulted in non-linear preamp operation during gimbal recovery, thus increasing settling time. Measurement made during testing showed -6 volt peak values of reverse bias on the base of Q2.

The saturation recovery test is performed by positioning the platform gimbals, such that the gyro gimbals are rotated against their stops, just prior to switching to the Fine Align mode. Maximum output (equivalent to ± 1 degree through ± 4 degrees of D20 gyro gimbal angle) is thus obtained from the gyro signal generator to insure worst case recovery conditions. Switching from Coarse to Fine Align cause the platform gimbals to rotate until the gyro error signal is nulled. During recovery, the gimbals pass through null at a faster rate than the discharge time of C2. When the gyro error signal amplitude is less than the negative charge on C2, Q2 remained cut off, passing no error information. Loss of the gyro error signal near null gave the rate network false information, resulting in intermittent loss of correct torque motor commands. In linear loop operation, the rate network reversed motor torque before the gimbal passed through null, putting a brake on the gimbal before it reached the desired position. This reduced the amount of overshoot. However, the

erroneous torque motor signal, resulting from saturated conditions, reduced the desired braking action, allowing greater overshoot, and hence increased recovery time.

A proposed solution to the problem was to insert a diode from the base of Q2 to ground to provide a low resistive path to discharge C2, correcting the non-linearity and eliminating the overstress condition on the Q2 base to emitter junction. However, with the advent of the D26 gyros having small stop angles (± 0.3 degree to ± 0.9 degree), the probability of hard saturation of the preamps was reduced to a minimum and a hardware modification was not required. Hard saturation requires gyro excursions of 0.8 degree or more, and a study of fourteen D26 gyros showed the greatest stop angle of the group to be 0.7 degree. Of the fourteen gyros examined, the mean stop angle was found to be +0.52 degree, -0.58 degree (for positive and negative gyro gimbal angles, respectively).

In addition to the above described effect, another contributor to long recovery time was found to be unrealistic cable capacitance and recorder loading in the test set. Unlike the short cables of the flight hardware, the test equipment loads were found to change the loop gains and phase lags, which increased loop recovery times. The test sets and recording methods were modified to eliminate the undesirable loading effects.

2.7.6. The Improved Centaur Preamplifier Design (1967). - The inertial sensor preamplifiers for the Improved Centaur MGS (IMG) will contain both discrete and integrated circuit components and will be packaged into potted modules. A preamplifier design using only discrete components was considered but the integrated circuit design was chosen as the best alternative, primarily due to the smaller physical size, higher reliability, and lower cost factors.

Capacitive decoupling will be provided within each module (reference Figures 2.7-2 and 2.7-3) to reduce sensitivity to injected power line noise. Further, the use of integrated circuit components will provide for good common mode noise rejection. Amplifier gain will be set by a selected, fixed resistor within a feedback loop. This will preclude the use of potentiometers, thereby avoiding potential potentiometer problems such as those encountered with the Temperature Control Amplifiers during the Centaur IGS development (reference Topic 2.8).

Worst-case circuit analyses and parts stressing techniques are being applied to the IMG preamplifier design to insure that all parameter values are properly design-centered and operating conditions are derated. The

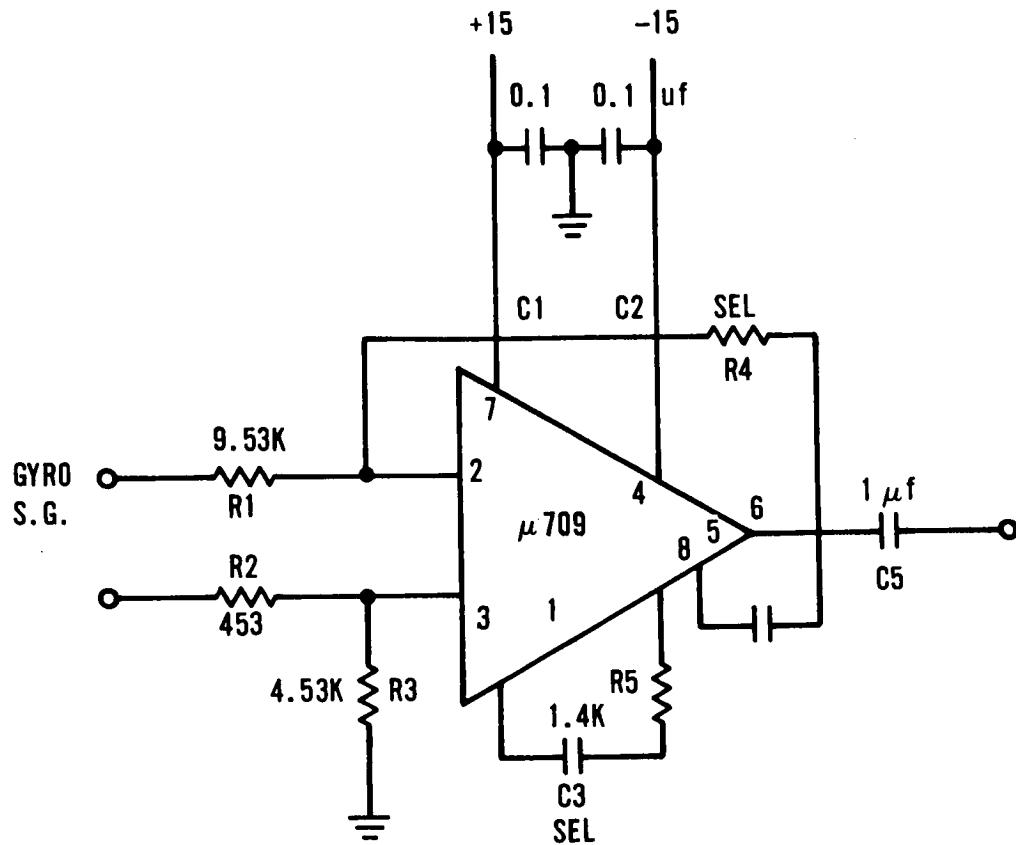


FIGURE 2.7-2. GYRO PREAMPLIFIER (IMG)

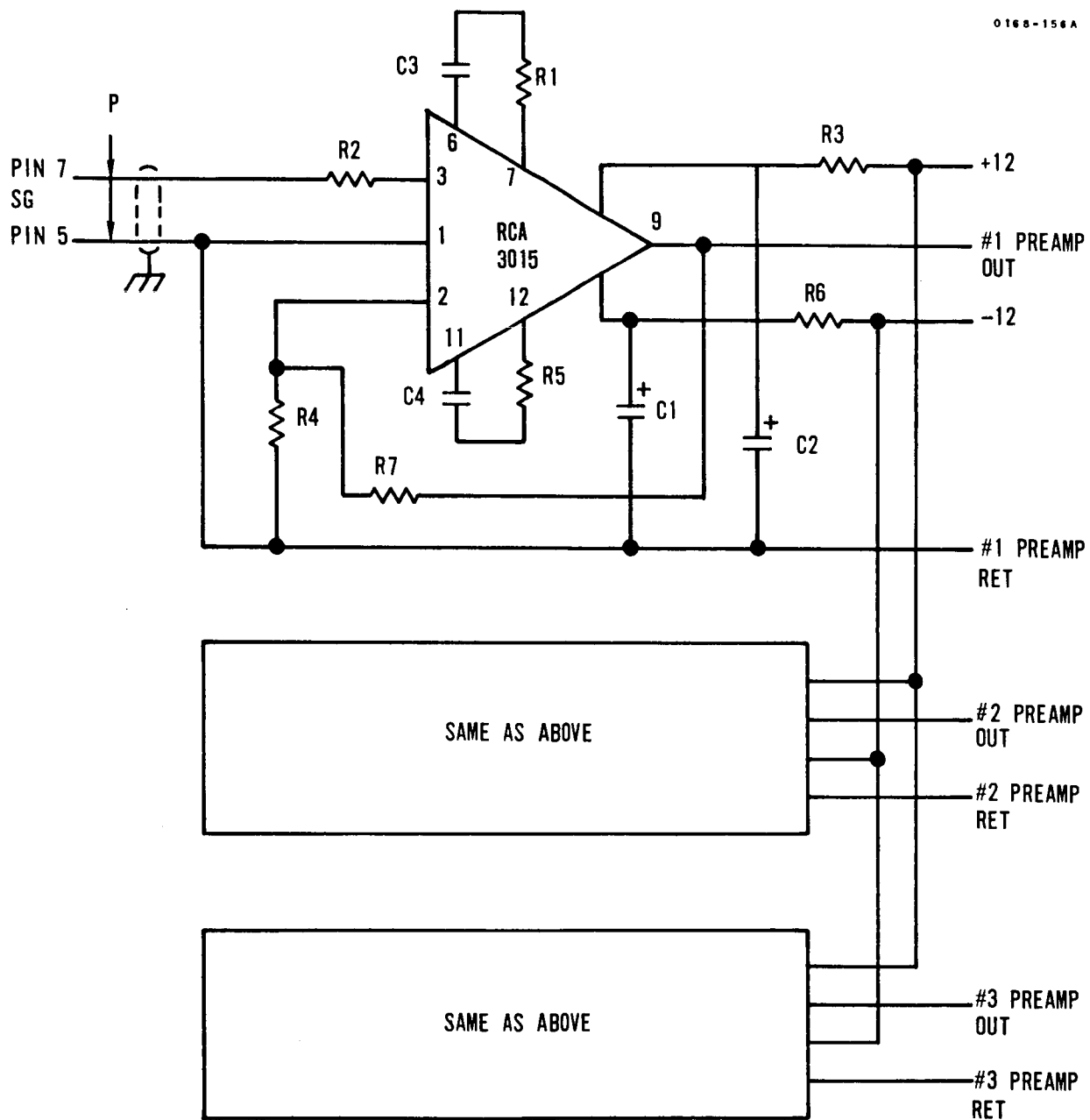


FIGURE 2.7-3. ACCELEROMETER PREAMPLIFIER (IMG-PRE)
(FIRST STAGE ON INERTIAL BLOCK)

preamplifier will also be subjected to design evaluation tests required to further prove design integrity.

2.7.7. Conclusions. - The discrete component gyro and accelerometer preamplifiers used in the Centaur platform since the start of the program, have exhibited good reliability and relatively few problems have been encountered with this design even though they did not undergo a rigorous worst-case circuit analysis. However, for future designs, worst-case analysis is recommended. In addition, care should be exercised in the areas of wire routing and shielding to avoid noise coupling from other circuits.

Topic 2.8

Platform Temperature Control Amplifiers

2.8.1. Summary. - The material herein is covered in the chronological sequence of hardware development since 1959. Emphasis is placed on the problems encountered and the lessons learned. During the development of the Platform temperature control amplifiers (TCA's) problems were encountered with:

1. All attitude temperature control of the inertial components in the early Centaur platforms.
2. Block heater control relay cycling.
3. TCA output transistor location.
4. Potential transistor overstress problems.
5. Circuit instability problems.
6. High frequency oscillations in the TCA output circuit.
7. Low frequency oscillations in the TCA output circuit.
8. Potentiometer reliability problems.

These problems could be avoided in future TCA designs by:

1. Generation of a mathematical model of platform thermal characteristics.
2. Thermal mapping tests of the platform on early prototypes.
3. Elimination of relay control circuits associated with the TCA loop.
4. Implementation of worst-case circuit analysis and parts stressing techniques.
5. Thorough and early analysis of TCA interfaces with other IGS circuits and test equipment.
6. Careful selection of passive and active electronic parts (e. g., use of fixed resistors instead of potentiometers).

The following paragraphs contain a discussion of these problems, alternative and chosen solutions, and the lessons learned during the Centaur platform TCA development. This discussion begins with a general description of the TCA and its functions, followed by a recap of the -1 and -3 program experience (1959-1967), and closes with the approach being used today in the TCA development for the next generation Centaur IGS.

2.8.2. General Description. - To achieve the desired guidance system accuracy and stability, it is necessary that the platform's gyros and accelerometers be maintained at specific temperatures, regardless of changing thermal environment outside the platform or inertial component during Centaur operations. (See Topic 6.10.) Each inertial component is maintained at the required temperature by a proportional type, Temperature Control Amplifier (TCA) which delivers power to the component as a function of the component's own sensor resistance value. Two triple TCA Assemblies are used in the Centaur Inertial Platform. One assembly contains TCA's for the accelerometers; the other has the gyro TCA's. The TCA assemblies are mounted in the Inertial Platform on the first gimbal assembly, except for the power output transistors, which are now mounted in the platform (case) end bells.

Each temperature control amplifier (TCA) circuit (ref. Figure 2.8-1) is a four-stage, transistorized amplifier, which receives its input signal from a bridge circuit, one leg of which is a Balco wire temperature sensor on the gyro or accelerometer case, adjacent to the component's control heater. The TCA output controls the dc current through the control heater winding at a level proportional to the bridge error signal to maintain the proper internal operation temperature for the gyro or accelerometer.

The gyro/accelerometer temperature sensor winding and the gyro/accelerometer control heater are on the component's case and enclosed within the dust cover. TCA adjustment potentiometers are mounted adjacent to the triple TCA assembly on the platform's first gimbal. The 26-volt rms, 400 Hz excitation transformer (T1) is also mounted on the first gimbal. The TCA's are adjusted in a completed platform so that the inertial component temperatures are maintained at $180^{\circ}\text{F} \pm 0.5^{\circ}\text{F}$ (as defined by the inertial component sensor resistance). This is accomplished by selecting resistor R8 and adjusting potentiometer R9 in each TCA to produce midrange output at the 180°F measured value of the sensor resistance of each inertial component.

The input signal for each TCA is obtained from an individual bridge circuit where two legs of the bridge are made up by the center-tapped secondary of T1. The bridge circuit is completed by the total resistance of R8 plus the TCA potentiometer acting as a third leg and the gyro/accelerometer temperature sensor winding acting as the variable fourth leg of the bridge. When the inertial component temperature drops, the resistance of the sensor winding decreases and 400 Hz signal information is coupled to the base of Q1, the input stage of the amplifier. The 400 Hz signal is amplified through stages Q1 and Q2 and is coupled through capacitor C3 to the 400 Hz demodulator, composed of CR1 and CR2. The

0463-01A

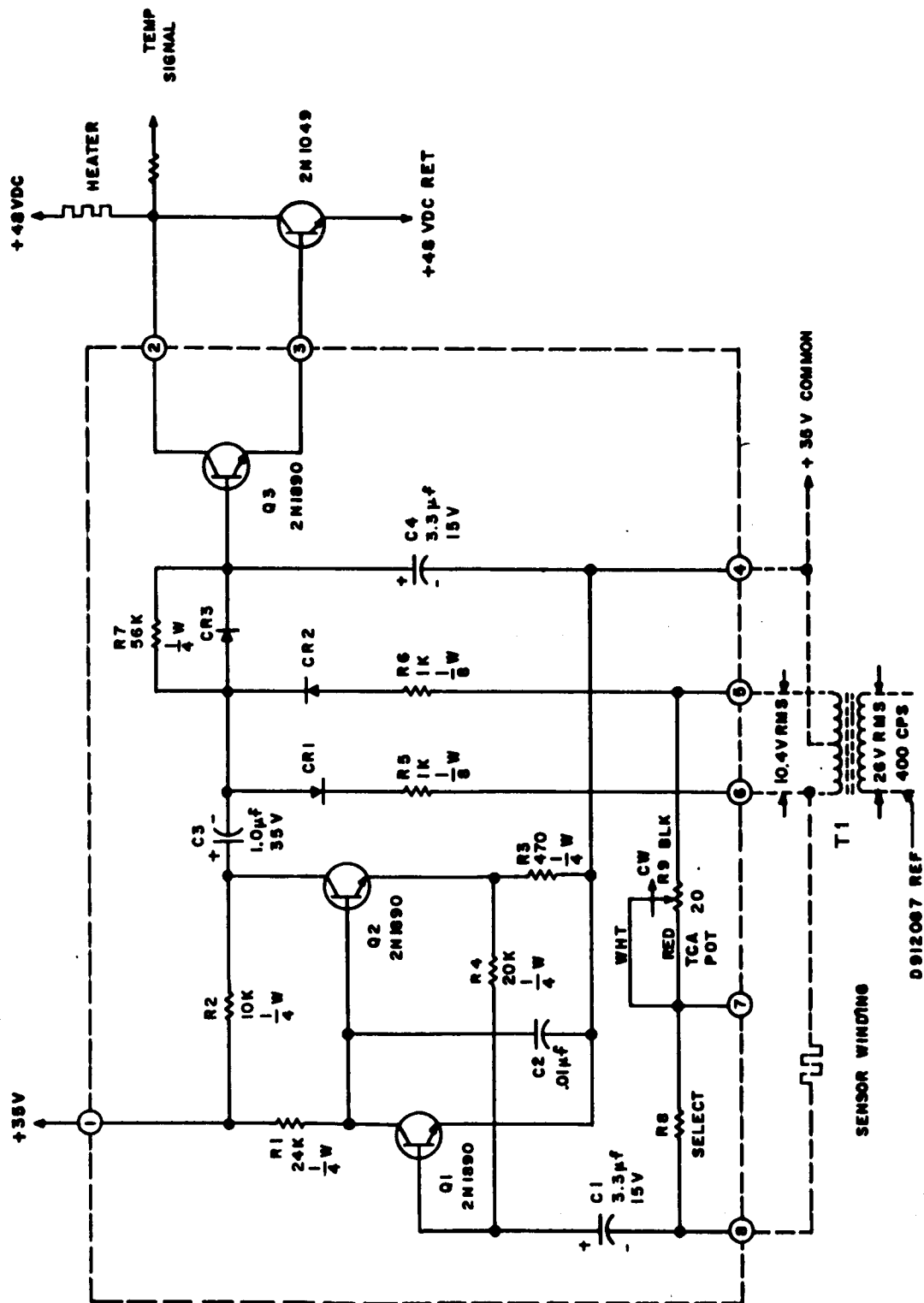


FIGURE 2.8-1. TEMPERATURE CONTROL AMPLIFIER SCHEMATIC

demodulator is driven or controlled by the 400 Hz signal derived from T1 and applied to terminals 5 and 6 of the TCA. When the inertial component is below operating temperature, the positive half-wave rectified voltage will result in C4 being charged to a positive potential -- positive from base of Q3 to the 35-volt return. When the inertial component is above the nominal operating temperature of 180°F, the voltage developed across C4 is negative -- negative from the base of Q4 to the 35-volt return.

When the base of transistor Q3 is positive, it is conducting, and the base of Q4, the power control transistor in the platform, is also positive and conducting. Transistors Q3 and Q4 operate as a Darlington pair. In this manner a change in sensor resistance, due to a variance in inertial component temperature, controls the current through the heaters on a proportional basis. The maximum output across each heater can be 43 volts dc. Each TCA is capable of controlling the temperature of its respective inertial component to within $\pm 0.5^\circ \text{F}$.

2.8.3. Centaur -1 System Temperature Control (1959-1962 Period). -

The original AC proportional control/dc output TCA circuit used in the Centaur platform was similar to circuits previously designed for use in platforms built by Honeywell for Fairchild Aircraft and Republic Aviation surveillance drone programs for the Army Signal Corps. These were the first transistorized TCA circuits for individual inertial components used by Aero-Florida. The capabilities of the original design were limited due to limitations in available space in the platform, circuit assembly techniques, and the state of the art of transistor technology in 1959. The basic design (see Figure 2.8-1) is still used in the IGS today, but significant design improvements have been developed and implemented.

Tests on the early -1 Centaur system showed that all attitude temperature control could not be maintained with the 28 volt TCA's without supplementary block heaters being installed in the Platform. Block heaters were required because the maximum heater power available from the TCA's was not sufficient to maintain the inertial components at proper operating temperature over the low range of specified operating environment ($+30^\circ \text{F}$ platform skin temperature). The block heaters were relay-controlled and their cycling caused the following problems:

1. Caused noise transients in other circuits when the relay circuits opened and closed.
2. Caused short term variations in inertial component performance with block temperature and position variations, which caused and altered thermal gradients across the flanges of the inertial components.

3. The V accelerometer TCA was used to control the block heater relay. The other inertial component temperatures were controlled by TCA's with their limited power output capability. As a result, individual component temperatures were at times forced out of their desired control region due to (a) the V accelerometer heater power requirement being high enough to hold the block heaters on so long as to cause other components to overheat slightly during the cycle period, or (b) the V accelerometer heater power requirement being low enough to keep the block heaters off while other components required heater power in excess of their TCA capability to maintain correct operating temperatures. In other words, some gyros or accelerometers could underheat or overheat because of the block heaters.

The above problems were complicated by variations in ambient temperature and positions in which the platform was required to operate and variations in thermal characteristics of the individual inertial components (different optimum operating temperatures and thermal sensitivity coefficients). Further, the TCA output transistors dissipating heat to the azimuth block constituted point heat sources on the azimuth block which contributed to thermal gradient changes.

During the -1 system design, the TCA output transistor was changed from a 2N549 to a 2N1049 to obtain improved power dissipation capability and improved reliability. The output transistors were moved from the azimuth block to the second gimbal to obtain a better heat sink and to reduce operating temperature control and thermal gradient problems due to TCA circuit power dissipation to the azimuth block. These changes were incorporated in all -1 platforms. They helped, but did not cure, the overall thermal control problems.

A basic limitation during this period was the lack of a good analytical platform thermal model. Empirical models were developed, but accuracy of the parameters (gradients, specific temperatures, etc.) was such that only limited improvements, such as those discussed in the following paragraphs, could be defined. (Reference Topic 2.10.)

2.8.4. Centaur -3 System Temperature Control (1961-present IGS). - In 1961-62, the Platform TCA's were modified for the -3 guidance system to solve problems from the -1 program and improve TCA performance and reliability. An alternative to upgrading the existing -1 TCA considered at that time was the use of an SCR controlled "bang-bang" (on-off control) type TCA. However, due to the possibility of feedthrough into the signal output pickoff within the inertial components, this design was not considered suited for Centaur.

For -3, the supply voltage used for control heater power was increased from +28 volts to +40 volts. This, combined with component heater winding changes, resulted in increased heater power available and eliminated the requirement for supplementary heater power from the block heaters which in turn eliminated the relay noise problem.

Even after they were relocated to the No. 2 gimbal, the TCA output transistors in the -1 Centaur system were too close to the stable element (azimuth block). This still caused problems with (1) TCA control at high case temperatures, and (2) gradient changes across the azimuth block. To relieve the problem, the output transistors were moved to the end bells (case) of the Platform. (This was made possible by a new slipring design, increasing the number of available slipring circuits.) The end bell location not only alleviated the high temperature control problem, but also provided a better heat sink for the transistors. In conjunction with this modification, the temperature readout was changed to monitor the TCA output transistor collector voltage directly. This allowed circuit simplification by deleting the temperature readout circuit board on the azimuth block.

The -3 TCA design eliminated a former reliability problem encountered with the -1 TCA input circuit. The emitter to base breakdown voltage rating of the 2N336 input transistor used in the -1 circuit was 0.5V. A high or low resistance (approaching an open or short) in the sensor bridge circuit would cause the negative swing of the input signal to the TCA to exceed the emitter to base breakdown voltage of the 2N336. This would overstress the transistor and could result in immediate or ultimate catastrophic failure of the transistor. Improvements in transistor technology allowed a change to another transistor (2N1890) with an emitter to base breakdown voltage rating of 7.5 volts for the -3 circuit. However, use of present-day worst-case circuit analysis and parts stressing techniques during the design cycle could have reduced the original -1 transistor problem in the first place.

2.8.5. Initial -3 TCA Instability and Power Problems. - In 1962, during the -3 TCA development, a resistor (R7) was added to the base circuit of the output transistor (Q3) to properly bias Q3 and prevent instability of the TCA output stage voltage encountered in some TCA's. Further in late 1963, it was found that an increase in heater power was required to provide proper TCA control margin when the platform skin temperature was held at the lower spec limit. To solve this problem, the output supply voltage was increased from +40 volts to +48 volts. Other alternatives, such as changing gyro/accelerometer control heater impedances, were considered. However, because of the long lead times in inertial component

delivery schedules, and the current status of the -3 Coupler design (which supplied the +40 or +48 volts), the output supply voltage was chosen as the best overall alternative. Again, a computerized thermal math model of the Centaur platform could have been used to good advantage in analyzing this problem and evaluating the alternate design changes prior to implementation into the hardware.

2.8.6. High Frequency TCA Oscillations. - During the latter part of 1963, several platforms exhibited TCA oscillations when operated with the subsystem and platform test equipment. These oscillations were evidenced by a continual variation of the TCA monitor voltage. The TCA monitor voltage would vary within the range of ± 1 or 2 volts, with some values reading in excess of ± 5 volts. During investigation of the problem, it was found that the impedance of the lines between the GSE +48 volt dc power supply and the platform caused the effective power supply source impedance at the TCA to be relatively high. A low source impedance is needed for proper TCA operation.

The high frequency oscillation problem was solved by decoupling the output of the GSE +48 volt dc power supply with a 2 microfarad capacitor, effectively lowering the power supply source impedance to the TCA's. The capacitor was installed in the GSE cable at the platform connector. Other alternatives considered were (1) installing a decoupling capacitor within the Platform closer to the TCA's or (2) installing individual decoupling capacitors on each TCA board. Both alternatives presented mechanical (space) problems and would have required extensive rework resulting in increased implementation cost.

2.8.7. Low Frequency TCA Oscillations. - In early 1964, low frequency oscillations were observed on the TCA readouts of several platforms. This was the first time these oscillations had been observed. The readouts showed the TCA's to oscillate from full off to full on at approximately 1.2 Hz. These oscillations were intermittent and random, sometimes not appearing for hours.

All previous platform changes pertaining to the TCA loop were investigated. The only significant change to the TCA loop was a TCA power transistor change. The power transistor, used in a Darlington configuration, was changed from a 2N1049 to a 2N1049A. The original reason for the change was to obtain solderable transistor leads not specified in the transistor spec, MIL-S-19500/176. The 2N1049 transistor vendor, Texas Instruments (TI), at that time did not manufacture this transistor with the required lead solderability, and hence an "equivalent" part (2N1049A) was purchased from Silicon Transistor Corp (STC).

Investigations proved that the TI transistor, 2N1049, was a double diffused type whereas the STC transistor, 2N1049A, was a mesa type. The transistor parameter, h_{ib} , was not specified by either vendor, but it was a major factor in the Darlington gain equation. The h_{ib} of the STC transistor was much lower than that of the TI transistor, and consequently resulted in a higher TCA gain, as there were no provisions in the Darlington circuit for gain control. This higher gain (sensitivity) caused the TCA loop to break into oscillations.

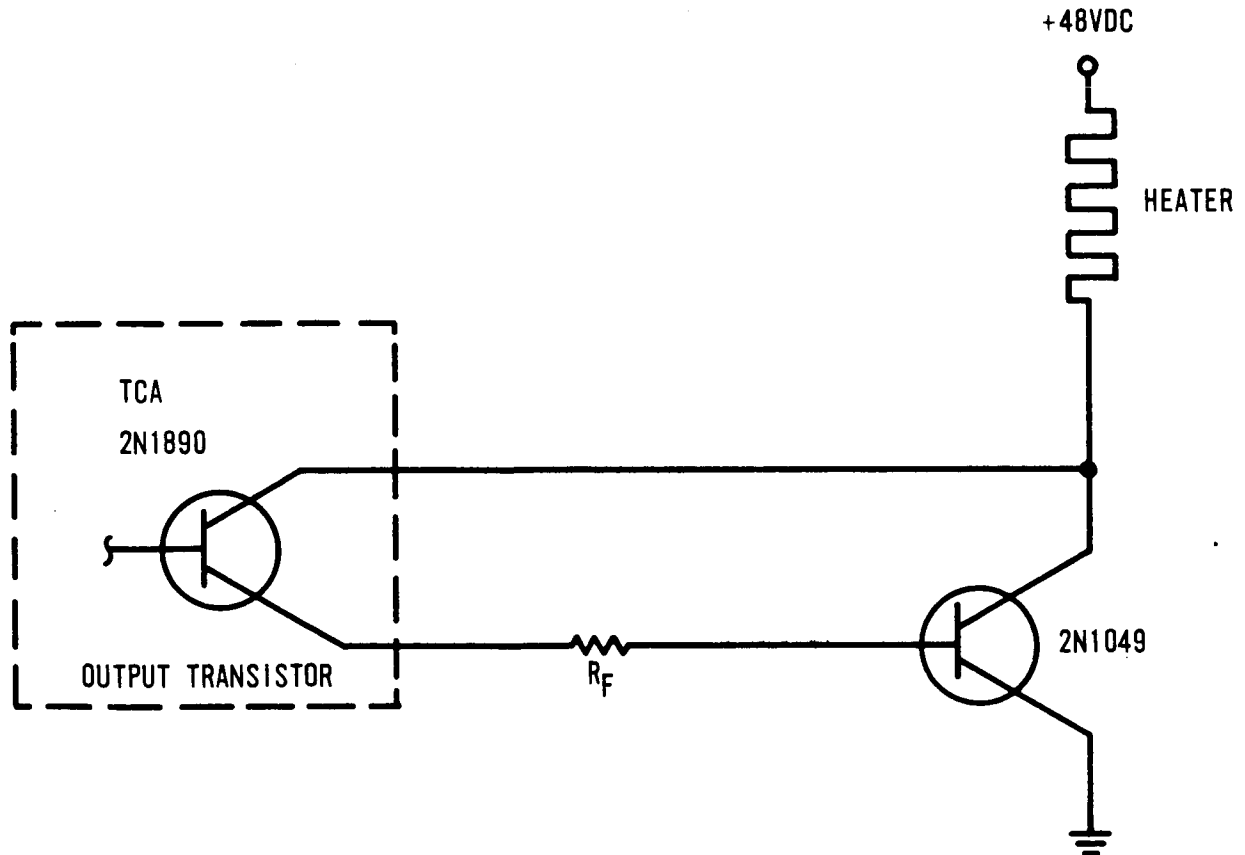
Correction of the TCA low frequency oscillation problem was accomplished by:

1. A selected resistor was added in the base of the TCA power transistor to control the gain of the Darlington stage (refer to Figure 2.8-2), and lower the overall TCA open loop gain. This change was added to three platforms and the TCA oscillations observed on all three stopped. At the time the change was incorporated, a very short investigation and computer analysis was performed to prove the fix valid. Subsequently, more data was obtained to prove the validity of the fix.
2. Because higher TCA gain (sensitivity) caused the TCA loop to oscillate, the TCA adjustment spec was changed from "1.2 ohms maximum change in sensor resistance to turn TCA from full on (43 volts across heater) to full off (5 volts across heater)", which controlled only minimum gain, to "from 0.8 to 1.2 ohms change in sensor---". This established a limit on maximum gain as well as minimum gain and could be controlled by selection of the added base resistor. All units adjusted to these limits were proven stable.

After analyzing the data obtained in lab verification tests and investigating the component temperature control requirements dictated by the system error analysis, the TCA sensitivity range was again changed to "from 1.0 to 1.4 ohms change in sensor---" to provide a greater stability margin.

Other alternatives considered as possible solutions to the low frequency oscillation problem were:

1. Addition of a resistor in the emitter of the 2N1049A power transistor. This would lower the gain and improve stability. However, the resistor would have to be of high wattage and large physical size and would cause a space problem and a mechanical redesign.

FIGURE 2.8-2. TCA MODIFICATION (ADDITION OF R_F)

2. TCA redesign to obtain maximum stability and minimize the effect of different power transistors.
3. Select power transistors for optimum parameters to obtain maximum stability, or revert back to using the 2N1049 TCA power transistor, which produced only marginal stability.

The resistor addition to the power transistor base circuit was implemented since extensive rework was not required, resulting in lower cost and elimination of potential mechanical problems.

2.8.8. Potentiometer Problems. - During 1966, erratic TCA operation was observed where the TCA control point shifted excessively and resetting was in some cases impossible. The problem was traced to the potentiometer (R9) in the TCA circuit. Testing of 30 potentiometers from stock showed that the resistance of the pot would change as a function of current passing through it. In addition, some mechanical discrepancies were noted upon disassembly, such as self lead failure, non-engagement of adjustment screw, and resistive element not secure.

This problem was solved through a redesign of the potentiometer by the vendor. The presently used Daystrom Pacific Co (P/N 313-60H-20) potentiometer has proven to be satisfactory. Other alternatives, such as replacement of the pot with a fixed resistor, were considered. However, the basic problem was a function of individual potentiometer quality, rather than a critical or marginal application. Also, to change the mechanization this late in the production program, would result in serious production and flight schedule impacts. Therefore, upgrading of the potentiometer was selected as the best overall solution. On a new design, the preferred approach would be to eliminate the use of potentiometers, use fixed resistors instead, and hence avoid reliability problems of this nature.

2.8.9. TCA Evaluation. - During one period of the -3 Centaur Program (1964-65) three basic developments took place to increase confidence and evaluate the design changes involving the Platform TCA's. These developments were:

1. Generation of a computerized thermal math model of the Centaur platform, using nodal analysis techniques. With this model, the quantity and distribution of heat flow throughout the entire platform could be determined, and potential design changes could be analyzed. This model included transient and steady-state conditions.

2. Complete internal thermal mapping of the Platform, which supported the development of and then confirmed the results of the math model.
3. Environmental testing of the platform and TCA performance under specified extremes of skin temperature, solar exposure, and various platform fill gases to insure that sufficient temperature control range and proper inertial component performance resulted.

2.8.10. "Doing It Over Today" - The Improved Centaur TCA Design (1967). - The TCA being used for the Improved Centaur MGS (also known as IMG*) is a DC proportional control/DC output type design. Other mechanizations considered were AC proportional control and "bang-bang" (on-off control) types. Some of the primary advantages of the DC proportional control TCA over the AC proportional configuration are (1) low power line noise injection and (2) the need for a coupling capacitor and an excitation transformer is eliminated. A disadvantage of the DC proportional TCA is its low power stage efficiency. The "bang-bang" design exhibits high power efficiency but power line noise injection and noise radiation is excessive. Particularly of concern was the possibility of feedthrough into the signal output pickoff within the inertial components with TCA's of this type.

The DC proportional TCA design was chosen as the best alternative primarily for compliance with the prevailing EMC specifications on power line noise injection and radiated noise, as well as utilization of the existing dc power source in the IMG. An ac proportional control device would have required the addition of an ac power source to the IMG. Mechanization of the TCA loop for the IMG is shown in Figure 2.8-3 and described in the following paragraphs. This design is proceeding with full use of the thermal math model described above in addition to full-scale implementation of worst-case circuit analysis and parts stressing techniques to insure that all parameter values are properly design-centered and operating conditions are derated. This TCA will also be subjected to the full range of design evaluation tests, as was done with IGS in the 1964-65 period.

Significant design considerations being employed in the development of the IMG TCA are:

1. The linear integrated circuit amplifier inherently has common mode noise rejection.

* IMG-Inertial Measurement Group

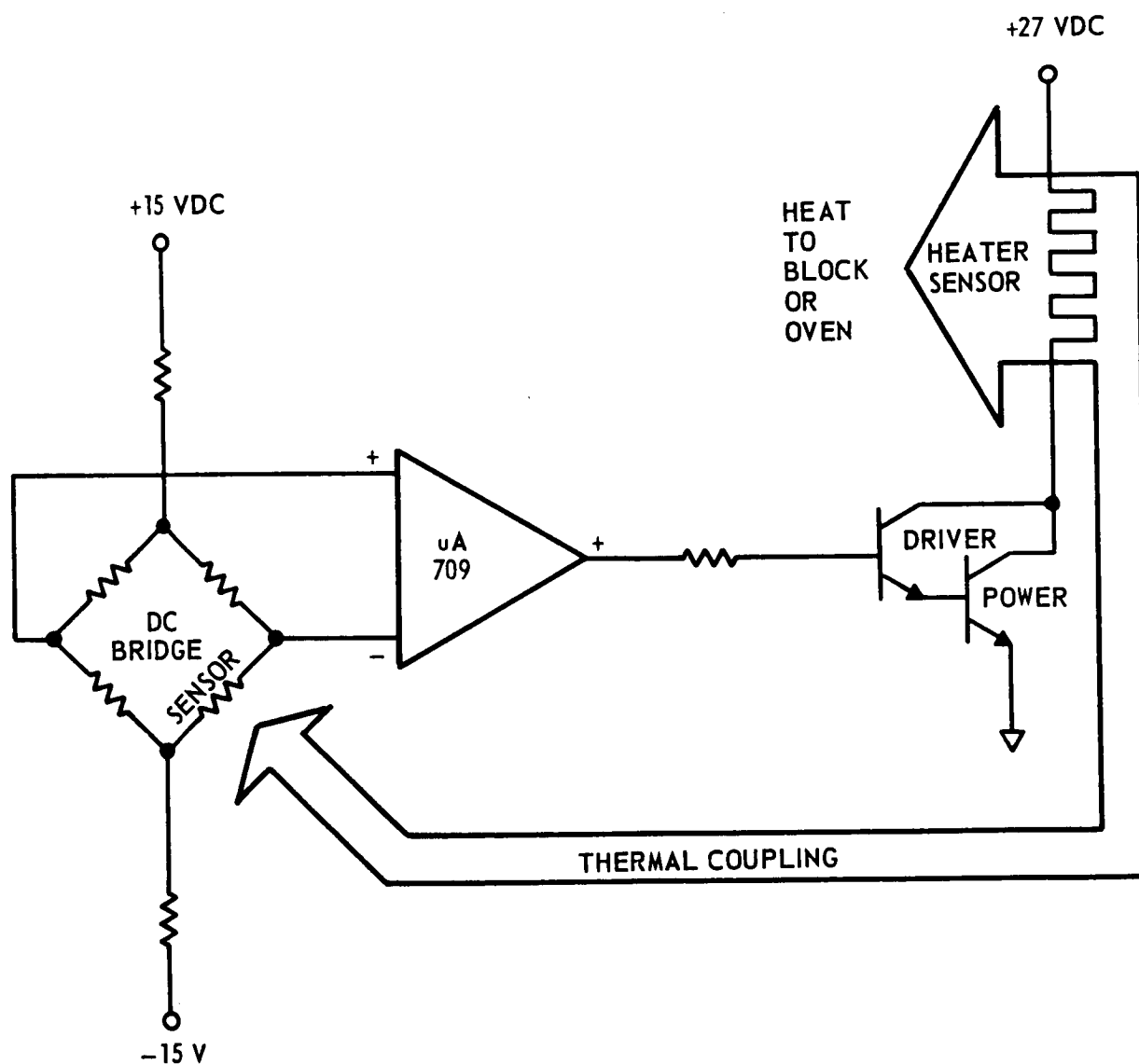


FIGURE 2.8-3. CENTAUR IMG TEMPERATURE CONTROL AMPLIFIER LOOP

2. The bridge and amplifier are individually decoupled from any power line noise (to reduce sensitivity to injected power line noise such as was encountered during the IGS development). The circuit is being designed to comply with a conservative noise budget.
3. The transfer characteristics of the sensor to heater combination were measured. Loop roll-off characteristics were set to optimize loop stability with minimum complication (to avoid control circuit instability such as encountered in the 1963-64 period).

2.8.11. Circuit Description. - An error signal is derived from the temperature sensor bridge whenever the gyro or accelerometer sensor moves away from its nominal value of 780 ohms. This dc error signal is fed to the integrated circuit preamp and in turn is amplified by a power output stage. The inertial component heaters are in the collector circuit of the power output transistors. The heaters then provide the thermal feedback loop to the sensors providing a rebalancing of each TCA loop to its normal null position. As a reliability design goal, if this circuit fails, it should do so in the "OFF" condition, thus degrading, rather than destroying the inertial component performance.

2.8.12. Conclusions from the TCA Development. - The requirements of the system in which the TCA will be used should be thoroughly studied so that the best TCA design for the application can be chosen; i. e., dc proportional control, ac proportional control, or "bang-bang" (on-off control) configurations. The "bang-bang" TCA is the most efficient design, but its high power line noise injection and radiated noise characteristics should be considered in light of EMC requirements for the particular system. The ac and dc proportional TCA's are less efficient (operations: approximately 50 percent) with the dc proportional being more advantageous from the standpoint of generated noise and elimination of components such as coupling capacitors and transformers which are needed for an ac proportional design.

During the development of the Centaur Platform TCA's, much has been learned with respect to the approach which should be taken in future TCA design and development. For future platform TCA designs, many problems resulting in rework, excess testing, and/or circuit redesign can be avoided through generation and proper application of design tools such as worst-case circuit analyses, parts stressing techniques, a mathematical model of platform thermal characteristics, and a platform thermal map. Further, noise problems could be reduced by avoiding

the use of relay control circuits associated with the TCA loop and the selection of active circuit components, possessing inherent common mode noise rejection, such as is evidenced in some types of integrated circuit amplifiers. Careful selection of passive circuit components is also important to preclude the use of reliability risk items such as potentiometers or non-hi-rel parts. In addition, early in the design phase, interface characteristics and requirements should be thoroughly examined with special emphasis on source/load impedance definition and electromagnetic compatibility considerations.

Topic 2.9

Platform Mechanical Design

2.9.1. Summary. - The discussion presented in this portion of the report will be directed toward the unique mechanical design considerations given to the platform. This topic is subdivided into three subjects-- the platform gimbal structures, rotary components, and gimbal housing (platform case). Operating environmental requirements imposed upon the platform, as well as other physical constraints, which influenced the design, will be covered. The discussion includes the problems and the redesign efforts to correct these problems. The development of a simplified computer simulation, based upon a nine degree-of-freedom vibration math model is discussed, and a comparison of computer simulation data to actual test data is made.

From the Centaur Program experience, the following lessons have been learned and have application to future designs:

1. Platform structural designs are primarily dictated by environmental and physical (sizing) design restraints, but too much emphasis on minimum overall size can create costly and unnecessary problems.
2. Complex gimbal structures can and should be simulated by the analogous spring - mass - damper math model to predict structural characteristics with reasonable accuracy, prior to hardware development.
3. Actual hardware test data should be obtained as early as possible for comparison with the computer simulation runs in order to evaluate the accuracy of the model as well as the hardware design and test setup.
4. Due to state of the art advancements in both materials and components, smaller, lighter, more rigid packaging is feasible for future platform designs. Again, however, minimum size and weight should not become an overriding criterion.

5. Future platform structural designs can be enhanced if special attention is paid to:
 - a. Detailed requirements, properly documented, prior to the start of hardware design.
 - b. A vibration computer simulation run as soon as initial design configuration is defined.

2.9.2. General Description. - The Centaur Platform is a four gimballed structure, contained in an outer housing. The gimbals are cast of a high damping capacity, magnesium alloy (K1A) which has the following desirable properties:

1. Mechanically stable.
2. Easily cast and machined.
3. Requires no aging or heat treating for stress relief although artificial aging does enhance dimensional stability.
4. High structural damping capacity (important if material is in stress after assembly or during environmental exposure).
5. Lightweight.

Rigid gimbal suspension system "stiffness" is obtained by using preloaded pairs of bearings ("duplex pairs"), contained in the gimbal resolver and torque motor assemblies. In assembling the gimbals, shims are used to increase pre-load slightly and further reduce the possibility of axial or radial gimbal movement. The gimbal design and assembly technique results in a high and nearly equal stiffness along each major axis.

A resolver or torque motor is mounted on each end of each gimbal. The relatively large diameters of the resolvers and torque motors, with their rotors mounted as integral parts of the gimbals, provide optimum accuracy of the gimbal angle pickoff.

In analyzing the Platform from a structural view point, the total assembly can be subdivided into three distinct structural elements, namely:

1. Gimbal structures.
2. Rotary Components (DC torquers and gimbal angle resolvers).
3. Outer housing structure (case).

For analytical purposes, a structural model of the platform can be approximated by the classic spring-mass-damper analogy. Since it is not the purpose of this report to go into a tutorial discussion of the techniques of structural analysis, the discussion will be limited to what has been done, why it was done, and the results.

2.9.3. Environmental Constraints. - Platform structural designs are predominantly dictated by two constraints, these being:

1. Environmental Requirements-

- | | | |
|-------------------|----------------|-------------|
| a. Vibration | d. Humidity | g. Pressure |
| b. Shock | e. Temperature | |
| c. Acoustic Noise | f. Radiation | |

2. Physical Requirements-

- a. Size
- b. Weight
- c. Power Consumption

The Centaur operating environmental requirements are as follows:

1. Vibration: Combined random and sinusoidal vibration input, simultaneously applied. The random component is described by Figure 2.9-1, in terms of Power Spectral Density. The sinusoidal component inputs are-

5 to 11 Hz at 0.25 inches, single amplitude
11 to 2000 Hz at 3g (peak).

The time duration of the operating vibration is twenty minutes, with the sinusoidal portion being applied at a constant octave sweep rate. The platform must be capable of operating while being subjected to the combined vibration environment along each of three mutually orthogonal axes.

2. Shock: 10g (undefined waveform); 100g, half sinusoidal waveform of 400 microsecond duration.
3. Acoustic Noise: 144 db referenced to 0.0002 dyne/cm².
4. Pressure Change: 14.7 PSIA to 1.1×10^{-10} PSIA.

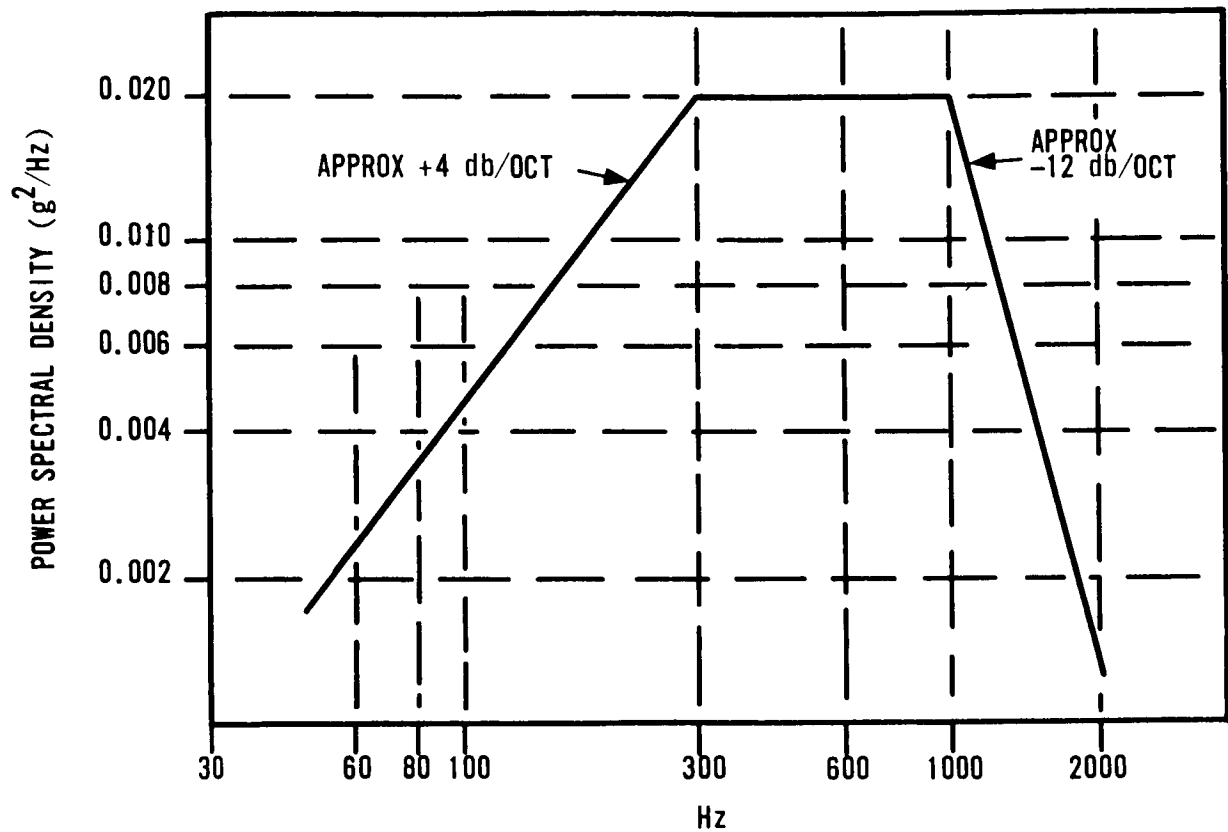


FIGURE 2.9-1. RANDOM VIBRATION INPUT VERSUS POWER SPECTRAL DENSITY

5. Humidity: Relative humidity of 100 percent.
6. Temperature: 400 minutes at +50 to +120° F (case skin).
7. Total Radiation Exposure: 2×10^{12} (3's/cm² plus 5×10^7 protons/cm²).

2.9.4. Physical Design Constraints. - Typical physical restraints, representative of -3 Centaur platform requirements, are as follows:

1. Size (outline dimensions): (11.94 x 9.6 x 13.42) inches.
2. Weight: 30.5 lbs.
3. Volume: 0.9 cubic foot (approximately a rectangular envelope).
4. Power: 70 watts (nominal).

2.9.5. Centaur Design Approach. - In view of the design constraints imposed by environmental and physical requirements, design tradeoffs were required. Materials studies were needed to meet the structural margin of safety for the overall design. Since weight is a prime factor in any space application packaging design, structural and weight considerations were inseparable. Heat sinking and thermal exchange through gimbal-to-gimbal conduction were also considered. Studies were made of heat conduction through rotary components (gimbal-to-gimbal) as a function of rotary component bearing configuration. Compromise between optimum rotary component stiffness, gimbal friction, and optimum thermal coupling had to be considered. Torque motor sizing studies (torque versus power), in conjunction with gimbal scaling (inertias), were also included in the tradeoff studies. Gear driven versus electromagnetic torquers, the advantages and disadvantages of each, were evaluated and weighed accordingly.

As hardware definition became firmed up and mechanization began, certain areas of the design became of immediate interest. In early 1960, a structural stress analysis was initiated to determine the margin of safety exhibited by the main housing and the covers (top, bottom, and end bells) of the platform, while under shock and pressurization loading. Since the platform housing and covers form a closed vessel, which under normal intended use would be pressurized, the structural integrity of this entire assembly was of immediate interest. Stress analysis studies were performed, the analysis being concentrated on the following types of stress loading:

1. Stress due to shock loading (20g).
2. Stress due to pressurization (24 PSIG).
3. Stress due to combination shock and pressurization.

To simplify this analysis, actual form factors were approximated by simple forms and shapes. Although this analysis was not considered all encompassing, it did provide sufficient information to indicate that, from stress loading alone, an adequate margin of safety did exist in the -1 platform design.

Design changes occurred, in the 1961-62 period, in going from -1 Centaur to -3 Centaur. These changes were brought about when the Temperature Control Amplifier Output power transistors were moved from the second gimbal to the end bells of the platform (reference platform TCA Topic 2.8). To facilitate this change, a design change in the end bell covers also was required. The redesigned covers had a heat sink cemented to the interior, and the output power transistors were mounted on the heat sink. An aluminum filled epoxy with high thermal conductivity was used to cement the heat sink to the cover. It was found that during vibration, the new cover design "oil canned", and the heat sink separated from the cover. The end cover was then redesigned to eliminate the "oil canning" previously observed. This alternative was preferable to that of moving the power transistors and heat sink because of heat dissipation problems. The heat sink was then mounted with screws to the new cover, thus eliminating the potential separation problem.

As the -3 Centaur Program evolved in 1961, the need for additional structural analysis and testing, particularly in the area of rotary components, became evident. In order to realize the most from the test and analysis efforts, a program was defined with the following broad objectives:

1. Determine where improvement is needed in the design.
2. Determine the influencing coefficients for unit axial, radial and moment loading.

With these objectives in mind, test and analysis efforts were directed toward determination of rotary components' spring rates and structural damping of the gimbal structures. Isolator damping and spring restraints, and their contribution to the overall structural behavior, were part of this study.

Testing to determine rotary component spring rates was performed on an Instron testing machine. This machine is capable of providing controlled axial, radial, and moment loading, while providing accurate

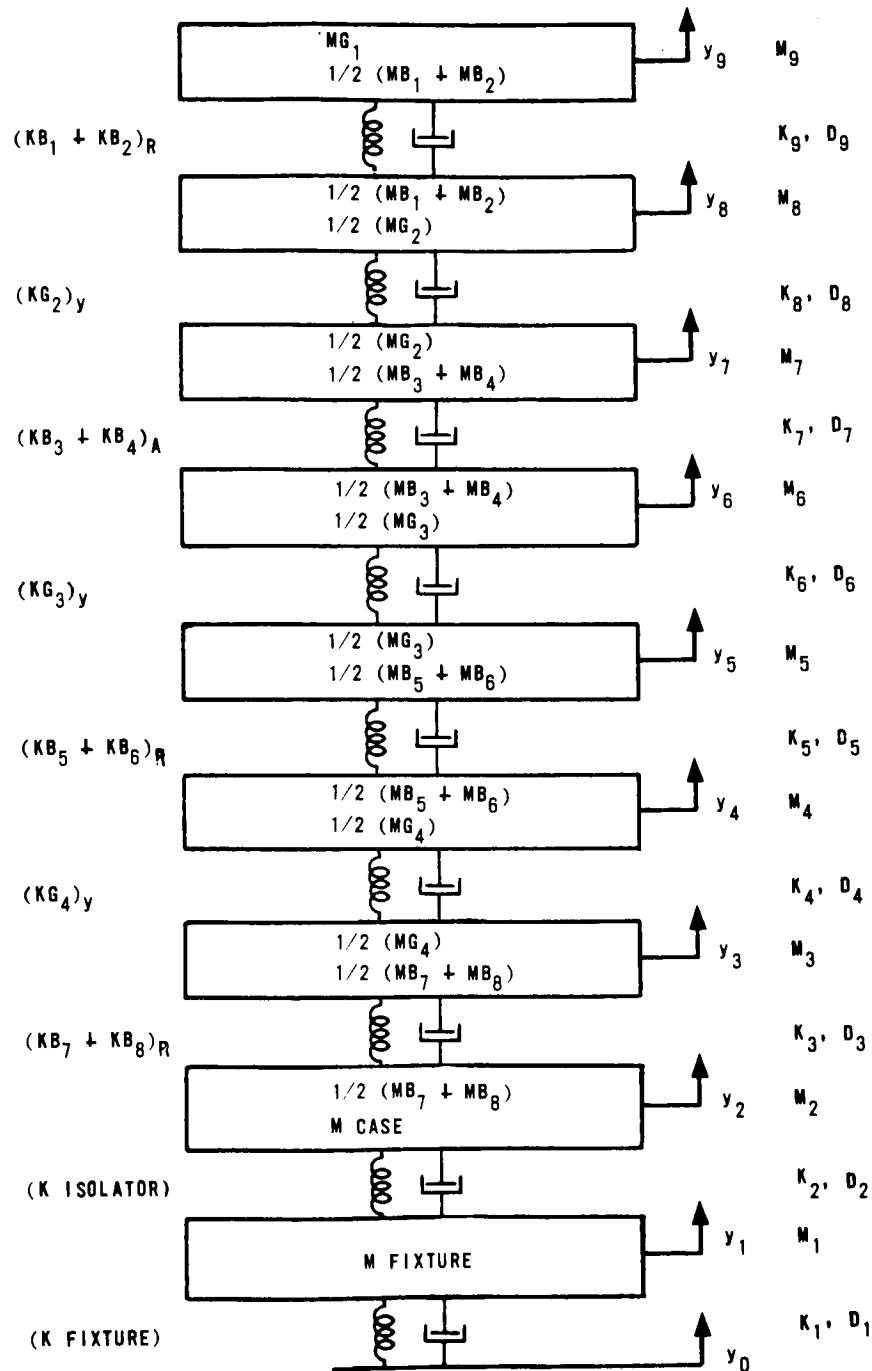
readout for spring rate determination. General conclusions based upon these test results indicated:

1. Rotary components used were too compliant to permit optimum performance for use in an inertial platform.
2. The rotary components exhibited non-linear spring rates (particularly the resolvers) which varied from unit to unit in an unpredictable pattern.

Prompted by these test results, redesign studies of the rotary components were initiated. Primary emphasis in the redesign effort was directed toward increasing the rotary component stiffness (increase spring rate or make less compliant) and to match spring rates and mass in the components (make isoelastic). Results of this study showed the bearing retainer snap ring was losing axial loading during vibration. This resulted in end play as well as radial "slop". To correct for the snap ring design deficiencies, the resolver housing was redesigned. The previous wedge fit, bearing retainer snap ring was replaced with a pre-load plate, retained by screws. In addition to replacing the snap ring, the housing configuration was changed to add greater stiffness to the unit and also incorporate an improved pilot diameter for the slip ring-resolver bore concentricity, thus eliminating slip ring side loading. Through the incorporation of these changes, less compliant components with more linear and repeatable spring rates resulted.

2.9.6. Vibration Math Model. - In addition to the rotary component redesign studies, it became evident that additional analysis and testing was needed to determine the dynamic structural characteristics of the platform. To facilitate meeting these goals, a vibration mathematical model of the Centaur platform was developed. The math model developed was a simplified nine-node (9 degrees-of-freedom) model based upon the "Y" axis only. The "Y" axis was chosen since it represented the "softer" and more vulnerable axis, insofar as vibration was concerned. From this model, equations were developed and programmed on the Honeywell 800 computer. Figure 2.9-2 illustrates the simplified model; Figure 2.9-3 illustrates axis definition and gimbal configuration.

The nine-node model, shown by Figure 2.9-2, is represented as a unidirectional spring-mass-damper model. Each structural element (gimbal, central axis of rotary components, set of isolators, and fixture) were considered as an effective spring and damper, separated by equally divided masses. Hysteresis damping was used in the model to represent structural damping. The damping coefficient (D) was expressed in terms



Notation: $G_1 - G_4$ (Gimbal); $B_1 - B_8$ (Rotary Component); A (Axial); R (Radial); M (Mass); k (Spring Rate); D (Hysteresis Damping Coefficient).

FIGURE 2.9-2. SIMPLIFIED MATH VIBRATION MODEL OF CENTAUR PLATFORM (Y AXIS)

0168-1058

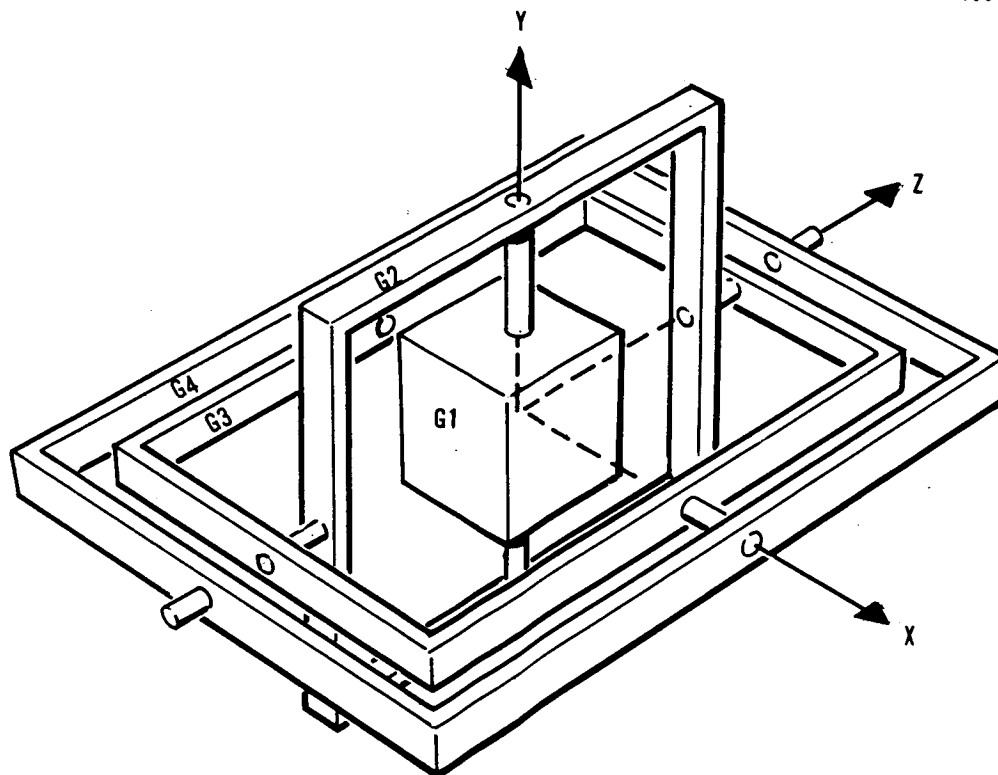


FIGURE 2.9-3. GIMBAL CONFIGURATION

of a loss factor (η) where η is the ratio of the real spring rate over the imaginary spring rate. The choice of hysteresis damping over viscous damping in the model was based upon the fact that hysteresis damping is independent of the forcing frequency, therefore resulting in realistic values of transmissibilities at the various resonant frequencies.

A comparison of vibration test data and computer simulation results, based upon the math model, is presented in Table 2.9-I. The test data and computer simulation were based upon using a platform mounted on isolators, thence on the vehicle platform mounting fixture. A computer simulation and hardware test data were also run for a "hardmount" configuration (no isolators), and a standard Honeywell platform mounting fixture. This information is also shown in Table 2.9-I.

TABLE 2.9-I
VIBRATION TEST DATA

Type Mounting	Data Source	First Resonance (fr_1)		Second Resonance (fr_2)	
		Freq. (Hz) (fr_1)	(Q_{14})	Freq. (Hz) (fr_2)	(Q_{24})
Isolators	Test	34	3.4	170	1
	Computer Simulation	33	3.2	180	0.9
"Hard" Mount	Test	103	25	311	10
	Computer Simulation	102	26	290	6

Conclusions reached as a result of the vibration test and analysis studies which included the redesigned resolver, were as follows:

1. The simplified, nine-node math model accurately simulated the first and second resonant frequency and transmissibility characteristics for both "hard" and "soft" mount configuration.
2. Computer simulation with redesigned (stiffer) rotary components would result in the following:
 - a. No change in the frequency of first resonance point (≈ 33 Hz)
 - b. Slight reduction in number one gimbal transmissibility at (Q_1) first resonance.

- c. Second resonance would move up to ≈ 210 Hz.
- d. Approximately 30 percent reduction in number one gimbal transmissibility at second resonance (Q2).

In late 1965, it was discovered that the second gimbal exhibited a flexural resonance with a center frequency of 395 Hz. Mapping of the second gimbal with a crystal accelerometer pickup revealed a very high "Q", narrow bandwidth flexural resonance. The fundamental flexural mode of the number two gimbal exhibited a "Q" of 20 for a 1 "g" peak input. This resonance produced orientation sensitive, Synchronized Vibration Induced Torques (SVIT) about the gyro output axis (reference Gyro Topic 2.2). Depending upon spin motor static and dynamic unbalance (which produced self induced vibration) and the phase relationship of spin motor excitation with respect to the self induced vibration, large shifts in acceleration insensitive gyro drift with relative gimbal orientation resulted. To eliminate these shifts, the second gimbal resonant frequency was detuned away from the operating frequency of the gyro spin motors (400 Hz).

To detune the second gimbal from its center frequency, mass was added to the corners of the gimbal. With the added mass, the resultant natural flexural resonance of the second gimbal was lowered to near 375 Hz. Detuning the mechanical resonance away from the synchronous gyro operating frequency significantly reduced the "SVIT" effect (as noted in the platform gyro topic, reduction of the vibration source within the gyro was the final "coup de grace" which solved the problem).

2.9.7. Problem Sizing and Producibility Problems. - Another problem which has reappeared frequently through the platform build and modification programs on Centaur, is gimbal interference and/or friction problems. In some cases the latter are due to specific rotary component problems, but frequently the source has been due to a stackup of mechanical tolerances in the mechanical structures (gimbals, shims, etc.) and the wire bundles or harnesses installed on the gimbals. In each case, the problem has been correctable by improved workmanship or slight process changes. However, the frequent recurrence has been costly throughout the years, and it could have been avoided, or at least greatly reduced, by a slight relaxation of the overall platform and gimbal sizing constraints. Too much attention was paid, in the initial design, to achieving a "small" platform, rather than a "producible" one. Trading off the size and weight penalty less than one inch on each major outline dimension and 2-3 pounds of additional weight against the improved producibility could have resulted in a much better balanced design. This is, of course, the application of

"20-20 hindsight". However, it points up an important factor, which is being considered in the IMG platform, and should be considered in the beginning of any new platform design.

2.9.8. Centaur IMG Platform Design. - For the Improved Centaur Platform magnesium (AZ91C) material is being used. This alloy possesses a lower damping capacity than K1A but a significant improvement in yield strength and tensile strength is realized. Computer simulation showed that stress due to actual displacement in the platform is small, thereby rendering damping capacity relatively insignificant. Ease of casting and machining AZ91C, resulting in cost reductions, presented further advantages, and thus the change to AZ91C. In addition to the gimbal material change, the Improved Centaur Platform now contains the gyro stabilization loop electronics, accelerometer loop electronics, plus the precision timing generator. These components are mounted in the separate PE and Coupler in the Present (-3) design. With the new packaging concept, size, weight, power and volume reductions have resulted in the overall guidance set, but without undue penalties on platform producibility.

2.9.9. Conclusions from Centaur Experience. - To summarize, the following may be concluded:

1. Platform gimbal and gimbal housing structures have two predominant design constraints to contend with, namely, those imposed by operating and nonoperating environmental requirements and those imposed by physical limits. However, size reductions can be overdone and should be traded off carefully against producibility and cost.
2. Optimum platform structural design begins with detailed specification of requirements. Proper weighing of these requirements in the design tradeoffs is an important part of the design evolution.
3. Complex gimbal structures can be broken down to simple geometric forms and effectively represented in the form of a math model by the spring-mass-and-damper analogy.
4. Rotary component compliance under complex loading is an important design consideration in a gimballed platform structural design. Bearing configuration and pre-loading play an important part in this consideration.
5. Early and realistic testing of gimbal structures is important to achieving a well-balanced, reliable platform design.

6. Care should be taken to avoid a "stack-up" of amplification of parts having the same resonant frequencies within the gimbal structures. This is particularly true in the areas of critical frequencies of specific components, such as gyro spin motor excitation frequency.

Topic 2.10

Platform Thermal Environment and Control

2.10.1. Introduction and Summary. - This topic discusses the design evolution of the Centaur Platform in meeting the thermal environmental requirements. Problems were encountered, throughout the -1 Program and well into the -3 Program, in maintaining proportional temperature control of the inertial sensors over the required platform thermal environment. Investigations of these problems are classified into four main categories:

1. Temperature Control Amplifiers (Reference Topic 2.8).
2. Platform case surface finish.
3. Platform fill gas and purge-fill procedures.
4. Inertial component-Platform thermal interface.

It must be recognized, when discussing the thermal environment and control problems, that the four preceding categories are highly interdependent and therefore almost inseparable.

The thermal environment for the -1 Centaur missions reflected a platform case skin temperature range requirement of +30°F to +120°F. That is, the proper operating temperature control of the inertial components had to be maintained in a final configuration platform over the temperature range of +30°F to +120°F, where these temperatures represented "average skin" temperatures at the extremes of the platform thermal environment. This range was later changed, during the -3 program, to a range of +50°F to +120°F.

Design problems that occurred, either directly or indirectly, as a result of the temperature requirements specified for the Platform were as follows:

1. Inability to maintain proper thermal control at the lower ambient environment (+30°F).
2. Marginal temperature control at upper ambient environmental temperature (+120°F).
3. Thermal overshoot in inertial components.
4. Large thermal gradients across inertial component mounting flange.

5. Thermal gradient changes with gimbal reorientation.
6. Platform purging - pressurization and seal techniques.
7. Optimization of Platform fill gas mixture for control range specified.

In reviewing the nature of the above problems and the complex dependency or interaction of the factors involved, future problems of this type may be reduced to a minimum by implementing the following action:

1. Initiation of detailed Technical Development Specifications (TDS) at an early stage in the design phase of the program.
2. Perform a detailed thermal analysis (to include dynamic as well as steady state) on the platform early in the design stage of the program. Update, as required, based upon actual test results and changes in operational concepts and mission requirements.
3. Supplement thermal analysis with a detailed thermal test program.
4. Develop and implement detailed process and procedural controls prior to design release.

A discussion of the problems encountered in providing proper temperature control of the inertial components, along with factors considered in arriving at solutions to the problems, can be found under the individual sub-topics. Alternate solutions and tradeoff considerations are also presented.

2.10.2. Temperature Control Problems Oriented Toward TCA Operation. - Platform thermal control problems that were either directly or indirectly associated with TCA performance occurred early in the Centaur -1 program. These problems were observed as follows:

1. Thermal overshoot of inertial components.
2. Large drift rates, associated with "block heater" cycling.
3. Loss of temperature control at +30°F platform exterior skin temperature.

The thermal configuration of the -1 Inertial Platform differed from later versions. Three DGG49D6 gyros and three DGG116A2 accelerometers were used in the -1 Platform. Each inertial component had an integral wound heater-sensor in which the sensor formed one leg of a bridge circuit. The sensors, with positive temperature coefficients of approximately +1.5 ohms/°F, were precisely padded with trim resistances such that at a composite sensor resistance of 780 ohms, the component would be at its proper operating temperature. Heater power to each

component control heater winding was provided on a proportional basis, controlled by individual +28 VDC temperature control amplifiers (TCAs) and their respective bridge circuit. In addition to the control heater winding, the gyro and accelerometers contained warm-up heater windings to bring the components rapidly up to operating temperature from a power-off condition. The fast warm-up heaters were excited by the GSE through a thermostat mounted on the platform first gimbal. When the first gimbal thermostat reached +160°F, the thermostat would open, dropping out fast heat. The proportional control TCAs would then take over.

In addition to the TCA control and GSE fast heat, three cartridge type heaters were mounted in the first gimbal and energized by a relay, controlled by the "V" accelerometer TCA. The "block heater" as it was known, was capable of supplying an additional seven watts of power to the platform any time the V accelerometer sensor resistance dropped below approximately 778 ohms.

In summary three modes of thermal control were available in the -1 configuration:

1. Fast Warm-Up Mode -
 - a. TCA Controlled heaters.
 - b. Cartridge or "Block" heaters.
 - c. Fast warm-up (GSE Supplied) thermostat controlled heaters.
2. Stand-By Mode -
 - a. Fast warm-up heaters, same as (c) above.
3. Normal Mode -
 - a. TCA controlled heaters.
 - b. Cartridge or "Block" heaters.

2.10.2.1. Block Heater Cycling Problem. - The use of fast heat warm up in conjunction with the block heaters caused large thermal overshoots in the inertial components. The overshoots were attributed to thermal lags that existed between the fast heat thermostat and the V accelerometer which, as discussed earlier, controlled the block heater through a relay in the V accelerometer TCA circuit. Associated with the thermal overshoot was large limit cycle variation in TCA power. Due to the complex heat paths in the first gimbal assembly, the individual inertial components interacted differently for every gimbal orientation. Stated another way, a particular component (with respect to another) may act as a heat

source or sink, depending upon the position of the gimbals. Large gyro drift rates were encountered as a result of block heater cycling.

2.10.2.2. Under-powered TCAs. - The basic problem associated with -1 platform thermal control was due to insufficient power from the TCAs. As mentioned earlier, the maximum output voltage to the inertial component heaters under proportional control was +28 VDC. The control heater windings were 132 ohms for the Gyro and 160 ohms for the Accelerometer. With the platform sealed and filled with air, but not pressurized, loss of temperature control resulted at the +30°F case skin temperature limit.

In general, the thermal control problem at the +30°F skin temperature exhibited itself as a lack of power to maintain proportional control by the TCAs. Depending upon relative gimbal orientations with respect to each other, fill gas, and the initial procedure and criteria used in setting up the TCAs, different TCAs would lose control.

Since the ability to maintain thermal control of the inertial components at +30°F was a problem, various techniques were used to set up the temperature control loops (Inertial component sensors-bridge-TCA), in an attempt to balance out thermal loads and regain control. At +30°F it was found that the U and V gyros were as much as 10 degrees below the desired operating point, with their respective TCAs full-on (maximum power to heaters), while the W gyro and all three accelerometers were marginally in control. Even though 92/8 fill gas was specified, all testing was performed during the -1 program with the platform containing ambient air as a fill gas. This condition existed since problems were frequent in the -1 platform, and to purge-fill and pressurize it with 92/8 gas mixture each time the cover was removed would have resulted in a costly, time consuming operation.

Several unsuccessful attempts were made to balance the TCA power and obtain proportional control over the desired temperature range by operating the components at different temperatures. This not only proved to be unsuccessful in bringing about overall thermal control but it also produced large thermal gradients in the first gimbal assembly. Reorientation of the gimbals with respect to each other produced gradient changes which produced large drift rate changes in the gyros. Other attempts on an experimental basis to balance TCA power requirements at +30°F included:

1. Thermally conductive greases between the component flange and first gimbal mounting surface, and

2. Thermal isolation shims under the flange of the "cold" operating components.

The thermal interface changes that were tried were steps in the right direction, but the degree of improvement was not adequate nor were they necessarily compatible with overall platform operation.

From the discussion of the general thermal control problem with the -1 platform, it becomes apparent that a solution to the +30°F case skin thermal control problem only tended to aggravate the control problem at the +120°F end and conversely. The modes of heat transfer and the means of controlling the heat transfer differ at the two temperature extremes. The -1 program TCA readout data and monitored component sensor resistance data showed that for the +30°F lower limit, more power must be delivered to the inertial component heaters. The block heaters were shown to cause large temperature overshoots in the inertial components; the particular components which exhibited the overshoot and the magnitude of the overshoot was dependent upon gimbal orientation. In mid 1961, it was shown that large drift shifts occurred with cycling of the block heaters. It was therefore concluded from -1 program data that the next design generation (-3 Centaur) should delete the block heaters and increase the maximum available control heater power to the inertial components.

2.10.3. -3 Platform Thermal Control. - In late 1961 the Centaur -3 configuration evolved. The changes made at this time to increase available inertial component heater power were:

1. Increased TCA output from +28VDC to +40VDC.
2. Deletion of block heaters (heaters embedded in first gimbal).
3. Decreased control heater resistance of the accelerometers from 160 ohms to 110 ohms.
4. Decreased fast heat (warm up) heater resistance on the accelerometer from 200 ohms to 30 ohms.

Letting the maximum available TCA output voltage be designated as E_{max} and the control heater resistance be designated R_{CH} , it is readily seen that available power to the inertial components was appreciably increased (E_{max}^2/R_{CH}). A comparison of available power to the inertial component from the TCAs for the -1 and -3 configurations is shown in Table 2.10-I.

TABLE 2.10-I

CONTROL HEATER POWER COMPARISON BETWEEN
CENTAUR -1 AND -3 CONFIGURATION

Maximum Available TCA Power (watts)		
	Centaur -1 (28VDC TCAs)	Centaur (Early -3) (40VDC TCAs)
3 Gyro	15.3	33*
3 Accelerometer	12.6	40.5

*Heater resistances the same as for -1

Because of TCA output transistor cutoff levels, the maximum available watts shown in Table 2.10-I were based on 26VDC of the available 28VDC and 38VDC, of the available 40VDC going to the heaters. A net increase of approximately 46 watts resulted from the -1 to the -3 configuration.

All of the material up to this point has been presented in an attempt to point out problems that developed during the -1 program. Emphasis has been placed on problems encountered at the +30°F skin temperature extreme. It must be emphasized that formal thermal analysis and testing up to this point was limited.

At the beginning of the -3 program, changes to the hardware were implemented. Also, refinements in build processes and procedures were beginning to materialize. However, up to this point in time, no thermal tests had been performed on the platform at +30°F with the platform pressurized with the 92 percent helium - 8 percent nitrogen fill gas mixture. Early in 1962, the first -3 platform was pressurized at 3.5 PSIG with the 92/8 gas mixture. It was immediately shown that at the +30°F platform case skin temperature, the new 40 volt TCAs were not capable of maintaining proportional control when the platform was pressurized. Once again the components that lost control (TCA full on, providing maximum available power) depended upon relative gimbal orientations. Loss of control, at +30°F was attributed to the difference in the conduction coefficient of ambient air and helium. The conduction coefficient for helium

is approximately five times greater than that of air. Tests with the platform operating with air for the fill gas indicated an adequate margin of control at +30°F. These early observations in the -3 testing revealed that incompatibility still existed between the thermal requirements for the hardware and the actual hardware design, when operated with the pressurized helium/nitrogen environment.

To correct this situation, several approaches were considered. Some of the possible solutions were:

1. Further reduce heater winding resistances of the gyro and accelerometer.
2. Increase supply voltage to TCAs.
3. Consider changes to platform ambient requirements such that a higher case skin temperature specification could be realized (i. e., raise +30°F spec.).
4. Change fill gas to one with a lesser conduction coefficient (help at +30°F, adverse effect at +120°F end).

After carefully evaluating each of the above, in terms of their short range as well as long range impact, a decision was made to increase the TCA supply voltage. Tests and analysis were conducted with this change in mind in late 1962. It was shown that in order to provide proportional control at +30°F case skin temperature (with the platform pressurized with 92/8 Helium-Nitrogen) the TCA output supply voltage should be raised from +40VDC to +48VDC.

In late 1963, a design change was made to increase the +40VDC supply to +48VDC. However, the second Atlas-Centaur (AC-2) flight was scheduled for November 1963. Before this launch, it was observed that the skin temperature of the gold-plated platform was running at +59°F. It was also noted at the same time that the "W" gyro TCA was "full-on", indicating loss of thermal control. This platform was equipped with the +40VDC TCAs. A decision had to be made to correct the immediate situation for AC-2. Several solutions were considered. These included:

1. Increasing the guidance compartment cooling air from +38°F to +60°F while on the launch pad.
2. Limiting the volume of the air flow through the compartment.
3. A combination of both 1 and 2.
4. Change the gas fill mixture from 92% He/8% Ni to pure nitrogen.

It was decided that the compartment cooling air would be modified and that the platform would be pressurized with 100 percent nitrogen for the AC-2 flight. At launch time, all TCAs were in control and the platform case skin was running at +90°F. These changes for AC-2 flight were considered as "quick fixes". No sacrifice in performance for this particular flight was foreseen (approximately 40 minute duration flight), but for future flights of longer duration, problems could be encountered with these "quick fixes".

At this point it became obvious that, in order to realize compatibility between the hardware and the operational requirements, a complete thermal analysis and test program was needed. Hardware thermal incompatibilities, up to this point had all become evident when tests such as a calibration run on the TCAs were performed. In the case of the temperature gradient changes, large changes in TCA power requirements were noted upon gimbal reorientation during normal gyro and accelerometer calibration modes. As the thermal control problems associated with the platform became more appreciated, more attention was directed towards their solution. In order to assess the total platform thermal control problem and to develop a program that would produce the most useful information for costs expended, the following questions needed to be answered:

1. Can the +30°F, +120°F thermal environment be maintained for the platform with a gold finish? If it can, what changes need be made to realize TCA control?
2. How is heat transfer through conduction, convection, and radiation distributed as a function of mission profile?
3. What are the predominant factors in the platform that control or influence the means in which heat is transferred from components to platform case?
4. What is the relationship between inertial component thermal gradients, case skin temperature, and TCA power?

With these basic questions in mind, the analytical and test program was formulated.

2.10.4. Thermal Transient Analysis. - In early 1962, space simulation tests were performed by GD/C. This test was conducted on a gold-plated, -1 configuration platform. The primary objectives of this test were to provide baseline data on guidance compartment thermal environment as a

function of time from pre-launch through extended orbit. Data from this test helped to remove some of the previous uncertainty inherent in the prediction of the thermal environment within the vehicle guidance compartment. Since this test was run with a -1 Platform, the results were not directly applicable, insofar as providing answers to the previous questions. However, the GD/C test did provide information on some of the primary environmental parameters that would be expected from orbital flight. Temperature gradients to be expected in the various sections of the vehicle, that would in turn influence the MGS thermal performance, were determined. This information proved helpful in setting up future tests at Honeywell. A limited space simulation test was conducted by Honeywell in late 1963 on a completed Missile Guidance Set (MGS). In setting up for the test, the environmental simulation was divided into the following two, highly important, factors:

1. Temperature gradients set up by the vehicle compartment in which the MGS is mounted.
2. Solar energy experienced during extended orbit.

Temperature gradients in the guidance compartment of the vehicle result from several causes. For the particular system under study, the MGS is located in close proximity to liquid hydrogen fuel tanks. Prior to launch, forced air correction is used to maintain the MGS equipment at approximately +80°F. At launch time (t_0), the compartment containing the MGS experiences a definite temperature and pressure change. Profiles of temperature changes were defined from t_0 through the orbital phase of flight. The test showed that temperatures in the compartment bulkhead, at the foil surface, adjacent to the Platform Electronics Unit, varied from +70°F to -250°F. Solar simulation tests conducted by Honeywell used a test fixture, which simulated a quarter section of the Centaur vehicle. Included in this fixture were the payload adapter, equipment mounting shelf, and the bulkhead. Calibrated quartz lamps and cooling coils were located on the test fixture to simulate temperature gradients seen by the MGS in orbit due to alternate sun and dark side of the Earth exposure.

Solar loading expected during orbital flight was previously determined to be cyclic in nature, with 40 minutes at 500 BTU/hr-ft², followed by 50 minutes of 65 BTU/hr-ft². GD/C performed a thermal analysis, predicated on a gold finish for the platform. Results of this analysis predicated a case skin temperature in excess of the +120°F upper limit during orbital flight. To enhance meeting the +120°F skin temperature requirement GD/C recommended the platform be painted with aluminized enamel

over the present gold finish. The Honeywell solar simulation test was thus run on a gold plated platform painted with an aluminized enamel. The results of the Honeywell solar simulation test indicated that for a simulated day launch, the aluminized enamel finished platform would exceed +120°F case skin temperature approximately 32 minutes after launch.

As a result of the solar simulation tests, studies were initiated by Honeywell to investigate different surface finishes to obtain a finish which was thermally compatible with existing requirements as well as containing desirable bonding characteristics. As a result of this study a polyurethane white enamel finish was recommended by Honeywell.

This recommendation was made to GD/C in late 1963. Initial concern was expressed by GD/C that for minimum solar heating, the platform skin temperature might be too cold. To fully evaluate the effect of changing surface finish, a transient thermal analysis was deemed necessary. Transient and steady state analysis later showed no basis for concern, indicating the platform would run with a skin temperature of +61°F for zero solar loading and approximately +71°F for the minimum 65 BTU/hr-ft² exposure.

In early 1964, a computer transient thermal analysis program was run. In setting up this program certain basic assumptions were made. A list of these assumptions is as follows:

1. Heat transfer between inertial platform and adjacent electronic hardware is negligible.
2. External heat inputs other than solar radiation can be averaged, added to true solar radiation, and treated as such with negligible error.
3. No thermal gradients exist within any node of the thermal matrix.
4. Heat conducted from the platform to the Centaur vehicle (or test fixture) through the platform mounts is negligible.
5. Conduction across the platform fill-gas blanket is negligible.
6. Thermal conductivity and surface emissivity are insensitive to temperature within the limits of this investigation.
7. All inertial components operate at the same temperature and their thermal outputs can be consolidated as a single program input without incurring excessive error.
8. Radiant heat transfer between inertial components and gimbal 1 is negligible.

9. Free convection heat transfer coefficients in a one g gravity field for a 92 percent helium 8 percent nitrogen (by volume) mixture can be based on the properties of pure-helium without incurring significant error.
10. Free convection effects in a zero g gravity field are negligible.
11. Platform wiring not specifically affixed to inertial components and gimbals is at the temperature of the case.
12. Hemispherical radiation emissivity of deep space (or test chamber cryo-wall) is equal to unity ($\epsilon_0 = 1$).
13. Twenty-three percent of the platform external surface area "sees" the Centaur vehicle (or test fixture).

In order to develop the solar simulation thermal equations, heat sources and heat sinks were defined. Platform heat sources and sinks are shown by Figure 2.10-1, where definition of symbols is as follows:

q_{ST} = External solar radiation heat source
 Q_{AL} = Solar radiation reflected from the Moon and Earth
 Q_A = Aerodynamic Energy
 Q_I = Energy generated within the Platform
 Q_F = Adjacent Area of Centaur Vehicle (External heat sink)
 Q_O = Deep Space (heat sink)
 Q_E = Earth } may act as either heat sink or source depending
 Q_M = Moon } upon relative temperatures
 Q_R = Reflected solar energy from the IMU
 Q_{SN} = Net absorbed solar energy (Function of Absorptivity - emissivity coefficients)

Since the heat sources shown by Figure 2.10-1a are difficult to analyze and moreover impractical to simulate, Figure 2.10-1b was used to develop the equations for the transient analysis. Due to solar radiation being an order of magnitude greater than the heat inputs attributed to other sources, the error resulting from using Figure 2.10-1b should be small. This point is mentioned since heat inputs other than solar radiation are not dependent upon the absorptivity (α) of the surface finish.

The following heat balance equation was written for the platform:

$$Q_S + Q_I = Q_F + Q_O + \frac{(W_p C_p)(T_p' - T_p)}{\Delta \theta}$$

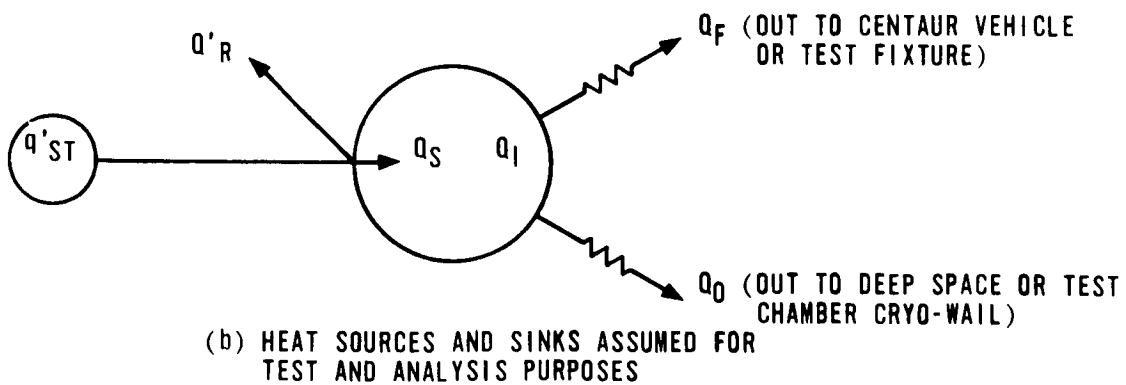
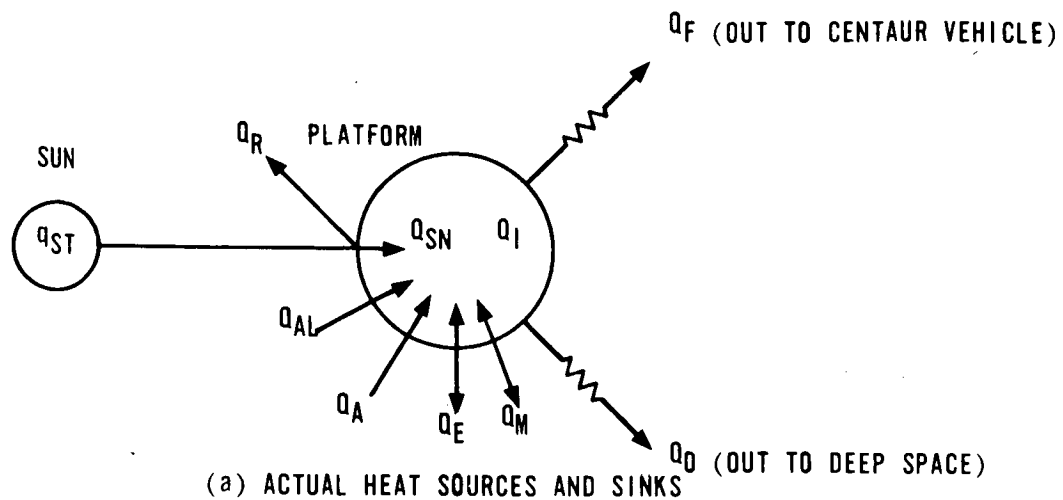


FIGURE 2.10-1. PLATFORM HEAT BALANCE

where:

W_p (The platform mass) = The summation of its component masses

C_p (Platform Specific Heat) = The summation of the platform components weighted specific heats

θ = time interval

T_p and T'_p = Temperatures in degrees Rankins

The basis for the entire thermal program and transient analysis was defined upon this equation. Three particular forms of the equation were of unique interest:

1. when $Q_S + Q_I > Q_F + Q_O$ (heat input > heat output) for this condition $T'_p > T_p$ and the platform temperature increases with time
2. when $Q_S + Q_I < Q_F + Q_O$ (heat input < heat output) then $T'_p < T_p$ and the platform cools with increasing time
3. when $Q_S + Q_I = Q_F + Q_O$ the $T'_p = T_p$ indicating thermal equilibrium

For purposes of this analysis only conditions outside of the Earth's near atmosphere were treated. This was done for two reasons:

1. On launch pad, case temperature is controlled by forced-convection.
2. The t_0 + (time interval between launch and orbit) is short and can be neglected without introducing significant error.

Based upon heat transfer between the platform and its surroundings being through radiation alone, for orbital flight, the equivalent solar input was written as:

$$Q_S = q'_{ST} a A_p$$

where:

α = The platform surface finish absorptivity coefficient

A_p = Projected platform area which is assumed to project on the sun

The previous material has been concerned only with external heat flux. No attempt to evaluate temperature gradients within the platform has been made up to this point. To perform this task a thermal mathematical model was developed. This model when integrated with the model for external heat flux is shown by Figure 2.10-2. The equations defining this thermal model are beyond the scope of this report. Only the basic equations upon which the analysis was based will be presented.

This model considers internal heat flux in terms of the three basic mechanisms of heat transfer, namely:

1. Conduction (Fourier equation).
2. Radiation (Stefan-Boltzmann Equation).
3. Free Convection.

Application of this model was realized by Programming the equations developed on the Honeywell 800 Computer. In applying the computer program necessary constants were either empirically determined or predicted for the given equations involved.

Results of the computer runs indicated that the accuracy of the mathematical model was limited by the validity of the assumptions previously listed, on which the model was developed. Among the assumptions made, those considered contributing more to accuracy limitations were:

1. Neglect of thermal gradients across nodes.
2. Neglect of conduction across the fill-gas blanket.
3. Neglect of absolute temperature effects on free convection "constants".
4. Treatment of fast-heat power as a special case of TCA power.
5. Neglect of the effect of launch pad 6-position platform calibration on warmup thermal regime.
6. Neglect of natural convection heat transfer from platform case to surroundings.
7. Accuracy of some of the thermal constants.

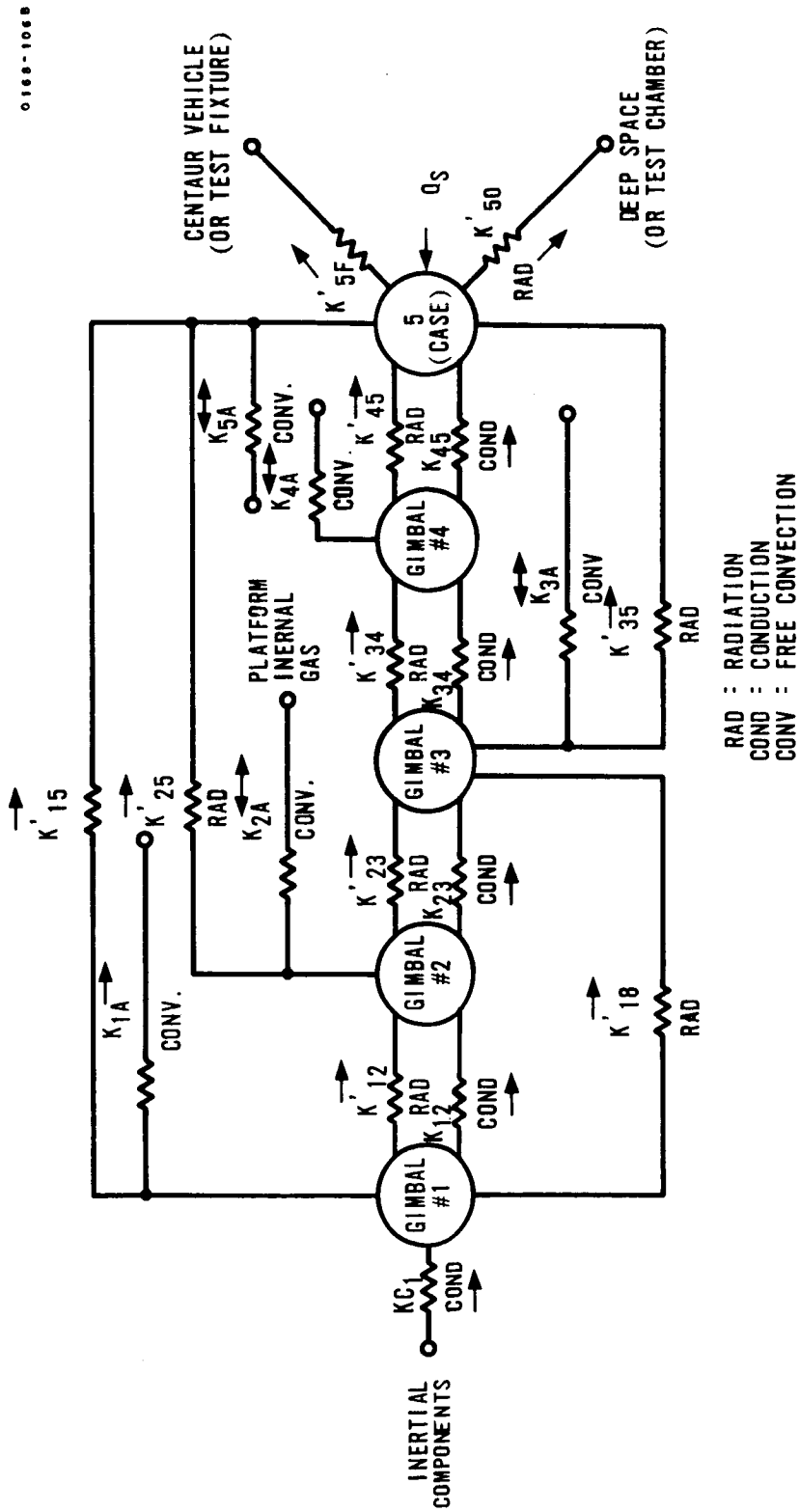


FIGURE 2.10-2. PLATFORM THERMAL RESISTANCE NETWORK

Detailed comments on the effect of each of the above limitations is beyond the scope of this report. However, some improvements can be achieved with a minimal effort.

2.10.4.1. Conclusions. - It was concluded from the analysis that aluminized enamel finished platforms would exceed the +120°F upper case skin temperature requirement when subjected to the solar loading expected from orbital flight. When the appropriate constants in the math model were adjusted to correspond to polyurethane enamel finish and the computer program re-run, results indicated an adequate margin of control. (Refer to Figure 2.10-3.) It was therefore recommended by Honeywell that the platform surface finish be changed to white polyurethane enamel. In early 1964, a change was incorporated to paint all platforms with the white polyurethane enamel.

For purposes of predicting inertial platform temperatures under transient thermal loading, the basic concepts used in this analysis are considered adequate. It is, however, concluded that in order to improve the accuracy of the math model and in turn realize improved accuracy of the analysis, the following changes should be made:

1. The mathematical model should be modified to include the effects of conduction across the fill-gas blanket.
2. The basic computer program should be modified to permit a more precise fast-heat analysis.
3. A term to cover free convection from the platform case to the surroundings should be added to the mathematical model.

2.10.5. Platform Thermal Model; Computer Simulation. - Problems associated with TCAs as they were reflected into overall platform thermal control have been presented. Platform surface finish studies, including test and computer simulation results, have been discussed. The next few pages will discuss the development of the Platform thermal model, why it was needed, how it was developed and how it was used.

Thermal gradient tests were run in early 1964 on a platform. Data obtained from this test provided a gross indication of the gradients one might expect. Further conclusions based upon this test were not made due to the hardware problems encountered and the problems encountered with temperature monitoring. Accurate determination of thermal gradients as a function of case skin temperature TCA power and gimbal orientation were successfully accomplished in mid-1965. The results of this test will be discussed later in this report.

0168-176A

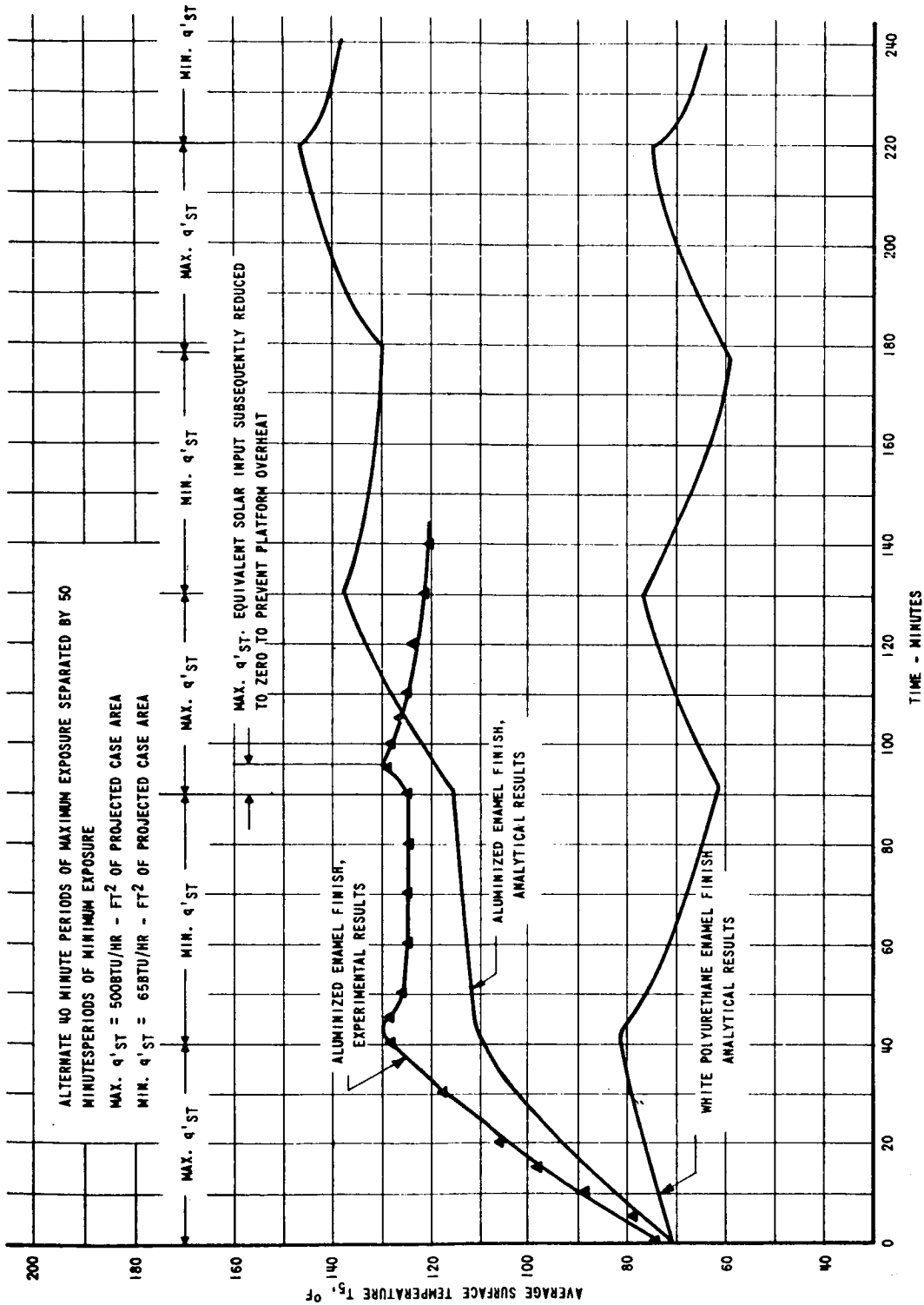


FIGURE 2.10-3. COMPARISON OF PLATFORM SURFACE TEMPERATURE PROFILES;
CYCLIC EQUIVALENT SOLAR INPUT

For the purpose of improving platform thermal control, process and procedure changes as well as design changes, were implemented. In late 1963 the 48VDC TCAs were introduced and in early 1964 the platforms were painted with white polyurethane enamel. In late 1963 a procedural change was made in setting up the TCAs with their respective inertial components. It was shown that in order to reduce gradients in the platform, all inertial components should be set to operate at their respective operating temperature ($+180^{\circ}\text{F} \pm 0.5^{\circ}\text{F}$). Prior to this change TCAs were set up so as to provide a balance of power among the six TCAs. This latter process resulted in all components running at different temperatures (gyros could operate from 177°F to 183°F and accelerometers, 175°F to 185°F). In mid-1963, the lower platform case skin temperature requirement was raised from $+30^{\circ}\text{F}$ to $+50^{\circ}\text{F}$. This provided considerable relief to the design.

In 1963 and early 1964, the method used to purge, fill and pressurize the Platform was investigated. This was prompted by several factors. One concern which lead to this investigation was the possibility of moisture in the Platform due to insufficient purging. Another factor which instigated questioning the purge and fill procedure came about indirectly during calibration of the TCAs. As a result of the purge and fill studies a new purge and fill procedure was implemented whereby the 92 percent helium-8 percent nitrogen mixture was purged through the Platform until a dew point reading of -30°F or lower was realized at the outlet valve. The new purge and fill procedure went into effect in June of 1964. Prior to implementing this procedural change, TCA control was achieved at $+50^{\circ}\text{F}$ by operating the "W" gyro below its desired operating temperature. After the new purge-fill procedure was initiated a significant increase in power was required to maintain inertial components at their operating temperature. The increase in power was attributed to a more thorough purge resulting in a more complete helium fill. Prior to the dew point requirement, insufficient purging left ambient air in the platform decreasing overall gaseous conduction, thus requiring less TCA power.

In mid-1964 the Platform configuration contained the 48VDC TCAs, white polyurethane enamel finish and 92 percent helium - 8 percent nitrogen fill gas, purged to meet the -30°F dew point requirement. With this configuration and all inertial components set to operate at $+180^{\circ}\text{F}$, difficulty was still encountered in meeting the $+50^{\circ}\text{F}$ case skin temperature requirement. In addition to the hardware and procedural changes just mentioned, a detailed 27 mode platform thermal analysis program was initiated. In early 1964 consideration was being given to replace the DGG116A6 accelerometer with the DGG177 accelerometer. For this

reason the thermal analysis computer simulation was performed for both a DGG116 and a DGG177 configuration platform. To further the usefulness of the analysis, different gas mixtures were compared. Previous studies, substantiated by test data taken in a 1 "g" environment, indicated that 100 percent nitrogen fill gas would result in loss of thermal control during orbital flight at the upper temperature limit (+120°F). After extensive testing the gas mixture most likely to result in optimum thermal balance over the temperature range of interest was determined to be 30 percent helium 70 percent nitrogen by volume. Since considerable thermal data was already available with a 92 percent helium 8 percent nitrogen fill, the constants for this gas mixture were also used in the analysis. By using the gas constants for the 92/8 mixture, a check of the accuracy of the model against actual data was afforded.

To better understand the thermal model illustrated by Figure 2.10-4, a brief discussion of the factors considered in its development will be presented. The particular thermal control problem under study is extremely complex. All modes of heat transfer are utilized. The following represents some of the factors taken into consideration in the development of the model:

1. Thermal contact conductances of metallic interfaces and the influence of atmospheric environment on same.
2. Emissivity factors for various metallic surfaces.
3. Heat transfer through gaseous conduction and factors influencing such transfer.
4. Heat transfer through rotary component bearings.
5. Intermodal thermal reaction and its influence upon heat transfer.
6. Gas blanket conduction as a function of gap distances and the effect of free convection upon same.

The preceding factors represent some of the more important consideration taken into account in the development of the thermal model. To include all of the factors that went into the development of this model is beyond the scope of this report. It should be noted that assumptions previously used in the surface finish studies were updated for this model where the previously used assumptions were shown to be in error.

To facilitate the development of useful thermal model, both empirical and analytical inputs were used. The model has been divided into discrete nodes. The basic nodal separation is as follows:

1. Inertial sensors.
2. Rotary Components.

3. Gimbals.
4. Case.

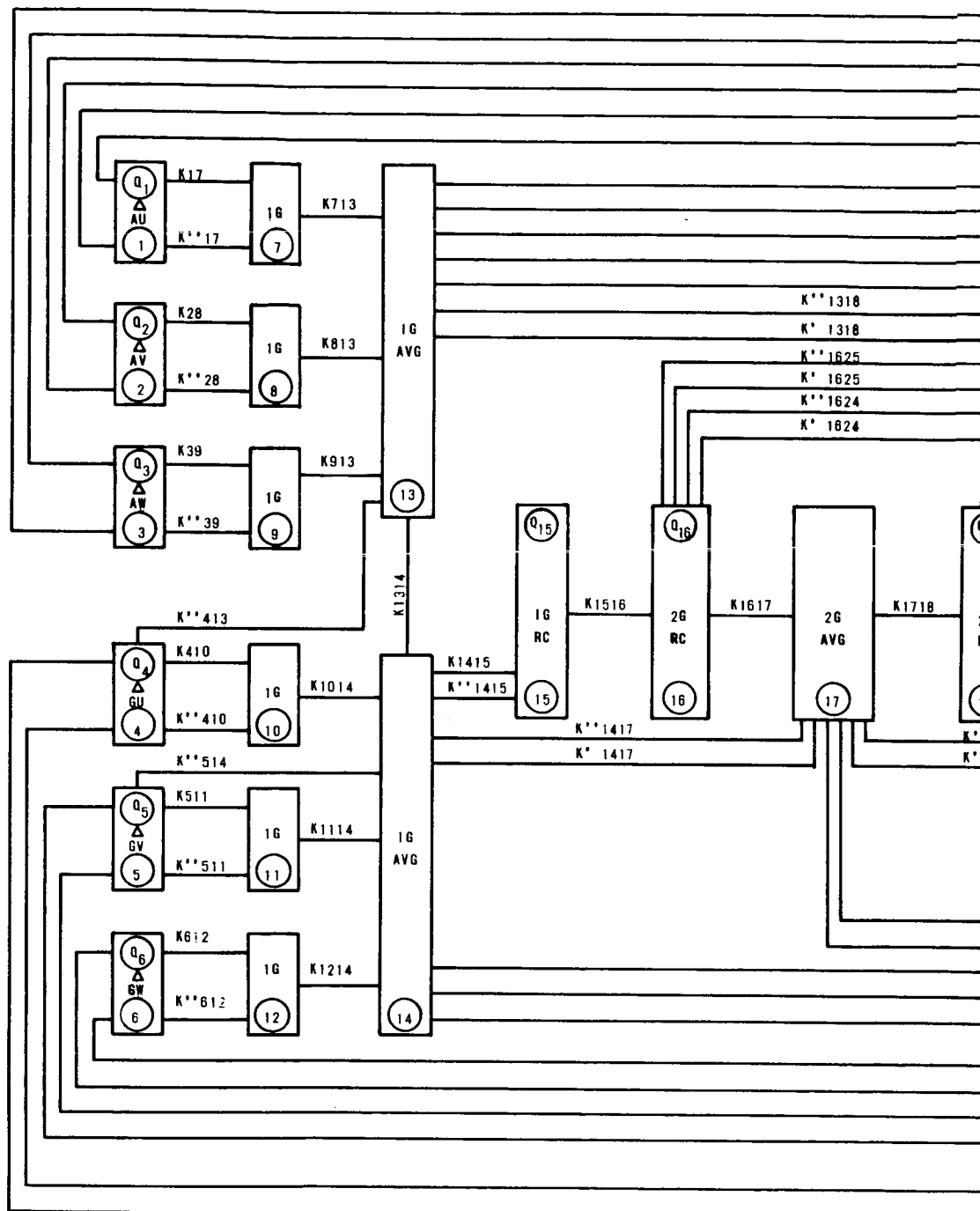
A brief explanation of symbols used in Figure 2.10-4 is as follows:

<u>Symbol</u>	<u>Transfer Mechanism</u>
Unprimed letters (K)	Conduction
Single Prime letters (K')	Radiation
Double Prime letters (K'')	Gas

The symbol K17 for example indicates the heat transfer from node 1 (the U accelerometer) to node 7 (the first gimbal) and the transfer is through conduction.

Results of the computer run indicate loss of thermal control of the U gyro and V gyro at a case skin temperature of +120°F when subjected to a zero "g" environment with a 30/70 fill gas mixture. This was true for both the DGG116 as well as DGG177J1 configuration platform. This observation appears to be pessimistic when compared to actual data collected from several DGG116 platforms. A worst case approach has been purposely used throughout the computer program which tends to produce conservative results. In the computer program the "g" sensitive convection coefficients were set to zero at t=0 (launch) rather than using a ramp or ramp to step function, thus again adding to the pessimistic observation. In actual tests, thermal control of a DGG116 accelerometer configuration platform filled with 30/70 mixture was achieved up to +145°F skin temperature (at 145°F skin temperature all inertial component TCAs were still in proportional control).

All DGG116 configuration platforms were operated with stainless steel tapered shims between the gyro and accelerometer flange and first gimbal mounting surface. These shims were primarily for purposes of alignment of the component input axis in the platform. The shims also influenced the heat transfer characteristics from the respective components. With the DGG177 design sufficient control of the Input Axis Alignment with respect to the flange mounting plane deleted the need for the alignment shim. The DGG177 configuration platform computer simulation was thus set up for a no shim configuration accelerometer with shims remaining under all of the gyros.



△ TCA HEATER INPUT
 ◇ TCA OUTPUT TRANSISTOR INPUT
 RC ROTARY COMPONENTS

FOLDOUT FRAME

2-10-21

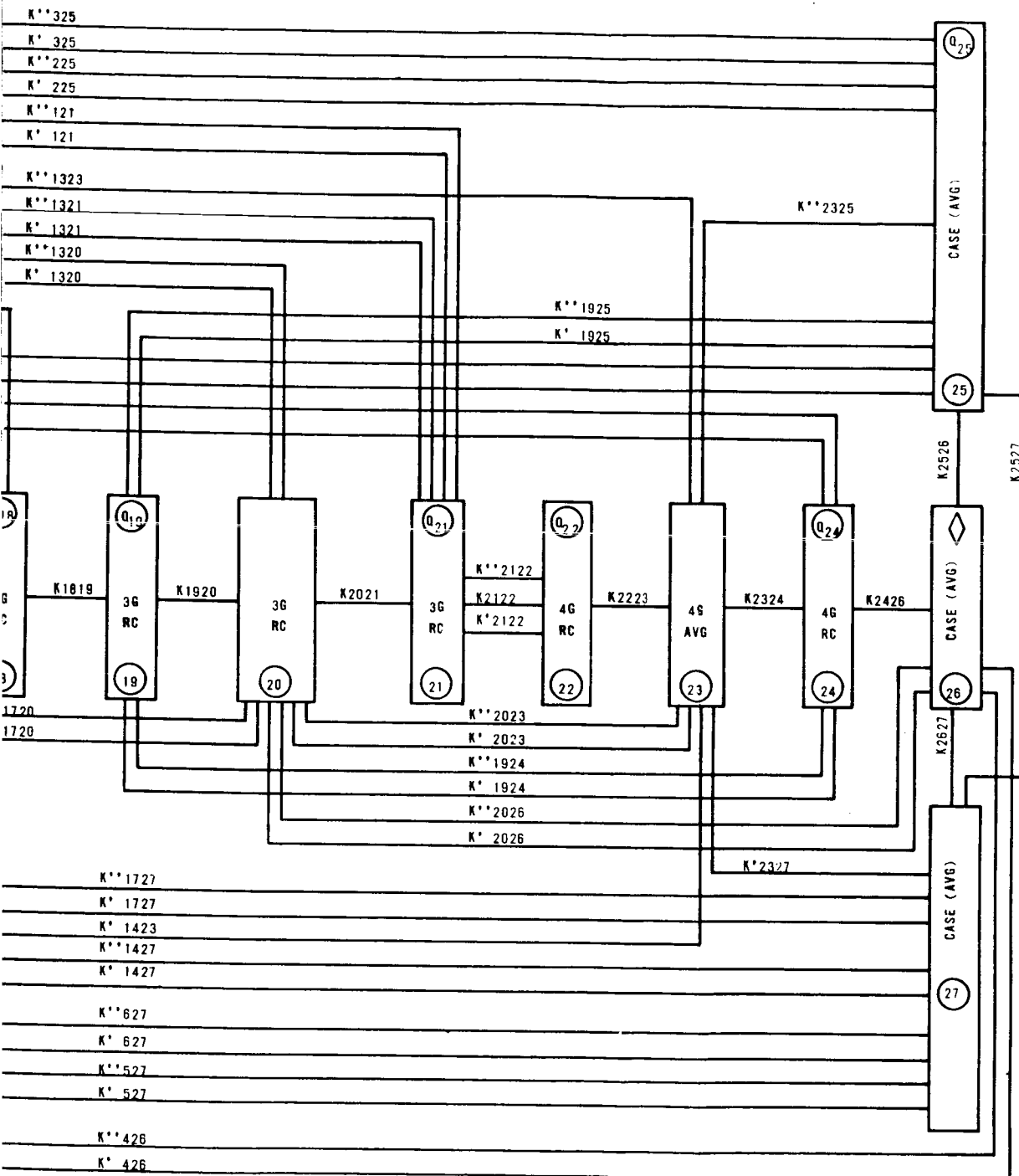


FIGURE 2.10-4. CENTAUR PLATFORM
THERMAL MODEL SCHEMATIC OF 27-NODE

2.10.5.1. Conclusions. - To summarize, the 27 node platform thermal analysis program proved to be invaluable. For the first time the complex thermal paths of the platform were defined and treated in such a manner as to totally encompass launch through orbit parameter dependency. Conclusions based upon this analysis have since proven to be technically correct as evidenced by the present DGG177 configuration platform and the thermal balance now being maintained.

Conclusions regarding the overall platform thermal effect by removing the accelerometer shims based upon 30/70 gas mixture were:

1. Shimless configuration improved accelerometer control margin at +120°F, while decreasing accelerometer control margin at +50°F end. Neither control margin was close to losing control.
2. Shimless configuration tends to improve gyro control margin at the +50°F end while decreasing the control margin for the +120°F limit.
3. The overall low temperature control advantages of the unshimmed accelerometer configuration were greater than the high temperature disadvantages. An overall net improvement in thermal control results with shim removal.

2.10.6. Inertial Component-Platform Mechanical Interface. - In mid-1965 the first production built DGG177 configuration platform went through thermal tests and demonstrated a safe margin of control at both the +50°F and +120°F. Since the inception of the DGG177 program the fill gas has been 30 percent helium 70 percent nitrogen, with no shims used under the accelerometers. Although evaluation of a shim and no shim gyro configuration was not actually run on the computer, conclusions based upon expected results indicated that further improvement in thermal balance in the platform could be realized by removing the shims from the "U" and "V" gyro. The net effect would be to smooth out the power requirement differentials between the inertial components.

Based upon expected results, the DGG177 platforms were to be built without shims under all components except the "W" gyro. This decision was rescinded due to some concern that gradient changes from on pad calibration through launch might be increased. Any large gradient changes would produce adverse drift rate changes, degrading overall system accuracy. In mid-1965 detailed tests were conducted at the systems level for both shim and shimless "U" and "V" gyro configurations. The two configurations were otherwise identical, i. e., in both test configurations the

accelerometers were operated without shims and the "Wg" was always operated with a shim. The objectives of the test were:

1. Determine inertial component flange gradient changes, as a function of relative platform gimbal angles, for discrete steady state platform case skin temperatures, covering the range from +50°F to +120°F for both shimmed and no shim U and V gyro configuration.
2. Determine degree of correlation between drift rate change with gradient change.
3. Determine the steady state relationship between Δ case skin temperature, Δ heater power and Δ gradient.
4. Evaluate overall thermal balance of the platform while under TCA control at the two extreme case skin temperatures for the shimmed and no shim configuration.

To achieve these objectives in the most meaningful manner, the system was operated in its normal configuration. The platform was purged, dew pointed and pressurized with 30/70 gas mixture. Utilization was made of the CAT-8 system calibration program to calibrate gyro and accelerometer terms. The test sequence consisted of going through a complete system calibration at each discrete platform case skin temperature, starting at +50°F and progressing to +120°F in 25°F increments. In addition to obtaining system calibration data, flange gradient data and heater power consumption were measured. To obtain gradient information, calibrated differentially connected copper-constantan thermocouples were used. These thermocouples were embedded in the gyro mounting flange to provide intimate thermal contact. The thermocouples were located along the +IA and -IA as well as +SRA and -SRA for each gyro. In addition to the differential temperature measurements, an absolute flange temperature measurement was obtained for each gyro. Gyro and accelerometer TCA power calculations were obtained by measuring the TCA voltage directly across each of the component heater windings. Knowing precisely the winding resistance of each component heater, the TCA power in watts was calculated (E^2/R).

2.10.6.1. Conclusions. - In reviewing the results of this test, the following observations and conclusions were made:

1. A linear relationship between flange gradient magnitude and control heater power exists for the range of temperatures covered.

2. Poor correlation was evidenced between drift rate change and gradient change indicating the probability of a still greater error forcing function "masking or swamping" out the true thermal effects (this forcing function was later identified as the SVT effect).
3. Overall improvement in thermal balance results when the Ug and Vg shims are removed. This observation is basically a result of a reduction in the "U" and "V" gyro flange - block thermal interface resistance. The U and V gyro now "pump" more heat into the block, thus the block acts as a lesser heat sink for the Wg and accelerometers.

Since the DGG177 program was underway prior to completion of the gyro shim - no shim thermal study, shims were used throughout until the 1967 follow-on build contract. Present platform build contains a shim under the W gyro only.

2.10.7. Conclusions and Future Considerations. - From this discussion the challenge that platform thermal control has presented to design is evident. Design evolution from the -1 Centaur configuration to the present Phase II PIP configuration has resulted in a Platform that is thermally compatible with all presently defined mission requirements. Further reduction of gradient changes with reorientation of the gimbals is always a goal.

Much has been learned in the treatment of thermal problems. Perhaps even more important is what has been learned to help prevent them in the future.

To prevent or reduce the possibility of occurrence of similar problems in future designs, the following should be considered:

1. Thorough and accurate definition of requirements.
2. Early computer simulation studies based upon detailed thermal model.
3. Augmented thermal test program early in the program for purposes of comparing actual data against simulations.
4. Initiate and implement good process and control procedures early in program.
5. Implement timely periodic design reviews.

Topic 2.11

Platform Electronics Gimbal Stabilization Electronics

2.11.1. Introduction. - The portions of the gimbal stabilization loops contained in the Platform Electronics Unit (PE) have been the subject of frequent problems on the Centaur program. The following problems were encountered:

1. Amplifiers saturated at low levels.
2. Gain and phase margins have been inadequate.
3. Overall gain was low.
4. Minor temperature effects on loop null.

Future designs could avoid these problems by:

1. Designing a gimbal control amplifier (GCA) for a particular purpose, rather than adapting a previous design.
2. Avoiding amplifiers with low saturation levels.
3. Adequately specifying overall loop gains at design inception.

2.11.2. Description. - The Centaur gimbal stabilization electronics design was adapted from previous Honeywell designs. The gyro-controlled loop electronics is shown in the following block diagram (Figure 2.11-1).

The front end of the gimbal control amplifier (GCA) is contained on a single circuit board (A1). The power amplifier section of the GCA is on the A2 board, which together with the A1 board comprise a module assembly. The rate network and attenuator are contained on a component board, which is located elsewhere in the platform electronics unit (not in the GCA module) because of component size. The fourth gimbal GCA is similar to the above block diagram, except that its input signal is derived from the second gimbal resolver, with phasing information supplied by the third gimbal resolver.

2.11.3. Original -1 and -3 Design (1959-62). - The major effort in adapting a Honeywell GCA design to Centaur was in modifying the rate network and redistributing loop gains to attain the specified static and dynamic loop accuracies. The previous design, from which this design was adapted, possessed static accuracies on the order of four arc-seconds, but was only required to exhibit relatively loose dynamic accuracy. Centaur requires static accuracies of ± 15 arc-seconds, and dynamic accuracies of ± 60 arc-seconds.

0168-134A

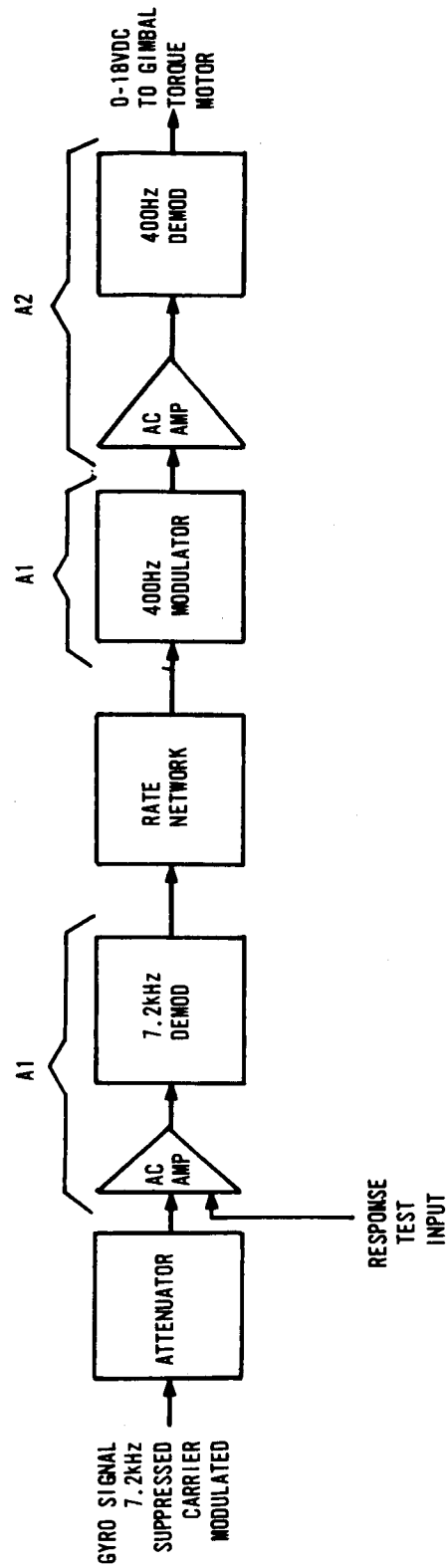


FIGURE 2.11-1. GIMBAL 1, 2, 3 GCA BLOCK DIAGRAM

The preceding block diagram shows an input to the 7.2 kHz amplifier for a response test. This feature was incorporated so that a sealed platform could be periodically tested for adequate gimbal servo response to a disturbance input. A 7.2 kHz error signal injected at this point will cause an angular offset of the gimbal. When the error signal is removed, the gimbal will return to its initial position in a manner analogous to a response from a disturbance torque. Each gimbal loop (excluding the fourth) has provision for individual adjustment of the error signal so that the offset angle input can be controlled.

2.11.4. Rate Network Change (February 1962). - The gimbal control loops had inadequate gain and phase margins, coupled with light damping. The problem was most pronounced during vibration testing of the platform. Oscillations were present at 30 to 40 Hz in the three gyro loops. The rate-compensation networks were redesigned, resulting in better gain and phase margins.

2.11.5. First Gimbal Loop Saturation Recovery Problem (February 1962). - The saturation levels of the first gimbal loop components are such that the A1 and A2 amplifiers are saturated at fairly small gyro displacements. The result is that the loop will almost certainly be saturated when the platform is switched from coarse alignment to gyro stabilization modes. The loop then experiences a loss of rate information (because the A1 amplifier is saturated), and non-linear oscillations result. To overcome this problem a diode clipper circuit was added to the attenuator (shown in Figure 2.11-3). The A1 amplifier was prevented from saturating by this means, and recovery time was reduced.

2.11.6. 400 Hz Modulator Null Problem (June 1962). - The 400 Hz modulator (see Figure 2.11-2) contained a 1.9K ohm resistor in each leg of the bridges. These resistors originally were included to minimize the differences in forward diode resistances. In practice, the heating produced by current in these resistors caused more unbalance than was present without them. The obvious solution was to remove the 1.9K ohm resistors. Results were good, with null variations of the modulator being significantly reduced.

2.11.7. Design of -3B DC Amplifier for Gimbal Control (1962-1964). - The problems encountered to date with the loop electronics pointed to the need for a completely new design. The solutions discussed above were mostly stop-gap in nature, and there was a definite need to increase loop gain and stability margins. The block diagram in Figure 2.11-4 depicts the new design, which became known as the "-3B" design.

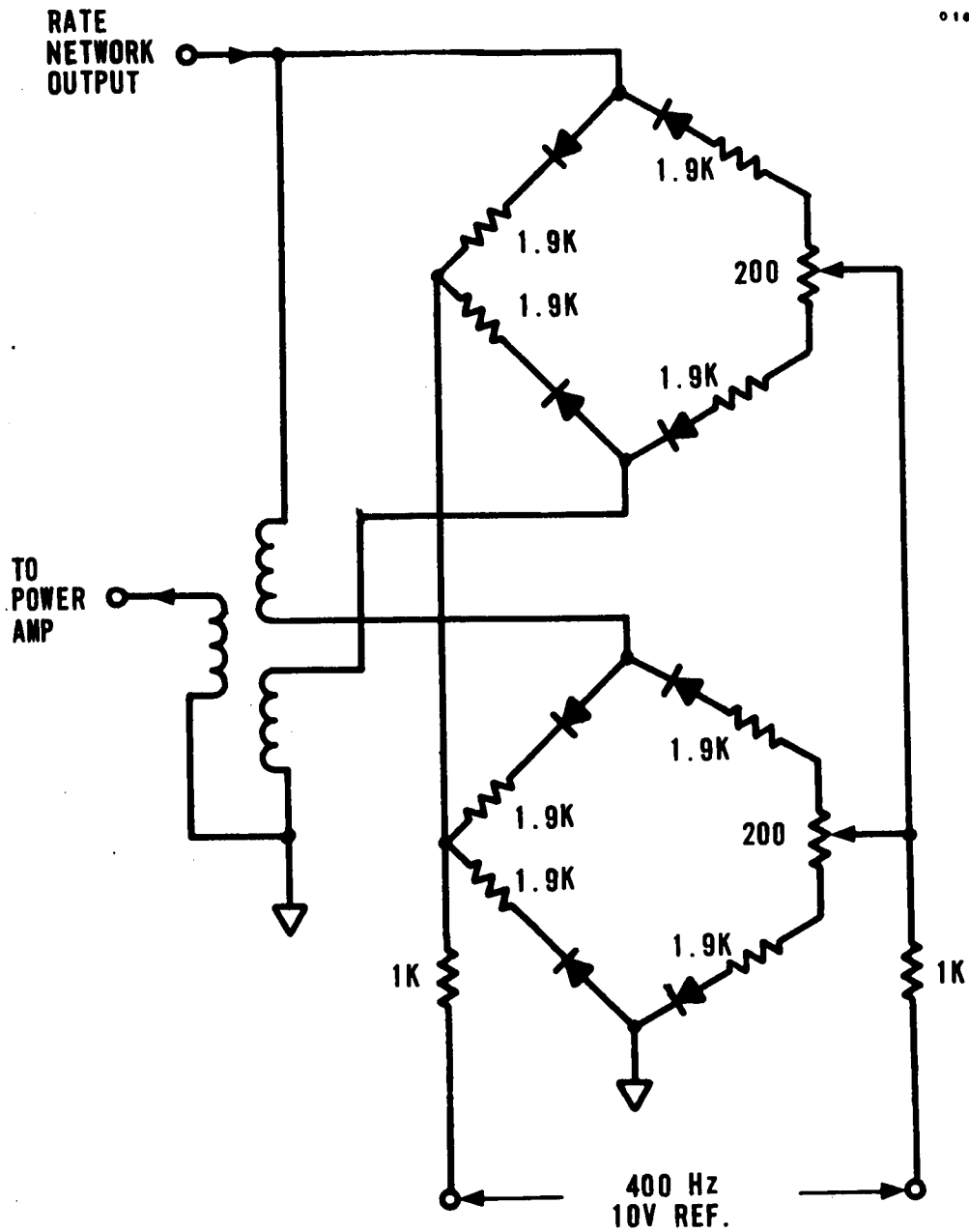


FIGURE 2.11-2. 400 Hz MODULATOR

0169-116A

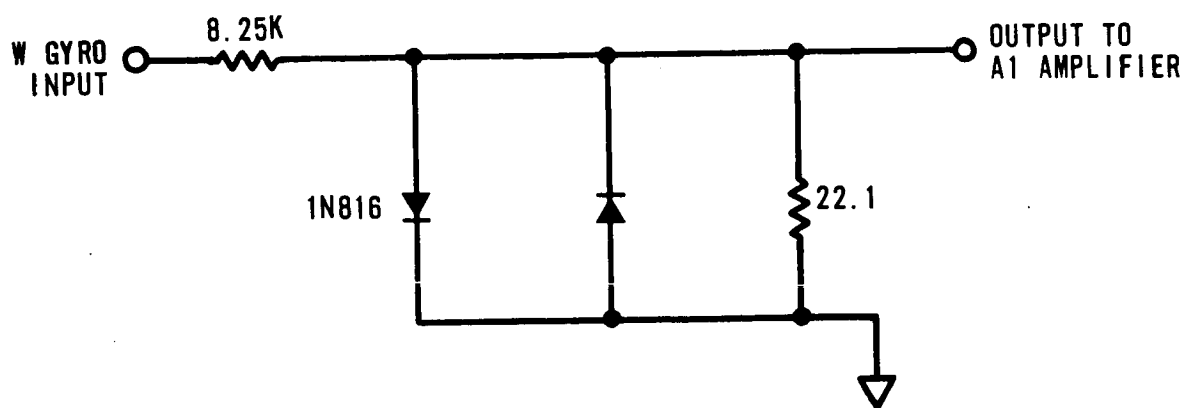


FIGURE 2.11-3. DIODE CLIPPING CIRCUIT

0166-131A

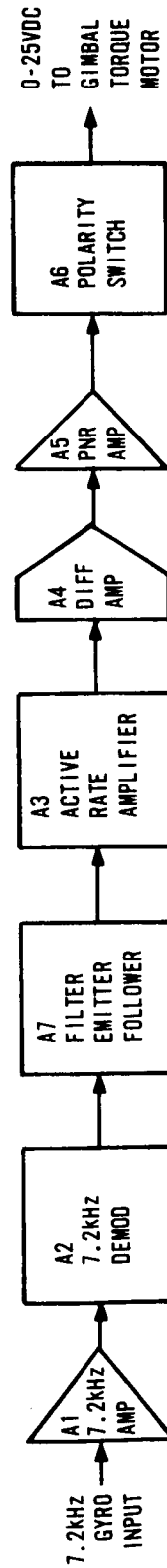


FIGURE 2.11-4. -3B STABILIZATION ELECTRONICS DESIGN

All welded modules (A1 through A7) were put on a single assembly, which replaced the previous printed circuit board assembly. Saturation levels were generally higher and 500 ma output current was provided. The higher output current (-3 design has 350 ma maximum output) enabled better utilization of torque motor capability. This design was not implemented because of program funding limitations. However, other Honeywell systems have successfully used designs similar to the Centaur -3B GCA.

2.11.8. First Gimbal Loop Gain Change (March 1965). - As a result of additional servo analysis, and concurrent with other major MGS changes, the gain of the first gimbal loop was reduced. The servo analysis predicted that better stability could be achieved, with little loss of loop accuracy, if the gain were reduced. The GCA input attenuator scale factor was changed from 0.616 V/V to 0.442 V/V. This has been contemplated previously, but a thorough servo analysis was a prerequisite to the change.

2.11.9. Recurrence of Loop Saturation Problems (March 1967). - As one step in product improvement of the GG49 Honeywell gyro, the gimbal output axis stop angles were reduced to ± 0.6 degree from ± 3 degrees. Soon thereafter, PE/Platform tests showed non-linear saturation recovery problems in the first gimbal loop. (Refer to discussion of this topic under Topic 6.5.)

Alternatives which included gyro stop angle changes, preamplifier modifications, and GCA redesign were considered. However, an approach similar to that used in 1962 was found to be the most simple solution. The A2 amplifier was protected from saturation by clipping diodes placed within the rate network. The schematics in Figures 2.11-5 and 2.11-6 give the details of the network change.

The saturation recovery of the first loop was greatly improved by this rate network change, and threshold gain (which controls static and dynamic accuracy) was essentially unaffected. However, this problem would not have occurred if the dc GCA had been implemented in 1963. The low saturation levels of the stages in the present GCA and the poor gain distribution among the stages have been major problem sources throughout the program.

2.11.10. IMG Design Approach. - The IMG gimbal control electronics (GCE) is an adaptation of the -3B design. (See Figure 2.11-7.) The higher saturation levels and better gain distributions of the -3B GCA were retained, and total loop gain (static stiffness) was raised almost 2.5 times above the present IGS loop gain. The IMG-GCE features integrated circuit

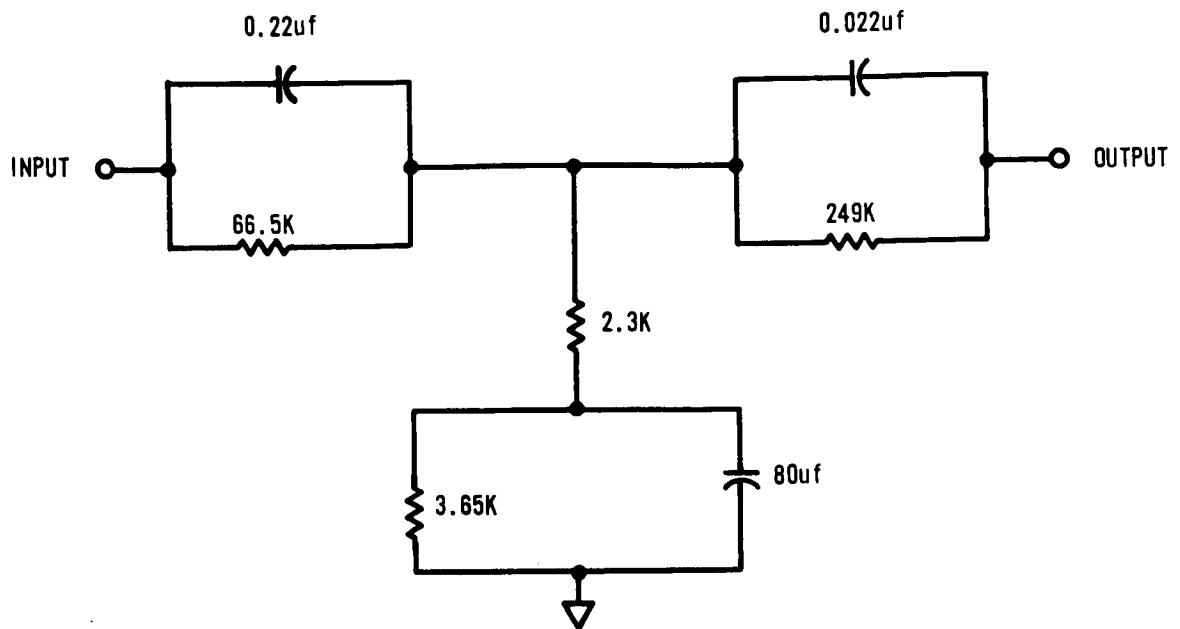


FIGURE 2.11-5. -3 RATE NETWORK (Before)

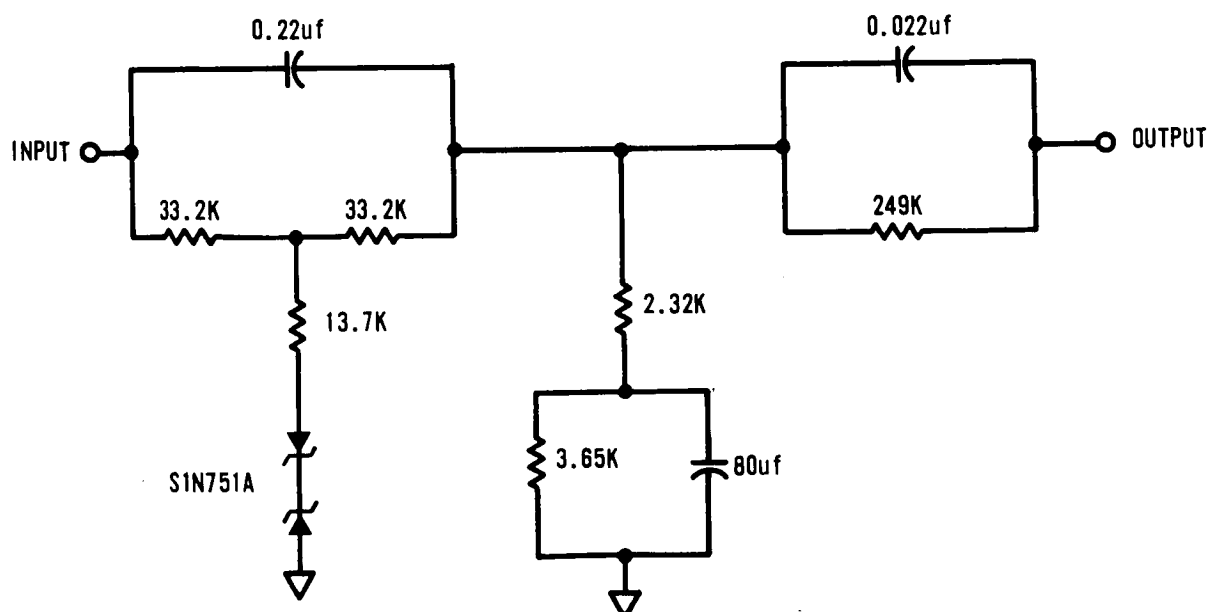


FIGURE 2.11-6. -3 LIMITING RATE NETWORK (After)

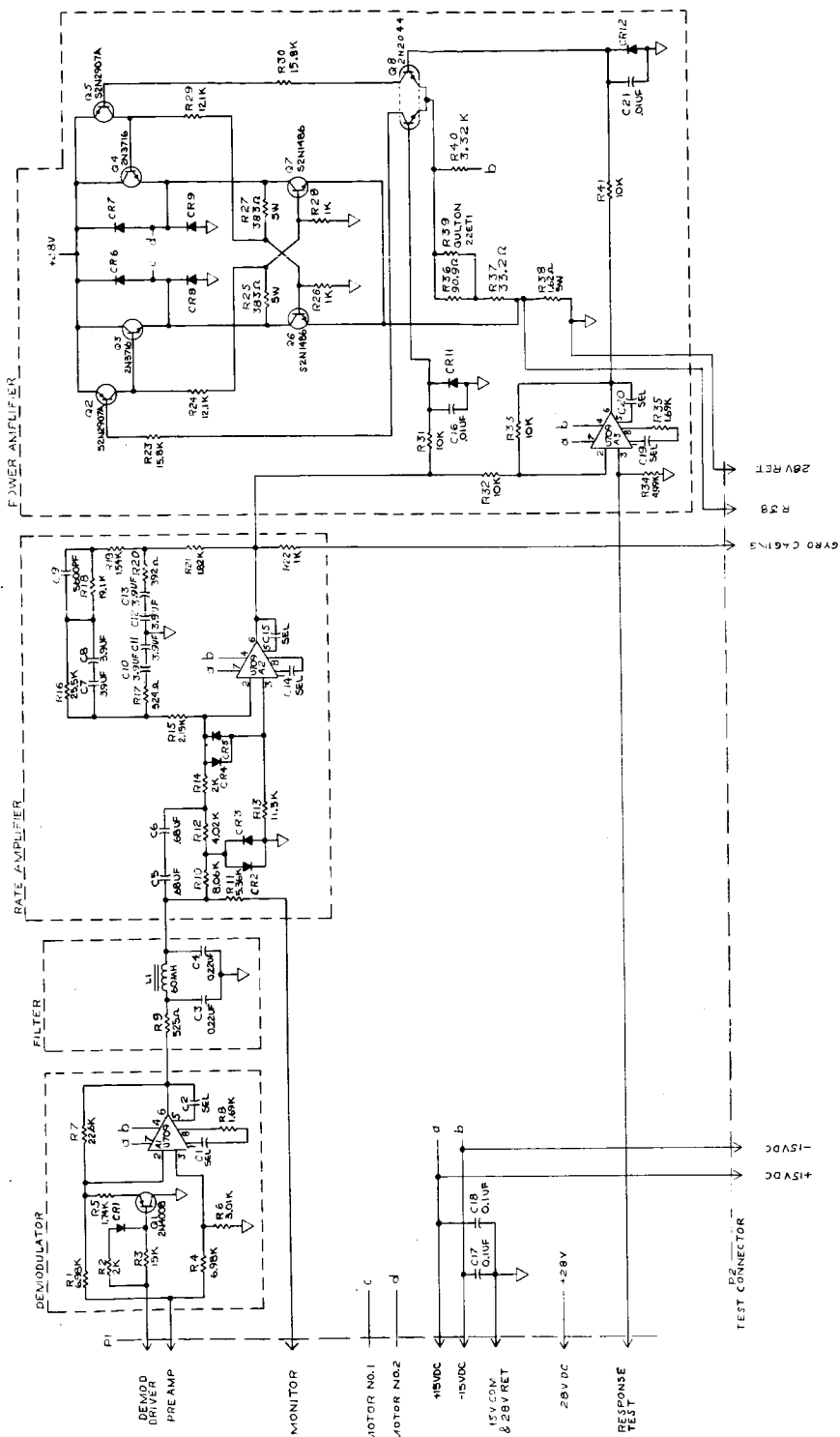


FIGURE 2.11-7. GIMBAL CONTROL ELECTRONICS

amplifiers for voltage gain and operational functions. The GCE module construction continues to be a soldered, printed circuit board assembly. (This has been a relatively trouble-free packaging design.) Two useful testing features have been added in the new design:

1. The GYRO CAGING output (refer to Figure 2.11-7) contains loop rate information suitable for nulling the gyro on itself. Previously, this function was generated in a panel in a platform-level test station for gyro testing. With 28VDC removed from the assembly, the power section of the GCE is disabled and no signal is sent to the torque motor while the gyro is in a rate loop.
2. The voltage measured across R38 (see Figure 2.11-7) is proportional to the current flowing in the torque motor. This monitor point will enable determination of adequate Platform gimbal clearance and proper friction levels. In the present IGS, this information must come from a voltage reading across the torque motor itself. (This is undesirable because of unit-to-unit resistance variation and temperature effects which invalidate all but very gross gimbal friction interpretations.)

2.11.11. Conclusions. - The primary problems associated with the Platform Electronics portion of the Centaur IGS gimbal stabilization loop have been:

1. Improper amplifier saturation levels, resulting in non-linear oscillation.
2. Low overall gain capability.
3. Low gain and phase margins at desired gain levels.

The lessons learned from seven years of developing the stabilization loop electronics include:

1. The first design should be the best possible; little should be left to the later stages of development. Although the solutions to loop problems may be obvious at a later date, the funding and schedules frequently do not allow the solution to be implemented.
2. The loop electronics should be designed not only for operation at, or near, loop null, but considerable attention must be focused on recovery from large loop error signals. The effects of amplifier saturation can be major problems in the stabilization loop electronics.

3. Establishment of loop specification requirements should include adequate regions of amplifier linear operation (saturation levels). Throughout Centaur development phases, the loop electronics were unable to utilize full gimbal torque motor capability.
4. To accomplish the above recommendations, requires the early performance of rigorous servo loop analyses (Topic 6.5) as well as thorough worst case analysis of the stabilization electronics circuits (Topic 6.18.2).

Topic 2.12

Platform Electronics Resolver Electronics

2.12.1. Resolver Chain Electronics. - The Platform Electronics unit (PE) contains the electronics circuitry for isolating the coordinate transformation resolver chain from interfacing computer and autopilot circuits. Three identical resolver chain input isolation amplifiers isolate the resolver chain from the computer and amplify the computer derived steering signals (U, V, W), which represent steering signal vectors in the inertial system coordinates. The computer derived steering signals have a frequency of 400 cps and an amplitude ranging from 0 to 13.5 volts rms. All three resolver chain input isolation amplifiers are packaged on a plug-in, printed circuit module. The input isolation amplifier outputs (sinusoidal with a frequency of 400 Hz and an amplitude ranging from 0 to 20 volts rms) are fed into the platform resolver chain.

The outputs of the resolver chain are obtained from the two stator coils of the fourth gimbal platform resolver. These signals represent pitch and yaw in airframe coordinates, and are fed into two output isolation amplifiers (one signal to each). These amplifiers each have a gain of 2.0 volts/volt and isolate the resolver chain from the autopilot gyro package. There is no roll information available from the resolver chain, as it is now mechanized.

2.12.2. Coarse Align Electronics. - The coarse align and caging mode operation of the platform electronics circuitry is used to place the inertial platform in the various orientations required to calibrate the gyros and accelerometers. For the coarse align and cage mode, relays within the platform electronics unit connect the gimbal control servo loops (reference Topic 6.5) in such a manner that the platform gimbals can be controlled from the GSE (reference Topic 6.6). The relays provide switching that connects the platform resolvers to the alignment reference unit to obtain independent control of Gimbals 1, 3 and 4. Gimbal 2 is caged on itself during the coarse align mode. The total coarse align function is detailed in Topic 6.6. The relays have not been a significant problem for the IGS. However, their existence, and the added complexity in the PE are not necessary in today's state of the art.

2.12.3. Problem Areas. - Problem areas within the resolver electronics have been few. In late 1962, the 1.8K ohm resistor in the input isolation amplifier was changed to 4.0K ohm resistor in an attempt to lower heat dissipation. This change resulted in this amplifier becoming marginally stable when driving the load provided by the resolver. This problem was primarily corrected by returning to the 1.8K ohm resistor and removing the first gimbal rotor compensation shunt capacitors. These changes were effective, and the stability problem has not recurred.

2.12.4. IMG Resolver Electronics. - The IMG resolver chain utilizes an actively compensated mechanization. Microcircuit buffer amplifiers are used between resolvers as well as for performing the input and output amplifier functions. The overall gain of the IMG resolver chain is unity.

The same electronics design practices (parts derating, worst-case circuit analysis, etc.) are being used on the IMG buffer amplifiers, as is being done for other IMG circuits. For the resolver electronics function, the result should be a simple and reliable design.

There will be no "Coarse Align" function in the IMG since platform gimbals will be torqued through the gyros. The overall mechanization will be greatly simplified, in comparison to the IGS, through the elimination of the many coarse align relays which now "clutter up" the present PE.

2.12.5. Conclusions. - The resolver chain electronics, excluding the resolver and its compensation networks, have been relatively trouble-free. The only major problem, the input amplifier oscillation problem, was self-induced and easily corrected by returning to the original design and removing the resolver rotor shunt capacitor. The overall resolver chain mechanization, however, has been changed in the IMG design to preclude deficiencies in the vendor purchased resolver and its compensation.

Topic 2.13

Signal Conditioners

2.13.1. Introduction. - The Signal Conditioners, like all the other IGS units, have been through several phases of modification. Some of the modifications were due to design deficiencies and others were due to the need to telemeter additional MGS signals, which were considered more important than those originally selected. There have been three phases of major modification that resulted in four distinct Signal Conditioner configurations. They are as follows:

1. Original Design,
2. Primary,
3. Auxiliary Signal Conditioners,
4. Operational Signal Conditioner.

A brief description of each of the phases will be presented. Also, each of the IGS signals that are conditioned are discussed, with a brief description and history of their conditioning circuits.

2.13.2. Design Approach. - The basic philosophy behind the Centaur IGS Signal Conditioner is to condition selected signals within an acceptable voltage range (0-5VDC) for the Centaur vehicle telemetry package. These signals represent portions of the major IGS control loops and are used to help evaluate the performance of the system during flight. Table 2.13-I shows the signals that were selected in the "original" Signal Conditioner. The major difference between the "original" and the "Primary and Auxiliary" Signal Conditioners is the addition of nine new signals. The original signals were evaluated against their future replacements during the Primary and Auxiliary phase of SC redesign. After the R&D flight program, the new circuits were packaged into what is now termed the Operational Signal Conditioner (see Figure 2.13-1).

2.13.3. Conditioned Signals. - There are some IGS signals that require only a voltage divider network for a conditioning circuit, whereas others require an amplifier and/or demodulator circuit. The following is a description of each of the signals that are modified either for the GSE or Centaur telemetry system.

TABLE 2.13-I

SELECTED SIGNALS FOR CONDITIONING

Original	Primary	Auxiliary	Operational
4 Gimbal Torque Motors	4 Gimbal Torque Motors	4 Gimbal 7.2 kHz Demods	4 Gimbal 7.2 kHz Servos
3 Gyro Torquers	3 Gyro Torquers		3 Gyro Torquers
3 Accel DC Amplifiers	3 Accel DC Amplifiers	3 Accel 14.4 kHz Demods	3 Accel 14.4 kHz Demods
3 Steering Inputs	3 Steering Inputs		3 Steering Inputs
2 Steering Outputs	2 Steering Outputs		2 Steering Outputs
3 + ΔV 's	3 + ΔV 's		3 + ΔV 's
3 - ΔV 's	3 - ΔV 's		3 - ΔV 's
2 Gyro TCA's	2 Gyro TCA's		3 Gyro TCA's
1 Accel TCA	1 Accel TCA		3 Accel TCA's
1 Gimbal 4 Cage	1 Gimbal 4 Cage		1 Gimbal 4 Cage
1 +35 VDC	1 +35VDC		1 +35 VDC
		1 22.2 VDC	1 Coupler Oven TCA
		1 Gyro TCA's	
		2 Accel TCA's	
		4 Gimbal Phase SW	
26 Channels	35 Channels		30 Channels

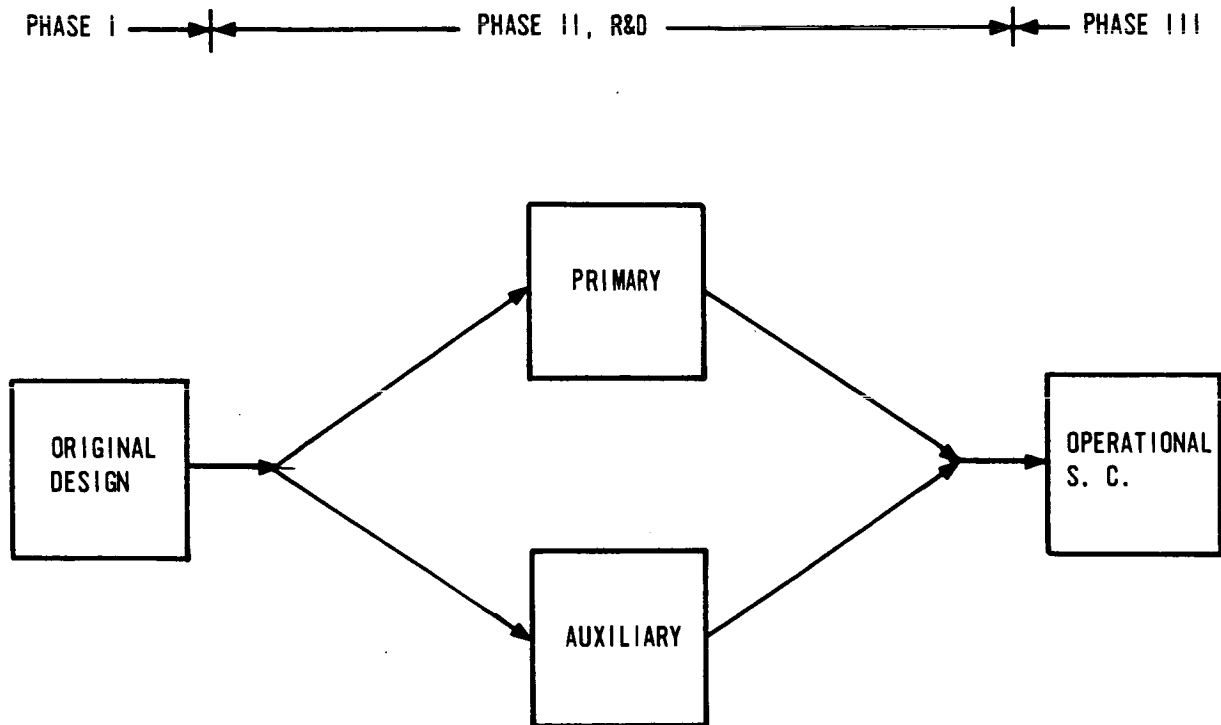


FIGURE 2.13-1. FLOW DIAGRAM OF THREE PHASES OF SIGNAL CONDITIONERS

2.13.3.1. +35 Volt Power Supply. - The +35 Volt supply is a secondary supply which provides DC voltages for many circuits in the MGS. This signal is voltage divided down to a 0-5VDC range for telemetry purposes.

2.13.3.2. Computer Telemetry. - This digital signal requires no conditioning. It originates in the Computer and is routed straight through the Signal Conditioner to the A/B telemetry package.

2.13.3.3. Gimbal Stabilization Loop Demod. - The Gimbal Demod signal is monitored to obtain platform gimbal displacement. This signal was first monitored in the second phase of Signal Conditioners (i. e. , Auxiliary and then Operational). It was adopted over the Gimbal Servo signal because the latter had a high noise content.

The gimbal demod conditioning circuit consists of a two stage amplifier. It has a common base input and a common emitter output. The output signal is resolved about 2.5 VDC. A positive current input causes an output voltage to increase above 2.5 VDC. There were no known reliability problems with these channels.

2.13.3.4. Steering Signals. - There are five steering channels; three steering inputs, and two steering outputs. The three input channels are the flight computer steering potentiometer outputs. The two output channels are the resolver chain outputs after a coordinate transformation and amplification. All five signals are 400 Hz. The basic circuit is the same for each of the channels with the exception of the voltage dividers on the inputs of the circuits.

The basic circuit consists of a one-stage amplifier with negative feedback whose output is transformer coupled to a phase sensitive bridge demodulator. A 400 Hz reference is also applied to the bridge. The demodulator output is filtered. With zero input the output is adjusted to 2.5 volts.

There have been no problems with the Steering Channels in any of the three phases of Signal Conditioners.

2.13.3.5. Gimbal Servo Signals. - In the original design Signal Conditioner, the gimbal servo signals were monitored as an indication of platform gimbal displacement. This signal is a DC signal (the phase sensitive power demodulator output) which drives the gimbal torque motor. This signal has characteristically been noisy, possibly due to the ripple content of the rectified wave. The conditioning circuit in the signal conditioner

was a voltage divider network. Since this signal was used to analyze the dynamic response of the gimbal loop, sufficient noise filtering would change the settling time of the wave form thus possibly masking a problem. With the advent of the Auxiliary Signal Conditioner, the Gimbal Stabilization Demod signal was also monitored. This signal is up stream in the same loop but it is a cleaner signal (7.2 kHz Demodulator output). The Operational Signal Conditioner eliminated the Gimbal Servo signal for telemetry use.

2.13.3.6. PRE Demod (14.4 kHz). - The 14.4 kHz demodulator channels were first used in the Auxiliary Signal Conditioner. The old design signal conditioner contained nine channels in which to monitor the accelerometer loop performance (six ΔV Channels, and three DC Amp Channels). Of these nine channels, only the ΔV channels contained worthwhile information. The DC Amplifier signal is an aggregate signal composed of accelerometer pendulum signal and a digital rate feedback signal. Better information on pendulum position can be obtained up stream from this summing point. Thus, the 14.4 kHz demodulator output was selected as a better monitor point.

The circuit used in the Auxiliary Signal Conditioner is a twin amplifier configuration with a filtered output. The configuration is the common base input-emitter follower output, similar to the Gimbal Stabilization Loop Demodulator Channel, except there are two connected in tandem. This design was far from ideal, yet, it was in keeping with a program groundrule not to develop new circuitry. The Operational Signal Conditioner contains only one (common base input-emitter follower output) amplifier. It was discovered that the desired output impedance and gain could be obtained using a single amplifier. This circuit has been very reliable; no failures have been recorded with this circuit.

2.13.3.7. Gimbal 4 Caging Relay Monitor. - This signal indicates the caging status of the fourth gimbal. This two-state signal is divided down from a 0-13 VDC signal to a 0-5 VDC signal. This circuit has been unchanged for all Signal Conditioners.

2.13.3.8. TCA Monitors. - There are six temperature control amplifiers (TCA's) in the Platform - three for accelerometers and three for gyros. In the original Signal Conditioner the Ug, Wg and Va TCA's were the only ones conditioned for telemetry. Later, with the Auxiliary the Ua, Vg and Wa TCA's were added. Finally, the Operational Signal Conditioner includes all six TCA's, yet only the Wg and Va are telemetered. This is because, during launch, the coolest inertial components are the Va and Wg. The

purpose of monitoring these signals is to verify that the TCA's can maintain control through the flight. All of these signals are conditioned by voltage divider networks. No problems have been encountered in this area.

2.13.3.9. ΔV Modules. - The ΔV signals are incremental velocities from the accelerometer digital loops. There are three accelerometer loops, and for each loop there is a plus and a minus ΔV . There are six flip-flops in the Signal Conditioner. For each ΔV pulse from the PRE, there is a change of state of the Signal Conditioner flip-flop.

There have been many problems with these flip-flops spuriously triggering on noise. The original Design Signal Conditioner flip-flop was re-designed to eliminate the false triggering. Yet, even in the Primary Signal and Operational Conditioners the false counting or triggering still existed. Another proposal for re-design was submitted to the customer, but was rejected. The ΔV signals are no longer telemetered, thus the need for a new circuit was reduced to a minimum.

The ΔV signals are used to check the flight computers' calculations of the inertial components parameters. Transients caused by GSE switching are found to falsely trigger the ΔV flip-flops. During the calibration of the system, no GSE switching is allowed so that the check on the computer may be made.

2.13.3.10. Gyro Torquing. - Prior to Phase II PIP, the gyros were torqued to compensate for inherent drift during flight. These torquing signals were telemetered during flight. Later with the operational phase of the IGS development, in-flight torquing was eliminated. The flight computer program was written to mathematically compensate for the inherent gyro drift. Yet the signals are available in the Operational Signal Conditioners.

The circuit used to condition the torquing signals is the same common base input-emitter follower output circuit that is discussed in the Gimbal Stabilization Demodulator section.

2.13.4. Conclusion. - In general, the Signal Conditioners have had relatively few problems. Since these units are not part of the major control loops, it is understandable that so few problems are encountered. The only problem area that still exists is the delta V circuit. The delta V circuits (two different designs) have always been susceptible to noise. Since they are used to cross check the flight computer's accumulations of delta V's and also used to monitor PRE loops, they certainly should be reliable. Many times during laboratory testing, the Limit Cycle

Monitor (GSE) would indicate an excessive limit cycle. Before it was determined to be a Signal Conditioner problem, the test personnel suspected the coupler. Even today a decision is necessary for new personnel who may be unfamiliar with spurious triggering of the Signal Conditioner. The point here being that it costs money and time to have this type of design deficiency.

Topic 2.14

Platform Electronics and Signal Conditioner Unit Packaging Design

2.14.1. Summary and Introduction. - This topic is concerned with three basic areas. These are:

1. Basic design concept as it relates to:
 - a. Environmental constraints-
 - (1) Vibration
 - (2) Shock
 - (3) Acoustic noise
 - (4) Humidity
 - (5) Thermal
 - (6) Radiation
 - (7) Pressure
 - b. Physical constraints-
 - (1) Size
 - (2) Weight
2. Problem areas and how they were overcome:
 - a. PE Internal temperature "hot-spot".
 - b. PE Cable breakage during vibration.
 - c. PE Resolver output amplifier vibration problem.
3. Recommendations to aid in future designs:
 - a. Consider the thermal relationship between modules or sub-assemblies very carefully when performing the initial design.
 - b. Perform thermal analysis concurrent with the design, or as early as possible after the design is complete, to identify potential internal problem areas.
 - c. Thermally map all devices internally as soon as possible.
 - d. Pay particular attention to cable support brackets, tie holes, etc., during the original design.
 - e. Pay particular attention to possible high vibration resonance areas during the original design.
 - f. Measure internal transmissibilities in areas of high resonance (per the analysis).

2.14.2. Packaging Design Constraints. - The original -1 Platform electronics and Signal Conditioner designs were constrained by the following requirements:

1. Environmental constraints-
 - a. Vibration: Combined random and sinusoidal vibration along each of three mutually orthogonal axes. The random Power Spectral Density is described in Topic 6.15. The sinusoidal component is also described therein.
 - b. Shock, acoustic noise, humidity, radiation, and pressure are also defined in Topic 6.15.
 - c. Thermal: 400 minutes at 30°F to 130°F skin temperature.
2. Physical constraints-
 - a. Size: The size was limited to a rectangular envelope of 16.8 x 8.0 x 7.78 inches for the Platform Electronics and 10 x 8 x 7.78 inches for the Signal Conditioner. (See Figure 2.14-1.)
 - b. Weight: Weight minimization was required for competitiveness with the total MGS weight constraint. The final weight of the Platform Electronics Unit was 19 pounds while the Signal Conditioner was 10 pounds. The Auxiliary Signal Conditioner weighed only 9 pounds.

2.14.3. Physical Description and Design Tradeoffs. - The housing is a cylindrical aluminum weldment with removable, domed, O-ring sealed, end covers. The mounting feet are welded directly to the cylinder. This device is hard-mounted on the vehicle, with the result that internal construction must be designed for both low and high frequency vibration exposure. A structural analysis was performed on the outer housing during the -1 program. The analysis considered combined shock and pressurization effects up to 24 psig, and confirmed that adequate design safety margin existed.

The housing was originally gold plated for heat transfer in the space environment. Subsequent tests and analysis showed that overheating of the PE could occur under orbital solar exposure. This problem was solved by a surface finish change to white polyurethane paint which increased the amount of solar heat emitted by the PE package. Internally,

0168-159A

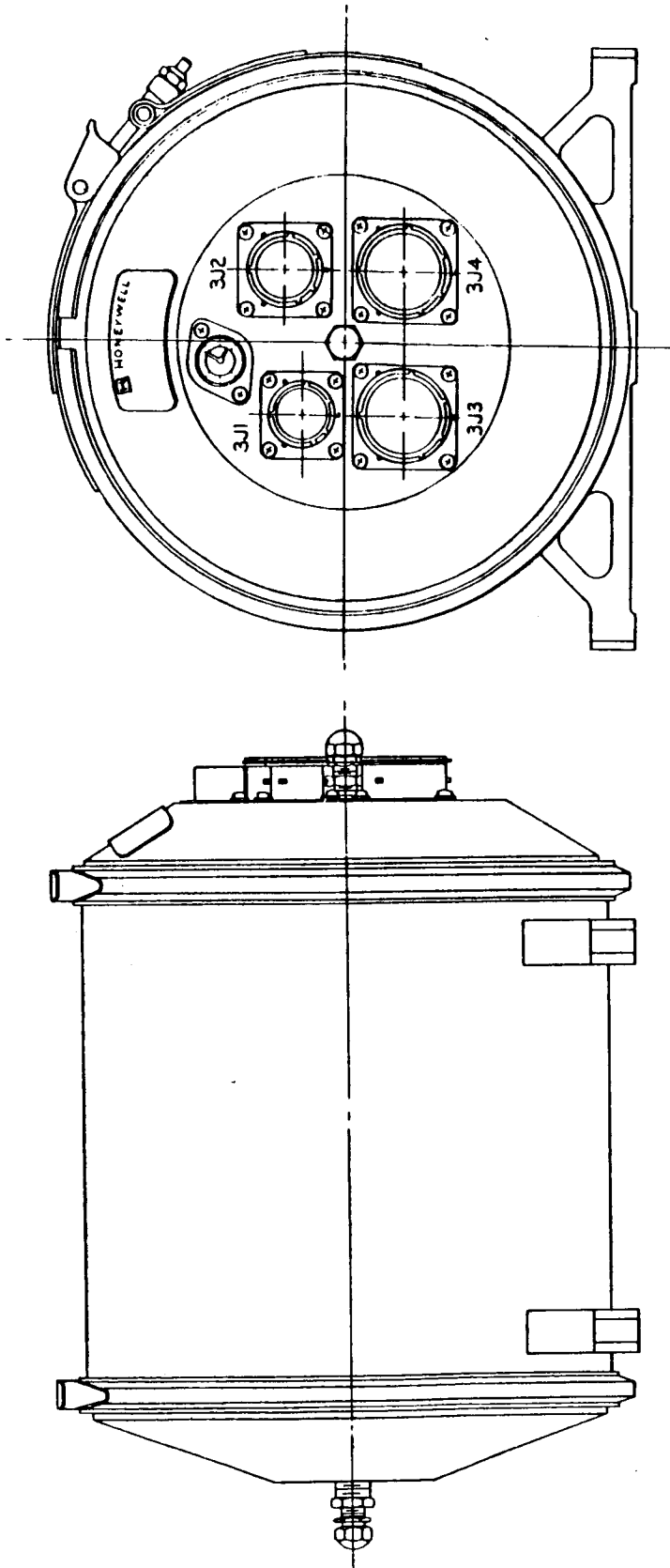


FIGURE 2.14-1. SIGNAL CONDITIONER

the PE is thermally controlled, by conduction and through use of a 92 percent Helium, 8 percent Nitrogen fill gas which is continuously circulated by a fan to provide forced convection cooling of the circuit boards and modules.

The Signal Conditioner is also filled with 92 percent Helium 8 percent Nitrogen fill gas. Due to the low heat dissipation of the internal electronics, the Signal Conditioner requires no circulation for cooling in orbit, and in actuality, requires supplementary heating to maintain the skin temperature above 30°F.

The inner chassis is a "U"-shaped, sheet aluminum channel (looking axially along the unit), with connectors spaced along the axial direction, in the bottom of the channel. Printed circuit modules slide on guide rails and are plugged into the connectors. A sheet aluminum cover completes the inner chassis assembly and makes it rigid by providing the fourth side of a box section. This assembly is then mounted in tension in the outer cylindrical housing. Housing and inner chassis assembly vibration resonances are decreased by the tension mounting technique. Cooling air holes are provided through the inner chassis wall for forced convection cooling of the modules.

Cabling, terminal boards, and other associated electronics are mounted on the sides of the inner chassis. External signals are brought out through Bendix connectors in one of the end covers.

2.14.4. Problem Areas. - The Centaur Signal Conditioner and PE structure have been relatively troublefree. However, there were three significant problems during the development of the PE.

Internal "hot-spot". - After the first prototype PE's were fabricated, it was discovered that the close physical proximity of the power input transistor on two of the modules was causing excessive "hot-spots". A shield was incorporated to serve as a heat sink to the chassis wall and reduce the heat transfer between the modules. This approach was preferable to the alternative of a major relocation of the modules.

2.14.5. Cable breakage. - Vibration testing of the PE disclosed several deficiencies in the design, regarding the securing of cables. Some large cables were flexing enough to break wires at termination points. Tie brackets and tie holes were added, and these corrected the problem.

2.14.6. PE Resolver Output Amplifier Vibration Problem. - The inner chassis cover, which was mentioned above, was found to have high vibration amplitude resonance points. The resolver chain output amplifier is mounted on this cover via standoffs. At resonant frequencies, the amplifier board was being flexed excessively in the cross-axis. This resulted in component lead breakage. Stiffeners were added to the cover and to the amplifier board. These effectively corrected the problem.

2.14.7. IMG Design. - There is no separate Platform Electronics Unit or Signal Conditioner in the IMG. The functions of the IGS PE and SC have been incorporated either into the IRU or SEU for the IMG mechanization. However, the lessons in packaging design, learned during the IGS PE and Signal Conditioner development, are being applied to both the IRU and SEU packaging design.

2.14.8 Conclusions. - The experience gained during the development of the Centaur Platform Electronics and Signal Conditioner Units have emphasized both the benefits of good initial design practice and the penalties of not taking special precautions in the areas of thermal and vibration characteristics. For future packaging design, the following format should be used:

1. Determine the thermal relationship between modules and sub-assemblies.
2. Perform thermal analyses, including the use of computer-aided techniques, before committing the unit to production build.
3. Thermally map all devices internally.
4. Perform internal vibration mapping as soon as possible in the development program.
5. Secure and support all internal assemblies to reduce failures caused by vibration.

Topic 2.15

Pulse Rebalance Accelerometer Loop Electronics

2.15.1. Theory of Operation. - The following paragraphs contain a tutorial discussion of the detailed theory of operation of the Phase II PIP Accelerometer Pulse Rebalance Electronics (PRE). If the reader is not familiar with this mechanization, he is urged to study this treatment before delving into the topics on the evolution of the IGS PRE loop (subject 2.15.3).

Maintaining the accelerometers at null by closing a digital loop around each one provided a measure of the acceleration being sensed. The three IGS accelerometer servo loops are electrically identical and operate simultaneously; therefore, the following discussion will be limited to one loop. A block diagram of the present (Phase II PIP) accelerometer servo loop is shown in Figure 2.15-1. Accelerometer pendulum position is obtained from the signal generator output.

The amplitude of the 14.4 KC accelerometer signal modulation is proportional to the angular displacement of the pendulum from the null position, and its phase is dependent on the direction of displacement from null. The accelerometer signal is amplified by the platform accelerometer preamplifier and then fed into the coupler PRE, where it is phase detected, filtered, rate compensated, and amplified.

Next, a tunnel diode level discriminator, controlled by the analog chain output signal amplitude and polarity, activates one of two logic states within the logic network. The logic network, in turn, performs two operations. Both of these operations are a function of the logic state set by the level discriminator. First, incremental velocity (ΔV) pulses are sent to the computer via the ΔV output modules. These pulses represent either positive or negative velocity increments, and each pulse has a weight of 0.1 ft/sec. Second, the logic network closes the appropriate gates in the master gate and current bridge, so that rebalance torquing pulses of the proper polarity are fed to the accelerometer. Torquing pulses of the same polarity will be applied to the accelerometer until the polarity of the error signal changes; then the polarity of the torquing pulses will also change. When there is zero vehicle acceleration, the PRE provides a train of alternate two positive and two negative current pulses to the accelerometer torque generator. As vehicle acceleration

The diagram illustrates the system architecture for vehicle acceleration measurement, divided into three main functional areas: **VEHICLE ACCELERATION**, **COUPLER**, and **TORQUING CURRENT**.

- VEHICLE ACCELERATION:** This section contains the **ACCELEROMETER**, which consists of a stack of three blocks labeled **T**, **P**, and **SG**. An input arrow labeled **VEHICLE ACCELERATION** points to the **T** block. The output of the **SG** block is connected to a **PRE AMP** (represented by a triangle symbol).
- COUPLER:** This central section contains the core processing and control logic.
 - The output of the **PRE AMP** is fed into the **ANALOG CHAIN**.
 - The **ANALOG CHAIN** is connected to the **LEVEL DISC**.
 - The **LEVEL DISC** is connected to the **LOGIC** block.
 - A **DIGITAL RATE FEEDBACK** line connects the **LOGIC** block back to the **ANALOG CHAIN**.
 - The **LOGIC** block is also connected to the **PRECISION TIMING** block.
 - The **PRECISION TIMING** block is connected to the **CURRENT BRIDGE MASTER AND GATE DUMMY LOAD** block.
 - The **LOGIC** block is also connected to the **Δ V OUTPUTS** block.
 - The **Δ V OUTPUTS** block is connected to the **Δ V** outputs of the **DIGITAL COMPUTER** and the **SIGNAL CONDITIONER**.
 - The **Δ V OUTPUTS** block is also connected to the **Δ V** inputs of the **SIGNAL CONDITIONER**.
 - The **LOGIC** block is connected to the **ARC S** block.
 - The **ARC S** block is connected to the **PVR** block.
 - The **PVR** block is connected to the **CURRENT BRIDGE MASTER AND GATE DUMMY LOAD** block.
 - The **CURRENT BRIDGE MASTER AND GATE DUMMY LOAD** block is connected to a ground symbol.
- TORQUING CURRENT:** This section is indicated by a label at the bottom right, representing the output of the system.

FIGURE 2.15-1. VELOCITY LOOP FUNCTIONAL INTERFACE

is experienced, either the positive or negative current pulse pattern, which is related to the acceleration sensed, begins to increase. The rebalance torquing pulses in the Phase II PIP PRE operate on a 50 percent duty cycle. Switching in the current bridge is such that the accelerometer torquing coil receives a precise current for half a 3,600 Hz period. A dummy load receives the same current magnitude for the other half period. This precision current is supplied by the accelerometer rebalance current supply (ARCS). Switching time is precisely controlled by clock pulses from the Precision Timing Generator (reference Topic 2.16).

2.15.1.1. Analog PRE Section. - A block diagram of the analog electronics is shown in Figure 2.15-2. A 14.4 KC signal, modulated by pendulum displacement and phase information, is received by the carrier amplifier. The carrier amplifier attenuates all frequencies other than the 14.4 kHz signal carrier and its sidebands ($\pm 1,800$ Hz). The signal is amplified and routed to the diode bridge demodulator.

The signal is full-wave rectified by the demodulator. The polarity of the output from the demodulator depends upon the relative phase of the carrier signal with respect to the demodulator driver reference voltage. The amplitude and phase of the demodulator output signal indicates the accelerometer pendulum position at any given time. The demodulator reference is provided by a pair of 14.4 kHz square waves, 180 degrees out-of-phase and referenced to the signal generator excitation.

The signal from the demodulator is routed through a filter which removes the 14.4 kHz carrier and all harmonics thereof. The filtered signal is then fed to a rate network which compensates for the lead-lag characteristics of the accelerometer. This signal is then summed with the integrating rate feed-back signal and amplified by the dc amplifier before being sent to the digital logic section.

The integrating rate signal through the rate network provides a synchronous idling mode, when the input signal from the demodulator is near null (accelerometer sensing zero acceleration). At zero g, the output of the dc amplifier will be an alternately positive and negative 900 Hz signal. This signal will cause the digital section to provide a train of alternately two positive and two negative ΔV pulses. The maximum signal output of the integrating rate network is limited to the maximum value of the pulse input. As vehicle acceleration increases the accelerometer analog signal magnitude increases, overriding the digital rate signal. Hence, above approximately 1.5g the integrating rate signal has negligible effect on the level discriminator input. By

0685-273A

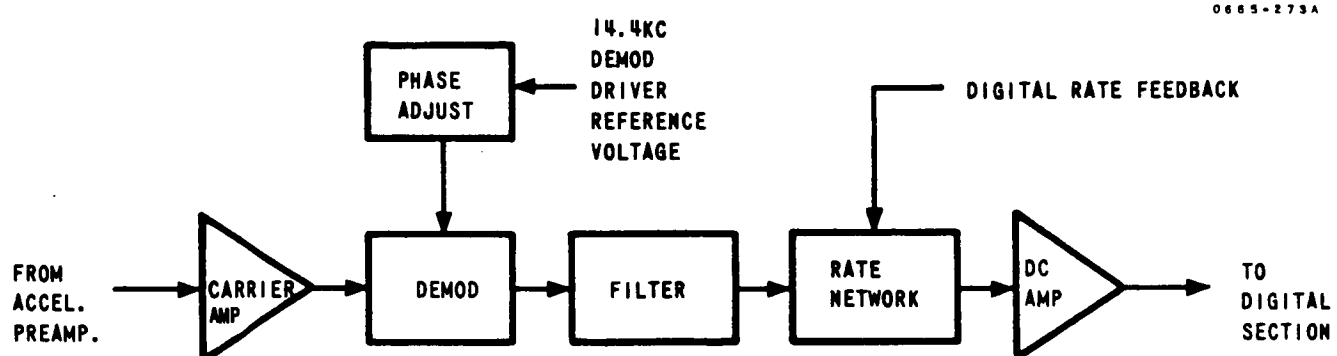


FIGURE 2.15-2. VELOCITY LOOP ANALOG SECTION

employing this technique the lead network and gain bandwidth requirements are reduced, and the signal-to-noise ratio is improved.

In summary, the analog chain receives a modulated 14.4 kHz signal. The phase and amplitude of this signal represents the direction and magnitude of the accelerometer pendulum deflection from the null position. The output of the dc amplifier is an analog signal which is proportional to this phase and amplitude information.

2.15.1.2. Digital Section. - A block diagram of the digital section is shown in Figure 2.15-3. The signal from the dc amplifier in the analog section is applied to the level discriminator. The level discriminator detects the amplitude and polarity of the signal. If this signal exceeds either of its two threshold levels (± 145 mv), an output pulse of the same polarity as the dc amplifier is obtained. Two pulse amplifiers are used to amplify the output pulses, one pulse amplifier is activated by the positive pulses and the other by the negative pulses. The outputs from these two pulse amplifiers are the input signals to the first flip-flop in the logic circuitry. Hence, the level discriminator converts the analog signal into digital information.

The logic circuitry controls the polarity of torquing current pulses required for pendulum rebalance and sends pulses to the ΔV output circuitry representing positive and negative increments of velocity.

The first flip-flop changes state each time the pulses from the level detector change in polarity. The output of the first flip-flop is sampled by two AND gates at C2 time and applied to the second flip-flop. Therefore, the second flip-flop changes state at C2 time only. At C2d times the output of the second flip-flop is sampled by the second two AND gates. The resulting P (positive) or N (negative) signal is amplified by its respective pulse amplifier and routed to the appropriate flip-flops which set the current gates for the proper direction of current flow. At C3 time all of the current gate flip-flops are reset.

The master gate performs the rapid switching of the constant current from the accelerometer rebalance current supply. The current is switched alternately between the current bridge and a dummy load at a fixed repetition rate. During the time the current is flowing through the dummy load, the logic sets the proper gates in preparation for the next master gate cycle.

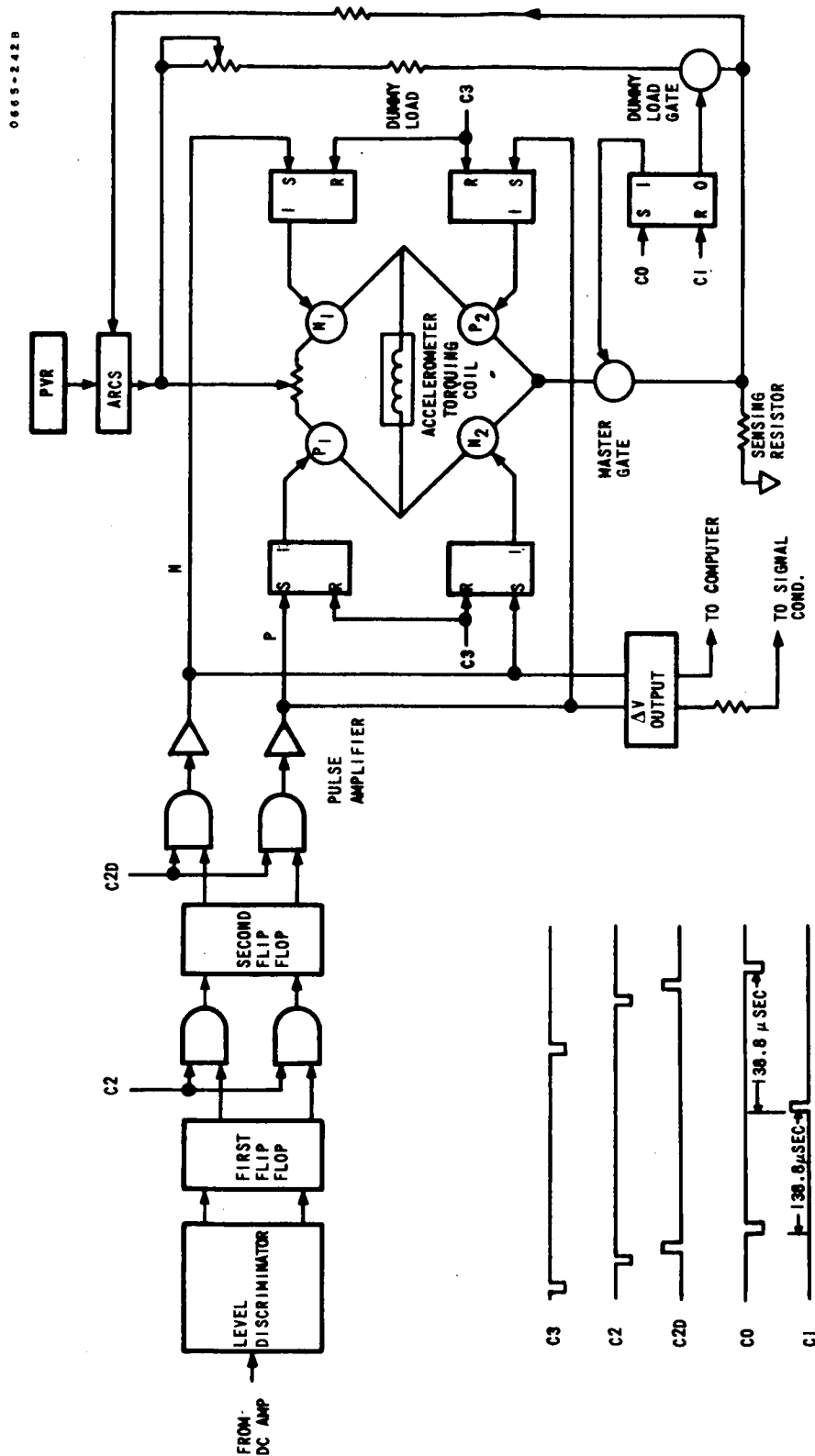


FIGURE 2.15-3. DIGITAL SECTION BLOCK DIAGRAM

A block diagram of the accelerometer current bridge is shown in Figure 2.15-4. Note that the P pulses from the logic block trigger P_1 and P_2 gates simultaneously while the N pulses trigger the N_1 and N_2 gates simultaneously. A P command pulse will close a path from left to right through the torquer coil while an N command pulse will close a path from right to left. The current direction through the accelerometer torquer coil (which is physically located in the accelerometer), and thus the resultant torque on the pendulum is a function of P_1 , P_2 , N_1 and N_2 gates. The master gate flip-flop, triggered by CP0 and CP1, fixes the duration that current will flow through the bridge and dummy load. The clock pulses insure that events will occur in the proper time sequence. Clock pulse CP3 resets the P and N flip-flops after CP1 has reset the master gate flip-flop.

The time relationships between the five accelerometer clock pulses CP2, CP2d, CP0, CP1 and CP3 are shown in Figure 2.15-5. Also shown is a simulated level discriminator output and the resulting states for logic and current bridge flip-flops.

A step-by-step description of the bridge gates under all switching conditions is given along with Figures 2.15-6 through 2.15-14. There are three master gate and current bridge circuits in the coupler; one each for the u, v and w loops.

The accelerometer pendulum is continually torqued at a 3,600 cps rate. The algebraic sum of the positive and negative torques equals zero when no acceleration is sensed. Since a ΔV is produced each time a torquing pulse is applied to the pendulum, the net ΔV 's will also be zero when there is no acceleration.

The ΔV output circuitry generates pulses representing positive and negative increments of velocity for the digital computer and signal conditioner (and GSE during calibration). The input signals are pulses from the logic which are generated at the same time as the P or N signals, which set the current gate flip-flops at C2d time. For each input pulse received, two output pulses are generated, one for use in the digital computer and the other for the signal conditioner. The output incremental velocity information is routed to both units on six lines (two per velocity loop channel), by the voltage pulses, the algebraic sum of which is proportional to the acceleration being experienced by the accelerometer.

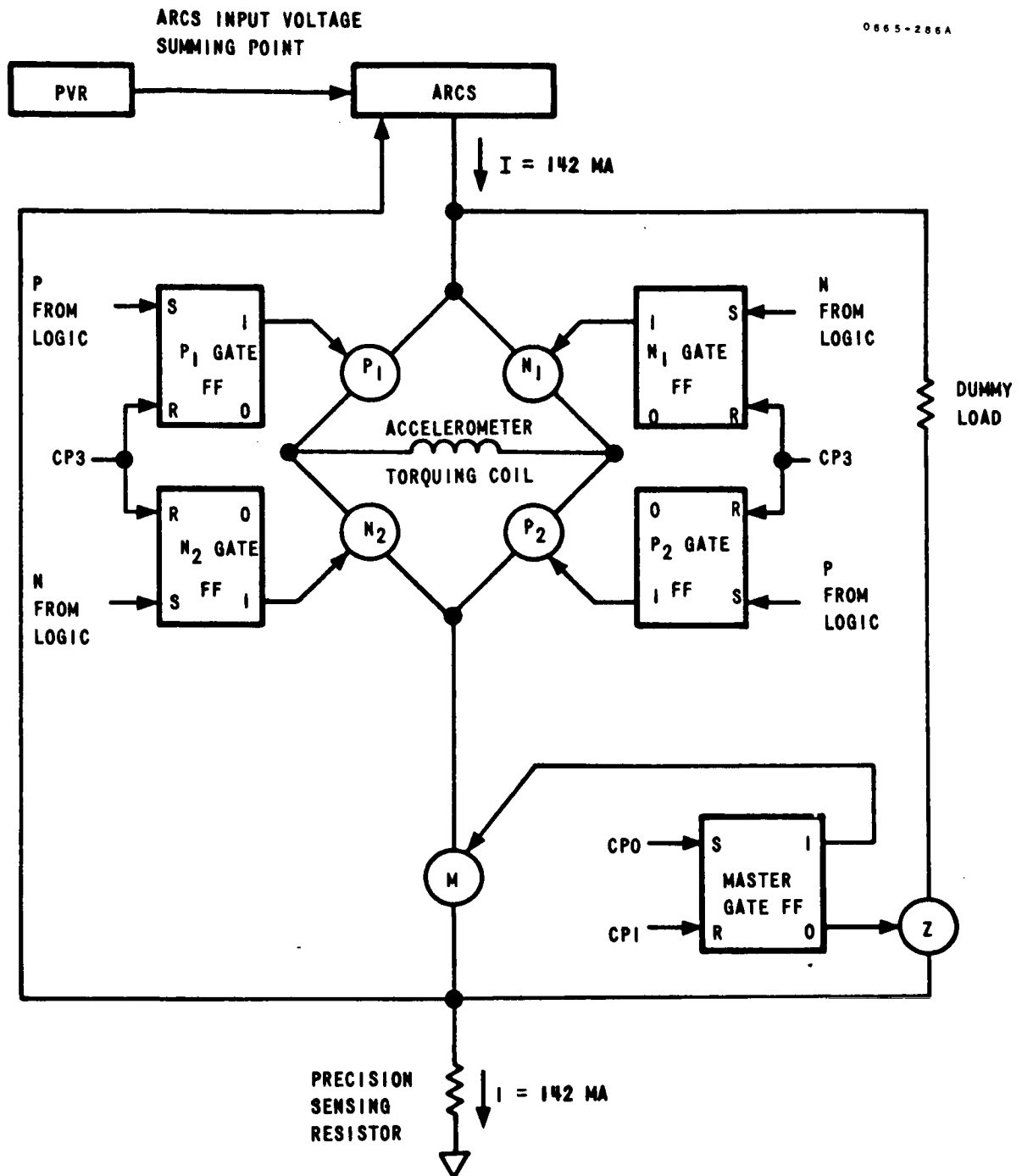


FIGURE 2.15-4. ACCELEROMETER PULSE REBALANCE
CURRENT BRIDGE LOGIC DIAGRAM

0500-4100

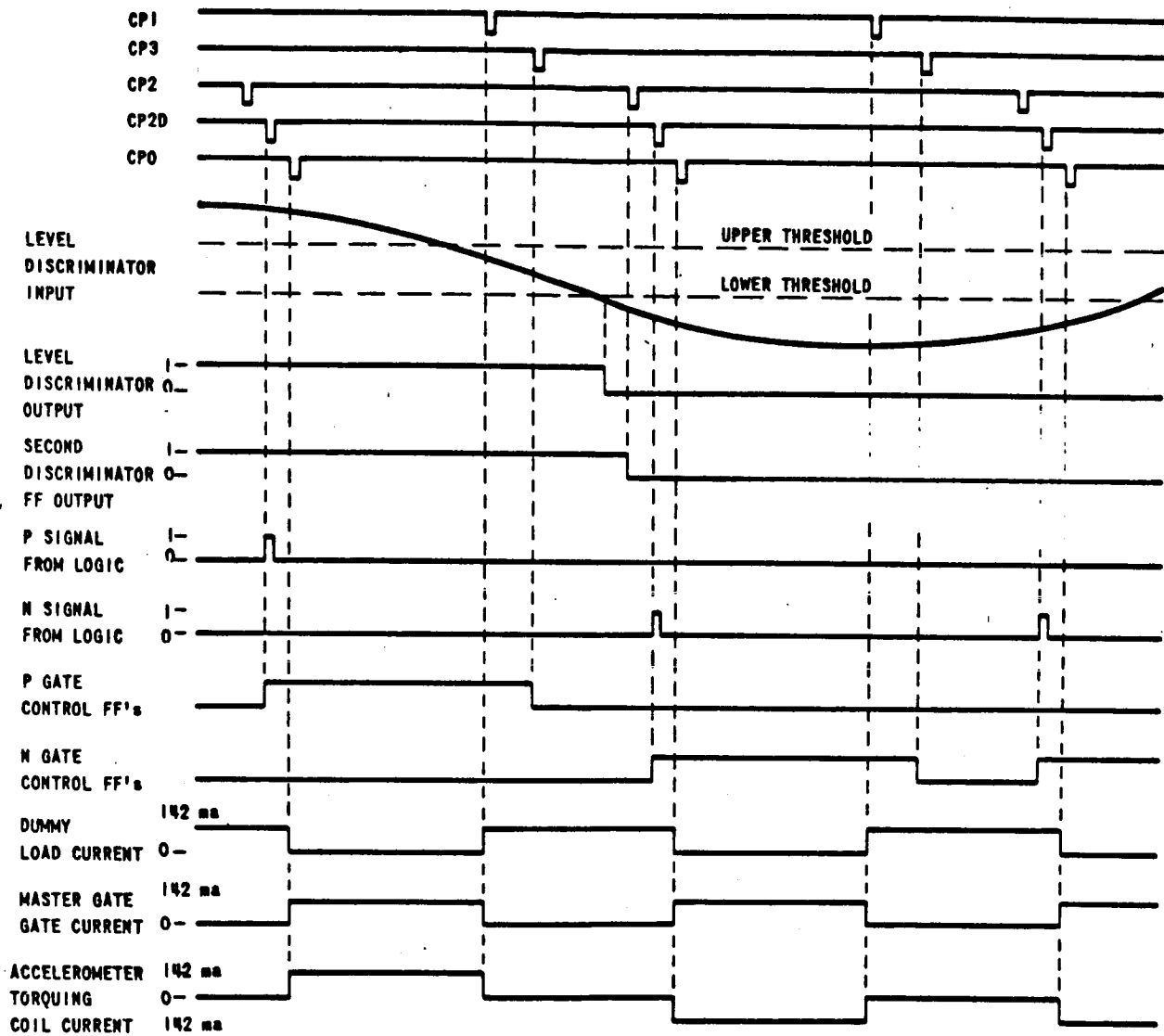


FIGURE 2.15-5. ACCELEROMETER PULSE

First, assume that all control flip-flops are in the "0" state. (Refer to the accelerometer current bridge logic diagram, Figure 2.15-4.) In this condition, current flows from the accelerometer rebalance current supply (ARCS) through the dummy load control gate, bypassing the bridge.

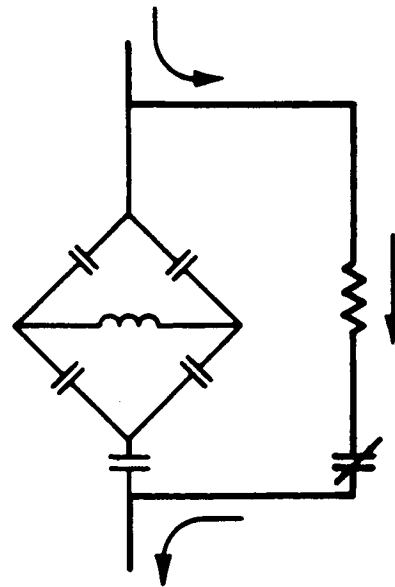


FIGURE 2.15-6

The P_1 and P_2 gate control flip-flops have been set by the control logic. Current continues to flow through the dummy load since the state of the master gate control flip-flop is unchanged at this time.

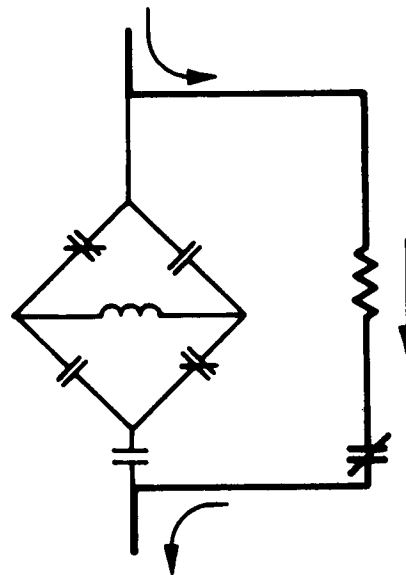


FIGURE 2.15-7

The master gate control flip-flop has been set. Current now flows through the master gate, through the P_1 gate, the accelerometer torquer coil, and the P_2 gate to the sensing resistor. The current through the accelerometer torquer coil produces a positive torque on the accelerometer pendulum.

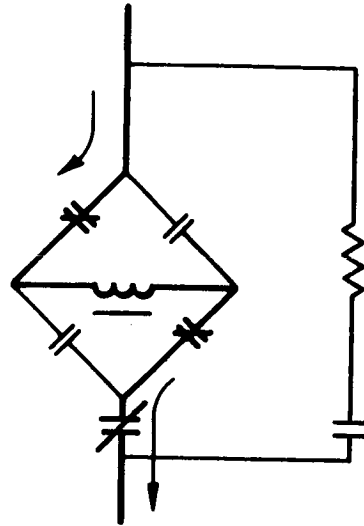


FIGURE 2.15-8

The master gate control flip-flop has been reset. Current has been switched back to the dummy load, since the Z gate switch is again closed.

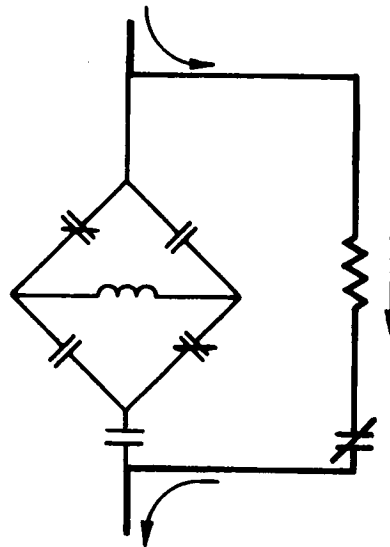


FIGURE 2.15-9

The P_1 and P_2 gate control flip-flops have been reset by the control logic. Current continues to flow through the dummy load since the state of the master gate flip-flop is unchanged at this time.

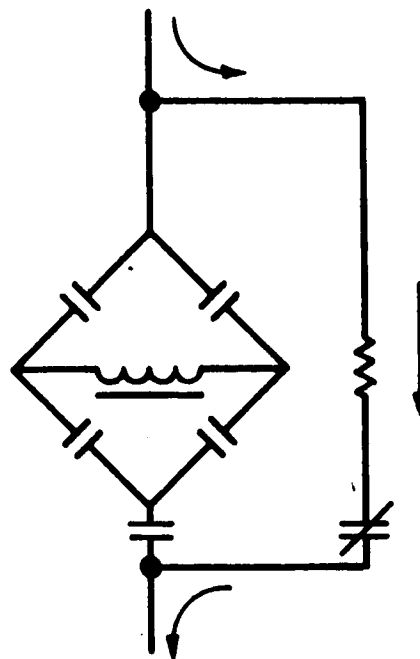


FIGURE 2.15-10

The N_1 and N_2 gate control flip-flops have been set by the control logic. Current continues to flow through the dummy load.

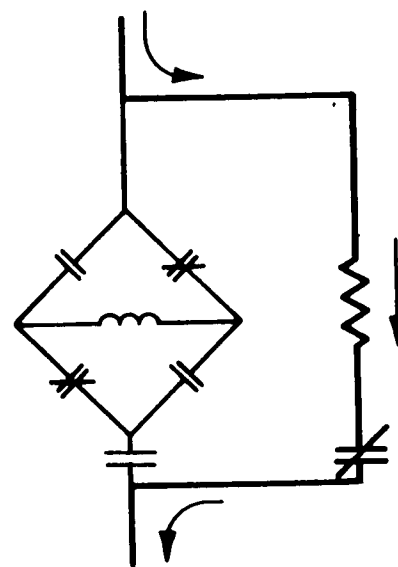


FIGURE 2.15-11

The master gate control flip-flop has been set. Current now flows through the master gate, N_1 gate, accelerometer torquer coil, and N_2 gate to the sensing resistor. Current through the accelerometer torquer coil produces a negative torque on the accelerometer pendulum.

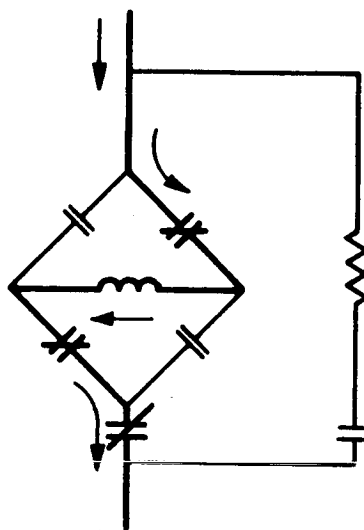


FIGURE 2.15-12

The master gate control flip-flop has been reset by the control logic and again current flows through the dummy load.

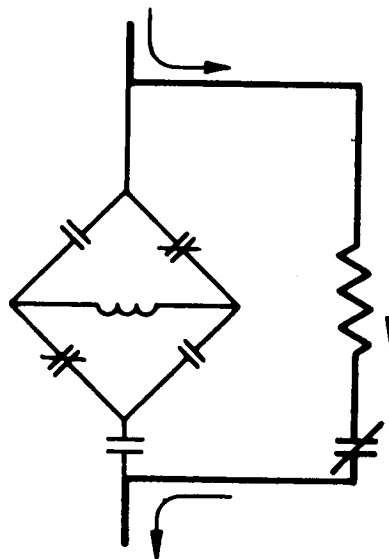


FIGURE 2.15-13

The N_1 and N_2 gate control flip-flops have been reset by the control logic. Current continues to flow through the dummy load.

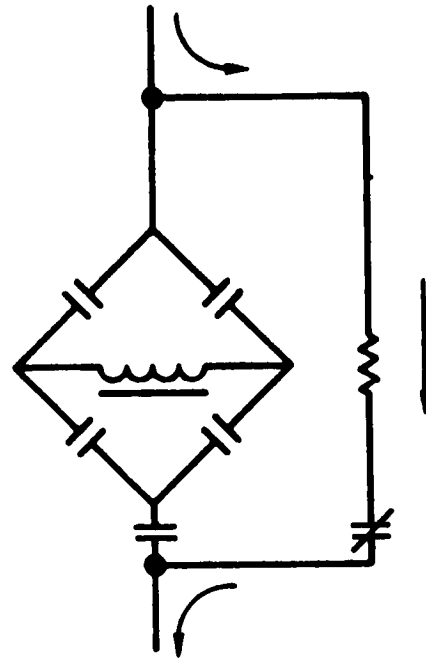


FIGURE 2.15-14

2.15.2. Description of Major Elements of the PRE. -

2.15.2.1. Carrier Amplifier and Demodulator. - This circuit amplifies and demodulates the accelerometer output. The characteristics of the amplifier, gain rolloff of 20 db per octave, with breaks at 14.4 kHz and 144 kHz, provide suitable amplification for the carrier and sidebands. The amplifier has a nominal gain of 1.6V/V, and the demodulator has a gain of 0.88 volt dc/volt rms, for an overall gain of 1.4 volts dc/volts rms. There are three identical channels on the one board, one for each velocity loop. Only one channel will be discussed.

The carrier amplifier receives its 14.4 kHz input signal from the accelerometer preamplifier. The input impedance of the amplifier is 20K ohms or greater and the output impedance is less than 1.1K ohms. The input signal is amplified by two class A stages and transformer coupled into the full wave demodulator.

The reference for the demodulator is provided by the 14.4 kHz demodulator driver. The driver generates two 14.4 kHz square waves 180 degrees out-of-phase with each other. The output of the demodulator is sent to the dc amplifier and networks assembly.

2.15.2.2. DC Amplifier and Networks. - The purpose of the dc amplifier and networks assembly is to:

1. Provide the necessary filtering of the 14.4 kHz carrier and its harmonics.
2. Provide the necessary phase relationships for accelerometer rebalance loop stability.
3. Provide additional gain to the accelerometer loop.
4. Provide the summing capability for combining the accelerometer analog output and the integrated rate feed-back signal from the level discriminator.

There are three dc amplifier and network assemblies in the system; one for each accelerometer loop.

The amplifier is a conventional operational amplifier with two inputs (see Figure 2.15-15). The input from the carrier amplifier and demodulator is through the forward loop networks. This network provides the

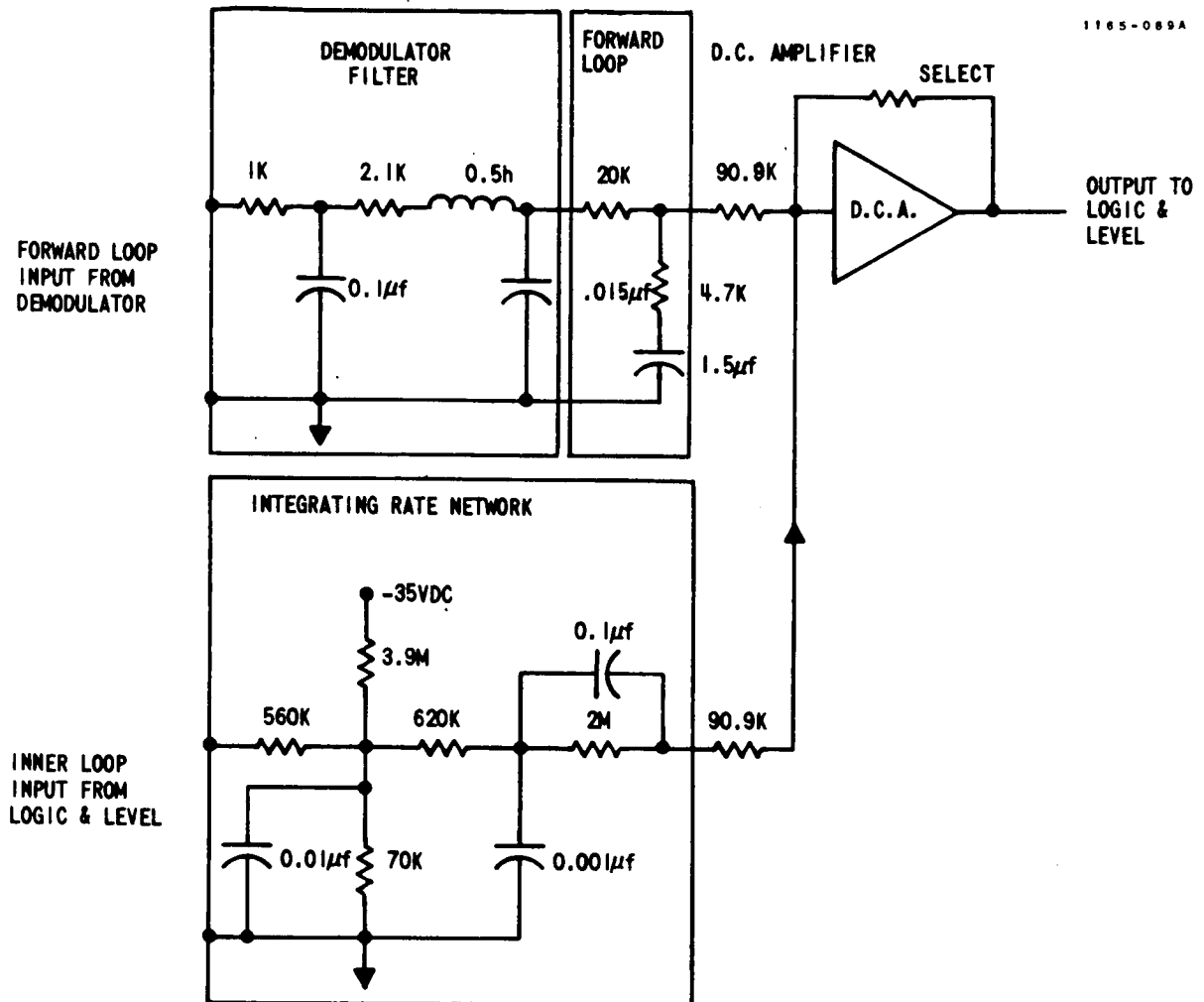


FIGURE 2.15-15. DC AMPLIFIER BLOCK DIAGRAM

necessary gain characteristics for the pulse rebalance velocity loop as well as removing the 14.4 kHz and all harmonics thereof. The other input to the amplifier from the rebalance logic and level discriminator is through the integrating rate network. This input is used, in conjunction with other electronics, to achieve improved pulse rebalance velocity loop operation at low inputs to the loop. The operational amplifier is a direct-coupled amplifier without any chopping and demodulation scheme employed. It has a wide passband, and, therefore, has no effect on the frequency characteristics of the amplifier assembly as determined by the networks.

2.15.2.3. Accelerometer Rebalance Logic and Level Discriminator. - This device controls the polarity of the torquing pulses in accordance with signals from the dc amplifier and provides pulses to the ΔV output board, representing positive and negative increments of velocity.

A block diagram of the accelerometer rebalance logic and level discriminator is shown in Figure 2.15-16. The basic function of the circuit is to sample the dc level of the demodulated and amplified input signal and thereby control the gates (P and N) in the current bridge. A secondary function is to supply the ΔV output circuit with pulses proportional to the length of time between changes of polarity in the input dc level (velocity increments). Amplitude detection is accomplished by a tunnel-diode level detector circuit. Pulse amplifier 1 (see Figure 2.15-16) is triggered to give negative pulses to the \bar{A} side of the A-A flip-flop when an input A-A voltage greater than the positive threshold voltage is applied to the input. Conversely, pulse amplifier 2 feeds negative pulses to the A side of the flip-flop when the input signal is greater than the negative threshold voltage. At C2 time, flip-flop B-B is gated as a function of the state at A-A. Gates 1 and 2 are AND gates. They provide a negative output when both inputs are negative. Gates 3 and 4 are NOT-AND gates. They provide positive output when both inputs are negative. At C2D time, pulse amplifier 3 or 4 receives an input if there is a B or \bar{B} output respectively. Assuming a B output, the output of pulse amplifier 4 will set the current gate control flip-flops P0-P $\bar{0}$ and P1-P $\bar{1}$ to the P0 and P1 states respectively, thus providing a positive accelerometer torquer pulse. The same output provides a $-\Delta V$ pulse to the $+\Delta V$ output circuit.

The converse is true for pulse amplifier 3 outputs and $+\Delta V$ outputs. At C3 time, the current gate control flip-flops are reset thereby assuring that there will be no accelerometer torquer current pulses until the next C2D pulse occurs. Figure 2.15-5 shows the effect of the accelerometer signals and clock pulses on the accelerometer rebalance logic and level discriminator.

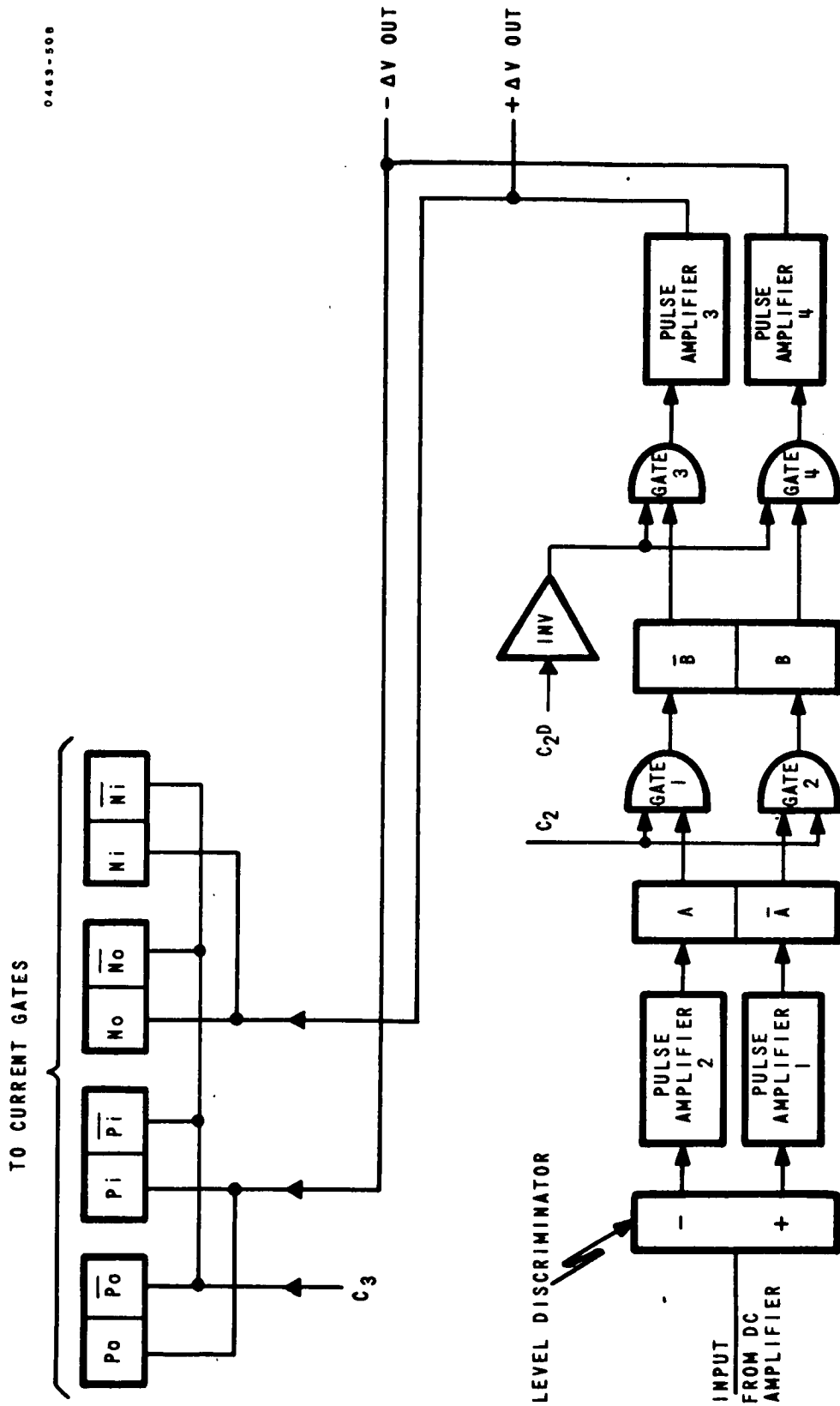


FIGURE 2.15-16. ACCELEROMETER REBALANCE LOGIC AND
LEVEL DISCRIMINATOR BLOCK DIAGRAM

2.15.2.4. Master Gate and Current Bridge. - The purpose of the master gate and current bridge is to switch the constant current provided by the ARCS between the accelerometer torquer coil and the dummy load. There are three master gate and current bridge boards in the system; one for each accelerometer loop. A simplified block diagram of the current bridge is shown in Figure 2.15-17.

The current bridge directs the pulse of torquing current through the accelerometer coil as directed by the current gate control flip-flops located in the velocity loop logic and level discriminator. The circuit consists of two pairs of transistor switches: P_0 and P_1 , N_0 and N_1 . The P and N gating levels are applied to diagonally opposite steering switches. The N or P gating levels from the current control flip-flops close the respective switches. Since only P levels or N levels are received, only one pair of switches is closed at a given time. The bridge is then set at C_{2D} to direct the current through the torquer coil when the master gate is closed at C_0 . At C_1 time the master gate flip-flop is reset, and the master gate opens. At C_3 time, the current control flip-flops are reset. The cycle is then complete.

The master gate, shown in block form in Figure 2.15-18 sets the duration of the current pulse through the torquer coil. The current gate control flip-flops set up the current bridge at C_{2D} time which precedes C_0 by 17.4 microseconds. This is sufficient time to allow switching transients to decay before the torquing current is applied.

The master gate flip-flop determines the signal levels of transistor gates Q_{10} and Q_4 . At C_0 time, the signal level at Q_{10} is high permitting current to flow through the current bridge, which directs the current flow through the torquer coil, and the signal level at Q_4 is low, cutting off current flow to the dummy load. At C_1 time, the signal levels are reversed and current flows through the dummy load.

A sensing resistor in series with the output line is connected to test points, which permit monitoring of the presence and polarity of torquing current pulses. The series RC network across the output lines compensates for the inductance of the accelerometer torquer coils. The variable resistor permits exact matching of the resistance of each torquer winding. Variable resistors are included in each of the current paths to permit balancing of the resistances through the three current paths. A capacitance is connected in series with the resistance to balance the torquer coil inductance.

0765-162A

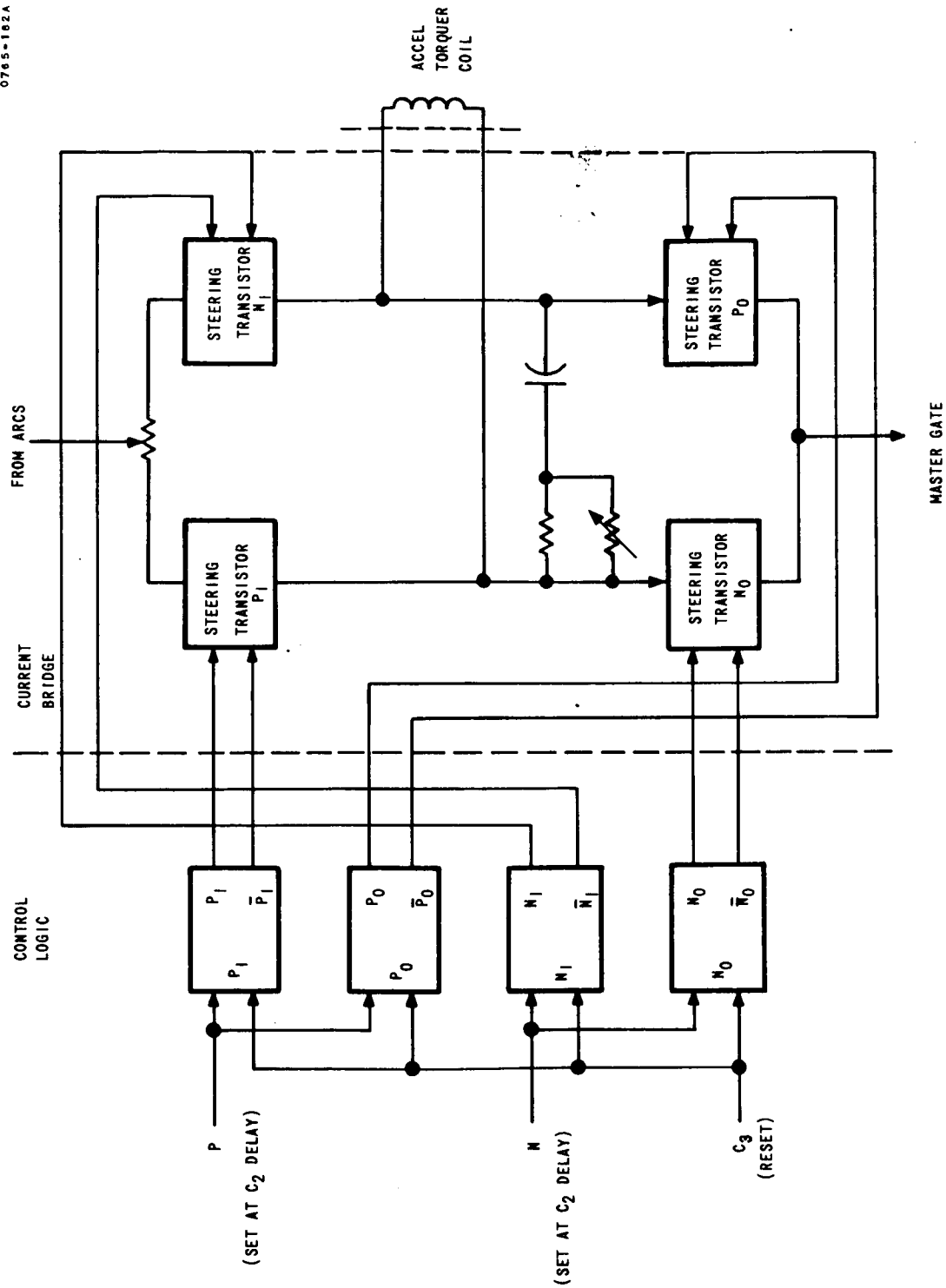


FIGURE 2.15-17. CONTROL LOGIC AND CURRENT BRIDGE BLOCK DIAGRAM

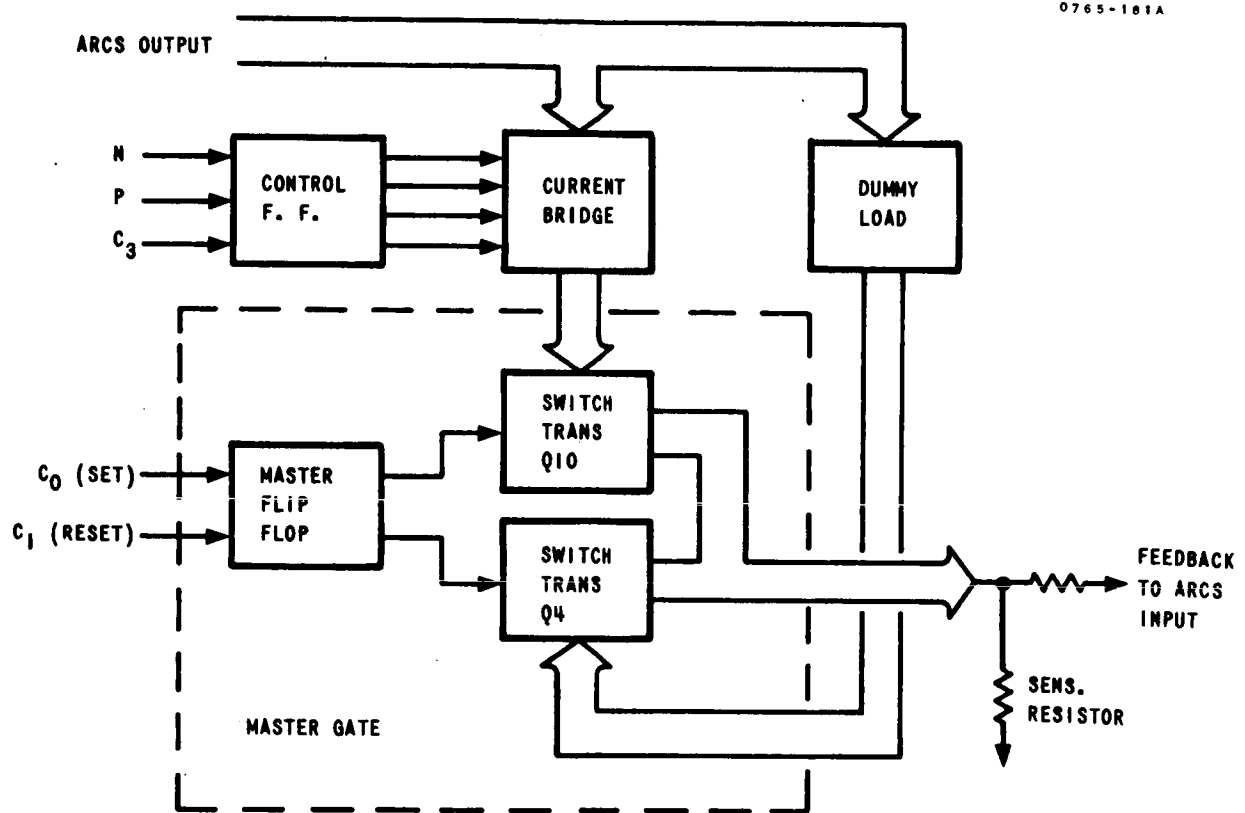


FIGURE 2.15-18. MASTER GATE BLOCK DIAGRAM

2.15.2.5. ΔV Outputs. - This device accepts signals from the accelerometer rebalance logic and level discriminator and conditions these pulses to a form acceptable to the Navigation Computer. As there are three accelerometer loops and each loop may have two direction signals, there must be six ΔV output circuits. Each circuit, which is identical, serves to lengthen a ΔV pulse in time and to amplify the pulse in voltage and power.

Each circuit consists of a one-shot multivibrator which is triggered by input pulses, and a two-stage ac-coupled amplifier. The output pulses are transformer coupled to the computer and the signal conditioner.

2.15.2.6. 14.4 kHz Demodulator Driver. - This unit supplies the drive signal for the diode demodulator on the carrier amplifier assembly. As shown in Figure 2.15-19, the unit consists of a common buffer amplifier, a phase shift and squaring network, and a drive network for each of the three outputs.

The input for the circuit is 6.0 volts rms, 14.4 kHz sine wave, synchronized with the accelerometer signal generator primary excitation.

2.15.2.7. Accelerometer Rebalance Current Supply (ARCS). - This unit provides a constant current (142 ma) to the accelerometer torque coil or the dummy load, depending on the setting of the master gate and the dummy load gate of the current bridge circuit. The dummy load provides the ARCS with an equivalent load during the off portion of the torque cycle.

There are three ARCS units, one for each accelerometer loop. The ARCS units are mounted in a temperature controlled oven along with a precision voltage reference that provides the ARCS unit with a highly regulated input voltage. This voltage determines the value of the constant current. The oven temperature is controlled to within $\pm 1.0^\circ\text{C}$ of a value near 100°C .

The torque current passes through a precision sensing resistor (also located in the oven) to ground, developing a voltage across the resistor. This voltage is summed with the reference voltage input and the resulting summed voltage is applied to the ARCS input as a feed-back signal to maintain the current constant. The function of the ARCS unit is shown in Figure 2.15-20.

2.15.3. Summary of PRE Velocity Loop Evolution. - From the beginning of the Centaur Program, considerable effort has been expended to improve the velocity loop associated with the inertial guidance system (IGS). More

0666-095A

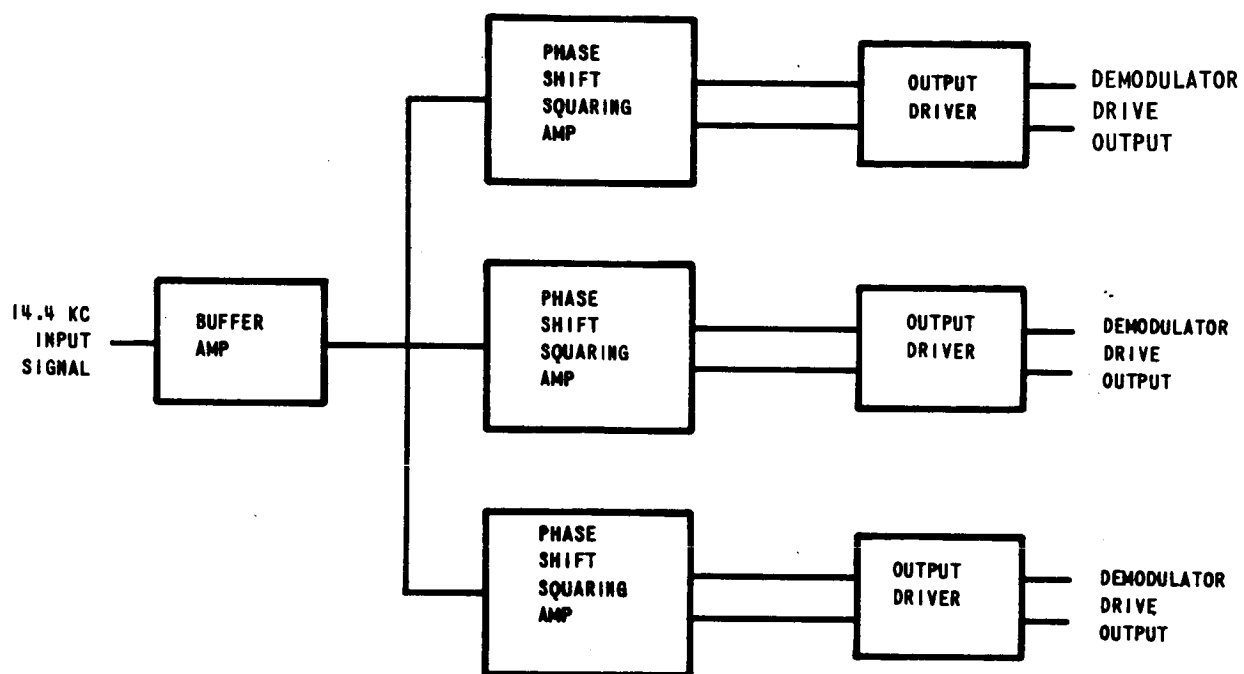


FIGURE 2.15-19. 14.4 KC DEMODULATOR DRIVER

0566-405A

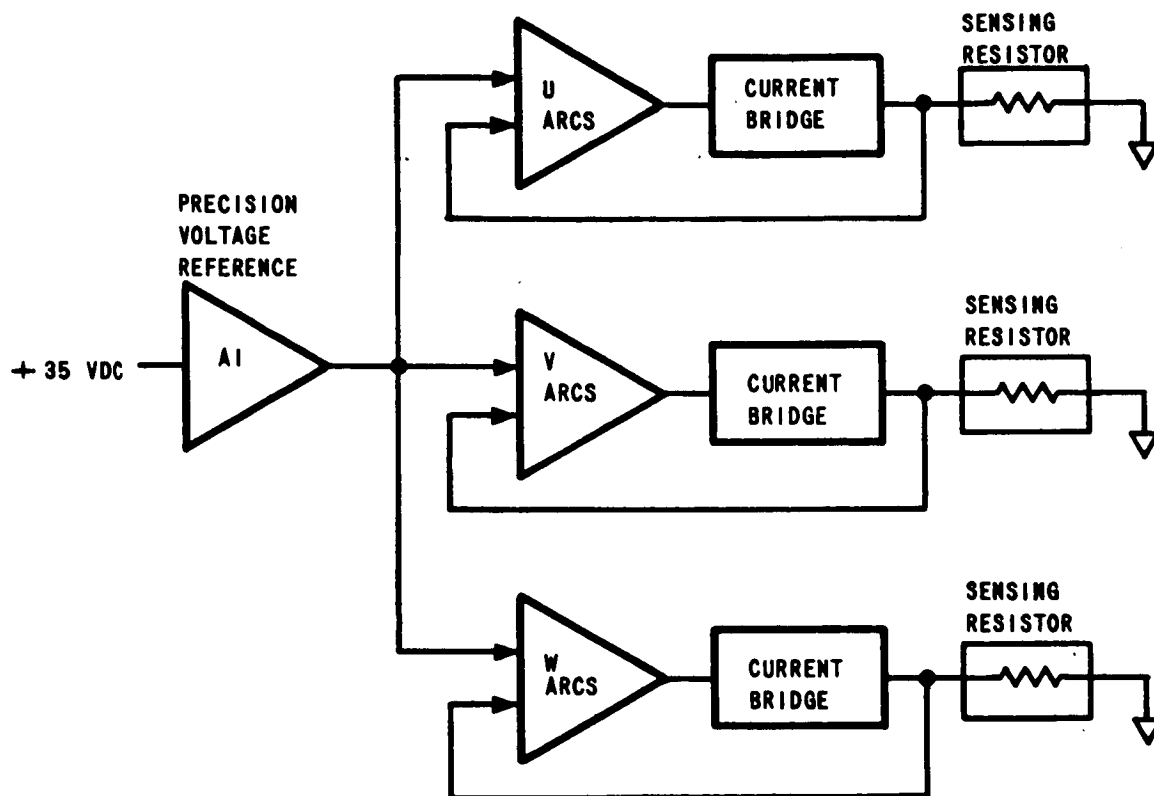


FIGURE 2.15-20. PRECISION VOLTAGE SUPPLY AND
ACCELEROMETER REBALANCE CURRENT SUPPLIES

8. Gate capacitors were changed from mylar to ceramic to eliminate erratic performance caused by intermittent opens in mylar units.

2.15.5. -3 Centaur Program. - The -3 program incorporated most of the major design changes to the velocity loop (excluding the accelerometer). The initial changes made to the velocity loop at the beginning of the -3 program were:

1. The output capacity of ARCS was increased by changing transistor type to permit operation at lower stress level.
2. The phase shifter and buffer amplifiers of the 14.4 kHz demodulator driver were moved from the interconnect board to a plug-in module to reduce wire runs and noise pickup.
3. Logic and level discriminator was redesigned to:
 - a. Replace unstable Schmidt trigger, which was difficult to adjust, with stable tunnel diodes, requiring no adjustment.
 - b. Increase stability of flip-flops used to control current bridge and master gates.
 - c. Relocate 4 kHz rectifiers by removal from board to reduce noise level.
4. Master Gate was redesigned to:
 - a. Reduce number of adjustments required.
 - b. Reduce number of components required by taking advantage of advances in transistor gain and stability characteristics.
5. The delay requirements in logic reduced to two microseconds to permit elimination of one delay line unit.
6. The Oven for precision reference components redesigned to reduce temperature changes on precision components from $\pm 5^{\circ}\text{C}$ to $\pm 1^{\circ}\text{C}$.
7. The Heat Sink for output transistors on ARCS boards was redesigned to increase thermal conductivity.

design changes and retrofit efforts have been done in this area than any other in the IGS. The changes have been necessary for two reasons; (1) the inherent complexity of the loop and (2) the opportunities for improved performance offered by the improvements in electronic components. The chronological history or evolution of the major changes made in the velocity loop can be outlined as follows:

1. Changes during Centaur dash one (-1) effort.
2. Changes during Centaur dash three (-3) effort.
3. Phase I Product Improvement Program (PIP).
4. Phase II Product Improvement Program (PIP).

Some of the major changes incorporated into the Centaur IGS during the -1 and -3 efforts will be enumerated here. A detailed discussion of the problems and solutions will not be made at this time because similar problems were encountered with the Phase I PIP and Phase II PIP hardware.

2.15.4. Centaur (-1) Changes. - Major changes incorporated during the Centaur -1 effort are listed as follows:

1. The ARCS board was redesigned and repackaged to decrease the output tolerance from 0.1 percent to 0.03 percent.
2. The delta V output board was redesigned and repackaged to employ reliable circuits.
3. The phase shifter and buffer amplifier were redesigned to improve impedance match and phase variation between 14.4 kHz input and demodulator drive circuitry.
4. The digital filter was removed from the logic board to reduce circuitry and increase information obtained from delta V pulses.
5. The rate network was modified to increase dynamic operating range of accelerometer loop from 8 g's to the required 11 g's.
6. All potentiometers were removed from feed-back networks in the summing oven, to eliminate vibration induced noise and increase dependability.
7. Gate transistors were changed from mesa type to planar type to reduce gate leakage.

The lower limit cycle provides increased resolution and decreased pendulum swing. The reduced pendulum swing, in turn, reduces cross coupling of "g" inputs along the pendulum axis. In addition, the more predictable loop performance of the new loop, in turn, permits more predictable system performance.

With the new configuration, it was possible to increase the gain of the forward loop so that there was less standoff or pendulum displacement under all values of steady "g" inputs.

2.15.6.1. Basic Operation. - Figure 2.15-21 is a block diagram of the -3 Centaur velocity loop. The accelerometer signal generator output is amplified on the platform, amplified again in the coupler, demodulated, filtered, sent through a rate network, amplified in the dc amplifier and this voltage applied to the logic and level discriminator. Here a decision is made on which polarity of torquer pulse is required to bring the accelerometer pendulum back to null. Any time the voltage into the level discriminator exceeds 0.1 volt, it triggers the discriminator input circuitry and sets a flip-flop, either positive or negative, depending on the polarity of the input voltage.

The state of this flip-flop is checked at discrete times, referred to as C2. C2 occurs 3,600 times per second. The state of the flip-flop at time C2 sets the state of a second flip-flop, which in turn determines the polarity of the next torquer pulse, which is triggered 28 microseconds later. As can be determined from Figure 2.15-21, the dc gain for the previous Centaur -3 Velocity Loop between the output of accelerometer signal generator and the input to the level discriminator was 182 volts/volt. At frequencies above 2,400 Hz, due to the lead compensation, the gain was 1,820 volts/volt. (The reason for the lead compensation was to provide stability margin.) This value of gain means that 55 microvolts at the platform is sufficient to trigger the logic and explains the high noise sensitivity of the loop.

Figure 2.15-22 is a block diagram of the Integrated Rate Velocity loop. The signal is amplified on the platform, amplified again in the coupler, demodulated, filtered, sent through a lag network and summed with a feed-back signal from the logic and level discriminator. Note that, except for increased gain, the new loop is similar to the previous Centaur loop up through demodulation. The logic and pulse generation circuits are the same as in the previous Dash Three Centaur.

8. All tantalum type B (85°C) capacitors were replaced with type C (125°C) where possible to reduce failure rates.
9. A stress analysis was run on electrical components to find and replace parts too highly stressed for dependable operation.
10. Re-packaging of the ARCS in the existing oven to permit use of simple, direct-coupled amplifier in place of chopper-stabilized amplifiers. Parts count reduced from 468 to 78.
11. The use of simple, direct-coupled zener reference as replacement for precision voltage reference requiring two chopper-stabilized high gain amplifiers. Parts count reduced from approximately 150 to 10.
12. The redesign of the rate network to improve loop accuracy and stiffness.

2.15.6. Integrated Rate Loop. - Late in 1962, a modification to the velocity loop was conceived which would make the loop less sensitive to noise input and more predictable in performance. During 1963, this modification, after testing, was installed in the Centaur velocity loop. This modification provided a new way to stabilize the accelerometer (or velocity) loop not by lead networks which were previously used but by an inner damping loop which integrated the output from a flip-flop, whose state was a function of torquing pulse polarity. This "inner loop" signal was summed with the forward loop signal from the accelerometer at the input to the dc amplifier. This method of obtaining damping, as compared to the use of lead compensation in the forward loop, resulted in an accelerometer loop which was less sensitive to noise.

Also, a temporary opening of the forward loop, between accelerometer and the dc amplifier, (such as open slip rings) does not remove damping from the loop. This prevents the loop from being driven hard over by the torquer rebalance signal. Thus, a temporary opening of the loop does not result in a loss of information if the time involved is sufficiently short so the "g" input being sensed by the accelerometer does not drive the pendulum to the stops.

The basic limit cycle with the configuration near null is two pulses. However, when the accelerometer is sensing any "g" level greater than 0.5×10^{-5} , the limit cycle will exhibit one, two, and three pulses in succession, depending on whether the basic two pulse drops or adds a pulse to provide information.

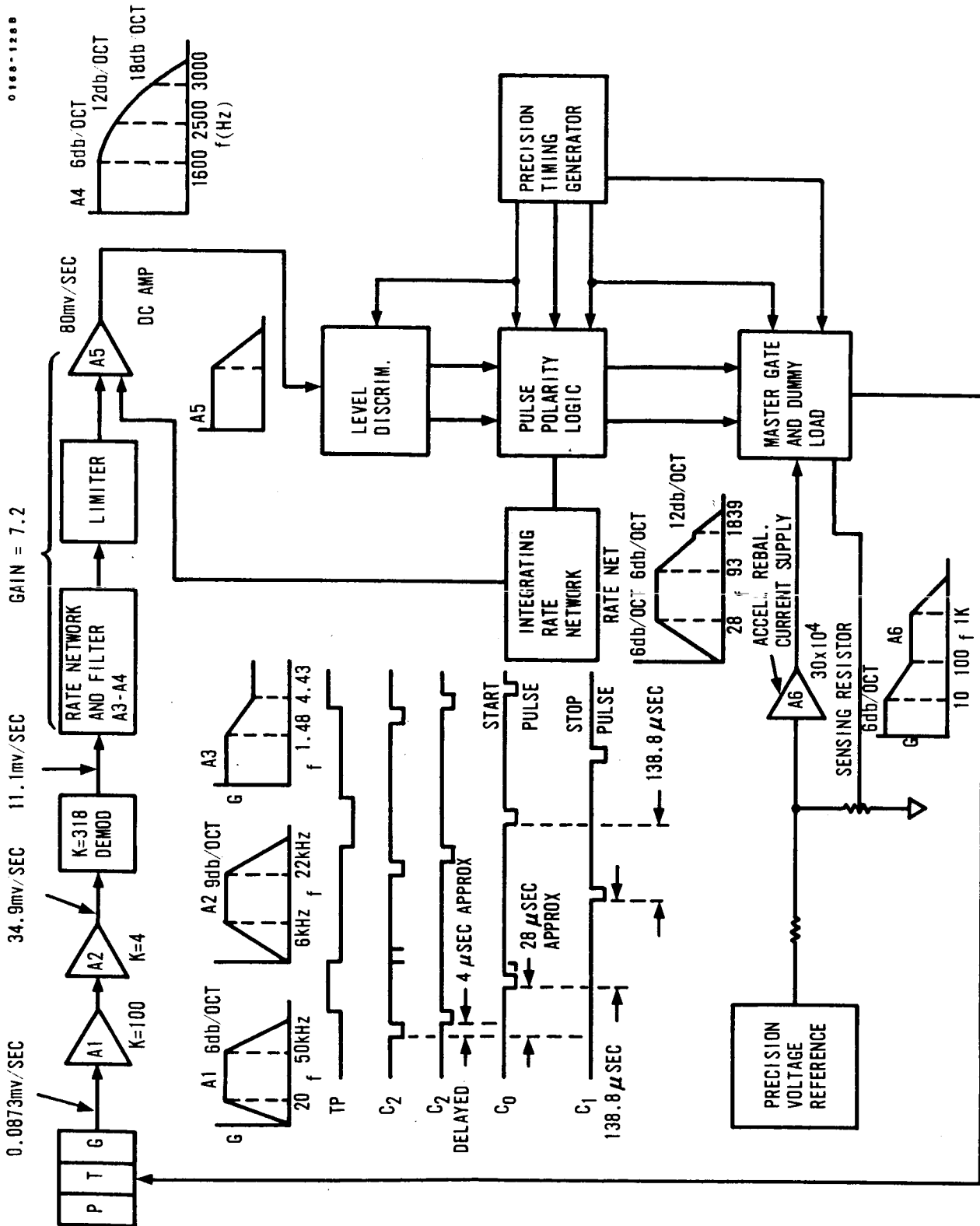


FIGURE 2.15-22. INTEGRATED RATE LOOP BLOCK DIAGRAM

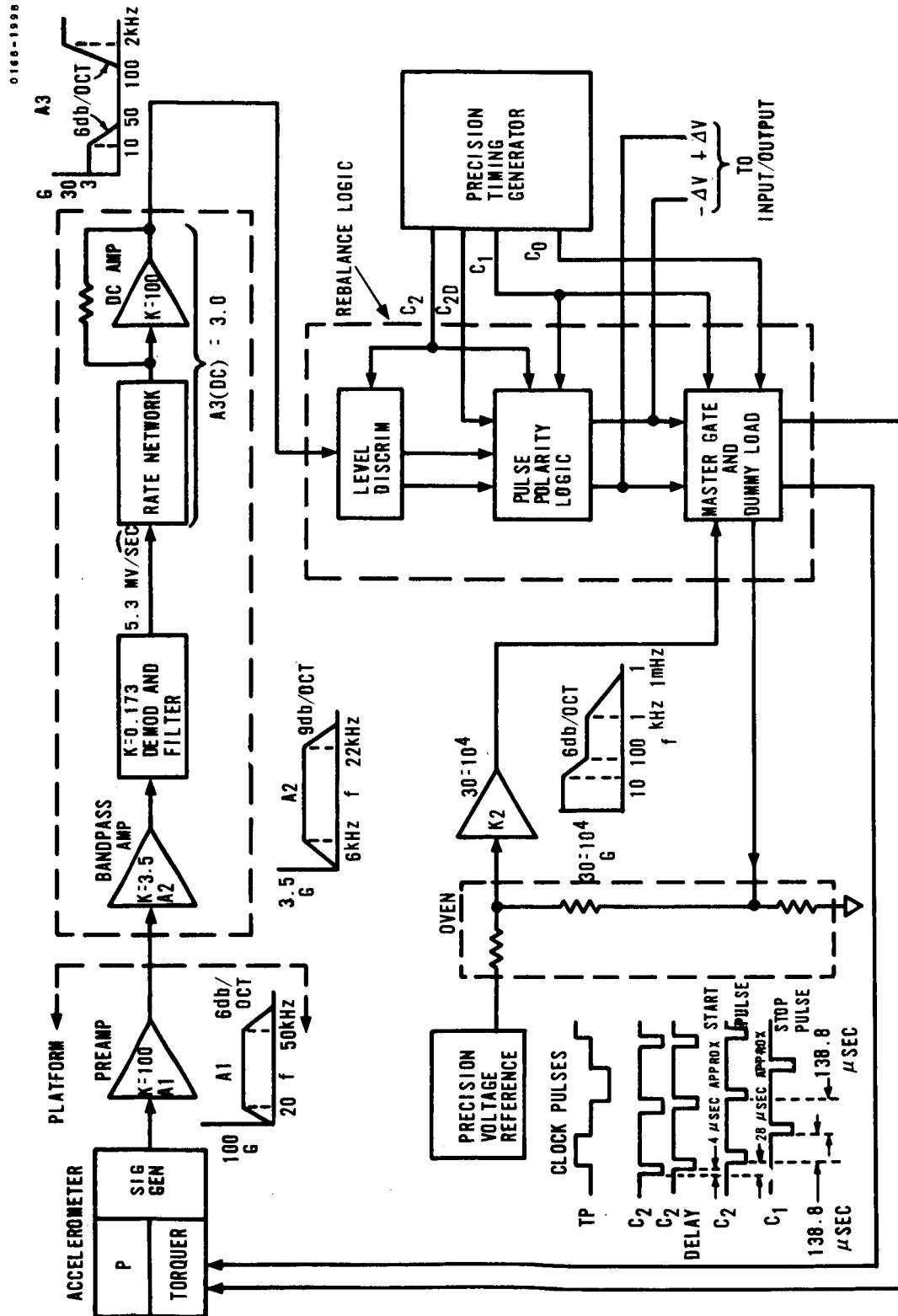


FIGURE 2.15-21. -3 CENTAUR VELOCITY LOOP

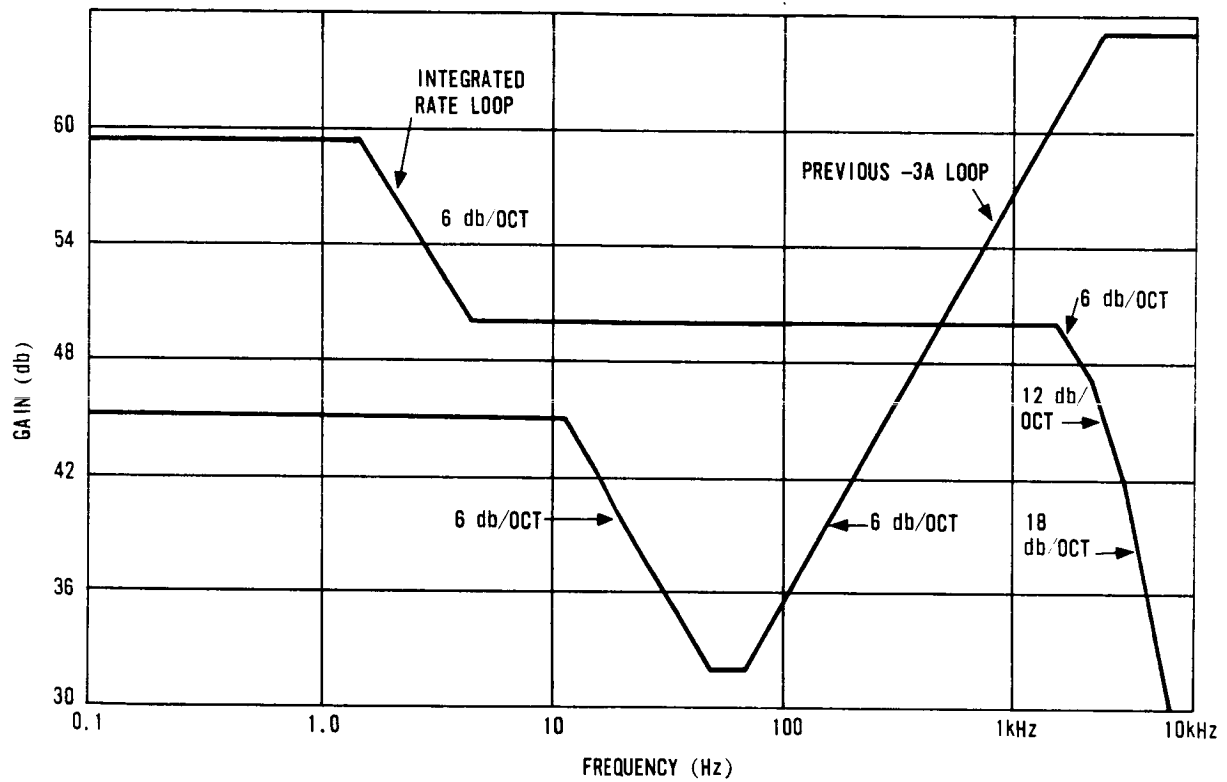


FIGURE 2.15-23. GAIN FROM SIGNAL GENERATOR
TO LOGIC INPUT

The differences between the two loops are (a) the absence of any lead compensation in the forward path of the new loop and (b) the feed-back path through a network from the pulse polarity logic to the dc amplifier input. The feedback provides the damping signal required for stability so that lead compensation in the forward loop is not required. It is therefore possible to have a loop which is much less sensitive to noise as shown by Figure 2.15-23, which shows a comparison of the analog section frequency response (asymptotes only) of the integrated rate loop with the previous Centaur loop. Note that while the integrated rate loop has higher gain at dc and through the low frequency range, it has much less gain at the higher frequencies, 1.8 kHz up, where noise is introduced.

2.15.6.2. The "Pure Rate" Analogy. - To gain insight into the operation of the new loop, note that at zero g input, a voltage proportional to the rate of the pendulum can be obtained by passing the torquer pulses through the proper lag time constant. In Figure 2.15-24, if the pendulum position is denoted by θ and θ is dependent only on the torquer pulses (0 g-input), then θ as a function of torquer pulse input is:

$$\frac{\theta}{T} = \frac{3.7}{S(S+281)} \text{ rad/ma}$$

if it is known what θ is doing, the torquer pulse input can be expressed in terms of θ by:

$$T = \frac{S(S+281)}{3.7} \times \theta$$

If this signal is passed through a lag,

$$\frac{3.7}{S+281},$$

the resultant signal is $S\theta$ or $\dot{\theta}$. Thus a signal which is proportional to $\dot{\theta}$, or rate, has been developed by lagging or integrating the torque pulses--hence the name, integrated rate loop. This signal can now be used for loop stabilization. However, this new damping signal bypasses the tremendous high frequency attenuation of the accelerometer. Therefore, as compared to a rate signal obtained by differentiation of θ (a lead network) it is much less susceptible to noise.

0188-109A

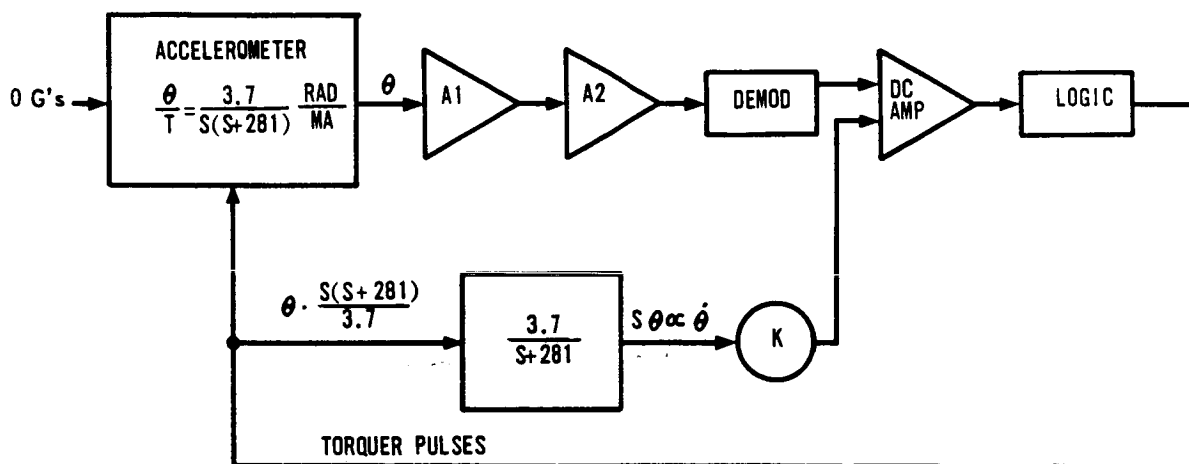


FIGURE 2.15-24. "PURE RATE" DERIVATION AT ZERO G INPUT

Figure 2.15-24 is a block diagram illustrating the above principle. Figure 2.15-25 is a block diagram of actual loop transfer functions including the inner loop.

2.15.6.3. The -3 Velocity Loop in Retrospect. - The original design goals for the integrated rate loop were as follows:

1. Reduce the loop noise sensitivity.
2. Increase static gain.
3. Reduce pendulum swing.
4. Provide a predictable null limit cycle.
5. Not degrade other performance characteristics.

How well each of the above objectives were met and the validity of each will now be examined.

The construction and packaging of the -3 Velocity Loop was exceedingly dense in order to meet the size/weight requirements. EMC (Electro-magnetic Compatibility) in the original design was inadequate. Noise was indeed a problem. Previously, system delivery schedules were seriously impaired by the time required to reduce the velocity loop noise. The integrated rate modification made the loop less susceptible to noise by reducing loop gain at higher frequencies.

Static gain was increased by a factor of five to one; however, the correspondingly smaller loop threshold, which was expected to result, was not realized. Some threshold improvement was accomplished. However, other factors were found to obscure the actual threshold.

Pendulum swing at null, and at static "g" levels out to ten "g's", was reduced by a factor of ten to one, primarily due to the gain and response of the loop.

The null limit cycle was lowered from a rather random combination of numbers from 1 through 8 to predominately 1-2-3. This was a big improvement; however, the limit cycle was not predictable in some cases.

Performance was degraded by the integrated loop in one area. Loop gain was reduced at higher frequencies in order to reduce loop susceptibility to noise. This reduction of loop gain occurred over part of the vibration

frequency range. This caused the loop to be more susceptible to vibropendulous errors*. The vibration levels measured during the first Centaur flight indicated that this was not a critical problem.

A tradeoff study should have been conducted and a compromise made between velocity loop susceptibility to noise and susceptibility to vibration. During later design improvements, the sources of noise were eliminated with no penalty in system performance.

The elimination of these noise sources, however, required almost a complete loop redesign and layout, as was later determined during Phase II PIP. The mandatory support of a flight schedule required a system that would meet the requirements at the time of the flight, whether or not it was an optimum system.

2.15.6.4. Conclusions. - A necessary and novel modification to the -3 velocity loop was conceived during 1962 and 1963, in the form of a better way to dampen the loop. Essentially the damping was done by a "derived rate" feed-back signal. The rate was derived by integrating the digital signal, which was fed to the torquing gates by the level discriminator. This rate signal was summed with the forward loop signal and fed into the dc amplifier input as a positive feed-back signal.

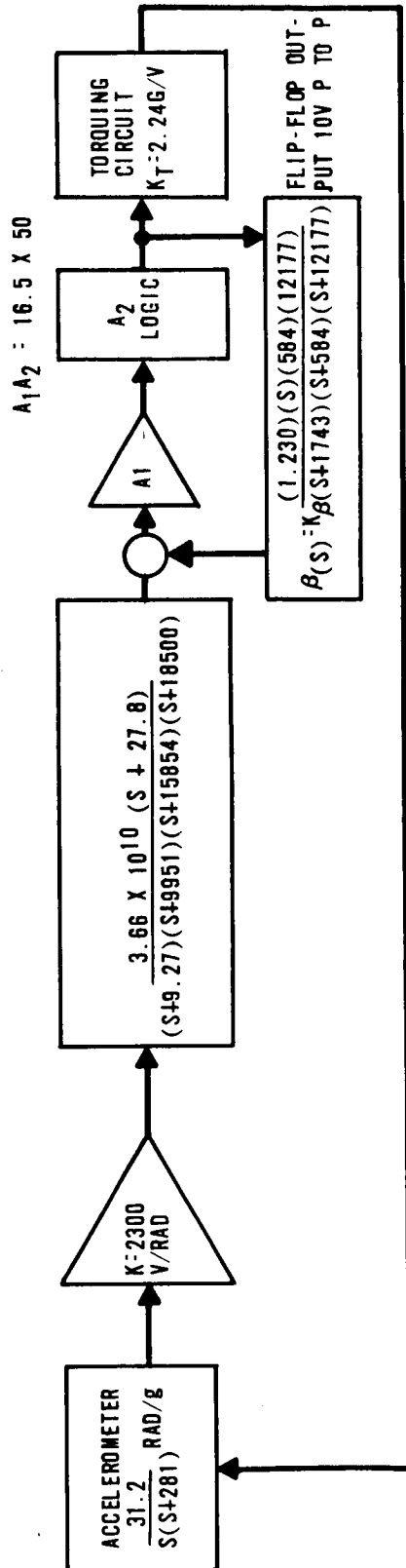
The advantages of this mechanization were:

1. Loop less susceptible to noise.
2. Lower limit cycle.
3. Less pendulum swing.
4. Loop control maintained during short openings.
5. Increased static gain.

Since loop gain over the vibration frequency range was reduced, the error due to the vibropendulous effect was increased. Any future loop design should include a tradeoff study of noise susceptibility versus vibration susceptibility in order to determine an optimum forward loop frequency response.

* When a pendulum is vibrated, it will have an oscillation motion which, under certain conditions, will cause an average torque (other than zero) to be developed about the pivot axis.

0166-1108



TORQUING PULSES

22.4 G's 50% OF TIME OR EQUIVALENT 11.2 G's PER PULSE

$$K_T = \frac{11.2 \text{ G's (EQUIV. TORQUER PULSE)}}{5V(\text{FLIP-FLOP SWING AROUND AVERAGE})} = 2.24 \text{ G/V}$$

TOTAL LOW FREQUENCY OPEN LOOP TRANSFER FUNCTION (G(S))

$$G(S) = \frac{(31.2)(2300)(0.15)(S+27.8)(5+174.3)(S+584)(2.24)}{S(S+4.1)(S+281)(S+9.27)(584)(0.075)K_\beta}$$

$$K_\beta = 0.67 \text{ (VALUE FOR BEST FIT)}$$

FIGURE 2.15-25. LINEAR ANALOGY OF INTEGRATED RATE LOOP

circuit to reject quadrature. After trying various circuit combinations the best quadrature rejection was obtained by placing a selected resistor in parallel with one-half of the primary coil. This balanced the impedance of the signal generator and reduced the quadrature voltage to acceptable levels.

It was necessary to tune the secondary of the accelerometer signal generator in order to reject unwanted signals. This tuning was done by placing a capacitor across the signal generator secondary. Calculations were performed to ensure that the combination of inductance of the signal generator, the input impedance of the preamplifier, and the tuning capacitor were of such values as to form a tuned circuit that has a resonant frequency of 14.4 kHz and a roll-off rate of 12 db per octave with the proper damping factor. Engineering tests were performed to assure that these criteria were met. Signal side band attenuation by the tuned circuit was also examined.

Previously, the secondary of the signal generator was tuned with a parallel combination of a capacitor and transformer. This method served two purposes; it provided the necessary tuning and it served as an isolation element for common mode rejection of the accelerometer torquer signals. This rejection was needed because of the close proximity of signal generator and torquer leads. In the GG177 Accelerometer, care had been taken to route the torquer and the signal generator leads so that pick-up was minimized. As a result, the isolation transformer was eliminated.

The signal generator output impedances of the GG177 Accelerometers and the previously used GG116 Accelerometer differ extensively. The output impedances of the GG177 and GG116 at 14.4 kHz, respectively, were $51 + j82$ ohms and $1,000 + j14,400$ ohms. Because of this difference the stability of the preamplifier could have been affected. The preamplifier was analyzed to determine its margin of stability, and the analysis confirmed by engineering testing.

The accelerometer signal generator excitation source must provide approximately three times more power to the GG177 Accelerometer than was needed for the GG116 Accelerometer. Also, the excitation voltage is 2.0 V rms for a single GG177 Accelerometer, whereas 6.2 V rms is required for a single GG116. Because of these requirements, the signal generator excitation source had to be changed.

2.15.7. Phase I PIP and GG177/DR Retrofit. -

2.15.7.1. Introduction. - In order to raise the level of performance and reliability of the Centaur velocity loop, Honeywell proposed a Product Improvement Program to NASA. Upon NASA concurrence, Honeywell was authorized to go ahead with the solution of these problems. The program became known as the Production Improvement Program (PIP) and later known as Phase I PIP. It was recognized that the program was no panacea, but several serious Centaur problems were solved. Several other problem areas were uncovered by reducing errors to a degree where minor errors could be analyzed.

The incorporation of the GG177 Accelerometer into the Centaur system required certain modifications of the velocity loop in both the Platform and Coupler. The functional aspects of these changes are described below.

2.15.7.2. Required Modifications. -

2.15.7.2.1. Accelerometer Signal Generator Circuit Design. - The GG116 Accelerometer used 6.2 volts rms, 14.4 kHz for signal generator excitation. The GG177 requirement is nominally 2 volts rms at 14.4 kHz. Two methods of obtaining the required excitation were evaluated. These methods were:

1. To connect the three accelerometer signal generator primaries in series and use the 6.2 volt source with minor modifications, or
2. Redesign the excitation supply for a nominal 2 volts and connect the primaries in parallel.

The series configuration was decided upon since it was less susceptible to noise.

Other areas where redesign was required for proper signal generator excitation were signal generator quadrature rejection, signal generator secondary tuning, and the effects of signal generator output impedance on accelerator preamplifier stability.

Quadrature voltage in the accelerometer signal generator is due to a mismatch of impedance from one-half of the center tapped primary to the other half. Various combinations of capacitive and resistive elements were connected to the signal generator primary to determine the best

With the GG177 Accelerometer signal generators connected in the parallel configuration, two components were removed. An output transformer was added for impedance transformation and to obtain the required output voltage. Component values of the filter network were changed to obtain an optimum filter.

Using the series configuration of the accelerometer signal generators, the required excitation voltage was obtained across each accelerometer using the existing excitation source concept. Component values of the filter network were changed to obtain an optimum filter.

After extensive testing, the series configuration for the accelerometer signal generators was selected. An analysis and additional breadboard testing was also conducted on the signal generator excitation source.

2.15.7.2.4. 14.4 kHz Demodulator Driver. - The 14.4 kHz accelerometer signal generator source is also used as a reference for obtaining the 14.4 kHz demodulating signal used in the velocity loop. The input stages of the 14.4 kHz demodulator driver circuit required modification to operate properly with the different voltage levels of the signal generator excitation used during the digital interface test. Modifications to the accelerometer signal generator circuitry in the platform required additional modifications to the demodulator driver circuit to generate the demodulating signal having the proper phase relationship with the output of the platform.

2.15.7.2.5. DC Amplifier. - The DC Amplifier used in the velocity loop was a modification of the amplifier used in the GG116 pulse rebalance loop. The primary modification was that of changing the loop compensation network that precedes the operational amplifier. This change was made necessary by the dynamic response of the GG177 Accelerometer. Specifically, one lead-lag network was modified and a second lead-lag network was removed. This, in turn, caused a change in loop gain. To establish the desired gain with the above mentioned network changes, the feedback resistor around the DC amplifier had to be changed. The components which comprised the signal limiting network were also removed.

2.15.7.3. Analysis of Results. - In addition to the analyses required by all the changes described above, new loop gain and frequency response requirements were needed to insure that the loop would work with the new accelerometer. The loop gain and compensation network were selected for adequate GG177 Accelerometer pendulum control with the Centaur

All new and changed electrical components were selected from NASA preferred parts lists.

2.15.7.2.2. Summing Oven. - The coupler, in its GG116 configuration, supplied 184 ma through the torquer coil of the GG116 Accelerometers. A resistor was used to sense the amount of current flowing through the accelerometer torquer coil. The sensing resistor voltage, in conjunction with the input signal, maintains the torquing current at a constant value.

With the incorporation of the GG177 Accelerometer, the required torquing current was changed to 150 ma. Minimum modification to accomplish this change was to change the value of the sensing resistor. To maintain the accelerometer torquing current at a constant value over the specified environmental conditions, the sensing resistors of each of the three loops (U, V, and W loop) were placed in a temperature controlled environment. The Summing Oven Assembly operating at $100^{\circ}\text{C} \pm 1^{\circ}\text{C}$ provides the temperature controlled environment.

After the requirements were determined, an analysis was performed on the circuit to determine the effect of the sensing resistor value change on the torquing current and current supply loop dynamics.

The rebalance torquing current through the accelerometer torquer coil is operated at a 50 percent duty cycle. It is required that the coupler furnish a dummy load to the accelerometer rebalance current supply (ARCS) during the time that the accelerometer is not being torqued. The dummy load must match the accelerometer branch of the rebalance loop.

With the incorporation of the GG177 Accelerometer, the impedance of the accelerometer branch of the ARCS loop was increased due to the increase in DC resistance of the accelerometer and padding resistor. This requires a change in a resistor value in the dummy load.

The GG177 Accelerometer incorporation also required a change in the resistor-capacitor network used to form a tuned load with the accelerometer torquer coil due to the difference in the resistance and inductance of the torquer coil. This tuned load presented a resistive load to the ARCS.

2.15.7.2.3. Filter Module. - To determine the final mechanization of three GG177 Accelerometer signal generators, digital interface tests were performed to determine the optimum configuration. The 14.4 kHz signal generator excitation circuit had to be redesigned for the various configurations tested.

The old DC Amplifier was vulnerable to oscillations with large inputs, to change in output load, and to power supply variations. The objective was to design a new amplifier that had improved stability (less gain change, lower drift, and improved loop frequency response). The old DC Amplifier was made up of transistors which had high leakage, required mechanical choppers for converting the low level DC to AC and was AC coupled between stages by capacitors.

During Phase I PIP, this amplifier was replaced by an improved design and improved components. Each stage was stabilized with feedback. The leakage problem was reduced to an acceptable level by using planar transistors to replace the 1959 vintage devices. The mechanical choppers were replaced by solid state units. The overall amplifier was stable and not as susceptible to noise.

3. Logic and Level Discrimination Circuit Problems. - The function of the Logic and Level Discriminator is to sample the signal from the DC Amplifier and convert it to a two-state level. If the signal from the DC Amplifier is positive and equal to or greater than the threshold level, the Logic and Level Discriminator output is a "1", likewise it is a "0" output for a negative signal which is equal to or greater than the negative threshold level.

The above logic function is achieved in the level discriminator by a front-to-back pair of tunnel diodes on the input. The input signal is applied to the two tunnel diodes and if the signal exceeds the peak voltage of either tunnel diode, the rapid change to the valley voltage level of the tunnel diode is coupled inductively to the set/reset inputs of a flip-flop. Thus, the state of the flip-flop is made to change when the polarity of the input signal changes. The state of this flip-flop is sampled by a clock pulse which, in turn, sets/resets another flip-flop. The second flip-flop is set by a clock pulse and its state is, therefore, changed only at clock times. This enables the loop to be synchronized by the precision clock pulses.

The logic and level discriminator had two problems:

- a. The threshold levels were temperature sensitive, which caused the loop to have a bias level that was temperature sensitive.

vibration and acceleration profiles. The entire velocity loop was simulated on the H-800 computer.

2.15.7.4. Conclusion and Analysis of Program. - A step increase in velocity loop performance and some increase in reliability was accomplished during the program which incorporated the GG177 Accelerometer. Until this era of Centaur guidance, the analytical effort was inadequate. For the first time, for instance, it was established analytically that the accelerometer loop would not open, under the Centaur vibration and accelerometer mission inputs, by mathematical simulation of the loop on the H-800 computer. Previously, this was established empirically on the centrifuge. Previously, the GG116 Accelerometer and its velocity loop were not adequately described mathematically. Worst-case analysis for circuit design was used during the GG177 program but not exclusively because of the time required and a short schedule. If the H-800 computer (which was available) was used, it required a separate program and was usually very time consuming. Consequently, much of the analysis was done by hand calculation from data obtained empirically.

2.15.7.5. Problem Areas. - The following problem areas were identified and corrected during Phase I PIP.

1. Bias and Scale Factor Shifts, Master Gate and Current Bridge. - The transistor type 2N1711 that was used as a switching transistor in the Master Gate and Current Bridge had large (approximately 11 ohms) saturation resistance. This resistance varied greatly with temperature. This phenomena detrimentally affected the ARCS ability to maintain a constant current for torquing the accelerometers. This problem was corrected by using better transistors (low saturation resistance) and to redesign the dummy load and temperature compensation network to match the actual load.
2. Forward Loop Instability. - This refers to the analog portion of the velocity loop, located between the accelerometer output and the level detector input. The big contributor to this instability in this region was the DC Amplifier. This amplifier contained a separate section for amplifying AC and DC. The amplified AC and DC signals were then combined and further amplified by an output stage. The amplifier had a frequency response which was shaped by resistive and capacitive components in the feedback network.

- e. The output impedance (open loop) was too low and the bandwidth too narrow for the required regulation.
- f. There was sufficient noise on the front end to cause an output error.
- g. The use of floating test points made the circuit susceptible to permanent damage if the points were grounded.
- h. The amplifier was subject to oscillations.
- i. The output wave form exhibited a damped voltage transient during accelerometer torquing.

These problems were of a critical nature and required redesign to improve overall loop performance.

2.15.7.6. Coupler Thermal Tests. - In late 1964, a Coupler Temperature Profile Testing program was started. After incorporation of this test, the yield of ARCS boards dropped to an intolerable low rate due to ARCS oscillations. Extensive reliability and design investigations in early 1965 identified the possible causes for the oscillations.

The conclusions drawn from these investigations were as follows:

1. An AC analysis did not show any conclusive evidence that the oscillations were caused by an overall ARCS stability problem.
2. A DC analysis detected several areas of marginal design that could have caused oscillations by blocking the high frequency amplifier. However, test results did not verify this condition.
3. The addition of a 178K ohm resistor from pin 3 (the input pin) to ground of the module stopped the oscillations. A feedback loop existed around the amplifier module which was probably due to coupling through the ground leads or due to stray capacitance between input and output. The 178K ohm resistor stopped the oscillations by altering the characteristics of the unknown feedback loop. With the 178K ohm resistor in the circuit, it required approximately four times as much capacitance from output to input to cause oscillations.

Although the above fix in Step 3 did not in all cases prevent the oscillations, the yield on ARCS boards was increased. The decision was made early in Phase I PIP to try to "fix" the ARCS board rather than replace it. The basic ARCS problems remained in the system until Phase II PIP.

- b. There was the possibility of component failure because several of the components were overstressed during operation.

An acceptable redesign was achieved by changing and tightening the specifications for the tunnel diodes and replacing components in the circuit which were susceptible to failure due to overstress.

- 4. Arc Suppression. - The coupler relays were inducing large voltage transients on to the power lines due to their inductances. These large voltage transients caused a potential reliability problem since they caused many of the maximum voltage ratings of the semiconductors to be exceeded. This transient problem was eliminated by placing a diode in parallel with the coil of each relay.
- 5. Bias and Scale Factor Stability, ARCS. - The ARCS is an operational amplifier with a high output impedance in order to approximate a current source. The AC and DC sections were summed and amplified by an output stage. Mechanical choppers were used to convert the DC signal level to AC.

The output of the ARCS is switched in both directions through the accelerometer torquing coil by the Master Gate and Current Bridge. The current is then returned through a sensing resistor. The voltage drop across the sensing resistor is compared with a precision reference voltage. The difference between the two voltages is an error signal and is used to close the loop.

The ARCS had basic concept and circuit problems. Most of the problems were manifested as scale factor and bias instabilities. Analysis of the total ARCS circuitry revealed the following problems:

- a. The bias levels in the DC amplifier section and differential amplifier section were not stable with temperature.
- b. The gain of the AC amplifier, which was affected by the potentiometer setting, varied as much as 40 db. Frequency roll-off was also affected.
- c. The summing of the AC and DC signals was nonlinear with amplitude changes and with different potentiometer settings.
- d. The output impedance (open loop) was too low to approximate a current source.

2.15.8. Phase II Product Improvement Plan (PIP). -

2.15.8.1. Introduction. - The major purpose of the Phase II PIP program was to improve Coupler reliability. The original Phase II PIP task included a partial solution to outstanding problem areas. However, the task description was amended to include all of the known PRE problem areas. Phase II PIP was the first step on the Centaur IGS program towards improving velocity loop performance and reliability using formal worst-case circuit analysis and test techniques. Worst case circuit analysis was utilized on Phase II redesigned circuits and on non-PIP II circuits in the Coupler. The Phase II PIP program, in essence continued to improve the velocity loop where the Phase I PIP program left off. This topic discusses the technical hardware aspects of Phase II PIP. Just as significant was the worst case design process, which is discussed in Topic 6.18.

2.15.8.2. Redesign Phase II PIP Circuits. - The circuits included in this topic represent the heart of the velocity loop and the secondary power supplies which energize it. Following is a discussion of these circuits.

2.15.8.3. Isolated Power Supplies (IPS). - The design of the IPS for the Phase II PIP program resulted from several problem areas. These include:

Overstressed Components,
High noise sources in the Coupler,
Specification requirements were not met.

1. Tradeoffs. - Three different IPS mechanizations were evaluated during the course of the Phase II PIP program. All three provided the required 15 isolated dc output voltages. The three approaches are discussed in chronological order.

First Design (Non-Synchronous 15 kHz Power Converter). - This was a standard DC/DC power converter similar to the original 4 KC converter. The new version operated at 15 kHz and used LC rather than RC filter networks to achieve better regulation and efficiency. This approach still possessed the disadvantages of not having the frequency synchronized with PRE timing functions. Hence "beat frequency effects" could still occur and cause PRE loop performance degradation in the form of pulse dropping and large dead zones.

2.15.7.7. New Problems Discovered as a By-Product of Phase I PIP. -

1. Pulse Dropping. - The base currents of the transistors, which compose the Master Gate and Current Bridge (described previously), are obtained from flip-flops. Long lines exist between the Current Gate and the ARCS load. The load is the accelerometer torquing coil and is located in the platform rather than in the Coupler where the velocity loop electronics is located. An R-C network is shunted across these torquing lines in order to tune them to look like a pure resistive load to the ARCS. Noise spikes, which were on the torquing lines due to both pick-up and to switching transients, were coupled back to the flip-flops, which controlled the bias of the switching transistors. This sometimes caused the control switching flip-flops to change states and, in turn, caused a dropping of the torquing pulse to the accelerometer. If the R-C tuning network was tuned capacitive, this acted as a filter and no pulse dropping occurred.

This problem was actually made more severe during Phase I PIP, since the switching and flip-flop transistors were replaced by newer, faster transistors, and since no noise floor was designed in, they were more susceptible to fast rise time transients.

This design error occurred because the interface into which the new design was to work was not properly considered.

2. Dead Zone. - This refers to the area around accelerometer electrical and mechanical null. The accelerometer input axis could be moved ± 50 arc-seconds before an output could be detected from the velocity loop. It was resolved that part of the problem was caused by noise spikes from the "Isolated Power Supply (IPS)" being coupled into the torquing lines. This small signal was superimposed on to the digital rebalance current where it rebalanced the loop in an analog, rather than a digital, fashion.

The dead zone was reduced to an acceptable level by removing the above noise level through the IPS module redesign (reference Topic 2.15.8).

1.8 kHz Driver Amplifier. - This circuit provides isolation and amplification of the 1.8 kHz signal between the frequency divider and power converter. The amplifier has an input circuit (Zener diode) which decouples the noise from the supply line to prevent it entering the frequency divider. All transistors are operated class S and a coupling capacitor is used in the output to prevent transistor damage for a loss of input signal.

Frequency Divider. - This is a PTG bistable multivibrator design used here to convert a 3.6 kHz pulse to a 1.8 kHz square wave. The multivibrator contains power supply and input signal noise rejection circuits. Clamps, decoupling and bias are obtained from the Power Supply Module.

Power Supply Module. - This is a PTG power supply design which was used here to provide noise rejection for the frequency divider. The bias voltage is also used by the 14.4 kHz amplifier. The supply is comprised of an LC filter and Zener diode shunt regulators.

20 VDC Line Filter. - This filter is a low-pass " π type" filter. This filter is used to decouple the noise, generated by the IPS, from the 20 VDC supply. This filter also decouples the noise generated by the 7.2 kHz Driver Amplifier in the 7.2 kHz Supply (not shown in Figure 2.15-26). The filter is designed to attenuate the lowest operating frequency into a one ohm source impedance. The attenuation is sufficient to keep the 20 VDC supply ripple less than 50 mv peak.

14.4 kHz Amplifier. - This amplifier is located in the IPS assembly because of a lack of space to package it on the 14.4 kHz and 7.2 kHz Power Supply board. This amplifier provides isolation and converts a PTG square wave to a push-pull, class S drive signal to the power amplifiers in the 14.4 kHz supply.

3. Worst Cast Analysis (WCC) was performed on the selected 1.8 kHz IPS design. The analyses included error analysis, stress analysis, and true worst case circuit analysis. All component parameters were taken from the Honeywell Centaur Preferred Parts List and derated according to the Centaur Derating Policy. (Ref. Topic 6.18.)

Initially, all circuits were to be analyzed using the NET-1 computer program. It was abandoned for the IPS design after encountering several program problems. However, sufficient data was obtained from this program to complete the 14.4 kHz amplifier circuit analysis.

Second Design (Synchronous 14.4 kHz Power Converter). - The second design consisted of power amplifying a 14.4 kHz precision square wave signal from the PTG and converting it to DC. This approach avoided the problem of asynchronous noise generation and the resulting PRE loop errors. Closer investigation, however, revealed that while a synchronous power converter is required, the 14.4 kHz converter still inherently possessed noise problems.

Synchronous 1.8 kHz Power Converter. - In this approach the dc output voltages are generated by a power converter operated push-pull, class S, and driven by a precision frequency square wave signal of 1.8 kHz. The 1.8K power converter drive is achieved by frequency dividing a 3.6 kHz PTG pulse and power amplifying the 1.8 kHz square wave output from the frequency divider. The power amplifier's square wave is transformer coupled and the secondary voltages are rectified and filtered to obtain the DC output voltages. Isolation between outputs is provided by the transformer. (Reference Figure 2.15-26.)

Results of the system evaluation of the 1.8 kHz and 15 kHz power converters led to the selection of the 1.8 kHz operated power converter design because of the reduced noise levels on the torquer current and ARCS output. The reasons for this noise reduction is attributed to the fact that IPS switching occurs during dummy load time, and the use of slower switching speed power transistors.

2. Circuit Description. -

The following paragraphs continue the description of the major blocks of the 1.8 kHz supply, plus the worst case analysis and test results which led to an acceptable design for the Phase II PIP Coupler. The factors considered and problems encountered, along with their solutions, were typical of the Phase II PIP design.

The two power transformers have 15 secondaries, each of which has a full wave bridge rectifier and RC filter network to convert the secondary square wave voltage to a DC voltage.

The two power transistors in the power amplifier are transformer driven push-pull, class S. This transformer is excited by a capacitor coupled square wave signal from the 1.8 kHz Driver Amplifier.

The attempt to use the NET-1 program to analyze the 1.8 kHz amplifier resulted in computer mathematical instability. This also occurred on the 14.4 kHz amplifier analysis, but involved only the last computer run. Many attempts were made to eliminate the NET-1 program as the source of the problem. The parameters, equivalent circuits, and program inputs were examined and modified without success. The conclusion, based upon the program results, is that the mathematical instability in the NET-1 computer, at this time, resulted from too large a spread between circuit time constants. (Note: This experience with NET-1 was not necessarily typical of other Phase II PIP circuits. It does emphasize the point, however, that NET-1, or ECAP, cannot just be "blindly" applied.)

1.8 kHz Driver Amplifier and Power Converter Error Analysis. - This analysis consisted of computing the maximum error in output voltage due to line, load, environment, and component tolerances.

Three cases were computed for the error analysis: nominal, minimum, and maximum output voltage. The nominal case verified the equivalent circuit using nominal parameters. The other two cases consisted of selecting the parameters for a maximum or minimum output voltage condition. The analysis results showed the 15V output could slightly exceed specification. However, tightening of the power transformer's resistance tolerances and exciting current brought the output back into specification.

The results are summarized below:

	Typical Beta	Minimum Circuit Beta Requirement
Transistor Beta	67	24
Forced Beta	12	28

The inadequate forced Beta condition was due primarily to the large tolerances on V_{BE} . Several solutions to this problem were available. One was to change the base drive resistor. This required a slight module modification. Another solution was to control V_{BE} more closely. Because of schedule, the problem was overcome by specifying a maximum V_{BE} .

X

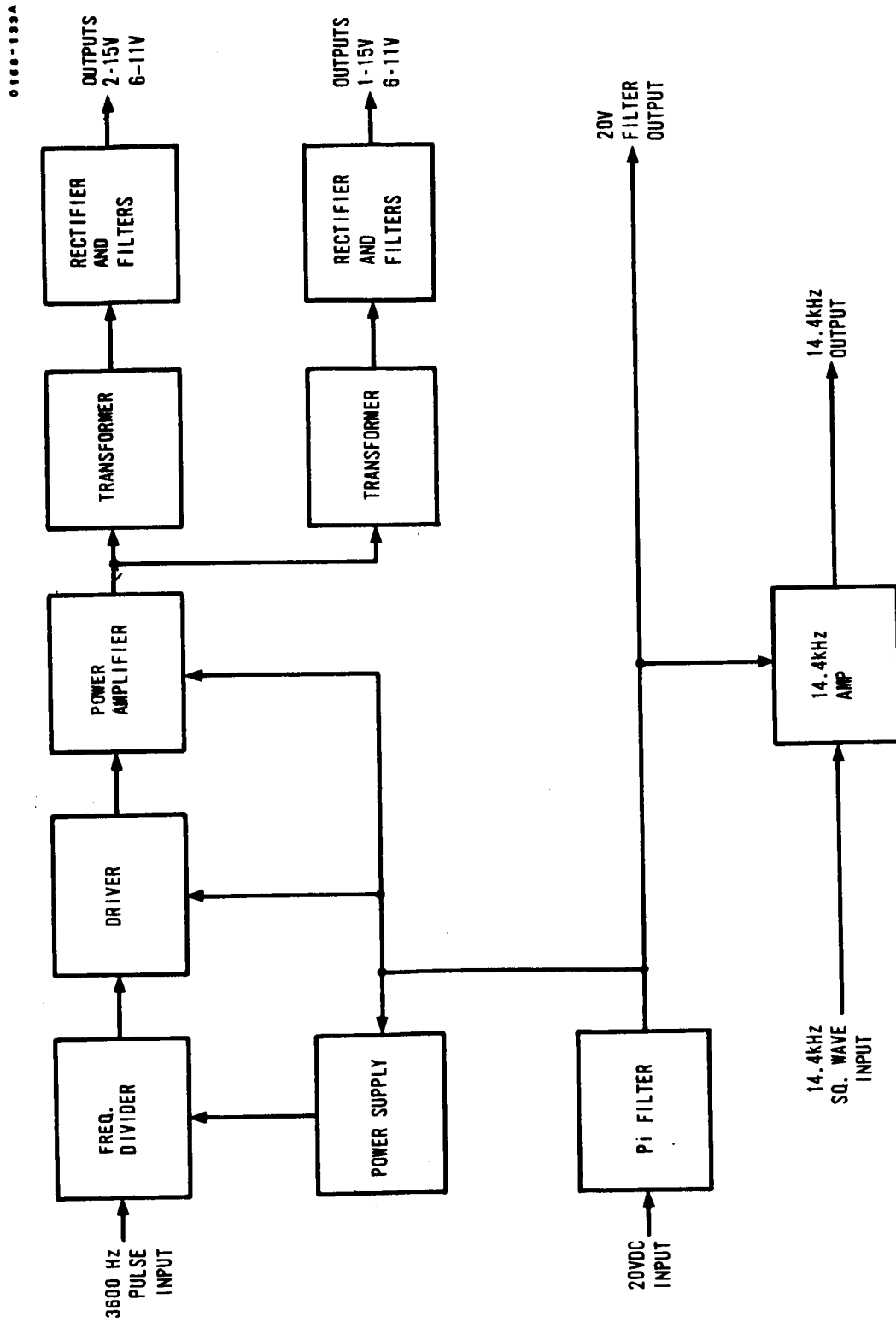


FIGURE 2.15-26. 1.8 kHz ISOLATED POWER SUPPLY BLOCK DIAGRAM

TABLE 2.15-I

14.4 KHZ AMPLIFIER WORST CASE ANALYSIS RESULTS

Parameter	Specification	Worst Case Analysis
Output Voltage	3V Peak $\pm 1V$	3.01V to 3.64V
Square Wave		
Amplitude	14.4 kHz ± 100 ppm	---
Frequency	1.0 μ sec max.	0.5 μ sec
Rise and Fall Time	$\pm 5 \mu$ sec	3.5 μ sec
Symmetry	-4 ma max. during down level	2.7 ma
Input Impedance	-5 ma max. during up level	6 μ A

TABLE 2.15-II

POWER CONVERTER WORST CASE ERROR ANALYSIS RESULTS

Output	Specification (%)	Analysis Error (%)	Parameter Conditions (Cases)
11V	± 18.2	-16.3 - 0.9 +15.4	Minimum Voltage Nominal Voltage Maximum Voltage
15V	± 13.4	-12 - 1.3 + 7.4	Minimum Voltage Nominal Voltage Maximum Voltage

14.4 kHz Amplifier. - The NET-1 computer program was used here to analyze the circuit. (See Table 2.15-I.) Hand computations were also used to confirm the results.

1.8 kHz Amplifier and Power Converter Stress Analysis. - The voltages, currents and power dissipations were computed for each component. The analysis showed several component ratings exceeded slightly but they were not considered reliability risks.

Worst Case Analysis Results. -

1.8 kHz Driver Amplifier and Power Converter. - The error analysis results are shown in Table 2.15-II and compared with the specification, which was met.

The ac analysis results are shown in Table 2.15-III and compared with the specification. In this case, noise is the maximum noise from 20 volt line to 11V or 15V output. This is added to the measured noise of each output resulting from switching and rectification. NET-1 analysis on this could not be performed because of the NET-1 mathematical instability problems encountered. However, the results of the analysis, that was performed, are satisfactory.

4. Breadboard Test. - Tests were performed to obtain actual performance numbers. These results were compared to specification limits and to the worst case analysis results. Regulation, output noise, temperature and stability tests were performed for each supply, and compared with the requirements in each case. The results were satisfactory. Tests of the output voltages versus time and power turn-on and turn-off conditions were performed. The conditions were:

Nominal line voltage, load, and temperature. A nine day stability test was performed where power is turned on at the beginning of each day and voltages monitored. The results showed the IPS to be stable under these conditions.

The IPS breadboard was then installed in a Phase II PIP Coupler and tested. The results showed no abnormal transients, in either the current or voltage during sustained operation for power on-off operation.

Circuit Mechanization. - A block diagram showing the circuit mechanization and a circuit schematic of the 14.4 kHz is shown in Figure 2.15-27.

The mechanization is the same for both circuits. The square wave input signal (this signal is conditioned by a buffer amplifier on the 14.4 kHz Supply to generate a two phase square wave) drives the Class S, push-pull transistors of the power amplifier. The square wave output is transformer coupled into a filter which attenuates the harmonics giving a sine wave output. The amplitude of the output voltage is regulated by transformer coupling the output and demodulating the signal with a full wave bridge. An RC filter then attenuates the carrier frequency, passing the low frequency error signal into a DC Regulator whose output supplies power to the center tap of the Power Amplifier transformer. The frequency response of the loop is controlled by the Regulator roll-off network and the demodulator filter.

Approach and Procedure. - The analysis made on the ac power supply was a combination of computer calculations, using the ac and dc programs of the Circuit Computer Program, and hand calculations. The AC Analysis Program provided frequency response information such as node voltages, currents, gain and phase angle. The DC Analysis Program provided the capability of calculating node voltages, currents, power dissipations and partial derivatives of each node voltage with respect to all parameters. The Centaur derating policy was used for all component derating.

AC Analysis Computer runs at the fundamental frequency were made on the Power Amplifier using nominal, minimum, and maximum component values of the filter and load. The results of these runs provided the worst case power, and the voltage and current range requirements of the DC Regulator.

Filter Analysis. - Frequency responses of the filters were calculated with nominal, minimum, and maximum component values using the AC Computer Program.

Loop Frequency Response. - The Open Loop AB gain curves were calculated by AC computer runs using minimum gain parameters with maximum time constant roll-off networks and maximum gain parameters with minimum time constant roll-off networks.

Output Voltage Stability. - The amplitude stability was calculated using closed loop equations. DC computer runs were made on the closed loop regulator circuit using minimum gain transistor parameters. The

TABLE 2.15-III

NOISE ANALYSIS RESULTS (20VDC LINE TO LOAD)

Output	Noise Source	Maximum Noise	Specification
11V	20V Line *Internal	35 mv peak, 2.4 kHz <u>200 mv peak</u> 235 mv peak total	550 mv peak
15V	20V Line *Internal	2 mv peak, 2.4 kHz <u>200 mv peak</u> 202 mv peak total	750 mv peak

*Internal noise is due to switching and rectification. The values are test data. No analysis performed on internal noise source.

5. Conclusions from IPS Redesign. - The conclusions reached by this redesign were that the IPS demonstrated, by analysis and test, that it performed within the established specifications.

The technical report approach taken to the IPS redesign was detailed in depth to give the reader a thorough understanding of the scope of design and analysis used throughout the Phase II PIP program. The remaining PRE Phase II circuit redesigns will not be treated with the same detail as IPS. However, each topic will detail the "whys" and "hows" of the redesign.

2.15.8.4. AC Supplies. - The function of the ac power supply is to provide 14.4 kHz excitation voltage to the three accelerometers in the platform and to provide a reference voltage to the 14.4 kHz demodulator driver. The ac supply also provides a 7.2 kHz signal to Platform Electronics (PE) for use as a gyro and resolver excitation and as a demodulator reference voltage. The 14.4 kHz portion of the supply will be covered in this section.

Circuit Concept. - The circuit requirements for voltage regulation with the worst case line voltage and load variations of the 14.4 kHz and 7.2 kHz supplies necessitated a regulated supply using some feedback technique. The square wave drive, class S supply, with a filtered output was chosen because of its simplicity and low distortion characteristics.

G168-114A

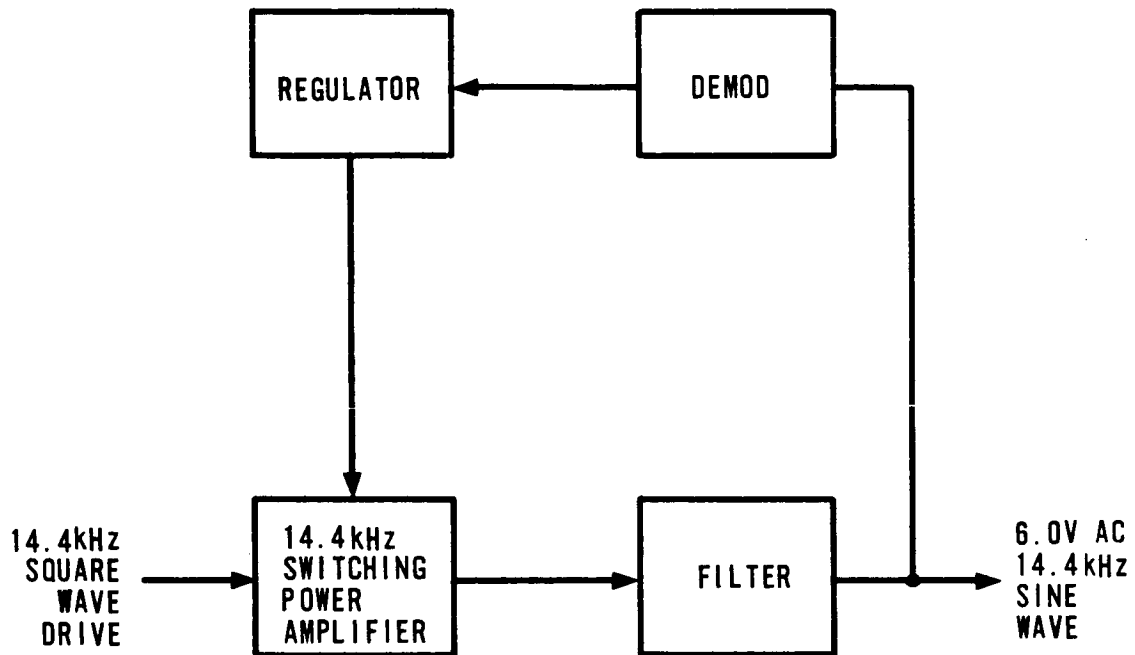


FIGURE 2.15-27. ACCELEROMETER SIGNAL GENERATOR EXCITATION

partial derivatives were used to determine the input error due to components changes of less than 1 percent such as resistor and zener references. The input error due to changes in small signal parameters, leakage currents and ΔV_{be} were to be determined by making runs with minimum gain parameter values at 0°C, then at 85°C.

Buffer Amplifier. - The analysis of the Buffer Amplifier was done by hand calculations.

Power Dissipation Calculations. - Worst case power dissipation of all components was calculated using the worst case voltages and currents obtained from the computer runs.

Noise Susceptibility and Generation. - The noise susceptibility and generation data in this report is empirical data. The combination of linear and non-linear circuits with large and small time constants made a computer analysis unrealistic.

Worst Case Analysis Results. - The ac power supply meets all the circuit requirements under worst case conditions. However, a noise problem did occur in the 14.4 kHz supply when the circuit was packaged on a printed circuit board. Noise was coupled into the 14.4 kHz regulator from the ground path, causing excessive noise on the 20 volt power supply. The problem was eliminated by adding a high frequency roll-off capacitor to the differential amplifier stage of the regulator, and a decoupling capacitor across the 20 volt supply on the board.

This problem verifies the fact that circuits are not packaged on "paper", but on printed circuit boards or modules that have undefined capacitances and inductance. Worst case analysis therefore is not the end, but only the beginning of sound design practice. Applying WCCA involves a shift of emphasis to "analysis before testing", but it does not preclude the necessity to perform the testing.

2.15.8.5. Temperature Control Amplifier (TCA). -

Circuit Function. - The Temperature Control Amplifier is part of a proportional controller whose function is to maintain the temperature of a component oven within specific limits. It provides ac amplification demodulation and drive for the power stage of the controller. The input signal is derived from a resistance bridge, one leg of which is the oven temperature sensor.

The heaters in the component oven constitute the load for the temperature control amplifier.

This device consists of an ac amplifier, a half wave demodulator, and a dc power amplifier. See Figure 2.15-28. This is essentially the same circuit as used on Centaur prior to the Phase II PIP effort, the primary change being a reduction in gain to insure stable loop operation. In addition to the circuitry located on the temperature control amplifier board, the sensor bridge which is located in the oven is considered to be part of this circuit.

Sensor Bridge Mechanization. - The sensor bridge consists of three RNR 60E resistors and a platinum wire sensor connected to form a bridge. The three resistors are in a potted module in the oven assembly and the sensor is located between the heater board and the inner wall of the oven.

AC Amplifier Mechanization. - The ac amplifier consists of two feedback doublets and has a nominal gain of 57 db. This amplifier originally had a small capacitor from the base of the first stage to ground to attenuate noise. This resulted in a very little attenuation due to the low input impedance and was therefore replaced by a 0.01 μ fd capacitor from collector to base of the third stage. No other changes were made in the ac amplifier portion of the TCA.

Demodulator Mechanization. - The demodulator is a half wave diode ring with a sinusoidal drive. The drive is obtained from a transformer which also provides the sensor bridge excitation. The coupling capacitor between the ac amplifier and the demodulator provides a voltage doubling effect and the demodulator gain is 0.9 volt dc per volt rms rather than 0.45 which is the usual gain of a half wave demodulator.

DC Amplifier Mechanization. - The dc amplifier consists of a PNP common emitter amplifier driving a Darlington emitter follower. The nominal gain of the dc section is 18 db. The gain reduction which was required to insure loop stability was accomplished by changing the values of the emitter and collector resistors in the common emitter amplifier stage.

Mechanical Configuration. - The temperature control amplifier circuitry, with the exception of the dc amplifier output power transistor, is packaged on a glass epoxy printed circuit board. The output power transistor is mounted on the heat sink assembly in the coupler.

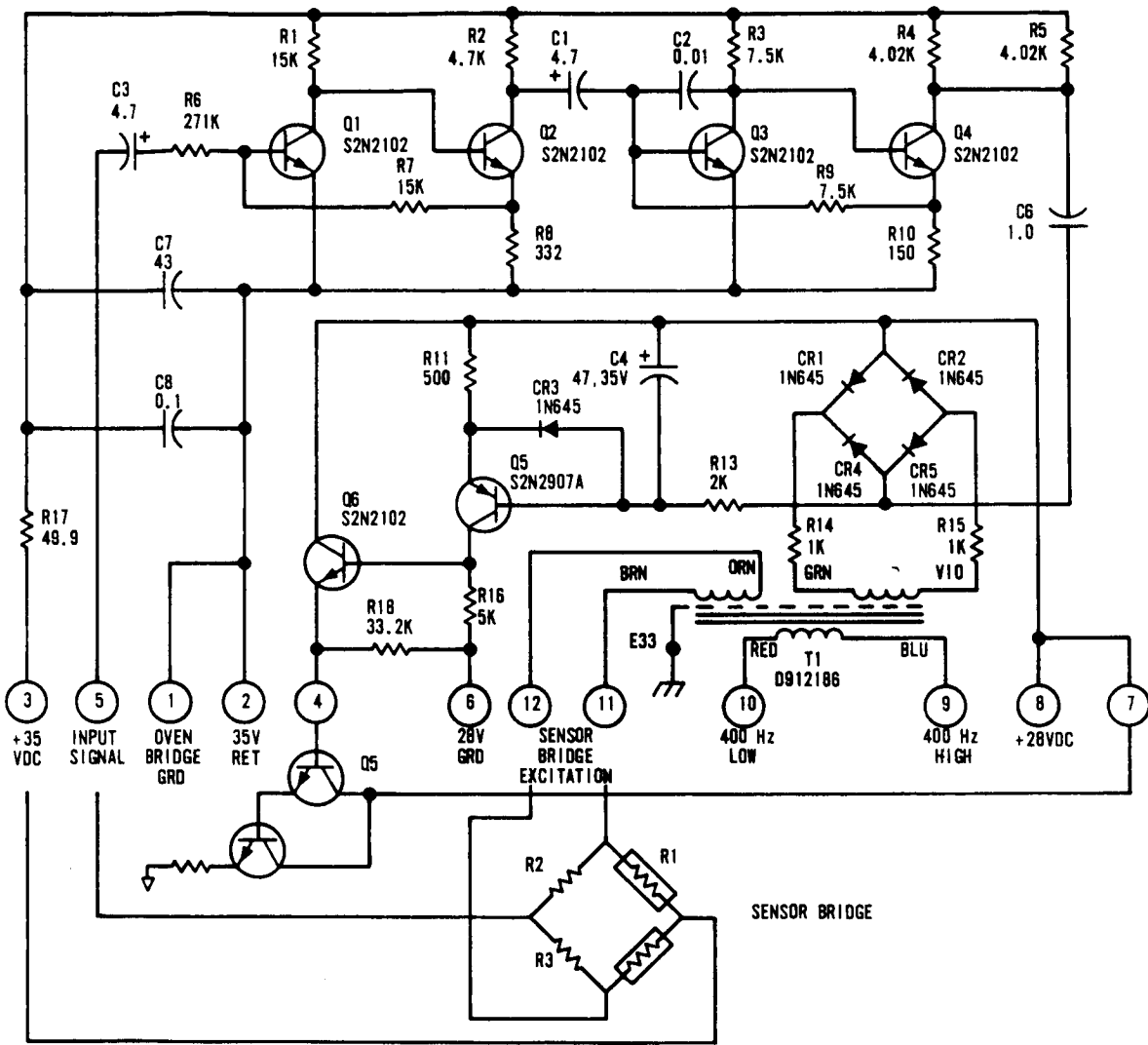


FIGURE 2.15-28. TEMPERATURE CONTROL AMPLIFIER,
ELECTRICAL SCHEMATIC

Worst Case Analysis. -

Approach and Procedure. - The ac amplifier analysis consisted of both an ac and dc analysis run on the Univac computer with the Circuit Program. The results of the dc analysis were used to determine the component stresses and the ac results provided the gain values that were needed for the loop analysis. The loop analysis and analysis of the demodulator and dc amplifier were hand calculations.

The analysis of the sensor bridge was performed using the H-800 computer and a Fortran program written to solve the bridge loop current equations.

Breadboard Tests. - Since the temperature control amplifier was only modified and not redesigned, there was no extensive circuit development testing. Almost all the tests performed were closed loop tests with the oven. The breadboard test data consisted of a series of turn-on transients versus gain, which were used to determine the loop gain margin.

Computer analysis was not used for design optimization. For this reason the circuit had some areas which could be improved, especially in the ac amplifier section.

The circuit performs its desired function reliably so there was no need for redesign or additional modification.

2.15.8.6. Carrier Amplifier. - This circuit provides amplification and demodulation of the accelerometer signal. The input is obtained from the accelerometer preamplifier located in the platform and the output drives the filter and forward loop equalizer module on the dc amplifier board. This circuit was a replacement for the Bandpass Amplifier previously used in the Centaur System.

Circuit Concept. - This device consists of a Class A amplifier and a full wave demodulator. See Figure 2.15-29. The full wave demodulator was selected to provide a constant output impedance, driving the filter module from a half wave demodulator with its periodically varying output impedance would result in a periodically varying filter corner frequency. The class A amplifier is required to provide gain and impedance matching between the preamplifier output and the demodulator.

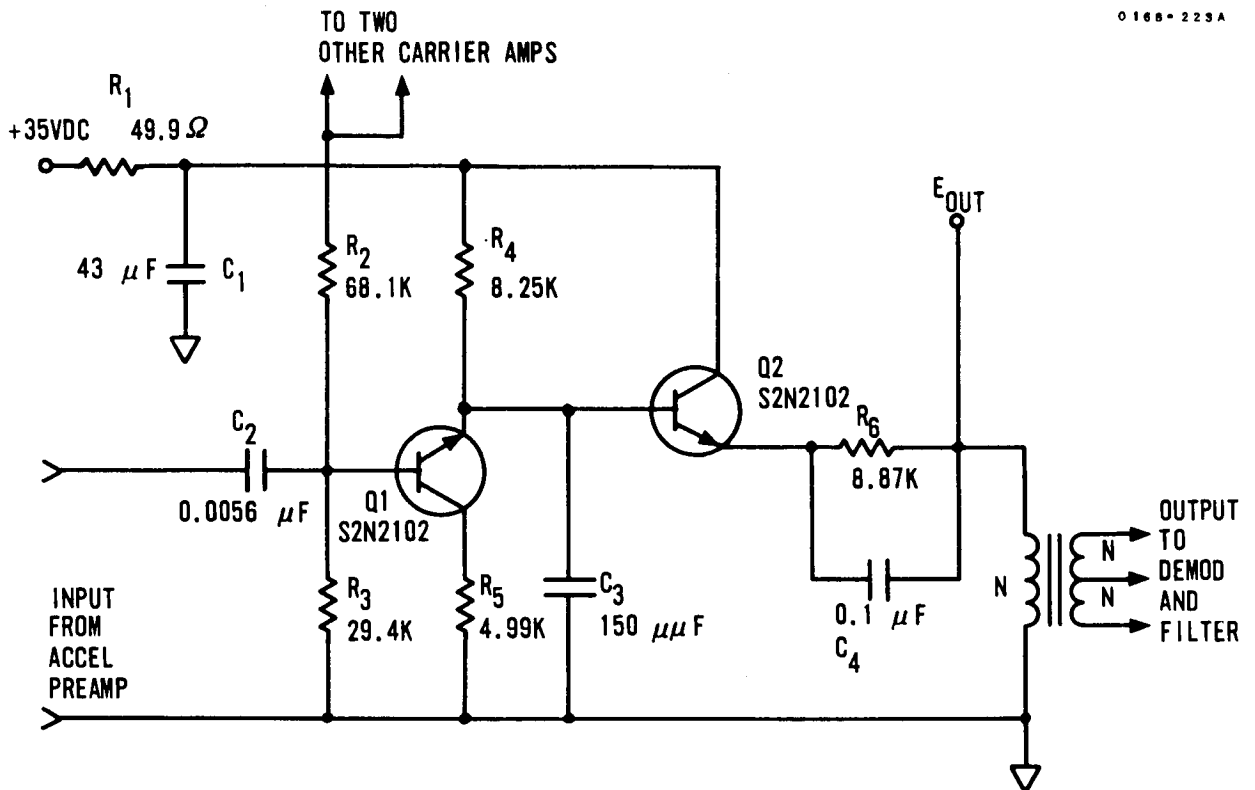


FIGURE 2.15-29. CARRIER AMPLIFIER SCHEMATIC

Circuit Mechanization. -

Demodulator Mechanization. - The full wave demodulator consists of two diode rings which are coupled to the amplifier output by a transformer having a 1.2 turns ratio and a center tapped secondary. The diode rings are matched quad assemblies to insure low offset voltages.

Amplifier Mechanization. - The amplifier has a common emitter stage to provide the required gain and an emitter follower to provide the power gain needed to drive the demodulator transformer.

The low frequency response is limited by the coupling capacitor and the input impedance to the first stage, the resulting corner being 1.4 kHz. The high frequency corner at 14.4 kHz is determined by the output impedance of the first stage and the 150 pf capacitor which is connected from the first stage collector to ground. This passband was selected to provide a linear phase characteristic with low slope in the range of $14.4 \text{ kHz} \pm 1.8 \text{ kHz}$ and approximately zero phase shift at 14.4 kHz.

Mechanical Configuration and Decoupling. - Three carrier amplifier and demodulator channels are packaged on a printed circuit board. In addition to the three channels, there is also a decoupling network on the circuit board. This network isolates the circuit from noise on the 35 volt line and has a corner frequency at 76 Hz and an attenuation of 6 db per octave above that corner.

Worst Case Analysis. -

Approach and Procedure. - The amplifier and demodulator sections were analyzed separately, with the transformer considered as part of the demodulator. The amplifier analysis consisted of both a dc and an ac analysis run on the UNIVAC computer with the circuit program.

The demodulator analysis was done by hand since this type of circuit is not easily handled by any of the presently available computer programs.

Worst case analysis of this circuit insured that all specification requirements were met and all components operated within the limitations imposed by the derating policy. Prototype testing verified this, with the exception of the demodulated gain. Tests indicated a gain of 1.1 volts dc/volt rms, rather than the expected gain of 0.88 volt dc/volt rms when loaded with an RC filter composed of a 1K resistor and a 0.1 mfd capacitor. This excessive gain was due to distortion in the transformer increasing the dc component of the output.

Since the system will operate satisfactorily with this demodulator gain and the schedule did not allow further design modification at this time, the specification was changed to allow a gain of 1.0 ± 20 percent.

2.15.8.7. 14.4 kHz Demodulator Driver. - The 14.4 kHz demodulator driver performs the function of generating the drive signal required by the demodulator circuits in the Carrier Amplifier Assembly. Three drive signals are required, with the phase of each one independently variable.

Design Philosophy. -

Circuit Concept. - The circuit shown in the block diagram (See Figure 2.15-30) was selected to meet the circuit requirements for one input and three isolated outputs. The nominal phase shift was incorporated in the buffer amplifier. Isolation was secured by using an emitter follower to drive three phase splitter circuits. The signals from the phase splitter are applied to a bridge circuit to yield the variable phase shift as required. Symmetry was achieved in the zero crossing detector by using a pnp-npn pair. The output is then squared in the digital circuits. The output circuits used permit short circuit protection and dissipated less power on the board than a flip-flop design. The use of phase splitters eliminated the inter-action between bridge circuits that was present when a transformer drive was used on the original circuit.

Worst Case Analysis. -

Approach and Procedure. - The circuit operation was analyzed for worst case conditions using the ac and dc programs of the Circuit Computer Program on the Univac computer at Phoenix, Arizona for the analog portion and steady state conditions of the digital section. The NET-1 program on the IBM computer at Boston was used for the transient analysis of the digital section.

Worst Case Transient Analysis. - The following analysis was conducted to determine:

1. Worst case waveform dissymmetry.
2. Worst case rise times (10 percent to 90 percent).
3. Line noise rejection.

0168-136A

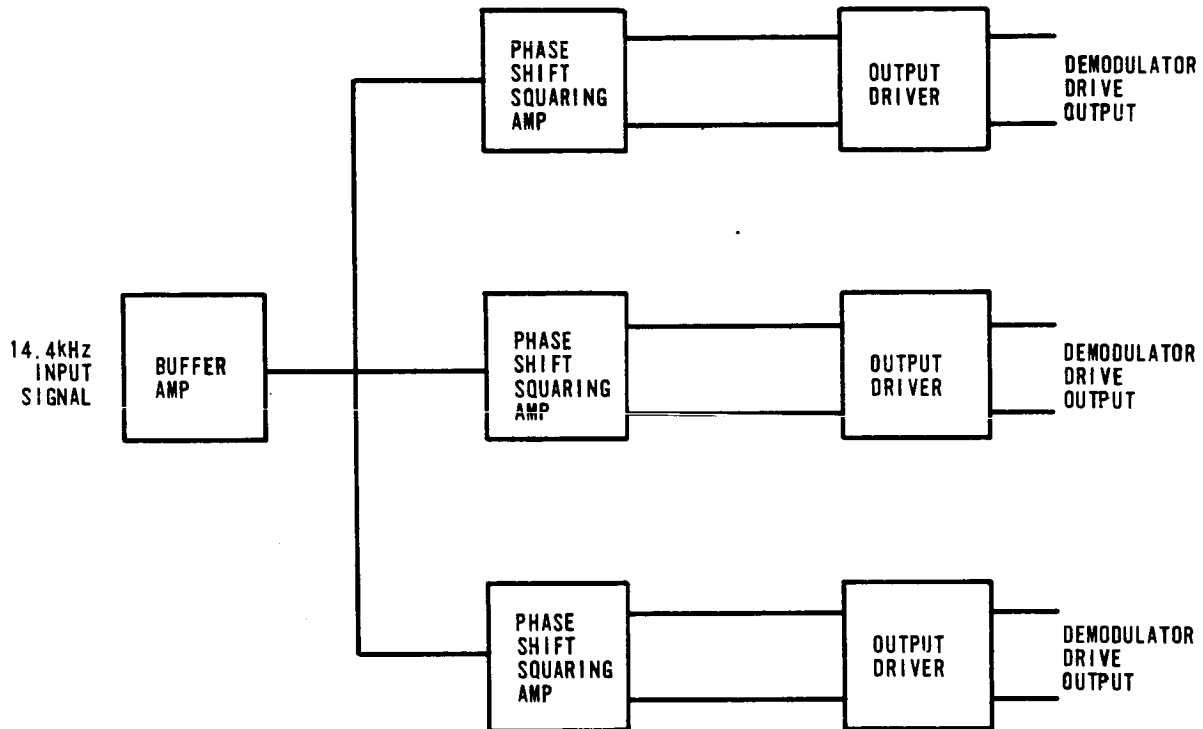


FIGURE 2.15-30. 14.4 KHZ DEMODULATOR DRIVER

The NET-1 computer program was used to perform the analysis. The transistor model utilized by NET-1 required the specification of bulk resistivities, leakage resistances, normal and inverse Beta's V_{BE} and V_{BC} characteristics (reverse bias saturation currents, and slope coefficients), normal and inverse alpha cutoff frequencies, transition capacitance coefficients and diffusion capacitance coefficients. Of these, only those parameters which affected the speed (time delay, rise time, storage time, and fall time) of the device were varied in the analysis. The parameters were calculated from both data sheet and test data. Two areas where improvements could have been made, had the schedule permitted, are the phase splitter and the output module.

The phase splitter saturated if the input signal exceeded the specification limit. This saturation will result in a loss of symmetry. A redesign with a negative bias voltage would have given a more comfortable margin of safety.

The output section exhibited no problems in the breadboard. However, when packaged in a module on the prototype circuit, stray capacitances caused the switching times to exceed specification. This was corrected by the addition of a zener and a diode on the base-emitter circuit. A different packaging approach may have eliminated the need for these additional components.

2.15.8.8. Design Changes - Phase I PIP to Phase II PIP Accelerometer Rebalance Current Supply (ARCS). - Following the Phase I redesign effort and while the Production build phase of the effort was proceeding, numerous problems with the ARCS developed. A brief description of the problems encountered with the Phase I PIP ARCS is given here, and a more extensive description of the more major problems is presented in subsequent paragraphs.

1. ARCS board oscillation problems were a constant source of trouble. At one point in the Phase I effort, 25 loops in nine couplers were lacking completely stable ARCS boards.
2. The long lead wires between the mechanical choppers and the ARCS amplifier input proved to be a source of noise.
3. The summing resistor high impedance lines transversed the back of the PRE, thus being subjected to injected noise.

4. ARCS units that did not have stability problems in the normal coupler ambient would not necessarily pass thermal tests.

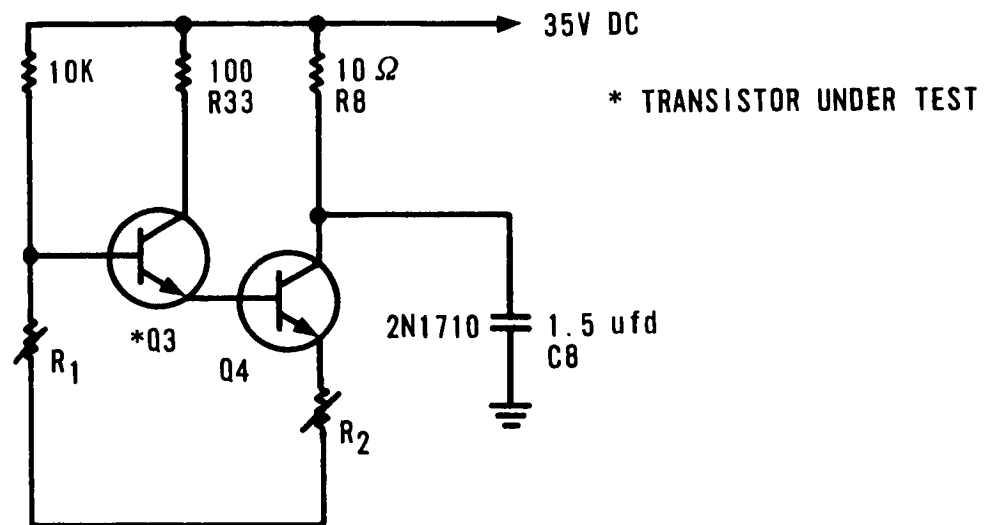
ARCS Board Oscillations. - During the Phase I configuration period, four distinct oscillation frequencies were observed.

1. 15-40 Hz oscillations occurred primarily at the coupler level after a cold soak at 30°F. In most cases, the oscillations would damp out as the coupler warmed up.
2. 160 to 260 kHz oscillations occurred in bursts.
3. 1 to 5 mHz oscillations were observed on the torquing pulses and ARCS output, but these were only observed at the coupler level.
4. 1 to 8 Hz were observed at both the board level and the coupler level.

The engineering effort was initiated to determine the source or cause of the oscillations. Isolation of the problem proved to be extremely difficult because it was difficult to duplicate the exact environment the ARCS board experienced inside the coupler. Tests did show a continuous relaxation type oscillation of approximately 5 Hz. Additional testing by Engineering showed that this oscillation was related to the collector breakdown voltage of Q3. When higher voltage devices such as 2N930 or selected 2N753 transistors were used, the oscillation did not occur. See Figure 2.15-31.

Testing was started on the coupler level, using 17 couplers in a temperature chamber. It was found that the following conditions had some effect in causing the 15 to 40 Hz and 160 to 260 kHz oscillations:

1. Temperature - Oscillation would normally start at a turn-on after a cold soak at 30°F. However, some boards oscillated at room temperature.
2. Position of shield between ARCS boards - By pulling shield out approximately 1-1/4 inches, some boards would start oscillating at room temperature.
3. Installation of heat sink plate that covers the coupler bay in which the ARCS boards are housed would sometimes cause oscillation.



R₁ VARIES BIAS LEVEL ON Q3
R₂ VARIES LOAD (SET AT 130Ω)

FIGURE 2.15-31. TEST CIRCUIT

The following items had little or no effect on oscillations:

1. -10V reference supply. An external reference source was wired directly into the coupler and oscillations still occurred.
2. Logic and Level boards and Master Gate boards were interchanged and had no effect on oscillations.
3. Oscillations occur with accelerometer load, simulated accelerometer load in coupler test station, and with pure resistive load.

The above findings indicated that the oscillation problem was definitely caused by the ARCS circuit itself, by mechanical layout of the ARCS and coupler, or by noise and transients in the coupler. Open loop frequency response was measured on several ARCS which were known oscillators. Response was measured with the heat sink plate on and off. No significant difference was found. Phase margin at the zero db crossover was approximately 46°. No indication of instability was seen at the crossover point between the high frequency amplifier and the low frequency amplifier. Frequency response was measured on an ARCS which did not oscillate. No significant difference was observed between the frequency response of the oscillating ARCS and the non-oscillating ARCS. Many different circuit components and combinations of components were tried and evaluated by test. After an extensive analytical effort was expended, it was concluded that the probability of obtaining a properly functioning ARCS was discouragingly low. A major redesign of the ARCS electronics was planned for the Phase II PIP Program.

Phase II PIP Accelerometer Rebalance Current Supply Design Goals. - Because of the major problems encountered with the Phase I ARCS, a new approach to the requirements of supplying a precision current source for the accelerometers was conceived. The Phase II PIP design placed the Precision Voltage Reference Supply, the three ARCS and the ARCS sensing resistors in one Oven Assembly. The design had been previously tried on another program and proven successful. The new design approach also provided the following improvements:

1. A single PVR is used and built as a potted module.
2. Three ARCS' s using the single PVR as a reference are each a separate module.
3. All the modules are mounted in a temperature controlled oven to obtain the required low level of dc offset and drift. Also, the open loop gain of the ARCS' s and the PVR voltage are held quite stable by the constant temperature environment.

The distinct advantages of the Phase II ARCS over the Phase I ARCS are given here:

1. Three 400 cps mechanical choppers were eliminated.
2. 400 cps demodulator drive circuit (15 watts) was eliminated.
3. Parts count reduction of 215.
4. Only minor changes required on an existing, proven design.
5. Oscillation problems were avoided.

ARCS Worst Case Circuit Analysis and Test Results. - The WCCA on the Phase II PIP design was completed before any attempt to proceed with test or production was considered. The WCCA was divided into four parts as follows:

1. DC Analysis of unit to unit performance, effects of three ARCS's being referenced to one PVR, and short term unit stability.
2. AC Analysis of unit to unit gain and phase margin variations.
3. AC Analysis of line noise attenuation.
4. DC Analysis of output variations resulting from load variations.

Following the WCCA, the Phase II PIP PVR, ARCS and associated electronics were breadboarded and tested extensively. The performance of the new ARCS, throughout the Phase II Production phase, has proven that the earlier problems were solved and that the new design and design approach were sound.

2.15.8.9. Conclusions. - The Phase II PIP redesign greatly improved the PRE velocity loop performance and reliability. The Phase II PIP was the first real attempt to utilize computer aided worst case circuit analysis techniques. Much was learned from and about the different techniques. Although there were several instances where packaging and environment problems caused redesign, after the worst case analysis was performed, for the most part, this aid proved beneficial in the design process.

By correcting major problem areas during Phase II PIP, Honeywell was able to obtain insight into minor undetectable problems that were present but masked.

The excellent flight performance and improved reliability obtained with the Phase II PIP systems, paved the way for the Centaur IGS being utilized on new missions such as the ATS, Mariner, and OGO.

Phase I PIP was no panacea, but it and Phase II PIP provided the largest single step to improve performance and reliability of the PRE velocity loop and the entire Coupler unit.

2.15.9. Improved Centaur PRE. -

2.15.9.1. Introduction. - Following loop candidate trade-off studies, a continuous torque (100 percent duty cycle) accelerometer Pulse Rebalance Electronics (PRE) loop concept was selected to perform the velocity measurement function within the Improved IMG.

The selected loop mechanization, which preserves the carrier sampling technique and null pattern control to minimize TGRT error effects, eliminates the need for Isolated Power Supplies and Dummy Loads within the loop. It requires only simplified timing interfaces and relieves a significant error source associated with pulse to pulse initial conditions as encountered in duty cycle loops.

The principal goal established for the PRE mechanization was reliability improvement as achieved through the elimination and simplification of functions, simplification of circuitry, use of integrated circuits where practical and reduction of error margins by providing improved and predictable performance.

2.15.9.2. Requirements. - The following summary identifies the more significant performance requirements for the velocity measurement function:

<u>Item</u>	<u>Requirement</u>
Accelerometer	GG177J3 with modified heater
Bias	25,000 μg maximum (absolute)
Bias Stability	190 μg
Digital Scale Factor	0.12 ft/sec/pulse nominal or finer
Measurement Range	50 μg to 12.5 g ± 10 percent
Threshold	$\pm 50 \mu g$
Non-Linearity	50 μg maximum

2.15.9.3. Trade-Off Study. - A number of accelerometer rebalance loop concepts may be mechanized to perform the desired velocity measurement function. Loop techniques which have been effectively demonstrated with the GG177 accelerometer include:

1. Analog rebalance
2. On/Off ("bang-bang") pulse torque rebalance
3. Continuous torque or pulse width modulate torque rebalance
4. Quasi-linear or pulse on demand rebalance

Three of these approaches received serious consideration during the study phase. The analog rebalance/digitizer configuration, which was investigated, is shown in Figure 2.15-32. A simplified block diagram of the loop adopted during the study, which is shown in Figure 2.15-33, is a 93.75 percent duty cycle "bang-bang" loop. This loop, patterned after previously used 50 percent duty cycle concepts (Centaur/Gemini) and time-shared (33-1/3 percent duty cycle), preferred state rebalance loops, combined ac sampling and preferred state logic features with reduced pulse voltage/current transients resulting from the use of 93.75 percent duty cycle. A simplified diagram of the 100 percent duty cycle continuous torque loop approach is shown in Figure 2.15-34.

Each of the three candidates possessed relative advantages and disadvantages. The following commentary reviews more significant trade-off results and identifies the principal basis for rejection/selection of the final approach.

Of the three loops, the analog loop approach offers the greatest potential advantages. The loop features analog rebalance circuitry, which could be directly packaged on the stable element in close proximity to the accelerometer. It also features A/D conversion circuitry which provides properly scaled digital "Delta V" velocity output data for the guidance computer. It offers maximum flexibility with regard to accelerometer type used, pulse rate, scale factor or output digital data format. Analog torquing has merit with respect to leveling, and if properly used, advantages could be gained from analog torquing the gyro during initial alignment. Size, reliability, and cost advantages exist as the loop is the simplest of the three candidates. Also, it offers simplified timing interfaces, has the lowest parts count, and is amenable to large scale integration.

The analog loop, though potentially strong, also imposes the most severe mechanization problems and carries the highest technical risks of the three candidates. No "in-depth" analysis supports the loop concept and very limited development history exists. Unresolved circuit mechanization problems were present within the preliminary breadboard development phase and no temperature/environmental/noise tests were conducted on the loop. Unexplored TGRT effects under a proportional torque mode and undefined effects of gimbal dead zones on leveling create a significant performance risk. In addition, the 6 ma/g scale factor of the GG177J3 accelerometer also creates an undue burden on the forward loop; for optimum operation, the torquer scale factor would have to be lowered. The analog loop concept was, therefore, abandoned early in the study

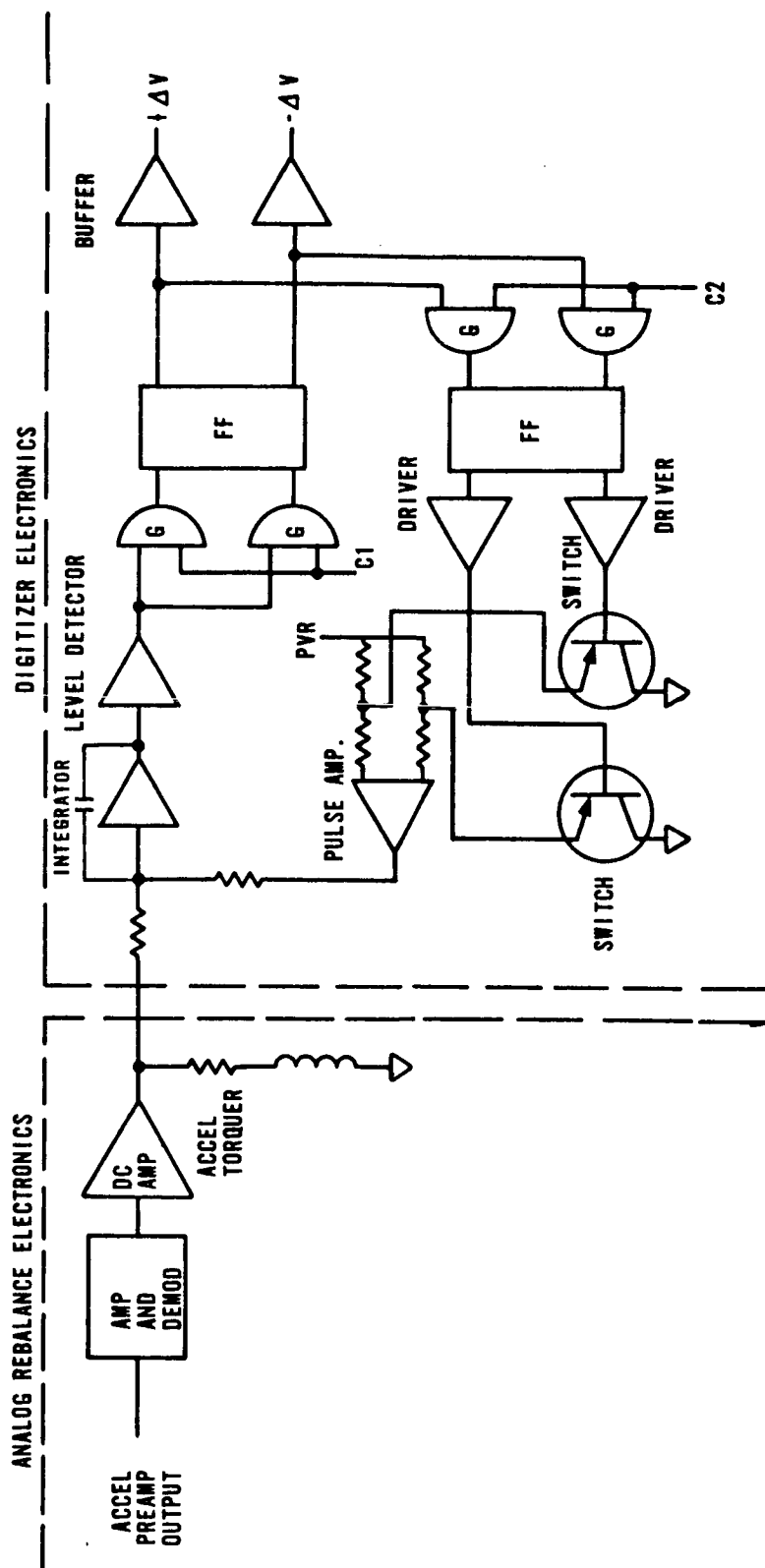


FIGURE 2. 15-32.
ANALOG ACCELEROMETER LOOP

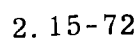


FIGURE 2. 15-33.
SEU LOGIC AND GATING

0167-228A

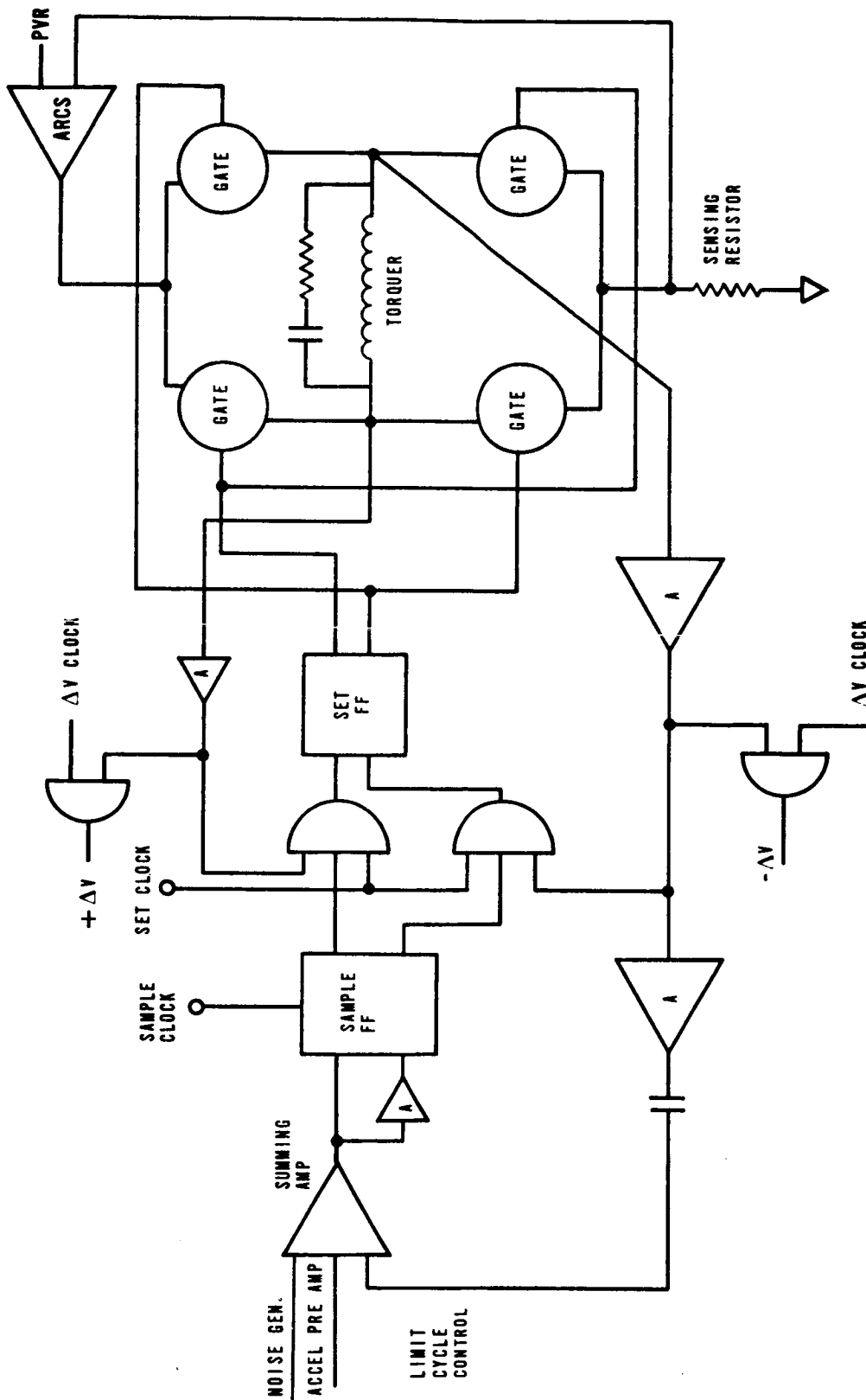


FIGURE 2.15-34.
ONE HUNDRED PERCENT DUTY CYCLE LOOP

program since it reflects relatively less proven technology and demanded a minimum four to six months of detailed analysis and development to establish feasibility. In addition, during this interval, other system concept approaches would be unduly constrained.

The second candidate, the 93.75 percent duty cycle loop, offers a concept of known technology with detailed breadboard and analytical history. The loop employs ac sampling of the accelerometer signal, a preferred state logic concept and a 93.75 percent duty cycle pulse torque mode. It features a one pulse limit cycle inhibit and asynchronous noise input to minimize loop frequency "lock-in" conditions and resulting TGRT problems. The loop concept presents no radical departure from Honeywell's history in PRE and possesses creditable reliability, cost, and performance. Performance capability of the loop has been demonstrated to fall within Improved System requirements; however, minor mechanization problems exist. These deficiencies, however, were well defined and, thus, the approach presents a loop concept demanding a relatively short term analysis/development cycle to completely validate the approach.

The 93.75 percent loop mechanization requires an Isolated Power Supply (IPS) for current bridge circuits and requires selection of a number of matched components; reduced performance characteristics with time is evidenced unless components possess the same drift behavior.

During this study phase, potential circuit simplifications were pursued within analog, gating and Delta V interface circuit areas. Use of field effect transistors within the lower gate sections of the loop could permit elimination of isolated power supplies with only minor additional circuit complexity in the current bridge.

The 93.75 percent duty cycle loop, thus offered a valid concept approach for the Improved System; however, it was subsequently rejected in favor of the continuous torque (100 percent duty cycle loop) which, in trade-off exercises, exhibited equivalent reliability, producibility and cost advantages while also providing extra performance margin, simpler interfaces and less critical circuit design requirements.

During re-examination and extended evaluation of the 93.75 percent duty cycle loop, predominant scale factor and/or bias sources were identified. Whereas gate leakage, voltage/current reference variations and loop gain/offset/limit cycle variations produce error effects, the largest scale factor and bias stability error source is the change of torque current pulse width due to changes in transistor switching speeds. One way to

relieve this problem is to have one serial pulse control the gating function such that a change in switching speed does not change the time between pulses. The 93.75 percent duty cycle loop partially utilizes this concept via use of a master gate control whereby the lower bridge gate and the transistor controlling the upper gates are preset; master gate switching speed change thus introduces only scale factor error.

Bias stability error will depend primarily upon the difference in switching speed changes of the upper gating transistors with respect to dummy load transistor switching speed. Since the transistors are prevented from operating in the saturated mode, the large change due to temperature is fall time.

Scale factor error has two main sources; the storage time change in the master gate flip-flop, and the difference in fall time change of the transistor and the dummy load.

Assuming use of transistors matched for switching speed to within 20 percent, calculations of possible switching speed variations over a 50°C temperature range could produce approximately 62 ppm scale factor error and 140 μ g's bias error.

A loop concept offering immediate relief of the switching error problems is the continuous torque, or 100 percent duty cycle loop approach. This concept reduces scale factor error due to switching by use of one serial pulse to gate the torquer signal. Gating transistors are connected as a flip-flop so that the single binary pulse can be used. Regeneration provided by the flip-flop connection increases circuit speed; although changes in fall time over temperature remains the predominant error cause. Transistors matched for switching speed may still be advantageous but not mandatory. A 20 percent match provides far less error than the 93.75 percent loop example given due to the regenerative mechanization and the effective doubling of the torquer pulse width. Aside from better switching control and improved bias/scale factor stability, mechanization of the concept offers other significant advantages.

1. The loop contains no isolated power supplies.
2. More settling time for the switching transient is allowed between pulses. This improves control of initial torque current conditions from pulse-to-pulse and provides better bias stability, improved linearity and better thresholds.
3. The loop concept effectively eliminates the possibility of pulse reset (that is, pulse dropping) of the torquing bridge.

4. Only two clocks are required for the mechanization, which simplifies the PTG.
5. Leakage currents are reduced.
6. No dummy load is required.
7. Parts count is reduced.

Potential adverse features exist. Larger voltages are switched in the loop; therefore, higher voltage gating transistors are required. Noise generated due to switching is increased and the larger voltage drop across the bridge increases the dynamic response demand of the current supply. Torquing loop analysis and development testing established that these conditions present no problem to the current supply or the remainder of the PRE. Based upon these final results, the 100 percent duty cycle loop was selected as the best concept for the Improved IMG.

In summary, the selected concept, 100 percent duty cycle loop, preserves the carrier sampling techniques and null pattern control feature of the 93.75 percent duty cycle loop. It permits simplification of the precision timing function and requires no Isolated Power Supply, dummy load or master control flip-flop. The loop, like the second candidate, presents no radical departure from prior Honeywell PRE technological approaches and, as evidenced by developmental and analytical study, provides performance capability within established requirements.

A summary of empirical data established during the preliminary concept study of the 100 percent loop is tabulated on the following page. Comparable data obtained with two separate breadboard loops was judged sufficient to validate the concept approach and influenced the final candidate selection.

<u>Parameter</u>	<u>Requirement</u>	<u>Test Data</u>	<u>Conditions</u>
Threshold	$\pm 50 \mu g$	Dead zone range from $< 25 \mu g$ to $50 \mu g$	Several runs made on two breadboards
Linearity	$50 \mu g$ max deviation	$49 \mu g$ maximum deviation over $\pm 1g$ range; $18.7 \mu g$ rms deviation	Two breadboards
$\pm 1g$ Repeatability	--	25 ppm max	Several runs
<u>Parameter Stability</u>			
Scale Factor	160 ppm	7.5 to 15 ppm	30 to $150^{\circ}F$ Several runs
Bias	$190 \mu g$	52 to $225 \mu g^*$	30 to $150^{\circ}F$ Several runs

* $225 \mu g$ (obtained in one data run only) was during investigation of logic/gating simplified circuit approaches. This value is not considered representative and is included for completeness only.

2.15.9.4. Functional Loop Mechanization Study. - Reliability is increased in the improved system by giving proper consideration in the present design to previous Centaur problem areas. These considerations are reflected by the following design accomplishments in the 100 percent duty cycle loop.

1. Elimination of the requirement for isolated power supplies removes the existence of former parasitic parameter error sources to isolated ground lines. In addition, noise injection within the torquing circuit through isolated power lines is non-existent.
2. The positive bistable gate technique prohibits the possibility of a "pulse drop" mode. Derivation of velocity output data directly from the bridge ensures proper torquer/delta V pulse correlation.
3. Integration of the PRE within the same unit enclosure as the accelerometer minimizes wiring capability problems and parameter variations due to cable capacity variations.
4. A functional loop package approach creates no severance of critical internal interfaces, permits positive control of parasitic parameters within the logic/gate interface (that is, "modal bias shift") and permits improved producibility and PRE interchangeability.
5. Placement of torquer tuning network components within the azimuth block minimizes thermal drift effects of components and the resulting PRE parameter instability.
6. Location control of ARCS outputs with respect to PRE assemblies within the Inertial Reference Unit (IRU) base mount provides added assurance that inherent ARCS stability is not jeopardized.

2.15.9.5. Description of One Hundred Percent Duty Cycle PRE. - The function of the PRE is to provide incremental velocity information to the guidance computer. A block diagram of the PRE is shown in Figure 2.15-35. Basically, each loop consists of an analog section, level detector, logic section, a bridge and a current supply. In addition, there is a precision voltage reference and precision timing generator common to all loops.

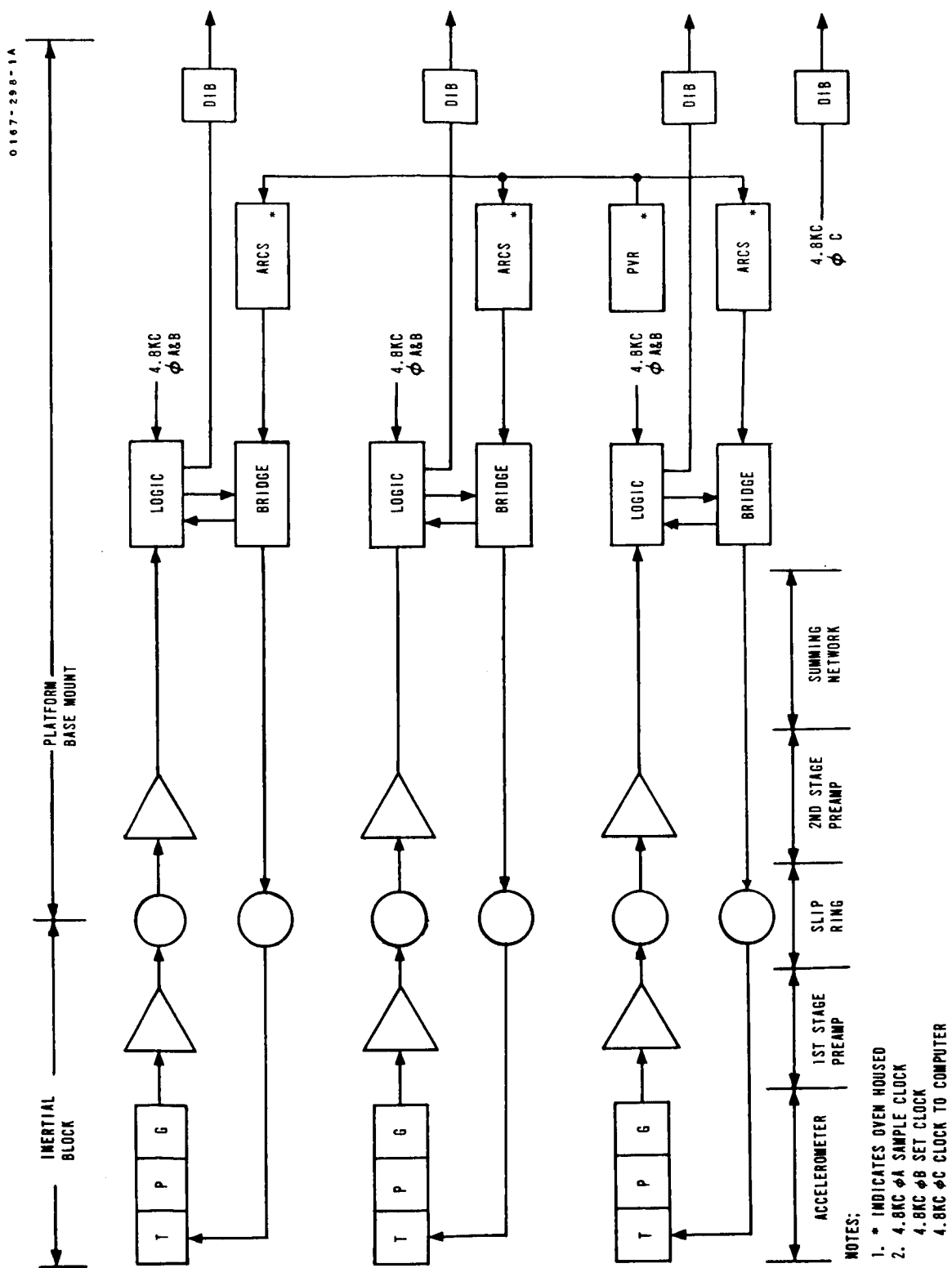


FIGURE 2.15-35. PULSE REBALANCE ELECTRONICS BLOCK DIAGRAM

To obtain the desired mission accuracy, the PRE must be designed to stay within a certain error allotment. From Honeywell's experience in rebalance electronics, the areas of potential error sources are well defined. The error sources and anticipated error contributions are contained in Table 2.15-IV. The table reflects the spread of error to fall within the total error as allocated by systems analysis.

1. Pulse Rebalance Forward Loop. - Under an imposed forcing function, the output of the accelerometer is a suppressed carrier modulated signal. The forward loop accepts this signal from the accelerometer signal generator, amplifies it, sums it with the appropriate pattern control signal and provides a level detection such that a logical decision can be made as to which direction the accelerometer must be torqued to rebalance the external applied forcing function. The hardware design will now be described.
2. Preamplifier. - The preamplifier provides the necessary impedance matching, gain and drive capability to permit the accelerometer signal to be transmitted to the main body of the PRE. The preamplifier is a two-stage amplifier with the first stage located on the platform and the second stage located in the base mount near the remainder of the PRE.

As previously indicated, a gain compensation in the preamplifier will be required if gain limitations are to be met. A two-stage preamplifier represents the most desirable manner of accomplishing this.

In order to meet the size requirements of the platform, the first stage preamplifier is an integrated circuit amplifier. The amplifier with its frequency compensation and gain control elements can be packaged in about one-third the volume of a comparable discrete component amplifier.

Test data indicates that the DGG177 accelerometer gain varies significantly with loading, particularly if the load is less than 10K ohms. Therefore, to minimize the loading effects, the first stage preamplifier was connected as a non-inverting amplifier resulting in an input impedance greater than 100K ohms.

Preamplifier gain was set at 30 volt/volt. This provides the amplifier with a GH of about 40. Thus, the amplifier has an adequate gain stability with time, temperature and unit-to-unit. Further, the dynamic output impedance is lowered by a factor of GH, which makes this amplifier suitable as a preamplifier.

TABLE 2.15-IV. VELOCITY LOOP ERROR BUDGET

Loop Function	Stability			Absolute		
	Bias		Scale Factor	Bias		Scale Factor
	Error Allot	Design Param.	Error Allot	Error Allot	Design Param.	Error Allot
PVR	NA	NA	40 ppm	NA	NA	1.8% Ref Zener: 1.4% Other: 0.4%
ARCS	NA (Reflected in bridge)	NA	100 ppm	NA	NA	1% Diff Amp Gain
Timing Generator	NA	NA Single Clock Fire both sides	40 ppm	NA	NA	0.1% tolerance on base crystal clock
Logic and Gate (Leak)	0.88×10^{-5} g's	Max 100 n Amp	1.5 ppm	7×10^{-5} g's	max 600 n amp	
Logic and Gate (Switch Time)	12.2×10^{-5} g's	4 n sec variation in switch time	20 ppm	100×10^{-5} g's	max 43 n sec	0.2%
Logic and Gate (ΔR)	6×10^{-5} g's	Max 3 Leg to leg ($2 \times 10^{-5} g/\Omega$)	30 ppm	20×10^{-5} g's	10 Ω unbalance	NA
Forward Loop	1.5×10^{-5} g's	Sig Gen: $\pm 15\%$ assume 5% excit Amp: $\pm 5\%$ Level Det: $\pm 5\%$ Note: Ratio of signal to pattern control noise must be maintained to $\pm 20\%$.	NA	10×10^{-5} g's		NA
Sensing Resistor	NA	NA	20 ppm	NA	NA	

3. Second-Stage Preamplifier. - The function of the second-stage preamplifier is to provide additional loop gain and to provide a means of adjusting the loop gain. The gain adjustment is required to compensate for signal generator gain variations. The gain adjustment is effected by means of selecting a feedback resistor for the amplifier. It is presently felt that a selection of one of five resistor values will be sufficient to bring the forward loop gain to its required value. It should be pointed out that the second-stage preamplifier is located in the base mount of the platform which makes it readily accessible for making the gain adjustment.

The second-stage preamplifier is of the same type and configuration as the first stage.

4. PRE Logic. - The PRE Logic takes inputs from the summing network and the bridge and makes a logical decision as to whether or not to change the direction of torquer current. If the decision is to reverse the torquer current, a pulse is transmitted to the bridge. Conversely, if the decision is made not to reverse the torque current, no pulse is transmitted.

The PRE Logic consists of a level detector, a holding flip-flop and "NAND" gates.

The level detector is the most important part of the PRE logic as it is at this point that the full transition from analog to digital is made and represents the last point where an "error" can occur in the forward loop. The logic following the level detector is essentially error free once drive levels, etc., are established. The level detector configuration essentially eliminates the error sources while retaining the basic simplicity required for reliability and size.

The level detector is an integrated circuit amplifier of the same type as used in the preamplifier and the summing network.

A holding flip-flop is set when a sample pulse is coincident with a high output of the level detector. Conversely the flip-flop is reset when a sample clock is coincident with a low output of the level detector. It should be pointed out that the phasing of the sample clock and the accelerometer output is such that a sample

clock always occurs at the peak of the carrier waveform. Thus, when a sample clock occurs, the level detector is either high or low and never in a transient state.

The output of the flip-flop is therefore a quantized pulse width modulated signal that indicates the position or phasing of the pendulum. Further, the output of the flip-flop indicates the direction the pendulum should be torqued. Then at "set" time a pulse is transmitted to the bridge if the State of the Bridge (SOB) does not agree with the flip-flop. If the flip-flop and the bridge are in the same state no pulse is transmitted to the bridge.

5. PRE Bridge. - The PRE Bridge represents the largest potential bias error source in the loop and therefore requires very careful attention to detail. In addition to providing the proper steering of the accelerometer torque current the bridge must do this in an extremely fast and stable manner with a minimum of impeding variations from "side to side". One of the salient features of the bridge is that this mechanization eliminates the need for an isolated power supply, as was required by previous velocity loops. Isolation between the torquer current and the master flip-flop is effected by means of very low-leakage diodes and the self-biased lower gates of the slave flip-flop.
6. ARCS. - The constant current supply (ARCS) is a high gain, wide bandwidth dc amplifier. The amplifier is connected in such a manner as to maintain a constant voltage across a precision sensing resistor. Since the sensing resistor is in series with the load the amplifier maintains a constant current in the load. It should be noted that the ARCS is the same as used on previous programs; it is a rescaled version of the one presently in use in the Phase II PIP Coupler, and has a proven history of reliability and performance. Anticipated errors all fall within the budgeted values.
7. PVR. - The precision voltage reference is designed around a highly stable zener reference diode. The diode bias current is derived from a constant current source, resulting in an output voltage that is very stable and independent of line voltage variations.

The PVR, like the ARCS, is a proven circuit from previous programs, including the Phase II PIP Coupler. It possesses proven performance history along with predictable error potential.

2.15.9.6. Error Budget Backup. - The following discussion summarizes the rationale governing the error budget developed. The primary factors considered in the preliminary error budget are absolute bias and scale factor and bias and scale factor stability. The 100 percent velocity loop has been adjudged the best loop for consideration.

Errors that affect only pulses of one polarity are taken as bias errors. Those factors affecting pulses of both polarities are taken as scale factor errors. The errors and associated design parameters shown in the error budget are considered as the total allotment allocated for time and temperature as dictated by mission requirements (assume approximately $\Delta 70^\circ\text{F}$ and 20-hour mission, including calibration).

The specified error totals that the error budget falls within are derived from the total error allowable for successful mission completion. The TDS indicated:

Scale factor absolute:	0.084 \pm 10 percent
Scale factor stability:	160 ppm
Bias absolute:	25,000 $\mu\text{g}'\text{s}$
Bias stability:	190 $\mu\text{g}'\text{s}$

Out of the totals indicated above, certain device stability figures must be "washed out" such that figures for the PRE electronics can be obtained. Following is a table of the primary factors and error contributions that were deleted from the total allowable error. These figures are based on systems studies and sensitivities developed by the System Group. RSS figures are used as the errors have been shown to be noncorrelated.

Scale factor stability:	
Thermal effects	20 ppm
magnetic	40 ppm
Accelerometer stability:	40 ppm
Null uncertainty	20 ppm
Vibration	<u>60 ppm</u>
RSS =	87.2

$$\sqrt{160_{\text{spec}}^2 - 87.2^2} = 134 \text{ ppm for PRE (RSS)}$$

Bias stability:

Temperature effect	90 μ g
Magnetic	15 μ g
Null uncertainty	20 μ g
Stability	40 μ g
Vibration	<u>50 μg</u>

RSS = 113 μ g

$$\sqrt{190_{\text{spec}}^2 - 113^2} = 152 \mu\text{g (RSS)}$$

Following is a brief discussion of the pertinent factors in the PRE loop. The numbers in the majority of cases were developed from discussions with the cognizant designers and past circuit performance under similar environmental and operational conditions. The error allocations for the functions were then adjudged as to their "fit" in their overall budget.

- A. Loop Function (1) PVR. - Errors in the Precision Voltage Reference result only in scale factor errors. Errors in regulation, stability, etc., result in errors to both P and N pulses.

This circuit has an excellent stability history over similar environment and operational conditions.

Error sources:	Zener TC
	Parameter variations

Allocated scale factor error: 40 ppm

- B. Loop Function (2) ARCS. - The ARCS can contribute both bias and scale factor errors-- bias errors, however, are related to the bridge resistance variations and are reflected in that portion of the error budget.

Error sources:	Gain
	Drift
	Regulation

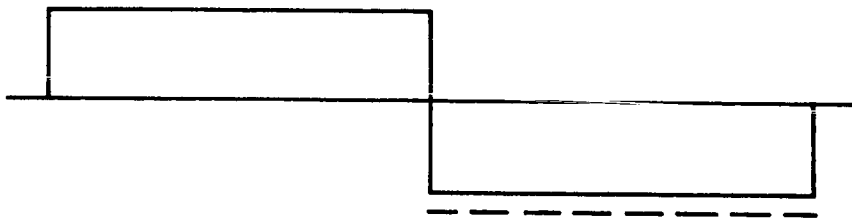
Allocated scale factor error: 100 ppm

- C. Loop Function (3) Timing Generator. - For the 100 percent loop the gates are "fired" simultaneously by definition. Therefore, errors arising from a difference in torque on-torque off pulses cannot exist. Thus, bias errors from this source are eliminated. Scale factor errors, however, can be created and are directly related to clock stability.

Allocated error: 40 ppm (Clock Stability)

- D. Loop Function (4) Logic and Gating Leakage. - Bias changes due to leakage can be attributed to a variation in pulse amplitude. As the diodes and gates will be matched to some degree, a maximum leakage figure of 100 nanoamp has been taken.

Consider:



Leakage results in error only on one polarity pulse over a given time.

$$\frac{2(208 \mu\text{sec}) 100 \times 10^{-9}}{4(208 \mu\text{sec}) 5.7 \times 10^{-3}} \times 1g = \frac{50}{5.7} \times 10^{-6} = 0.88 \times 10^{-5} g's$$

Scale factor change due to 100 nanoamp leakage

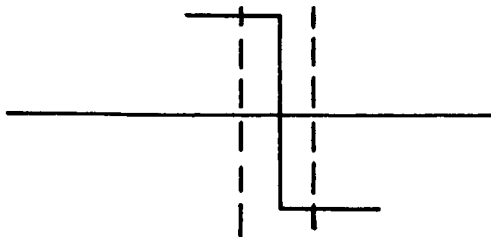
$$\frac{\text{Torquer current change}}{\text{Torquer Current}} = \frac{100 \times 10^{-9} \text{ amp}}{72 \times 10^{-3} \text{ amp}} = 1.4 \text{ ppm}$$

- E. Loop Function (5) Switch Time Variations. - Errors in switch time result in a variation in pulse width. This error source is the greatest single error source in the loop.

A worst case variation in switch time must be considered over two pulse periods. This configuration of pulses can occur, and

represents the most serious potential degradation in performance; any other pattern will result in an effective integration over a longer period of time and will reduce the error due to switch time.

Consider:



Assume four nanosecond variation maximum.

$$\frac{4 \times 10^{-9} \text{ sec}}{2 \times 208 \times 10^{-6} \text{ sec}} \times \frac{72}{5.7} \times 1g = \frac{144}{(5.7)(208)} \times 10^{-3}$$

$$= 12.2 \times 10^{-5} g's.$$

Tied directly to this bias error is an effective scale factor error resulting from this variation in pulse width.

$$\frac{\text{Pulse Width Change}}{\text{Pulse Width}} = \frac{4 \times 10^{-9}}{208 \times 10^{-6}} = 20 \text{ ppm}$$

The bias error required is the predominant factor in this case.

- F. Loop Function (6) Change in Bridge Resistance. - Changes in bridge resistance result in both bias and scale factor errors. The controlling factor in this case is the ARCS sensitivity to variations in load. Previous efforts with the ARCS have shown that sensitivities of $2 \times 10^{-5} g/\Omega$ for bias and $10 \text{ ppm}/\Omega$ for scale factor. Based on previous experience, it appears that one could expect something less than 3 ohms of change over temperature.

Based on this then:

$$\begin{aligned} \text{Bias budget:} \quad & 6 \times 10^{-5} \text{ g' s} \\ & (2 \times 10^{-5} \text{ g}/\Omega)(3\Omega) = 6 \times 10^{-5} \text{ g' s} \end{aligned}$$

$$\text{Scale factor:} \quad (10 \text{ ppm}/\Omega)(3\Omega) = 30 \text{ ppm}$$

- G. Loop Function (7) Forward Loop. - The variations in the forward loop represent bias changes only and not scale factor changes.

Based on existing figures for signal generator excitation and forward loop gain, a change of less than one arc-second of pendulum swing can be expected. Allocated scale factor error - $1.5 \times 10^{-5} \text{ g' s}$.

- H. Loop Function (8) Sensing Resistor. - The last significant error contribution in the table is the scale factor change due to variation in the sensing resistor.

Allocated scale factor error: 20 ppm

2.15.9.7. Task Analysis in Retrospect. - The Improved System is still in the design phase at this time (December 1967). There have been and will be design changes as analysis and test results show potential areas of weakness. One such change that has taken place is null pattern control. The original design incorporated a null pattern control supply, which provided a nonsynchronous triangular wave that was algebraically summed with the preamplifier output. Analysis and test results showed that this technique of maintaining a "two-two" limit cycle at accelerometer null was not as effective as the presently used feedback technique discussed under the Integrated Rate subtopic 2.15.6 (page 2.15-27). Subsequently, the null pattern control supply and its associated circuitry were deleted from the design and replaced with the time tested technique.

Topic 2.16

Coupler Precision Timing Functions

2.16.1. Introduction. - The purpose of the Precision Timing Generator (PTG) is to provide precisely timed pulses to control the electronics associated with the accelerometers. The timed pulses control the PRE Logic and Level Discriminator, Current Bridge Gates, and the Current-Master Gates. The Phase II and Improved Centaur PTG's are quite different in concept and design. Each of these three timing generators will be discussed in detail.

2.16.2 Clock Pulse Generator-Original Unit. - In the -1 and early -3 Couplers, precision timing was developed by the Clock Pulse Generator (CPG). The Clock Pulse Generator consisted of four blocking oscillators, three flip-flop modules, two differentiator and amplifier modules, and a phantastron delay circuit, which were connected as shown in Figure 2.16-1. The Frequency Standard fundamental frequency of 28.8 kHz was applied as the primary input to the A6 (Figure 2.16-1) module where it was differentiated and amplified. The output of the A6 module was applied to the Clock Pulse Blocking Oscillator, which generated a triggering pulse at 2π intervals of 28.8 kHz. The output of the A6 module provided the basic timing function for the precision timing pulses that control the accelerometers.

A 7.2 KC input was applied to the A7 module where it was amplified. The output of A7 module was then used to drive the 3600 flip-flop (A12). One output of the A12 module was differentiated and used to trigger the ACP0 flip-flop (A14) and the second output of A12 was differentiated to trigger the ACP1 flip-flop (A13). The ACP0 and ACP1 nomenclature indicates "Assembly" for Clock Pulse Zero and "Assembly" for Clock Pulse One respectively. The clock pulse was "ANDed" with the output of A14 to trigger the ACP0 Blocking Oscillator A4. The output of A4 then retrigged A14 which would remain reset until the next trigger from A12. In a similar manner, the clock pulse was "ANDed" with the output of A13 to trigger ACP1 Blocking Oscillator A5 whose output was fed back to reset A13. The outputs of A4 and A5 were negative pulses which were precisely timed and 138.8 microseconds apart.

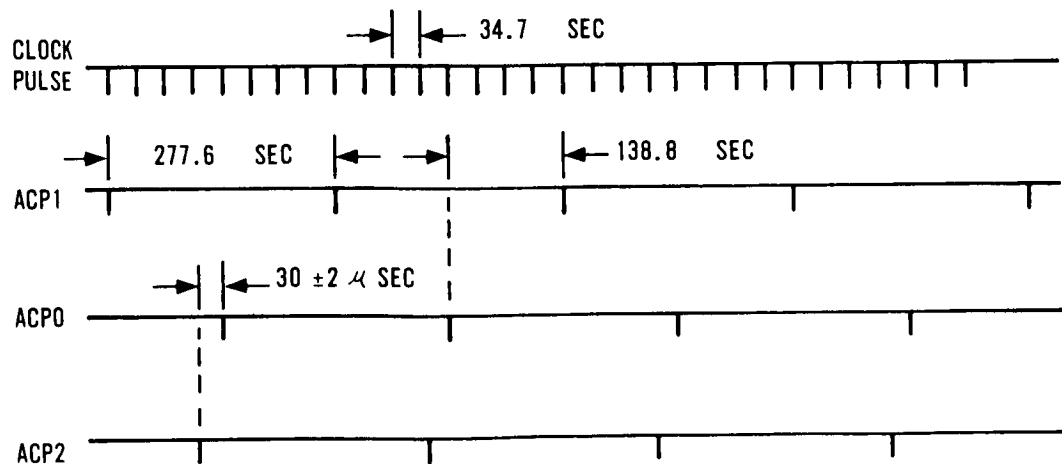
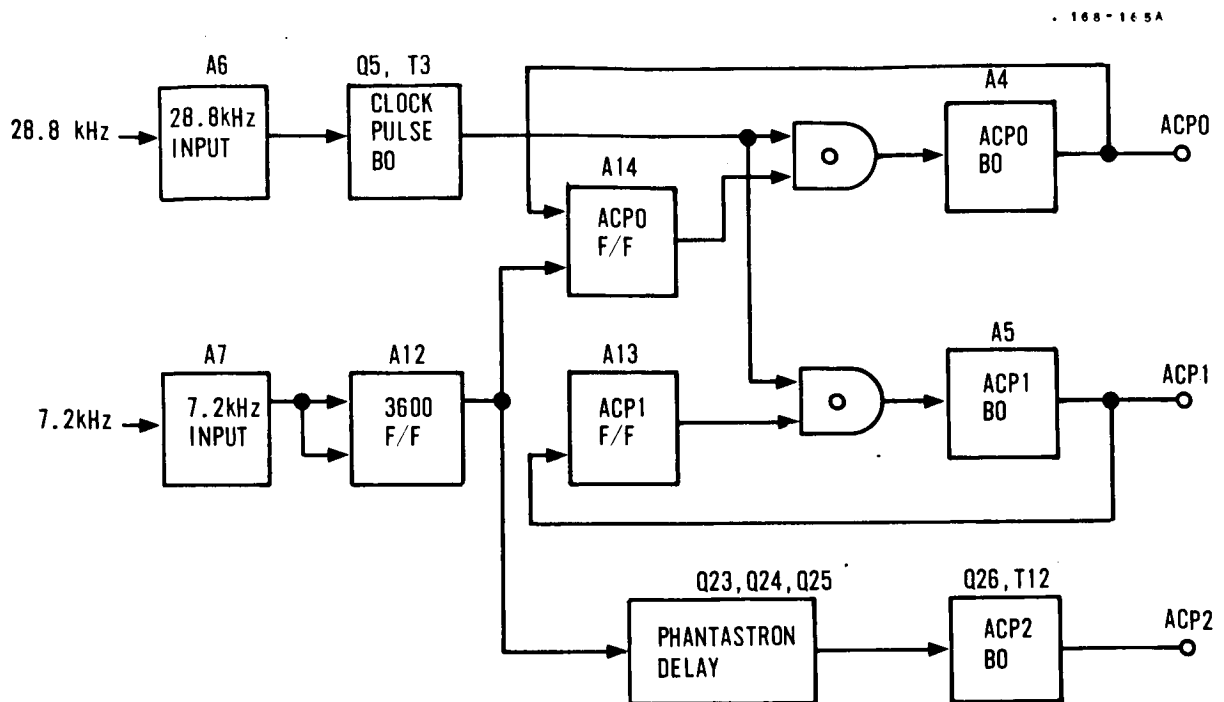


FIGURE 2.16-1. PRECISION TIMING GENERATOR BLOCK DIAGRAM AND TIMING PULSES

The output of the A12 used to trigger the A14 module would change state nominally 34 microseconds preceding a particular clock pulse (ACP0). This output from A12 would also trigger the phantastron delay circuit which would sweep approximately every 3.5 microseconds. The output of the phantastron was a negative gate having a duration of 3.5 microseconds. The trailing edge of this gate was differentiated and used to trigger the ACP2 block oscillator. The ACP2 output preceded the ACP0 output by approximately 30 microseconds. The precision timing functions are shown pictorially in Figure 2.16-1.

2.16.2.1. Problems Encountered with the Clock Pulse Generator. - There were three basic problems associated with the Clock Pulse Generator. The three problems are identified here and discussed in some detail in the following paragraphs.

1. Variable pulse width as a function of calibration.
2. Time stability or jitter of the precision timing pulses.
3. Past reliability problems inherent in original design.

2.16.2.2. Pulse Width as a Function of Calibration. - During the early Coupler calibration sequence, three adjustments were required to set the pulse width of the precision timing pulses. The timing pulses were used as follows to control the pulse-rebalanced accelerometers.

CP0 - Set the Master Gate Current Bridge and established accelerometer "torquer-on" time. The CP0 pulse was adjusted as follows:

Amplitude: 8.0 ± 1.2 volts
 Width: 1.4 ± 1.0 microseconds
 -0.4

CP1 - Master Gate and Polarity Gate reset pulse. The pulse amplitude and pulse width requirements were the same as CP0.

CP2 - The CP2 pulse was used to sample the polarity (indicative of pendulum position) of the Accelerometer Logic and Level Discriminator. The characteristics of CP2 were as follows:

Amplitude: 8.0 ± 1.2 volts
 Width: 1.4 ± 0.4 microseconds

The polarity or state Logic and Level discriminator was sampled during the time interval or duration of the CP2 pulse. As indicated by the pulse characteristics, the calibration requirements were stringent.

2.16.2.3. Time Stability or Jitter. - Because of the noise levels in the early -1 and -3 Couplers, and the fact that no worst case analysis had been performed, the timing of the precision clock pulses was difficult to establish and control. The relative timing or jitter of the clock pulses was checked during coupler calibration, and it was a requirement that pulse tolerances be maintained when the ± 35 volt power supplies were varied ± 1 percent during the calibration. Despite the repeated and extensive checks of the clock pulses during coupler calibration, the time stability of the timing pulses proved to be a problem.

2.16.2.4. Reliability. - The inherent complexity of the original CPG design plus the fact the device required calibration led to poor performance and reliability. The calibration requirement necessitated the use of variable potentiometers. The frequent adjustment of these potentiometers resulted in an abnormally high failure rate, and once the potentiometer had been adjusted, the calibration would frequently change with vibration or shock. In later PTG design efforts, the elimination of variable potentiometers led to improved PTG reliability.

2.16.3 Description of Phase II PIP Design. - The Precision Timing Generator previously described had problems both with marginal circuits and with fundamental design. During the Phase II Product Improvement Program, this board was replaced by one which was new in both concept and design. Since the type of timing pulses generated are different, its function will be re-described.

The Precision Timing Generator (PTG), provides the precision clock pulses used for timing control in the accelerometer pulse rebalance electronics. Five such pulses are provided for this purpose labelled C0, C1, C2, C3, and C2D. The PTG also provides 14.4 KC and 7.2 KC square waves to the AC Power supplies, which in turn provide the excitations for the gyro and accelerometer signal generators and servo amp demods. The ultimate reference frequency for the PTG is an ultra stable 28.8 kHz sinewave from a crystal controlled oscillator.

2.16.3.1. Clock Functions. - The demodulated accelerometer input to the level detector is asynchronous and must be stored before it can be further processed. The information in the level detector is dumped into a storage flip-flop at C2 time. The complete transfer is made during the width of the clock.

C2D Clock - The information in the storage flip-flop determines which pair of Current Bridge Control flip-flops are activated and is gated to these

control flip-flops at C2D time. Also at this time, a ΔV pulse is generated and sent to the computer. Again, complete transfer of information is accomplished during the width of the clock. C2D clock nominally occurs 17.3 microseconds after C2 clock and 17.4 microseconds prior to C0 clock.

C0 and C1 Clocks. - The C0 and C1 clocks control the length of time the Current Bridge supplies rebalance current to the accelerometer torque coil. Since this function directly affects system accuracy, the delay between and delay stability of these two clocks must be very precisely controlled. The Current Bridge turns "on" at C0 time and "off" at C1 time.

C3 Clock - C3 Clock resets the Current Bridge Control flip-flops. It nominally occurs 34.7 microseconds after C1 time.

2.16.3.2. Design Concept. - Refer to the Block and Timing Diagram of the PTG in Figures 2.16-2, -3, and -4. The buffer shaper amplifier is an emitter-follower and double inverter which produces complimentary 28.8 kHz square waves from the 28.8 kHz sine wave out of the frequency standard. This is counted down by 3 flip-flops to 14.4, 7.2, and 3.6 kHz. These signals provide the proper logic functions to gate the master clock pulse to the proper output inverter. The frequency dividers that set up the output gates are triggered on the compliment of the signal that triggers the master clock generator, such that no race conditions can exist.

Inherent in this scheme is the provision for the control of the C0 to C1 delay stability which is the most critical requirement of the unit. Since the master clock generates both output pulses and is merely gated out at different times, any changes in delay in the circuits leading to the generation of the master clock are serial changes, adding to both output pulses, their relative delay remaining unchanged. Such changes would include changes in the trigger levels in the buffer shaper amplifier or master clock generator with temperature or component aging. The situation which would not add the same delay to both output pulses is one where the input signal is high-frequency modulated, but every precaution has been taken to keep this signal clean and free from noise. The remaining possible error contributing circuits are the output gates and inverters which are the only parallel paths the output pulses must take. Every consideration was given these circuits to produce an adequate, stable, circuit design. The circuits are identical and are packaged in the same welded potted module for temperature tracking.

0168-164A

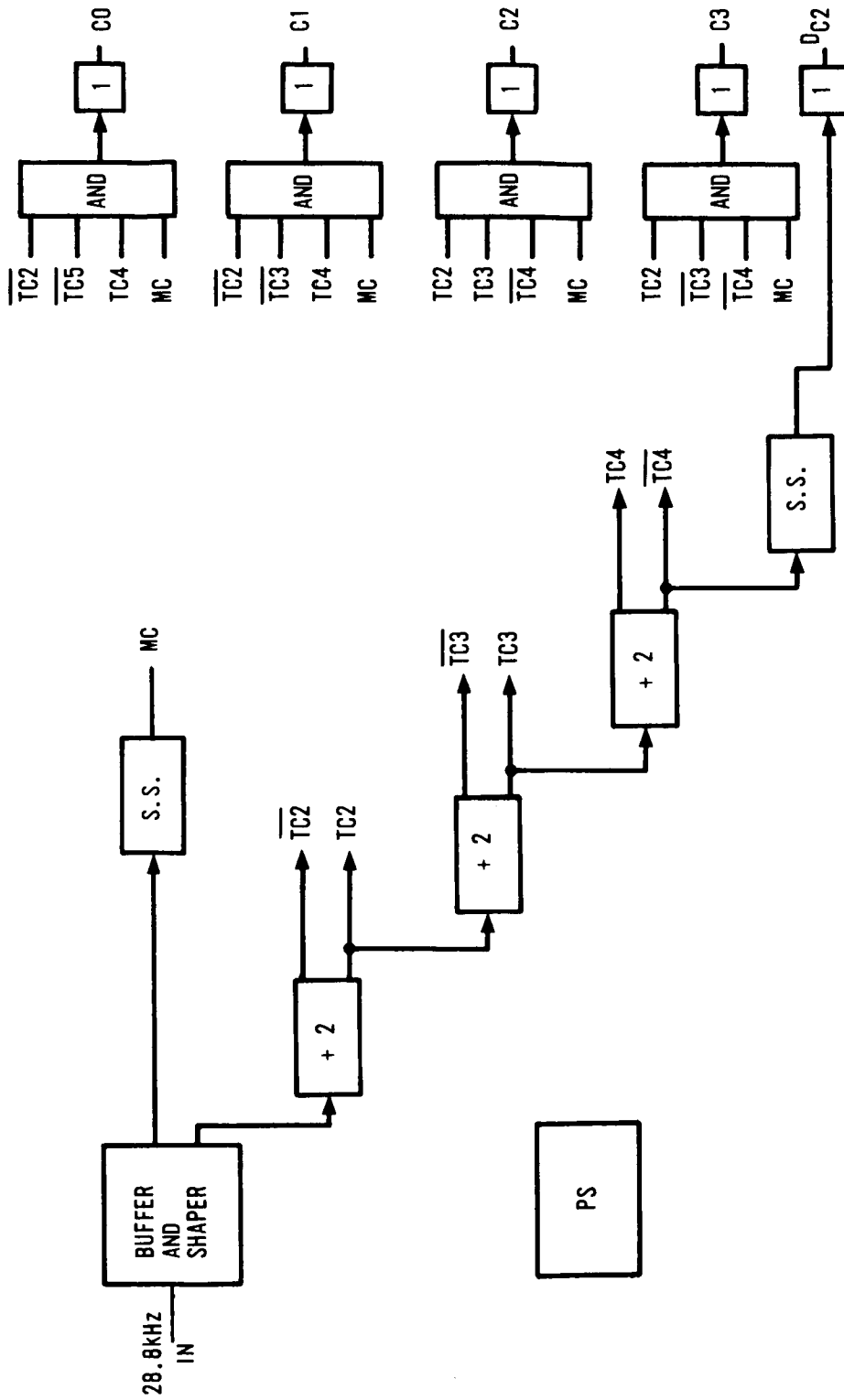
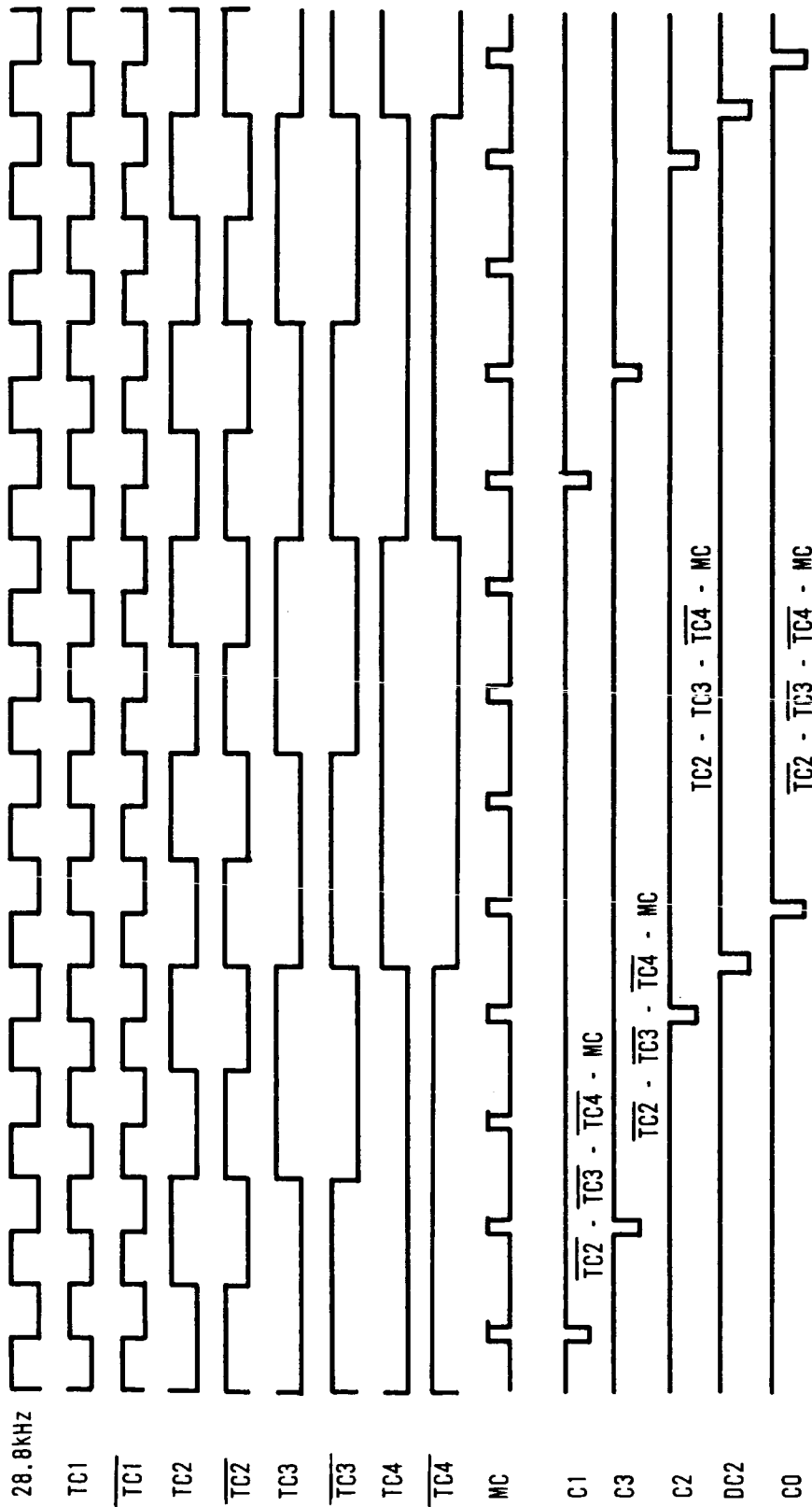


FIGURE 2.16-2. PRECISION TIMING GENERATOR BLOCK DIAGRAM

0166-186A

FIGURE 2.16-3. TIMING, FREQUENCY DIVIDER AND
CLOCK PULSE GENERATOR

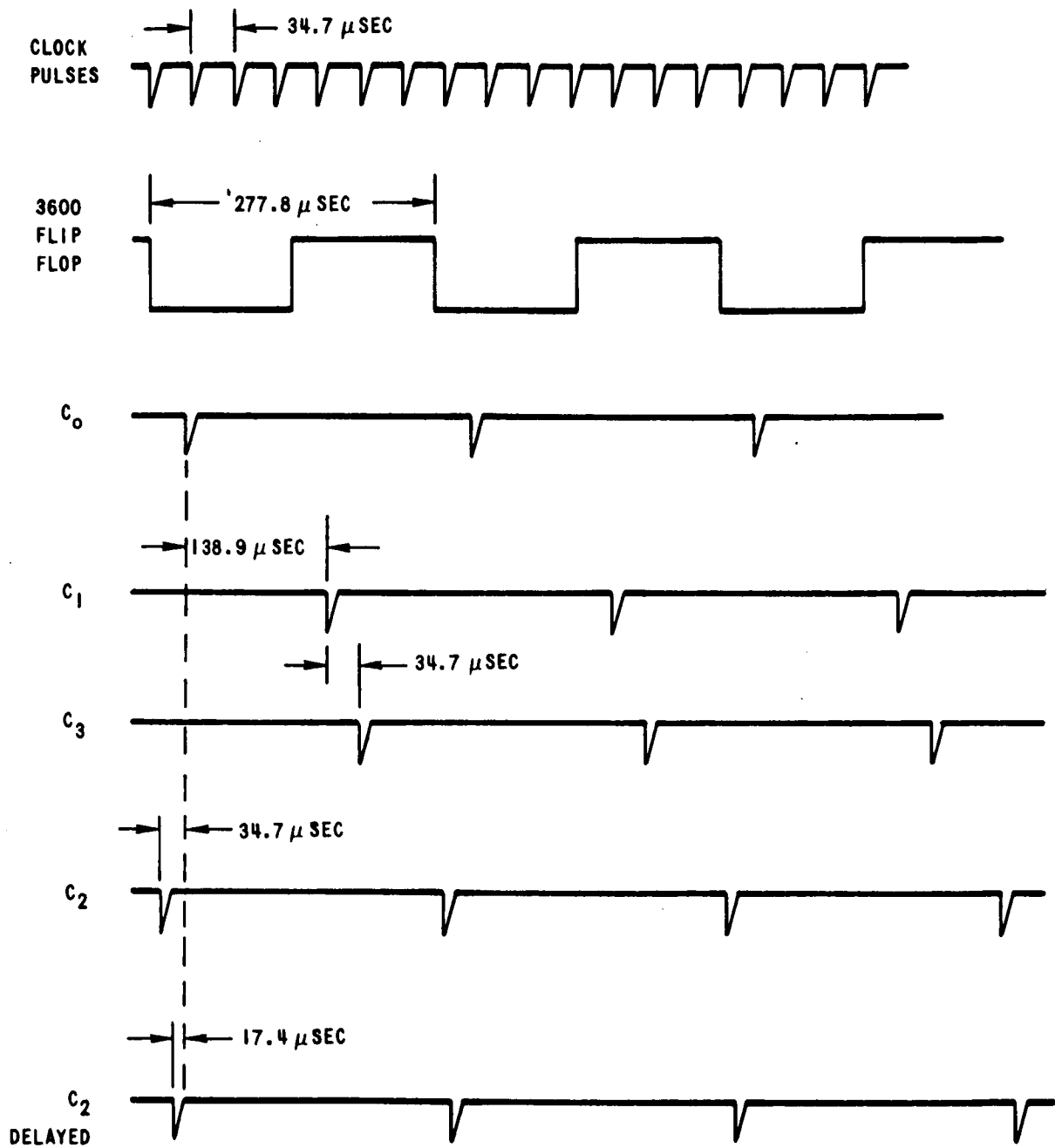


FIGURE 2.16-4. VELOCITY LOOP TIMING PULSES

C2 and C3 are generated in like manner to C0 and C1 though their position and stability are not at all critical. C2D is generated by a separate single shot and inverter triggered from TC4 to allow C2 to be generated as close to C0 as one timing bit would allow.

The 14.4 KC and 7.2 KC square waves required by the ac power supplies are direct outputs of the frequency divider flip-flops.

2.16.3.3. Mechanization. - The basic operation of the PTG circuitry for Phase II PIP is shown in Figure 2.16-5. Since there is nothing unique about this mechanization, a detailed explanation of the circuitry will not be included. The plus and minus 3V dc required by the internal circuitry is generated by means of zener diodes and is heavily filtered. The +25V dc input power is both low and high frequency decoupled and while the -35V dc input line is not decoupled, it is well isolated from the internal circuitry because of the manner in which it is used.

The PTG circuitry is packaged cordwood fashion in potted welded modules and mounted on a printed circuit board. Ten modules make up one unit. The circuits are broken up into modules on the basis of function. Each functional block as seen in the block diagram in Figure 2.16-2 makes up one module with the following exceptions:

1. C0 and C1 AND Gates and Inverters are packaged in one module.
2. C2 and C3 AND Gates and Inverters are packaged in one module.

C2D Inverter makes up a module by itself. Electrical connection is made with the board by means of Elco pin contacts.

2.16.3.4. Worst Case Analysis. - Approach - The Net 1 Circuit Analysis Computer Program was primarily used to perform the worst case analysis of the PTG circuitry. This program, with its dynamic semiconductor models, is ideally suited to transient analysis, and transient conditions can be considered the normal operation of the switching circuits of the PTG.

It is not at all practical, however, to put the entire PTG design on the computer at one time. Instead, the analysis was performed on the individual building blocks and emphasized three major conditions:

1. Worst case stability.
2. Worst case stress.
3. Worst case switching.

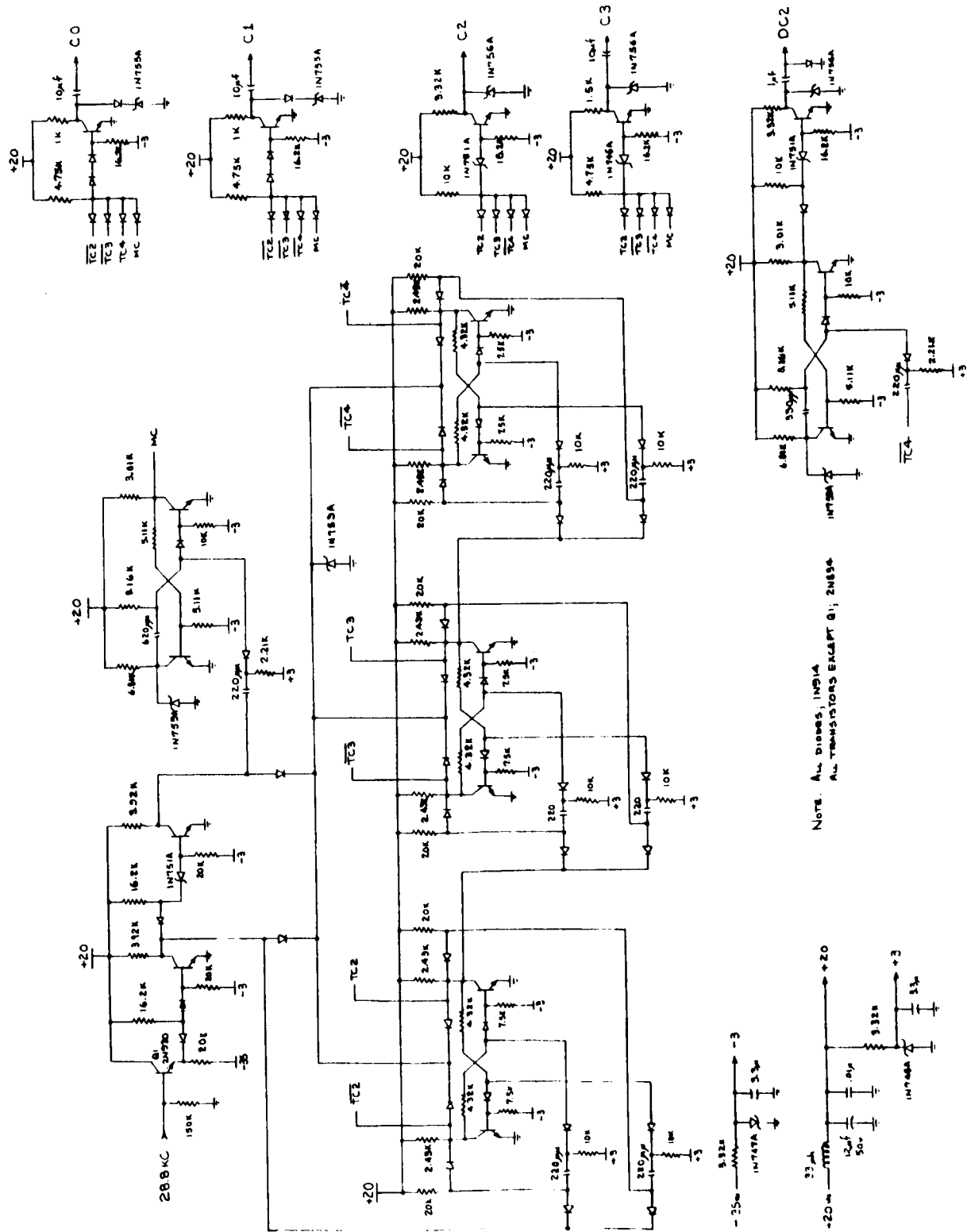


FIGURE 2.16-5. PRECISION TIMING GENERATOR

The worst case analysis using computer techniques confirmed the soundness of the design. The breadboard PTG test results follow the results of the worst case analysis. All unique dc and switching parameters were measured with the breadboard subjected to ambient temperatures of -25, 0, 25, 100, and 125°C, which are substantially beyond the required operating temperature limits. No "out-of-spec" conditions were noted.

2.16.4. Precision Timing Generator for the IMG. - The Precision Timing Generator (PTG) consists of two functional areas:

1. A frequency standard.
2. Frequency divider and gating.

On previous timing sources, these were two separate assemblies.

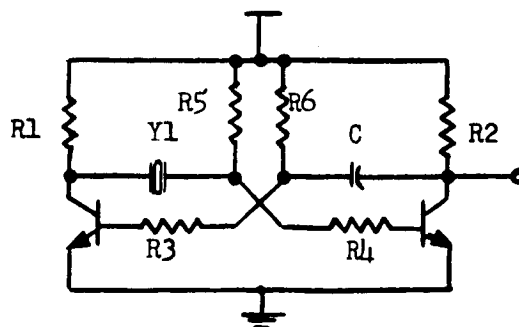
The following chart summarizes the IMG operating frequency outputs required of the PTG. Frequency selections were established via parameter studies associated with each of the IMG functional control loops and on the basis of compatibility with logical countdown approaches within the PTG. Output frequency tolerance and stability requirements were governed by error budget allocations associated with the most critical load; the accelerometer rebalance loop.

<u>Frequency</u>	<u>Stability</u>	<u>Form and Function</u>
57.6 kHz ±0.1 percent	40 ppm	Square-wave signal providing power supply section frequency for accelerometer signal generator excitation.
14.4 kHz ±0.1 percent	40 ppm	Square-wave signal providing power supply section frequency for gyro signal generator excitation.
9.6 kHz ±0.1 percent	40 ppm	Square-wave signal providing power supply section frequency to be used for DC-DC power converter.
4.8 kHz ±0.1 percent	40 ppm	<ol style="list-style-type: none"> 1. Square-wave signal providing PRE with the gating frequency required for pulse repetition rate of loop. 2. Three clock pulses 1.1 microsec in width occurring at the stated frequency.

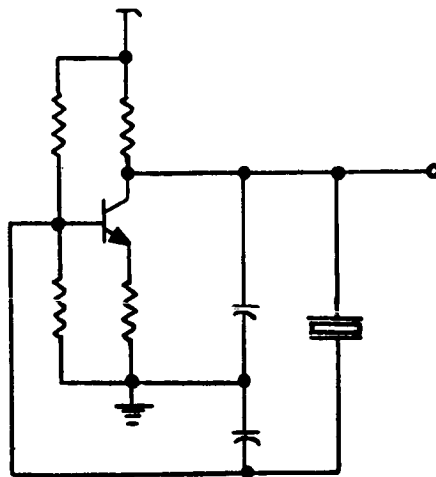
<u>Frequency</u>	<u>Stability</u>	<u>Form and Function</u>
4.8 kHz (Continued)		These frequencies are to be used as the sampling, set and ΔV output clocks in the velocity measurement loop.
3.2 kHz ± 0.1 percent	40 ppm	Square-wave signals providing power supply section the frequency to be used for resolver excitation.
2.4 kHz ± 0.1 percent	40 ppm	
0.4 kHz ± 0.1 percent	40 ppm	Square-wave signal providing power supply section the frequency to be used for gyro spin motor excitation. Only one phase will be provided.

2.16.4.1. Frequency Standard Selection. - Three different types of oscillators were evaluated versus requirements set for the oscillator in the Technical Specification. Tradeoffs considered the following characteristics:

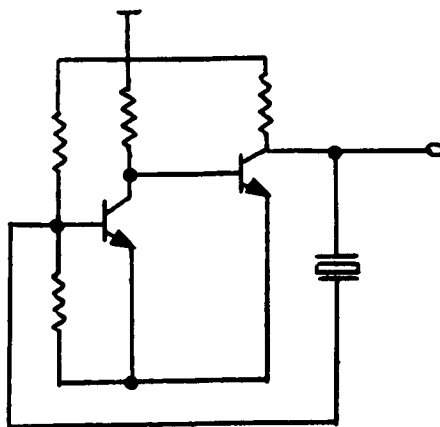
1. Type of Oscillator (see Figure 2.16-6)
 - Two-stage amplifier with positive feedback.
 - Single-stage amplifier with tuned tank circuit that provides positive feedback (Clapp Oscillator type).
 - Single-stage amplifier with RC networks on the output sufficient to provide positive feedback.
2. Type of Oscillator Control
 - Crystal control.
 - Reactive components (inductors, capacitors).
3. Basic Operating Frequency
 - 460.8 kHz.
 - 230.4 kHz.
 - 115.2 kHz.



Alternative A - Multi-Vibrator (Crystal Controlled)



Alternative B - Clapp Oscillator (Crystal Controlled)



Alternative C - Two Stage Amplifier with Positive Feedback

FIGURE 2.16-6. BASIC OSCILLATOR TYPES

4. Type of Environment Control

Constant temperature.

The first decision made was that a crystal-controlled oscillator would be used. The reasons for this decision being:

1. Crystals provide highly reliable equivalent series-parallel resonance circuits with circuit Q's much higher than those available with reactive component resonance circuits.
2. Crystals provide high frequency stability when specifications are imposed to assure same.
3. Crystals with high reliability, good selectivity of frequencies, and high stability are relatively inexpensive.

The choice of oscillator type was influenced by the decision to use crystal frequency control. Specifically, the crystal must be in an oven for temperature control, and the oscillator must be in or near the oven.

Of the three basic types of oscillators previously cited, the third type (RC positive feedback-single stage) is not directly applicable to crystal controlled circuits. The second type (tuned-tank circuit-single stage) was excluded from further consideration due to its need of reactive components other than the crystal to control frequency. The first type (multivibrator type) was chosen since the crystal exclusively controls the frequency if the temperature and power supply voltage is maintained constant within required limits. This two stage amplifier (multivibrator type) design offers high stability, since the stability is entirely dependent on the crystal. This integrated circuit also offers cost and size savings and improved reliability.

A requirement exists that the sample pulse must maintain a distinct angular relationship with the signal generator excitation voltage. Use of 460.8 kHz as the oscillator frequency provided the ability to set the sampling network (of the velocity loop) in the correct phase angle relationship with the excitation in question. The use of a Schmidt trigger and a lower frequency oscillator was rejected since the Schmidt trigger timing is dependent upon reactive components, which are more susceptible to error causes (temperature and time variations on the RC components setting the pulse time constant) than those associated with the basic crystal.

Based upon the tradeoff study, a multivibrator type crystal-controlled oscillator, which will be oven housed, was chosen as the best mechanization for this application. A power supply regulation circuit was included to optimize the multivibrator circuit.

2.16.4.2. Proposed Mechanization. - The IMG mechanization is shown in Figure 2.16-7. This particular circuit employs an integrated circuit to provide the transistors for the multivibrator. It was recommended that integrated circuits be used because of their small size, and improved reliability over discrete components. Figure 2.16-8 shows the circuit in the more familiar form of a multivibrator circuit but still using the particular integrated circuit.

The crystal is started into oscillations at turn-on of the power supply and is sustained at the resonance frequency of the crystal. The crystal allows feedback only at its resonance frequency. At any other frequency the crystal's impedance is reactive, therefore precluding positive feedback operation. The R2C2 time constant provides the symmetry adjustment capability in the circuit. The circuit has both power supply regulation and noise rejection sufficient to provide the highly stable frequency desired.

2.16.4.3. Frequency Divider and Gating Section. - System requirements specify that the frequencies shown in Figure 2.16-9 must be supplied by the frequency divider and gating section. Tradeoffs conducted for this section include:

1. Establishment of optimum countdown sequence.
2. Establishment of a circuit design approach to reduce jitter to acceptable limits.
3. Selection of the type of circuit components employed:
 - Integrated circuits.
 - Discrete components.

The countdown sequence was selected by logical design processes. Figure 2.16-10 shows the mechanization that evolved from the study. This approach is considered an optimum mechanization to provide the required frequencies with a minimum number of logic components.

A must in the design of the frequency division section was that stability be maintained between required output clock pulses. This problem was solved by selection of a countdown circuit design approach, which interlocks all frequency. Figure 2.16-11 shows the timing diagram that was evolved from the use of the mechanization of Figure 2.16-10. Close inspection of the diagram will show that each frequency division is initiated

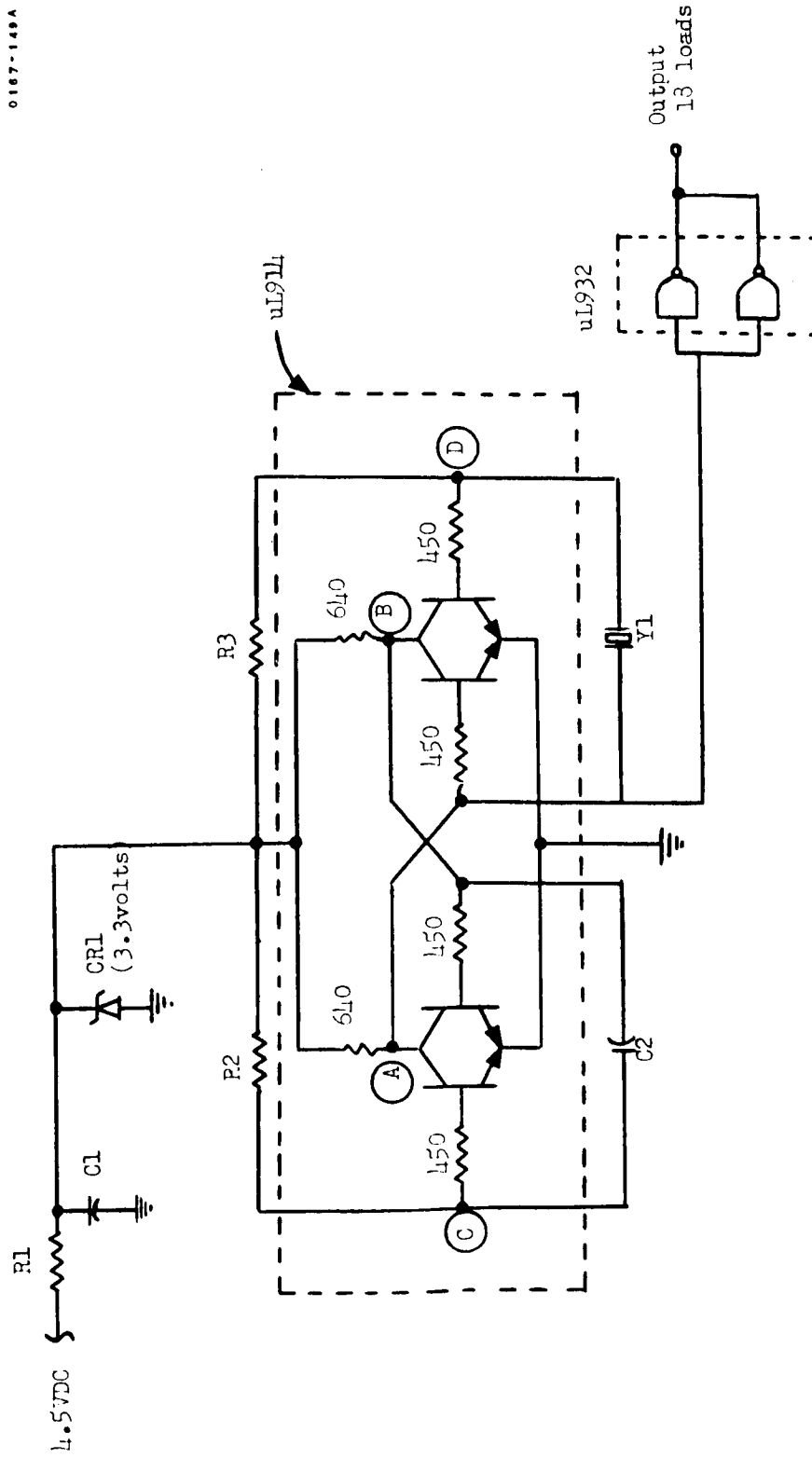


FIGURE 2.16-7. CRYSTAL CONTROLLED OSCILLATOR

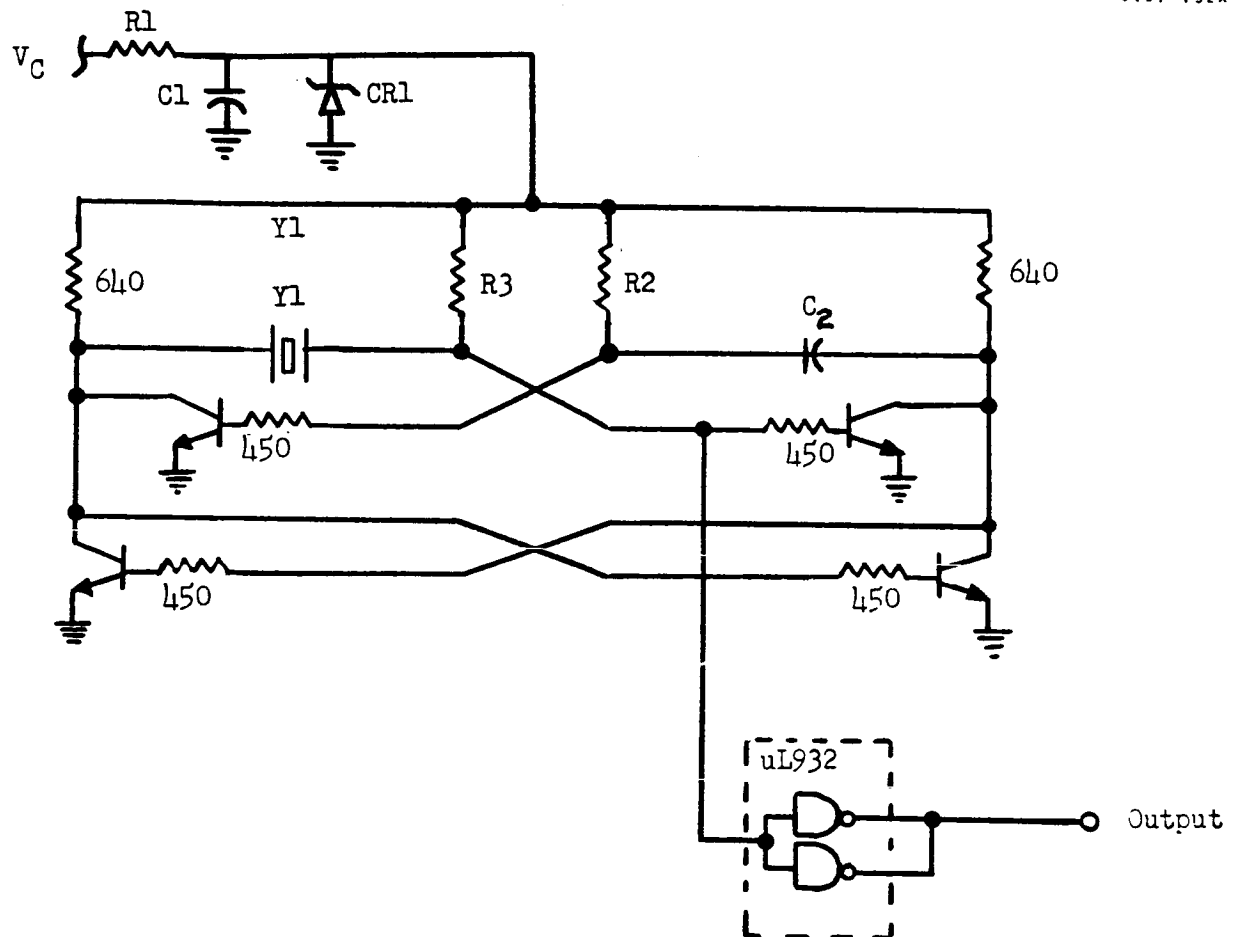


FIGURE 2.16-8. CRYSTAL CONTROLLED OSCILLATOR REDRAWN

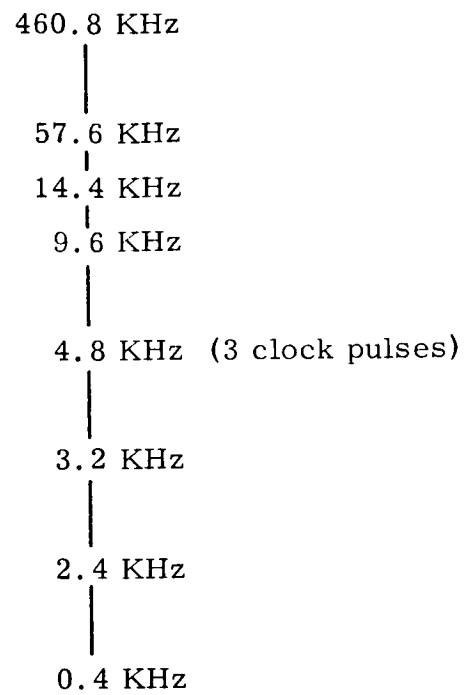


FIGURE 2.16-9. REQUIRED PRECISION FREQUENCIES

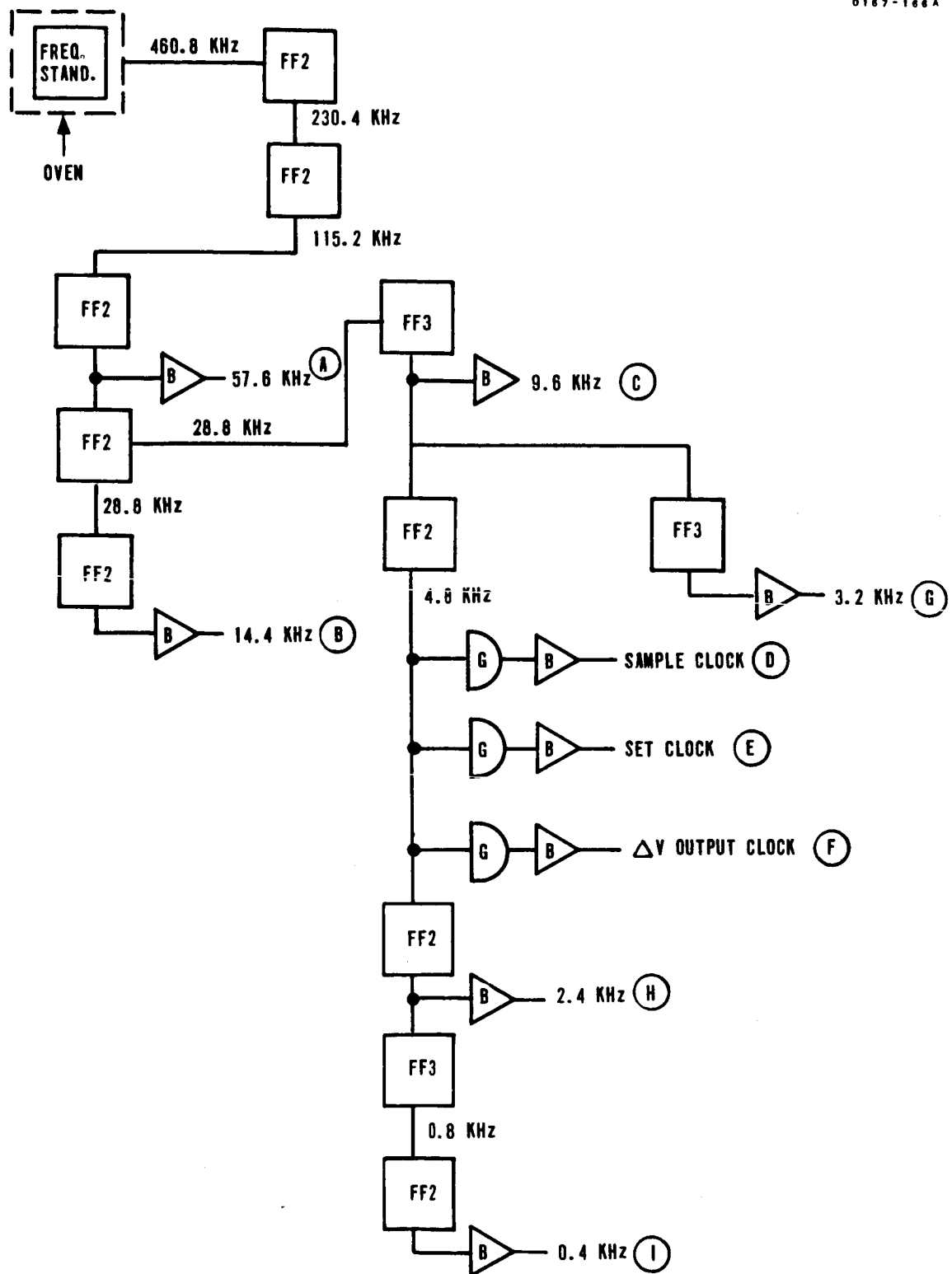


FIGURE 2.16-10. PROPOSED COUNTDOWN MECHANIZATION

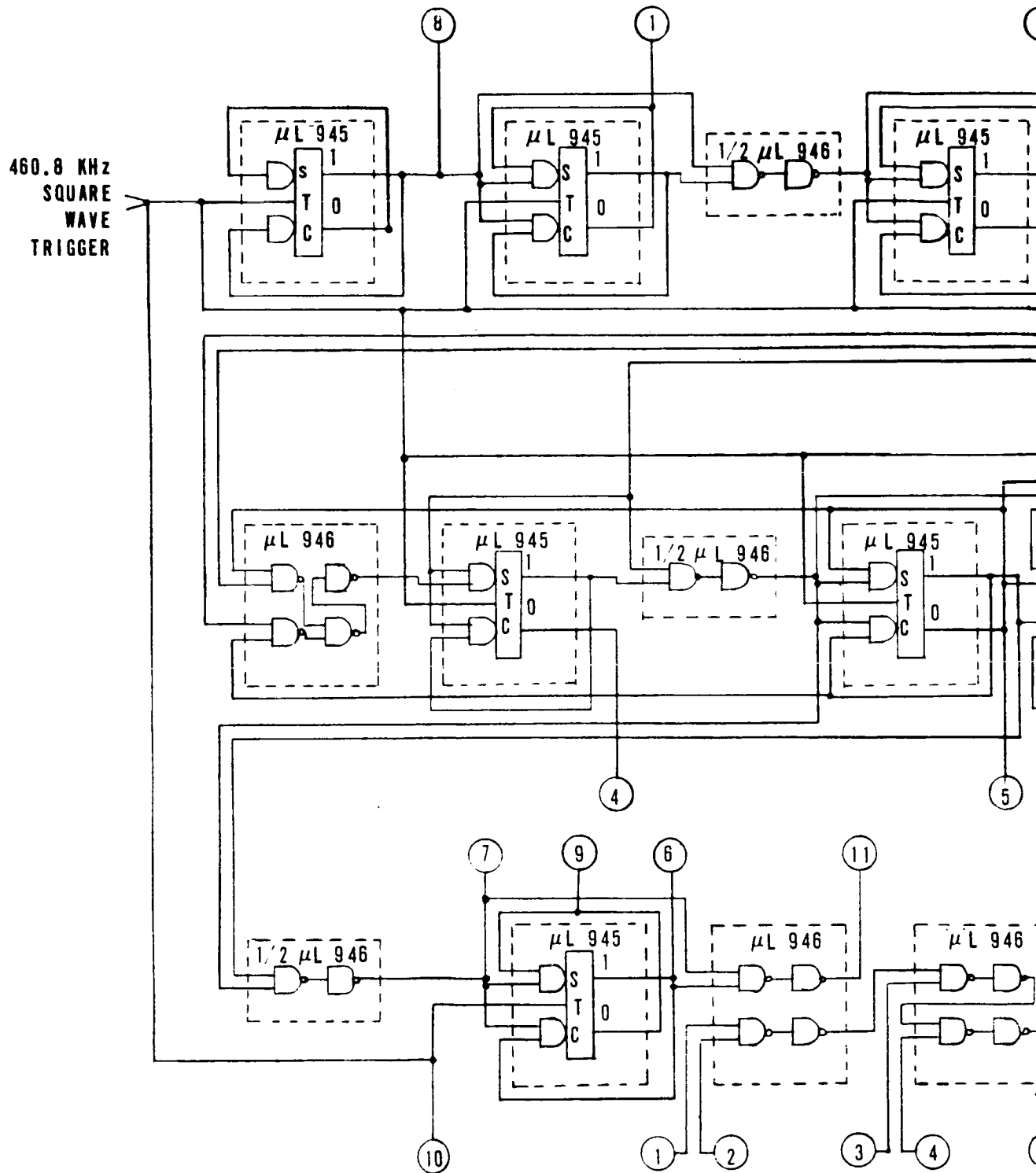
only when all previous frequencies are in a "high" (positive logic "1") state and a negative going trigger (460.8 kHz) occurs. This is accomplished by sequentially "ANDing" each frequency into the next frequency division stage and then letting the negative trigger accomplish the frequency division. This eliminates any jitter between frequencies that could be caused by delay times within the countdown circuitry. The stability between pulses is as good as the frequency standard stability which is required to be 40 parts per million. Any instability between pulses due to the frequency standard should be of a random nature, thus the error introduced is insignificant.

Size reduction alone would dictate the use of integrated circuits for this application. Integrated circuits of the 930 series have also proven to be reliable, therefore, it was recommended that integrated circuits of the 930 series be used in this application rather than digital circuits constructed from discrete components. The integrated circuits can provide the required rise times and fall times and will provide completely satisfactory operation in this application.

2.16.4.4. Proposed Mechanization. - Figures 2.16-11 and 12 show the circuit diagram of the recommended mechanization shown in Figure 2.16-10. Three types of integrated circuits can be used for the complete design of the circuit. Basic logic division techniques were used in obtaining the divide by two and divide by three circuits shown. The timing diagram (Figure 2.16-12) is a visual representation of the logic equation necessary to provide the required outputs. The timing diagram and the schematic are cross-referenced as far as definition of output signals are concerned. At present, the circuit design appears to be the optimum design for the selected mechanization.

2.16.5. Precision Timing in Retrospect. - The Precision Timing Generator for both Phase II PIP and for the IMG are adequate designs in all respects. The IMG takes advantage of improved components. The early Centaur timing generator, however, would certainly have improvements if it were designed today. The following improvements would be made:

1. Since the distance between C0 and C1 are the starting and stopping points of accelerometer torquing, this is one of the basic factors which determines system accuracy. The time of occurrence of these two pulses would be determined by using the same clock source so that any jitter which occurred on one clock pulse would also occur on the second pulse. The



9167-2000

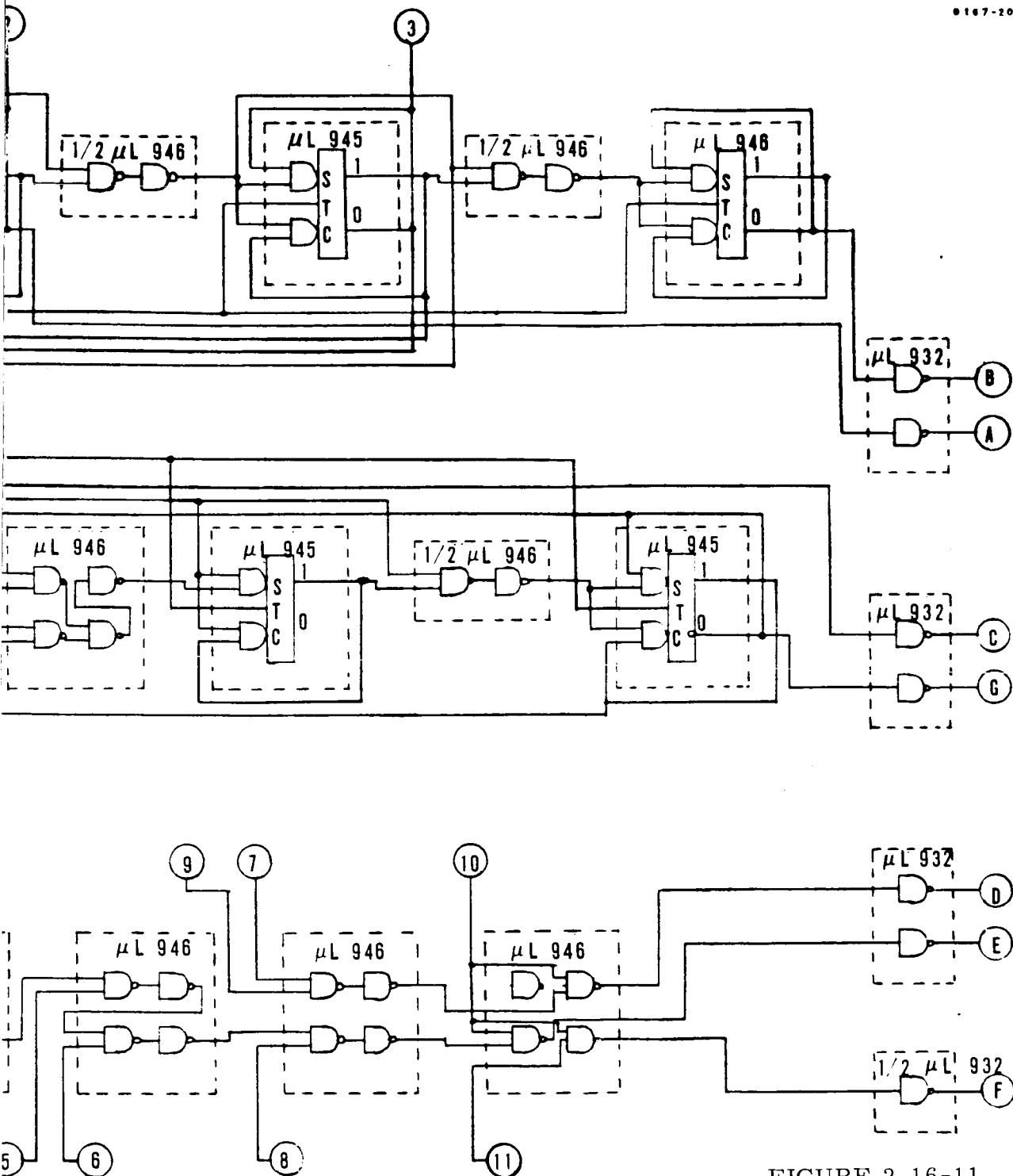
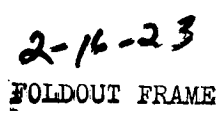


FIGURE 2.16-11
PRECISION TIMING GENERATOR -
FREQUENCY DIVISION
(Sheet 1 of 2)



FOLDOUT FRAME

2167-207B

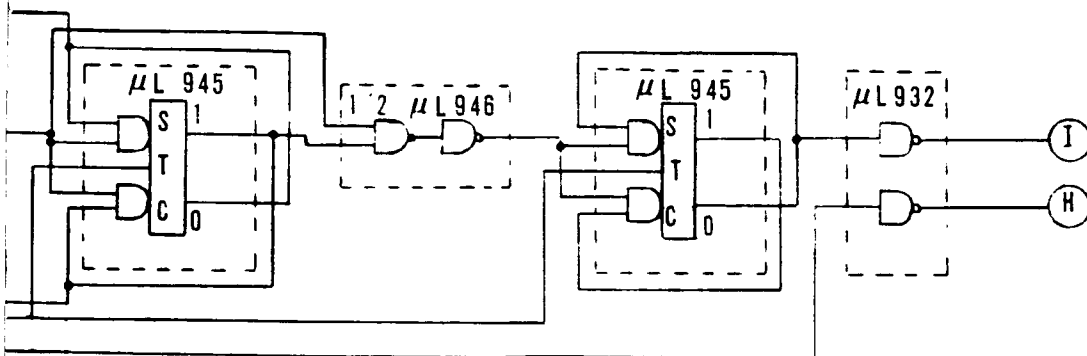


FIGURE 2.16-11
PRECISION TIMING GENERATOR -
FREQUENCY DIVISION
(Sheet 2 of 2)

~~2.16-23~~
2.16-24

FOLDOUT FRAME

480.0 KHz

230.4 KHz

115.2 KHz

57.6 KHz

28.8 KHz

14.4 KHz

9.6 KHz

4.8 KHz

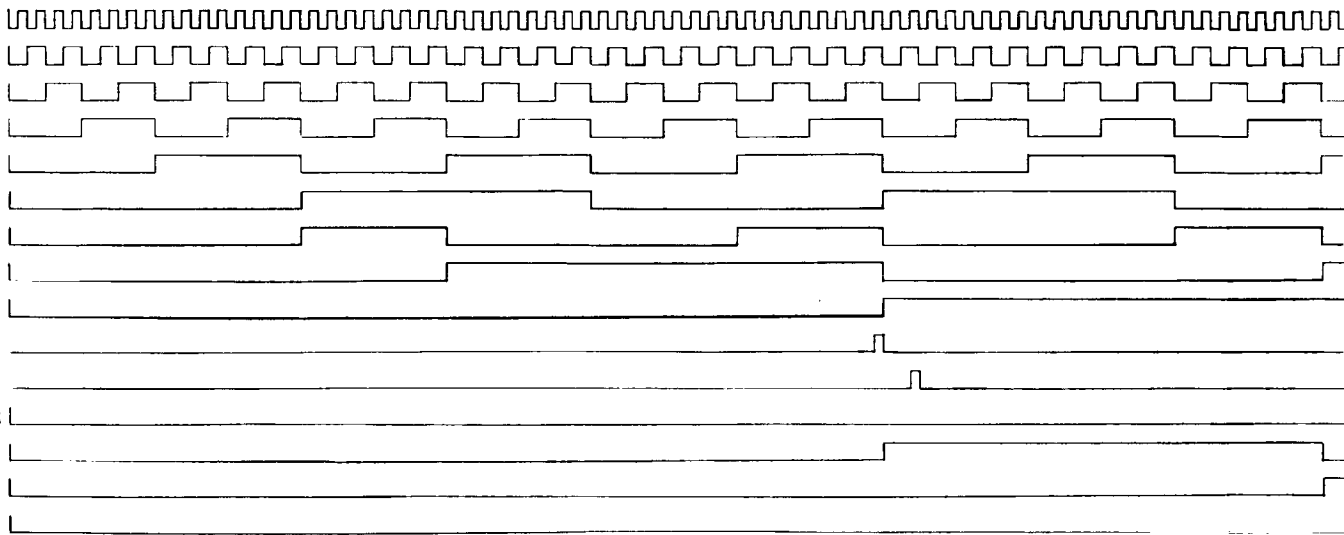
SAMPLE CLOCK

SET CLOCK

ΔV OUTPUT CLOCK

3.2 KHz

2.4 KHz



2-16-25

FOLDOUT FRAME

0167-211B

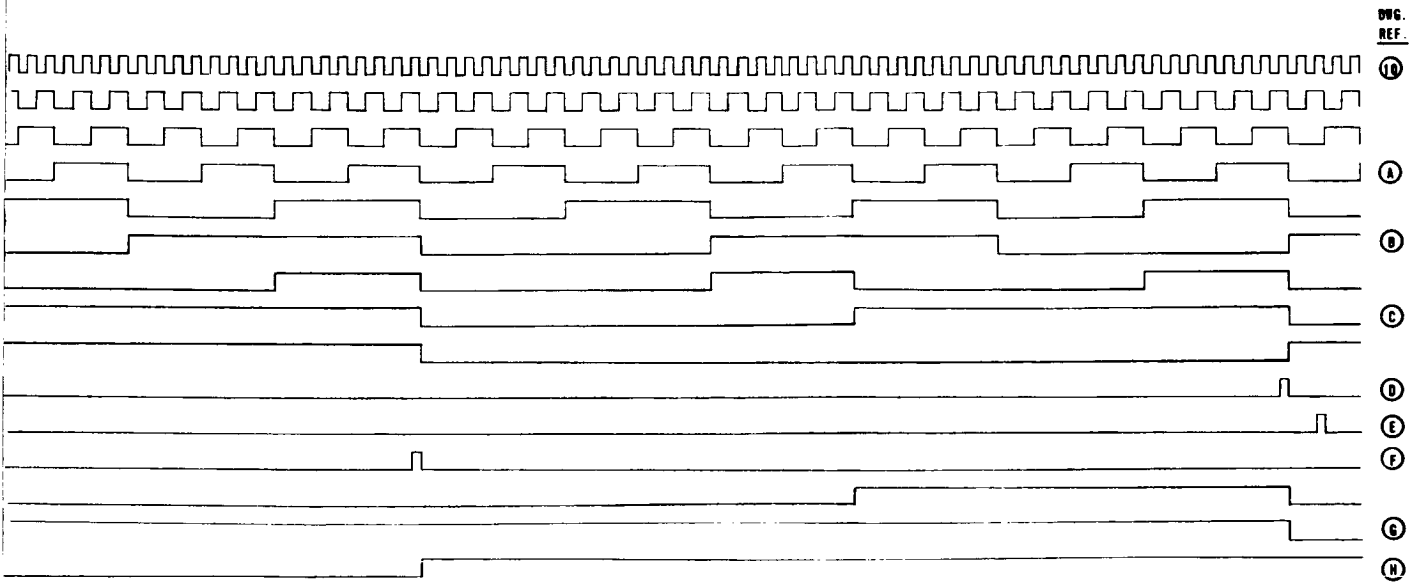


FIGURE 2.16-12
TIMING DIAGRAM FOR
PRECISION TIMING GENERATOR

~~2.16-25~~
2.16-26

FOLDOUT FRAME

relative distance between C0 and C1 is rather constant. For the early design, this distance between C0 and C1 was determined by separate RC time constants.

2. Worst case circuit analysis would be used.
3. The basic clock outputs would be amplified by a power amplifier, instead of a blocking oscillator, as an output medium to maintain a more constant pulse width with load and temperature changes.

2.16.6. Conclusions. - The purpose of this Precision Timing Generator is to provide precisely timed pulses to the Accelerometer Rebalance Logic, and Accelerometer Rebalance Current Gates. This unit in the original design was unreliable because of the available components and the lack of worst case design. It also contributed to system error by allowing the distance between C0 and C1 (torquing pulses) to jitter. Errors were also caused by the width of the clock pulses, which changed pulse width as temperature and loading varied.

A new design was completed in 1965 for Phase II PIP. A second new design was completed for the IMG in 1967. Both of these designs are fully successful in meeting their performance and reliability objectives. The Improved Centaur PTG gating is designed with the more reliable integrated components and has a frequency standard which is less susceptible to jitter than the Phase I PIP and other previous designs.

The high precision clock and timing pulses provided in the IMU can be made available for use external to the IMU. In future vehicle designs, consideration should be given to their use for precision clocking of other vehicle subsystems in order to eliminate duplicate functions on the vehicle.

Topic 2.17

Gyro Torquing Electronics

2.17.1. General. - Gyro torquing is necessary for two reasons. First, each gyro is subject to unwanted forces which tend to turn it from its desired position. Second, it is necessary to torque the gyros to position the platform in all preflight modes except coarse align. The requirement for gyro torquing is to maintain a stable platform reference, or because it is desired to change to a new reference. Torquing to maintain a stable reference is required because gyros are not perfect devices. All command gyro torquing is obtained from the torquing potentiometers in the digital computer and from the optical torquing signal from the GSE. The mechanization of gyro torquing is detailed in Topic 6.11.

2.17.2. Computer Torquing Description. - The computer contains three digital torquing modules. Each torquing module provides an analog output from a 20 turn 10K potentiometer. The torquing potentiometer (Figure 2.17-1) is supplied with precision +22VDC and -22VDC from the Coupler.

The computer calculates the required gyro torquing rates and compares it with the actual torquing rate in the error determining logic. Any difference generates an error signal which is sent to the error hold circuit, which stores and maintains it as an input to the servo amplifier, until a new signal is received. The servo amplifier will cause the motor to drive to reduce the error. The motor positions the potentiometer and an encoder through a gear train. The encoder is an analog to digital converter whose output represents the actual torquing rate. The serial scan matrix converts this signal to serial form and routes it to the error determining logic where it is again compared with the required torquing rate.

This cycle continues until the actual torquing rate equals the required torquing rate. The error hold circuit will then receive a no error signal causing it to change the stored error signal and stop the motor. A brake holds the gear train in a fixed position during power transfer and inflight coast phases.

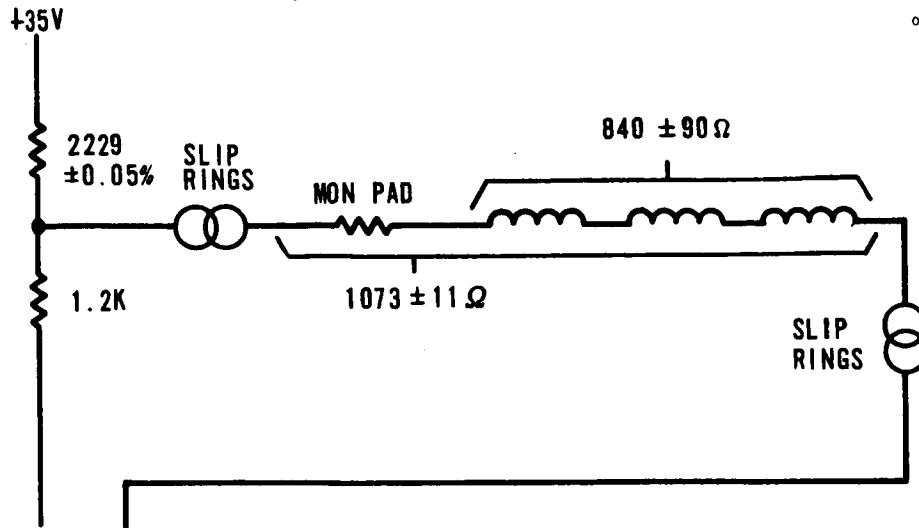


FIGURE 2.17-1a. GYRO PATTERN FIELD SUPPLY

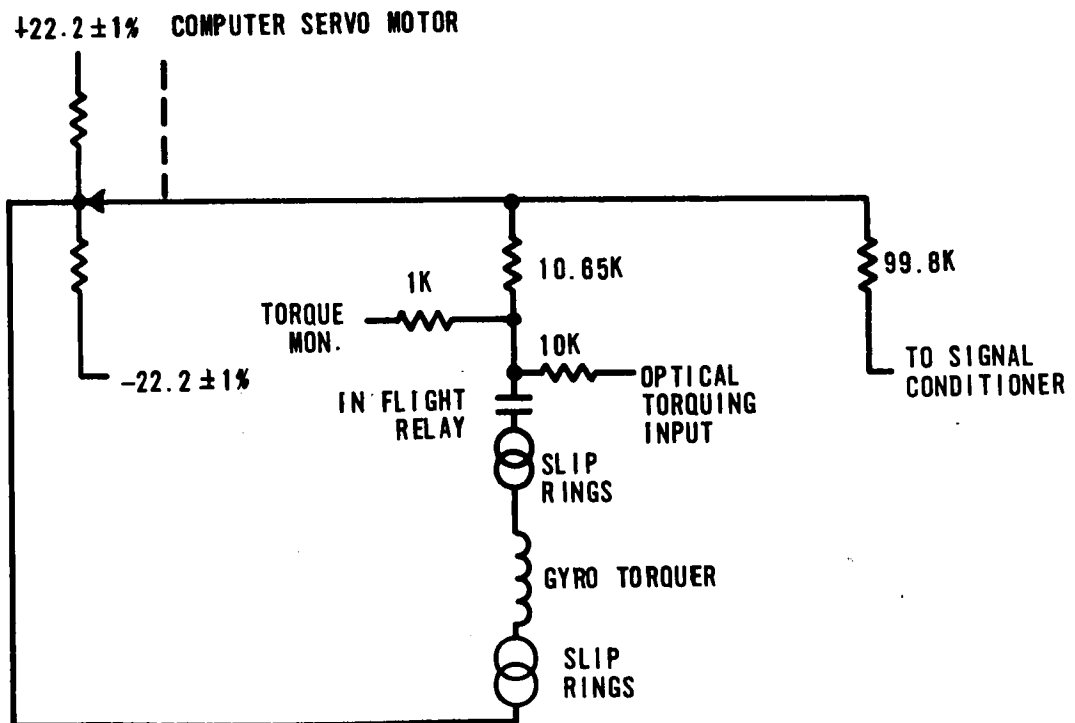


FIGURE 2.17-1b. GYRO CONTROL FIELD CIRCUITRY

2.17.3. Coupler Circuitry. - The Coupler circuitry required to provide gyro torquing consists of:

1. Gyro Pattern Field Supply.
2. Gyro Control Field Excitation.

The present Gyro Pattern Field Supply is simply a scaled down voltage output from the +35VDC supply to provide 10.6 ma. The circuit is shown in Figure 2.17-1a. The +35VDC supply is detailed in Topic 3.26. All the pattern fields are in series and are padded to 107 ± 11 ohms.

The Control Field Supply is shown in Figure 2.17-1b. The control field of each gyro is excited from the output of the potentiometer in the computer. The gyro control field current is linearly proportional to the rotation of the arm from the center tap, which is at signal ground. In series with each gyro winding is a resistance of 10.65K ohms in the Coupler. This resistance is proportional such that, for each gyro, the effective loading on the potentiometer is 10K ohms. The loading of the signal conditioner circuits on this arm is approximately 100K ohms, hence, the 11.1K ohms in the gyro circuit in parallel with the 100K ohms yields an effective load of 10K ohms, providing 2 ma of control field torquing current.

The + and - 22VDC precision regulators each supply 18 ma to the gyro torquer potentiometers located in the computer. The regulator is a conventional, series type having the impedance of the series element controlled by the magnitude of the output voltage. A portion of the output voltage is compared against a zener diode reference voltage by means of a differential amplifier. The output of the differential amplifier is then applied to a dc amplifier to control the operating point of the series element. Phasing is such that as the output voltage drops, the impedance of the series element is reduced, thus reducing the voltage drop across the series element and raising the output voltage.

2.17.4. Changes to Gyro Torquing Circuitry. - In late 1965 a conditional, parasitic oscillation involving the -22.2 volt regulator was discovered. Investigation and analysis pinpointed the problem cause to be a tuned circuit, created by a capacitor and the printed circuit wiring paths. The capacitor was removed from the circuit, eliminating the problem. A computer study was performed to demonstrate the stability under maximum and minimum gain conditions with the capacitor removed.

The Phase II PIP retrofit changed the Gyro Pattern Field Supply. The original supply provided $10.6 \text{ ma} \pm 33 \mu\text{a}$ to the gyro pattern field windings. The voltage across the sensing resistor was fed back to the input of a constant current supply for precise regulation. The unit was made up of a chopper-stabilized dc amplifier, an ac hum-reducing amplifier, and a direct-coupled series regulator. A constant reference voltage was obtained from a temperature-controlled bridge with a zener diode in one leg. Across the bridge was a stabilized voltage reference amplifier, which provided a constant output to the current supply. This technique is similar to that now used in the ARCS. The output of the current supply was applied as the input to the gyro pattern field supply.

The reasons the Phase II PIP change was made were twofold:

1. The Phase II PIP technique utilizes fewer and simplified components, and increases the circuit reliability.
2. The accuracy provided by the -3 supply was not needed when the inflight torquing requirement was eliminated (prior to Phase II PIP).

It was determined through analysis and test results that the computer could store and operate on the predetermined gyro terms more accurately and reliably than by actually torquing the gyro. A relay was added to the circuitry in series with the gyro torquer to disable the control torquing loop at vehicle lift off. The provision was also made to allow inflight torquing if necessitated by a mission change, etc.

2.17.5. Gyro Torquing in the IMG. - The IMG gyro torquing technique is being changed to -

1. Simplify hardware.
2. Increase reliability.
3. Eliminate coarse align gimbal positioning.
4. Minimize interface lines.

2.17.6. Background for IMG Torquing Electronics. - Since the need for inflight torquing and its accuracy requirements were dropped prior to the IMG, the way was paved for a simplified torquing circuit. In the past, the necessity to demagnetize the dualsyn of the DGG49 gyro, after exceeding 2 ma of control field current, had imposed torquing design and mechanization difficulties. In an effort to relieve or eliminate these difficulties, the dualsyn of the gyro was analyzed and tested further to find a torquing mechanization that did not require demagnetization after high rate torquing.

Gyro testing has demonstrated that demagnetization is not necessary for the gyro uncertainty due to electrical hysteresis to be within an acceptable band of 0.05 degree/hour, if both pattern field current and control field current are removed. The removal of both currents is compatible with both flight and calibration since drift compensation is not required. The torquing mechanization to command gimbal reorientation and position hold is shown in Figure 2.17-2. This mechanization offers the following advantages over the present mechanization:

1. Minimum interface lines since the analog information is carried on the steering input lines.
2. Simple interface with dc isolation by returning the low side of the input transformers and the low side of the control relays to the source.
3. Minimum sliprings since the low side of each pattern and control field is common on the first gimbal and returned through a single slipring.

2.17.7. Requirements for IMG Torquing Electronics. - The basic requirements for the design and mechanization of the IMG gyro torquing loop are:

1. Variable torquing levels, but capable of $\pm 3,200$ degrees/hour for coarse alignment and a lower value (0 to 40 degrees/hour) during fine alignment and drift compensation.
2. Individual on-off Control of U, V, and W Gyro Torquing Function.

2.17.8. IMG Circuit Considerations. - Four basic configurations were developed to meet the requirements for gyro torquing. The particulars of each circuit are discussed here.

1. Control and Pattern Fields controlled by the same amplifier.
2. Separate excitation for Pattern and Control Fields.
3. Control and Pattern Fields controlled by same amplifier but using analog inputs from existing steering lines.
4. Separate excitation for Pattern and Control Fields but using analog inputs from existing steering lines.

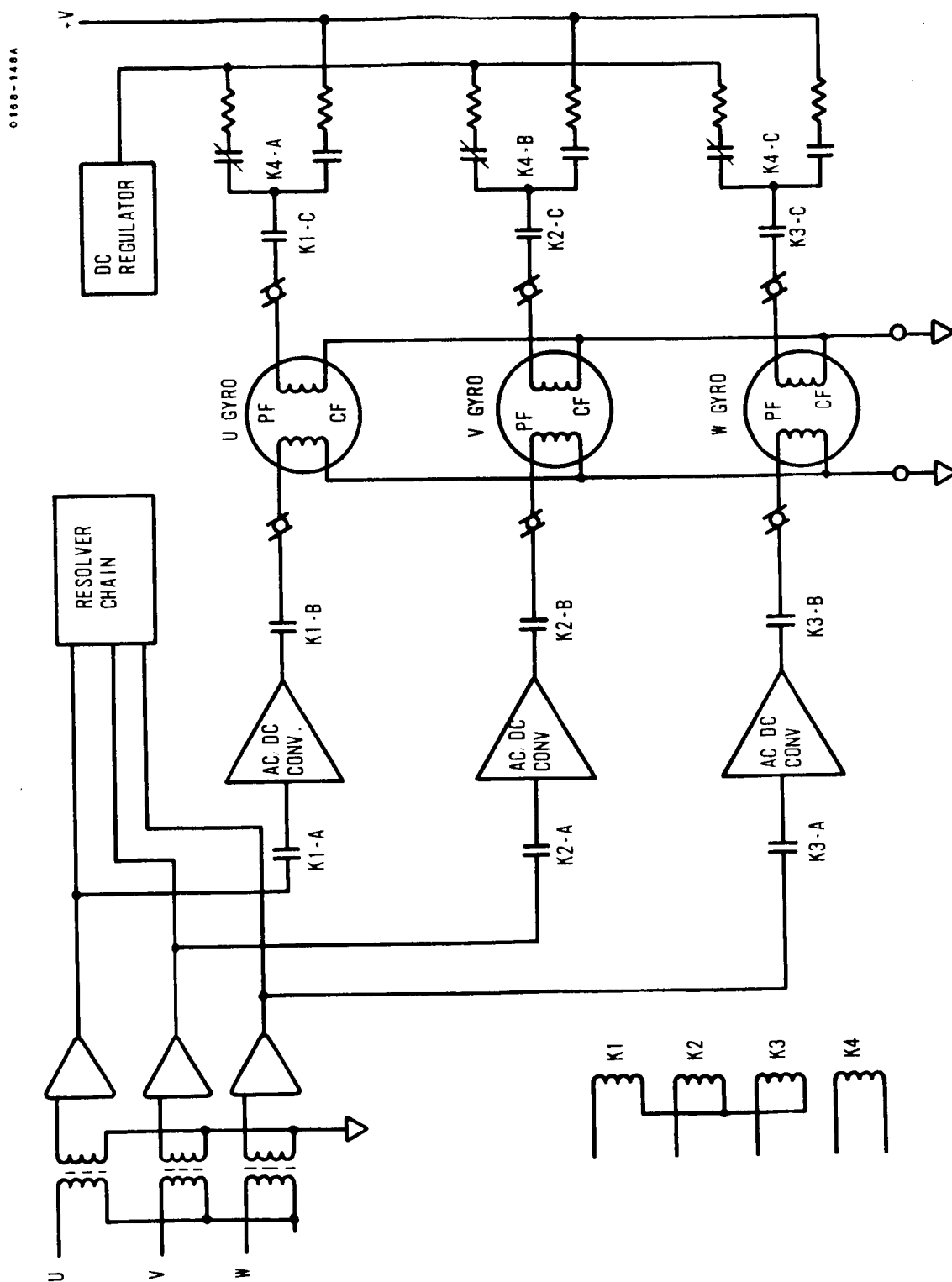


FIGURE 2.17-2. IMG GYRO TORQUING MECHANIZATION

Configuration 4 is the optimum analog torquing mechanization. This decision was arrived at in the following manner:

1. Configurations 1 and 2 were eliminated for the following reasons:
 - a. Greatest number of sliprings required.
 - b. Complexity of computer software.
 - c. Inherent noise and ripple problem associated with driving both windings from a common source.
2. In comparing configurations 3 and 4, the logical selection was configuration 4 as it required the least interface circuitry, with all other requirements equal.

Configuration 4 involves the use of the mixed frequencies already carried to the IRU on the steering lines. In considering the circuit aspects of the torquing function, either of the two frequencies, 800 Hz or 1,600 Hz, may be used for gyro torquing information. Similarly, 800 Hz and 1,600 Hz are equally accurate for position vectors through the steering chain. The 1,600 Hz signal was arbitrarily selected for gyro torquing. A phase sensitive ac to dc converter will be required for polarity and magnitude control of the torquing rate. Since the two combined signals are synchronized and have the proper frequency ratio, the use of a full wave demodulator will provide zero average output from the 800 Hz position signal. The ac components, predominantly 400 Hz, due to the position signal must be adequately attenuated to prevent excessive modulation to the signal generator carrier and to minimize gyro heating.

2.17.9. Conclusions. - The gyro torquing electronics has provided relatively trouble-free performance since the beginning of the Centaur program.

The elimination of the inflight gyro torquing requirement permitted a much improved platform reorientation mechanization. Hardware benefits were also obtained in the IMG design as a result of no inflight torquing. They are:

1. A minimum number of interface lines.
2. Minimum sliprings.
3. DC isolation is achieved by returning the low side of the control relays to the source.

Topic 2.18

Coupler Excitation for Platform Sensors

2.18.1. Introduction and Summary. - The material presented in this topic will cover Coupler excitation sources for all platform electro-mechanical sensors. This will include the following excitations:

1. Accelerometer Signal Generator (14.4 kHz).
2. Gyro Signal Generator (7.2 kHz).
3. Gyro Spin Motor (400 Hz).
4. Resolvers (7.2 kHz for gimbal servo loops).

The above excitations originate from two separate sources. These sources and the excitation(s) from each source are as follows:

1. Coupler Unit (see Figure 2.18-1, Precision Frequency Supply)
 - a. Precision 14.4 kHz and 7.2 kHz.
 - b. Precision 400 Hz spin motor excitation (supplied to Coupler from Vehicle Inverter as 115V, 400, 3 phase power; step down transformer in Coupler reduces voltage to 26V).
2. Vehicle Inverter - Supplies 3 phase, 115V, 400 Hz excitation to Coupler from which 26V, 3 phase, 400 Hz spin motor excitation is obtained.

During the -1 Phase of MGS development, design problems were experienced in the Coupler with the generation of precision 7.2 kHz and 14.4 kHz excitations. These problems were related to thermal conditions and occurred during coupler testing under worst case conditions. Because of the attention required by more demanding problems, little was done in this area (except for thermal ramp testing) until the Phase II PIP design effort. Problem areas were identified, prior to the Phase II PIP redesign, in areas that affected precision excitations to the gyro, accelerometer, and resolver. The problem sources were overstressed components, under temperature extremes, on the Frequency Divider Board and in the Filter Module, both prime functional elements in the excitation power supplies. These problems were corrected in the Phase II PIP design.

0566-4108

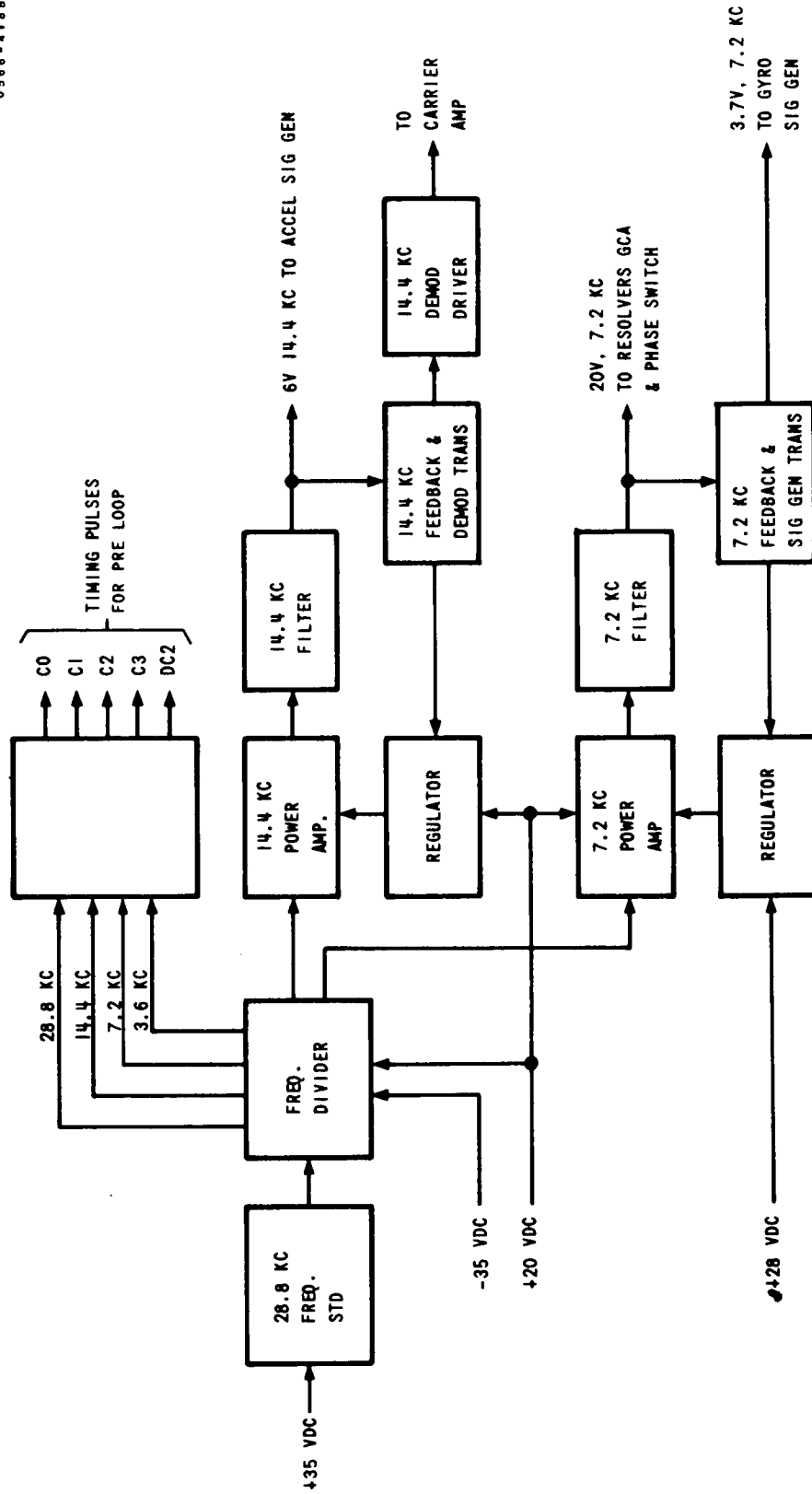


FIGURE 2.18-1. PRECISION FREQUENCY AND TIMING BLOCK DIAGRAM

Another excitation source, the vehicle inverter, was found to be inadequate insofar as providing stable 400 Hz, 3 phase, excitation for the gyro spin motors. As a result, the Vehicle Contractor (GD/C) found it necessary to replace the then existing rotary inverter with a solid state device in order to meet gyro spin motor excitation voltage and frequency stability requirements and other vehicle requirements. This change occurred in 1964.

2.18.2. General Description. - The 14.4 kHz and 7.2 kHz power supply furnishes precise frequency outputs for the gyro and accelerometer signal generators. The base frequency, 28.8 kHz, is obtained from a temperature-stabilized, quartz crystal, frequency standard. The output of the frequency standard is routed to a frequency divider. A 7.2 kHz square wave signal, derived from the frequency divider, is amplified in the 7.2 kHz power amplifier. The output of the power amplifier is then fed to the 7.2 kHz Harmonic Filter to produce a sinusoidal waveform. The 7.2 kHz is routed to the Platform and Platform Electronics Units, where it is used for gyro signal excitation and gimbal servo loop resolver excitation.

Precision 14.4 kHz is used as excitation for the accelerometer signal generators and Bandpass Amplifier Demodulators (in the -3 PRE loop, ref. Topic 2.15). From the Frequency Divider, the 14.4 kHz square wave is amplified by the 14.4 kHz Power Amplifier then filtered. Part of the filtered 14.4 kHz is routed to the 14.4 kHz Demodulator Driver through an isolation amplifier and transformer. Figure 2.18-1 shows a block diagram of the precision frequency and timing block as it exists today.

2.18.3. Detailed Characteristics. - The precision frequency standard receives a +28VDC input, furnished by batteries on the vehicle during vehicle operation or by GSE during testing in the lab. The frequency standard has the following characteristics:

Waveform: Sinusoidal

Frequency Accuracy: 28.8 kHz ± 10 PPM

Frequency Stability: ± 5 PPM

The 28.8 kHz is counted down in the frequency divider. The count down circuitry consists of transistorized flip-flops, which produce the following outputs:

1. 28.8 kHz
2. 14.4 kHz
3. 7.2 kHz
4. 3.6 kHz

The frequencies of primary interest in this discussion are the 14.4 kHz and 7.2 kHz excitations. The 14.4 kHz and 7.2 kHz Power Supply furnishes precise frequency outputs for the gyro signal generators, accelerometer signal generators and the 14.4 kHz demodulator driver. The precision timing generator provides a precise frequency input square wave at 7.2 kHz, and the isolated power supply provides a precise frequency input square wave at 14.4 kHz. The two frequencies are separately processed as previously discussed. The output characteristics of the 14.4 and 7.2 kHz power supply are as follows:

1. Frequency: 7.2 kHz ± 5 percent
Amplitude: 20 volts ± 0.5 percent
Distortion: Less than 5 percent
Usage: Resolver excitation
2. Frequency: 7.2 kHz ± 5 percent
Amplitude: 3.7 volts ± 3 percent
Distortion: Less than 5 percent
Usage: Gyro SG excitation
3. Frequency: 14.4 kHz ± 5 percent
Amplitude: 6 volts ± 0.5 percent
Distortion: Less than 5 percent
Usage: Accelerometer SG excitation
4. Frequency: 14.4 kHz ± 5 percent
Amplitude: 5.8 volts ± 5 percent
Distortion: Less than 5 percent
Usage: 14.4 kc demodulator driver excitation

The above requirements are realized when the Coupler unit is operated in an ambient environment, which produce coupler skin temperature extremes of $+30^{\circ}\text{F}$ to $+130^{\circ}\text{F}$. The above requirements are also applicable during operating environmental inputs (vibration, linear acceleration, etc.).

2.18.4. Problem Areas:- The primary problems that were indirectly associated with precision excitations to the platform sensors were in the Filter Module and Frequency Divider of the -1 and -3 Couplers. These boards were a part of the Precision Frequency Supply. Problems associated with these boards were temperature oriented and showed up during testing under worst case thermal environment (+30°F to +130°F skin temperatures).

The frequency divider board was redesigned as part of Phase II PIP. The new frequency divider design eliminated the previous thermal over-stress condition. This was accomplished by better packaging, and selection of components through implementation of derating policies and worst case analysis design techniques.

Similar problems were experienced with the filter module. New 14.4 kHz and 7.2 kHz power supplies were redesigned for Phase II PIP. The power stages previously part of the frequency divider were incorporated in the filter module. These changes were again made as a result of overstressed components at elevated temperatures. With the incorporation of these and other associated changes in Phase II PIP, the following results were obtained:

1. Elimination of 33 overstressed components.
2. Reduced power.
3. Reduced total parts count.
4. Increase predicted coupler MTBF.
5. Number of leads reduced.
6. Isolation of noisy circuits from circuits of high noise susceptibility.
7. Elimination of potential failures at unit level through module level acceptance tests.

Problems encountered in the area of precision excitation supplies could be reduced or avoided completely in future designs by incorporation of the following design disciplines.

1. Document detailed design requirements from unit level to board level.
2. Implement worst case circuit analysis early in the design cycle.
3. Implement parts stress analysis (also at an early point).
4. Define and implement a component derating policy.
5. Develop and implement module level testing.
6. Initiate periodic design reviews.
7. Design proof testing under worst case environmental conditions.

2.18.5. Spin Motor Precision Excitation. - The precision 3 phase, 400 Hz, 26V spin motor excitation is derived from the Coupler. The Coupler has a 115V, 3 phase, 400 Hz input, originating either from the Vehicle Inverter, as in the case of vehicle operation, or GSE during lab testing. This voltage is stepped down in the Coupler, through a transformer, to 26V. Throughout the -1 and well into -3 program, this power was supplied by a rotary inverter on the vehicle. Problems in platform gyro excitation developed in this area but they were caused by Vehicle Inverter characteristics. Therefore a discussion of these is presented in Topic 4.3, Primary Power Interface.

2.18.6. Considerations for Future Precision Power Supplies. - The problems encountered in the Centaur IGS precision power supplies have shown that the following factors should be considered in the design of future supplies for platform sensors:

1. Type of supply (Square Wave or Sine Wave).
2. Type of load (Tuned or Untuned).
3. Ripple Content on the Output.
4. Total Harmonic Distortion.
5. Stability.
6. Regulation.
7. Susceptibility to Environmental Changes.
8. Warm-up and Stabilization.
9. Phase lock all harmonically related frequencies.
10. Output Impedance and Frequency(s) of Interest.
11. Size, weight and Power Consumption.

The significance of each of the above factors for a given application must be thoroughly evaluated before an optimum choice in design can be realized.

2.18.7. Conclusions. - Problems encountered in the area of precision power supplies could be reduced or avoided in future designs by utilizing the following aids:

1. Detailed definition and documentation of all design requirements in the form of technical development specifications.
2. Implementation of timely design reviews at each stage of design and development.

3. Implement worst case analysis, parts stress analysis and component derating policies at inception of design.
4. Develop and implement module/board level performance and environmental tests.
5. Develop and implement a full design proof program early in the program.

Topic 2.19

Coupler Unit Packaging Design

2.19.1. Introduction. - The material discussed in this topic will be confined to the unit packaging design of the Coupler. Particular attention will be directed towards the packaging constraints imposed by environmental requirements. In addition, physical limitations as they affect packaging concepts will be considered.

2.19.2. Evolution of Coupler Packaging Design. - Throughout the -1 Program, the coupler packaging configuration remained relatively unchanged. In early 1961, the -3 Program began and major changes in packaging resulted. In the -3 Centaur Coupler, changes were made in the arrangement, location, and mounting of boards and modules. The exact position or location of a board or module was governed by many factors, some of which were: optimum heat paths; shortest practical wire routing to adjacent boards; separation of noisy circuits from circuits having a high susceptibility to noise; considerations for vibrational inputs; shock and other environment or physical design constraints. As with any design, tradeoff studies were required for the -3 Coupler.

Later in the -3 Program, other packaging changes were implemented during the Phase I and II Product Improvement Programs (PIP).

The first complete change in overall packaging design of the Centaur Coupler came about in late 1965, when the System Electronic Unit (SEU) was proposed. The SEU proposal was based upon a complete redesign of the coupler, including redistribution of certain functions contained in other units comprising the MGS.

In mid-1966, the Inertial Measurement Group (IMG) study was begun. New guidelines for hardware design were implemented, and from these the present configuration SEU resulted. The new SEU, in conjunction with the new IRU contains the coupler functions and signal conditioner functions as well as the Platform Electronics (reference Topics 2.11, 2.12, and 2.13).

2.19.3. Packaging Problems. - Problems associated with -3 Coupler packaging concepts in one form or another have been exhibited since 1961. These problems can be classified into five basic categories, namely:

1. Functional loops are split between several boxes.
2. Noise induced (electrical cross-coupling).
3. Vibration induced (structural damping or lack thereof).
4. Thermal induced.
5. Overstressed components due to (2) and/or (3).

Throughout the program, improvements in packaging concepts have been oriented towards reducing or eliminating these problem sources. Further details concerning these subjects are contained in the following paragraphs.

2.19.4. Description of Basic -1/-3 Couplers. - The Pulse Rebalance Gyro Torquer and Power Supply (Coupler) for the -1 and -3 Centaur configurations consisted of a magnesium casting (EZ33A) with removable top and bottom covers. The main housing contained three rows of plug-in boards or modules. Connection between the boards or modules to wiring inter-connect boards was made with Elco Pin connectors. A fourth row or section in the main housing contained a chassis to which was hard mounted the mechanical choppers, relays, filters, etc. The problems associated with vibration, and the subsequent repackaging in the hardmount area will be discussed later.

The primary functional requirements of the Coupler, as mechanized for the -1 and -3 configuration, were as follows:

1. Provide precision analog torquing to the control field windings of the platform gyros, in accordance with the output of precision potentiometers, located in the I/O of the computer.
2. Provide precision rebalance current pulses to the accelerometers and ΔV pulses to the Computer.
3. Provide the secondary supply voltages, route the prime source voltages, and provide frequencies and timing pulses to accomplish (1) and (2), in addition to providing precision frequencies to other MGS units.

4. Provide monitoring inputs to the Signal Conditioner and GSE for the following parameters:

- a. ΔV pulses.
- b. Prime electrical power inputs.
- c. Secondary power supply voltages.
- d. Accelerometer and gyro loop signals.

2.19.5. Environmental Requirements. - These functions were to be performed when the Coupler was subjected to certain environmental requirements. Packaging concepts therefore were in turn directly influenced by both the functional and environmental requirements. Environmental requirements for the Coupler are as follows:

1. Vibration. - Combined random and sinusoidal inputs simultaneously applied as described in Topic 6.15.
2. Shock, acoustic noise, humidity, and corrosive elements were specified to be the same as those in Topic 6.15.
3. Temperature: +30°F to +120°F (Flight) average skin temperature.
+40°F to +130°F (Launch) average skin temperature.

2.19.6. Physical Constraints. - In addition to the design constraints imposed by the environmental requirements, physical constraints impose further restrictions upon the packaging concepts. The physical constraints for the -3 type coupler configuration are:

1. Outline dimensions: 22.14 x 14.70 x 10.20 inches.
2. Weight: 63 lbs.

2.19.7. Mission Thermal Control Problems. - During the -1 and early -3 Programs, the Coupler Unit had an electroplated, gold over magnesium finish. In early 1963, GD/C initiated a request that the coupler surface finish be changed. This action was prompted by a thermal analysis which indicated that for the missions anticipated, the coupler case skin temperature would exceed the interface requirement (reference Topic 4.6). As a substitute for the gold electroplated finish, a white polyurethane enamel was proposed by Honeywell. The change to the new finish was approved and incorporated into the design in mid-1963. Once again (ref. Topic 1.5) choice of surface finish was primarily dictated by the absorptivity-emissivity characteristics. The solar absorptivity (α) constant for gold and polyurethane white enamel finish were approximately the same, but

the emissivity (ϵ) constant for the white polyurethane paint is approximately six times that of gold. Unlike the platform (ref. Topic 2.10), which had the white polyurethane enamel over gold incorporated in early 1964, the coupler finish incorporated white polyurethane enamel over magnesium (no gold plating). Comparison of absorptivity and emissivity constants for the two types of finishes is as follows:

Gold Plate		White Polyurethane	
ϵ	α	ϵ	α
0.13 - 0.15	0.28 - 0.4	0.86 - 0.93	0.25 - 0.29

2.19.8. Corrosion Problems. - Soon after the change from gold plating to the white polyurethane finish, corrosion problems were noted during DPT salt spray tests. The corrosion was limited to the unpainted (bare magnesium) cover-to-main-casting interface and around the connectors. It was desirable, from thermal consideration, to maintain this interface for the purpose of providing good thermal conductivity between the main housing and covers. To circumvent the corrosion problem and still maintain intimate casting-to-cover-contact, a bead of silastic material was used around the cover-casting interface. This material isolated the bare magnesium from exposure to the external environments, thus reducing the corrosion problem to a sufficient degree.

2.19.9. Vibration Problems. - As a result of design incompatibilities with environmental requirements other packaging changes were required. The original -1 coupler and early -3 configuration were "hard-mounted" (no shock and vibration isolators used). During vibration of the -3 coupler, transmissibilities exceeding the rated values of several assemblies occurred. In an effort to minimize this vibration amplification, shock mounts were installed for the purpose of damping the vibration being absorbed by the coupler. Addition of the shock mounts (Lord HT2-35 isolators) resulted in reduction in transmissibilities to acceptable limits for the printed circuit board assemblies. However, stresses persisted in the areas where components were internally "hard-mounted" to the coupler chassis, through sheet metal mounting brackets.

In mid-1963, a redesign and repackaging of the "hard-mounted" area of the coupler was initiated. This change was deemed necessary in order to insure flightworthy couplers. The design change resulted in hard-mounting mechanical choppers, relays, other components and modules to eliminate the high transmissibilities that resulted previously through the

sheet metal brackets. The chassis or frame to which the components were hard-mounted was machined from a magnesium alloy with a ribbed configuration for added structural strength and damping. Results of this investigation were as shown in Table 2.19-I.

TABLE 2.19-I

-3 COUPLER VIBRATION TRANSMISSIBILITIES

Component's Of Interest	Transmissibility			
	"Hard" Mount		(HT2-35) Isolator Mounted	
	Old Design	New Design	Old Design	New Design
Chopper (Bracket)	31.8	3.4	6.6	2.6
Relay	28.2	4.4	6.9	3.0
Chopper (Board Mount)	31.8	4.0	4.0	2.8
Printed Circuit Board	70.5	---	5.7	---

2.19.10. Plans for the IMG. - As was previously mentioned, minor packaging changes occurred during the Phase I and II Product Improvement Programs. The new IMG design represents the latest packaging concepts. The IMG design studies resulted in combining functions so the improved IMG could be reduced from a five "box" MGS to a three "box" configuration (computer included). Functions formerly in the coupler are now divided between the platform (part of the IRU) and SEU. In arriving at the present IMG packaging configuration, emphasis was placed upon reliability, producibility, maintainability, simplified guidance interface, reduced power, less weight, and smaller size. Vibration and thermal requirements, as well as isolation of noise susceptible circuits were also prime factors considered.

2.19.11. Conclusions. - To summarize, it may be concluded that the Coupler unit package design concept is highly influenced by the environment and physical constraints imposed. All factors should be considered during the initial design phase with individual weighting being applied in the final tradeoff study after completion of detailed computer simulation studies. Particular attention must be paid to vibration and thermal conditions, as was the case with the Platform Electronics Unit.

SECTION 3

COMPUTER EQUIPMENT

Topic 3.1

Introduction and Computer Development Summary

3.1.1. Introduction. - The Computer for the Centaur Inertial Guidance System is procured by Honeywell from Kearfott/San Marcos Division, previously Librascope. The Computer consists of a general purpose section and an Input/Output Unit. The general purpose section is a solid state, digital, serial operation computer with a rotating magnetic drum memory. The Input/Output Unit mechanizes the circuitry necessary to interface the Computer with the other units of the Inertial Guidance System and the vehicle flight control systems.

The general purpose section and the Input/Output units are mounted on a common base. Mounting to the vehicle is through vibration isolators. The packaging design provides for radiation cooling in the space environment.

3.1.2. Computer Development Summary. - The Computer development was accomplished in essentially three major phases:

1. Initial -1 Computer design (1959/1960).
2. -3 Computer redesign (1961/1962).
3. GPK32/GPK33 Computer redesign and retrofit (1965/1966).

Other redesign and retrofit efforts to correct specific design problems or reliability risks were accomplished in the time intervals between these three major redesigns.

3.1.2.1. -1 Computer Development. - The -1 Computer general purpose section was based on an existing prototype computer, designed by Kearfott (Librascope at that time) in 1957/1958. The basic circuits, flip-flops, read amp, write amp, etc., and the logic design and mechanization from the existing prototype were used for the Centaur Computer. The packaging was redesigned to provide for radiation cooling in the space environment.

The Input/Output Unit was a new design for the Centaur application. Thus, the -1 Computer design spanned a period from 1957 to 1960. The basic circuits were designed in the 1957 period and represent the state of the art transistor technology of that time. The input/output was designed in 1959 and reflects the state of the art of that time. The D/A conversion for example, is accomplished by an electro-mechanical servo loop with brush encoders and an output potentiometer.

3.1.2.2. -3 Computer Development. - The -3 Computer redesign provided increased computer capability and corrected several problem areas detected during the -1 development and test phase. The major redesign areas were:

1. Incorporation of seven additional permanent storage tracks and one additional temporary storage track on the memory drum. This provided increased memory storage capacity and additional "scratch pad" memory.
2. Redesigned the Write Amplifier and modified the Clock Generator - This redesign corrected operational problems with the Write Amplifier.
3. Modified the packaging to provide for pressurization of the general purpose section and the Input/Output unit with an inert gas. The pressurization was accomplished to eliminate corrosion problems encountered when operating in a humid environment.
4. Minor circuit modifications to the flip-flops and emitter followers to correct circuit operation problems.
5. Redesign of the torquing D/A converters to provide improved conversion accuracy.

3.1.2.3. GPK32/33 Computer Development. - The GPK32/GPK33 redesign and retrofit program was accomplished primarily to improve the Computer reliability by substitution of high reliability parts and removal of the unused "Coast Phase" logic and circuitry. Limited circuit redesign to meet worst case analysis was also accomplished and the operational capability was increased. The major redesign areas were:

1. Substitution of high reliability parts on all circuit cards and the power supply. All circuit cards and the power supply were built new for the GPK33 retrofit.
2. Removal of the "Coast Phase" logic circuitry. This circuitry provided the capability to turn off the major portion of the Computer during the parking orbit portion of flight and to

automatically turn on at the completion of the parking orbit. This capability was no longer required and a malfunction of this unused circuitry could cause an in-flight computer failure.

3. Redesign of the Input/Output circuit cards to provide additional output discretes (4 to 14) and to provide a two-state non-return-to-zero telemetry output in lieu of the three state telemetry.
4. Redesign of the memory select function to provide for solid state switching for all memory drum track selection. This effectively expanded the memory available for use in-flight by providing the capability to rapidly switch to all tracks.
5. Redesign of the power control circuitry such that all control lines and all relays were de-energized in the flight mode. The power control circuitry was simplified because the inflight turn on/turn off capability was no longer required.

3.1.2.4. Redesign for Individual Problems. - Other major redesign areas accomplished separately to solve specific problems were:

1. Changing the external finish from gold plating to white polyurethane paint to improve the radiation cooling in the space environment.
2. Redesign of the time standard to eliminate a vibration problem with the crystal mounting.
3. Redesign of the head select matrix to provide the capability to more readily reprogram the memory permanent storage, simplify the circuitry, reduce the parts count, and incorporate high reliability parts.
4. Modify the computer flip-flop to eliminate circuit design problems.

The specific problems encountered, alternates considered, and the detailed redesign and modifications accomplished are delineated in the body of this report.

3.1.3. Conclusion. - The redesign and development areas of the computer program can be grouped into three categories:

1. Redesign to provide increased functional capabilities.
2. Redesign to solve specific circuit design or environmental problems.
3. Redesign to improve reliability by parts substitution and to provide improved producibility and workmanship quality.

Redesign to provide increased functional capability will always be necessary on a program which continues for the length of time the Centaur Program has continued. Requirements are constantly being changed and redefined. This redesign, of course, can be minimized by initial selection of a computer with capabilities and capacity for expansion which are maximum consistent with trade-offs on size, weight, power, reliability and cost.

Circuit design problems in digital computers can be reduced by (1) worst case circuit analysis with particular attention to transient and switching analysis; (2) detailed logic and timing analysis; (3) utilization of all practical techniques to reduce computer and system level signal and ground noise; (4) detailed review of all part parameters, both specified and unspecified, prior to "direct substitution" into existing circuits; and (5) comprehensive prototype functional test and checkout at both the unit and system level and environmental test prior to production build; (6) comprehensive structural and thermal analysis.

The need to improve reliability by parts substitution and redesign to improve producibility, can be reduced, of course, only by proper initial parts selection (selecting the best available part) and by "designing in" producibility and maintainability in the initial design.

3.1.4. Computers Available Today. - Airborne digital computers of current 1967 state of the art are considerably different than the present Centaur Computer. These computers utilize integrated circuits and random access memories, core or thin film. The input/output functions of D/A and A/D conversion are performed by solid state converters. Operating speeds provide a vastly increased capability. Reliability is improved by the reduction in parts and interconnections and the elimination of moving parts.

Topic 3. 2

Computer Memory

3. 2. 1. Introduction. - The general purpose computer is a solid state, digital, serial operation computer with a magnetic drum memory. The general purpose computer basically consists of memory, control, and arithmetic sections. The memory section contains the program control necessary to systematically perform a mission, the control section mechanizes the logic required to systematically progress through the program, and the arithmetic section performs the computations specified by the program and mechanized by the control section.

3. 2. 2. Discussion. - General purpose computer operation is performed under timing control provided by a clock track on the memory drum. By this means, data contained in memory is serially provided at the same rate as the operations being performed, thus maintaining synchronization of all computer functions regardless of slight variations in memory drum speed.

The major overall control governing navigation computer operation is the stored program on the memory drum. The control section systematically accepts the stored program and directs its implementation. Initial synchronization to the program (main memory) is provided, stored data is located and brought out for operations as required, and results are stored in memory through the control section. By implementing systematic computer operation (phase control), considerable time sharing of circuits is applied.

Computer arithmetic is basically addition, subtraction, multiplication, and division; multiplication and division are accomplished by a series of additions and subtractions. The additions and subtractions are performed serially.

3. 2. 2. 1. Flip-Flops. The flip-flop performs the primary switching function of the computer general purpose section. The circuit is essentially a bi-stable Eccles-Jordan multivibrator with output buffers and power gain stages. Logically, it is a J-K type flip-flop with cross-coupling feedback from the output of one side to the input of the other side. All flip-flops in the computer general purpose section are clocked with the exception of those flip-flops used for velocity and time accumulation. The velocity and

time input pulses are asynchronous with respect to the computer clocking. In the case of these flip-flops, the input pulse simulates the computer clock. The basic flip-flop is also used in the read amplifier as the final output stage. The read amplifier flip-flops have a modified gating input of the ground emitter configuration that provides power gain.

The basic flip-flop circuit was designed about 1957 and reflected state of the art transistor technology of that time. That technology consisted of high voltage transistors, medium fast frequency response, high drive currents, and high bias levels. Today, integrated circuits would be utilized almost exclusively for computer flip-flops.

The flip-flop provides two complementary outputs of +9 volts and +35 volts dc with a one micro-second rise time and a 0.5 micro-second fall time. The track select flip-flops S1 through S5 have a low voltage of +3 volts dc and the S6 flip-flop has a low voltage of 0 volt dc. The flip-flop output is sufficient to drive 40 logic gates at 0.55 milliamps per gate. The flip-flop is set or reset when a clock pulse occurs provided that the logic gate inputs are high and the opposite side from that being set is also high. In quiescence, current flows in the input logic gate and through the trigger transformer when all inputs are high. The clock pulse interrupts the current flow through the primary of the trigger transformer and causes a positive voltage to be induced in the secondary. The transistor in the Eccles-Jordan section then switches, normal flip-flop action follows and the flip-flop stabilizes in the opposite state. The flip-flop will remain in this state until one bit time after the input logic and the opposite side goes high. A schematic of the typical flip-flop is shown in Figure 3.2-1.

3.2.2.1.1. Problems. Problems encountered with the basic computer flip-flop during the course of the Centaur Program were:

1. Marginal triggering.
2. Slow switching speed of the Eccles-Jordan section.
3. False triggering of the velocity accumulation of the flip-flops caused by noise.

These problems could have been reduced or eliminated by attention to the following areas during design process:

1. Worst case circuit analysis, particularly transient and switching analysis.
2. Improved internal grounding techniques.
3. Improved interface circuit design to specifically provide high noise level stand-off on interface lines.

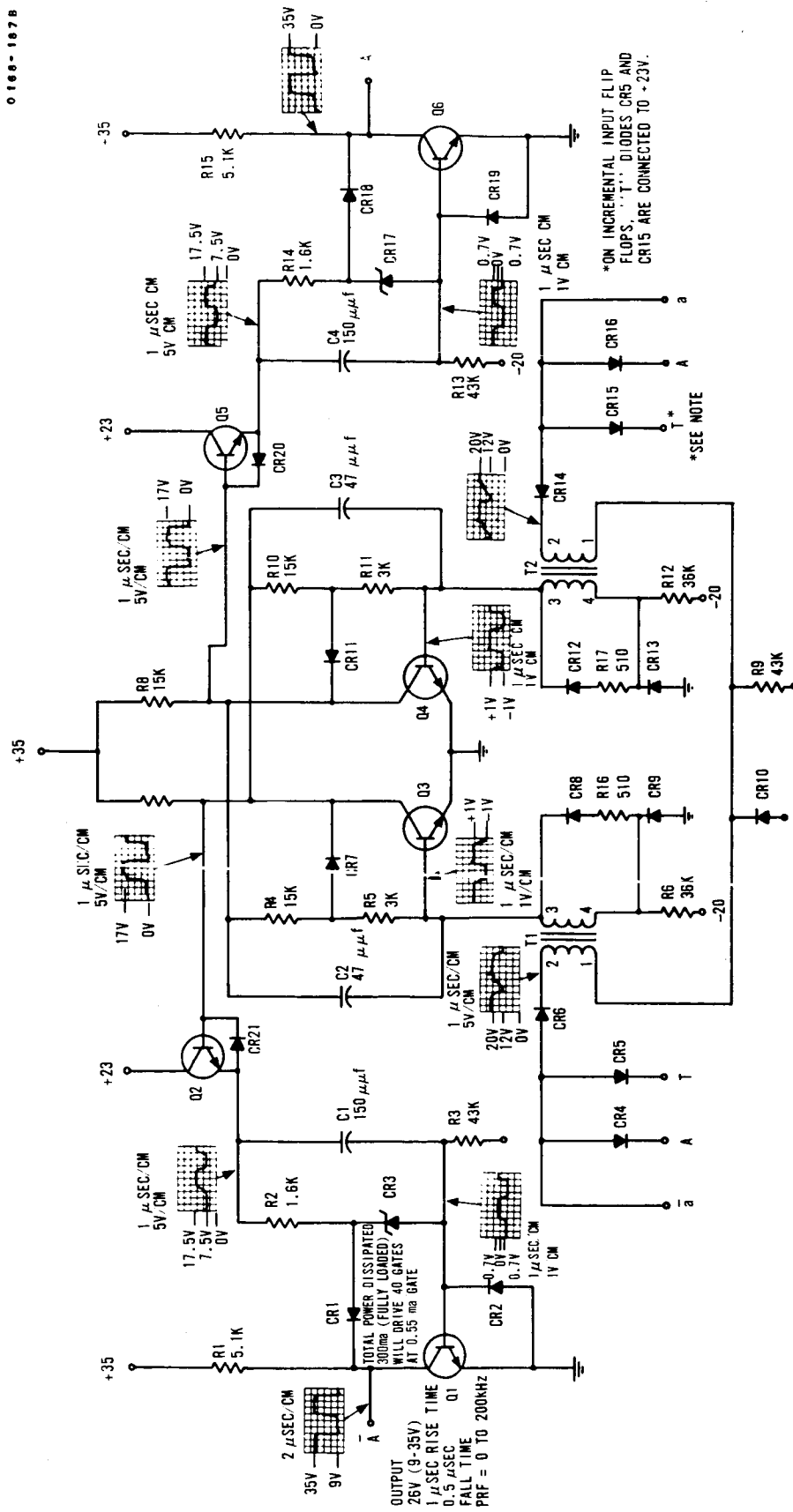


FIGURE 3.2-1. TYPICAL FLIP-FLOP SCHEMATIC DIAGRAM

3.2.2.1.2. Centaur -3 Solution of -1 Problems. In 1961-62, a minor modification was incorporated in the basic flip-flop trigger circuitry. The modification consisted of adding a 510 ohm resistor (1,000 ohms for the velocity accumulation flip-flops) in series with the reverse voltage suppression diode, across the secondary flip-flop trigger transformer. This provided limiting of the reverse current when the clock returned to the high state (+23 volts) and damped any resultant positive voltage overshoot which could cause the flip-flop to trigger.

3.2.2.1.3. Centaur -3 Problems. In 1964-65, investigations of problems associated with the computer jumping program, particularly at high temperatures, resulted in the conclusion that the flip-flop switching characteristics were marginal in response to normal input pulses. The initially "on" transistor in the Eccles-Jordan section was not switching off in the required period of time. The problem was particularly evident in the read amplifier due to its trigger input circuit. The marginal switching of the flip-flop resulted in the high output partially or fully returning to the low state. The storage time of the 2N37 transistors utilized in the basic flip-flop switching section was the primary parameter contributing to this condition. Of several minor redesign alternatives available to provide reliable flip-flop switching, substitution of a faster switching transistor was selected. Other alternatives considered were:

1. Complete flip-flop redesign-- this would have required a major repackaging effort and was rejected due to the extensive modification required.
2. Increase the cross-coupling current to switch the "off" transistor more rapidly. This did not improve the switching time significantly and only masked the transistor storage time problem.
3. Reduce the base drive so that the "on" transistor was not in heavy saturation. This would reduce the noise standoff characteristics of the flip-flop and was too variable to insure good safety margins under all operating conditions.

3.2.2.1.4. Velocity Accumulation False Triggering. In 1966, problems with false triggering of the velocity accumulation flip-flops were encountered. The false triggering was caused by a combination of noise on the velocity accumulation lines from the Coupler, computer internal ground noise, and the faster switching speed of the flip-flop which now used high reliability S2N2102 type transistors. The S2N2102 transistors had been incorporated as part of the high reliability parts substitution program associated with the GPK33 retrofit. The velocity accumulation flip-flops are more susceptible to input noise than the normal flip-flops because the delta V high signal level is +23 volts dc versus the normal computer high

logic level of +35 volts dc. Under nominal conditions, the flip-flop will start switching when the high input drops to +20 volts dc or below, thus a major portion of the 35 to 20 volt noise level standoff is not provided on the delta V inputs.

The redesign accomplished as the result of this problem was to improve the computer internal grounding configuration. This consisted of providing branch type grounding to the card frame on all circuit cards in lieu of a single wire daisy chain grounding configuration. The improvement was incorporated on all circuit cards with each branch ground wire containing no more than three flip-flops or two read amplifiers or two write amplifiers. This improved the grounding to the circuits by reducing the switching transients on the ground line. Other modifications considered were:

1. Redesign of the velocity accumulation input circuitry to provide improved noise standoff. This approach, although highly desirable, was rejected because of interchangeability considerations with unmodified units.
2. Redesign of the coupler delta V output circuitry to provide an input signal more closely simulating the +35 to +9 volt logic levels used in the computer general purpose section. This would increase system noise levels due to the higher pulse amplitudes and would effect interchangeability with unmodified units. The approach was rejected.

3.2.2.2. Emitter-Followers. Emitter-followers are utilized to provide power gain for large fan-out signals. The emitter-follower output follows its input with no significant time delay. The basic emitter-follower utilizes a NPN type transistor with negative pull down on the base and collector voltage of 35 volts dc. A typical emitter-follower schematic is shown in Figure 3.2-2.

3.2.2.2.1. -3 Design Changes. The original -1 emitter-follower was unclocked and the output was not isolated. -1 to -3 design changes incorporated the emitter-follower clock, T_e , and resistor isolation of the output signal. The incorporation of the T_e clock input to the emitter-follower provided faster rise and fall times of the emitter-follower output. The isolation resistors in series with the emitter-follower output provided protection against inadvertent shorting of the output causing component failures.

3.2.2.2.2. GPK33 Design Changes. In 1966, modifications to the T_e clock to eliminate unwanted voltage spikes on the emitter-follower outputs

0168-104A

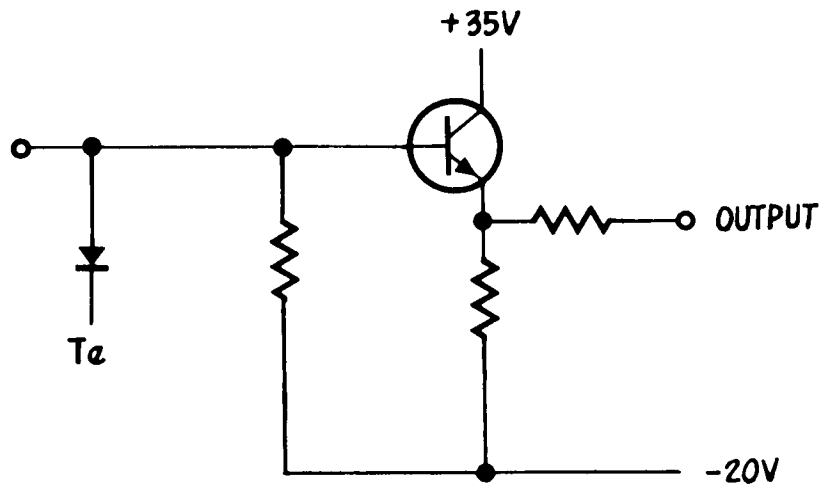


FIGURE 3.2-2. TYPICAL EMITTER-FOLLOWER SCHEMATIC DIAGRAM

were accomplished. The problem and solution are described in the clock generator section.

In 1967, a problem was noted with noise spikes on the output of the MECO discrete driver circuit. This discrete is used for generation of the main engine cutoff signal. The cause of the problem was determined to be logic overlap of the P_O and C3, $\overline{K4}$, and K5 logic terms to the unclocked MECO flip-flop. This was primarily caused by the slow fall time of the P_O emitter-follower which is very heavily loaded. Redesign of the P_O emitter-follower from an NPN to a PNP configuration provided a very fast fall while providing sufficiently fast rise. The situation was only critical to those flip-flops in the input/output section of the navigation computer which were unclocked.

This problem could have been avoided by a detailed timing analysis when the unclocked flip-flops in the I/O were designed.

3.2.2.3. Write Amplifiers. The write amplifiers associated with each of the ten write heads on the memory drum receive complementary inputs from the logic flip-flops and generate high current pulses to the associated write heads. The write amplifiers allow the recording of information on the magnetic drum temporary storage tracks, instruction and arithmetic registers, and the Sigmator.

The write amplifier switches current through the proper side of the write head coil at clock time to record either a one or a zero on the magnetic drum. The write amplifier clock, designated T_W , is generated by the clock amplifier. The complementary inputs are received from the computer input logic and determine whether a one or a zero shall be written at the particular bit time. The write current pulse is 300 milliamps for a duration of approximately two microseconds.

3.2.2.3.1. Centaur -1 Write Amplifier. The original write amplifier utilized in the Centaur -1 Computer contained two blocking oscillators, two intermediate power stages and output current driver stages. The write amplifiers were clocked by the general computer clock. The output current pulse width was determined by the blocking oscillators in each write amplifier circuit. Stability problems with the blocking oscillators and variations from write amplifier to write amplifier resulted in a complete redesign of the write amplifiers for the -3 configuration to eliminate the blocking oscillators.

3.2.2.3.2. Centaur -3 Write Amplifier. The -3 amplifier consists of a push-pull arrangement of two pairs of transistors connected in a

Darlington configuration to obtain high gain. Both stages are clocked. The critical timing and pulse duration function in the -3 computer is provided by the write amplifier clock, which is generated by the clock amplifier and is utilized by all write amplifiers. Instead of using the general computer clock as in the -1 configuration and providing the proper pulse width internal to the write amplifier, the clock amplifier was redesigned to provide a separate write amplifier clock with a 2.0 ± 0.1 microsecond pulse. This eliminated the write amplifier timing shifts associated with the individual blocking oscillators in the -1 write amplifiers. A schematic of the -3 write amplifier is shown in Figure 3.2-3.

3.2.2.3.3. Centaur -3 Write Amplifier Problems. In 1965, during the high reliability parts substitution program for the GPK33 computer configuration, intermittent writing of erroneous information at high temperature was noted. The cause of the problem was traced to the capacitance of the high reliability zener diodes which had been substituted into the write amplifier circuit. The zener diode capacitance was coupling current into the second stage of the write amplifier. Upon receipt of a clock pulse, the driver transistor would be triggered by the capacitor discharge on the fall of the clock pulse.

Tests of the high reliability zener diodes revealed that the capacitance was three to ten times higher than the capacitance of the same type diode per the MIL specification. Capacitance was an unspecified parameter for the high reliability components. A minor redesign to eliminate this problem consisted of replacing the input resistors on the first stage of the write amplifier with nine volt zener diodes. The addition of the zener diode on the input stage effectively dropped the nine volt normally low input logic level to 0 volts at the base of the input stage, and reduced the charge on the second zener diode capacitance to essentially 0 volts.

The problem encountered could have been eliminated by detailed circuit design analysis, particularly transient analysis and a detailed review of both specified and unspecified parameters when the high reliability components were substituted.

Other cases of unspecified parameters of the high reliability components being significantly different from the nominal parameters of the same type MIL part have been encountered. It is apparent that these differences in parameters must be taken into account when utilizing these parts. A detailed review of both specified and unspecified parameters should be conducted prior to substitution into previously designed circuits. The tendency to hold analysis to a minimum because of the supposed direct substitution may result in these types of problems.

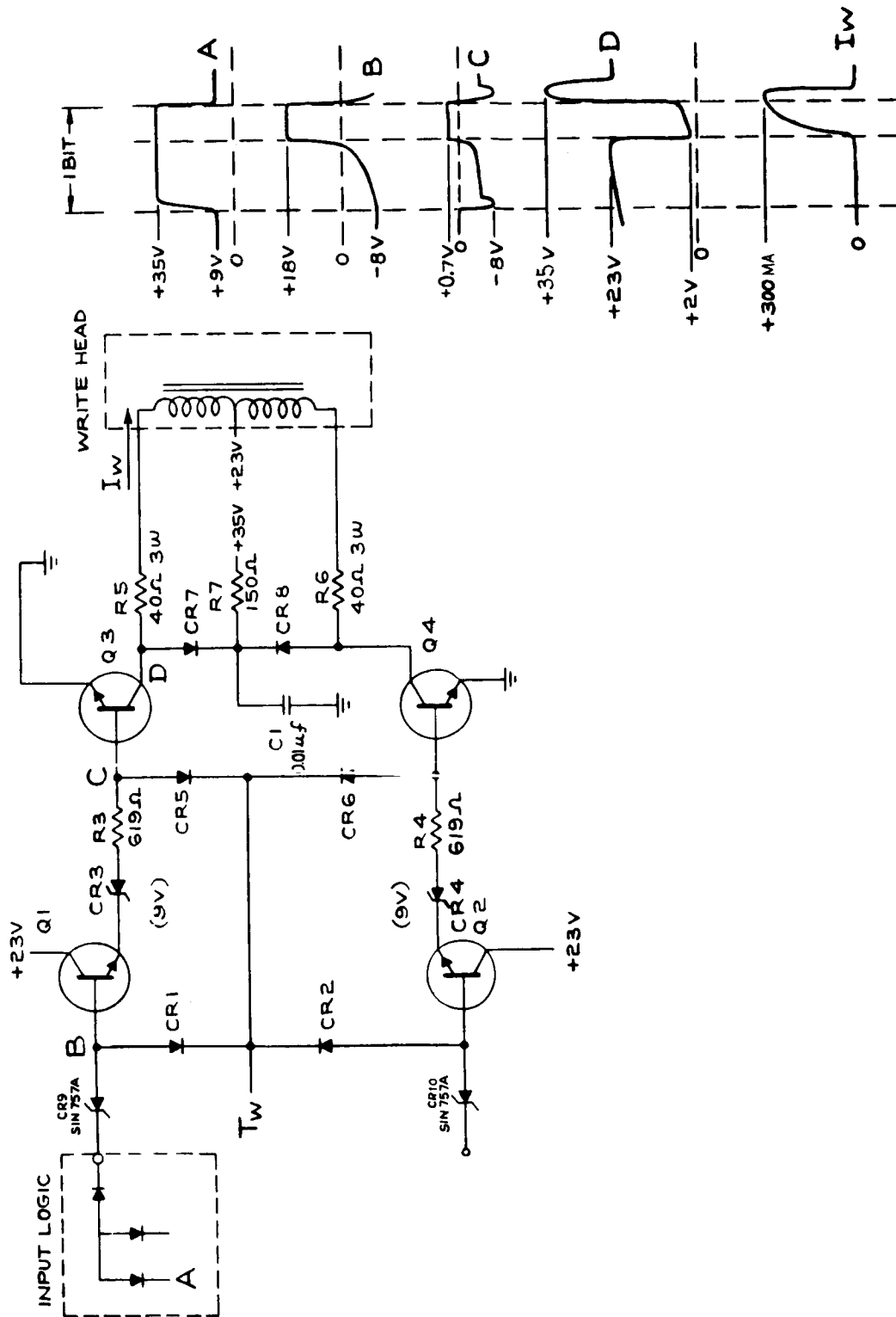


FIGURE 3.2-3. WRITE AMPLIFIER SCHEMATIC DIAGRAM

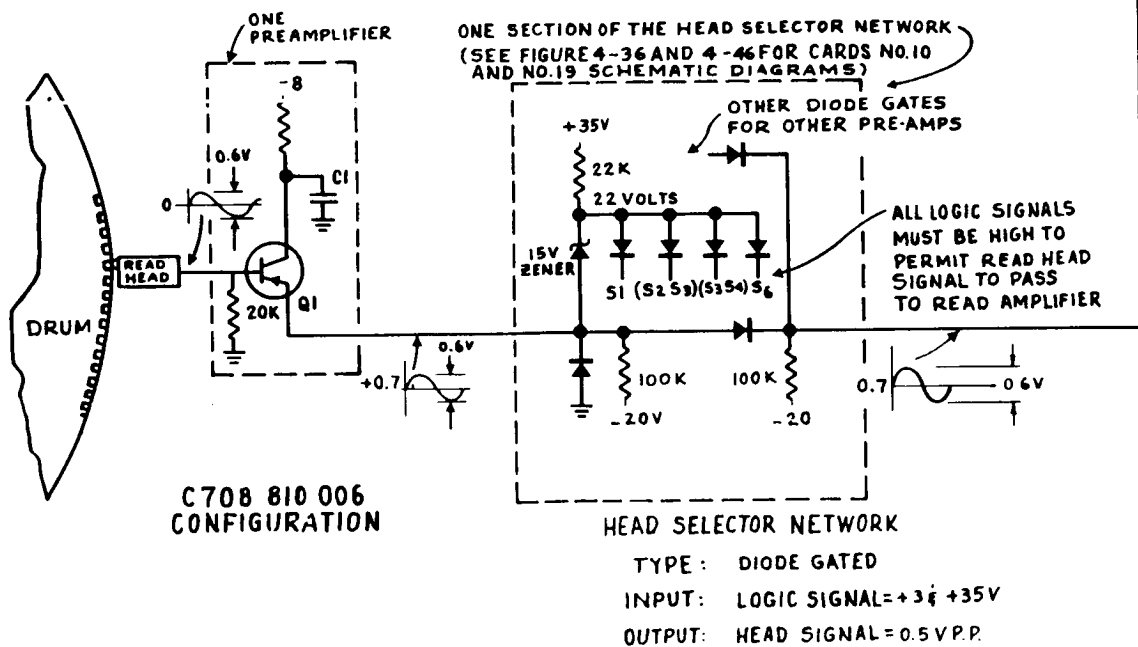
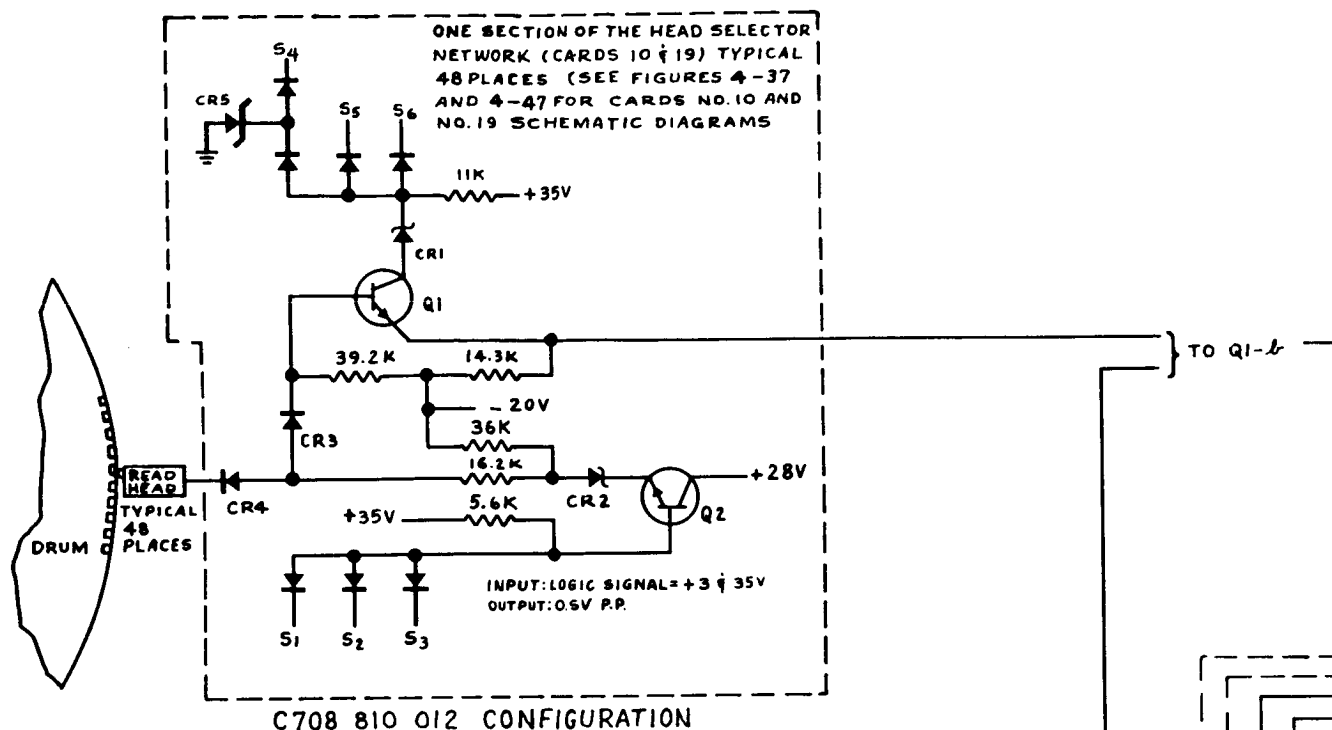
3.2.2.4. Read Amplifiers. The read amplifiers are used to read information previously recorded on the memory drum permanent storage tracks, temporary storage tracks, instruction and arithmetic registers, and the sigmator tracks. All temporary and permanent storage tracks utilize a common read amplifier with a head select matrix input. The arithmetic and instruction registers and one temporary storage track have separate read amplifiers as do the several read outputs from the sigmator tracks. The read amplifier receives an input from the associated read head and generates two complementary outputs. The amplifier section consists of four amplifier stages, two gating circuits, and the basic flip-flop. The signal from the head select network output, or the read head directly in those cases where the read amplifier is associated with one particular read head only, is amplified and clipped. The wave shaped signal then triggers the flip-flop. The operation of the flip-flop portion of the read amplifier is the same as that of the standard flip-flop except for the transistor gating input.

The read amplifier design has remained essentially unchanged from the initial -1 Centaur design. A schematic of the Read Amplifier is shown in Figures 3.2-4a and b.

3.2.2.4.1. Centaur -3 Problems. In 1965, with the substitution of the high reliability parts, a problem with triggering of the read amplifier on noise at the clock time was encountered. Noise on the ground was being amplified by the flip-flop section of the read amplifier and coupled to the output transistor through the speed up capacitors. The S2N2102 transistor which was substituted into the GPK33 design was providing this increased noise amplification over the previous read amplifier flip-flop design. This was due to the higher gain bandwidth product of the S2N2102. The part substitution thus made the read amplifier more sensitive to noise.

Of the several alternatives available to eliminate this noise problem, removal of the cross coupling of the output to the opposite side input of the read amplifier was selected. The cross coupling was not required because the read amplifier application did not require J-K flip-flop type operation. Elimination of the diodes prevented noise spikes on the output of one side of the flip-flop from coupling back and pulling the other input low. Also, the transistors in the Eccles-Jordan section of the flip-flop were now driven into saturation every clock time reducing the noise amplification capability.

The other alternative considered was reducing the speed of transistors in the flip-flop to slow the circuit operation and eliminate the amplification of the noise through the flip-flop section. Timing studies and analysis



3-2-1)

FOLDOUT FRAME

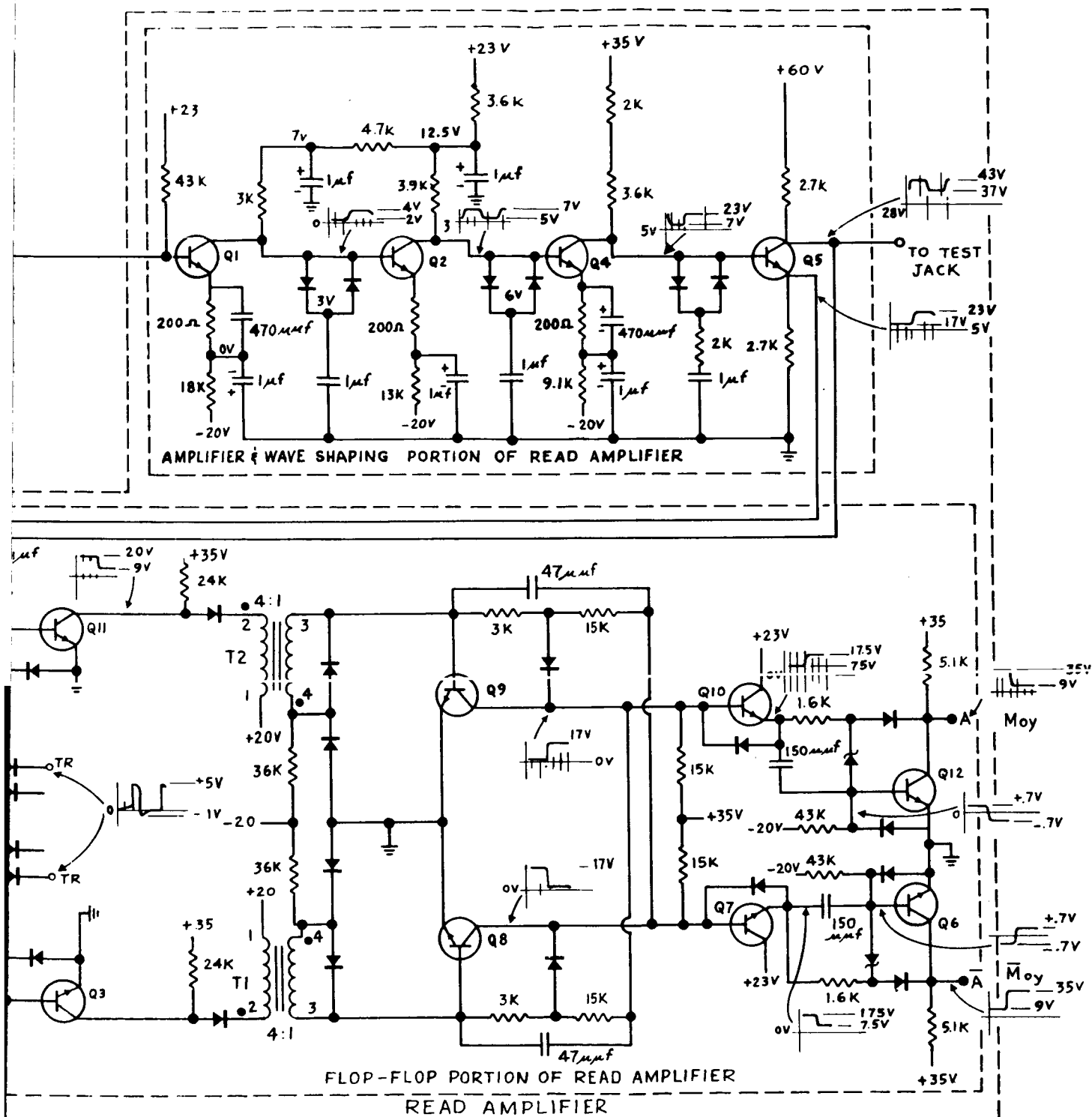


FIGURE 3.2-4. MAIN MEMORY SCHEMATIC DIAGRAM

indicated that this solution was not desirable in that the output of the flip-flop must switch within one microsecond.

3.2.2.5. Logic Networks. The general circuits that mechanize the computer logic are diode AND gates and OR gates. The type used in the computer general purpose section is the AND/OR pyramid to control flip-flops or amplifiers. Input voltage levels are +9 volts dc and +35 volts dc representing zero and one respectively. In some cases, +3 or 0 volts dc represent zero (F/F's S1 through S6). The AND gate output follows the lowest input; that is, when all inputs are high, the output is high, and when any or all inputs are low, the output is low. The OR gate follows its highest input voltage level; that is, when any or all inputs are high, the output of the gate is high and when all inputs are low, all outputs are low.

Logic mechanization as represented in the basic logic equations for the computer general purpose section has remained essentially unchanged throughout the Centaur program with the exception of the removal of the logic to provide in-flight turn-off/turn-on capability. Minor changes in component values were also made to meet worst case analysis requirements established during the course of the program.

3.2.2.5.1. Elimination of the Coast Phase Logic. In 1965, logic changes in the computer general purpose section were accomplished to eliminate the in-flight Coast Phase capability. This capability allowed a major portion of the computer to be powered down during extended coast phase portions of the original projected Centaur missions. Requirements for this type of mission no longer existed in 1965. Thus, all logic associated with this automatic power down and power up after a specified period of time was deleted. The removal of this logic was performed to improve the reliability of the computer by eliminating the associated parts and thus eliminating the possibility of a failure in this unused circuitry causing a mission failure.

3.2.2.5.2. Sigmator Logic Modification. One minor logic change was incorporated in the MECO and velocity accumulation logic associated with the sigmator. Adoption of a semi-automated computer self-test program associated with the GPK33 computer revealed a low probability condition whereby the MECO time and velocity accumulation could be erroneous. Certain logic conditions could cause an error of one bit each time the particular logic condition was satisfied. The logic operation resulting was caused by the fact that the MECO time pulses and velocity inputs are asynchronous with respect to the computer clock. The original logic mechanization did not consider this highly improbable logic condition. The

change incorporated into the logic mechanization eliminated this possibility. The physical change was limited to the addition of three diodes.

3.2.2.6. Memory Drum. The memory drum is the major information storing medium in the general purpose section of the computer.

The drum is a cylindrical motor driven unit which rotates at a nominal speed of 100 rps and has a permanent memory storage capacity of 2,816 words and a temporary memory storage capacity of 200 words. Recording is accomplished on 1,600 evenly spaced magnetic oxide grooves.

Utilizing a 25 bit word, the 1,600 grooves provide for 64 words located around the periphery of the drum. A read head defines a particular track around the drum which intersects each of the 1,600 grooves during one drum revolution. The permanent storage tracks contain read heads only, and the information is recorded on the drum through use of the read head as a write head during the filling operation only. The data is stored in a particular location with a north-south polarization representing a zero and a south-north polarization representing a one. The temporary storage tracks, the instruction and arithmetic registers, and the sigmator tracks, contain one or more read and write heads, depending upon the particular function of the track. A diagram of the memory drum showing the various tracks, read and write heads and amplifiers, and head select networks is contained in Figure 3.2-5.

The memory drum has proven very reliable in field operation. Modifications to the drum have been limited to a change from the -1 to -3 configuration which resulted in the addition of seven permanent storage tracks and one temporary storage track. This modification was accomplished to increase the computer memory storage capability. Problems encountered with the drum have been limited to the critical head gapping, alignment, and clocking operation which is performed during the manufacturing process. The adjustment and clocking operations are extremely critical and time consuming, requiring a high degree of skill and a considerable amount of testing to insure that all operations are proper prior to delivery of the computer. This is a producibility problem. Once the drum has been gapped, adjusted and properly clocked, operation in the field has been reliable.

3.2.2.7. Clock Generator. The clock generator supplies the basic timing for the general purpose computer. The clock amplifier receives an input from the clock track on the computer memory drum. The clock amplifier output supplies four clock pulses designated T , T_e , T_w and T_r . The T_w clock pulse gates the write amplifier, the T_e clock pulse gates the

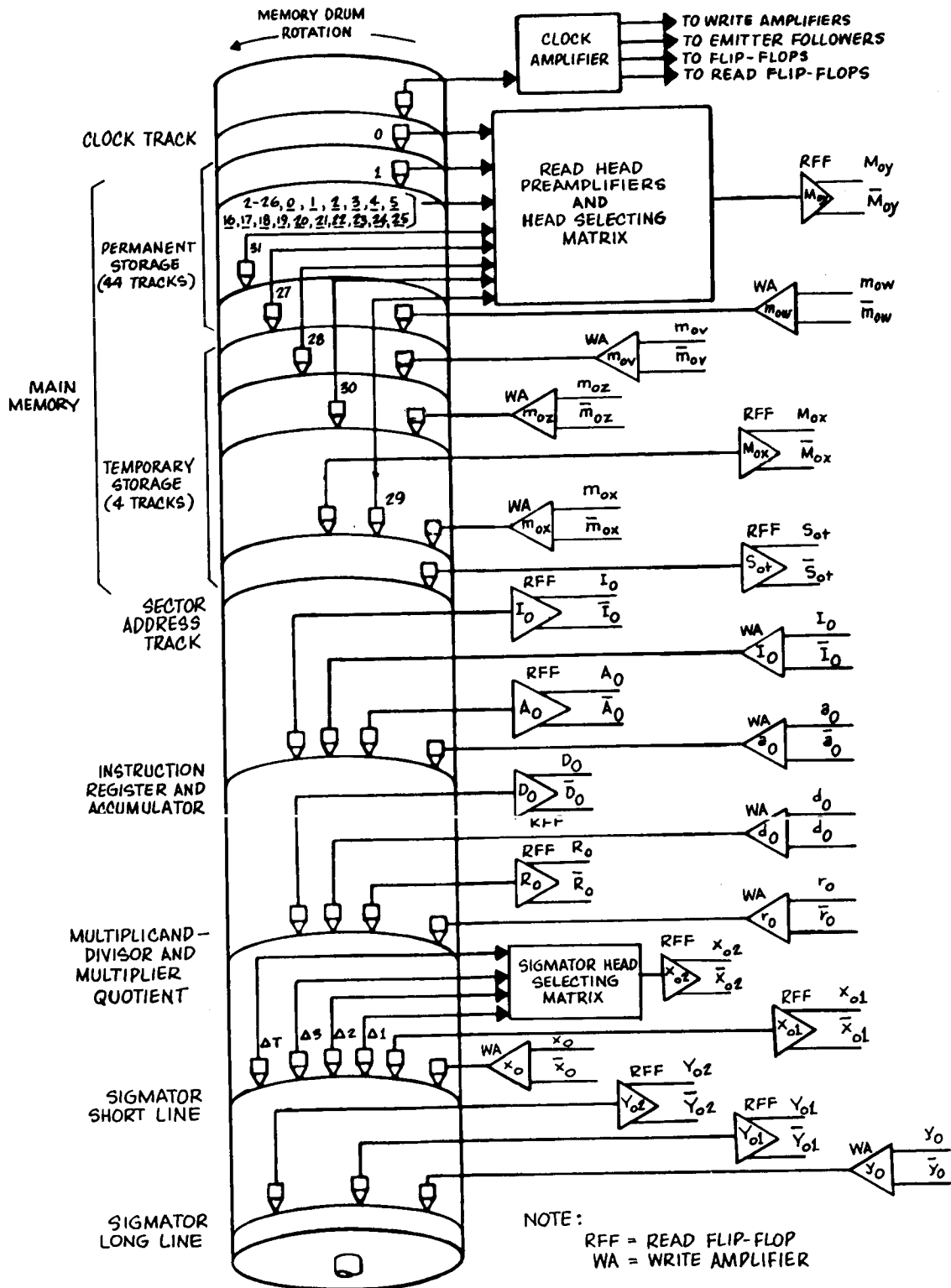


FIGURE 3.2-5. MEMORY DRUM TRACKS

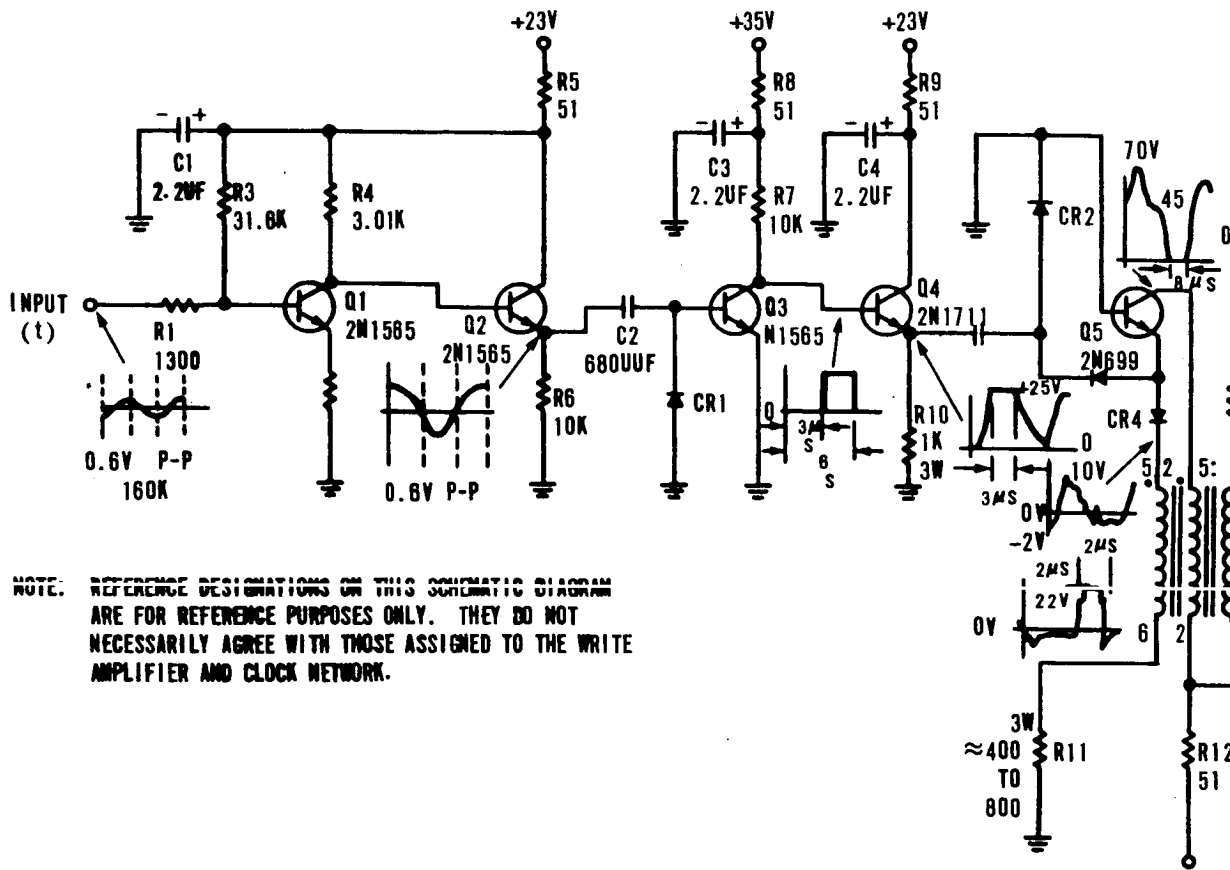
emitter-followers, the T clock pulse gates the general flip-flops, and the T_r clock pulse gates the read flip-flops. The clock amplifier consists of a DC preamplifier, a trigger shaping stage, two blocking oscillators, and power stages. The amplifier uses four transistor stages to amplify and shape an input signal into a suitable driving signal for the first blocking oscillator. The first blocking oscillator generates the T_w clock pulse. The trailing edge of the T_w clock pulse triggers the second blocking oscillator which generates the remaining three clock pulses. A clock amplifier schematic is shown in Figure 3.2-6.

3.2.2.7.1. Centaur -1 Clock Generator. The Centaur -1 clock generator was essentially the same as the present circuit; however, it did not provide the write amplifier clock or the emitter-follower clock. The -1 clock amplifier consisted of a DC amplifier, a trigger shaping stage, one blocking oscillator and a power stage. The clock generator redesign to incorporate the T_w write amplifier clock and the T_e emitter-follower clock was accomplished in the -1 to -3 redesign. The reason for incorporating these design changes into the clock amplifier are delineated in the write amplifier and emitter-follower sections of this report. The redesign was not occasioned by problems with the clock generator but rather to solve specific problems with the write amplifier and emitter-follower circuits.

3.2.2.7.2. -3 Clock Generator. Several minor modifications were incorporated into the clock generator circuit in the GPK32/33 redesign.

3.2.2.7.3. T_w Clock Modification. The modification of the write amplifiers consisting of replacement of the input resistors with zener diodes to eliminate false writing of the write amplifiers imposed an increased load on the T_w clock. To supply the increased current load, a PNP emitter-follower stage was added to the T_w output circuit. This alternative was selected over changing the loading on the blocking oscillator because it was a simple circuit change requiring only the addition of two diodes and one transistor, whereas modifying the blocking oscillator would have resulted in considerable circuit analysis and testing.

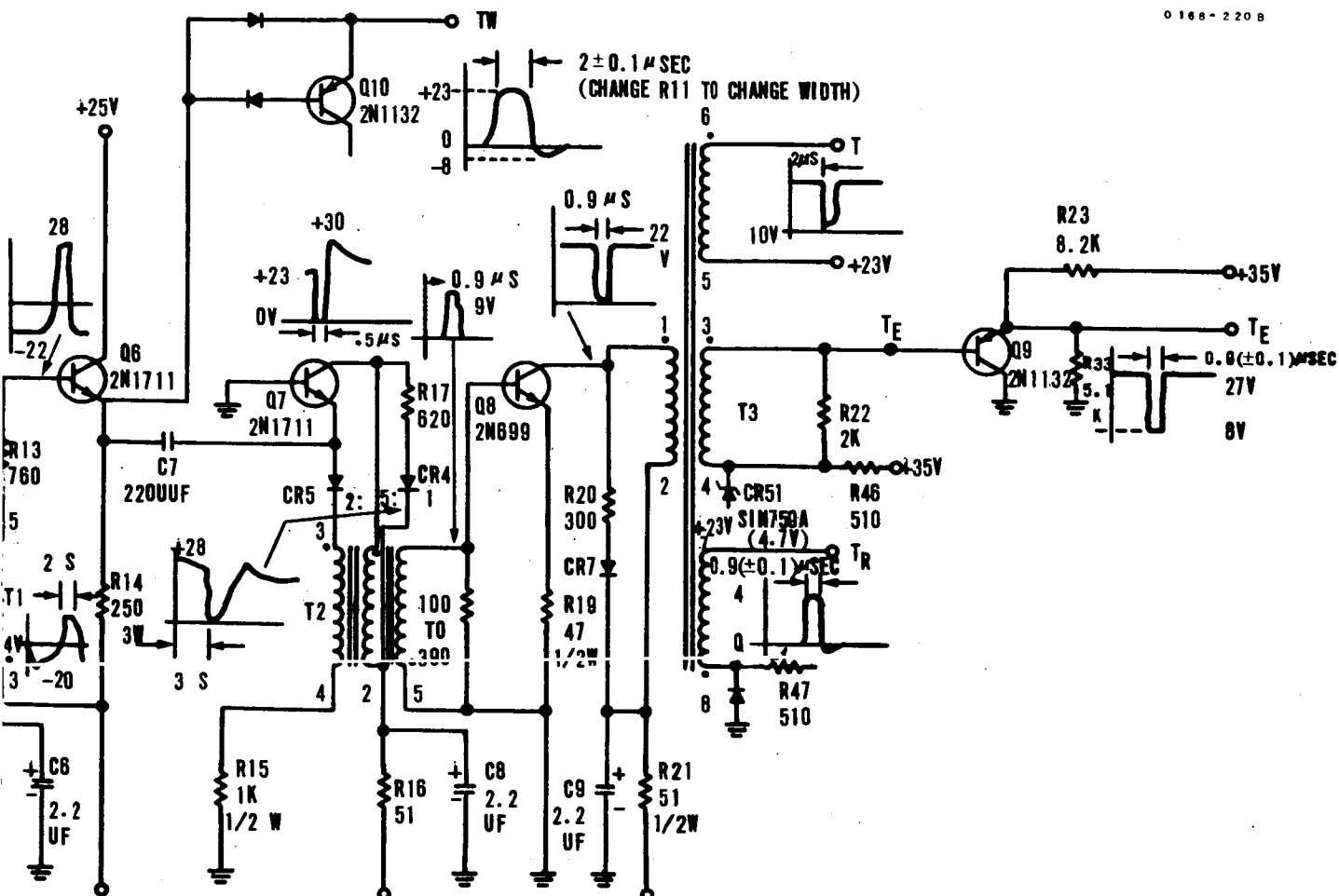
3.2.2.7.4. T_r Read Amplifier Clock. The circuit analysis during the GPK33 redesign revealed that the read amplifier clock low level noise margins could be improved by a minor change in the output circuitry of the read amplifier clock. The change consisted of adding a negative clamp to the output transformer stage of the read amplifier clock. A diode was used to clamp the low level of the T_r clock to a nominal negative 0.7 volt. The previous low level was ground. This change provided a greater noise margin for the read amplifier flip-flop trigger and was not accomplished in solution to any particular problem.



3-2-17

FOLDOUT FRAME

0 168 - 220 B

FIGURE 3.2-6. CLOCK AMPLIFIER
SCHEMATIC DIAGRAM~~3.2-17~~
3.2-18

FOLDOUT FRAME

3.2.2.7.5. T_e Clock Modifications. Problems with the emitter-followers resulted in a modification to the T_e clock output stage. The problem encountered resulted from the slow switching speed of the emitter-follower transistors. The observed anomaly was a positive going spike on the emitter-follower output following the return of the output to the nine volt low level. This positive going spike, if of sufficient magnitude, could cause false triggering of the flip-flops which accent the emitter-follower outputs. The emitter-follower output transistor was being operated in deep saturation and was not coming out of saturation within the one microsecond T_e clock pulse. This resulted in the transistor remaining on for some period of time after the clock pulse had returned to the high state. This condition was due to the large base drive on the emitter-follower transistor and the fact that its collector was at the same potential as the high logic input to the base (35 volts). The transistor then remained in hard saturation for most of the duty cycle, resulting in excess energy in the form of minority carriers being stored in the emitter to base and base to collector junctions. This excess energy was not being removed during the one microsecond T_e clock. Consequently, the remaining excess charge attempted to return the transistor to the high state at the end of the clock pulse and resulted in the abnormal voltage spike. The solution selected was to redesign the T_e clock output circuitry to provide a lower voltage level input to the transistor circuit, thus preventing the transistor from going into deep saturation. This provided a rebiasing of the emitter-follower base and insured that the transistor collector to base junction remained reversed biased at all times. The base is effectively clamped by the T_e clock which provided a 28 volt level versus the original 35 volt level and saturation of the transistor was prevented.

This design change was selected over the alternative of the modifying of all the emitter-followers due to simplicity.

3.2.2.8. Head Select Networks. Read back of information recorded on the 44 permanent storage tracks and four temporary storage tracks are provided via a common read amplifier. Track selection is accomplished by the head select network. The read back from the head on the memory drum is preamplified and then gated to the main read amplifier.

3.2.2.8.1. Centaur -1 and -3 Head Select Circuitry. The -1 and -3 head select circuitry consisted of a preamplifier and diode gating circuit for each head on the memory drum. The preamplifiers were contained in three plug-in packages mounted on the memory drum shroud to provide power gain and improved signal to noise ratio inputs to the head select circuitry. The head select network consisted of 48 diode gating circuits, one for each main memory track. Each selector network AND gate had a

specific gate code derived from the head select flip-flops S1 through S6. The gating provided for the electrical connection of the desired memory read head via the preamplifier to the read amplifier.

3.2.2.8.2. GPK33 Head Select Redesign. In 1966, the head select network was redesigned. This redesign was accomplished because the -1 and -3 computers were not designed to readily facilitate reprogramming of the computer memory permanent storage. However, during the Centaur program, the need developed to accomplish many program changes during the life of the computer. Loading of the permanent storage memory required removal of the preamplifiers.

There was inadequate space for the removal of the preamplifiers and thus, the possibility of damaging the delicate preamplifier pins and cabling to the preamplifiers existed. Intermittent or poor connections of the preamplifier pins or cabling will cause erroneous read back of the information in the computer memory. This occurrence is a critical failure. Instances of damaged or distorted connector pins were noted periodically during utilization of the -1 and -3 computers. Redesign also afforded the opportunity to utilize a matrix selection technique with a significant reduction in the number of components used. The redesigned head select also used high reliability parts and new design cards in accordance with NASA requirements.

The redesign of the head select circuitry consisted of removing the preamplifier for each read head and the use of matrix selection. The preamplifier in the new head select matrix is in the driver for the Y select gates. This reduced the number of preamplifiers from 48 to 8. The adoption of a diode matrix to perform the select function also reduced the number of gating diodes required. The new head select network is an 8 by 8 matrix with 16 codes unused.

Topic 3. 3

Computer Input/Output Unit

3. 3. 1. General Description. - The Input/Output Unit connects the Computer Memory to the other IGS units by adapting signals received from the IGS for transmission to and acceptance by the Computer Memory. The unit also extracts information from the Computer Memory and adapts it for transmission to the IGS. The navigation computer has the following inputs and outputs (see Figure 3. 3-1).

1. Inputs-

- a. Accelerometer Signals.
- b. Mode Control Signals.
- c. Mode Set Signal.
- d. Steering Alert Signal.

2. Outputs-

- a. Gyro Torquing Signals.
- b. Steering Signals.
- c. Discrete Signals.
- d. Telemetry Signals.

The Input/Output Unit consists of the following modules and assemblies.

3. 3. 1. 1. Steering Converter Modules. - The three steering converter modules are sealed plug-in assemblies. Each one contains a modulator, servoamplifier, motor generator, potentiometer, digital to analog converter, and a gear train to enable the motor to position the potentiometer and digital to analog converter shafts.

3. 3. 1. 2. Torquing Converter Modules. - The three torquing converter modules are sealed plug-in assemblies. Each one contains a modulator, servoamplifier, motor generator, potentiometer, digital-to-analog converter, and a gear train to enable the motor to position the potentiometer and digital to analog converter shafts. A brake is also included to hold the potentiometer in a fixed position.

3.3.1.3. Error Storage and Converter Selectors. - There are six error storage and converter selectors, one associated with each of the steering and torquing converter modules. They are plug-in circuit assemblies consisting of AND gates, a flip-flop and an emitter follower.

3.3.1.4. The 1.3 kHz Frequency Standard. - The frequency standard is a sealed unit consisting of a crystal-controlled oscillator with a temperature-controlled oven. The unit is energized by 28 VDC and supplies 1300 Hz.

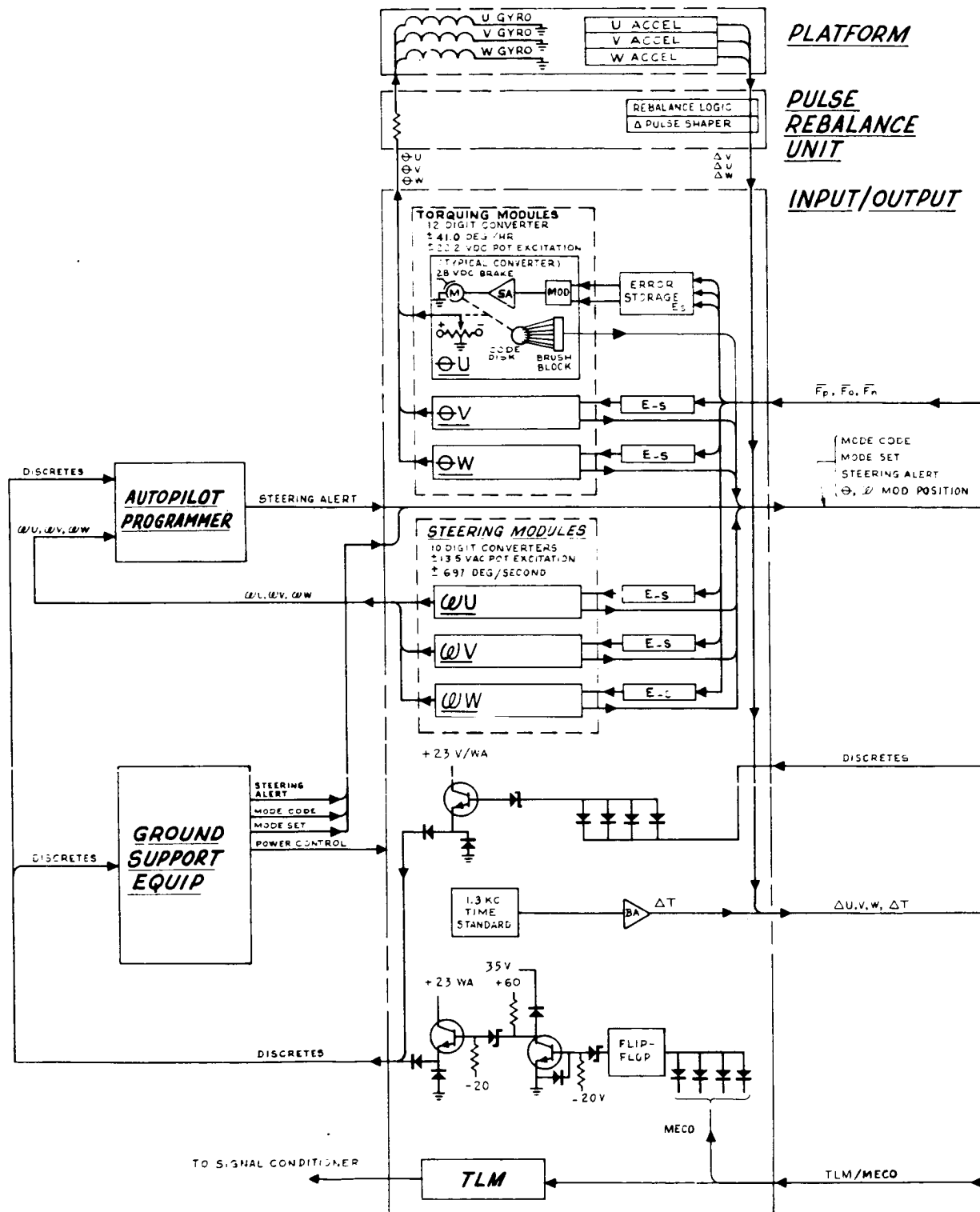
3.3.1.5. Input/Output Plug-In Card Assemblies. - The input/output contains two plug-in card assemblies; the Telemetry Network Card and the Discrete Driver Card.

3.3.1.6. Power Supply. - The power supply consists of a power transformer, power supply capacitor package assembly, power supply rectifier package assembly, and resistors and semiconductor devices mounted in the input/output subassembly.

3.3.2. Digital to Analog Conversion Gyro Torquing. - Prior to launch, the inherent drifts of the gyros are compensated for. Platform movement in three axes is detected by the accelerometers on the inertial guidance platform. These accelerometer signals are passed on to the pulse-rebalance unit which conditions them for acceptance by the navigation-computer. The incremental velocity inputs are received in the input/output and accumulated on the sigmator short and long lines via an adder-subtractor control circuit.

Various arithmetic computations are performed during the preflight alignment modes to establish corrections to the inertial guidance platform gyros and accelerometers. The digital corrections are then stored on the sigmator long line as outputs to the inertial guidance system. The digital information is then sent to the inertial guidance gyros via three digital to analog converters in the input/output. Each analog voltage is taken from the wiper arm of the ± 22.2 VDC excited, 10,000 ohm potentiometer in the D/A converter module. This potentiometer is load compensated. Three gyro torquing signals with the following characteristics are available:

Range: ± 41 degrees per hour.
Digital resolution: 12 bits including sign.



23-3

FOLDOUT FRAME

U 158-14-B

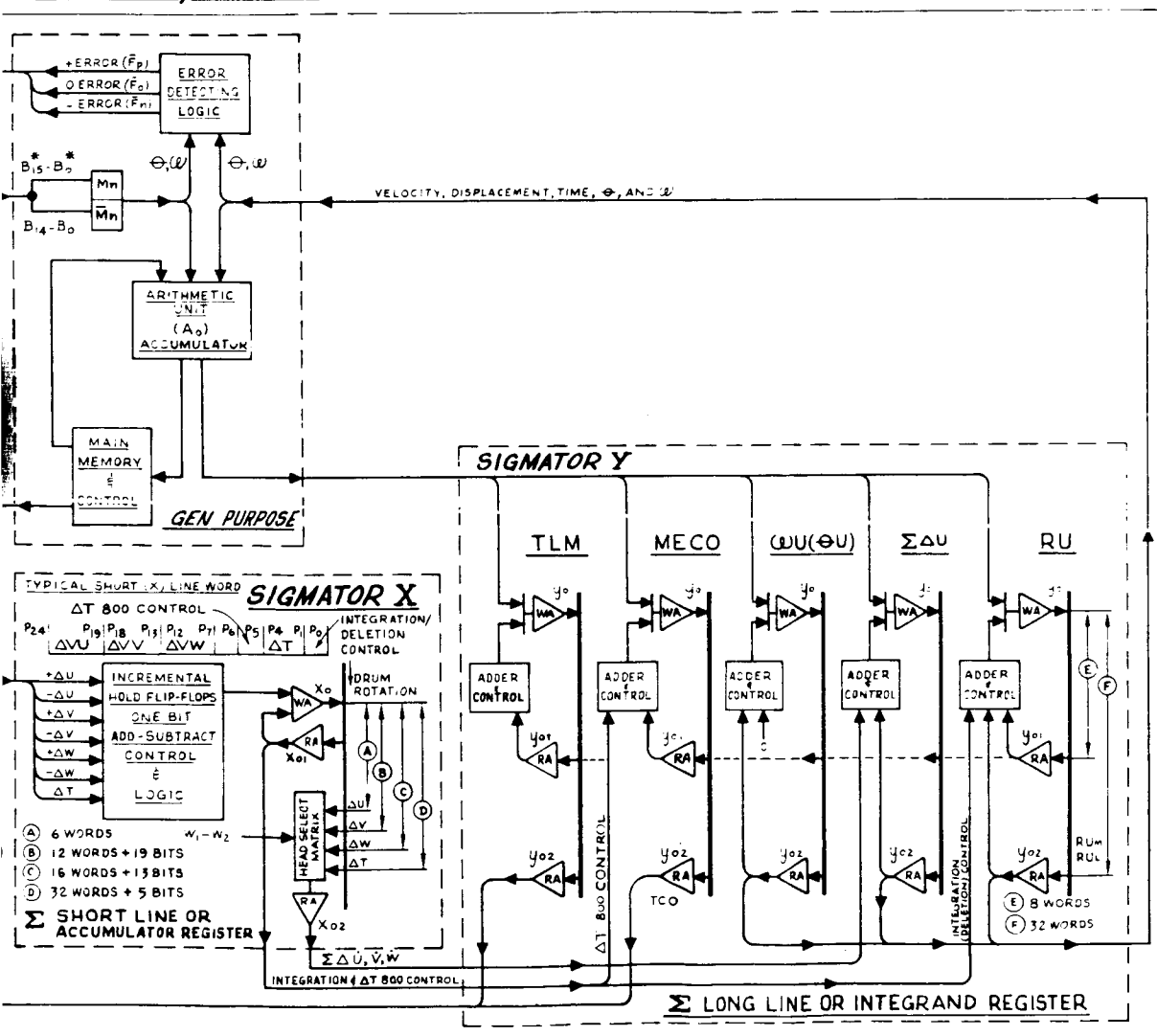
COMPUTER/MEMORY

FIGURE 3.3-1. NAVIGATION COMPUTER FUNCTIONAL DIAGRAM

3.3.2.1. Torquing Module Problems. - The torquing module is difficult to manufacture due to its space limitation and its electro-mechanical construction. Throughout the IGS development, the problem areas have been in the:

1. Torquing Potentiometer,
2. Alignment of Brush Block and Encoder Disc,
3. General Wear.

Attempted solutions to these problems have been to:

1. Replace the torquing potentiometer with a new design (1962) and subsequently redesign the new potentiometer.
2. Redesign the encoder disc and brush block assembly. This attempt failed and the manufacturer subsequently reverted to the old assembly.
3. Intensify quality control of parts assembly and alignment.

3.3.2.2. Torquing Potentiometer. - The torquing potentiometer in the -1 Centaur design did not provide the required resolution (accuracy). Therefore, for the -3 Centaur redesign effort, the potentiometer was changed from a 10 turn type to a 20 turn type built by another manufacturer. Procurement of the 20 turn potentiometer was a real state of the art problem due to size and accuracy requirements. No response was forthcoming from potential vendors on initial efforts to obtain a supplier. However, due to the evaluation of a similar potentiometer on another Honeywell program, a vendor was discovered.

The new potentiometer proved difficult to build to Centaur requirements. Problems which occurred were:

1. Failure of mechanical stops.
2. Flaking of winding coating.
3. Excessive wear of windings.

Each of the problem areas was worked out by intensive effort on the part of the vendor, Kearfott and Honeywell. At the present time the potentiometer is giving satisfactory performance.

3.3.2.3. Encoder Disc and Brush Block Assembly. - The encoder disc and brush block assembly shows wear characteristics with time. The wear contributes to misalignment of the brush block and encoder disc. While the problem is not acute and is one of the things which must be

tolerated with a mechanical device, an attempt was made to alleviate the problem in early 1967. A new assembly was designed for the ADD-6 program to improve the wear characteristics and to eliminate brush block vendor problems by using standard parts and processes.

The new assembly displayed more excessive wear than its predecessor. The only remaining alternative was to retrofit modules to the previous design after efforts to improve the new design failed.

3.3.2.4. General Wear. - This problem, as in the case of the above assembly, is typical of many electro-mechanical devices. Problems have arisen due to wear of moving parts in the torquing module assembly (gear trains, etc.). The general approach has been to use extra care in the cleanliness and accuracy of parts assembly. In addition, on the last major retrofit of modules, as discussed above, the modules were inspected for worn parts and completely refurbished, including replacement of certain torquing potentiometers which were installed prior to a certain date.

3.3.3. D/A Conversion - Steering. - During powered flight, missile acceleration in three axes is detected by the accelerometers in the inertial guidance platform, then are integrated and conditioned in the pulse-rebalance unit for input to the navigation computer. The incremental velocity inputs are accumulated and integrated in the sigmator portion of the computer to be used in the various arithmetic computations required to solve the in-flight steering equations. The digital steering corrections determined by the computer are then set to the resolver chain in the inertial guidance platform via the sigmator long line and three digital to analog converters in the input/output. Each analog voltage is taken from the wiper arm of the ± 13.5 VAC excited, 1000 ohm potentiometer in the module. This potentiometer is not load compensated. Three steering signals with the following characteristics are available:

Range: ± 6.97 degrees per second.
Digital resolution: 10 bit including sign.

The steering module is similar to the torquing module although the accuracy requirements are not as great as those for the torquing module. With the exception that the original steering module potentiometer has remained satisfactory, the discussion for the torquing module may be applied here.

3.3.4. Velocity Sampling. - Accelerometers mounted on the Centaur guidance system stable platform provide six pulse trains, each pulse being an increment of velocity. Another set of pulse trains are generated in the coupler ΔV output circuitry and intended to be equivalent to the true ΔV 's. The ΔV output pulse trains are applied to the computer input/output and have the following characteristics:

Repetition rate: 0 to 3600 pulses per second.
 Amplitude: 19 (± 4.75) volts.
 Scale Factor: 0.1 foot per second per pulse.

The velocity accumulation flip-flops in the general purpose computer experienced false triggering problems in 1966. The discussion of the problem and solution are discussed in a preceding Topic titled "Flip-Flops" (Topic 3.2).

3.3.5. Discretes. - Discrete signals are generated under navigation computer program control and are provided to the autopilot programmer and GSE. When received by the autopilot programmer, the discrete signals, except Computer GO, Mode Accept and Mode Complete, are used as commands to control the various phases of powered flights for the missile. When received by the GSE, the discrete signals are used to verify navigation computer functional performance. Discrete signals provided are as follows:

1. Ground Discretes. -

- a. Computer GO
- b. RL&R Frame Complete
- c. RL&R Operation Complete/Memory Sum OK
- d. Mode Accept
- e. Mode Complete
- f. Launch-on-Time Accept
- g. Flight Mode Accept.

2. Airborne Signals. -

- a. Booster Engine Cutoff (BECO)
- b. Sustainer Engine Cutoff (SECO)
- c. Main Engine Start (MES)
- d. Main Engine Cutoff (MECO)
- e. Vernier Cutoff (VCO)
- f. Reorient
- g. Separate Spacecraft.

The discrete signals have the following characteristics:

On level: 23 (± 3) volts.
Off level: 0 (± 1) volt.

In the -1 design only four discrete lines were available. These were time-shared to provide both GSE and airborne functions. The discrete orders are special orders, which may change with each application. As the Centaur program has evolved, more discrete functions have been required, and the available lines were increased to the present 14 in the GPK32/GPK33 redesign effort.

3.3.6. Telemetry Interface. - Outputs of the navigation computer pertaining to overall system functions are provided from the computer in a form suitable for telemetry. The computer telemetry output has the following characteristics:

Information rate: 800 bits per second.
ONE voltage level: 5.1 (± 0.5) volts (A/B).
5.1 (+0.5, -1.2) volts (GSE).
ZERO voltage level: 0 (+1, -0) volt.

The computer issues a telemetry marker pulse on the telemetry line, which is programmable to provide markers for separating information in real time. The pulse has the following characteristics:

ONE voltage level: 5.1 (± 0.5) volts.
ZERO voltage level: 0 (+1, -0) volt.

The telemetry output in the early design was a three-state, return to zero, format. In the GPK33 redesign the output was changed to the two-state, non-return to zero, format shown above. The reason for the change was to reduce the required bandwidth of the signal, thereby freeing higher bandwidth channels.

The output line was found to be susceptible to large transients, since no isolation was provided in the original design. The GPK33 redesign provided for an isolation diode. No problem has been experienced since the change.

3.3.7. Frequency Standard. - The frequency standard is a sealed unit, containing a crystal oscillator with a continuously temperature-controlled oven and countdown circuits. The unit is energized by 28 VDC and

transmits a square wave signal with a frequency of 1300 Hz. The output of the time standard is shaped and amplified (basically a Schmidt trigger). The in-phase amplified signal is applied to a flip-flop in the Computer Memory. It provides real time to the computer to be used in in-flight guidance calculations.

The frequency standard experienced a high failure rate on the initial design. The failures resulted from crystal mount failures under vibration, open circuits and a marginal output signal. A redesign incorporated a redesigned crystal mount, redesigned oscillator and foam potting of frequency divider flip-flops and cables to the output header. Problems were experienced with the new crystal mount during the requalification of the frequency standard. Honeywell at this time (August 1963) submitted a VCP for second sourcing which was disapproved by GD/C. The crystal mount in the meantime was redesigned and the new frequency standard requalified. The frequency standard has operated satisfactorily since the requalification. It has remained unchanged for subsequent computer redesigns.

3.3.8. Conclusions. - The lessons learned from the evolution of the Input/Output Unit relate in part to a design that is obsoleted by the present state of the art in solid state circuitry. The D/A conversion would be solid state in any new design thereby eliminating the potential problems associated with complex mechanical parts confined in a small space. The frequency standard in a new design would have a structural analysis and environmental testing along with worst case circuit analysis. The remaining circuitry of the Input/Output Unit would have worst case circuit analysis.

The IMU and Navigation Computer for the present MGS utilize separate real time clocks (frequency standards). For future systems, simplification of the design can be realized with the use of one frequency standard for the IMU, Computer, and perhaps other vehicle systems. Such is the case with the Centaur IMG design. The Digital Computer Unit (DCU) will have a real time clock signal available, provided by the frequency standard located in the IMG.

Topic 3. 4

Input/Output Functional Characteristics

3. 4. 1. Introduction. - This topic is included to assist the reader in understanding the total functions and format of the Centaur IGS Computer. The discussion is primarily descriptive in nature. However, understanding the functions will help the reader in reviewing the computer hardware development, its problems and solutions, and the lessons learned for application to future programs.

3. 4. 2. Basic Numbering and Word Construction. - Instruction words and data words are written on the memory drum. A word consists of 25 consecutive magnetic segments on a particular track. The location of a word on a track is called a sector. The track and sector location of a particular word is called the address.

Each instruction word of 25 bits supplies:

1. The order code of the current operation (3 bits).
2. Binary address of the current operand to be used (11 bits).
3. Binary address of the succeeding instruction word (11 bits).

Table 3. 4-I shows the distribution of bits in an instruction word.

Each data word format, also 25 bits long, is a binary equivalent of a decimal number. The least significant digit appears at position P24, the most significant digit at position P1. The sign digit is located at P0 and a binary point exists between P0 and P1, supplying a fixed reference. See Table 3. 4-II. In the sign position, a "0" denotes a positive sign and a "1" denotes a negative sign. All quantities must be scaled less than 1.

3. 4. 3. Arithmetic Functions. - The arithmetic section of the computer consists of three recirculatory registers (Ao, Do, Ro), two delay flip-flops (A1 and D1), a serial adder with its carry flip-flop (Ca), and control flip-flop (Kc). Some of the flip-flops from the control section are also used on a time shared basis for arithmetic operations.

INSTRUCTION WORD FORMAT

DATA WORD FORMAT

P24 = Least significant bit position
P1 = Most significant bit position
P0 = Sign bit position

The accumulator (Ao) recirculating register is exactly one word long, 24 bits on the memory drum and one bit in the A1 flip-flop. It contains the results of addition, subtraction, extract, multiplication and division after completion of the operation. The Do register is used to hold the multiplicand or divisor during the multiplication or division operations. This register is 24 bits long. Recirculation is obtained by using a time shared track selector flip-flop, S2, to make this register 25 bits long. The Ro register is 24 bits long and holds the multiplier or the quotient. During multiply the multiplier is left shifted by forming a 26 bit register consisting of the Ro register and S3 and S4 flip-flops.

The arithmetic section can accomplish eight basic operations as shown in Table 3.4-III.

3.4.3.1. Clear and Add (At). - Clear and add operation is completed during the first word (FW) phase. The accumulator is cleared of its previous value by setting the A1 flip-flop to zero at the same time that the main memory word is being copied by the D1 flip-flop. This is then transferred into the Ao register.

3.4.3.2. Add. - The add order (Ad) forms the sum of the number contained in the accumulator (Ao) and the operand from the main memory. The contents of the accumulator are added to the number specified by the β address of the instruction. Addition is completed in one word time during the FW phase.

3.4.3.3. Subtract. - The subtract order (Su) takes the difference of the number in the accumulator and the number from main memory. The contents of the accumulator are subtracted from the contents of main memory during the FW phase.

3.4.3.4. Multiplication. - The multiplication order (Mu) forms the product of the number in the accumulator and the number in main memory. The contents of the accumulator represent the multiplier whereas the multiplicand from main memory is located by the β address of the instruction. Multiplication is started in the first word (FW) phase, continues through the additional word phase (AW) and is completed during the last word (LW) phase. The number of additional word operations formed is determined by the sector address of the next instruction. The feature allows the multiplication operation to be terminated when the desired accuracy has been obtained in the product. This is made possible because the most significant digits of the product are generated first. The most significant digit of the multiplier is used in the first step and in successive

TABLE 3.4-III
ARITHMETIC OPERATIONS

Order	Order Code P2 P1 P0	Order Abbrev.	T β Code P19P18P17P16P15	Order Description
Clear Add	000	At	- - -	Clear the accumulator to 0 and to it add the contents of the beta address Moy.
Extract	001	Ex	- - -	Compare the contents of Ao to contents of Moy. Resultant contains 1 where 1 occurred in both Ao and Moy.
Multiply	010	Mu	- - -	Multiply the contents of Moy by the contents of Ao.
Conditional	011	Tc	- - -	If the sign of Ao is negative, take the next instruction from the alpha address of the current instruction. If the sign of Ao is positive, take the next instruction from the beta address of the current instruction.
Add	100	Ad	- - -	Add the contents of the beta address Moy to the contents of the accumulator Ao.
Divide	101	Dv	- - -	Divide Ao by Moy.
Subtract	110	Su	- - -	Subtract the contents of Ao from the contents of Moy.
Store	111	Sr	00000	Store Ao into Yo.
Store	111	Sr	10000	Store Ao into Mov.

steps the multiplier is shifted left so that the digits are used in decreasing order of significance. The multiplicand is shifted right one bit per step and a bit is dropped from the least significant end of the word for each step.

3.4.3.5. Division. - The division order (Dv) forms the quotient of the number stored in the main memory (the divisor), and the number in the accumulator register (Ao). The length of the quotient is equal to the number of additional word phases. During the FW phase, the divisor is read into the Do register, and the quotient is established in the Ro register. During additional words, the quotient digits are determined and inserted in the Ro register at a position determined by the quotient index digit. The index digit shifts right one position per additional word, therefore assembling the successive quotient digits in descending order of significance. During the LW phase, the quotient is shifted into the Ao register. The quotient is incorrect during the divide process and the roundoff necessary to correct the quotient is performed during the LW phase. All five track selector flip-flops are used during division in addition to the elements in the arithmetic section.

3.4.3.6. Extract. - The extract order (Ex) is normally used to modify instructions by changing the address portion of the instruction. The operation will write a "1" in the accumulator whenever a "1" appears in both Ao and main memory and will write 0's everywhere else. Therefore, data contained in part of a word can be selected or extracted by using a control word containing 1's at the desired bit location. The control word may be located on the accumulator register (Ao) or read from main memory as both numbers in this operation are treated identically. This operation is completed during the FW phase.

3.4.3.7. Conditional Transfer. - The conditional transfer (Tc) operation selects one of two addresses for the next instruction based on the sign digit of the number in the accumulator. If the sign is negative, the location of the next instruction is taken from α address of the present instruction. If the sign of the accumulator is positive (equal to zero) the next instruction is taken from the β address of the present instruction. The Tc order does not modify the contents of Ao. These operations are initiated in the W β control phase.

3.4.3.8. Store Order. - The store order (Sr) defines a class of special operations. The β track address is used to specify particular operations. Normal storage of a number in the accumulator on any one of the temporary storage tracks or the signator track is accomplished during the FW

phase. The sector storage location is the sector of the present instruction. The track storage location is specified by a code in the β track portion of the instruction. Add, subtract, extract, clear add and normal store orders are said to be first word (FW) operations. The conditional transfer order is a non-arithmetic operation, so it has no limits on duration. The multiply, divide and some modified store orders are additional word (AW) operations and vary in length.

3.4.4. Sigmator Functions. - The sigmator is an independent, high speed, programmable, real time integrator used to sum, store, and process high frequency incremental inputs from external sources. The inputs (positive or negative increments of velocity in three channels) are asynchronous with respect to navigation computer operation, but memory drum speed limits the rate of input to 6200 pulses per second at a nominal drum speed of 6000 revolutions per minute. Where the general purpose computer uses the clock track (drum speed, variable with ac frequency) as a time standard, the sigmator uses the frequency standard described above for real time integration control. Input data is retained by logic so as to be transferred to the sigmator at specific times, permitting the asynchronous input to be synchronized with the navigation computer.

External information received is in the form of pulses which arrive at random intervals, asynchronous with the machine time of the navigation computer. This information is stored in flip-flops, the outputs of which are controlled by gating with computer time. Included with the pulses from the inertial guidance system is the time pulse from the real time oscillator. This pulse is a positive increment added to the velocity pulses and represents an adjustment of the summation processes to real time determinations.

The positive or negative incremental information is added algebraically, through a one-bit adder, to a memory drum register (sigmator short line) through the operation of two carry flip-flops (one for positive increments and one for negative increments). The carry flip-flops form an incremental adder, which places the additive result of the plus and minus outputs of the carry flip-flops into the sigmator short line. These increments are then recirculated via the incremental adder to be added to the new increment pulses. This occurs once for each of the four incremental inputs Δu , Δv , Δw , and Δt . The sigmator short line word receives pulse information at four separate intervals and is correspondingly divided by the spacing of read heads into four information divisions. There is also a one word (25 bit) spacing between the write head and the first read head (Xo1). The inputs of pulses stored momentarily on the sigmator short

line are fed back to the incremental adder through read head Xo1 and added to the new pulse increments. The new sum is returned to the short line. At intervals of the accumulated function, quantities stored in the four divisions of the short line are transmitted additively to another memory drum register (sigmator long line) via the serial (two-bit) adder. The sigmator short line makes it possible to accumulate pulses more rapidly than they could be accommodated if brought directly to the sigmator long line, since each of the four input functions accumulated on the short line can be accepted and accumulated in consecutive divisions of the sigmator short line word. If transmitted directly to the long line, each function would have to wait its turn for one-half drum revolution (since the sigmator long line track is divided into two 32 word sections).

The sigmator long line, or integrand register, is a 32 word register which cycles twice each drum revolution. The sigmator long line receives inputs as programmed from the accumulator and from the sigmator serial (two bit) adder. In the process of integration, or otherwise, the contents of the long line are recirculated cyclically through the serial (two bit) adder, thus periodically adding the contents of the long line, augmented by inputs from the short line, to themselves, thus completing an accumulative summation, or integration, of the incremental inputs. The contents of the long line are transferred programmably to the accumulator, and vice versa.

In addition to performing integration, the long line is used to provide a real time countdown for generation of a main engine cutoff (MECO) signal and the serial shifting out of binary information for telemetry.

3.4.5. Mode Control. - The calibration of inertial components in the IGS is accomplished by placing the platform stable element in various positions, or modes. While in each of these modes the computer program provides for an automatic sequence which measures appropriate terms. For each position of the stable element there is a computer routine which is commanded by logic lines into the computer. The logic (Mode Control Signals) is set up externally by the GSE and initiated upon activation of a Mode Set Signal.

3.4.6. Power Control. - The power control network consists of three relays that connect or disconnect certain voltages to the navigation computer and cause various actions within the navigation computer in a definite sequential pattern. A definite sequence is required to prevent erasing data recorded on the temporary storage tracks and to place the navigation computer in the proper phase to start operations. Since the shutdown circuit is not used during flight, the relay coils are de-energized

any time the navigation computer is in normal operation. During normal operation, two of the relays are released and the third relay, a latching relay, is reset. The controls for power sequencing the navigation computer are located in the GSE. The computer was originally designed to meet the requirement of an "In-flight Coast Phase" turn-off/turn-on function. This allowed the computer to internally control the computer power during the long coast periods required by the early mission concepts. This one requirement made necessary a complicated power control network requiring an excess of 300 discrete components and, at least, eight relays. This same circuitry because of the requirement, was mechanized for use both in normal operation and the coast phase portion of the flight. Failure in either the control logic or the relay network could cause the effective computer circuitry to operate as if the computer were in the coast phase portion of the flight. The power control circuitry had two undesirable characteristics:

1. A major portion of the relays were energized during flight.
2. The control lines from the GSE through the umbilical were energized at the time of the umbilical eject.

These two facts increased the computer susceptibility to umbilical disconnect transients; thus, increasing the possibility of control network malfunctions at that time.

When the Centaur requirements were reoriented towards Surveyor missions the complicated power control circuitry was no longer necessary. An interim modification was made to the computer to expand the minimum effort necessary to provide a more reliable power control network. Unused circuit elements were disabled or physically removed as required to accomplish the end requirement. Later, as an updating of the computer to the GPK33 configuration the power control circuit was redesigned to minimize the number of airborne relays and wires in the interface, to physically remove all unused circuitry and to render the power control relays in the relaxed state during the "run" mode.

Topic 3.5

Software Design and Control

3.5.1. Introduction. - Two distinct stages of programming are used in the Centaur spaceborne computer. The first is the "ground tape program" stage used for computer and guidance system test prior to loading of the flight program. The second is the "flight program" stage, which includes all of the programming needed in the spaceborne computer to support guidance system test and calibration during pre-flight and flight operations at ETR.

The "flight program" is generated by GD/C, with analytical support and review provided by TRW Systems. All flight equations are under the control of a Guidance Equations Review Board (GERB), with members from each organization participating in the Centaur project. This paper will not attempt to further delineate the content or control of the flight program.

The "ground tape program" is currently used in a form known as UGT, Universal Ground Tape. The UGT contains the computer unit test programs, the MGS calibration and alignment programs, the Earth Spin Test (earth-bound navigation test), Remote Load and Read programs, and an Integrated Test which includes check of the MGS/Autopilot and MGS/Launch-On-Time interfaces. In general principle, a detailed flow chart for the computer test and all MGS tests other than Autopilot and LOT interface is prepared by Honeywell. Actual coding of the UGT used at Kearfott and Honeywell may differ somewhat from that used at GD/C, but the UGT procedures and test parameters are alike at all sites.

Historically, all coding of computer programs-- flight and pre-flight-- was originally done by Librascope under contract to Honeywell, with specifications for flight programs supplied by GD/C. This practice was followed on the original Model Program and on the revised "Code A" program, which separated flight and pre-flight routines shared by the Model Program. By the time of actual Centaur launches, program coding had evolved to the mode where flight programs were coded as well as specified by GD/C, and MGS calibration, alignment and test programs used prior to delivery of the MGS were coded by Honeywell.

By the time of the AC-2 flight, a fairly sophisticated computer program had evolved and the AC-2 Preflight program became the accepted program for IGS production testing and selloff. By July 1964, however,

certain shortcomings in the AC-2 Preflight program had become increasingly noticeable, and a fair amount of experimental programming work was started beginning with SCATE III (Shortened Calibration, Alignment, Test and Evaluation) to accommodate the need for revised platform orientations, Final Align and Functional Test. This effort was followed in fairly rapid succession by a series of pre-flight program revisions known as SCATE IV, 3ACT2C, 177-3ACT, CAT8, CAT9, UGT (H), UGT 33 R0 and subsequent revisions to the now current UGT 33R3.

3.5.2. General Concept of Preflight Calibration. - The basic object of preflight calibration is to solve for the three accelerometer scale factor and bias terms, and the three gyro constant torque terms and the mass unbalance terms about the input and spin axes. Supplementary preflight functions include computer selftests, Final Align, Earth Spin Test, functional test, Remote Load and Read, etc., and each contributes an additional MGS test capability. To carry out MGS calibration, a set of six platform alignments are performed such that each accelerometer input axis is oriented up and down, and at the same time, each gyro input axis is oriented north or south while the output axis is oriented vertical or horizontal such that g-sensitive torques will be inactive or active. For each of the six orientations the north axis is held level, while the platform is allowed to drift about the north axis. The East accelerometer output gives a measure of the amount of drift during the measurement period, while the vertical accelerometer output is stored for subsequent use in computing accelerometer scale factor and bias. Refinements of the basic method involve the choice of: the particular platform orientations to be used, the order in which each inertial component is calibrated, the compensation of the north gyro for Earth's rate and/or best known drift rates, partial compensation, or no compensation, etc.

Assuming the platform remains within about 1/2 degree of the true north-east-vertical orientation during the drift measurement period the drift measurement is basically,

$$W_N = \frac{V_E}{g t^2}$$

Separation of g-sensitive torques from non-g-sensitive torques is accomplished by differencing the drift measurement of an OA vertical orientation (non-g-sensitive) from the drift measurement of an OA horizontal orientation (combined "constant" and g-sensitive).

Accelerometer scale factor and bias are computed from the pairs of accelerometer input axis up-down data as compared with the known local gravity acceleration which would be sensed by a "nominal" accelerometer.

$$SF = g \frac{2g}{V_{UP} - V_{DOWN}} K_{NOM}.$$

$$Bias = g \frac{V_{UP} + V_{DOWN}}{V_{DOWN} - V_{UP}}.$$

Variations and refinements to these basic equations will result from appreciable deviation from the assumption that the platform remains within 1/2 degree of the north-east-vertical orientation and other special conditions.

In the past two or three years, measurement and compensation for accelerometer misalignment angles and gyro mass unbalance about the spin axis (MUSA) have been added to the preflight and flight programs. Originally measured optically, misalignment angles are now measured "automatically" using three special additional platform orientations. Gyro MUSA is still measured optically, although several attempts are being made to "automate" this measurement also.

3.5.3. Historical Development of Preflight Calibration Programs. - More specific detail on the revisions introduced into the calibration programs is provided in the following paragraphs.

3.5.3.1. AC-2 Preflight. - Orientations used in this program established the following order of calibration:

Mode 1	U_{CT}	$+V_W$
Mode 2	W_{CT}	$-V_U$
Mode 3	V_{CT}	$-V_W$
Mode 4	W_{MUIA}	$+V_V$
Mode 5	U_{MUIA}	$-V_V$
Mode 6	V_{MUIA}	$-V_U$

The north gyro torquer was set to zero during the measurement phases, azimuth gyro was torqued at best known drift plus Earth's rate compensation, east gyro was in level hold loop to keep the north axis at level.

The platform was positioned off-level about the north axis in such a direction as to cause the platform to drift through level, finishing the ten minute measurement period approximately the same amount off level on the other side. Appropriate adjustments in the accelerometer data for scale factor and bias were made to compensate for the platform being more than 1/2 degree off-level.

3.5.3.2. AC-3 (SCATE III Preflight). - Orientations

Mode 1	U_{CT}	$+V_W$
Mode 2	W_{CT}	$-V_U$
Mode 3	V_{CT}	$-V_W$
Mode 4	W_{MUIA}	$+V_V$
Mode 5	U_{MUIA}	$-V_V$
Mode 6	V_{MUIA}	$-V_U$

No basic change in calibration method over AC-2.

3.5.3.3. SCATE IV. - Same platform orientations.

Revised velocity pick-up to coincide with time pick-up. Increased resolution in velocity computation by updating previous accumulation with change from last compute cycle.

Revised torquing output and torquing to position platform for measurement phases.

Display of velocity via steering outputs for better system performance monitoring.

Greatly simplified scale factor and bias computation.

3.5.3.4. CAT-8. - Several intermediate experimental programs were tested; program CAT-8 evolved from these. At this period preparations were laid down to accommodate the change from GG116 Accelerometers to GG177's and a less arbitrary choice of platform orientations were being debated, tested out, and decided upon but not incorporated. Particular stress was put forth to meet the requirements of the AC-8 mission. Beginning with this program, a series of computer unit level tests were incorporated to allow acceptance testing of the computer as well as the IGS without any changes in the contents of permanent memory being required. Preloaded geophysical parameters were incorporated to allow use of this program at each of the four main operational sites. An Earth Spin test was included. During the measurement phases, the north gyro was compensated for gyro constant torque and MUIA or MUSA (best known).

CAT-8 also incorporated a set of programs extending the scope of the computer unit acceptance test programs. These additions made it easier for the operator to perform the tests, and at the same time provided increased test capability. In some cases the capability provided was not previously obtainable, using the old manual procedures. The integration test is an example of this, since it was not possible to check the integration function of the sigmator manually to the desired degree of accuracy. Tests of telemetry outputs and discrete outputs were expanded to allow measurement of pulse width and amplitude instead of just repetition rate. The Temporary Storage Validity test was expanded to include operations on every cell of temporary storage instead of only 20 locations previously checked. The original time accumulation test was computer controlled, but the program had to be hand loaded into temporary storage. This test is now in permanent storage and has been expanded to check MECO timing also.

3.5.3.5. CAT-9. - Several additional important changes were incorporated into this program. Three new align modes were added to calibrate accelerometer misalignment factors, d4,5 and 6. The order of calibration became as follows:

Mode 1	$(W_{CT} + W_{MUIA})$	$+V_v$
Mode 2	$(U_{CT} + U_{MUIA})$	$-V_v$
Mode 3	U_{CT}, U_{MUIA}	$-V_w$
Mode 4	V_{CT}	$+V_w$
Mode 5	V_{MUIA}	$+V_u$

Mode 6	W_{CT} , W_{MULA}	$-V_u$
Mode 7		D4
Mode 8		D5
Mode 9		D6

The Earth Spin Test was revised to compute platform drift as a result of not torquing the gyros. During the measurement phases the north gyro torquer was set to zero. A velocity filter, consisting of a 25 point averaging technique, was added to reduce the effects of velocity noise on the calibration. This program is essentially the one in use at the present time, except for minor changes.

3.5.3.6. UGT 33 R3. - This is the program currently in use. Changes from CAT-9 are: (1) expanded order code test allowing separation of arithmetic tests from temporary storage tests; (2) addition of D-sum test routine; (3) safeguards against garbled transmissions causing undesirable load operations during Remote Load and Read; (4) display output resolution limited to 0.3 fps to prevent excessive wear of steering pots during the velocity display routine; and (5) addition of certain MGS/vehicle interface tests. The development of the UGT program has achieved standardization of MGS test procedures and parameters at all sites prior to loading of the flight program. The present UGT has available several hundred unused locations in permanent memory, so that the potential exists for expansion as further tests are found necessary.

UGT has also established improved control over the computer program. Changes in parameters or procedures are coordinated between all contractors through NASA LeRC. In order to assure conformance to the UGT standard, the actual computer coding has been placed under drawing configuration control at Honeywell. A controlled tape is loaded into the computer at Kearfott at the time of manufacture and remains unchanged in memory until after shipment to GD/C.

3.5.3.7. Future Revisions of UGT 33. - Modifications in process currently are (1) revised scaling of D-values, and (2) revised unit level integration test, both due to new requirements for AC-16 and beyond.

3.5.4. Ground Test Programming Problems. - A few problem areas can be selected for special note from the experience in programming the computer for test of the MGS.

Limitations in availability of memory in the computer have always created problems in generation of the desired programs. Under the UGT scheme, the ground test functions have been separated to the greatest practical extent from the flight and immediate pre-flight functions, at least temporarily making sufficient memory available for the MGS ground test functions.

Severe problems have always been associated with the unique programming problems associated with optimizing memory access in the drum computer program. This problem reflects in programming costs as well as in difficulty in making required changes to the program.

Finally, mention can be made of the difficulties inherent in coordinating programming efforts of several contractors all concerned with the same computer test programs. Achievement of coordination in this regard was one of the prime reasons for undertaking of the UGT revision. The UGT effort and the separation of the UGT from the flight program appear to have been reasonably successful in achieving workable programming coordination.

3.5.5. The Improved Centaur IMG. - The improved system will use a different airborne computer and ground checkout of the IMG will be performed with a commercial computer, at least during the prototype phase. Design of programs for these computers will become for the most part, completely new designs as dictated by the particular computer groundrules and IMC specifications, although the basic calibration methods will remain the same. Computer program changes will be made to accommodate improved calibration procedures such as automatic MUSA computation, and changed system specifications such as a new technique for inputting ΔV 's and the precision time reference to the computer.

3.5.6. Conclusions. - Centaur experience in programming the spaceborne computer for MGS test indicates the following conclusions:

1. Programming change can be anticipated as long as performance improvements are a goal, as well as for changes in mission requirements.
2. Programming costs and effort can be minimized by provision for adequate computer memory and performance capability.

3. Provision should be made for a programming structure conducive to effective coordination between the government agency and computer, MGS, and vehicle contractors. This structure should assign responsibilities consistent with the inherent obligations and capabilities of the respective organizations. A method should exist for monitoring and controlling program changes.

Topic 3.6

Computer Packaging Design

3.6.1. Introduction. - The computer consists of two major subassemblies. The computer memory section which contains the general purpose computer, and the input-output unit, which contains the necessary circuitry to interface with the Centaur Inertial Measurement Unit and the vehicle flight control electronics. The computer memory and input-output unit are mounted as a single assembly on mounting rails. Mounting to the vehicle is through vibration isolators.

3.6.2. General Purpose Computer Section. - The general purpose computer section has a volume of 0.55 cubic foot and weighs approximately 38 pounds. The chassis is machined and fabricated from magnesium to combine high strength with lightweight. The computer memory section contains the memory drum assembly and 19 plug-in circuit card assemblies. The memory drum is described in detail in another section of this report. The plug-in circuit card assemblies are a combination of printed and hand-wired circuits. Each card contains circuitry associated with its particular function. There are nine large or double cards, 9-1/2 by 6 inches and 10 small or single cards 4 by 6 inches. Each double card has two 37-pin connectors, each single card has one 37-pin connector for input-output signals to the particular card. Each card is unique with no interchangeability or commonality between circuit card assemblies. The cards are divided into six specific categories: flip-flop cards, write amplifiers, read amplifiers, head select cards, emitter-follower network cards, and a clock generator card.

3.6.3. Input/Output Unit. - The Input/Output Unit occupies a volume of 0.28 cubic foot and weighs approximately 21 pounds. The chassis is machined and fabricated from magnesium to combine high strength with lightweight. The major components mounted on or within the input/output chassis are steering converter modules, torquing converter modules, error storage and converter select assemblies, 1.3 kc frequency standard, plug-in card assemblies, power supply, and power transformer. The plug-in circuit cards, power supply, and error storage and converter select units mount within an L-shaped chassis. The frequency standard, power transformer, and six converter modules consisting of three torquing and three steering converters mount on the chassis.

3.6.4. -1 to -3 Packaging Design Changes. - The original -1 computer general purpose section and input/output section were unpressurized units. Utilization of the first -1 computers in the humid environment at the ETR launch site revealed a corrosion problem. To eliminate this corrosion problem, the -3 computer packaging was redesigned to provide sealing for pressurization with an inert gas to an internal pressure of 2.5 psig. The existing packaging design, particularly the input-output unit, was a poor configuration for pressurization. The sealing configuration resulted in numerous problems in retaining pressurization. Due to the large number of subassemblies which mount into the input/output chassis and the number of sealing surfaces associated with the L-shaped chassis configuration, the input/output unit has eleven separate sealing surfaces. This pressurization design was selected at the time of the -3 redesign to limit the amount of repackaging associated with the pressurization requirement. Redesign today would be based on placing a shroud over the entire input/output assembly with a maximum of two sealing surfaces. Additionally, the original design -3 pressurization fill and relief valve configuration did not provide efficient purging of the units. Also, the valve locations were not optimum under end usage conditions. With the computer mounted on the vehicle, access to the fill valves was limited and required the removal of cables. Future designs should take into consideration fill and relief valve configuration and location. This is particularly important for use on the vehicle, where access space may be limited.

The original -1 computers were gold-plated. Thermal analysis and testing revealed that a more suitable surface finish for the radiation cooling requirements would be a white polyurethane base paint. In 1963-1964, all computers were painted with this white polyurethane paint.

The use of magnesium for chassis and covers has resulted in corrosion problems. Corrosion of the magnesium prior to, during, and after fabrication is a constant problem. The requirement for metal to metal mating surfaces on the computer covers to obtain RFI shielding presents the possibility of corrosion. The bare metal surfaces required to provide this RFI shielding are presently protected by a grease, Shell Alvania Composition No. 2.

Producibility problems during the manufacturing of the assemblies from magnesium has also been encountered, particularly where welding of the magnesium is required. Machining and preparing detailed parts for custom welding of the magnesium requires elaborate coordination between the welder and the machinist. This fabrication cannot be achieved properly if the units are processed through normal production processes. Stress, warpage, shrinkage, and resultant pressure leakage problems have been encountered due to welding of the magnesium. Conversion to aluminum has been accomplished on several covers. However, the basic chassis and primary cover plates for the Input/Output Unit and the memory are manufactured from magnesium.

Unit packaging design on future build should consider the use of aluminum to eliminate the corrosion and producibility problems associated with magnesium. The increased weight of aluminum, of course, is a critical tradeoff factor that must be considered for each individual application.

3.6.5. Specialized Packaging. - The computer contains a number of subassemblies which were specially packaged for this application, that is, assemblies which are special build utilizing non-standard parts to accomplish reduced weight and volume. These subassemblies are the torquing and steering converters in the Input/Output unit. These converters are an electromechanical assembly requiring numerous gears, two brush encoders, a motor generator and a potentiometer. The packaging is extremely dense to conserve volume. Producibility and maintainability problems have been continually encountered with the steering and torquing converters.

Special packaging and build should be avoided wherever possible to eliminate producibility and maintainability problems. Where possible, standard packaging arrangements as available in assembled units from a vendor should be utilized. Attention should be given to all packaging arrangements to insure that a high degree of producibility and maintainability can be accomplished during the fabrication and repair. If this is assured, improved reliability will result.

SECTION 4

ACTIVATION AND VEHICLE INTERFACE

Topic 4.1

Introduction

The interface of the IGS with the other subsystems of the Atlas-Centaur vehicle is discussed in the following topics. The various interface considerations (electrical, mechanical, thermal, etc.) help define the design constraints for the IGS. In this context the IGS may be considered as a "black box" with a specific input and environment, and a required output, consistent with the total Atlas-Centaur mission requirement.

Topic 4.2

IGS/IMG - Autopilot Interface

4.2.1. Present IGS - Autopilot Interface. - The present IGS-Autopilot interface signals are as follows:

1. IGS-Atlas
 - a. Booster Steering Augmentation
 - b. BECO Discretes
 - c. Sustainer Steering (pitch and yaw)
 - d. SECO Backup Discrete
2. IGS-Centaur
 - a. Steering (pitch and yaw)
 - b. MECO Discrete
 - c. VECO Discrete
 - d. MES Discrete
 - e. MECO Discrete

The above signals are explained in the following typical signal sequence.

At liftoff, the Atlas autopilot utilizes programmed pitch and roll sequences. These sequences take into account nominal wind conditions for the specific season of the year. To provide vehicle flexibility in launching over a range of wind conditions, delta steering assists are provided in the pitch and yaw axes by the IGS. The steering pots in the input-output D/A converter modules are set to the desired delta values at intervals during the boost period of flight. These delta values provide augmentation to Booster Steering.

The Atlas vehicle booster engine continues to burn until a preset acceleration level is detected by the IGS, at which point a discrete called Booster Engine Cutoff (BECO) is generated by the IGS. This discrete is used by the Atlas autopilot to start a sequence, which includes shutting down the two (outboard) booster engines and separating them from the Atlas vehicle.

After booster separation (sustainer still burning) IGS Steering is admitted by the autopilot. The steering signals, in inertial coordinates, are calculated as a function of velocity to be gained and are outputted as attitude steering commands. They are transformed to pitch and yaw vehicle coordinates via the IMU resolver chain.

The Atlas sustainer engine burns until fuel depletion, at which time the autopilot issues a Sustainer Engine Cutoff (SECO) discrete. This discrete starts the sequence which provides Atlas/Centaur separation. Should the primary SECO not be issued by the autopilot the IGS issues a backup SECO discrete upon sensing a preset negative acceleration level.

The Centaur autopilot programmer, utilizing the SECO discrete, commands the start of the Centaur main engine after which IGS Steering is admitted by the autopilot. The steering is as described above.

Upon determination by the IGS that the required velocity vector has been attained, the IGS issues a Main Engine Cutoff (MECO) discrete to the autopilot.

If an additional main engine firing is to take place, the autopilot starts vernier engines to settle out the Centaur fuel. After a nominal on-time, the IGS issues a Vernier Engine Cutoff (VECO) discrete. Small ullage engines keep the fuel settled during the remainder of the coast period at which time the vernier engines again fire to assure fuel stability.

At the end of the coast period, the IGS issues a Main Engine Start (MES) discrete. After engine start, IGS Steering is again admitted by the autopilot.

Upon the attainment of the required velocity vector, the MECO discrete is again issued by the IGS.

The autopilot commands the main engine off and the separation of the spacecraft from the Centaur vehicle. The IGS then changes the Steering vector to the autopilot. The Centaur vehicle is turned around and excess propellants are released through the engines by the autopilot sequencer.

4.2.2. Major Developments in the IGS-Autopilot Interface. - The number of discrete lines has changed during the course of the Centaur Program (reference Topic 3.3). These lines, however, are under the control of the IGS Computer program, thereby providing a great deal of flexibility in the issuing of discrettes. The discrettes used for any particular flight are a function of that flight.

The steering interface has changed as follows: Prior to flight AC-8 (AC-7 was fired after AC-8), the inertial coordinate steering lines went to the Centaur autopilot. The autopilot was able to select either the IGS steering or nominal Centaur programmer signals. The signals selected

were then routed back to the IGS resolver chain for transformation to vehicle coordinates. The programmed steering signals were used for flights AC-2 and AC-3 and during the sustainer phase of flight as well as booster phase for flights AC-4 and AC-5.

The Booster Steering Augmentation inputs were added for flight AC-9. This function is programmable by the IGS Computer and therefore has wide flexibility. The result of this change has been to provide the ETR launch team with much greater flexibility with regard to upper atmosphere wind conditions.

The expansion of Atlas/Centaur mission applications from Surveyor to ATS, OAO, etc., has imposed stricter requirements on the MGS. ATS mission requirements require tighter accuracy in the MGS/resolver chain - autopilot interface.

The MGS design requirement for resolver chain accuracy has been two degrees. The ATS mission requires that the resolver chain output be accurate to 0.6 degree. A Honeywell design study, performed in the Fall of 1967, indicates that the present MGS hardware can meet this additional requirement if systematic resolver chain errors are compensated for in the flight equations. Flight platforms will be tested to measure these errors and insure their capability for meeting the tightened resolver chain accuracy requirement.

4.2.3 IMG - Autopilot Interface. - The additional functions required of the IMG, in conjunction with the Digital Computer Unit (DCU), are three-axis steering signals and vehicle rates. The vehicle steering interface will be between the DCU and the autopilot. The most significant improvement is that a full, three-axis steering capability will be available, from lift-off, with the IMG.

The steering ability of the IMG will include vehicle rate measurement as well as the three-axis transformation of inertial coordinates into vehicle coordinates. Vehicle rate measurement has been accomplished thus far by a gyro unit in the autopilot. The IMG will measure vehicle rates by differentiating the dc signals, representing roll, pitch, and yaw at the end of the resolver chain.

The dc steering outputs from the chain are themselves a change from the MGS 400 Hz steering concept. The signals from the resolver are demodulated and filtered before going to A/D converters in the DCU.

In the DCU, three steering signals and three rate signals will be inputs for the vehicle dynamic control equations. The vehicle control interface between the DCU and autopilot for advanced Centaur has not been completely defined. However, it is conceivable that the DCU can provide signals suitable for direct engine gimbal control or vernier engine control.

4.2.4. Problem Areas. - The IGS/Autopilot steering interface has been straightforward and not presented many problems. However, in recent years there have been two unresolved interface areas. They are:

1. A low beat frequency is present on the IGS resolver chain outputs throughout the Centaur mission. This problem is caused by coupling between the 400 Hz resolver chain excitation and the precision 7200 Hz, used in the stabilization loops (reference Topic 2.4). The magnitude of the problem is greater during the Atlas boost phase, until SECO, because the 400 Hz steering excitation comes from the Atlas inverter. The Atlas inverter is not a precision inverter, thus creating greater frequency variations. After SECO, the 400 Hz steering excitation comes from a precision 400 Hz Centaur inverter, thus reducing the magnitude of the beat frequency. There is no easy solution to this problem as the autopilot incorporates a demodulator which must use the steering chain excitation, regardless of source, as its reference. A possible solution to the problem would be to excite all affected functions with precision 400 Hz IGS excitation. This solution, however, would require IGS changes, as well as a more complex interface with regard to switching requirements. Thus far, the magnitude of this "beat" has been low enough on flight hardware to avoid any real vehicle control problems.
2. Resolver Chain Null Voltage. The specification limit for the composite resolver chain null is 150 mv rms. The autopilot input amplifier worst case analysis shows this amplifier can saturate below 150 mv. When the autopilot input amplifier saturates, the overall gain of the autopilot loop is reduced, resulting in sluggish performance. Normally, the problem is not acute because the average platform null voltage is less than 100 mv. Resolver chain phase shift also manifests itself as an overall gain reduction, due to the demodulation process used by the autopilot. The gain reduction is $(1 - \cosine)$ of the phase

angle between the steering chain output and the demodulator reference. The solution to these problems is to develop more compatible interface specification requirements between the IGS and the autopilot, trading off the error sources on both sides of the interface. On future programs, this should be done before the hardware designs are "frozen".

Topic 4.3

Primary Power Interface

4.3.1. Description of Present Interfaces. - The IGS receives primary power from the Centaur Vehicle 400 Hz Inverter and the 28 VDC Vehicle Battery. Power is routed from these sources, via the autopilot, to the MGS. The power characteristics are as follows:

1. Alternating current - three-phase (A, B, and C) 400 Hz, 115 volts rms line-to-neutral.
 - a. The Phase A, B, and C voltages are 115 volts ± 1.5 percent with a 12-hour stability of ± 1.0 percent within the 115 volts ± 1.5 percent band.
 - b. The frequency of the alternating current supply is 400 Hz ± 1 percent.
 - c. Phase accuracy and balance, 120 degrees ± 2 degrees between any two phases.
 - d. 100-millisecond regulation response time, provided that the voltage variation from the nominal 115-volt values does not exceed ± 15 volts rms.
 - e. Transients, 100 microseconds duration, plus and minus 20 volts, one per second rate.
 - f. Maximum total harmonic distortion 5 percent.
2. Direct Current - 25 to 30 volts.
 - a. Transients: 200-microsecond maximum duration, +10, -5 volts on any dc level between and including 25 to 30 volts, 1 per second maximum occurrence rate.
 - b. Ripple: 1.5 volts peak-to-peak, with 2400 Hz frequency predominating.

In addition to the prime power, the steering command excitation is supplied by the autopilot to the IGS. Original sources are the Atlas Inverter, during Boost and Sustainer flight phases, and the Centaur Inverter thereafter. Characteristics of the steering potentiometer and demodulator excitations are alternating current at 115 volts ± 1.75 percent, 400 Hz ± 6 Hz, single phase.

4.3.2. Original Power Interface. - The interface specifications prior to the current Phase II PIP (ADD-6 procurement) program were not as well defined. That is, no transient specifications were considered. The primary power specifications were:

1. Alternating Current - three-phase, 400 Hz, 115 volts rms line-to-neutral.
 - a. The three-phase voltages will be 115 volts ± 1.5 percent (combines repeatability, stability and accuracy).
 - b. The frequency of the alternating current supply will be 400 Hz ± 6 Hz.
2. Direct Current - 25-30 volts dc.

The additional power interface specifications for steering potentiometer and demodulator excitation were-- alternating current at 115 volts ± 1.75 percent, 400 Hz ± 6 Hz, single phase.

4.3.3. Power Interface Problems. - Original power requirements for the 400 Hz prime power did not specify a separate stability requirement either for voltage or frequency. As error models for the inertial sensors and system developed, it became evident that both gyro frequency and voltage error sources, if not adequately controlled, could produce large errors in the overall system accuracy. Revised voltage and frequency stability requirements were recommended by Honeywell based upon the following conditions:

1. System calibration without verification (airborne inverter requirement) ≈ 12 -hour stability.
2. Allocated gyro errors, based upon system calibration.

After reviewing the gyro error contributions, the total allotted error for gyro spin motor excitation instability during calibration was allotted as ± 0.02 deg/hr (3-sigma). This error source allocation would require a voltage stability requirement of ± 0.75 percent. The requirement was determined by using the nominal gyro sensitivity to Δ spin motor excitation (0.1 deg/hr/volt) and a nominal spin motor line to neutral excitation of 26 volts.

In addition to voltage stability, frequency stability was considered. Since the wheel is synchronous at the operating frequency applied, any deviations in this frequency will be reflected as a change in H_W . It is

thus seen that during the free drift calibration mode, platform drift (W_p) that results from internal gyro torques are a direct function of frequency. For the Centaur gyros, this relationship results in a frequency sensitivity of 4 deg/hr ($\% \Delta f$) where 4 deg/hr represents specification maximum drift rate in a 1 "g" test environment. The system error budget allocation to gyro error due to Δ spin motor frequency is ± 0.02 deg/hr or a 0.04 deg/hr 6-sigma band. To accomplish this, a frequency stability of ± 1 percent or better is required. In 1964, the MGS specifications were changed to incorporate both a voltage and frequency stability requirement. To meet the MGS voltage and frequency requirement as well as other vehicle requirements, the previously used rotary inverter was replaced with a solid-state inverter.

A serious problem developed with the original design of the new inverter. Intermittent 400 Hz prime power drop-outs with durations up to 200 milliseconds were observed during MGS checkout on the vehicle. Prime power loss of this time duration could not be tolerated by the MGS without computer program jumping or unacceptable IMU performance degradation. The source of this intermittent power outage was ultimately isolated to an overload protection device within the inverter. The cause, however, was not due to inverter overloading, but susceptibility of the control device to noise. A minor redesign eliminated this problem. The present vehicle "high-reliability" inverter avoided this problem prior to its qualification for flight use.

For a discussion of power control and power interlock interfaces of the MGS, refer to Topic 6.13.

4.3.4. Improved IMG Power Interface. - The IMG primary power interface will consist of 27.5 volts dc ± 2.5 volts dc only. The regulation of this voltage will maintain the input within the specified limits except for the following transient conditions:

Duration:	100 microseconds maximum.
Magnitude:	± 50 volts maximum.
Occurrence Rate:	1 per second maximum.

Topic 4.4

Telemetry Interface

4.4.1. Summary. - The guidance instrumentation in the early -1 and -3 phases of the Centaur Program was inadequate for an accurate analysis of IGS system flight and sled test performance. There were two limitations: (1) Signal Conditioner corner frequencies, and (2) the bandwidth of the telemetry, which was limited by the use of commutated instead of continuous monitoring.

4.4.2. Discussion. - During the earlier R&D flights, it was discovered that an accurate analysis of the IGS system could not be made due to the instrumentation bandwidth being so low (3 Hz). The "original" Signal Conditioner design had low frequency filters on all of the analog channels. Coupled with this, the signals were commutated at a sample rate of 40 samples per second or less. This problem was recognized during sled testing and also in the earlier flights.

A couple of examples will be mentioned to give a better understanding of the problem. The platform gimbal control amplifiers (four total) were conditioned and commutated to pass 0-3 Hz only. The frequencies of interest had a bandwidth of from 0 to 80 Hz since the platform shock mount resonance frequency was within a range from 38 to 66 Hz. It was believed that the effect of this energy on the stabilization loops must be evaluated.

The three accelerometer dc amplifier signals had a corner frequency of 3.7 Hz. Much higher bandwidth was desired. Extending the bandwidth frequency to pass 300-400 Hz (or at least 160 Hz, since the playback bandwidth could be opened) would permit a gross determination of accelerometer pendulum motion. It would be necessary, however, to have an understanding of the rate network characteristics and their correlation with input excitation (as determined from vibration measurement and stabilization loop measurement traces). The higher frequency response would also allow a more precise determination of the proper operation of the pulse polarity logic than was presently available with a 3 Hz Signal Conditioner filter.

Before the third Centaur flight, Honeywell proposed a filter modification to three sets of signals: (1) gimbal servo signals, (2) accelerometer

dc amplifiers, and (3) steering inputs and outputs. This proposal was rejected. Later, the need for monitoring additional signals arose and this brought about the new design of the Auxiliary Signal Conditioner and a modification of the "original" Signal Conditioner. This was an ideal time to modify the filters on the Primary Signal Conditioner (modified from "original") and also design the new Auxiliary Signal Conditioner with fairly wideband channels (specifically for the accelerometer 14.4 kHz demodulator signals). This pair of signal conditioners was flown on the remaining R&D vehicles. Some of the telemetry assignments were changed to continuous TM channels and others were changed to different commutation rates.

Today, the Centaur vehicle is operational. With it is the final-design, operational signal conditioner. The corner frequencies have returned to approximately their original points. There was no need for the wider bandwidths on operational flights. The telemetry assignments have also returned to commutated TM allocation.

4.4.3. Conclusion. - If it is desirable in the R&D phase of an inertial guidance system to accurately monitor specific signals for detailed analysis of the system's performance, then the frequency range under dynamic conditions should be considered before designing the signal conditioner filters. The bandwidth of the input device (to the telemetry package) dictates the accuracy to which the signal can be transmitted, with respect to the commutation rate. Therefore, a transition from one signal conditioner to another or some other way to switch filter frequencies would offer a more flexible approach for the R&D flights.

Topic 4.5

Electromagnetic Compatibility

4.5.1. Present Centaur MGS. - In 1963, Honeywell proposed that a series of Radio Frequency Interference (RFI) tests be completed to evaluate the performance of the Centaur MGS. These tests were not performed at that time, but in 1964, RFI tests were performed as a part of the MGS design proof tests. These tests indicated that the MGS was susceptible to low level audio signals of approximately 7 kHz and 21 kHz in all power lines with the exception of phase A. High susceptibility was also apparent throughout the entire range of the audio conducted test in the 400 Hz neutral. Further, the MGS was susceptible to high power radiation in the telemetry band of frequencies.

During 1965, electromagnetic compatibility (EMC) tests were performed on the Phase I PIP system which contained GG177 accelerometers. These tests showed that the MGS with the GG177 accelerometers was susceptible at generally the same frequencies and thresholds as the GG116 accelerometer configured MGS tested in 1964. Transients on the power lines did not affect MGS performance or accuracy. This conclusion was based upon the condition that the transient characteristics were within the EMC test limits. The following conclusions on AF susceptibility resulted from the 1965 EMC tests:

1. The Centaur MGS was susceptible to audio frequencies on phases A, B, and C of the 400 Hz power lines. The Platform stabilization loops were susceptible at 7.2 kHz at a threshold of 1.0 vrms. Gimbal oscillations of 10 arc sec p-p occurred when 2.6 to 3.0 vrms were injected on these 400 Hz lines at 7.2 kHz or the odd harmonics of the 7.2 kHz signal at 21.6 kHz or 36 kHz.
2. The Missile Guidance Set was also susceptible to 7.2 kHz and the third (21.6 kHz) and fifth (36 kHz) harmonics on the 400 Hz neutral power line. Minor susceptibility was noted at 55 mv at 22 kHz and 57 mv at 37 kHz. Major susceptibility (GSI) occurred when the injected signal was increased to 0.3 vrms at 7.2 kHz.

3. The +28 VDC power line proved to be the most susceptible of the MGS power lines. Special tests performed in support of the AC-8 launch indicated MGS susceptibility to 2.4 kHz and 4.8 kHz. The Platform stabilization loops were also susceptible to audio frequencies on the +28 VDC power line, that is, at 7.2 kHz and 21.6 kHz and 36 kHz. The cause or mode of susceptibility to AF frequencies on the +28 VDC line was not readily apparent; the +28 VDC is not used in the Platform but it is used in the Platform Electronics. With 1.0 vrms, 7.2 kHz injected on the +28 VDC power line a Gimbal Spin Inhibit (GSI) was encountered.
4. Tests on the +28 VDC Return line indicated that the threshold of MGS susceptibility was much less (lower) on this line than on any other of the power lines. A GSI occurred at 0.5 vrms, 7.2 kHz with signal injection on the +28 VDC Return Line.
5. The Radio Noise Filter (RNF) in the Phase I PIP Coupler, provided little attenuation to the 7.2 kHz or the odd harmonics of the 7.2 kHz (21.6 kHz or 36 kHz). The new RNF in the Phase II PIP coupler, DDG8014H1, will provide attenuation to the harmonics of 7.2 kHz; the MGS susceptibility characteristics with the Phase II PIP device will be different.

The following conditions on RF susceptibility resulted from the 1965 EMC tests:

1. The MGS proved to be susceptible to RF radiated energy at frequencies between 210 mHz and 260 mHz. The threshold of susceptibility at 244 mHz proved to be as low as 0.5 to 1.0 watt, but the tests were completed with the RF energy radiated directly at the units of the MGS.
2. Tests with the Centaur Subsystem 4 Telepak indicated that the Missile Guidance Set is susceptible to the 240 mHz, FM/FM, RF energy. The V accelerometer loop of the MGS proved to be the most susceptible. During the EMC tests, the antenna was directed at the units of the Centaur MGS.

During the Phase II PIP effort (1965-66 period), modifications in the Coupler significantly improved the electromagnetic compatibility characteristics of the MGS. Because of these changes, further EMC tests were

initiated to evaluate the susceptibility problem areas noted during previous RFI or EMC tests. The following problem areas were investigated:

- Susceptibility - Audio Frequency, Power Line Conducted, 30 Hz to 150 kHz.
- Susceptibility - Transient, Power Line Conducted, Transient Repetition Rate = 1 PPS.
- Susceptibility - Radio Frequency (RF), High Power Radiated Tests using Telemetry (TLM) Band Frequencies 210 to 260 mHz.

A discussion of these EMC tests is given below.

AF Power Line Conducted Tests:

1. The Centaur MGS, with the Phase II PIP Coupler, was susceptible to audio frequencies injected into the 400 Hertz Phase B and C power lines. The susceptibility was designated major when frequencies of 7.2 kHz and harmonics of 7.2 kHz caused gimbal oscillations. Only minor susceptibility was noted when audio frequencies were injected into the Phase A, 115 volt rms, 400 Hz line.
2. The 400 Hz Power Line Neutral proved to be the most susceptible of the 400 Hz lines. Major susceptibility in the form of gimbal oscillations occurred when frequencies of 7.2 kHz, 300 mv rms, and 36 kHz, 100 mv rms were injected into the 400 Hz Power Line Neutral.
3. The guidance platform stabilization loops were susceptible to 7.2 kHz and its harmonics when audio frequencies were injected into the +28 VDC Power Line. A special Stab Loop investigation was completed during the EMC test period, and it was determined that the injected AF signal was being carried to the platform on more than one interface line. A large percentage of the injected signal was being carried on the gyro torquer lines into the gyro torquer and, hence, coupled into the gyro signal generator and stab loops. The stab signals (platform outputs) are affected by the injected signal, that is, the platform outputs have the same frequency as the injected signal. When the injected signal was 36 kHz, the platform preamp outputs were 36 kHz modulated with 7.2 kHz, and when the injected signal was 50.4 kHz, the preamp output was 50.4 kHz modulated with 7.2 kHz.

4. During the Stab Loop Susceptibility Investigation, it was noted that shorting or filtering MGS Signal Ground in the Coupler to the Coupler chassis significantly reduced stab loop susceptibility and stopped gimbal oscillations caused by injection of 2.0 V p-p of 21.6 kHz noise into the +28 VDC Power Line.
5. Stab loop susceptibility was checked with the Phase II PIP Coupler and the new Radio Noise Filter (RNF) using a frequency of 21.6 kHz, 2.0 Volts p-p and compared directly to a Phase I PIP device. At the test frequency, the susceptibility of the Phase II PIP configuration was less in terms of the magnitude of the gimbal oscillations.
6. The Phase II PIP configured MGS, programmed for the AC-9 flight, was tested for accelerometer scale factor and bias shifts when 2400 Hertz, 4800 Hertz, and 2400 Hertz Synchronous Noise was injected into the +28 VDC Line. Only minor accelerometer scale factor and bias shifts occurred when the magnitude of the injected signal was increased to 7.0 V p-p. No well defined threshold of susceptibility was noted.
7. The Phase II PIP configured MGS was tested with the Borg-Warner Controls Centaur Inverter. There were no large accelerometer scale factor or bias shifts noted when the Inverter noise was increased to 6.5 V p-p. No platform gimbal oscillations were noted when the Inverter noise was held at 6.5 V p-p on the 28V high line.

Transient Power Line Conducted Tests:

1. No indications of major MGS susceptibility were noted during the Phase II PIP Transient Tests.
2. No major susceptibility was noted when ± 20 volt transients of 325 microseconds were injected into the +28 VDC power line. Plus and minus 20 volt transients of 325 microsecond duration were also injected into the Phase A, B, and C power lines to the MGS with no indications of major susceptibility. Transients on the 400 Hertz Power Line Neutral were limited to ± 10 volts due to the difficulty of developing a voltage potential between the neutral and the Forward Ground Point (FGP).

RF High Power Radiated Tests:

1. The Centaur Phase II PIP MGS was susceptible to RF radiated energy at frequencies between 210 mHz and 260 mHz. The MGS signals that showed indications of susceptibility were the +22.2 VDC, the Gyro, the Gyro Torquing Signals, and the Accelerometer Demodulator monitor signals at the output of the Primary and Auxiliary Signal Conditioners. The threshold of susceptibility was determined to be 1.0 watt. The susceptibility indications are attributed to the Signal Conditioning units. The RF radiation did not affect MGS performance or accuracy.
2. Tests with the Centaur Subsystem (SS) 4 Telepak indicated the MGS was susceptible to the 240 mHz, FM/FM, RF energy. The energy radiated by the Telepak did not affect MGS performance or accuracy.

4.5.2. EMC for the IMG. - The general philosophy of interference/susceptibility control for the IMG, can be summarized as:

1. Provide a basic electrical design that has the best practical EMC noise/immunity characteristics consistent with the total equipment requirements.
2. Suitably reduce the transfer of electro-magnetic energy to and/or from the basic electrical circuits to be commensurate with the required EMC specification limits. This requires reduction of the undesired electromagnetic energy, by elimination, inclusion and/or exclusion, through the use of shielding and suppression components. The reduction will be accomplished at:
 - a. The equipment interface.
 - b. The separate areas of interference/susceptible (source/receiver) circuitry.

4.5.2.1. General Approach. - In order to provide (1) above, it was imperative, wherever practical, to avoid or minimize high current, or high voltage switching circuitry, and high impedance or high gain amplifier circuitry anywhere in the hardware. When tradeoffs required any of these EMC compromises to be utilized, care was taken to suitably isolate them from the system perimeter (radiated/conducted interface) by implementation of (2) above.

The minimization of a total equipment design to meet the EMC requirements is greatly dependent on where the reduction hardware of (2) above is applied. In general, it is best to enclose or suppress an interference source within as small a volume as practicable. Conversely, it is best to exclude a cause of susceptibility from as large a volume as practicable. Another general statement is that it is more economical to provide a singular reduction criteria applicable to a hardware grouping than to provide the equivalent for several or many individual portions thereof.

The above statements influenced the IMG EMC design in two basic ways:

1. Major portions of the IMG circuitry operate on (or from) digital, pulse and/or square wave signals. These many similar interference sources can most economically be enclosed (shielded to meet radiated limits) at the system perimeter. Thereby, the shielding is applied once at the system perimeter and suppression applied only on the applicable interface lines. (Outstanding interference sources, or susceptible circuitry, may have additional control measure applied directly at the problem circuitry.)
2. The inability to suitably reduce coupling (by twisting, shielding or spatial separation) between the many gimbal slip-ring circuits that are required by the IMG is a serious drawback to allowing the radiated or conducted energy of susceptibility signals to penetrate the system perimeter. When this is considered along with the inherent advantages (bilateral nature) of the interference reduction criteria of (1) above, the susceptibility signal reduction is (with few exceptions) most economically accomplished at the system perimeter.

4.5.2.2. EMC Design Aspects. - The aspects of EMC control design (shielding and suppression) are discussed in terms of the specific test methods and associated amplitude/frequency spectrum limits imposed on the IMG design. The discussion is divided into the three categories, i. e., Radiated Interface, Conducted Power Interface and Conducted Signal Interface. Figures 4.5-1, 2, 3, illustrate the applicable tests imposed on these interfaces.

4.5.2.3. Radiated Interface. - The total radiated interface (interference/susceptibility control problem) requires control of radiated energy transfer from the IMG below applicable radiated interference limits of the IMG

0168-194A

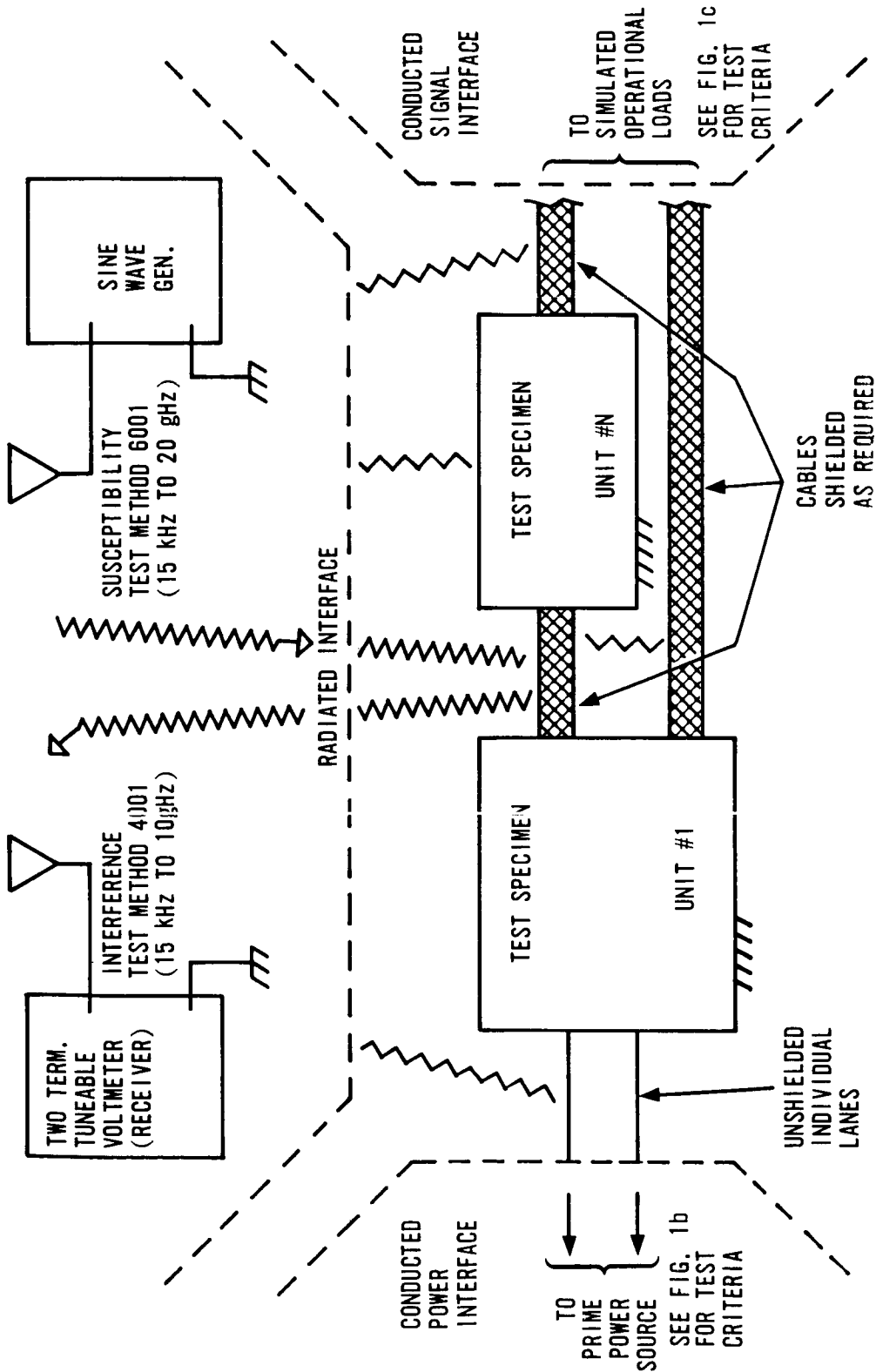


FIGURE 4.5-1. CS-EMC-1 TEST METHODS AS APPLIED TO THE SYSTEM INTERFACE

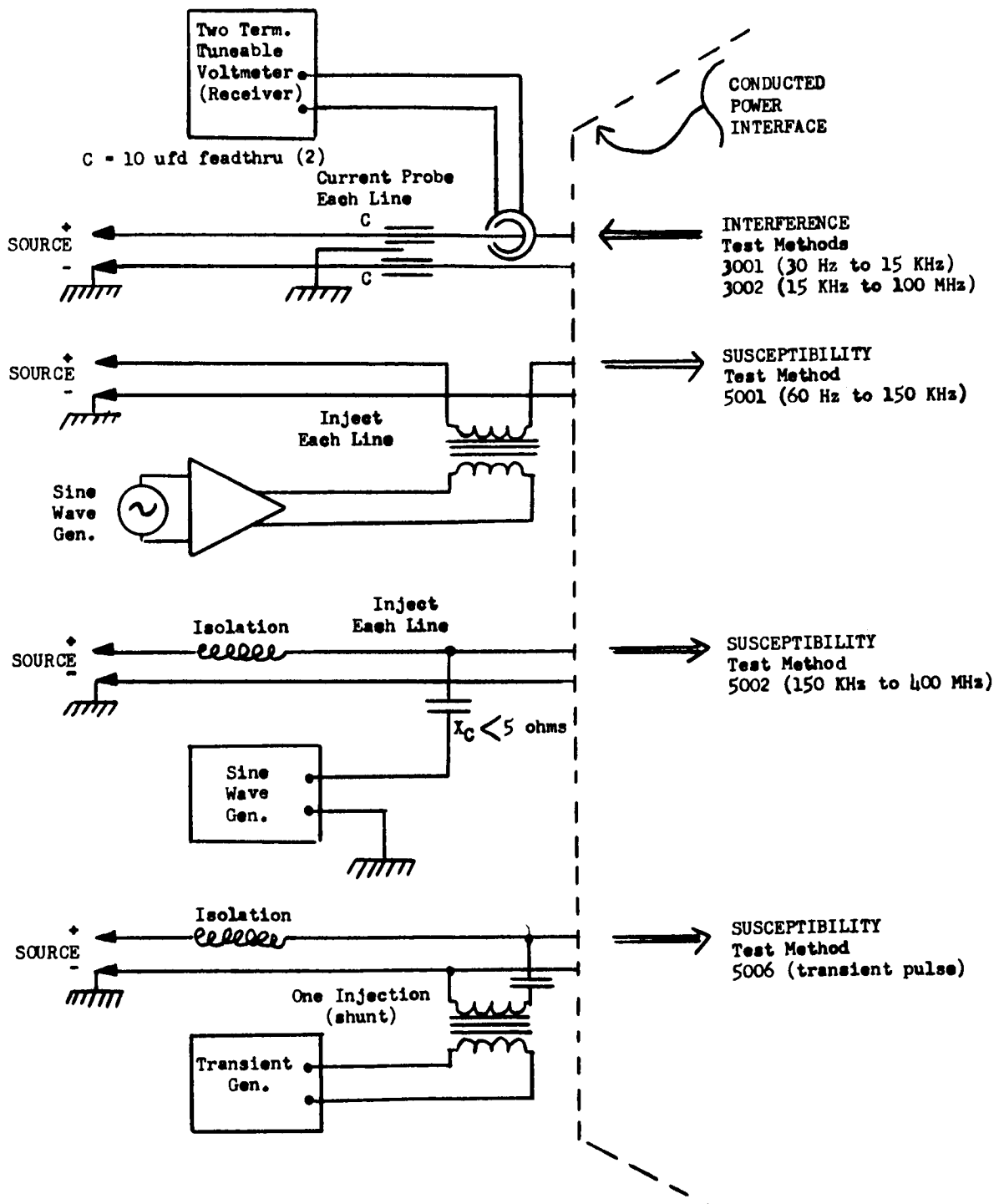


FIGURE 4.5-2. CONDUCTED POWER INTERFACE

0168-174A

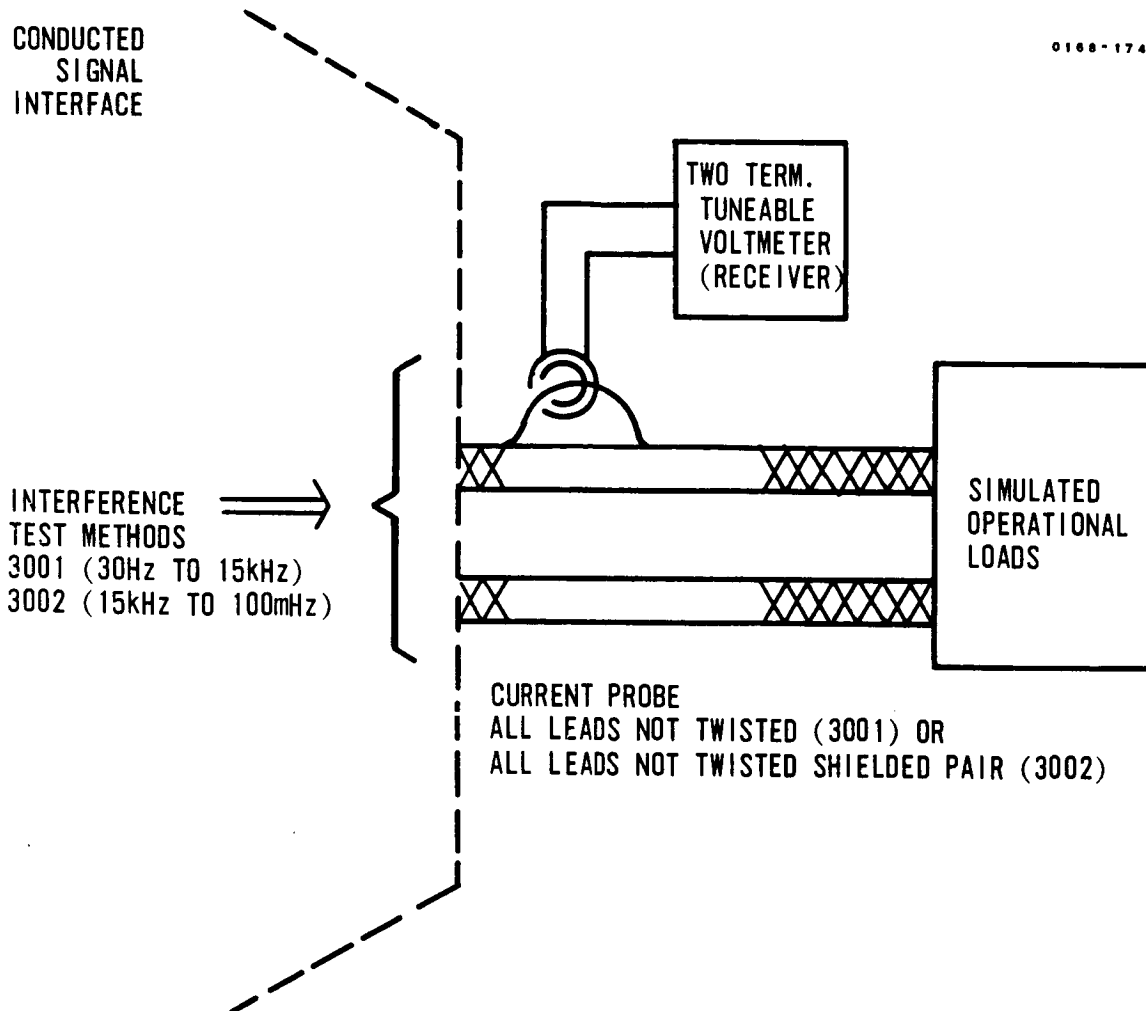


FIGURE 4. 5-3. CONDUCTED SIGNAL INTERFACE

EMC specification and to the IMG in order to protect against radiated susceptibility levels of the IMG EMC specification.

In that the basic IMG electrical circuit design is assumed to emit and be susceptible to the radiated levels up to the EMC specification, the radiated interface control problem involves:

1. The shielded integrity of unit enclosure.
2. The shielded integrity of exposed cabling.
3. The suppression of applicable conducted energy on inter-unit and interface lines that are not (or cannot be) sufficiently shielded in order to provide the necessary control of radiation through shielded integrity.

The shielded integrity of unit enclosures is the only practical means for reducing radiation to or from the many conductors, terminals, modules, etc. within the units. The necessary considerations are:

1. Enclosure "skin",
2. Joints, seams, covers, or access plates,
3. Uncovered openings.

The enclosure "skin" material/thickness has been selected to provide a shielded effectiveness goal of 60 db at 150 kHz. The aluminum parts of the enclosure "skin" are therefore a nominal minimum of 60 mils thickness. Magnesium parts are a minimum of 125 mils thick. Joints or seams in the enclosures are reduced to a minimum by castings and drawn on one-piece covers. The covers and access plates provide a nominal overlap of approximately 0.6 inch.

An uncovered opening (hole not covered by conductive shielding material) is present in the IRU "skin" due to optical access requirements. This opening size is 1.5 x 1.8 inches which is dictated by optical-mechanical geometry considerations. Such an opening does compromise the shielded integrity of the IMG. The applicable control methods were studied and rejected as tradeoffs with associated optical-mechanical problems.

The most workable tradeoff was to provide a waveguide tube "snout" which would have a cutoff frequency of 3.7 GHz as determined by the maximum cross-dimension of the tube. The attenuation below cutoff is essentially $\alpha \text{ (db)} = 32 \text{ l/d}$ where l = length of tube, and d = maximum cross-dimension, both in same units. (Actually, at half the cutoff frequency, the attenuation is 87 percent of maximum.) For 60 db attenuation, in the reject band, the length would have been 3.4 inches. The mechanical problem of mounting and clearances can readily be understood. The optical alignment problems would probably dictate a larger (or tapering) cross section of the "snout".

Except for prime power input lines, the exposed cabling outside IMG unit enclosures can be shielded to control radiated energy during spec compliance testing. This includes the cabling between IMG units and the cabling to interfacing systems. All shielding present in the compliance test configuration must be as specified in the operational installation.

Shielding will be provided in combination with suppression components to obtain the necessary control of radiated energy from these cables at minimum impact to the hardware design. The advantages of providing a suitable combination of maximum shielding and minimum suppression include lesser penalties in reliability, cost, weight, power and effect on circuit design.

Conductor shielding is normally provided by a braided sheath that is conductive, but non-ferrous and provides 90 to 95 percent area coverage. This can be provided on a single or grouped conductor basis or for an overall cable assembly. The conductive/non-ferrous properties provide good shielded effectiveness to electric fields (predominantly high impedance, high-frequency) but relatively little to magnetic fields (predominantly low-impedance, low-frequency). A single layer of this typical braided sheath will provide roughly 50 to 55 db of shielded effectiveness to electric fields (from 150 kHz to 100 MHz range) if properly terminated.

For interference control purposes, the external shield is necessarily terminated at both ends, shortly and directly to chassis or enclosure. Where this criteria presents compatibility problems with the enclosed signal(s) an additional, electrically independent shield is needed between the conductor of the incompatible signal and the interference shield. This internal shield is terminated by whatever method is determined necessary.

The special case of an overall cable shield can be used to great advantage. This means will be utilized to extend the shielded effectiveness from one IMG unit enclosure to another. This is of particular advantage as a replacement for many individual shields whose major purpose would be to provide compatibility with the external environment rather than to reduce crosstalk within the cable. Thus, one overall shield may replace many separate ones resulting in a reduction of weight, volume and wiring complexity. It may also eliminate the need for suppression of all or part of the extraneous waveform characteristics of a portion of the associated signals.

Another practical advantage of the overall cable shield is that special RF tight connector-shell termination hardware will be used and is available commercially. This termination hardware attaches to the connector back-shell and provides contact with the sheath around the entire circumference. Sheath termination is therefore shortly and directly to the enclosure via the connector shells at both ends of the cable. Proper usage of such hardware will provide a shielded effectiveness that could only be duplicated (on an individual conductor basis) by all coaxial connector pins or equivalent separate (BNC type) connectors. The lengths of unshielded conductor, as in the usual "pigtail" termination practices, are eliminated. The inherent shielded effectiveness of the braided sheath is thereby not compromised by the termination criteria.

The application of suppression components (generally, LC, RC, or C filters) to reduce undesired conducted energy had to be considered under the category of the radiated interface in that:

1. The radiated interference limits of the EMC specification extend to 10g Hz whereas the conducted interference limits extend only to 100 mHz. Therefore, the radiated interference limits are a governing factor on exposed cabling from 100 mHz to 100 Hz.
2. The exposed prime power input lines to the IMG are required to be unshielded per the specified test methods.
3. The radiated susceptibility limits of the EMC specification extend to 20g Hz whereas the conducted susceptibility limits extend only to 400 mHz. Therefore, the radiated susceptibility limits are a governing factor on interface (power) lines from 400 mHz to 20g Hz.

4. A suitable combination of suppression and shielding may provide the optimum hardware considerations for control of radiation to or from exposed cabling other than prime power lines.

In general, suppression to meet radiated requirements must reduce the transfer of energy which is referenced to the "ground plane" and hence to the enclosure of the Test Specimen. This presents two possibilities in the application of suppression components (filters) to control the radiation by reduction of undesired conducted noise. These are Line Filtering and Signal Filtering.

1. Line Filtering - This applies series impedance elements in the line and shunt elements from the line to enclosure. This method reduces the undesired conducted currents in that line beyond the point of application but may allow those currents to exist in the loop toward their origin. The characteristics of this type filtering apply well to the reduction of radiated energy throughout the RF spectrum of typical specifications. (Such radiated energy is invariably assumed referenced to the "ground plane".) This advantage, however, can only be gained with special attention to the choice of components and the installation design. In particular, feedthrough capacitors, and inductors with low distributed capacitance are necessary. The installation must be at the bulkhead which establishes the shielded effectiveness for direct radiation of energy from the item being controlled.

Indiscriminate application of line filtering can be detrimental due to the possibility of extraneous currents in the signal circuit caused by the additional reference to enclosure. The application to a pair of signal lines, balanced to enclosure reference, is ideal.

Where the return for a signal is the enclosure, line filtering can also accomplish signal filtering as below. Application of line filtering (balanced) on both a signal Hi and its return also accomplishes signal filtering.

2. Signal Filtering - This applies series impedance elements in the line and/or the associated return and applies shunt elements from the line to its return. This method reduces the undesired conducted currents in the signal loop beyond the point of application. The characteristics of this type filtering usually apply only to the bandpass of the signal or that bandpass over which

gain is present in the loop. This type of filtering is appropriate for reducing the generation of extraneous signal currents but its effect is severely limited outside that bandpass. In addition, the point of application is usually not critical, for the appropriate signal effect, and hence is not adapted to application of any specific filtering with respect to the enclosure.

4.5.2.4. Conducted Power Interface. - The conducted power interface (interference/susceptibility control problem) requires control of conducted energy transfer:

1. From the IMG-
 - a. Below the applicable conducted interference limits of the IMG EMC specification and,
 - b. In order to bring the radiation from these lines below the applicable radiated interference limits of the EMC specification. (It is mandatory that the prime power input lines be unshielded during compliance testing.)
2. To the IMG-
 - a. In order to protect against conducted (sine wave and transient) susceptibility levels of the EMC specification,
 - b. In order to protect against conducted susceptibility resulting from the pickup of radiated susceptibility levels of the EMC specification. (It is mandatory that the prime power input lines be unshielded.)

The conducted power interface control problem involves:

1. Suppression in the form of "line filtering" to control:
 - a. Current probed conducted interference levels.
 - b. RF conducted susceptibility levels.
 - c. The RF radiated interference levels.
 - d. The RF radiated susceptibility levels.
2. Suppression in the form of "signal filtering" to control:
 - a. AF conducted susceptibility levels.
 - b. Transient conducted susceptibility levels.

4.5.2.5. Conducted Signal Interface. - The EMC control aspects of the conducted signal interface have been handled by:

1. Twisting and shielding of all signals or groups of like signals and associated return.
2. Working out interface signal specifications that sufficiently cover noise characteristics of mutual concern to the interfacing systems.

Topic 4. 6

Structural Interface

4. 6. 1. Introduction. - A discussion of the Missile Guidance Set (MGS) structure interface with the Atlas/Centaur vehicle is presented herein. Consideration for shock and vibration at the interface level will be presented.

4. 6. 2. Description. - The Centaur MGS is located on top of the Centaur Vehicle in close proximity to the cryogenic fuel supply. A two tier equipment shelf on the Centaur Vehicle forward bulkhead is used to support the MGS. The guidance set installation arrangement is shown in Figures 1. 3-1 and 1. 3-2 of Topic 1. 3.

4. 6. 3. Shock and Vibration Exposure. - During certain stages of operation, the MGS is subjected to a high amplitude, short time duration shock pulse. In addition, the system must perform satisfactorily when exposed to simultaneous sinusoidal and random vibration inputs applied at the vehicle mounting interface (MGS-adapter mounting shelf). The vibration profile for both the random and sinusoidal component are as follows:

1. Combined random and sinusoidal input along any of three mutually orthogonal axes-
 - a. Sinusoidal: 5 to 11 Hz at 0.25 inch single amplitude
11 to 2000 Hz at 3g (peak).
 - b. Random Spectral Density as shown by Figure 4. 6-1.
2. The operational shock requirements are as follows-
 - a. 10g shock of undefined waveform.
 - b. 100g half sinusoidal waveform of 400 microseconds duration.

Operational in-flight shock results primarily from a shaped charge separation system. The Centaur vehicle uses a cryogenic fuel (LH2 and LO2). To minimize propellant boil-off during the Atlas boost phase, an external insulation panel system is employed. After the Centaur vehicle leaves the Earth's atmosphere, a shaped charge separation system is used to jettison the panels (refer to Figure 4. 6-2).

0168-190A

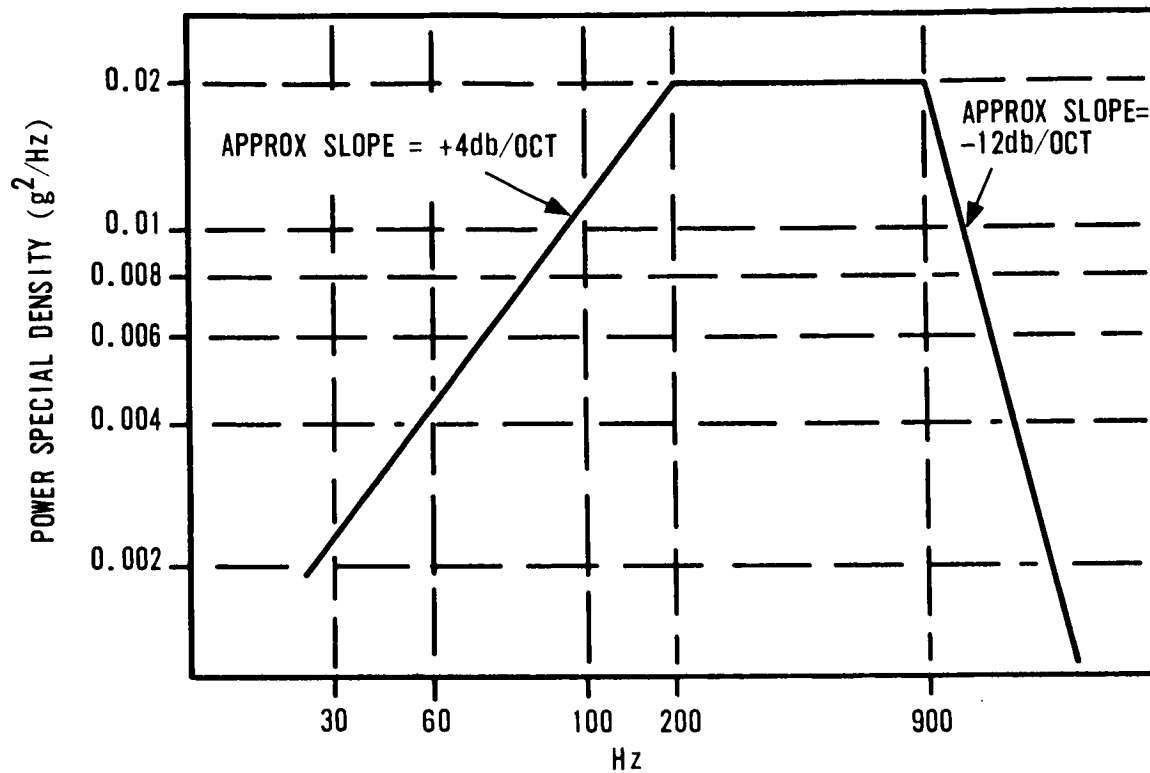


FIGURE 4.6-1. RANDOM NOISE POWER SPECTRAL DENSITY SPECIFICATION

0168-143A

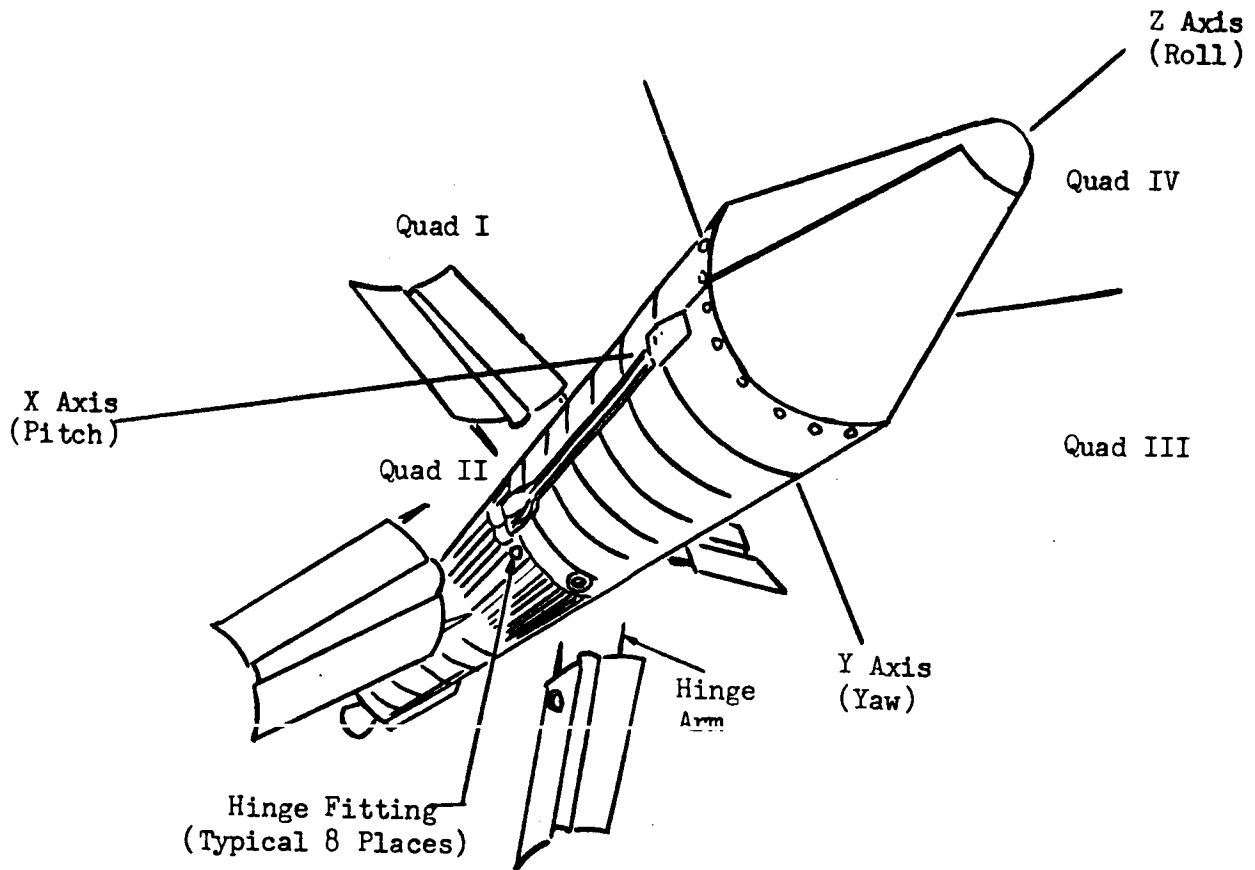


FIGURE 4.6-2. CENTAUR JETTISONABLE INSULATION SYSTEM

The shock spectra experienced by the equipment varies proportionally with increased distance from the charge separation system to the various equipment units. In the area of the MGS mounting high shock "g" levels are experienced in the frequency range of 700 to 1800 Hz. To provide shock isolation for the guidance equipment, some of the units making up the guidance set are shock mounted.

Typical isolator resonance for the type isolators used is below 100 Hz with high attenuation at the high "g" level shock frequencies mentioned. The MGS "Unit" level mounting configuration is as shown by Table 4.6-I.

TABLE 4.6-I
MGS UNIT TO VEHICLE MOUNTING

Unit	Type Mounting to Vehicle
Platform	Isolator
Pulse Rebalance Gyro Torquing and Power Supply	Isolator
Computer-Navigation	Isolator
Signal Conditioner	"Hard"
Platform Electronics	"Hard"

In addition to shock isolation, high frequency vibration attenuation is achieved through using isolators. Due to the nature of the unit physical characteristics (size, weight, structural damping), isolators were not deemed necessary for the Signal Conditioner and Platform Electronics Units. Problems were encountered in the Platform Electronics Unit during vibration testing of early -3 hardware. These problems were, however, eliminated by better cable tie down, better use of stress loops, and addition of stiffeners to the resolver output amplifier board (reference Topic 2.14). In addition problems associated with vibration were observed in the Coupler. These problems were eliminated by shock mounting the Coupler and redesigning the "hard" mount area (reference Topic 2.19). A brief discussion of vibration specification requirements versus vibration during flight is presented in Topic 6.15.

4.6.4. Summary. - The following interface considerations have had significant impact upon the Centaur MGS design:

1. The MGS is subjected to high "g" level shock during jettisoning of the Centaur insulation panels.

2. Shock isolators effectively attenuate the shock evidenced by the "soft" mounted units of the MGS.
3. The Signal Conditioner and Platform Electronics, due to size, weight and structural damping do not require shock isolators.

SECTION 5

CONTROL AND DISPLAY (SYSTEM AND COMPUTER GSE)

Topic 5.1

Introduction

At the onset of the Centaur program in mid-1959, funds were limited and an atmosphere of economic austerity prevailed. In addition, space programs were in their infancy and general design criteria for ground support equipment were not well established. Consequently, the requirements set forth for the Centaur GSE were of an extremely general nature. Specific technical requirements were left for Honeywell to define within funding limitations.

The general requirements set forth were that the GSE shall:

1. Support system level checkout and calibration of the guidance system in a laboratory test area, a hangar assembly area, and the launch control area.
2. Provide fault isolation to a major MGS assembly.
3. Be designed so that panels will be interchangeable among the sets in the three different test areas.
4. Be designed and produced employing a minimum cost approach.

By the end of 1959, these requirements had been expanded into detailed requirements, which Honeywell described in a technical specification issued during December 1959. This specification became the basis for the original GSE and maintenance equipment, which was subsequently designed and produced. This specification defined:

1. Broad test and calibration requirements.
2. Quantities of equipment.
3. Locations of all equipment.
4. Each subassembly of the GSE and its functional requirements.
5. Commercial test equipment requirements.
6. Construction and packaging requirements.
7. Power requirements.

8. All MGS-GSE interface signals with voltage amplitudes.
9. Monitoring requirements.
10. Customer-to-GSE interface.
11. Environment.
12. Reliability.

Prior to issuing the specification, close technical liaison was maintained between the customer and Honeywell, particularly in the areas of customer electrical interface, equipment deployment, and customer equipment installations where packaging configurations were important. This document represented mutual agreement as to the total support requirements, and was later reissued by GD/C under their control number 55-04099, as the contractual GSE requirements document.

In the following paragraphs, a description of the original GSE will be presented, followed by a discussion of subsequent modifications which made significant contributions to the evolution process. This will lead to the present day System GSE and the future IMG Test Set. Further, the Computer unit test equipment and the long-range optical azimuth alignment control equipment will be discussed.

A discussion will be given of significant technical problems experienced through the years, and solutions to those problems. Finally, looking back over the support equipment experiences from inception to date, the lessons learned from these experiences will be pointed out.

Topic 5.2

Systems GSE

5.2.1. Functional Requirements. - The functional requirements originally established for the GSE were, in general, to provide:

Control of MGS prime power and inertial component fast heat power.

Platform coarse alignment control.

MGS control switching and status indication.

Signal monitoring.

Spin motor power to the MGS gyros.

Buffer amplifiers in the transfer room for signals being monitored in the blockhouse.

Maintenance equipment capable of being used for system troubleshooting and fault isolation.

5.2.2. Original GSE Configurations. - In accordance with requirements established at the onset of the Centaur program, the items of Systems GSE listed below were designed and produced. By the fall of 1960, all items had been manufactured and put into operation.

5.2.2.1. Laboratory Rack Assembly. - The Laboratory Rack was to be used during test and calibration of the MGS in the laboratory area prior to installation in the missile, or integration with other subsystems.

The rack was a two-bay configuration, shown in Figure 5.2-1. Three Laboratory Rack assemblies were originally produced to be employed at (a) Honeywell lab, (b) Convair lab, (c) ETR lab. In addition to the rack assembly, each lab setup required a precision voltmeter (digital or differential) and a 4-channel chart recorder. At the Honeywell lab, capital equipment was employed for this purpose. At the other labs, Government-furnished equipment (GFE) was employed. Figure 5.2-2 is a flow diagram

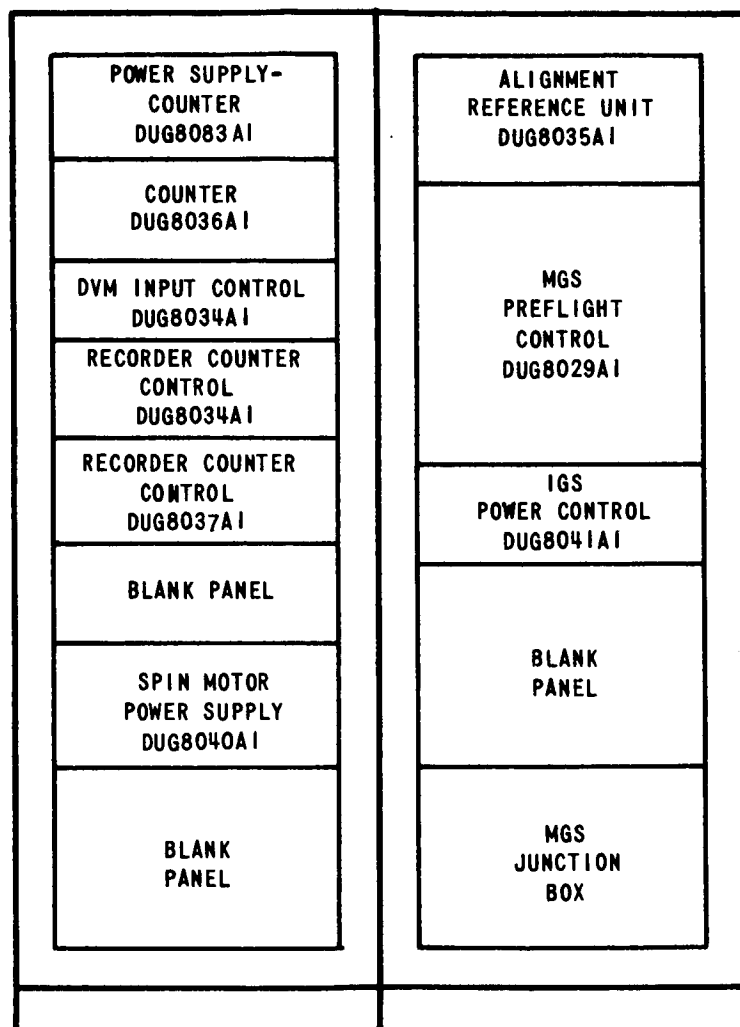


FIGURE 5.2-1. ORIGINAL CONFIGURATION OF LABORATORY RACK ASSEMBLY DUG8057A1

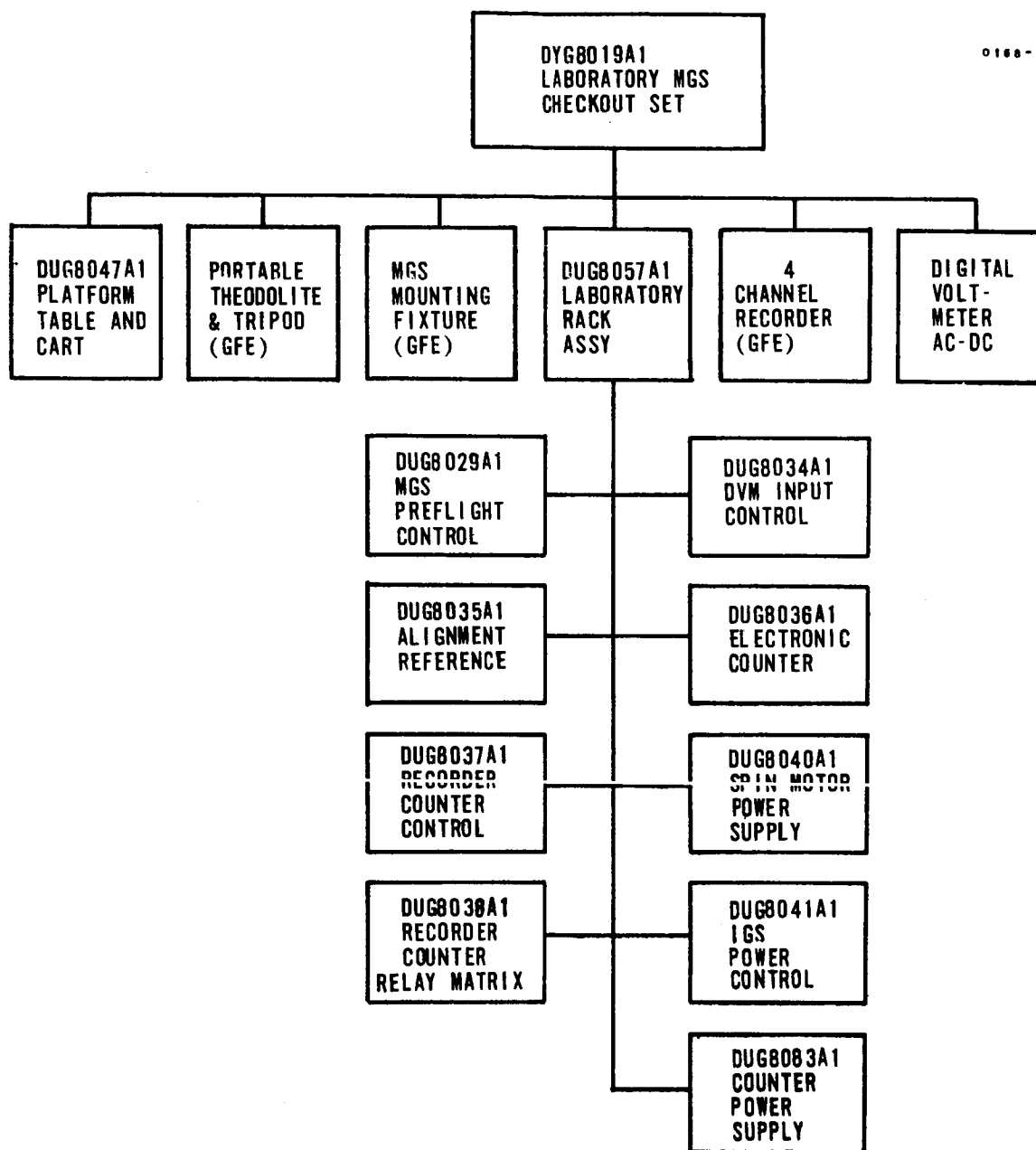


FIGURE 5.2-2. FLOW DIAGRAM OF COMPLETE LABORATORY CHECKOUT STATION

illustrating the laboratory rack with external instrumentation, plus other equipment necessary for complete laboratory check capability.

5.2.2.2. Trailer Rack Assembly. - The Trailer Rack assembly was to be used during test and calibration of the MGS after installation of the Centaur vehicle. This testing was to be accomplished in hangar assembly areas at San Diego, California, and at ETR. Two Trailer Rack assemblies were originally produced to support these two locations. The rack was a two-bay configuration, shown in Figure 5.2-3. The rack frame is shorter than normal and was specially defined by GD/C to be installed in their mobile trailer units.

In addition to the Trailer Rack Assembly, an external 4-channel chart recorder was required with each trailer checkout set. Figure 5.2-4 is a flow diagram illustrating the complete trailer checkout set.

5.2.2.3. Launch Site Checkout Equipment. - The Launch Site checkout equipment was designed for final MGS test and calibration in preparation for launch. The equipment consisted of a two-bay rack located in the blockhouse and a single-bay rack located in the transfer room adjacent to the launch pad. The Launch Site Equipment configuration is shown in Figure 5.2-5. Two sets of Launch Site Equipment were originally produced for use at: (a) the ETR and (b) the Sycamore Canyon, California, test sites. In addition, a 4-channel chart recorder was required with each Blockhouse Rack. The Figure 5.2-6 is a flow diagram illustrating the equipment necessary for complete launch site checkout capability.

5.2.2.4. Maintenance Equipment. - The maintenance equipment is a grouping of commercial test equipment and Honeywell fabricated fixtures, shown in the flow diagram of Figure 5.2-7. The equipment provided operating personnel with the capability of troubleshooting and isolating malfunctions to a major MGS assembly. Faulty assemblies would then be returned to the St. Petersburg plant for detailed troubleshooting and repair.

Three sets of maintenance equipment were originally produced. They were supplied to: (1) San Diego Guidance Lab, (2) Sycamore Canyon test site, and (3) ETR Lab.

5.2.3. GSE Evolution. -

5.2.3.1. Rearrangement of Launch GSE Control Functions. - As can be seen from Figure 5.2-5, the Alignment Reference Unit, the DVM Input

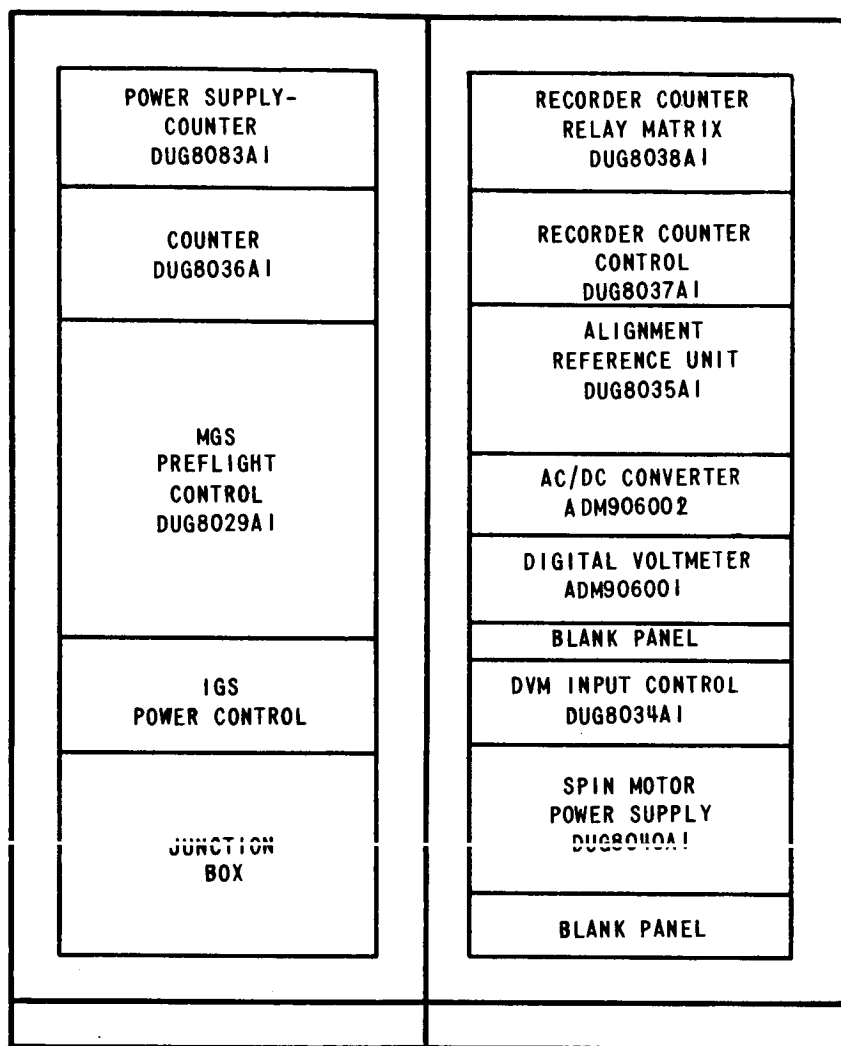


FIGURE 5.2-3. ORIGINAL CONFIGURATION OF TRAILER
RACK ASSEMBLY DUG8063A1

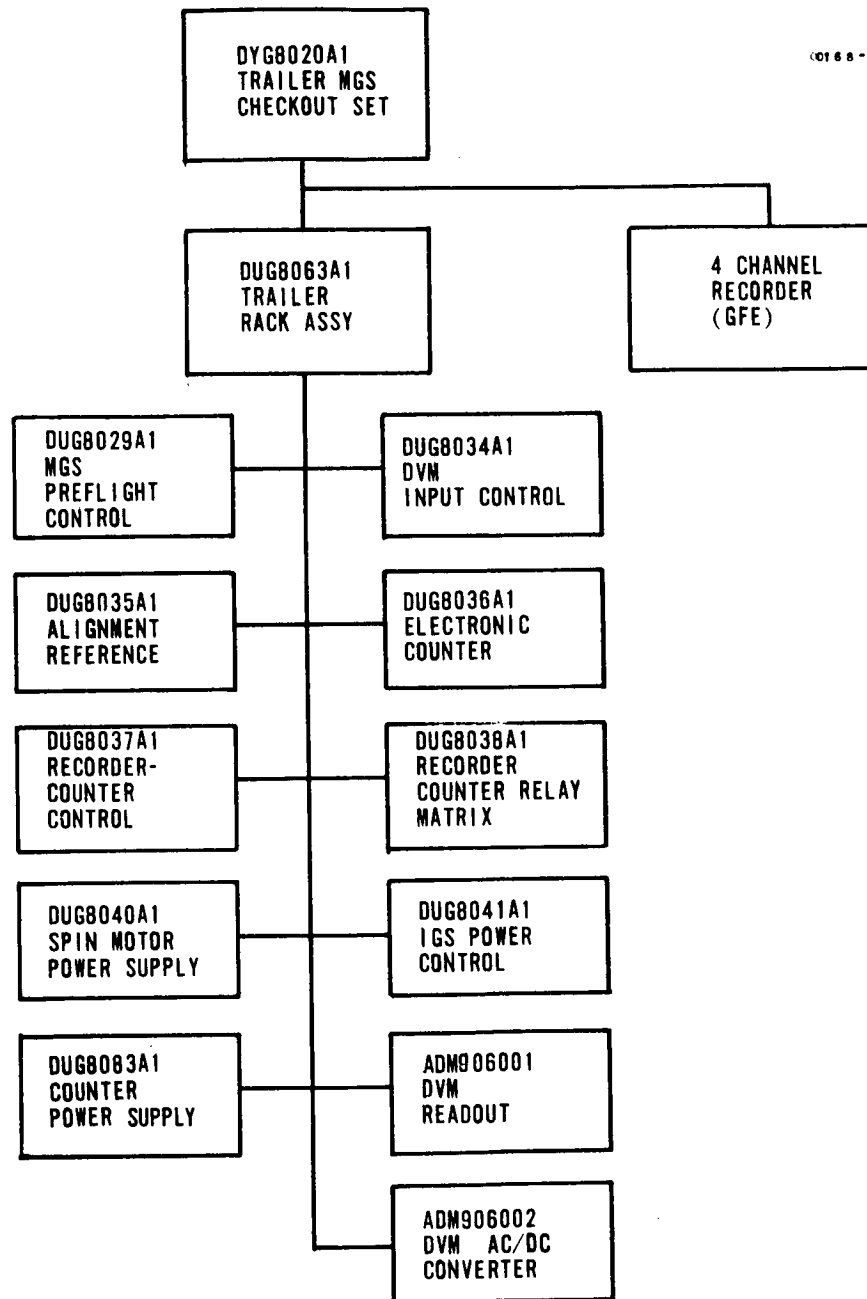


FIGURE 5.2-4. FLOW DIAGRAM OF COMPLETE TRAILER CHECKOUT STATION

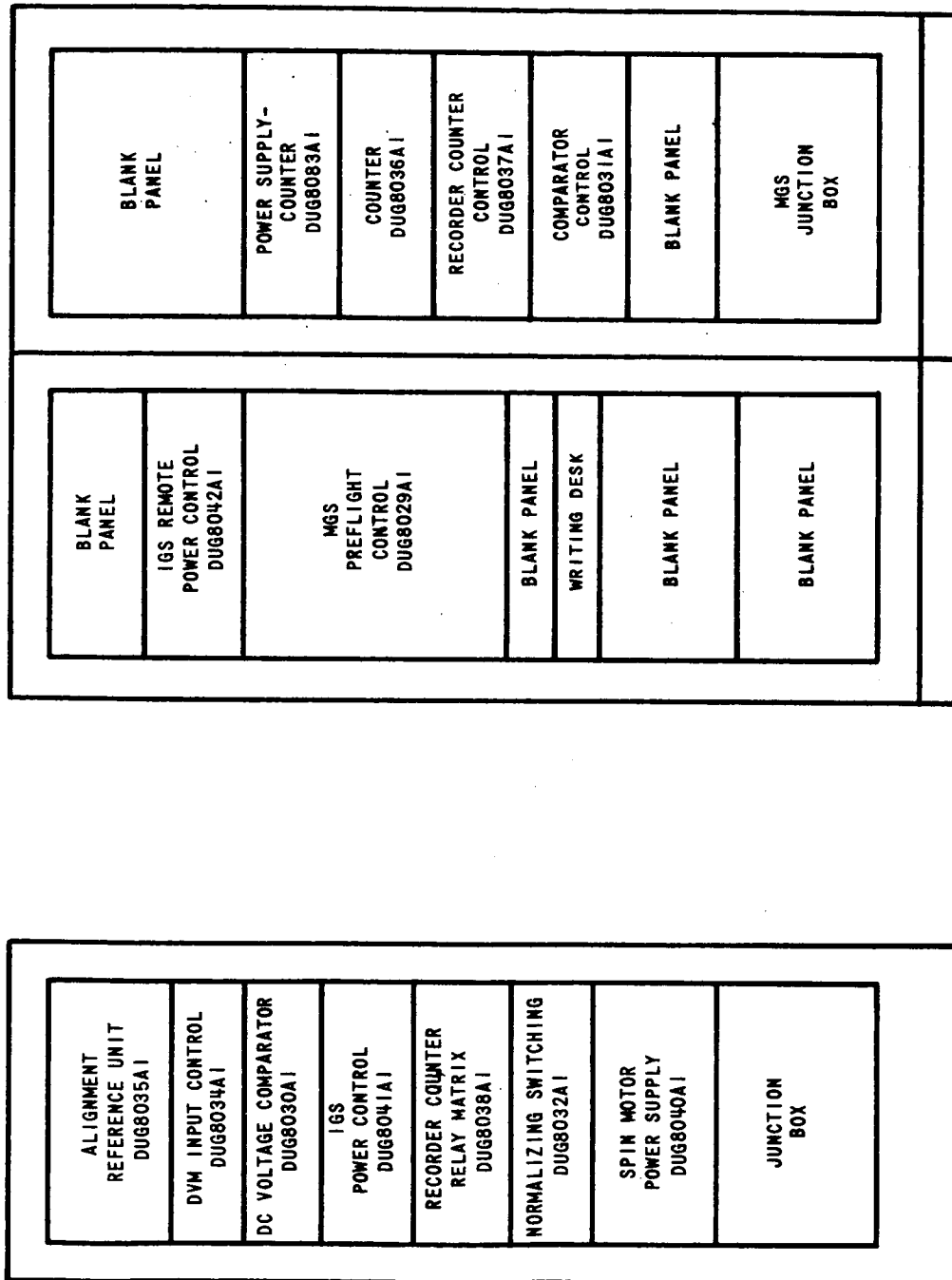


FIGURE 5.2-5. CONFIGURATION OF ORIGINAL LAUNCH CONTROL GSE

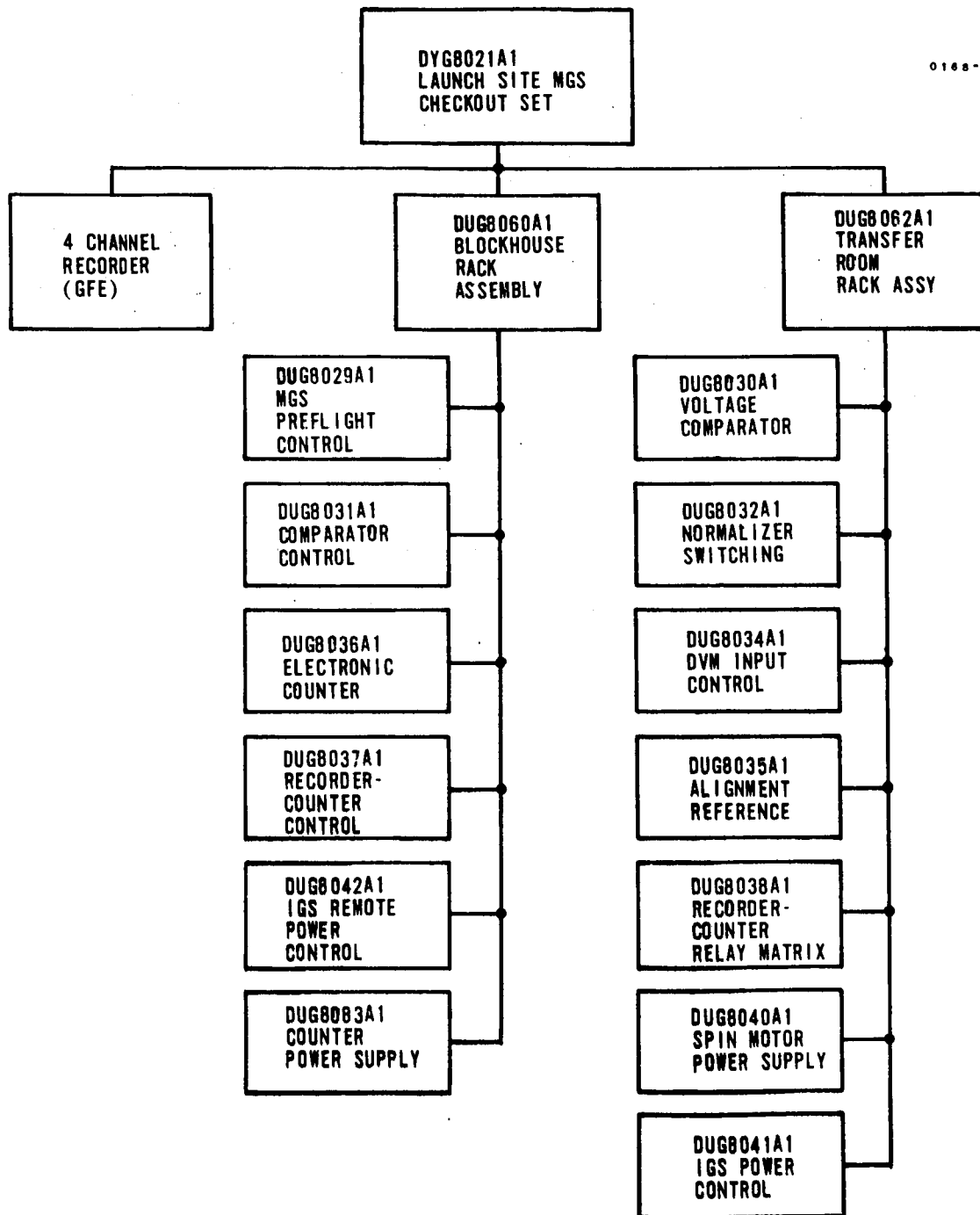


FIGURE 5.2-6. FLOW DIAGRAM OF COMPLETE LAUNCH SITE CHECKOUT EQUIPMENT

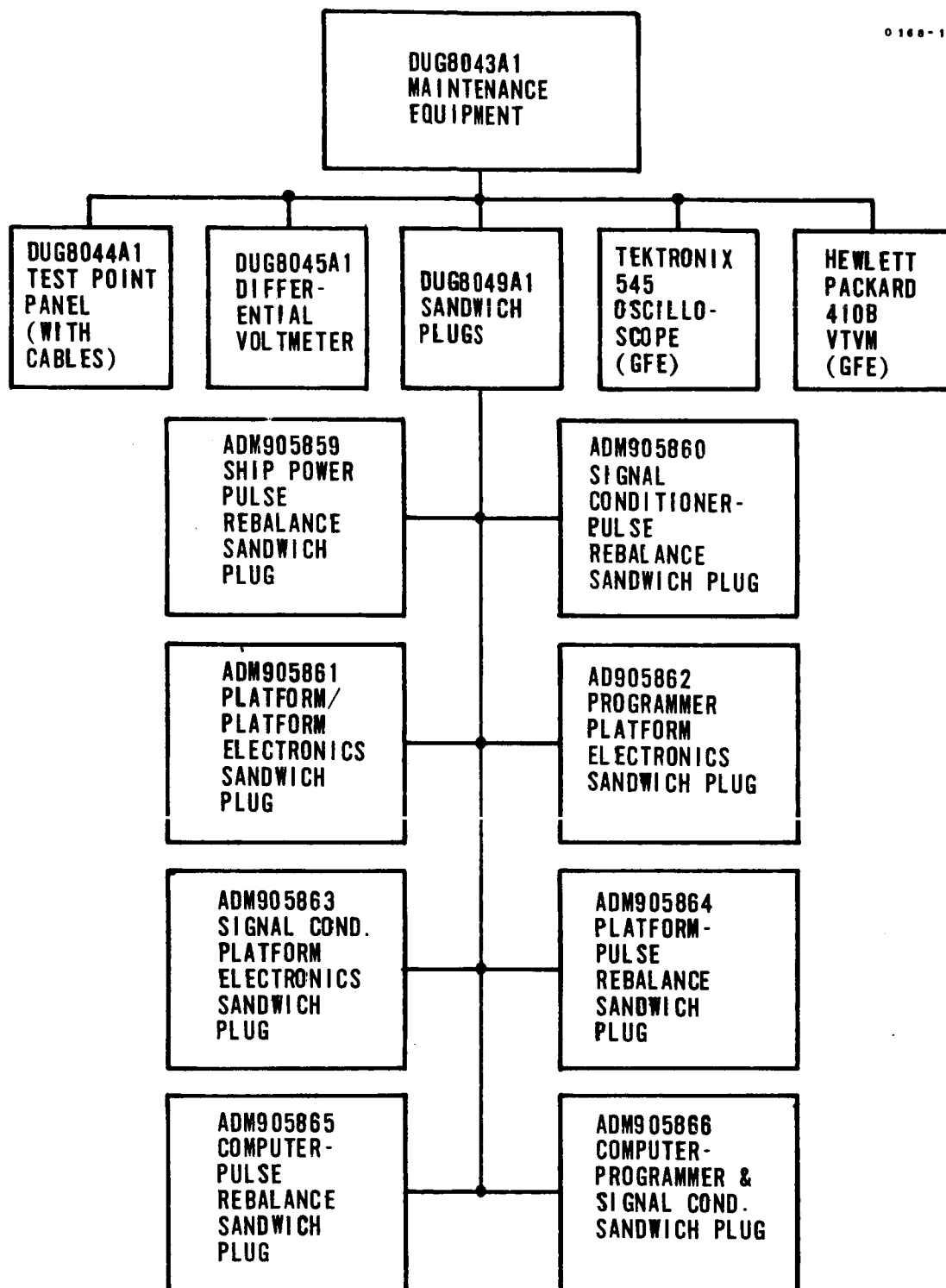


FIGURE 5.2-7. FLOW DIAGRAM OF COMPLETE SET OF MAINTENANCE EQUIPMENT

Control, and the Spin Motor Power Supply were originally located in the transfer room rack. This was done to place the coarse alignment, DVM monitoring, and precision power functions as close as possible to the MGS. It was believed that line loss, crosstalk, and phase shift precluded the installation of these units in the Blockhouse Rack. At the time of this design, many landline parameters were yet undefined, e.g., line length, wire types and sizes, equivalent lump constants, extent of noise and crosstalk, etc.

After the equipment had been put into operation, it became apparent that greater operational flexibility could be achieved by relocating the Alignment Reference Unit, DVM Input Control, and Spin Motor Power Supply to the Blockhouse Rack. This is because operators were needed during checkout at both the Blockhouse Rack and Transfer Room Rack location. This required direct communications between the two operators to communicate operations and responses.

In addition, it was necessary for personnel to clear the transfer room approximately two hours before launch for safety reasons. This rendered the Alignment Reference Unit and the DVM Input Control inaccessible from that time until after launch. The monitoring criteria was that only key signals would be monitored during that final period through the automatic voltage comparator and multiplexed chart recordings. However, anomalies or malfunctions could not be easily evaluated since the majority of the instrumentation signals were not available in the blockhouse.

In the fall of 1961, after approximately one year of operation, it was decided to relocate the Alignment Reference Unit, DVM input control, and Spin Motor Power Supply to the Blockhouse Rack. In addition, it was decided that a Digital Voltmeter would be purchased and installed in the Blockhouse Rack. Enough experience had been gained with the system by this time to afford confidence that the landline characteristics would not significantly degrade the signal characteristics.

This retrofit required an extensive amount of new landlines between transfer room and blockhouse, rearrangement of Blockhouse Rack panels and a complete rewiring of the Blockhouse Rack. A crash program was undertaken to accomplish the change in as short a time as possible with a minimum of downtime. New drawings were created, others modified, complete rack wiring harnesses were fabricated and installed in the Launch GSE before the end of that year. The GSE was out of service only long enough to pull out the old wiring harness, install the new, and rearrange and install the required panels-- a matter of only a few days.

The Launch Control GSE configuration after this modification was completed is shown in Figure 5.2-8. This change was the first major change to the GSE.

5.2.3.2. Additional GSE Sets. - During 1961, the program test schedules required that a fourth Laboratory Rack assembly be produced. The rack was fabricated and produced late in 1961. This increased the quantity of system level GSE sets from 7 to 8. Again, in early 1962, the program test schedules required that a third Trailer Rack assembly be produced to support the GD/C factory test activity. This set was fabricated and produced about mid-1962. This now increased the quantity of system level GSE sets from 8 to 9.

Both sets were manufactured to the latest configuration existing at that time.

5.2.3.3. Dash 1 to -3 GSE Modification. - With the introduction of the -3 MGS in 1962, a few MGS changes affected the MGS to GSE interface. It was recognized that both -1 and -3 systems would be in existence for several years in the future. The GSE, therefore, was required to be compatible with both systems, with a positive and foolproof means of switching from one interface configuration to the other.

It was decided that the switching would be accomplished by providing a jumper between two pins of the GSE connector on the -3 coupler. This would serve to complete a circuit to energize several relays in the GSE. The relays would switch to the proper interface configuration for operating the -3 MGS. The jumper would not be present in the -1 coupler, and the GSE relays would remain de-energized to provide the interface required to operate the -1 MGS.

MGS circuits which affected the interface were:

1. Fast heat control.
2. TCA monitoring.
3. Launch-on-time function.

It was 1965 before -1 systems were sufficiently phased out that the -1 capability was deleted from the GSE.

5.2.3.4. Addition of Gimbal Spin Inhibit Function. - Also in 1962, the requirement came about for a device to prevent the platform gimbals from going into an uncontrolled spin condition in the event of a stabilization

0188-170A

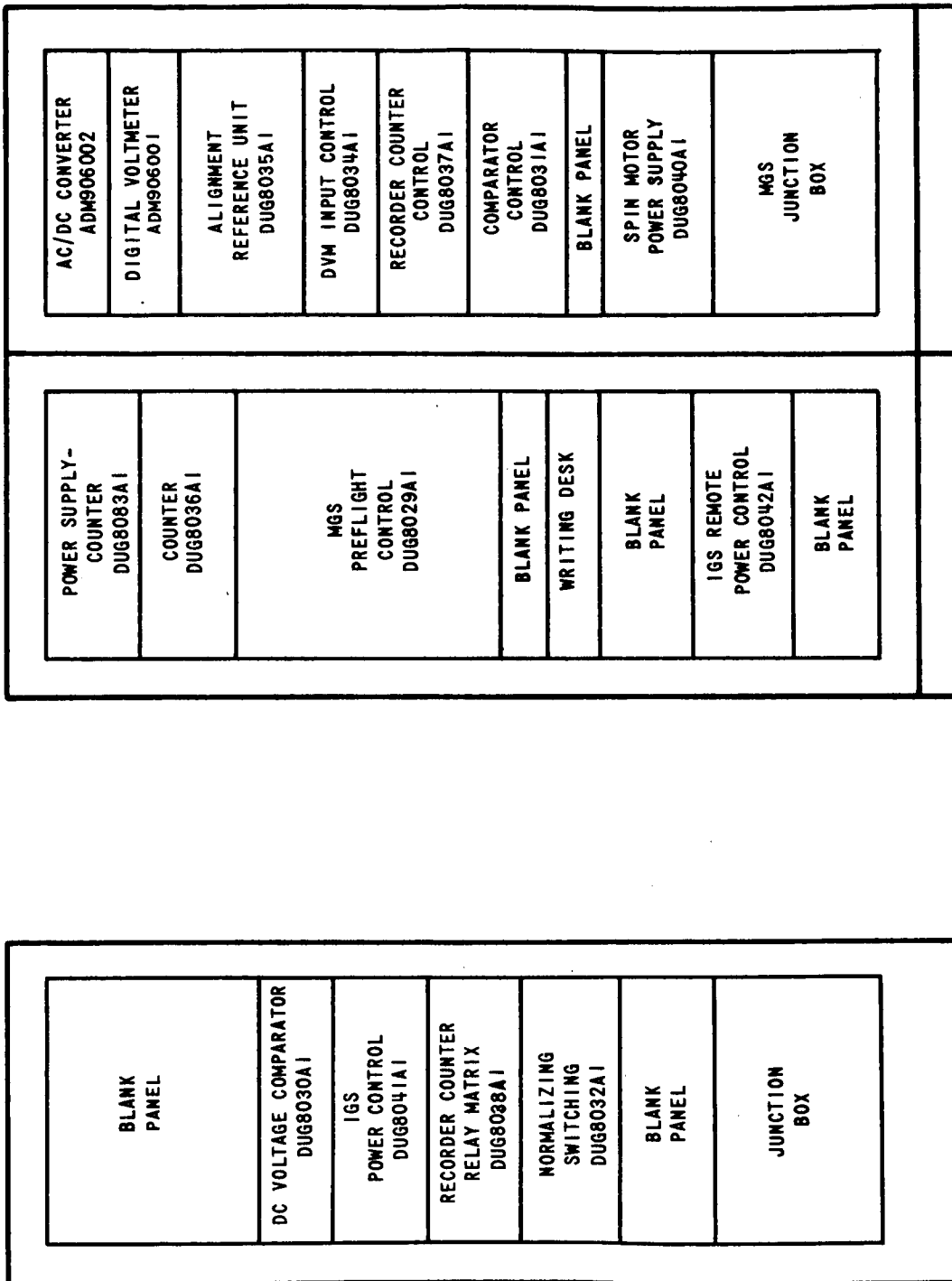


FIGURE 5.2-8. CONFIGURATION OF LAUNCH CONTROL GSE AFTER PANEL REARRANGEMENT

loop malfunction. The original requirement was to provide a detection of a spin condition, and then to act on the gimbal torque motor circuit to stop the spin. A technical investigation ensued to establish technical requirements for the device.

Design constraints were that the device operate with existing interface lines from the MGS, and be incorporated in all system level sets of GSE. With these constraints, the only interface lines available to provide an indication of a gimbal spin were the monitor lines for the gimbal torque motor excitation.

The signal on these lines is normally near zero volts when the gimbal loop is closed and functioning properly, but could swing between limits of +20 volts and -20 volts during a malfunction. This departure from null, or zero volts, could be the symptom of a spin condition. However, gimbal friction, slipping irregularities, loop transients, etc., could cause short-term transient departure from null which must be ignored. With these interface characteristics known, it was necessary then to establish a criterion for distinguishing between a normal, or permissible condition and a true spin condition.

Since the only information available to work with was a voltage rise from zero, the information needed for a criterion was:

- (a) What is the maximum permissible transient amplitude, above which a malfunction is certainly taking place, and
- (b) What is the maximum length of time this amplitude can be exceeded.

After searching existing records, it was concluded that very little analytical and experimental information was available to form the basis for a criterion. System test activity was less than two years old and all testing up to this time had been centered around other performance parameters. Little attention had been given to details surrounding gimbal spins.

A great deal of concern was not being placed on gimbal spin at this time and an inhibit function was wanted more or less as a "safety valve". An extensive analysis was not justifiable because all available effort was being applied to other more critical areas. From the information available and from opinions of people experienced in the platform engineering

and test, it was decided that criterion for operation of the gimbal spin inhibit function should be:

- (a) Signal amplitudes greater than 10 volts will be considered a malfunction condition, and
- (b) The signal must exceed this amplitude for more than 250 milliseconds.

This criterion was the basis for subsequent design and manufacture of the gimbal spin inhibit circuit. Modification of the GSE to incorporate the GSI function was accomplished concurrent with the -1 to -3 GSE modification.

5.2.3.5. Addition of Remote Load and Read Equipment (RL&R). - In the course of routine preflight tests on the Centaur guidance system, it is frequently desirable to communicate with the Navigation Computer to verify the existence of predetermined constants or to update specific information stored in temporary storage locations of the computer Memory Drum. As part of the original contract, the computer subcontractor supplied a Fill/Test Unit for this purpose.

The Fill/Test Unit was a portable, manually controlled unit that was carried to the computer and connected to it by short cables. This procedure was satisfactory in laboratory test installations but soon proved to be quite awkward for launch configuration checkout. It was necessary to carry the Fill/Test Unit to the guidance level of the gantry for use. This introduced delays in the guidance checkout. In addition, the vehicle was inaccessible for this function at certain times. This introduced further delays in the guidance checkout.

In 1962, technical discussions turned toward incorporating equipment in the blockhouse capable of communicating with the guidance computer on the vehicle. A contract was let to the computer supplier in the Fall of 1962, and in mid-1963, four sets of Remote Load and Read equipment were put into service and installed with both Launch Sets, the San Diego Guidance Lab Rack, and the Honeywell Lab Rack. The two labs were equipped with RL&R sets to provide a laboratory duplication of the launch control function. In addition, this afforded a source of spare equipment for the launch complex.

The RL&R equipment consists of a single-bay rack containing manual program controls and a visual indicator arranged in the computer word format; a Folded Paper Printer which selectively prints a permanent record of outputs from the computer; a Tape Reader to permit rapid filling and interrogation of the temporary storage tracks of the navigation computers Main Memory and necessary Power Supplies.

Existing signal and mode lines connected to the computer from the Ground Support Equipment were utilized to convey data or location inputs to the computer. Outputs from the computer were transmitted through a telemetry land line to the Remote Load and Read Test Set, where they were decoded, visually displayed, and recorded.

Figure 5.2-9 depicts the configuration of the RL&R equipment. Further discussion of the RL&R, including problem areas, is provided in Topic 5.3.

5.2.3.6. Spin Motor Power Supply Removal from Launch Control GSE. - In 1962, attention focused on the vehicle 400 Hz supply. The vehicle supply, up to this time, had been one of relatively poor regulation. Therefore, the original GSE design requirements called for a precision 400 Hz supply installed in the GSE to furnish precision power for the spin motors up to the time of power transfer. At that time, spin motor power would be switched from precision GSE power to vehicle power for launch and flight. Precision spin motor power supplies were furnished with all sets of GSE.

In 1962, the program decided to replace the existing vehicle 400 Hz inverter. The characteristics of the new, static inverter output were to be equal to or better than those of the GSE Precision 400 Hz Supply. The inverter would furnish all 400 Hz power for the MGS, including spin motor power. The GSE precision supply would then be removed from the system, and the GSE would control a power relay in the coupler to switch inverter power off or on to the spin motors.

By mid-1963, the inverter had been implemented in all vehicles, and the two sets of Launch GSE were modified to remove the spin motor power supply.

5.2.3.7. Optical Alignment Control. - In 1963, a highly significant change took place in the function of the GSE. This was the addition of optical azimuth alignment capability. Technical details surrounding the optical alignment requirement are covered more thoroughly in Topic 5.4, Optical Alignment Control Group.

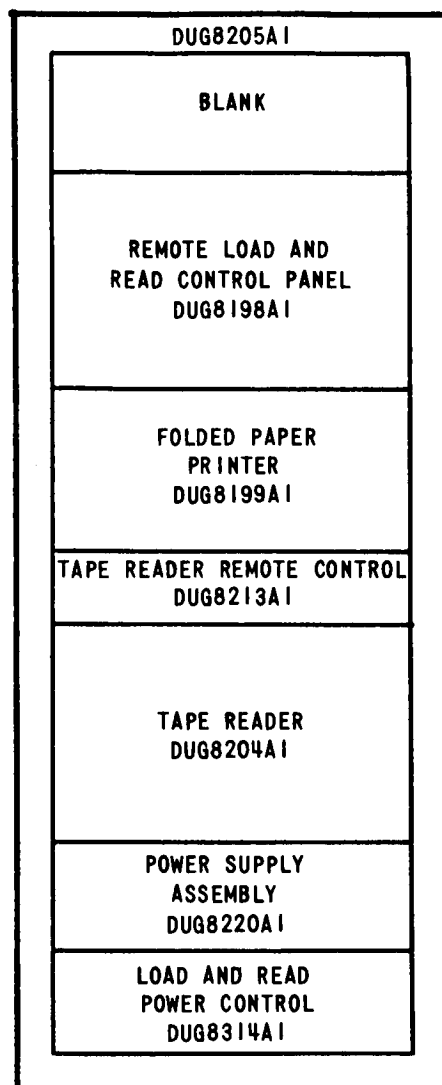


FIGURE 5.2-9. REMOTE LOAD AND READ TEST SET

After the need for optical alignment became apparent, several months followed before detail equipment design was started. During these months, technical specifications and requirements were generated and coordinated with GD/C, LeRC, and the supplier of the long-range theodolite. The first set of optical equipment was produced and delivered to complex 36A in March 1964. Immediately following, Honeywell was given an order for a second set of optical equipment for complex 36B. This set was delivered in July of 1964. Later, a third set was ordered for CSTS and delivered by the end of 1964.

The optical equipment was composed of several individual assemblies. Together, these assemblies were identified as the Optical Alignment Control Group (OACG). The assemblies of the group are shown in Figure 5.2-10.

A special optics building was constructed by NASA at a particular location with respect to the launch pad. This building was called the Guidance Optical Alignment Shelter (GOAS). The building was to contain the theodolite and associated electronics. The Remote Optical Control Panel (ROCP) was located in the Blockhouse Rack. The Blockhouse Rack also contained a complex modification to integrate the optical alignment function with the alignment and control functions already existing in the GSE. Control implementation permits operation of the OACG from either a local position in the GOAS or a remote position in the Blockhouse.

All three sets of optical equipment were identical, except the third set for CSTS was not furnished with the long-range theodolite and the associated autotheodolite control panel. For this site, the Government-furnished a short-range autotheodolite and electronics. The using contractor provided interface electronics for functional compatibility. Thus, all three sets were functionally identical.

5.2.3.8. Additional Laboratory Test Equipment. - In the early months of 1963, Honeywell was issued a contract for a test and evaluation (T&E) program. This contract called for the manufacture of two additional sets of system level test equipment. The sets were to be similar to Laboratory Racks except that they would also contain:

1. A digital voltmeter, and
2. A power interlock panel.

In addition, the bidirectional counter and spin motor power supply were replaced with units of improved design. Because of these deviations from

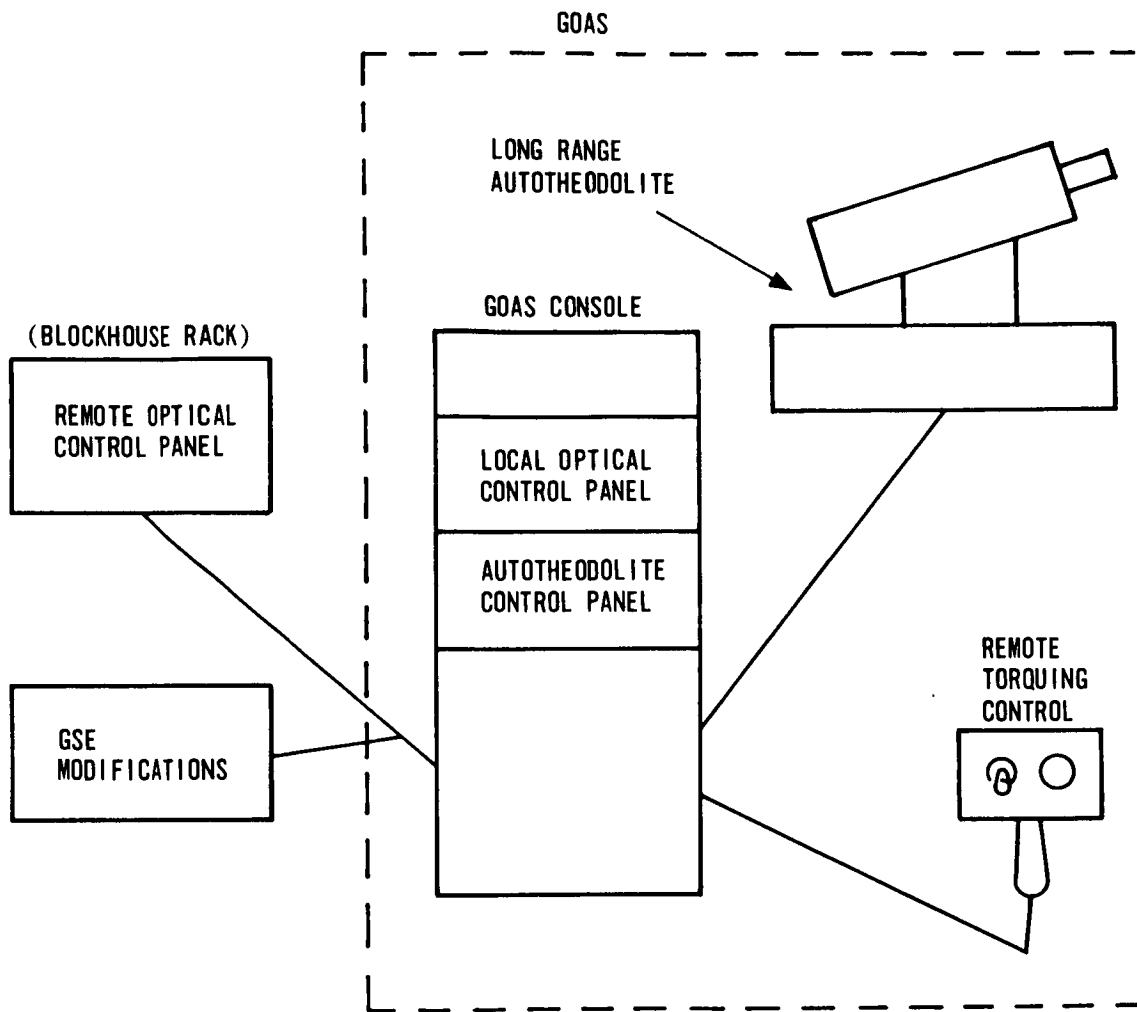


FIGURE 5.2-10. OPTICAL ALIGNMENT CONTROL GROUP

the documented Laboratory Rack configuration, these stations were documented and named "System Test Sets" to avoid confusion. These stations were produced in the Fall of 1963 and became GSE sets No. 10 and 11.

The function of the power interlock panel was to monitor gyro spin motor voltage and prime 28 volts, 60 Hz, and 400 Hz voltage to the IGS. If either the 28-volt or 400 Hz prime power should go outside, its voltage limits, high or low, circuitry within this panel will remove prime power from the MGS and GSE. If 60 Hz prime voltage or spin motor voltage should go outside its limits, circuitry within the panel will place the MGS into coarse align. All phases of ac power are monitored by the panel.

By the time these sets were produced, the total complement of system level GSE sets consisted of four Laboratory Racks, three Trailer Racks, two Launch Control Sets, and two Systems Test Sets plus two additional Laboratory Rack type sets manufactured for use by Honeywell production. With this many sets being used at four locations (i. e., Honeywell, GD/C, Sycamore, ETR), and with frequent exchanges and transfer of sets between locations, identification of sets was becoming increasingly more awkward and confusing in correspondence and discussions. Therefore, a numbering system was established whereby each individual set was assigned an identification number. The sets were then referred to by number in communications. The number assignments were as follows:

GSE	1	Production Set
	2	Production Set
	3	Laboratory Rack
	4	Laboratory Rack
	5	Laboratory Rack
	6	Launch Control Set
	7	Launch Control Set
	8	Trailer Rack
	9	Trailer Rack
	10	Trailer Rack
	11	Laboratory Rack
	12	System Test Set
	13	System Test Set

The number assignments were originally made to each set based on its specific location at that time. These numbers were later correlated to the set serial number since the locations were not necessarily permanent.

5.2.3.9. Deletion of Remaining Transfer Room Equipment. - In mid-1964, the Launch Control GSE was again modified to delete the Transfer Room rack of equipment. This was the first step in a two-step modification task which ultimately expanded the blockhouse GSE from a three-bay (including RL&R) to a five-bay configuration. This first step was termed an "interim configuration" and was accomplished to only one set of Launch Control GSE to support the AC-4 Launch.

This set of GSE, which, by the new numbering system, had been numbered GSE 7, was located at the Sycamore Test Site. This site was being de-activated and GSE 7 was shipped to St. Petersburg for modification. After the modification was accomplished, the set was shipped to ETR to support the AC-4 Launch.

This interim configuration modification consisted of:

1. Installation of mod kits into several GSE panels for operation with OACG.
2. Deletion of Transfer Room Rack Assembly, DUG8062B1, and installation of the IGS Power Control and Recorder-Counter Relay Matrix in the Blockhouse Rack assembly.
3. Installation of a modification kit to accommodate a GD/C furnished Accelerometer Limit Cycle Monitor panel, and
4. Installation of a Remote Optical Control Panel in the Blockhouse Rack.

In addition to these planned modifications, one other change was made. That was to replace the rotary switches used for mode selection on the MGS Preflight control with another type switch. The switches which were in use had become unreliable on several sets. (This problem is discussed subsequently in Topic 5.2.) Since this set was destined for ETR it was thought best to replace the switches with a more reliable type.

This same change had recently been accomplished on GSE 6 which was already at ETR. The change was accomplished, though, by simply exchanging MGS Preflight control panels with Trailer Rack No. 3. This set had been manufactured with the new type switch.

Prior to this "interim modification", the Launch Control GSE was configured as shown in Figure 5.2-8, except that the spin motor Power Supply had now been deleted and replaced with a blank panel. After the "interim modification", GSE 7 was configured as shown in Figure 5.2-11. Not shown in either figure is Bay 1, the Remote Load and Read equipment.

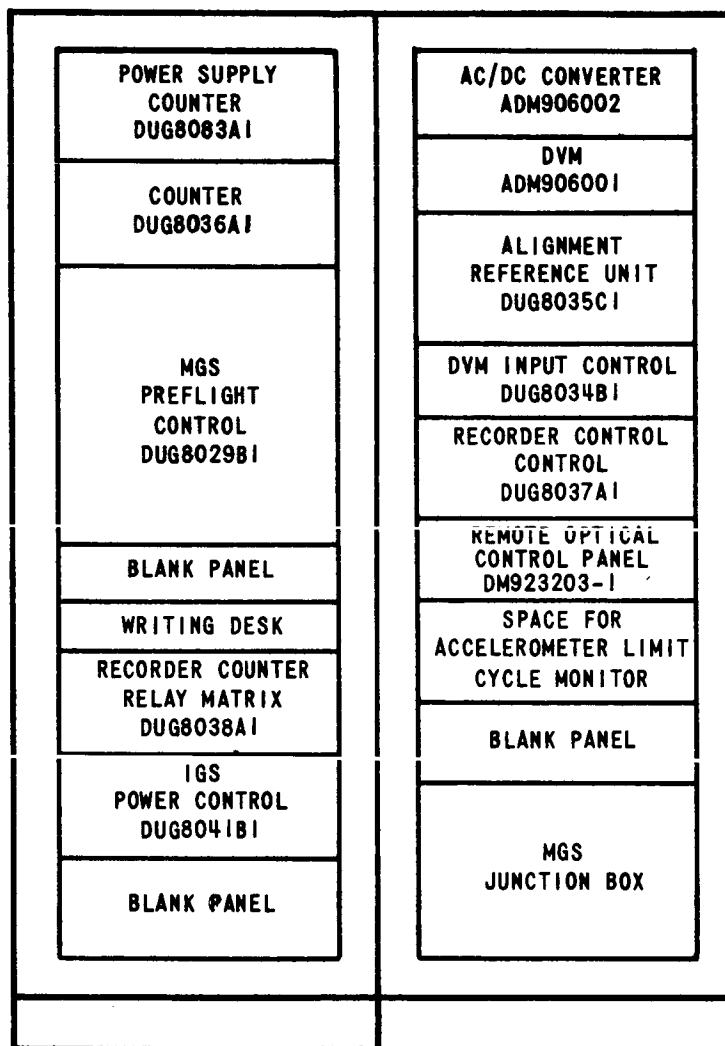


FIGURE 5.2-11. BAYS 2 AND 3 OF BLOCKHOUSE EQUIPMENT,
AFTER INTERIM CONFIGURATION

5.2.3.10. Five-Bay Launch Control GSE Configuration. - Immediately following the "interim configuration" modification in 1964, effort turned to the "final configuration" modification. This modification was another major change in the launch control GSE. The change expanded the blockhouse equipment from a three-bay to a five-bay configuration. This modification was accomplished to both GSE 6 and GSE 7. In addition, a third set of launch control GSE was manufactured. The three sets were to support launch configuration testing at:

1. ETR launch complex 36A,
2. Newly activated launch complex 36B, and
3. Newly activated Combined System Test Stand (CSTS) at San Diego.

The three launch sets were to be functionally identical but would have noticeable physical differences. Figure 5.2-11 reflects the latest launch control GSE configuration up to this time. This figure is that of GSE 7, as GSE 6 was still at an earlier configuration. Figures 5.2-12 and 5.2-13 illustrate the "final configuration" of GSE 6 and 7, respectively. Figure 5.2-14 illustrates the configuration of the newly manufactured launch set. This set was designated GSE 15 (Honeywell production had previously manufactured a third set for in-plant use which was designated GSE 14). The new five bay configuration was also given a new name, "Guidance Launch Control Equipment Group" (GLCEG).

Significant aspects of this modification were:

1. Manufacture of GSE 15.
2. Subcontract procurement of two Remote Load and Read Sets (Bay 1).
3. Manufacture of Bay 4 Assembly (LOT Decoder).
4. Manufacture of Bay 5 Assembly (Chart Recording Equipment).
5. Deletion of Recorder-Counter Relay Matrix and Recorder-Counter Control Panel.
6. Manufacture of new Counter Input Control for Bay 3.
7. Incorporation of newly developed bidirectional counter in Bay 2 of GSE 7 and 15.
8. Incorporation of a newly developed digital voltmeter in Bay 3 of GSE 15 only.
9. Incorporation of new color scheme in all newly purchased or newly manufactured equipment.

1166-2628

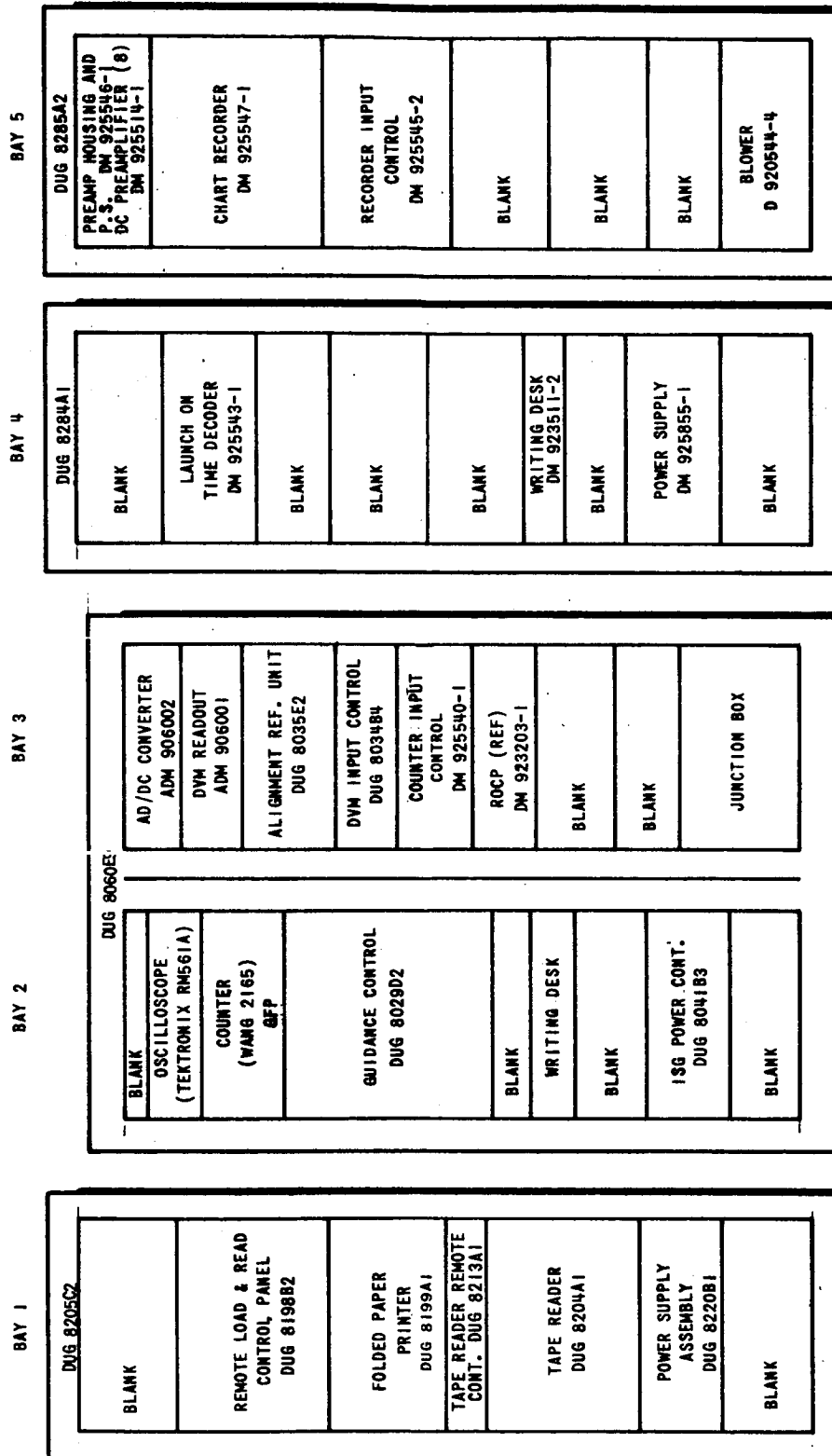


FIGURE 5.2-12. GUIDANCE LAUNCH CONTROL EQUIPMENT
GROUP FINAL CONFIGURATION, GSE 6

0168-1768

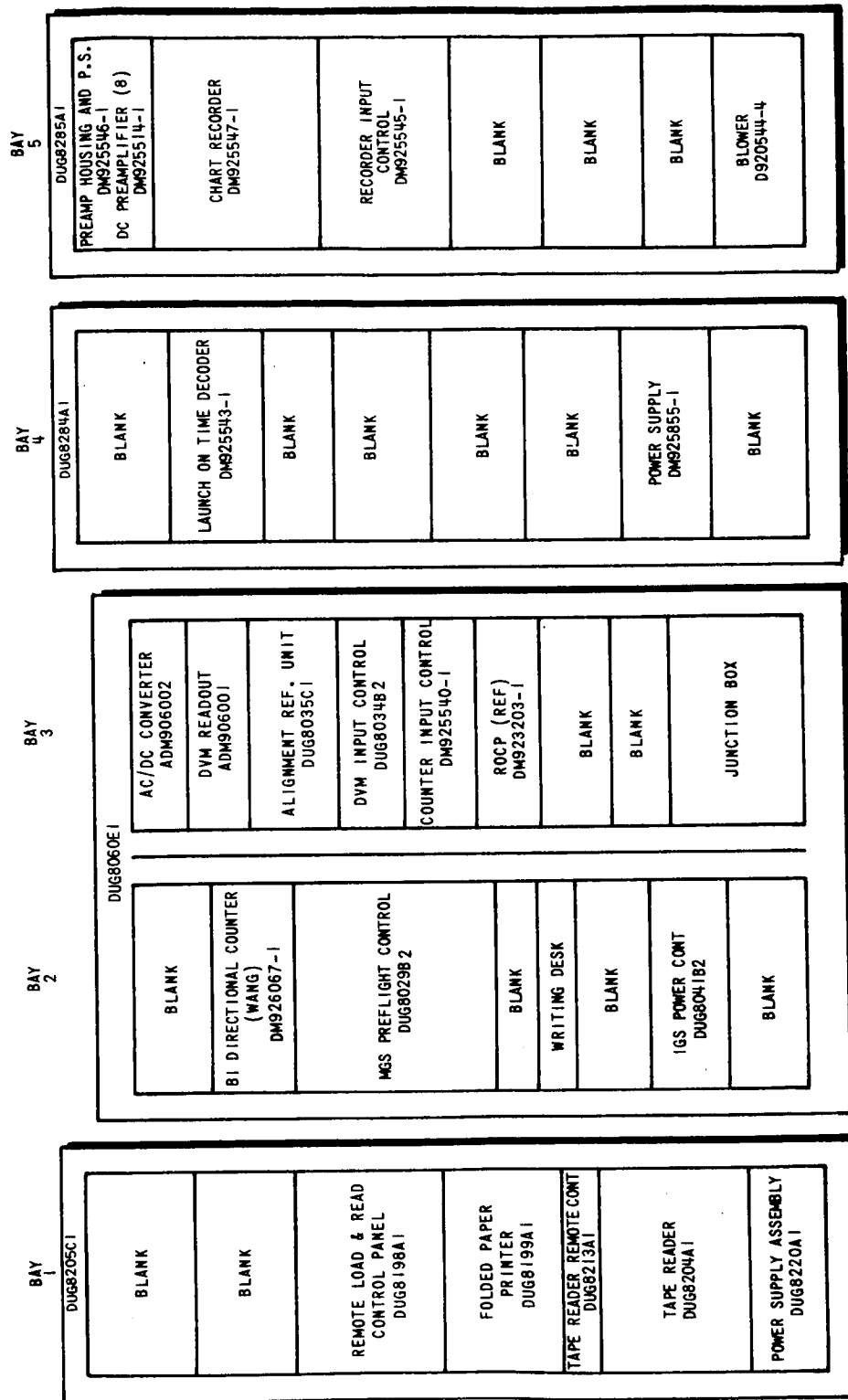


FIGURE 5.2-13. GUIDANCE LAUNCH CONTROL EQUIPMENT
GROUP FINAL CONFIGURATION, GSE 7

0168-224B

BAY	BAY	BAY	BAY	BAY
1	2	3	4	5
DUG 8205C1	DUG 8282A1	DUG 8283A1	DUG 8284A1	DUG 8285A1
BLANK	BLANK	DIGITAL VOLTMETER DM 925758-1	BLANK	PREAMP HOUSING AND P.S. DM 925546-1 DC PREAMPLIFIER (8) DM 925514-1
BLANK	BI-DIRECTIONAL COUNTER DM926067-1	BLANK	LAUNCH ON TIME DECODER DM 925543-1	CHART RECORDER DM 925547-1
REMOTE LOAD & READ CONTROL PANEL DUG 819881	MGS PREFLIGHT CONTROL DUG 8029C1	ALIGNMENT REF. UNIT DUG 8035C2	BLANK	RECORDER INPUT CONTROL DM 925545-1
FOLDED PAPER PRINTER DUG 8199A1	BLANK	DVM INPUT CONTROL DUG 8034B2	BLANK	BLANK
TAPE READER REMOTE CONT. DUG 8213A1	WRITING DESK	COUNTER INPUT CONTROL DM925540-1	BLANK	BLANK
TAPE READER DUG 8204A1	BLANK	R.O.C.P. - REF DM923203-1	BLANK	BLANK
POWER SUPPLY ASSEMBLY DUG 8220B1	IGS POWER CONTROL DUG 8041B2	BLANK	POWER SUPPLY DM925855-1	BLOWER D 920544-4

FIGURE 5.2-14. GUIDANCE LAUNCH CONTROL EQUIPMENT
GROUP NEW BUILD, GSE 15

The major physical differences between GSE 6, 7, and 15 are:

1. GSE 15 employed two individual racks for Bays 2 and 3 instead of one integral two-bay assembly as originally employed with GSE 6 and 7.
2. New build Bay 1's were used with GSE 7 and 15. An existing old build Bay 1 was used with GSE 6.
3. New bidirectional counters were used with GSE 7 and 15. The existing old style counter remained with GSE 6.
4. GSE 15 employed a new style digital voltmeter. The existing old style digital voltmeters remained with GSE 6 and 7.
5. GSE 15 employed the new color scheme throughout since it was entirely a new build. Therefore, all assemblies were uniform. GSE 6 and 7 employed the new color scheme only on new build assemblies. Therefore, these sets contained a mixture of old and new color schemes.

Bay 4, the LOT Decoder bay, was incorporated to provide a real-time reference signal to the Navigation Computer to modify flight equations. The LOT decoder decodes the ETR time code B1 signal, and at some precise, pre-selected time generates and transmits the reference signal to the computer.

The time at which it is desired to transmit the LOT pulse to the Computer is selected manually with thumbwheel switches on the front of the LOT Decoder panel. Upon depression of the start pushbutton switch, the time set on the thumbwheel switches is loaded into the preset register and the operation of the LOT decoder circuitry is enabled. From this point on, the operation of the LOT decoder is completely automatic.

Bay 5, the recorder bay, contained an eight-channel chart recorder with preamplifier, and a Recorder Input Control panel. This equipment provides the capability of manually selecting and displaying simultaneously any eight of 56 possible instrumentation signals. The recorder is a Sanborn Model 850 with plug-in preamplifiers.

5.2.3.11. Vehicle Guidance Simulator. - In 1964, a need also developed for a device to simulate as accurately as possible the electrical interface of the Centaur MGS and be electrically substitutable for the Centaur MGS. The simulator was required for validation and checkout of the guidance

site wiring and the guidance GSE. It would be connected to the landline wiring at the guidance level of the vehicle service tower at either:

1. The umbilical connectors, or
2. The MGS connectors within the guidance wiring harness of the vehicle.

The Vehicle Guidance Simulator was produced in mid-1964, and is shown in Figure 5.2-15. The device was manufactured in a standard 6-foot high, single-bay, weather-proof rack assembly, mounted on a four-wheeled carriage. The back and front doors and all other openings are sealed with neoprene weather stripping. Air intake and exhaust openings have drip-proof louvres.

The MGS Simulator contains signal sources, power supplies, resolver units, indicating devices, simulated loads, interconnecting cables, and other equipments required to provide the necessary discrete and response signals for validation of the GSE. All Guidance Launch Control GSE, including the Remote Load and Read portion and selected functions of the Optical Alignment Control Group, can be validated by the Vehicle Guidance Simulator.

The Simulator affords electrical simulation of the MGS, consisting of voltages, signal stimuli, stimuli responses, loads, grounding and shielding continuity. Simulation is primarily done by manual operations. Automatic or dynamic response circuits are used only for certain Remote Load and Read functions where it is necessary for accurate indication of proper RL&R operation.

5.2.3.12. AC-8 Modifications. - Computer modifications with effectivity beginning with the AC-8 flight reflected major hardware change requirements into the GSE. One of the primary change areas was the increase in the number of computer discrete signal lines from 4 to 15. This area in itself imposed an extensive redesign in the MGS Preflight Control circuitry. At the same time, the launch ladder operational sequence was evaluated and a complete redesign created.

The task was further complicated by a decision to remove all circuitry within the GSE that was associated with operation of -1 MGS. This was done as a reliability measure since by this time all -1 MGS's had been phased out of the Centaur flight plans. In addition, with the new computer interface, it was highly impractical to maintain -1 and -3 interface compatibility with the GSE. It was also decided that many of the new

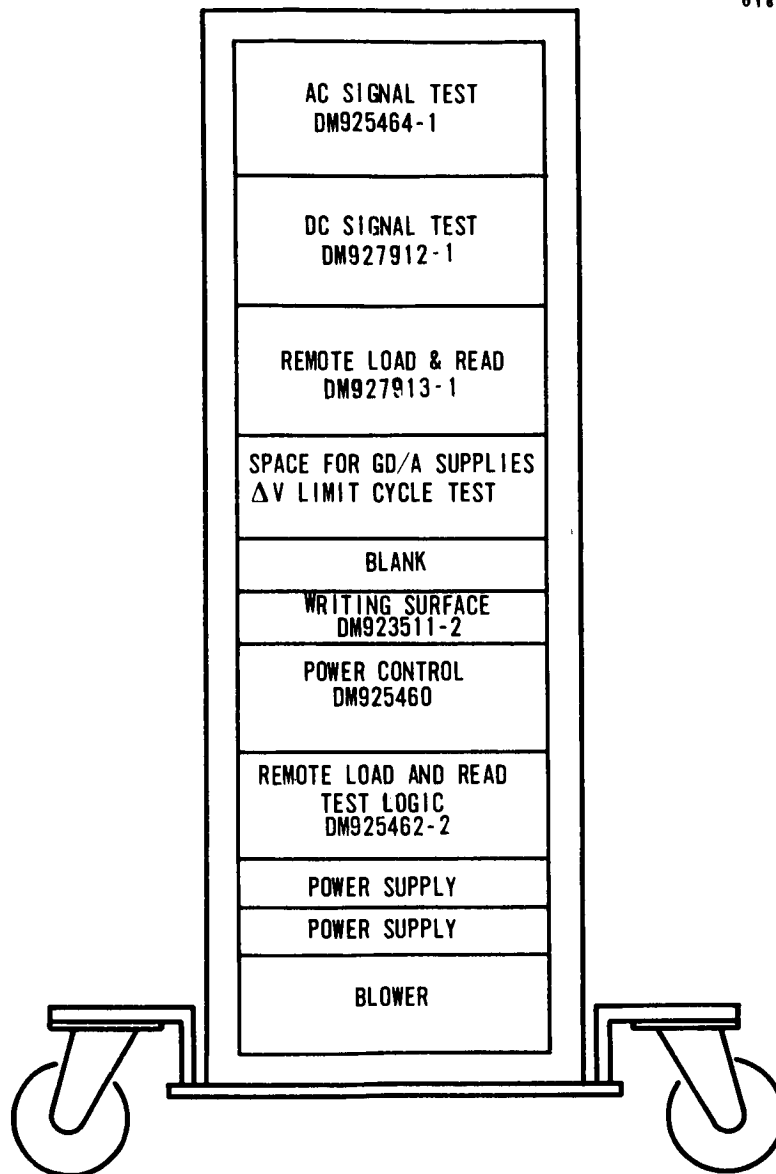


FIGURE 5.2-15. VEHICLE GUIDANCE SIMULATOR

control panel logic functions could easily be handled by semiconductors in this design rather than by relays-- another reliability improvement.

Two problem areas which had plagued the GSE for some time were also reviewed, and it was decided that this was an opportune time to provide a permanent solution. The problems were:

1. Unreliable Heinemann time delay relays, and
2. Malfunctions of the MGS Preflight Control align mode switches.

These problems are discussed in detail in Topic 5.2.4.

With the total amount of changes identified, the majority of the rework was centered in the MGS Preflight Control panel. The rework affected several other panels, but to a much lesser extent. The MGS Preflight Control panel redesign necessary was so extensive that it was decided to completely strip the panel of all wiring and parts and rebuild to the new design. In view of this, it was decided that rework this extensive should not be handled in the field. Therefore, a plan of rotation was set up whereby all MGS Preflight Control panels were routed to St. Petersburg, rebuilt and returned to the field. The plan involved keeping one or more panels moving through rework until all sets had been modified. As each set was completed, it would be packed with a modification kit for the remaining rack panels and shipped to its preplanned destination. The remaining rack modification would be accomplished by field support people.

The modifications to the MGS Preflight Control were so extensive that it was necessary to discard the front panel and manufacture a new one. All wiring was stripped from the unit, and all parts carefully removed, cleaned and retained.

During the rebuild, old parts were re-used when technically feasible to effect a cost savings. None of the Heinemann time delay relays or CDI printed circuit mode switches were re-used. More reliable components were employed for these functions in the rebuilt panels.

As part of the configuration change, the panel name was changed from "MGS Preflight Control" to "Guidance Control". This was done to better reflect its function. Figures 5.2-16 and 5.2-17, respectively, depict the old and the new front panel appearance.

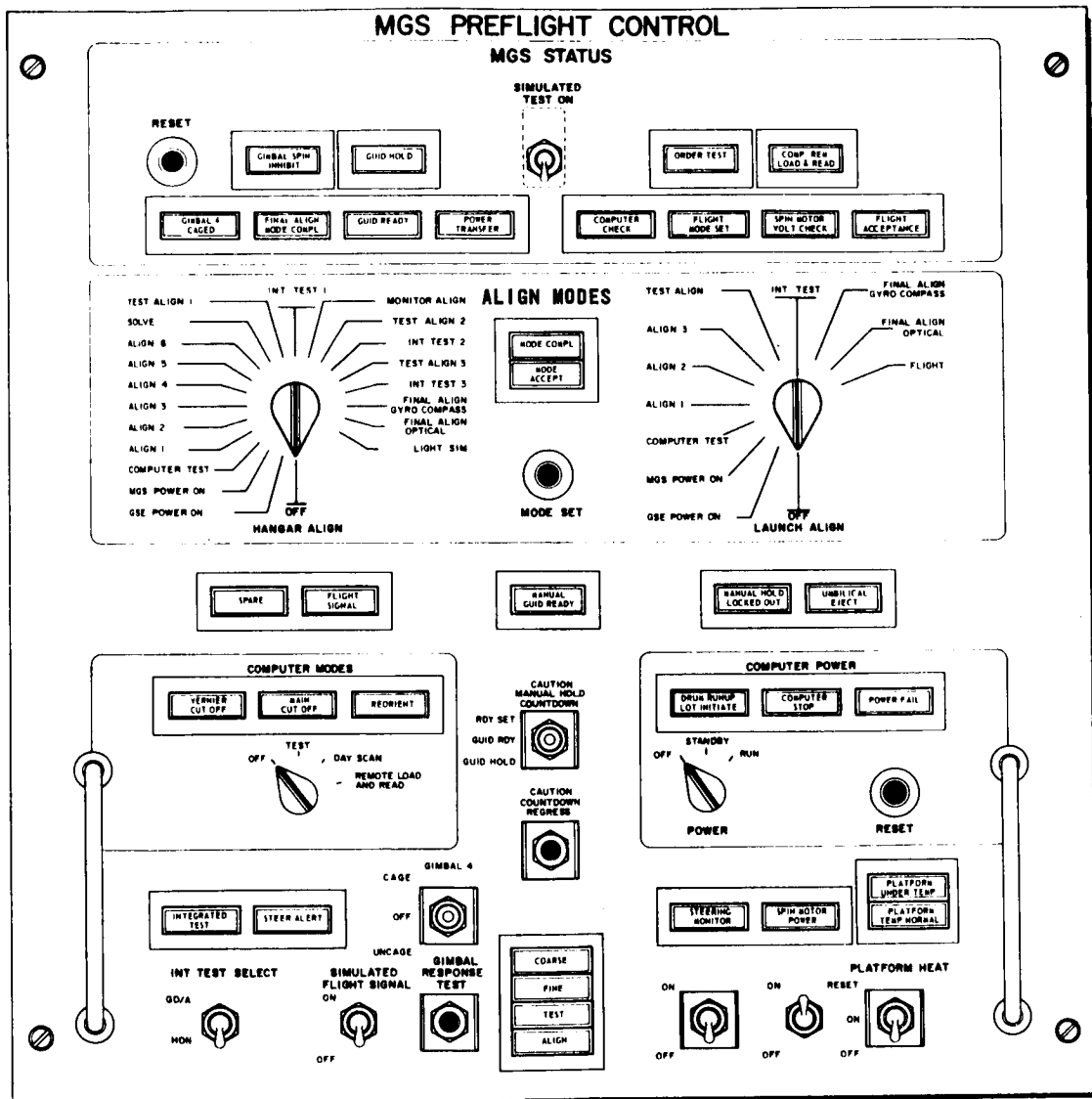


FIGURE 5.2-16. MGS PREFLIGHT CONTROL PANEL



The rebuild activity was spaced over a period of time from approximately mid-1965 to approximately the end of 1966. Two sets were exempt from rebuild, and these were GSE 7 at ETR and GSE 12 which was at LeRC. GSE 7 was being retired from use, and GSE 12 was being used entirely with a -1 system for engineering testing.

The lead time allocated to implement these changes was very short. Therefore, in order to support the flight schedules in certain critical areas, an interim design was undertaken. Interim hardware was provided in the form of an "add-on" panel to operate in conjunction with the MGS Preflight Control and rack wiring. Meanwhile the final design proceeded and as the final changes were incorporated, the interim modifications were phased out. This effort was the last major change in the Systems GSE configuration.

5.2.3.13. Delta-V Limit Cycle Monitor. - As the Centaur Program progressed, additional as well as improved monitoring equipment was needed in the system level test sets. In 1964, a requirement arose for a device to monitor the delta-V limit cycle and indicate whether the pulse patterns exceed predetermined limit cycle patterns. In addition, the device was required to indicate the occurrence of missing delta-V pulses. Although this was guidance oriented equipment, the Delta-V Limit Cycle Monitor was manufactured and supplied to the program by GD/C.

5.2.3.14. Instrumentation Changes. -

- a. Digital Voltmeters. - In 1965, it was decided to incorporate digital voltmeters (DVM's) in the laboratory racks. The voltmeter is an absolute necessity during guidance checkout, and up to this time, portable instruments had been used with laboratory racks. Trailer Racks incorporated DVM's in the original design, Launch Racks incorporated the instruments several years later, and the System Test Sets included DVM's in their design. This left only the Laboratory Racks without permanently installed voltmeters. Cost precluded incorporating the instruments in the original design. Since that time, however, NASA-LeRC has decided to provide three additional DVM's for GSE 3, 4, and 5.
- b. Bidirectional Counters. - Also in 1965, new improved bidirectional counters were provided to replace the now outdated Navcor counters. At the beginning of the Centaur Program in 1959, bidirectional counters which would meet the program needs were

not commercially available. The Navcor Company modified one of their standard counter designs to provide an up-down counter with a preset time base which would meet the program needs. The counter readout was given in binary in order to minimize the hardware required and the original costs. This solid-state unit required two separate assemblies, a power supply assembly and a counter assembly. The binary readout characteristic proved to be very awkward to use. With advances in the state-of-the-art, other highly reliable, smaller, solid-state bidirectional counters having decimal readouts became commercially available at a considerably lower cost than the Navcor units. Therefore, in late 1965, new commercial counters were procured and installed into each of the system level test stations.

Honeywell procured two units for GSE 7 and 15 as part of the "Final Configuration" modification discussed above. Later, the additional units were purchased by NASA and supplied to all other system test stations as GFE. In addition, Government-furnished counters were also supplied to some unit level test equipment employed by Honeywell Production.

When the counters were procured by NASA, Honeywell was contracted to establish a test program to provide a thorough performance test of each unit. A test plan was prepared and approved by NASA, and each unit was routed to St. Petersburg for testing prior to installation in the field.

- c. Oscilloscopes. - In 1966, oscilloscopes were installed in Launch and Trailer Sets. They are used to facilitate troubleshooting in the event of a suspected anomaly or malfunction. As an auxiliary oscilloscope is not always readily available in the Trailer and blockhouse areas, provisions were made to permanently install the oscilloscope in the equipment racks in these configurations.

5.2.3.15. Present System GSE - End of 1967. - Since completion of the AC-8 modifications, little further change has taken place in the system GSE. Several minor circuit changes have been incorporated to alter certain circuit functions. GSE's 6, 7, and 11 have been retired from service and placed in storage. All other sets remain in active service at this time.

It should be emphasized again that the modifications discussed above are only the more significant modifications since inception. There have

been scores of other, less significant, modifications incorporated through the years. To discuss all of these would contribute heavily to the volume of this report, but would contribute little more to its technical value.

5.2.3.16. Computer Control Launch Set. - The Computer Control Launch Set (CCLS) is an electronic system for automatic checkout and calibration of the Centaur guidance system at the launch complex. It was developed and integrated by GD/C.

The CCLS consists of:

1. An SDS 930 computer with special input/output capabilities for processing digital and analog signals.
2. A DD210 Display System, consisting of a display controller and three display stations.
3. Interface electronics, consisting of the circuitry required to properly mate computer, display system, guidance system, and launch equipment.
 - a. Background. - In early 1965, GD/C began a feasibility study for the implementation of a Computer Controlled Launch Set (CCLS) to check out and calibrate the Centaur Guidance System. The concept of CCLS testing was to check out and launch the guidance system employing a philosophy similar to the one being used with the manual GSE. A ground computer rather than the airborne computer would control the tests, thereby providing automatic data reduction with considerably increased signal monitoring, and more flexible control capabilities. By using CCLS to control MGS calibration, space in the flight computer could be freed for more explicit flight guidance equations. The limited space was a result of having to use temporary storage and large portions of permanent storage of the flight computer for the preflight calibration program. Some 1,000 memory cells could be freed for the flight program. This additional storage space would result in hardware simplifications and also allow ease and flexibility in programming the flight equations. Programming for more complex flights, requiring greater memory space, also becomes possible. The flight computer has a drum for storage. Much programming time is necessary in optimizing a program because access to and from a particular location is dependent upon the rotating drum. As more locations become available, the task of programming becomes correspondingly easier.

- b. General Description. - Figure 5.2-18 shows a block diagram of the CCLS and/or manual GSE interface with the vehicle. The heart of the Automatic Test Equipment, ATE-2230, is a Scientific Data Systems (SDS) 930 Computer-- a high speed, low cost, general purpose digital computer configured with 12,288 words of core storage. A priority interrupt system which is capable of suspending execution of the in-process program when guidance system or external timing signals demand immediate processing is provided. In addition, standard input/output devices, including magnetic tape units, a disc file storage unit, a teletypewriter, a card reader, and a paper tape reader and punch are provided. The ATE-2230 also includes digital-to-analog and analog-to-digital converters to allow the computer to process and control analog signals, as well as digital logic circuitry to allow both single- and 24-bit information to be processed into or out of the computer.

The system displays status and control information in alpha-numeric form on the face of a cathode ray tube. This information allows the operator to be completely informed of system test status, and provides him with the capability of manually executing control of the test, when he so desires, by entering commands via the display keyboard.

CCLS became operational for AC-13 launch on 8 September 1967. It replaced the manual Launch Blockhouse GSE. Six months prior to that, it monitored the flight computer digital telemetry signal during prelaunch and launch activities on AC-11 and 12. For the first three flight support tasks, CCLS was to essentially replace the test operator. The preflight calibration program still remained in the guidance flight computer. CCLS has not as yet accomplished one of its major goals-- the one of freeing the flight computer of the preflight calibration task.

The manual GSE is currently employed as a backup for the CCLS. Switchover between the manual and the automatic GSE is made possible by means of a patch panel located in the Blockhouse. In the event of a CCLS malfunction, the checkout control can be switched to the manual GSE and the launch countdown can be resumed at some convenient point, thereby minimizing the possibility of "scrubbing" the launch.

A Computer Control Launch Set has a very important place in vehicle launchings. It relieves the operator from having to make quick decisions during critical portions of the launch countdown. If properly programmed,

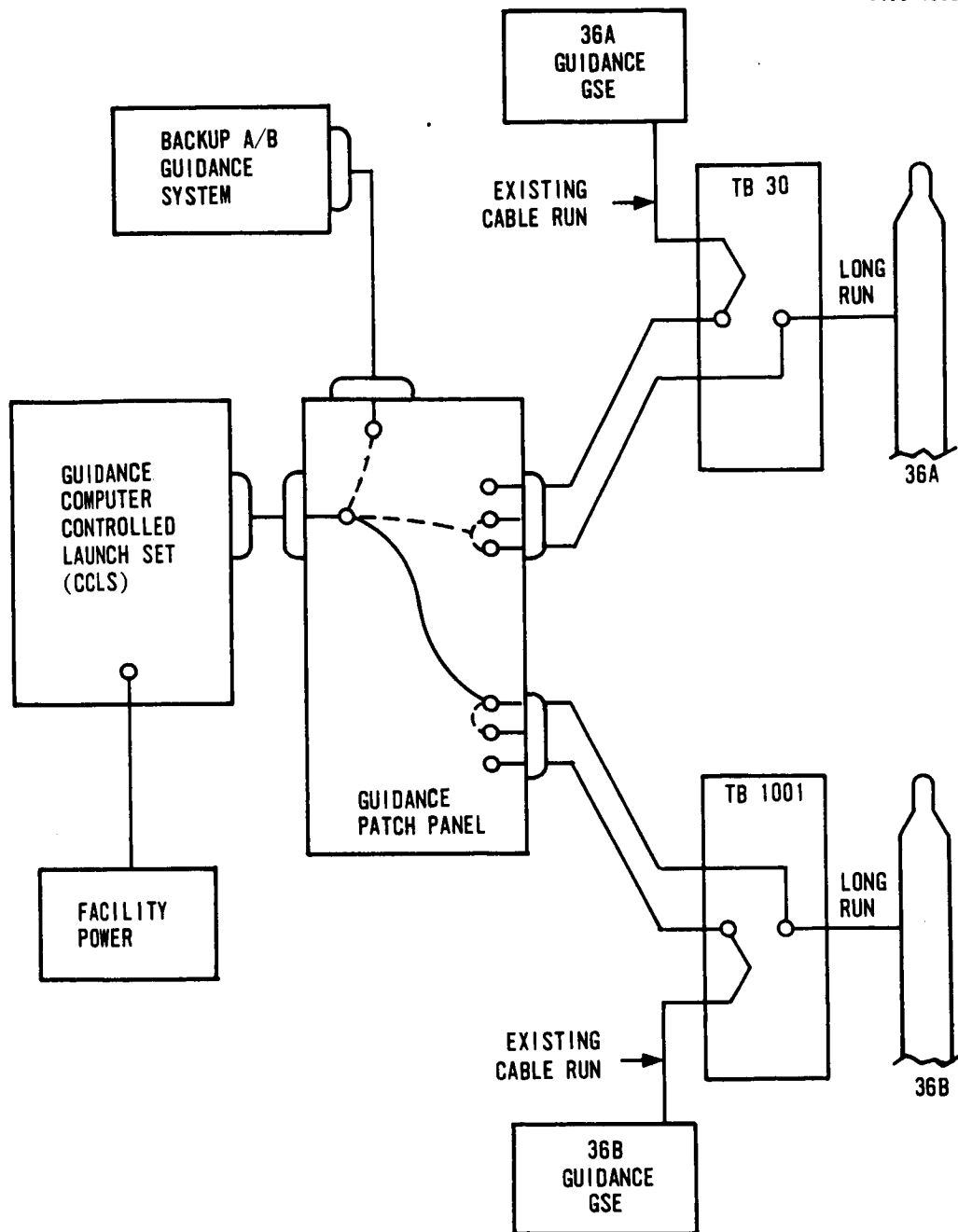


FIGURE 5.2-18. COMPUTER CONTROLLED LAUNCH SET INTERFACE

many emergencies may be automatically handled quickly and efficiently without the requirement for operator decision. Even though the original intent of the CCLS has not been accomplished, immediate goals have been set for 1968 completion date. This would allow CCLS to relieve the guidance flight computer of preflight calibration.

5.2.3.17. IMG Test Set. - As part of the conceptual design phase of the Improved IMG task, effort was directed to the choice of a manual or an automatic IMG test set, including the review of existing facilities and equipment, since these would be major contributing factors to the total cost. Three major categories were considered: (1) completely manual GSE, (2) manual GSE with on-line data processing capability, or (3) manual GSE with on-line data processing capability including provisions for automatic calibration of the IMG. A study of the GSE requirements resulted in the decision to provide the latter configuration for the Improved Centaur IMG support equipment. In reaching this decision, existing facilities and equipment were considered, including available Honeywell capital equipment, and equipment available from the present Centaur program, particularly the ADLE and ADPS hardware.

An ideal goal for test equipment is to provide a comprehensive test capability that can be duplicated from run to run and unit to unit, minimizing the dependence on the operator. Further, it should provide for automatic data acquisition, logging and reduction; have the flexibility to permit special testing; and do so at a cost that is not prohibitive. The selected configuration for the IMG Test Set approaches these goals. It provides a reasonable balance between manual and automatic capability, recognizing other program constraints.

Two important factors influenced the final decision on the recommended configuration, and support the reasonableness of the approach:

1. The availability of a compact reliable, low cost, computer including field-proven software.
2. The availability, from the present Centaur program, of high cost items required to prove the concepts involving automatic data acquisition and data logging. These items, available to the Improved Centaur System program at no additional cost, include the A/D Converter, Multiplexer, Time Code Generator, and Magnetic Tape Unit.

The IMG Test Set can be considered in two separate, but totally integrated facets, the Computer Subsystem and the Manual Equipment. Automatic control, data acquisition, data logging, data reduction, and calibration will be accomplished through the Computer Subsystem. System status, data printout, and input mode controls via a Teletype Unit provide a flexible man-machine communication link.

Ideally, the Computer Subsystem would exclusively provide all the requirements of the IMG Test Set. However, since the IMG program was initially concerned with one new prototype system, nominal manual capability backup was included. The manual capability will provide added test flexibility at minimal cost.

The test set design will be applicable to Production, but not necessarily identical to one designed specifically for Production testing. The manual provisions were considered as a valuable, flexible tool to be used during initial prototype program debugging and developmental testing. If additional test sets should be required for Production testing, the manual functions, having served their purpose in the prototype phase, would most probably be reduced or eliminated. A design feature of the test set, as conceived, includes a simple transition from either mode, manual or computer, by pushbutton switch selection, and the ability to operate manually with the computer disconnected.

The optimum configuration for the IMG Test Set to meet the needs of the IMG program requires both manual and automatic capability. Manual capability will enhance the test set flexibility during the prototype phase. The computer capability will permit the development of automatic techniques and programs for use in the production phase and for applicability to vehicle integration concepts. Although the initial hardware cost of a computerized GSE will exceed that of a total manual GSE, tradeoffs conducted during the study program indicate the advantages to the Improved IMG program will overcome the disadvantages. The advantages to be gained with an automatic computerized IMG Test Set include:

1. Reduced time required for test.
2. Reduced time required for data reduction.
3. Elimination of human errors.
4. Excellent repeatability due to inherent equipment stability and repeatability.
5. Reduced personnel skill levels in operators required.
6. Central programmer for control efficiency.
7. Development diagnostic test techniques.

8. Improved maintenance and fault isolation possible through self-testing techniques.
9. Automatic preparation of data packages.
10. Ability to dynamically control and monitor, thereby, providing better stimulation of the IMG operation in the Centaur System.
11. Development of software techniques for calibration, self-check, fault isolation, etc., and their ultimate use in Production and vehicle integration phases.

As stated above, the IMG Test Set will provide both manual and automatic capability. Data processing and automatic calibration will be accomplished by a digital processor (ground computer) and its associated input/output unit. Provisions will be incorporated into the design for the optional control of the IMG by the computer. The manual capability will not be a complex mechanization, duplicating the computer capability. It will, however, complement the computer functions with a minimum of redundant hardware, and yet provide sufficient capability to exercise the system without the ground computer.

The IMG Test Set will include the following functions:

1. Mode control and status monitoring.
2. Fault isolation.
3. Coarse and fine alignment.
4. Gimbal position readout.
5. Gyro torquing.
6. Calibration.
7. Data logging and data reduction.

All of the above functions will be provided in either mode of operation (manual or computer control) with the exception of automatic calibration, data logging and data reduction which will be provided only in the computer mode. Built-in test circuits and troubleshooting provisions will be incorporated into the test set whenever practical. With these fault isolation features included in the equipment, it will be possible for a failure to be readily localized to either the test set or the IMG when out-of-specification conditions occur. The ground computer will be capable of processing sample problems in a self-test routine to determine go/no-go status. Interlocks will be provided in the IMG Test Set to insure proper IMG power sequencing and system safety precautions.

5.2.3.18. Factory Test Station. - A separate discussion of this item of GSE is required because the equipment is non-deliverable, not subject to the same requirements and constraints as deliverable GSE, and must be tailored to factory test requirements.

The Factory Test Station (FTS) is very similar to the Laboratory Rack Assembly previously discussed. The FTS is used exclusively in the production test areas. There are five panels in the FTS which differ from the ones in the Laboratory Rack. They are:

- TCA Monitor Panel.
- Recorder Control Panel.
- Power Monitor Panel.
- Filter Panel.
- Counter Input Control Panel.

The TCA Monitor Panel and Power Monitor Panel are not used by any other GSE configuration. These panels evolved to provide safety interlocks in the event of TCA or prime power anomalies. The other panels are designed differently than their counterparts in other GSE configurations in order to better accommodate standard factory instrumentation.

Many problems were encountered in the earlier stages of the FTS evolution. There were two main reasons. One was poor workmanship on the stations. The factory build standards were significantly different from the build standards for the field GSE. Solder problems, layout problems, and mechanical problems caused many hours of down time. As time passed, the standards were upgraded. Today, workmanship problems are rarely encountered. The second problem was documentation. In 1961, two system test stations were built. Modifications to one station may not have been made to the other because of the poor movement of the documentation. There was no attempt to standardize both factory stations. The inter-rack wiring was different for each station per the drawings. Proper change controls were not in effect. Changes to the GSE's needed no formed concurrence from the engineering design groups. Thus, all documentation controls were open loop. Much progress has been made since 1961. Documentation procedures now contain effective controls. The drawings are now updated immediately and concurrence from the system design group is obtained before proceeding with any modification.

In 1965, all of the system test sets were modified to reflect the new design phase. In conjunction with the new panel designs, etc., a team of

system design, production, and instrumentation engineers revamped the grounding scheme for all factory sets. The philosophy of simulating the Vehicle grounding as nearly as possible was adopted. A forward ground plate, simulating the vehicle ground plate (to which all MGS units are bolted) was placed within the GSE rack. Prime power was referenced to this point. Monitoring lines from the MGS were referenced to a non-current carrying conductor (MGS signal ground). All of the existing ground loops were purged from the GSE's, and as a result all of the precision meter readings and Sanborn recordings are now tremendously improved. Revamping the grounding in the factory test stations is one of the most significant accomplishments ever made to the FTE's. Improvements which were made to the factory test stations were also made, if applicable, to the field GSE.

5.2.4. Significant Problem Areas in Systems GSE. -

5.2.4.1. Mode Switch Problem. - The two mode switches which were originally used in the MGS Preflight Control Panels had exhibited unreliable operation since early in the program. The switches were printed circuit, plug-in, multi-deck rotary types manufactured by Chicago Dynamic Industries. The switches were used to operate many control functions and also to generate the mode code signals which are transmitted to the computer. Figure 5.2-19 shows a typical rotary switch assembly, and Figure 5.2-20 shows a typical printed circuit switch wafer.

The first problem with these switches became apparent soon after the first GSE sets had been manufactured. This problem was that a very weak spring was used in the switch detent mechanism. The combined frictional drag of the rotors of all wafers in a housing was so great that it overcame the force of the detent spring. With this great amount of drag, the switch shaft would not fall into the detents without assistance. This problem was solved by installing a much stronger spring in all assemblies.

The second problem with the switches was also mechanical. As can be seen from Figures 5.2-19 and 5.2-20, an insertion slot extends from the bottom of the card to mid-way into the rotor. When the cards are inserted in the housing, the rotor slot is aligned with the stator slot. The switch shaft is then turned to a specific position and the card is inserted into the housing. When the card is fully seated in the housing socket, the switch shaft is seated entirely within the rotor. When the switch shaft is rotated approximately 180 degrees, the wafer rotor is in



FIGURE 5.2-19. TYPICAL MODE SWITCH ASSEMBLY

A6712-57

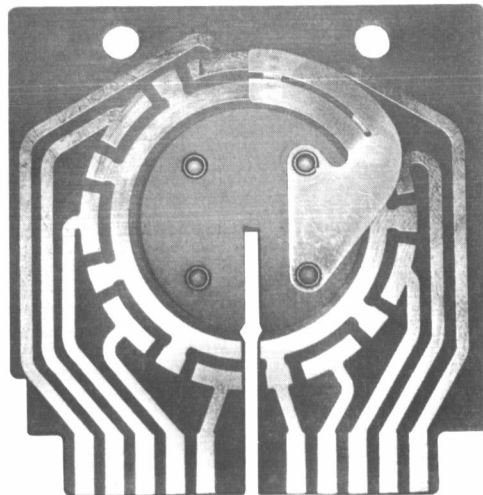


FIGURE 5.2-20. TYPICAL MODE SWITCH WAFER

the position shown in Figure 5.2-21. In this position, the buttons on the rotor contact arms would drop into the stator insertion slot. With all wafers in the assembly dropping into the slot simultaneously, the feel was as positive as a normal position detent. This "false" position was mid-way between two real positions.

This "false" position or detent was a constant annoyance to operators. The only solution was to completely disconnect the switch, rotate the rotor to a new reference position so that the slot did not fall in the usable portion of the switch travel, and rewire the switch according to a new wiring plan. This was considered to be too extensive a task at that time, so operators had to live with this defect.

The third problem which occurred sometime later was the occurrence of conductive bridges between positions on the wafer. The printed circuit paths on the wafers were fabricated with a relatively soft metal. The action of the switch wiper across the printed paths would erode small metal particles from the printed paths and deposit them on the epoxy gap between paths. Eventually, the metal deposits would accumulate sufficiently to bridge the insulation gap between adjacent positions and cause a short circuit. This, of course, resulted in equipment malfunctions. This bridge could be cleaned with a cleaning solvent, and periodic maintenance instructions were issued to all users of the equipment.

Sometime later, Honeywell was given direction to manufacture Trailer Rack No. 3 as discussed earlier. At this time, it was decided to incorporate different type switches in this equipment to eliminate the problems currently being experienced. Langevin rotary switches were selected as replacement mode switches and incorporated in this build. Figure 5.2-22 illustrates a typical Langevin switch.

Honeywell continued to pursue the printed circuit switch problem, and working with the vendor an improved wafer design was obtained. This wafer employed a hard nickel rhodium alloy for the printed circuit paths. This eliminated the problem of conductively bridging adjacent switch positions.

After using these wafers for a period of time, perhaps a year, a new problem arose. Constant wear from the wiper traveling through its arc of rotation began to break through the hard surface of the epoxy board at locations between the printed contacts. Once the hard surface was broken through, continued use and wear caused epoxy powder to accumulate on the metal contacts. This contamination caused poor contact and

A6712-58

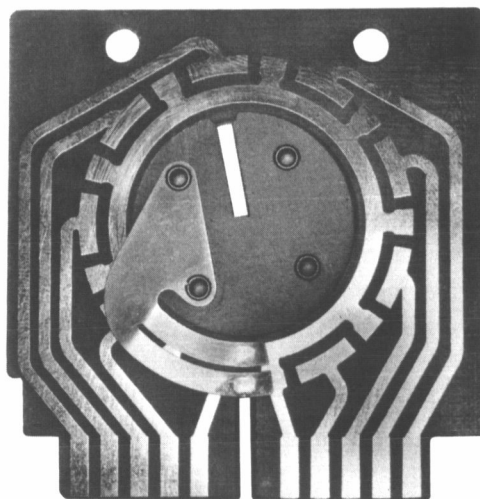


FIGURE 5.2-21. ILLUSTRATION OF WIPER
CONTACTS ACROSS INSERTION SLOT

0168-05

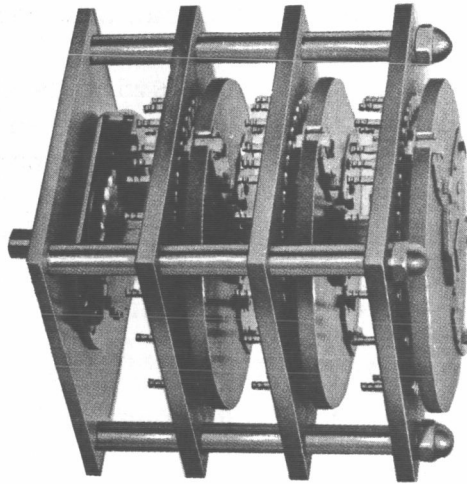


FIGURE 5.2-22. TYPICAL LANGEVIN SWITCH

intermittent operation. Periodic cleaning would again reduce this occurrence of malfunctions, but was still not a permanent solution to the problem.

Working with the switch vendor, other approaches were experimented with in an effort to provide a completely trouble-free switch. However, no satisfactory solution could be found. Thus, it was necessary to continue periodic cleaning as a preventative measure. But the cleaning did not guarantee trouble-free operation, as occasional failures still occurred.

It was obvious that as long as these switches demonstrated unreliable performance, they would pose a potential threat to a launch. Therefore, it was decided that these switches must be eliminated from the Launch GSE.

In February of 1964, MGS Preflight Control panels were exchanged between the launch set at ETR (GSE 6) and the newest Trailer Set (GSE 10). This was the set manufactured with the Langevin switch and was proving to be very reliable.

In mid-1964, GSE 7 was routed through St. Petersburg for rework, while in route from Sycamore, California, to the ETR. The mode switches were removed from the MGS Preflight Control panel at that time and replaced with the Langevin type. This provided both launch sets with the new type mode switch.

About this same time, plans were being made to ship GSE 6 to San Diego for use at CSTS. In view of this, it was decided that a backup panel should be provided at the ETR. Another exchange was then made between GSE 3 (ETR Lab Rack) and GSE 12 (recently built systems test set). Both GSE 12 and GSE 13 were manufactured with the new style switches. With this panel in GSE 3, a reliable backup was assured for the Launch Set in the event that an emergency exchange was needed during a launch countdown.

With this potential problem removed at the launch site, the remaining sets were not considered to be a serious problem. Regular periodic maintenance should greatly reduce the amount of failures. But should a failure occur, a serious impact would not necessarily result.

In 1965, the opportunity arose to replace the switches in all remaining sets as part of the AC-8 modification. Once this was accomplished, this problem area was completely corrected.

5.2.4.2. Heinemann Time Delay Relays. - The MGS Preflight Control originally required 10 general purpose time delay relays. Many of the functions controlled by the relays required double pole, double throw relay operation. The Heinemann relay was chosen since it was one of the few DPDT time delay relays available at the time of the original design. Electronic time delay relays were available, but their cost prohibited their use. The Heinemann relay employs a conventional hydraulic dash pot configuration to develop the time delay.

Some of the relays began to exhibit occasional malfunctions whereby they would either fail to pull-in or fail to drop out. A light tap on the case would usually relieve the malfunction and cause the relay to actuate. But it was found that once this type of failure occurred with a particular relay, it would often repeat at random. Therefore, it became a practice to replace a relay whenever a malfunction was first experienced.

Examination of the relays showed that the armature was free to move laterally by a small amount. By moving the armature to one lateral extreme, it could frequently be made to malfunction. As a result of not being properly centered on its pivot post, the armature would hang-up. The hang-up would occur either upon actuation or release. It was observed that as long as the armature remained roughly centered on its pivot post the relay would function properly. However, as long as the armature was free to move in this manner, shipping, handling, equipment maintenance, or other motion could cause the armature to move to one extreme and become a potential source of malfunction.

With the problem identified, the vendor did not take any immediate action to improve his design to prevent this type of malfunction. Therefore, a search was undertaken to find a better relay which could be used to replace the Heinemann relays as they failed. After a thorough survey of the market, a suitable replacement could not be found. This was primarily because of size and mounting constraints which were placed on a replacement.

A relay was found, however, which was suitable for new designs. This relay, an Agastat, exhibited a pneumatic dashpot time delay rather than hydraulic, and its cost was approximately 5 to 6 times that of the Heinemann. However, its reliability was far superior to the Heinemann model. This relay was incorporated in all future modifications and designs involving time delays.

In 1965, when the AC-8 modification was accomplished, advantage was taken of the opportunity to replace all Heinemann relays with the Agastats in the MGS preflight control. The design modifications, therefore, employed the new type relay for all time delay functions. Scores of the Agastat relays have been operating since that time and not one failure has occurred to date. One or two Heinemann relays are still in use in panels of the GSE which were not involved in the AC-8 modification. However, the relays are used in non-critical monitoring applications.

5.2.4.3. Alignment Reference Unit Servo Motor Problem. - The servo motors in the Alignment Reference Unit are 400 Hz units constructed with a fixed phase and a control phase winding. Both windings are operated from a single phase 400 Hz power source. The fixed phase voltage is shifted 90 degrees by means of a phase shifting network. Depending on the operational mode, these motors drive the Alignment Reference Unit resolvers to any desired orientation under manual control of the operator, or they drive the resolvers to servo loop nulls representing the platform gimbal positions.

In early 1962, a series of servo motor failures began to occur. These failures were characterized by extreme heating, changes in the speed of the motors, and a reduction of the winding dc resistance.

In the ARU panel design, 115 volts 400 Hz was continuously applied to the fixed phase winding. The motor drive switch controlled only the voltage to the fixed phase winding. The switch either applied excitation to the winding to "run", or shorted out the control phase winding to "stop". With excitation on the fixed phase winding and a short across the control phase, dynamic braking effected rapid stopping.

In use, the servo motor was only operated to drive the resolvers for a very small percentage of the total time. The problem could be solved by removing power from the fixed field during the normal standby period. However, another related problem source was noted. The motor inductance and the series phase shifting capacitive network used with the fixed field produced a resonant circuit which is tuned near 400 Hz. As a result of this, an undesirably high voltage appeared on the fixed phase winding terminals.

A modification was made to provide a new phase shifting network which would provide the required phase shift and yet maintain the voltage at the motor terminals within or near the motor rating. The modification removed the fixed phase voltage with a relay controlled by the motor drive

switch, but with a delayed drop out to maintain excitation for a short period after operation. The delayed drop out was required to provide dynamic braking. Without dynamic braking the resolver would coast for several degrees after the motor drive switch is turned off.

The dynamic braking time was empirically determined for several drive motors. Then a relay circuit, having adequate drop out time to allow the dynamic braking to occur, was incorporated into the circuit. After the relay drop out occurs, all excitation is removed from the drive motor. Figure 5.2-23 illustrates the redesigned circuit. There have been no servo motor failures recorded since this modification was incorporated.

5.2.4.4. Grounding and Shielding. - System operational measurements at the DVM Input Control have shown the presence of an appreciable noise content on several signal lines. Field tests indicate that significant noise reduction can be obtained by grounding signal line shields which are presently not grounded. The original laboratory shield termination philosophy was to ground the signal line shields at the airborne ground point. There presently appears to be a deviation to this shield treatment in the laboratory site cabling. In addition, the treatment of some shields and grounds within the laboratory racks differs from that shown on the drawings.

In order to better determine a solution, Honeywell performed a complete wiring checkout of laboratory racks at the ETR and at San Diego. The purpose of this was to identify all shield and ground connections as they currently exist, compare this with the drawings, and determine corrective modifications. Corrective modifications would provide site cabling and GSE wiring which is consistent with prevailing grounding philosophy. A discussion of specific IGS grounding and shielding problems and the prevailing philosophy is given in Topic 6.14, "IGS Electrical Interface and Grounding".

5.2.5. Conclusions. - During the past eight years extensive changes have been made to the Centaur GSE. The changes started only one year after the equipment was put into operation and continued for the next five years. For the most part, these changes were a result of:

Changes in MGS interface and control requirements,

Changes in system operating philosophy,

Changes in system status monitoring and data acquisition requirements.

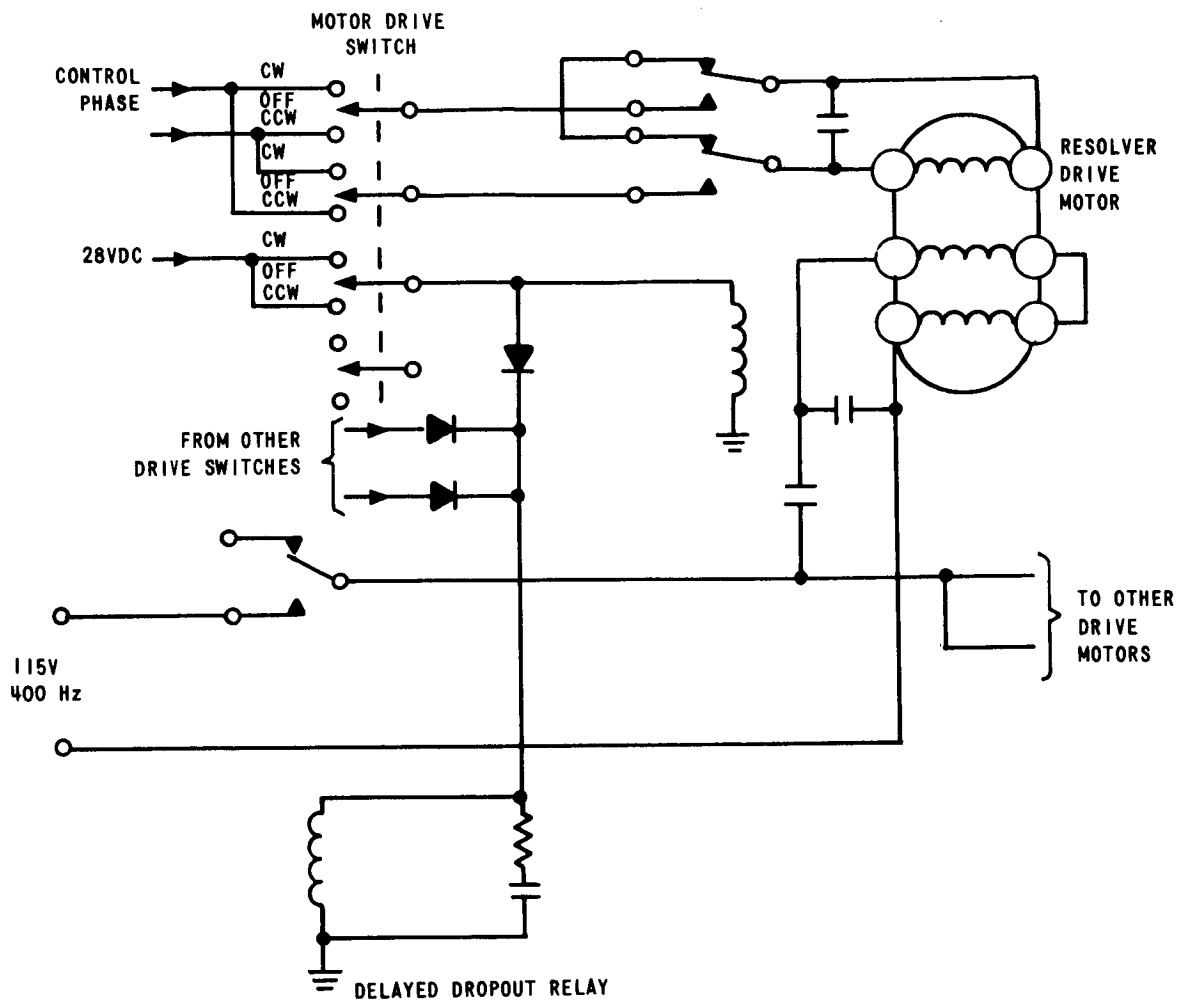


FIGURE 5.2-23. REVISED RESOLVER DRIVE MOTOR CIRCUIT

In retrospect, it can be seen that the program experienced progressive changes in mission and system requirements. Originally, cost was the prime consideration and the objective was to produce GSE hardware with a minimum of documentation and sophistication. As MGS requirements changed, greater documentation coverage and sophistication was required of the GSE. In short, the GSE experienced the evolution from a simple and inexpensive start to a relatively sophisticated program.

To obtain the greatest effectiveness and greatest value from a program, the ideal approach is to identify, at the very beginning the total GSE program requirements. A total IGS system approach should be adapted in planning the GSE program. The planning should include:

All testing programs - components, subsystems, systems, repair and maintenance, locations, schedules, etc.

Total support requirements - all test functions, repair and maintenance, performance, active sites, quantity, schedules, objectives, etc.

Personnel - quantity, locations, functions, education.

Documentation - drawings, analyses, manuals, reports, schedules.

Quality and reliability requirements.

In addition, the cost of the program should be geared to the requirements, rather than the requirements geared to the cost. Some compromises may be necessary, but these problems should be solved in the planning stages.

Once all requirements are identified in detail, prototype hardware should be manufactured and evaluated. The schedule should allow for this phase. The evaluation should include production processes as well as performance.

It was learned from the present program that accurate documentation and good configuration control practices are a must. With our rapidly changing technology, it should be recognized that equipment modifications and improvements will surely be made. The quantity of modifications will be, to some extent, a function of the program length. Preservation of all circuit design details is important to thoroughly executing future design modifications. With original design details available, the details and impact of modifications can be more accurately evaluated.

Topic 5.3

Computer Test Equipment

5.3.1. Introduction. - GSE for checkout and maintenance of the Navigation Computer Unit at the unit, subunit, and module levels has evolved during the course of the IGS development. Computer GSE has been developed and supplied by the Computer vendor except for a test set for in-house semi-automatic computer testing which was developed by Honeywell and uses facility equipment; and, a test set developed by the vehicle contractor for flight program checkout. Because the design and development of this equipment for the most part was accomplished outside of Honeywell, problem discussions are limited primarily to the interface and operational aspects of the equipment.

5.3.2. Fill and Test Unit. - The fill and test unit, in conjunction with other computer manual test equipment, is used to test and troubleshoot the navigation computer and to reprogram the main memory through the use of one word fills or a tape reader input. Operation of the unit is separated into two modes, the fill mode and the test mode. When in the fill mode, information may be entered and/or verified on the memory drum from a perforated tape via the tape reader. The fill mode submodes are as follows: (1) build index, (2) tape fill, (3) verify and (4) word fill.

The test mode permits verification of the computer's operating condition and facilitates computer test, troubleshooting, and maintenance. The test modes submodes are (1) loop, (2) one step, (3) instruction fill, (4) accumulator fill, (5) instruction sync, and (6) instruction stop. Synchronization is provided for monitoring various computer registers and memory locations and entering instructions or operands into the computer. Test points are also available for monitoring specific computer signals without removing the computer covers.

The fill and test unit was designed specifically for use at the computer level test only. The unit contains a large number of switches and buttons to allow performance of the intended operational functions. As such, it is conspicuously lacking in indicator lights or display aids to the operator. It has been found that a high degree of skill and capability is required to effectively operate and utilize the fill and test unit.

Future designs of control equipment for computer test functions should consider human engineering operating principles in providing readily definable controls and indicators to assist the operator in the utilization of the equipment.

5.3.3. Tape Reader. - The tape reader used in conjunction with the fill and test unit enters and verifies program information on the memory drum of the computer by reading a perforated paper tape. The tape reader uses mechanical pin sensing of perforated tape at a rate of one tape character every 125 milliseconds. The tape is advanced by a pin wheel which is automatically stepped immediately after the reading pins have been withdrawn from the tape. The major disadvantage of the mechanical tape reader is the extremely slow read rate. To load the 44 permanent storage tracks requires approximately four hours. Verification requires an additional four hours.

The tape reader operation has been found to be extremely reliable. No modifications have been required over the course of the program. However, today many varieties of high speed photo electric tape readers are available for this application.

5.3.4. Input/Output Test Set. - The input/output test set simulates computer input and output functions. This test set is used to perform checkout and acceptance test of the navigation computer. Specific functions provided by the input/output test set are: (1) computer power distribution and sequence control, (2) mode control, (3) monitoring of D/A conversion, (4) monitoring of telemetry outputs, (5) simulated loads, and (6) counter display of periodic signals. The input/output test set consists of a control panel which provides the power control, mode control, discrete indicators, generation of simulated incremental velocity inputs, and signal switching and monitoring functions. The remaining equipment is commercial and consists of a ratiometer to provide accurate voltage and ratio measurements of the output signals, a square wave generator to provide variable frequency velocity inputs, and a counter.

Modifications to the input/output test set have been limited to: (1) redesign of the delta V (velocity) input circuitry to provide the capability for multiple inputs. This redesign was performed to provide improved simulation of input signals generated by the IMU; (2) redesign of the input/output test set at the time of the GPK-33 computer redesign to: (a) provide the capability to monitor an increased number of discretes (4 to 16); (b) to replace the Hewlett-Packard model 522BR Frequency Counter with a Berkley Model 7360R Frequency Counter. The

Hewlett-Packard counters had been extremely unreliable and sensitive to noise triggering: (c) incorporate a commercial ratiometer to allow measurement of the dc power supply voltages, output signals, and provide an accurate ratio measurement of the D/A converter output. The ratiometer replaced a bridge balance system for the D/A converter measurements. The ratiometer provides a digital readout in decimal form which eliminated the possibility of human error in reading the null in balance system and reduces test time.

5.3.5. Card Checker. - The card checker provides the capability of testing the 21 computer plug-in circuit cards at the card level. The card checker tests all logic gates, flip-flops and other circuit sections functionally. The test can be performed under nominal or marginal voltage and frequency conditions. The card checker is used primarily at the manufacturer's facility for subassembly level tests prior to integration of the subassembly into the computer. Card checkers are available at each of the field sites; however, field use has been extremely limited. Troubleshooting with other unit level test equipment including input/output test set, fill and test unit, and the marginal test set have been found to be sufficient to isolate card level failures to particular functional sections or even the component level.

5.3.6. Marginal Test Set. - The marginal test set provides the capability to test the computer under both 400 Hz prime power amplitude and frequency variations and to test the general purpose section of the computer under simulated computer dc power variations. These tests are conducted under conditions exceeding those experienced under normal operation. The marginal test set consists of computer power control, output discrete monitor points, dc power supplies, and an ac prime power input control for both frequency and voltage level. During the prime power variation test, the navigation computer is assembled in its normal flight configuration. The 400 cycle ac prime power frequency and voltage levels are varied and computer performance is tested over ranges grossly exceeding the operating specification. The +28 volt dc prime power is also varied and the computer similarly tested. The marginal test computer dc voltage variation test consists of separating the general purpose section of the computer from the input/output section. The dc voltages which are normally supplied from the computer power supply located in the input/output unit are disconnected from the general purpose computer section. DC voltages from separate power supplies in the marginal test unit are supplied to the general purpose section of the computer. These dc voltages are varied in a non-tracking manner and the computer operation tested simulating worst case conditions for the dc power supply voltage variations. The input/output unit continues to operate from its self-contained dc power supplies during this test.

The marginal test unit was basically designed as factory test equipment to be utilized at the manufacturer's facility for production and pre-acceptance test only. In 1963, five marginal test units were procured and provided to the field sites for computer troubleshooting tests. The intent was to use the marginal test set to isolate known problems observed under normal computer operating conditions. However, during the course of the program, the marginal test evolved as a criteria for acceptance or rejection of the computer. The test was performed on a routine basis at the prime contractor's facility and at the Eastern Test Range on all computers prior to committing these units to flight. The marginal test set as designed for factory test equipment was subsequently found to be inadequate for this new function at the field sites. A major modification of the test set to correct the following conditions was accomplished in 1966:

1. The test set cabling was redesigned to more closely simulate the flight configuration cable loads on the signals between the computer general purpose section and the input/output unit.
2. Overvoltage protection for the marginal test unit dc power supplies to prevent excessive voltage input to the computer and possible damage was incorporated.
3. The control panel was redesigned to provide better control and indications to the operator and to eliminate all -1 computer and unused functions to reduce the possibility of computer damage through operator error.
4. The velocity simulation input circuitry was redesigned to provide simultaneous multiple positive and negative pulses to allow testing under conditions more closely simulating guidance system operation.
5. The control and adjustment of the dc power supplies was redesigned to provide increased accuracy of control of the input voltage levels.
6. Proper dummy loading for the input/output unit dc power supplies was provided.
7. The power distribution and control system was redesigned to provide positive computer control for I/O test set.
8. Additional test points and indicator devices were added.
9. Proper cooling was provided for the rack by the addition of a blower.

These types of problems can be eliminated in the future by establishment of test requirements and anticipation of future requirements for the test equipment at both the manufacturer and the field sites. Establishment of the types of tests and test requirements is a necessity for all test equipment prior to its final design and manufacture to insure that it will perform the intended and anticipated functions.

5.3.7. Remote Load and Read Test Set (RL&R). - The Remote Load and Read test set provides the capability of filling and reading the computer temporary storage. This fill and read can be performed manually by the use of push-button control switches and displayed on digital indicators or automatically by a tape fill and readout via a paper tape printer. The RL&R is used at the launch site for verification and fill of the temporary storage prior to launch, at the vehicle prime contractor's facility for vehicle guidance integration checkout, and at the guidance system manufacturer's facility for guidance system test and checkout.

The RL&R consists of a control and readout panel, a commercial photoelectric tape reader, a commercial paper tape printer, and a power supply assembly. The logic circuitry in the control panel is a standard CCC logic line used as building blocks to provide the basic logic functions. The digital readout indicators are commercial units. Problems encountered with the RL&R are: (1) unreliable operation of the digital display indicators; (2) intermittent operation of the logic and control functions due to noise.

The digital display indicator problems resulted in a retrofit of all the display units with units that were tested and built to stringent quality and workmanship standards in 1965/66. A test program was conducted on these standard commercial units to insure operation over the temperature and other environmental ranges experienced in the use of the test set. Circuit design and part changes were found to be required and accomplished. The design and part changes along with upgrading of the workmanship and quality standards provide reliable operation of the digital display indicators.

Intermittent operation of the logic and control circuitry was eliminated through a redesign of the test set grounding and signal distribution system. The primary effort involved was the isolation of all signal, power, and chassis grounds. This required the incorporation of isolated power supplies and a complete redesign of the test set signal and grounding distribution. This redesign proved satisfactory and provided reliable operation in the "noisy" launch site environment.

These problems could have been avoided by careful selection and evaluation, including testing, of commercial equipment. Test sets utilized in high noise environments such as those encountered at the launch site or complex checkout and test setups should be designed to insure that the test set is effectively isolated from other on-site noise sources.

5.3.8. Flight Function Generator. - Flight function generator equipment has been designed and used by GD/C to checkout each flight program in the flight computer. Installations of this equipment are located at San Diego and ETR.

The flight function generator provides velocity information which simulates the proposed mission (via delta V pulses) to the guidance computer. The velocity profiles for the particular mission are modifiable by pluggable panels. Thus, a nominal velocity profile can be generated, and non-nominal velocity profiles can be generated to check the flight program accuracy under both conditions. The performance of the program is determined by recording the computer's telemetry output on magnetic tape. (The telemetry output contains vehicle component velocities, discrete signals, and steering vector components.) The tape is then played back into a off-line general-purpose computer for analysis.

In addition to the program accuracy checks, the actual flight computer to be used (and any flight backup computers) are confirmed to be properly programmed and fully operational by this test equipment.

5.3.9. Semi-Automated Computer Testing. -

5.3.9.1. Summary. - In May 1966, Honeywell proposed to NASA that the GPK33 computer testing capabilities be improved by establishing an interface of the GPK33 test system with the existing Honeywell SDS 930 computer controlled test system. The operation was feasible because the Honeywell Automatic Data Acquisition and Conversion System (ADACS) was, and is, fully established and operational, and could be interfaced with the GPK33 test system by minor modifications and equipment additions. Honeywell was directed to proceed with the improved testing capability in July 1966, and the system became operational in November 1967.

The ADACS system is built around a centrally located Scientific Data Systems Model 930 computer capable of simultaneously accepting and processing data from four test sites (Satellite Stations). Only one satellite station is used for semiautomatic computer testing.

The GPK-33 Computer and I/O Test Set are mated to the ADACS by the Interface Test Set, comprised of an interface electronics unit, IBM Selectric input/output typewriter, digital voltmeter (DVM), and an AD/DC converter.

The automated test system provides SDS 930 control of the following functions:

- Control of GPK-33 input discretes.

- Monitoring and recording of the GPK-33:

 - Voltages,

 - Frequency standard,

 - Telemetry output,

 - Output discretes,

 - Mode status.

- Automatic print-out of proper procedural steps.

- Automatic print-out of test reports.

- Automatic recording of historical test data records.

5.3.9.2. Test Operation. - The operator has available five basic test modes as follows:

1. Marginal Test No. 1.
2. Marginal Test No. 2.
3. Unit Acceptance Test.
4. Long Duration Mode.
5. Operator Determined Test Sequence.

The first four modes are "canned" test modes. These modes are made up of various combinations of the basic GPK-33 test routines already programmed into the GPK-33 computer. In the case of the Marginal Test modes, the basic routines are performed under different combinations of power supply and frequency variations. The modes correspond to the existing Marginal Test and Unit Test procedures.

The fifth mode is available to the Operator to permit him to make up his own combination of GPK test routines.

Once an operator has selected a mode via an I/O typewriter command, the test proceeds under SDS control. When an operator action is required during the test, such as equipment setup or oscilloscope monitoring, this action is specified to the operator by the I/O typewriter. The operator can interrupt a mode and repeat GPK tests, change modes or merely

return to the program at the interrupted spot. A record of operator actions is kept by the SDS. If at any time the GPK fails a test due to improper discrete indications or an improper voltage condition the test is interrupted and the operator is notified of the discrepancy via the I/O typewriter.

The basic GPK-33 test routines are:

1. GO Test
2. Memory Sum Test
3. Discrete Output Test
4. Telemetry Output Test
5. Time Accumulation and MECO Test
6. Velocity Meter Test
7. Temporary Storage Validity Test
8. Integration Test
9. Mode Control Input Verification Test
10. Module Static Test
11. Module Slew Test
12. Module Sawtooth Slew Test.

The manual GPK-33 test is performed, using well-established programmed test routines under well documented procedures and sequences. The sequence of tests is under manual control, progress of the tests is monitored manually, and data resulting from the tests is manually recorded. There exists limitations in the manual test operation which are eliminated by automation of the procedures. Significant among these are:

1. Human operator errors in sequencing of tests is an ever present possibility. Occurrence of an operator error necessitates expensive retest and can incur doubt as to hardware validity.
2. Operator errors in observance or recording of test results can result in invalid acceptance of a test result. Such errors are known to have occurred with resulting delay and expense in correction.
3. Intermittent failures can be of a nature difficult to observe under manual surveillance of progress of the test. Automatic continuous monitoring speeds the detection of such failures, cutting test cost and eliminating return and retest in cases where the failure would otherwise escape detection.

5.3.9.3. Problems. - In general, the test set experienced problems of interface incompatibilities, program errors, faulty circuit layout, and faulty components. The problems were systematically corrected. The system at this time is fault free and completely operational.

The major problem areas in the design and development of interface equipment were:

1. Grounding. - The ADACS grounding was incompatible with the interface equipment. The problem was solved by a clean-up of interface circuitry.
2. Component Failures. - A marginal micrologic element in the typewriter receiving register caused a loss of information due to heat sensitivity. A marginal transistor in the decom-decode board of the digital electronics section caused excessive errors. In both instances, a replacement of components and clean-up of circuitry resulted in considerable improvement.
3. Noise. - After clearing up grounding and marginal component problems there still were information errors due to noise. Noise rejection was achieved by narrowing the window for choosing information format.

5.3.9.4. Conclusions. - Benefits of operation of GPK-33 test procedures under the automated system include the following:

1. Adherence to proper procedures is assured.
2. Precise, repeatable test limits and positive failure recognition is assured.
3. Continuous test monitoring increases probability of failure detection.
4. Costly test repetition due to error or unobserved failure is eliminated.
5. A given period of test time provides a much greater amount of actual computer test, since many manual operations are eliminated.

6. Test logs and test reports are prepared with greater speed and precision.
7. Test data history is automatically retrievable.

It is anticipated that the benefits of the automated method will directly result in a reduction in the number of computer RG's, with an attendant cost saving, and should provide an increase in confidence in those computers accepted by the automated test method.

Topic 5. 4

Optical Alignment Control Group

5. 4. 1. Introduction and Summary. - The Optical Alignment Control Group (OACG), a part of the Guidance Launch Control Equipment, is a set of electro-optical equipment which provides the capability at the launch complex to establish initial preflight azimuth alignment of the Inertial Platform by precision optics.

The following discussions pertain to the OACG hardware development and problem areas. The system aspects of optical azimuth alignment are covered in Topic 6. 9.

The OACG is comprised of a long range autotheodolite, associated electronics, operating controls and status displays. The heart of the OACG is the long range autotheodolite which was procured from Perkin-Elmer Corp. The electronics to properly interface the vendor supplied equipment with the IGS, and the operating controls and status displays were designed and manufactured by Honeywell.

During the development, test, and operational use of the OACG, problems encountered were:

1. Power line noise crosscoupling into the control loop.
2. Light spill-over within the detector assembly of the alignment optics which caused false indication of prism acquisition (capture).
3. Degradation of optical sensitivity of the alignment optics with time which reduced operating margin.

These problems were critical to proper operation, but were solved with minor redesign. The noise problem was unique in that it was experienced only in the 36B complex installation (both Complex 36A and 36B are equipped with identical OACG configurations). Although the problem emanated from differences in the 36A and 36B complex site wiring configurations, it was simply eliminated by minor cable changes in the OACG equipment rack located in the optics shelter.

The light spill-over problem in the autotheodolite was also unique in that it was experienced only with one of the units delivered by Perkin-Elmer; and, the problem did not occur until after the explosion of the AC-5 vehicle above the launch pad. Prior to that, the unit had successfully supported both the AC-4 and the AC-5 prelaunch operations. After internal masking adjustments and cleaning at the field site proved unsuccessful, the unit was returned to the Perkin-Elmer factory where replacement of the detector slit prism and the light source condenser mirrors; and, complete optical re-alignment eliminated the problem. The slit prism was replaced because of damage; the condenser mirrors as a precautionary measure. To what extent, if any, temperature and shock from the AC-5 catastrophe contributed to the damaged prism and internal optical alignment shifts could not be determined.

The problem experienced with marginal operation of the long range autotheodolite due to optical sensitivity degradation resulted from aging of the lead sulfide light detector at an abnormally fast rate. The problem source was traced to poor quality detectors supplied to Perkin-Elmer. As Perkin-Elmer was experiencing the same problem with similar instruments supplied to the Saturn program, a new source for the detectors had already been established, and replacement with the new detector alleviated the problem. Although discussion of vendor experiences is beyond the scope of this report, Perkin-Elmer had previously recognized the shortcomings of lead sulfide detectors and was studying (at the time sensitivity problems were encountered) the use of more stable type detectors, that is, phototransistors-- to eliminate problems associated with lead sulfide aging characteristics.

5.4.2. Discussion. - The Optical Alignment Control Group (OACG) is used in conjunction with the MGS and its associated GSE at the launch complex to establish the launch azimuth of the platform. The OACG with the MGS forms an automatic closed loop alignment control system which uses a Perkin-Elmer Model LR2B Long Range Autotheodolite as the alignment error detector. The collimated light beam from the LR2B intercepts the reflecting Porro prism mounted on the stable element of the inertial platform. Any deviation of the Porro prism from the predetermined azimuth reference established by the optical line of sight is detected by the autotheodolite and an electrical signal is produced to torque the stable element back to the required launch azimuth. The OACG is comprised of the following units:

Remote Optical Control Panel (ROCP)
Local Optical Control Panel (LOCP)

Remote Torquing Control (RTC)
Long Range Autotheodolite, LR2B
Autotheodolite Control Panel (ACP)
Equipment Rack.

All units of the OACG are located at the launch complex in the Guidance Optical Alignment Shelter (GOAS) with the exception of the ROCP. The ROCP is located in the Blockhouse. The block diagram in Figure 5.4-1 shows the electrical interface between the various units of the OACG, as well as the external OACG interface with the MGS, the guidance Preflight Control Panel, and contractor controlled equipment.

The ROCP was provided as the master control unit for operating the OACG. It provides all controls necessary for OACG operational use and visual indicators at the Blockhouse for continuous monitoring of the operating status. The design was simple, straightforward relay control logic, and there have been no problems experienced with either the design or use. There have been no changes to the original design. Today, the operational control and monitoring functions of the ROCP have been assumed by the CCLS; however, the ROCP is maintained as a backup.

The LOCP provides, at the GOAS, both operating and test controls for the OACG. In addition, the unit provides the necessary electronics to operate in conjunction with the ACP and/or the manual torquing controls. The following functional capabilities are provided:

Controls for normal OACG operation.

Controls for various test modes of operation to facilitate maintenance and calibration.

Controls for torquing the platform stable element to enable optical capture (acquisition) of the platform Porro prism.

Visual indicators to display OACG operating status.

Front panel controls of the LOCP are interlocked in such a manner that they can only be enabled for use by control from the Blockhouse via ROCP or CCLS control. In this manner, primary control of the OACG is always maintained at the Blockhouse.

A feature of the LOCP that has proven to be very useful is a "Calibration and Maintenance" front panel section. Various test modes of operation are

0166-1798

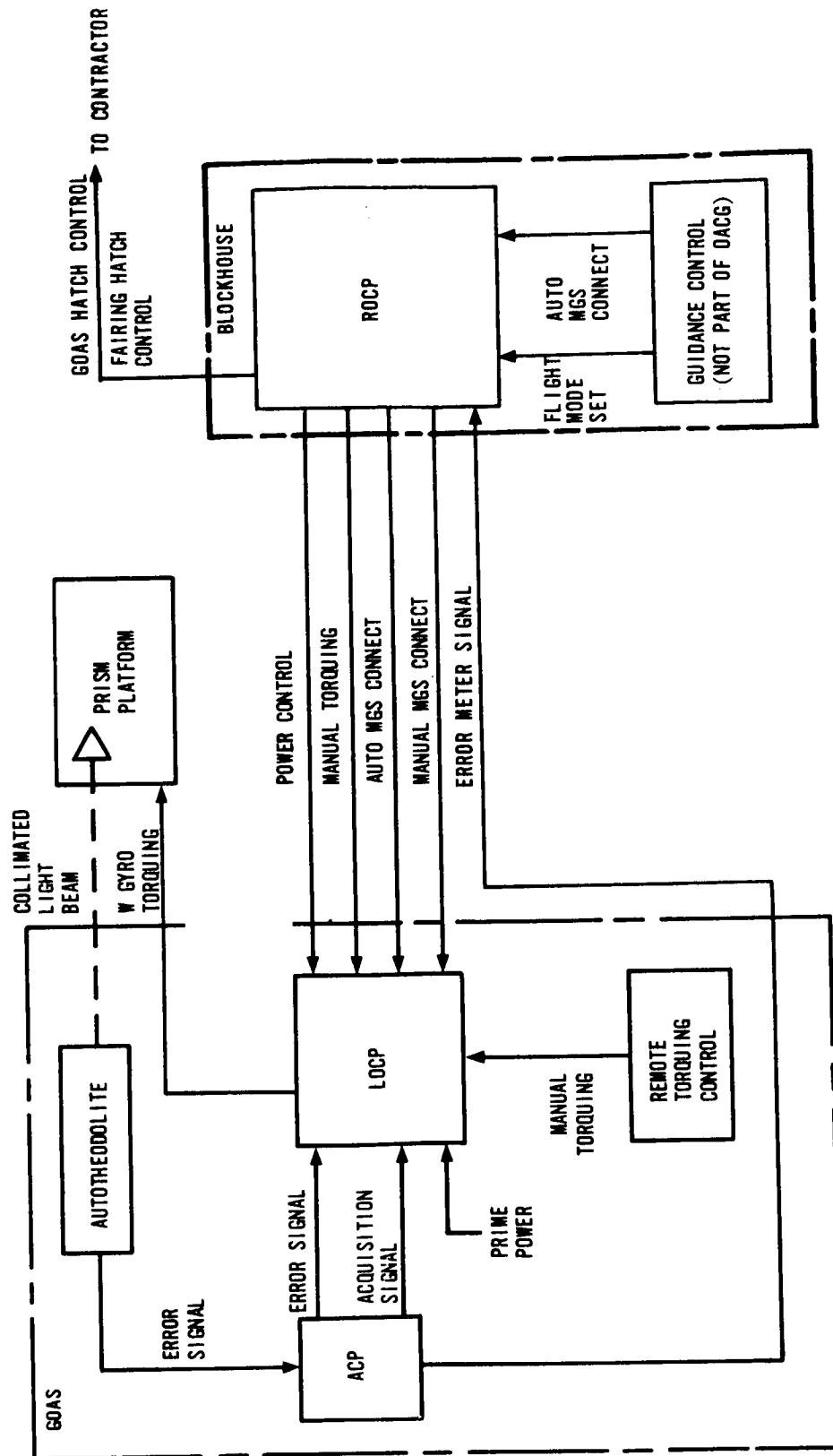


FIGURE 5.4-1. BLOCK DIAGRAM, OACG

programmed by relay logic within the panel which can be readily selected by front panel control. This capability in conjunction with the ready access to power and signal voltages afforded by front panel test points simplifies maintenance and calibration operations. Also provided for maintenance and checkout convenience is the RTC. When connected at the front panel of the LOCP, it provides a hand held manual torquing control so that the operator can control the azimuth orientation of the platform stable element while observing through the autotheodolite viewing optics. When not in use the RTC may be disconnected and stored.

In the LOCP design, vendor supplied modular operational amplifier and power supplies were selected for use. These ready developed devices had been proven by test and usage. Their use eliminated unnecessary development costs. The remaining portion of the LOCP design was straightforward relay control logic. There have been no major problems with the LOCP design. In four years of usage, one power supply failure and one relay failure have occurred in the LOCP (3 units are in service). One minor change has been made in the original LOCP design. This change was made to facilitate continuous recording of the alignment control signal at the Blockhouse. The original design provided for DVM monitoring only at the Blockhouse.

The Long Range Autotheodolite and its associated electronics (ACP) provides the electro-optical system for sensing platform azimuth misalignment. The autotheodolite consists of an autocollimator, mounting fixture, and a reference prism assembly, and provides the following functional capabilities:

The autocollimator transmits a collimated light beam to the platform Porro prism, monitors the reflected light, and provides an electrical output error signal proportional to the prism misalignment.

The mounting fixture supports the autocollimator and provides the means for azimuth, elevation, and translation alignment of the autocollimator for establishment of the optical line of sight.

The reference prism assembly provides the means for transferring the desired alignment heading from a survey instrument to the autocollimator.

The ACP contains the power supplies required for operation of the autocollimator and the necessary electronics, that is, demodulators, buffers, and acquisition control logic-- to interface with the LOCP and ROCP. In conjunction with the autotheodolite, the ACP provides the following functional capabilities:

A \pm dc voltage output proportional to platform prism misalignment and for control and monitoring purposes.

Front panel control for adjusting error voltage output scale factor (gain).

Front panel indicators for visual display of acquisition status.

The autotheodolite and its associated electronics of the OACG were developed outside of Honeywell. No attempt has been made in this report to cover the evolution and the development problem history of these devices. However, since the opto-electrical system of the LR2B unit used in the OACG is basically the same as the LR2A unit which was originally developed by Perkin-Elmer Corp. for the Saturn program, the reader is referred to the following report for supplemental autotheodolite development information:

Perkin-Elmer Engineering Report No. 7030B
Saturn Long Range Azimuth Alignment Theodolite (LR2A)
Dated 6 May 1963
Prepared for: George C. Marshall Space Flight Center, NASA,
Huntsville, Alabama.

5.4.3. Doing It Over Today. - The present OACG is planned for use at the launch complex for final azimuth alignment of the Improved IMG. However, as the IMG will afford no analog control signal interface to the GSE (by design constraint, IMG control will be via computer control), a control loop modification will be required for OACG/IMG interface compatibility. A/D conversion of the present OACG control signal has been recommended to achieve interface compatibility.

5.4.4. Conclusion. - From an operating and performance point of view, there were no major problems experienced with the OACG that would dictate any change in the basic developmental approach to a similar task today. However, a recognized shortcoming of the OACG pertaining to launch support logistics is a limited autotheodolite field repair capability. Therefore, in redoing the job today an effort should be made toward autotheodolite packaging design improvements so that a higher level of autotheodolite repair could be accomplished in the field.

SECTION 6

GUIDANCE AND CONTROL SYSTEM

Topic 6.1

Introduction

6.1.1. Requirements Definition. - System design effort begins with the interpretation of the customer's specification. A complete understanding of the functions to be performed by the system is required. In addition, interface requirements of the system with other systems or sub-systems must be thoroughly understood. This includes electrical, mechanical and environmental interface considerations, as well as mission requirements definition.

The implications of design constraints defined by the customer specification must be fully evaluated.

6.1.2. System Mechanization. - Once the total system requirements are understood, functional and major loop requirements are defined, feasible concepts identified, and mechanizations synthesized. In this stage of the design, it is very important that all pertinent factors are considered and properly weighed. This will include error budget considerations as well as physical and environmental constraints.

6.1.3. Systems Engineering in the Detailed Design Phase. - Systems design effort becomes involved in many areas of hardware design and development. Among some of the more important areas of involvement are:

1. Continued IGS control loop and error model analysis.
2. Electrical and mechanical design and analysis.
3. Power requirements and distribution.
4. Environmental requirements and constraints.
5. Testing and operational requirements and techniques.

In addition to these efforts, the systems engineer must work closely with supporting specialist groups in establishing reliability and design assurance programs compatible with the overall program requirements. A discussion of these and other system design efforts will be discussed in detail in the subsequent sub-topics. In Topics 6.2 through 6.19, emphasis is placed upon the technical aspects of systems design, particularly in terms of the problems, solutions, and significant development of the Centaur IGS evolution.

Topic 6.2

Error Budgeting, Analysis and Model Synthesis

6.2.1 Summary. - Error budgets should be developed for major error sources and detailed error sources at the beginning of a project as guides for designing the IGS and its components to meet mission accuracy requirements. As the design proceeds to the final configuration, the IGS hardware capability takes form and a synthesized error model can then be generated based on analysis and test data. Comparing this error model with the original error budgets provides a basis for guiding and evaluating the design results and design changes. This process is depicted in Figure 6.2-1.

6.2.2 General Description. - The error budget for the Centaur IGS is intended to specify and control the following parameters:

<u>Symbol</u>	<u>Description</u>
SFu	Accelerometer Loop Scale Factor along the U axis
SFv	Accelerometer Loop Scale Factor along the V axis
SFw	Accelerometer Loop Scale Factor along the W axis
ρ_{u-v}	Accelerometer Triad Non-orthogonality, V to U axes
ρ_{u-w}	Accelerometer Triad Non-orthogonality, W to U axes
ρ_{v-w}	Accelerometer Triad Non-orthogonality, W to V axes
β_u	Accelerometer Loop Bias along the U axis
β_v	Accelerometer Loop Bias along the V axis
β_w	Accelerometer Loop Bias along the W axis
CTu	Gyro Constant Torque Drift about the U axis
CTv	Gyro Constant Torque Drift about the V axis
CTw	Gyro Constant Torque Drift about the W axis
MUIAu	Drift due to Mass Unbalance along the U Gyro IA
MUIAv	Drift due to Mass Unbalance along the V Gyro IA
MUIAw	Drift due to Mass Unbalance along the W Gyro IA
MUSAu	Drift due to Mass Unbalance along the U Gyro SA
MUSAv	Drift due to Mass Unbalance along the V Gyro SA
MUSAw	Drift due to Mass Unbalance along the W Gyro SA

<u>Symbol</u>	<u>Description</u>
θ_u	Platform Misalignment about the U axis
θ_v	Platform Misalignment about the V axis
θ_w	Platform Misalignment about the W axis

The allowable uncertainty of each parameter is a function of the Centaur vehicle missions and the initial flight alignment of the inertial triad. The control of the parameters is a function of inertial component accuracy, associated circuitry accuracy, the method of calibration and compensation, when and where the final calibration is performed (that is, on the launch pad or in the lab), and the time stability required between final calibration and flight.

6.2.3. Evolution of Centaur Error Analyses. - The initial approach to establishing the -1 Centaur error budget was confused by the need for multi-mission capability, along with a lack of knowledge of all the error source magnitudes within the IGS. As a result, the initial performance requirements were quite rigid and poorly allocated among the parameters.

GD/C, Honeywell, and NASA recognized the shortcomings of the original performance requirements. Several error analyses were developed and published during the 1961-62 period on the -3 program. Some of these analyses, though limited in the scope of individual error source details, attempted to predict the accuracy which could be achieved by specific IGS design improvements (see Figure 6.2-2).

A major limitation to developing a complete error model (with error sources, mission sensitivity coefficients, etc.) was the definition of the missions and their overall requirements. The mission definition work was performed in late 1962 and early 1963 in order to properly define the IGS hardware and software requirements.

In November 1963, a formal Error Analysis Committee was formed with representatives from GD/C, Honeywell, NASA, and TRW. The committee was charged with the responsibility of developing a complete error analysis of the Centaur guidance hardware as it then existed. To accomplish this task, the committee developed an error model from available data and requested individual component and circuit tests where additional information was needed. The Committee assumed the added responsibility of recommending systems changes for both hardware and procedures, based upon the error model, and also recommending areas for further study of potential improvements. One recommended change, in 1964, was the replacement of the GG116 accelerometer with the GG177 model (ref. Topic 2.3).

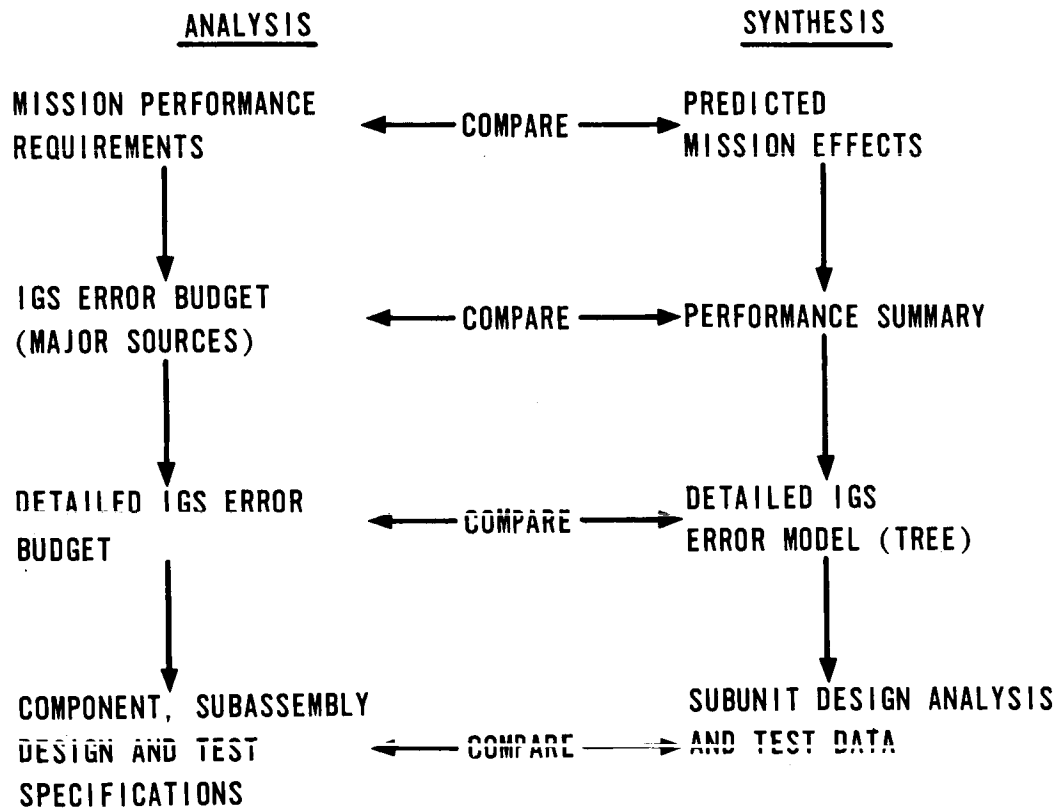


FIGURE 6.2-1. IGS ERROR SOURCE CONTROL
(PREFLIGHT AND FLIGHT)

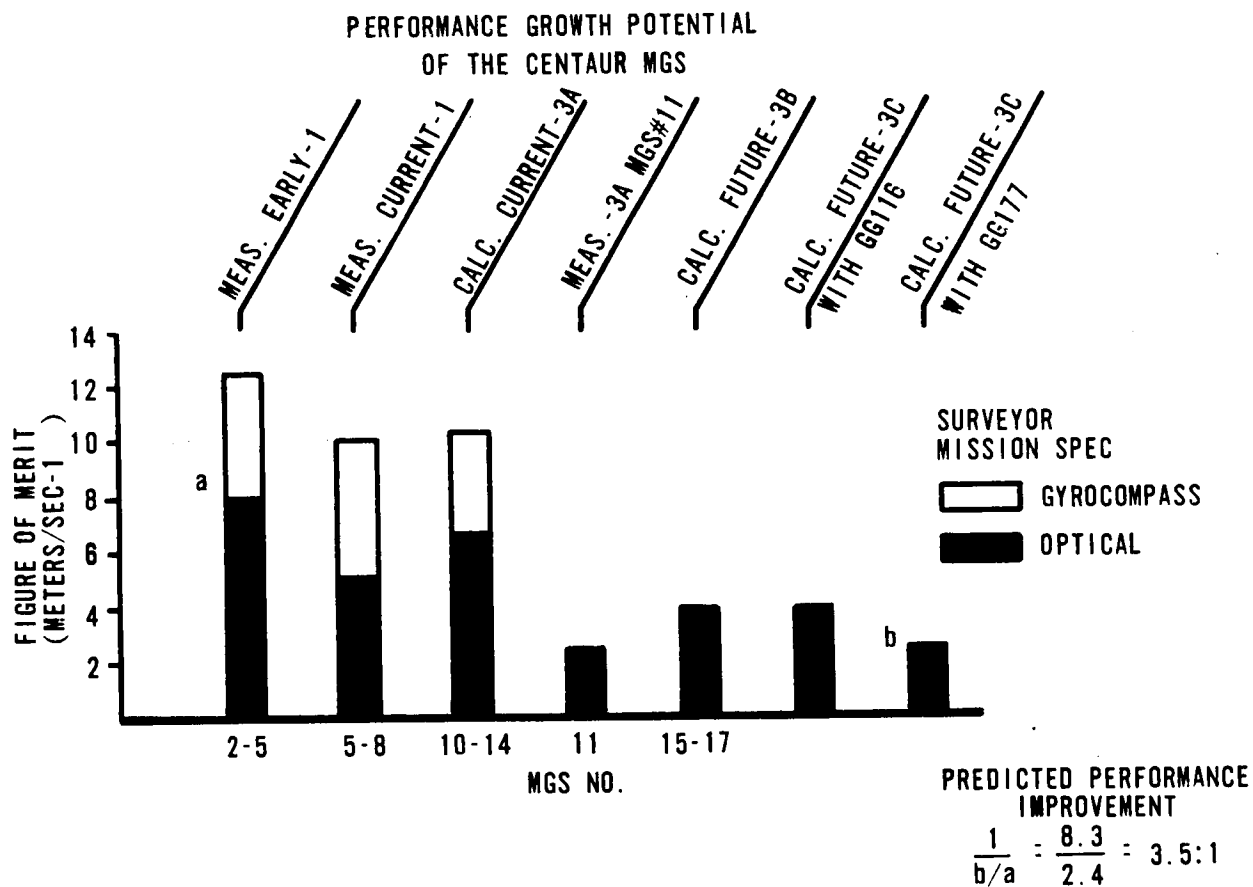


FIGURE 6.2-2. PREDICTION OF HARDWARE CAPABILITY
IMPROVEMENT MADE IN 1962

The Committee efforts resulted in a preliminary error analysis and a synthesized error model, which were published for the Committee, by Honeywell, in May 1964. As the guidance system was improved during the 1964-67 period, amendments to the original analysis were prepared by Honeywell, reviewed by the Committee*, and published. In June 1967 Honeywell published a completely revised error analysis and synthesized error model representing the present Phase II PIP system configuration and calibration procedures. The new document is self-contained and requires no reference to the previous editions. It is one of the most complete documents of its kind.

Use of system error budgeting techniques was made more meaningful through reference to the detailed error model. The Error Model itself was developed on a strong analytical base, but with the inclusion and interpretation of component, unit, and system level test data. As such, it provided a major design tool in the improvement of the IGS, so that efforts could be effectively directed toward providing the maximum performance improvement at minimum cost.

An Error Model construction diagram is shown in Figure 6.2-3. Error trees were generated for each significant error source. The error tree shows each factor which can be expected to contribute to the total error and/or uncertainty. In the construction of the error tree for a given parameter, the effects of manufacturing procedures and tolerances, testing and measuring errors, calibration errors, alignment errors, stabilities, and deviations caused by temperature changes, thermal gradients, magnetic fields, orientations, line transients, and vibrations are evaluated wherever applicable. Figure 6.2-3 indicates how the technique is employed. From the figure it will be noted that once the contributing error sources are evaluated and an error magnitude determined, mission sensitivities for each mission of interest are utilized to determine the velocity correction (δ FOM) due to each system error. Combining the δ FOMs for all the errors yields the predicted system performance capability when committed to the individual missions.

The model is divided into two sections, one for preflight error build-up and one for the inflight error contribution.

From the IGS error analysis, two other error analysis tools have evolved: (1) a synthesized shift error model and (2) an internal error budget. The shift error model is a tool for evaluating and updating

* By this time the committee had been given the formal title of LEAP (Lewis Error Analysis Panel).

preflight performance of the guidance system and provides a basis for assessing performance specifications. The internal error budget provides a control of parameters for each unit of the system such that, when integrated, the overall system requirements will be met.

Table 6.2-I shows the evolution of the performance shift requirements of the IGS from the -1 days to the IMG (1967). Using the -3 program (Surveyor) requirements as the baseline, the reader will note subsequent tightening of IGS performance requirements, which were accompanied by steady improvement in IGS hardware capability. That improvement may be seen in Figure 6.2-4, which shows calculated FOMs based on system acceptance data. The FOMs are shown accumulative by IGS for each phase of the Centaur Program in the 1964-1967 period. Also shown are actual Midcourse Correction Requirements (MCR) for Centaur flights during that time.

A representative direct ascent mission was used for the calculated FOMs. However, in evaluating IGS acceptance data, several missions, both direct ascent and two-burn, were commonly used. In addition, the acceptance data were combined in various ways to show the limits of calculated capability.

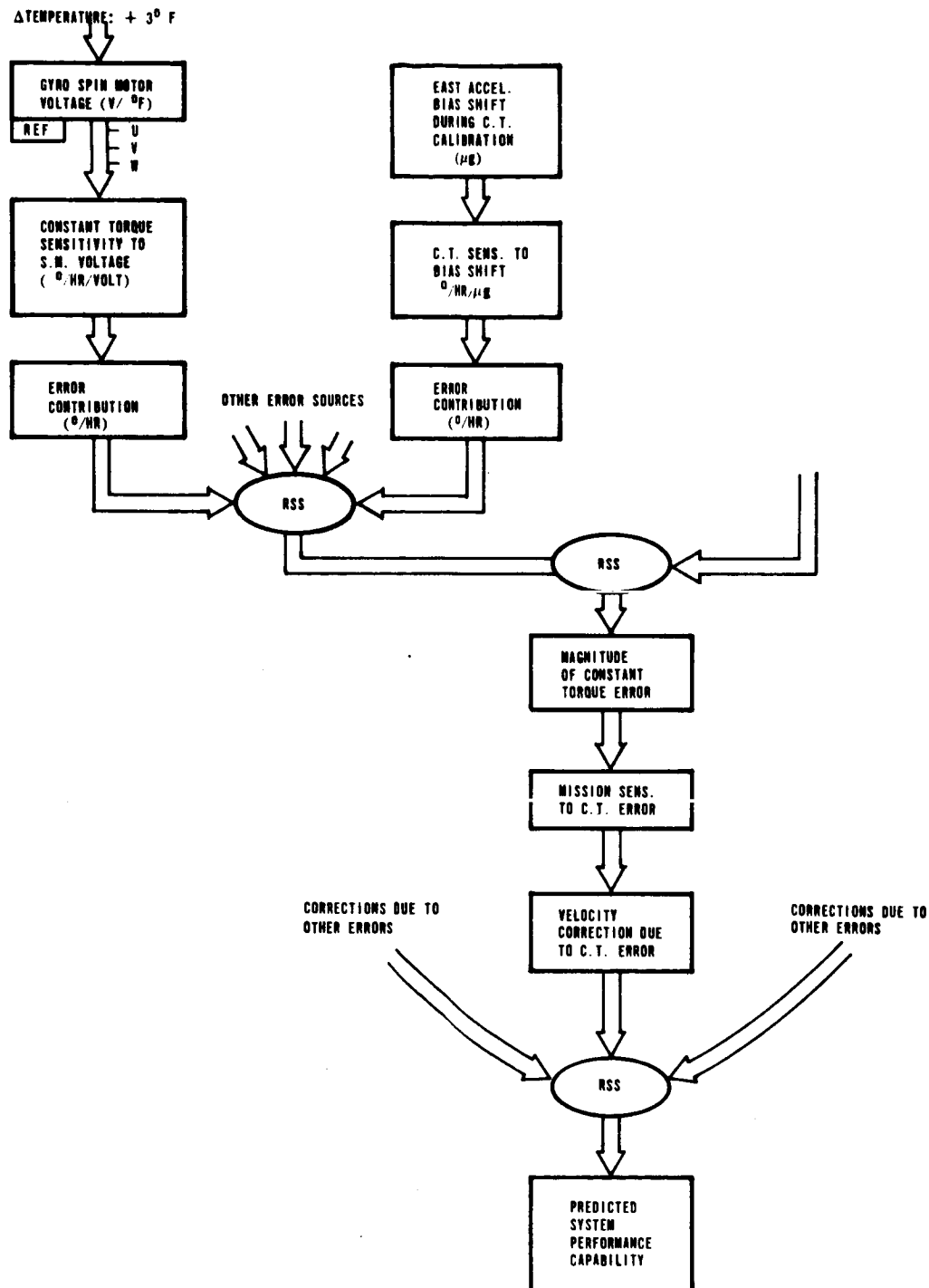
PREFLIGHT CONTRIBUTIONIN-FLIGHT CONTRIBUTION

FIGURE 6.2-3. ERROR MODEL CONSTRUCTION DIAGRAM

TABLE 6. 2-I
EVOLUTION OF PARAMETER SHIFT REQUIREMENTS (ACCEPTANCE TESTS)

Parameter	Dash-1 Early Dash-3		Later Dash-3 ‡		PIP Phase I		Original PIP Phase II		Late PIP Phase II (ADD-6 Contract)		Improved IMG		Unit
	NCD	CD	NCD	CD	NCD	CD	NCD	CD	NCD	CD	NCD	CD	
SFu	210	210	210	N/A	210	280	160	280	120	220	90	120	PPM
SFv	210	210	450	N/A	350	350	160	280	120	220	90	120	PPM
SFw	210	210	450	N/A	210	280	160	280	120	220	90	120	PPM
pu-v	120	120	450	450	450	450	238	340	185	270	175	175	μrad
pu-w	190	190	750	750	490	490	238	340	185	270	175	175	μrad
pv-w	190	190	1500	1500	490	490	238	340	185	270	175	175	μrad
βu	160	160	300	N/A	200	270	131	230	100	185	75	100	μg
βv	160	160	480	N/A	300	310	131	230	100	185	75	100	μg
βw	160	160	480	N/A	200	270	131	230	100	185	75	100	μg
CTu	0.12	0.135	0.36	N/A	0.35	0.52	0.19	0.36	0.15	0.29	0.11	0.17	°/hr
CTv	0.12	0.135	0.18	N/A	0.25	0.42	0.19	0.36	0.15	0.29	0.11	0.17	°/hr
CTw	0.12	0.135	0.36	N/A	0.35	0.52	0.19	0.36	0.15	0.29	0.11	0.17	°/hr
MUIAu	0.17	0.36	0.90	N/A	0.42	0.56	0.26	0.40	0.20	0.32	0.13	0.17	°/hr/g
MUIAv	0.17	0.36	0.36	N/A	0.25	0.42	0.26	0.40	0.20	0.32	0.13	0.17	°/hr/g
MUIAw	0.17	0.36	0.90	N/A	0.42	0.56	0.26	0.40	0.20	0.32	0.13	0.17	°/hr/g
MUSAu	0.17	0.63	0.63	0.63	0.40	0.60	0.38	0.46	0.30	0.36	0.30	0.37	°/hr/g
MUSAv	0.17	0.63	0.63	0.63	0.40	0.60	0.38	0.46	0.30	0.36	0.30	0.37	°/hr/g
MUSAw	0.17	0.63	1.20	1.20	0.40	0.60	0.38	0.46	0.30	0.36	0.30	0.37	°/hr/g
θu *	210	N/A	210	N/A	210	N/A	210	N/A	200	N/A	185	N/A	μrad
θv *	210	N/A	210	N/A	210	N/A	210	N/A	200	N/A	185	N/A	μrad
θw *	130	N/A	750	N/A	730	N/A	727	N/A	250	N/A	470 **	N/A	μrad

* Absolute values (not shifts)

** 120 day stability

NCD = No-Cooldown Shift

CD = Cooldown Shift

‡ From initial Surveyor mission requirements

0166-878

DA = DIRECT ASCENT MISSION
 2B = TWO BURN MISSION

CALCULATED PERFORMANCE IMPROVEMENT

$$\frac{1}{b/a} = \frac{2.9}{1.1} = 2.6:1$$

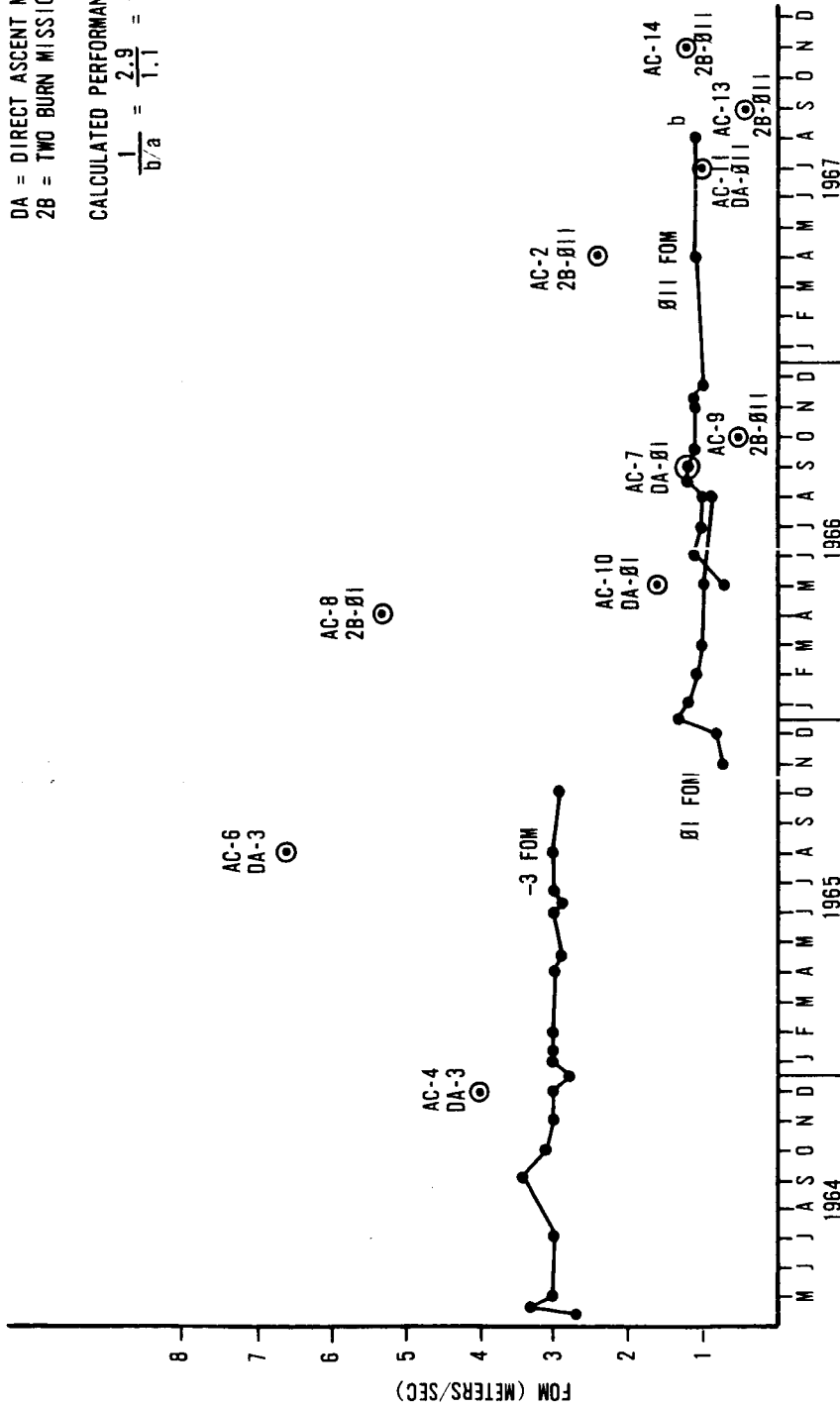


FIGURE 6.2-4. CALCULATED FOM'S FROM ACCEPTANCE DATE ACCUMULATIVE BY SYSTEM FOR EACH PHASE OF PROGRAM WITH ACTUAL FLIGHT MCR'S SUPERIMPOSED

Topic 6.3

Major IGS Control Loops

6.3.1. Introduction and Summary. - This topic discusses the evolution of major IGS control loops. The major loop functions are:

1. Velocity measurement.
2. Platform stabilization.
3. Platform coarse align.
4. Steering and coordinate transformation.
5. Automatic self leveling.
6. Final azimuth alignment.
7. Active temperature control loops.
8. Gyro torquing.
9. MGS and GSE mode control.

This introduction to the major IGS control loops explains the evolution of the analysis and synthesis techniques applied on the Centaur program, with a brief description of the effects on hardware mechanization and test procedures.

6.3.2. The -1 System. - The design of the -1 Centaur Inertial Guidance System was established early in 1959. This design included as its objectives, an all-attitude capability, operation in a space environment for an extended period of time, and capability for self-alignment about the vertical and level axes. At this time, Honeywell was pushing the "state of the art" in many of the control loop designs. Centaur, during the -1 program, was also plagued by a serious lack of test bed hardware with which to prove equipment capability and reliability and permit sound engineering approaches to identifying and solving design problems. This problem area was created by lack of funds, schedule problems, and a lack of programmed available hardware to support developmental tests. The -1 system was not subjected to formal, system level, design proofing tests. These tests generally consist of at least vibration and temperature/altitude tests. These tests, had they been performed, could have aided the analysis in defining the marginal conditions in the major IGS control loops. The -1 system, with regard to the control loops, was a system of marginal individual circuits, which combined to make up marginal control loops. There was some analysis

and testing done on the -1 IGS control loops. When the tests indicated weak areas in the original design, these circuits were redesigned using a more conservative design philosophy, with greater safety margins.

The -1 hardware analysis and test history shows a limited progression of initial advancements in test techniques and improvements in design. These included:

1. Nominal analysis to define loop/circuit requirements, followed by nominal circuit design and hardware build.
2. Initial definition of measuring and testing techniques.
3. Development of limited fault isolation processes.
4. Higher performance circuits were required, but only partially developed. Advancements in solid state components permitted circuit improvements in some areas, but component limitations precluded other improvements.
5. Several electrical and functional improvements were evolved:
 - a. The accelerometer rebalance current supply (ARCS) required higher gain, broader bandwidth, and better stability. Limited improvements were made but the problem was not completely solved. (Ref. Topic 2.15.4.)
 - b. Accelerometer loop rate networks were improved, permitting 11g operation. (Ref. Topic 2.15.4.)
 - c. Critical grounding, affecting control loop operation, was improved.
 - d. Testing of the -1 Coupler indicated that power being dissipated on the Frequency Divider Board was causing the 7.2 kHz gyro signal generator excitation to approach a thermal runaway condition. Transistors were removed from the board and hard mounted on the coupler housing to dissipate heat more effectively and prevent thermal runaway.
6. A new specification was written for all summing and sensing resistors to obtain more stable and reliable parts.
7. A partial thermal analysis and mapping test was performed on the -1 platform. This effort indicated major system performance degradation due to thermal gradients on the stable element, caused in part by block heater cycling. (Ref. Topics 2.8 and 2.10.)
8. A linear analysis of the -1 gimbal control loops revealed poor gain and phase margins in the first three gimbal loops. The analysis was confirmed by test. The problem was alleviated in the early -3 hardware, by redesigning the appropriate rate networks. The condition of "border-line" gain and phase margins was not eliminated, however. (Ref. Topic 6.5.)

6.3.3. The -3 System. - With the advent of the -3 System in 1961, Honeywell was able to correct some of the known deficiencies in the major control loops. However, the lack of complete loop analyses was still a drawback.

The year 1962 was the beginning of in-depth analysis and testing. An example of this was the accelerometer loop. A program was undertaken to develop an accelerometer loop which was less sensitive to noise input and more predictable in performance. This loop incorporated an inner loop which integrated rate (that is, used lag compensation), instead of increasing the lead compensation in the forward loop. Thus, the overall PRE loop was made much less sensitive to noise. Important contributions to the improved accelerometer loop were accomplished through:

1. Analysis and optimization, using known methods of linear analysis, resulted in a known transfer function for the entire loop.
2. Analog and digital computer simulation was used extensively before and after hardware testing, both to verify results obtained from the testing and to check areas that were difficult to test on actual hardware. An example of a difficult test item is a step "g" input to an accelerometer loop.
3. Measured data were obtained from:
 - a. Vibration tests.
 - b. Centrifuge tests.
 - c. Test Bed System operation in a static one "g" environment.

The "integrated rate" accelerometer loop, which was incorporated into all -3 flight systems, upgraded performance in the following areas:

1. The noise sensitivity of the accelerometer loop was reduced to a level where it was no longer an impairment to system delivery or flight success.
2. Static gain was increased by over five to one, reducing the steady-state pendulum offset and loop threshold.
3. Pendulum swing under transient acceleration inputs was reduced by factors greater than two to one.

Late in 1963, the Centaur program initiated a detailed error analysis program aimed at synthesizing all known or potential errors into a complete error model. The format was an "Error Tree" model, illustrating the manner in which each error source contributed to the total system error. Each "error tree" permitted propagation of forcing functions and

error sources throughout a given mission model to yield the probable mission effects. The error models were sufficiently flexible to permit examination of errors during any phase of calibration, as well as predicting in-flight errors for various missions.

All of the major performance errors in the IGS control loops were detailed in this error analysis. Among the forcing functions analyzed for each individual error source were:

1. Temperature.
2. Operating and storage time.
3. Magnetic fields (internal or external to MGS).
4. Line transients in prime power.
5. Preflight calibration techniques.

In 1964 and 1965, a detailed analysis was performed on the disturbing torques into and the performance of all four gimbal stabilization loops. These studies were performed utilizing a Honeywell 800 digital computer, a Bendix G-15 digital computer, and a PACE analog computer. Computer results were compared with test results from a test bed platform and platform electronics subsystem. The objectives of the analysis were to:

1. Detail loop parameters and servo loop response characteristics.
2. Detail the subsystem ability to meet static and dynamic accuracy specifications.
3. Investigate disturbance torque transmission, deadzone, and the spring effect phenomena.
4. Define and verify an optimum step response test to measure dynamic performance (response time and relative stability and margin) of the loops.
5. Establish the validity of the mathematical model and computer simulation by test results on test bed hardware.

The results of the analysis showed the servo characteristics were consistent with good servo loop design, except that complete worst case conditions (due to circuit parameter variations) were not evaluated.

A very detailed analysis of the -3 coarse alignment servo loops was performed in 1965. The purpose of this analysis was to summarize the loop mechanization, operation, and performance in relationship to overall guidance system requirements. Emphasis was placed on how the various

loop elements interface, rather than on detailed circuit description. Calculations were performed for:

1. Alignment accuracy.
2. Stability margin.
3. Frequency response.

The conclusion reached in this analysis was that the coarse alignment servo performance was adequate to meet the overall guidance system requirements. (Ref. Topic 6. 6.)

6.3.4. Phase I PIP Program. - Early in 1964, NASA and Honeywell initiated a product improvement program (PIP) to insure compatibility with the overall requirements of the planned missions. With regard to the major IGS control loops, upgrading of performance was to be accomplished by:

1. Incorporation of the more stable accelerometer into accelerometer loops.
2. Stabilization loop improvements.
3. Steering loop resolver chain analysis and test, including a complete worst case analysis, in order to bound, and if necessary, improve gain stability, reduce phase shift, and improve absolute accuracy.
4. A worst case analysis of the Gyro Pattern Field Supply.
5. A detailed thermal analysis of the Coupler.
6. Platform TCA analysis to ensure adequate control margins at the specified extremes of platform skin temperature.

The following items were proposed for formal analysis, but not performed during Phase I PIP:

1. Platform worst case circuit analysis.
2. Platform slip ring stress analysis.
3. Inertial component alignment study.
4. Platform Electronics worst case circuit analysis.

The original PIP proposal included incorporation of the GG177 accelerometer. Utilization of the 177 was delayed, though, by device evaluation testing, until after the product improvement program began. However, the flight hardware modifications did include the GG177 and Phase I PIP, and hence, the two were considered as one change to the system. A dual section fourth gimbal resolver was also added at that time.

6.3.5. Phase II PIP Program. - With the incorporation of the 177 accelerometer, Honeywell proposed a Phase II PIP program primarily for reliability improvements. This proposal was accepted by NASA and the resulting reliability performance and improvements to the major control loops were obtained by*:

1. An error analysis which was updated for the 177 accelerometer loop.
2. A revised Coupler thermal analysis and improved thermal distribution throughout the coupler improved PRE loop thermal stability.
3. Parts stress analysis and a new component derating policy, which reduced the likelihood of loop degradation or catastrophic failures.
4. Elimination of the gyro pattern field current supply board, which simplified the gyro torquing mechanization.
5. Additional prototype testing which insured that modified loops met all performance and environmental requirements before being committed to production.
6. Small stop angle gyros which improved gyro drift due to FLRT.

In early 1967, error analysis of the major IGS control loops was revised for the Phase II PIP guidance system configuration. The changes to the IGS covered in this error analysis* were:

1. Improved velocity measurement performance with the incorporation of GG177 accelerometer and Phase II PIP electronics (especially the new ARCS).
2. Smaller gyro gimbal stop angles and better balanced spin motors.
3. Automatic nonoptical measurement procedures for accelerometer misalignments.

In addition to evaluating the hardware changes, testing and analysis in the Phase II PIP Program more precisely defined the overall characteristics of the IGS hardware.

6.3.6. "Doing It Over Again" - The IMG. - The major control loops used in the IMG are being redesigned to upgrade performance, simplify circuitry, and increase reliability over the present configuration. Prior knowledge obtained from the IGS development, in terms of analysis, synthesis, and test procedures, is being applied to the IMG. Worst case

* For more details on these items, see specific topic in this report.

analysis techniques are being utilized for every major control loop function and circuit. Test requirements are being defined before actual testing begins, not after (see subject 6.17.2.6). Prototype units are undergoing tests prior to commitment of the final design to production build. Even though the present state of the art is again a consideration, the knowledge gained by previous IGS experience is being employed to circumvent the early IGS shortcomings. The objective is to gain an overall, better-balanced, more reliable design.

6.3.7. Conclusions. - From the above summary and from the detailed loop discussions in the following pages, it becomes readily apparent that many lessons on the timely use of analytical techniques have been learned during the Centaur IGS development. To sum it up, for any new guidance hardware program, the emphasis should be placed heavily on early and effective use of analytical tools, that is, "Homework before hardware!".

In the topics which follow, the reader will gain further insight into the individual IGS control loops, their evolution, problems and solutions thereto, throughout the Centaur IGS development program.

Topic 6.4

Velocity Measurement Loops

6.4.1. Velocity Measurements. - The use of the digital rebalance technique to close the accelerometer loops was relatively an innovation in the early Centaur days. Though many advantages were gained by this technique, there were some disadvantages. The main disadvantage, which is evident in the Phase II GG177 accelerometer configuration, is the accelerometer's Torque Generator Reaction Torque (TGRT). TGRT is a function of frequency and current into the torquer. TGRT is different for each accelerometer. The TGRT effect results in accelerometer bias changes with limit cycle pattern variations, which in turn are "g" sensitive. (See Topic 2.3, Platform Accelerometers, for details on TGRT.)

The concept of measuring velocity has not changed from the initial -1 Centaur design. The accelerometer digital rebalance loops simplify this task. The digital information is sent to the guidance computer in the form of "plus and minus" pulses that are defined in terms of velocity increments (0.1 fps). The computer then differentiates or integrates these net pulses with respect to time to get acceleration and position, respectively.

Included in this topic are:

1. History/evolution of the digital rebalance loop.
2. Functional description of the loop.
3. How the loop is calibrated.
4. Accelerometer Bias and Scale Factor equations.
5. Maximum capability of loop.
6. Conclusions.

6.4.2. Background Summary. - To properly understand velocity loops the background and evolution of accelerometer pulse rebalance loop development should be examined. First, several available inertial techniques were considered. They were:

1. PGA's - These devices compromised the platform size.
2. Vibrating string accelerometers - At that time they were relatively unstable and unproven.
3. Pendulous accelerometers - They were developed to the point of dependability and were available.

For the Centaur IGS, the pendulous accelerometer was chosen as the optimum method of achieving acceleration information in a digital form. Early planning requirements were limited by both electronic and inertial components. At that time the stability requirements were approximately 300 PPM. Nonlinearities were undefined, and no historical data was available. Analog techniques were considered, but A/D converter limitations were severe, the weight and power were high, plus the accuracy and stability were no better than 0.05 percent. Digital pulsing of the rebalance torquer, using a constant energy, "bang-bang" technique, eliminated A/D converter problems and presented other advantages: (1) (At that time), torquer generator reaction torque was thought to be constant; (2) torquer thermal input was constant; and, (3) pulse rebalancing offered low torquing rates, which minimized capacitance leakage problems. There was also a minimum amount of temperature control electronics necessary. Figure 6.4-1 shows a summary of the tradeoffs for the "bang-bang" rebalance technique. Figure 6.4-2 shows an alternate mechanization, a pulse-on-demand loop, which has good resolution, but poor linearity at high "g's" because of torquer heating effects.

Honeywell gained some of the original background for the pulse rebalance loop with the GG56 accelerometer operated in analog loops, when it found there was a need for a digital readout of velocity. While the GG56 was designed as an analog device, preliminary studies indicated that it could be rebalanced with pulses. Consideration of performance parameters of the GG56 and system requirements led to the choice of 0.1 ft/sec/pulse velocity resolution and 3,600 pulses/second as the pulse rate. At that time a study of potential sources of nonlinearities in the accelerometer led to the choice of bang-bang rebalancing to minimize effects of nonlinearities. Analytical work indicated that the loop could be mechanized as shown in Figure 6.4-3. Early analysis defined gain and servo compensation to achieve a $10^{-5}g$ threshold. Simulations of the loop on PACE analog and Bendix digital computers indicated satisfactory loop performance over the full 10g dynamic range.

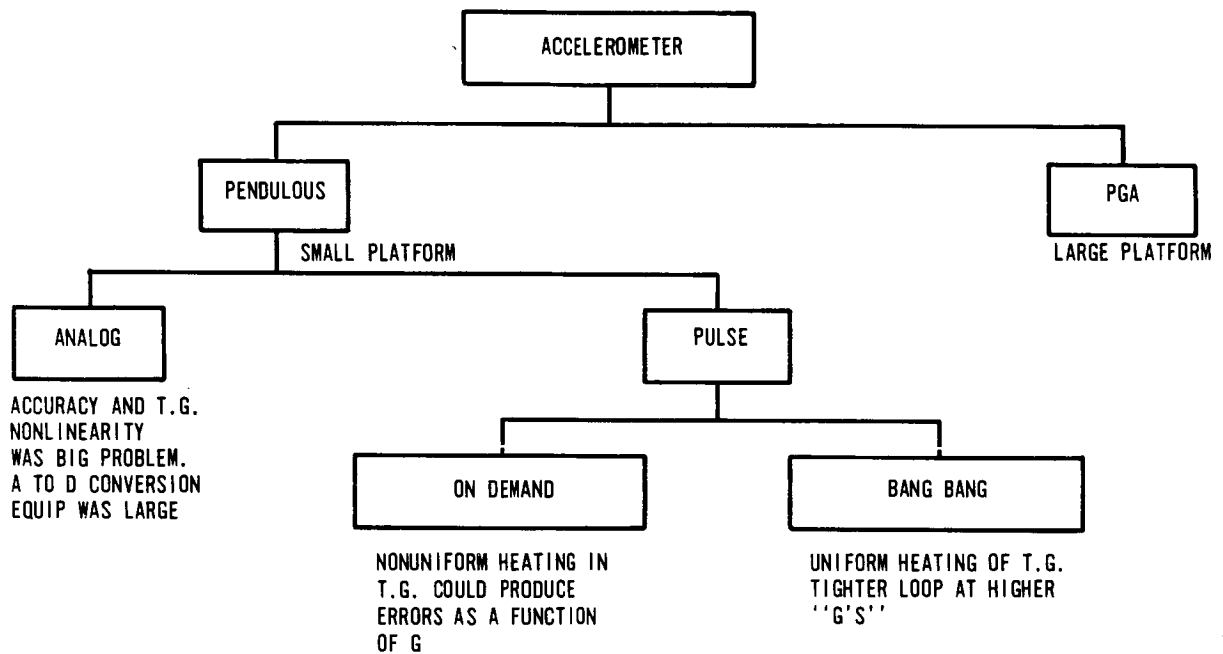


FIGURE 6.4-1. EVOLUTION TO BANG BANG REBALANCE TECHNIQUE

0168-1008

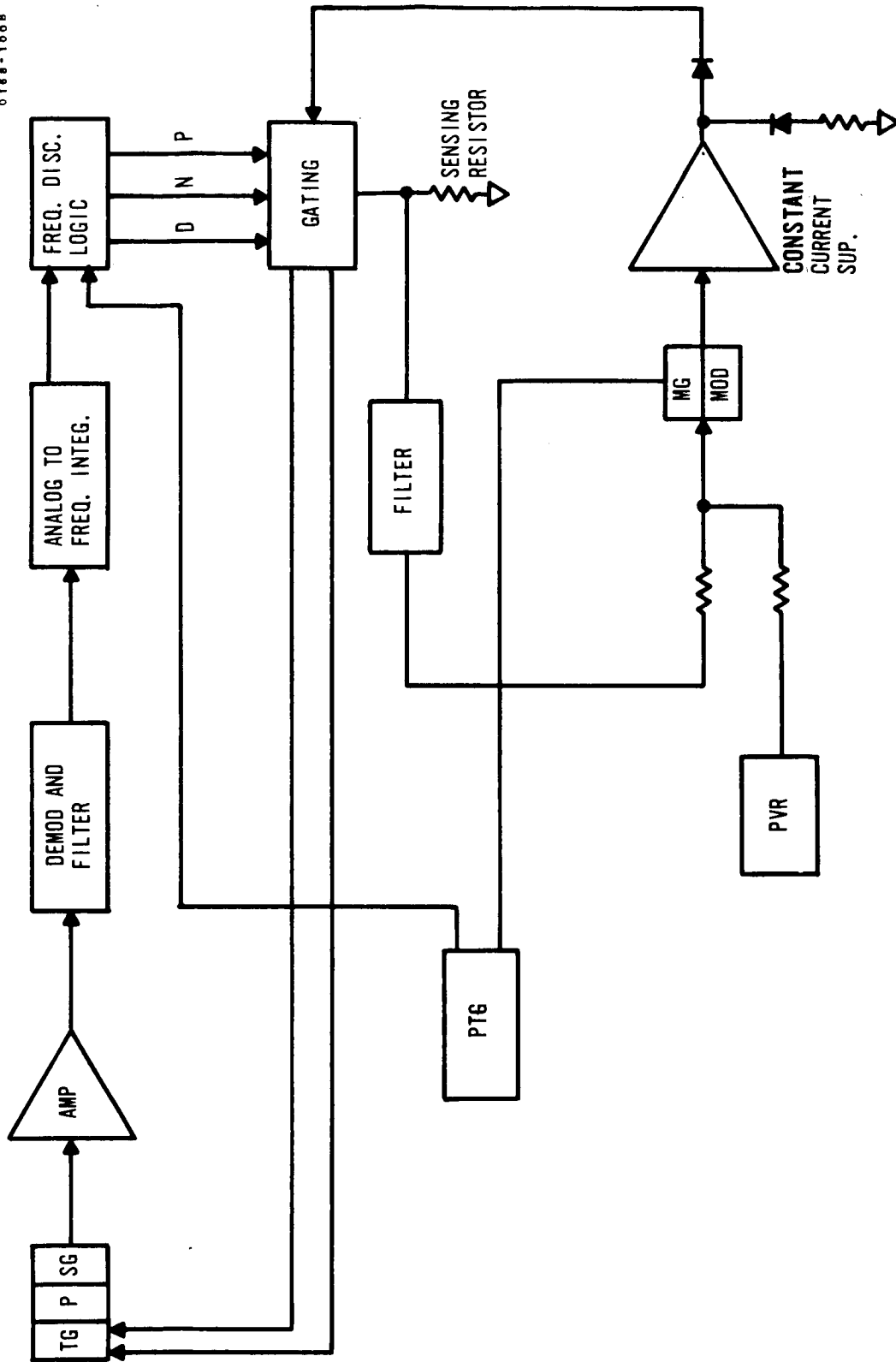


FIGURE 6.4-2. PULSE ON DEMAND LOOP

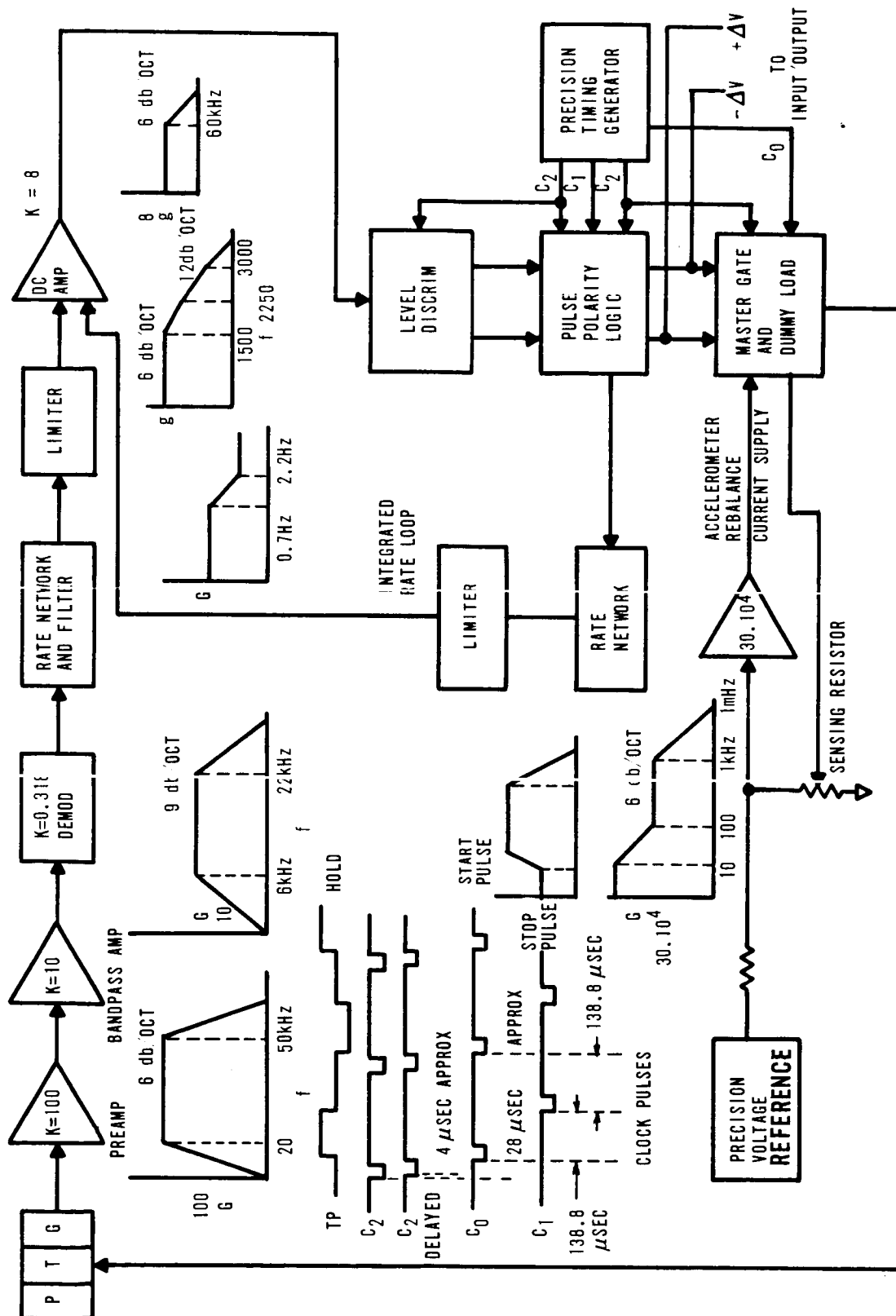


FIGURE 6.4-3. INTEGRATED RATE LOOP BLOCK DIAGRAM

Early in the -3 program period, investigations of other techniques showed the Honeywell system had significant advantages. M. I. T.'s loop utilized a constant current torquing technique with range, scale factor stability and null uncertainty less favorable than the Honeywell system. JPL's loop was a pulse-on-demand system with linearity and range equivalent to the Honeywell system, but the accuracy was an order of magnitude less than Honeywell's. The Bell system performance was comparable to the Honeywell system, but size, weight and power requirements were not comparable.

During the past years, several programs have contributed to improvement of Honeywell systems:

1. The Fairchild Drone Guidance system resulted in successful flight tests.
2. The Dyna-Soar system was ground tested, sled tested and in manned flight checkout when it was cancelled. The X-15 program benefited from this and has successfully used this system design for several years.
3. The Gemini guidance system has successfully completed its manned flight program.
4. The Centaur Guidance system has completed a successful R&D program and is now operationally supporting Surveyor lunar missions.

There have been four phases of design modifications with the Centaur IGS. They are the -1, -3, Phase I and the present Phase II PIP configurations. In each of these phases, the velocity loops have undergone modifications. Figure 6.4-4 shows a block diagram of the present (Phase II PIP) loop.

6.4.3. Functional Description. - There are three hinged pendulum accelerometers mounted on the inner gimbal of the inertial platform. Their sensitive axes are mounted to form an orthogonal triad, enabling linear acceleration to be sensed along three mutually perpendicular axes. The rebalance electronics loop is identical for each accelerometer.

To help understand the mechanization, assume that the accelerometer senses an acceleration. In the presence of this acceleration, the average displacement of the accelerometer pendulum will be away from the null position. When it reaches a certain magnitude, and the signal it generates exceeds the PRE's level detectors' triggering limits, logic will be set to enable successive current pulses of the same polarity to flow through the

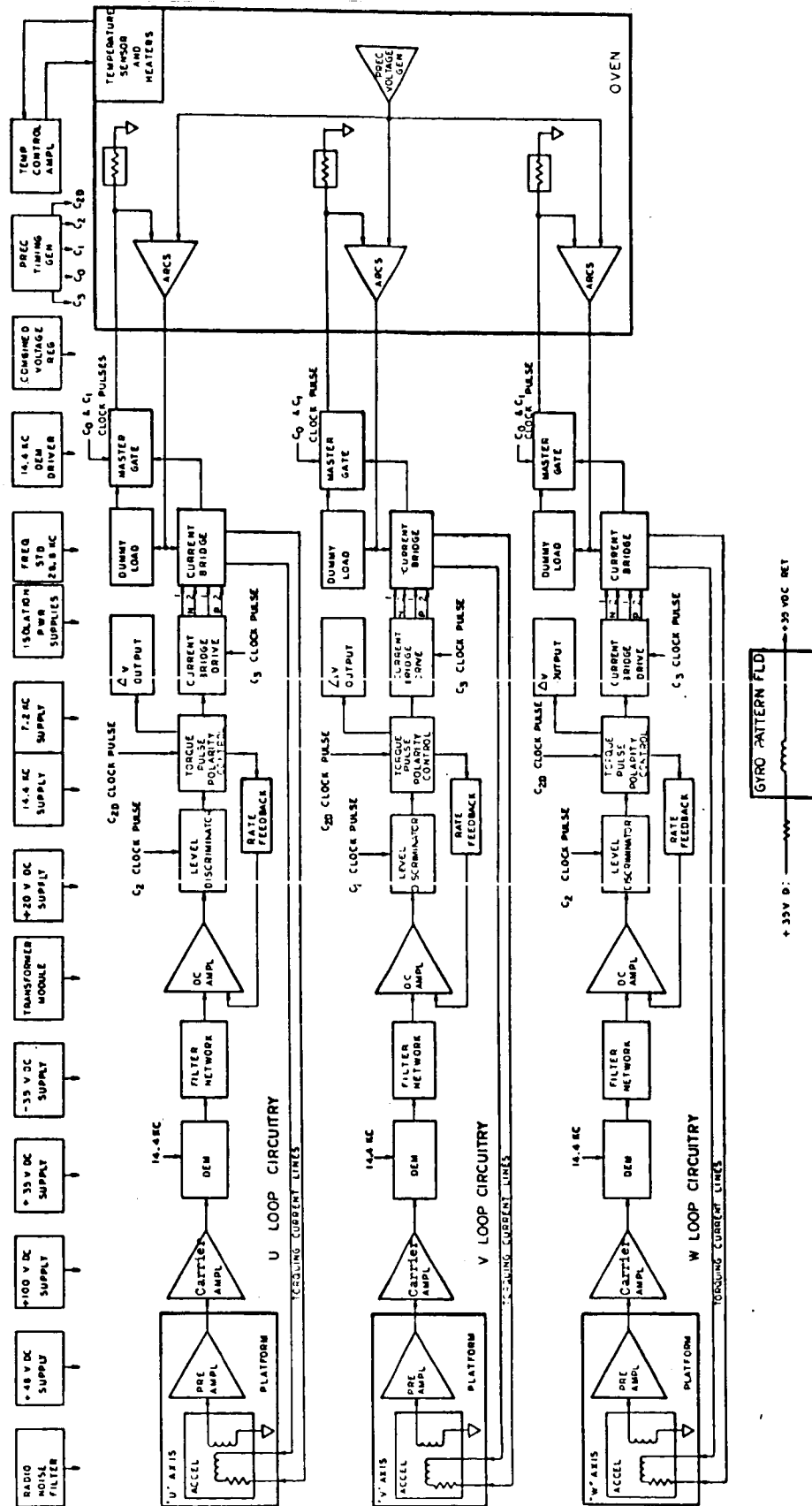


FIGURE 6. 4-4. COUPLER OPERATIONAL BLOCK BLOCK DIAGRAM

accelerometer torquer coil, in such a direction as to counteract the pendulum offset. Once back at null, the accelerometer loop (digital rate feedback) is designed to generate a plus-two pulses, then minus-two pulses, that is, a two pulse limit cycle. Aside from the main stream of the loop, incremental velocities (one-to-one ratio with the torquer pulses) are generated and sent to the flight computer as its basic delta V inputs.

In this plus-and-minus principle of torquing, the accelerometer torquer is excited with alternate pairs of positive and negative pulses when the accelerometer senses zero-g. These pulses are of such amplitude, width, and repetition rate as to produce a small amplitude oscillation of the pendulum about null.

6.4.4. Calibration. - An accelerometer is not a perfect device. Its parameters change slightly with environmental change. In order to minimize unnecessary errors, the inertial components are calibrated prior to a flight (or simulated flight). They are also calibrated periodically to gain an indication of their intermediate performance after shipment to the field sites. Historical performance data plots are maintained for each major parameter to aid in early analysis of potential problems.

The accelerometer loops are calibrated under control of the guidance computer. The calibration program is stored in the computer. The system is energized through the use of the Ground Support Equipment.

The inertial platform is coarse aligned to place the accelerometer input axis within two degrees of local vertical. From that point on, by command, the flight computer takes over and calibrates both the accelerometers and the gyros. The accelerometer ΔV 's are sampled for a 600 second interval. The computer receives both positive and negative counts, but only stores the net counts.

Two align modes are necessary to calibrate each set of bias and scale factor terms. At the end of the second align mode, the computer makes the necessary calculations and stores the results, so they are readily available to the operator.

Accelerometer Loop Bias and Scale Factor Determination. - The accelerometer bias and scale factor terms are determined by placing the input axis along the local vertical, into a plus and then minus "g" field. Ten minute counts are taken in both orientations. The scale factor is the slope of the "Input versus Output" curve and the bias is the finite output with zero "g's" input. See Figure 6.4-5.

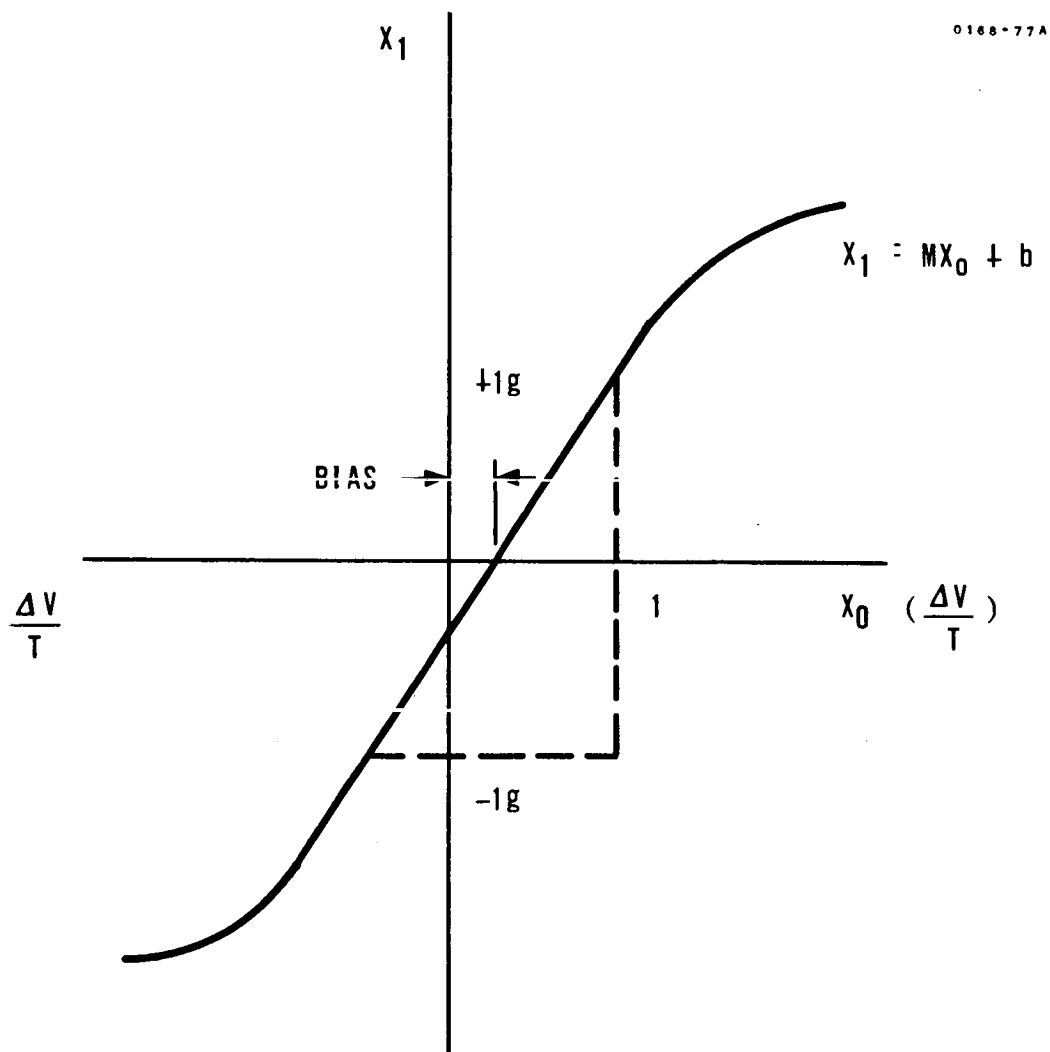


FIGURE 6.4-5. ACCELEROMETER BIAS AND SCALE
FACTOR CORRECTION COEFFICIENTS

From the curve, then the equation for scale factor is:

$$M = \frac{2g}{K (\Delta V_+ - \Delta V_-) \Delta T}$$

where M = Loop Scale factor

g = Acceleration due to gravity

K = 0.1 ft/sec/pulse

ΔV = Net Incremental Velocity pulses in 1G Field to the computer

ΔT = 600 seconds

The bias can be calculated as follows:

$$b = -g \frac{(\Delta V_+ + \Delta V_-)}{(\Delta V_+ - \Delta V_-)}$$

6.4.5. System "g" Capability. - The GG116 systems were designed to handle a maximum acceleration input of 11.2g's. With the GG177 retrofit, the maximum acceleration capability was increased to 12.4g's. It's interesting to note that the system specifications call for a maximum of 10g capability; however, a worst case tolerance buildup of 12 percent was calculated, thus dictating a possible "g" level greater than 10g's. The 12.5g level ensured sufficient margin to meet this requirement.

In order to determine the system "g" capability, it is necessary to know: (1) pulse repetition rate to the computer, (2) duty cycle and weight of each pulse, and (3) the accelerometer analog scale factor. The pulse repetition rate is usually restricted to the rate at which the computer can accept delta V's. The guidance computer was designed to accept 5,300 pulses/second, but the pulse rate presently used is 3,600 pulses/second. The weight of a GG177 loop pulse is 142 milliamperes with a 50 percent duty cycle. The accelerometer analog scale factor is 5.7 milliamperes per "g".

The weight of a torquer pulse or digital scale factor, D, is calculated from the following expression:

$$D = \frac{(Ktg)}{P} \cdot \frac{(Ip)}{2} \cdot (K1) \cdot (Tp)$$

where:

$\frac{Ktg}{P}$ is the inverse analog scale factor, $\frac{g}{ma}$

$\frac{I_p}{2}$ is the average torquer current ma

K1 is the gravity conversion $\frac{F/S^2}{g}$

T_p repetition rate pulse width plus dummy load $\frac{sec}{pulse}$

$$D = \frac{(1)}{5.7} \frac{(142)}{2} (32.125) \frac{(1)}{3600} = 0.111 \text{ ft/sec/pulse}$$

Now, knowing the weight of the pulse, one can determine the maximum g capability as follows:

$$A = (0.111 \frac{ft/sec}{pulse}) \left(\frac{1}{3600 \frac{pulse}{sec}} \right) \left(\frac{1g}{32.125 \text{ ft/sec}^2} \right)$$

$$A = 12.4g$$

acceleration	= A
digital scale factor	= 0.111 ft/sec/pulse
pulse repetition rate	= 3600 pulses/sec
conversion factor	= 1g/32.125 ft/sec ² *

* 32.125 ft/sec² is "g" at St. Petersburg, Florida

6.4.6. Conclusions. - The digital rebalance loop has been proven successful. Prior to designing the new IMG (improved Centaur), Honeywell again made tradeoff studies of accelerometer rebalance techniques. Honeywell again decided on the "Bang-Bang" concept. The main differences between the present and new system technique are loop simplification and a change in duty cycle. (See Topic 2.15 for details.) Finally, a thorough analysis (worst case) of modifications and/or new design has contributed greatly to the success of this rebalance technique on Centaur.

Topic 6.5

Platform Stabilization Loops

6.5.1. Summary. - The Centaur gyro stabilization loops were originally adapted from a previous Honeywell design. The major change during this adaptation was redesign of the rate compensation networks. Subsequent problems encountered were:

1. Insufficient damping.
2. Poor gain and phase margins.
3. Poor recovery from large error signals (non-linear operation).

These problems were solved only by "stop-gap" methods, when in reality a total loop redesign was required and should have been implemented in 1964.

Future stabilization loop designs could avoid problems of this type by:

1. Explicit specification of open and closed loop parameters.
2. Accounting for regions of non-linear operation through control of amplifier saturation levels.
3. Application of non-linear analysis techniques wherever possible.

6.5.2. Introduction. - A discussion of this topic should begin with a look at some of the initial operational and performance requirements imposed on the platform stabilization loops in 1959. The original purpose of the stabilization loops was to provide a three-axis, orthogonal reference for missions, which were intended to place a payload in a 300 nautical miles or 24-hour synchronous orbits. The reference was to be maintained in the platform by gimbaling about the inertial component assembly. The following are excerpted from the original -1 Missile Guidance Set specification:

1. Platform: The platform shall consist of an outer housing and a four-gimbal, all-attitude gimbal structure mounted on a vibration-isolation system.
2. Gimbaling: All gimbals shall be free of angular restraint about their own axes, except the inner middle gimbal which shall have

plus or minus 15 degrees of rotational freedom. Gimbaling shall be in the following order from inside to outside:

- a. Inner (shall include three GG49D6 gyros and three DGG116A2 accelerometers).
 - b. Inner middle.
 - c. Outer middle.
 - d. Outer.
3. Orientation of Gimbal Axes: The platform shall be mounted in the vehicle in conformance with the following:
- a. The platform outer gimbal axis shall be parallel to the vehicle roll axis.
 - b. The platform outer middle gimbal axis shall be parallel to the vehicle pitch axis when the angle between the platform outer gimbal and the platform case is zero degrees.
4. Platform Electronics: The platform electronics shall provide the electronic components and circuitry required for the stabilization of the platform gimbals.
5. Response to Angular Acceleration and Angular Velocities: The platform, when operated with its associated electronics equipment and vibration isolation system, shall maintain the stabilized reference about all three axes within a static accuracy of ± 10 seconds of arc (three sigma) and a dynamic accuracy of ± 40 seconds of arc (three sigma) with the platform subjected to the peak angular velocities or accelerations in any attitude as specified below:

	<u>Pitch</u>	<u>Roll</u>	<u>Yaw</u>
a. Attitude	$\pm 360^\circ$	$\pm 360^\circ$	$\pm 360^\circ$
b. Angular Velocity			
Peak (deg/sec)	14*	16*	7*
Duration (sec)	5*	5*	3*
Average (deg/sec)	5	5	5
c. Angular Acceleration			
Peak (deg/sec ²)	90	40	40

* Decaying sinusoid with $\omega_d = 1.4$ Hz

6. Residual Oscillation: Residual oscillation of the gyro-stabilized reference shall be less than ± 10 seconds of arc about any of the three axes, when operating at rest relative to the Earth.
7. Gimbal Flip: The outer gimbal shall change in orientation (Gimbal Flip) before the inner middle gimbal reaches its stops for all platform attitudes.
8. Outer Gimbal Caging: The platform shall provide means (caging) to prevent continuous rotation of the outer gimbal in either direction when the vehicle is pitched up 90 degrees, to simulate a vertically erected vehicle. The outer gimbal shall be uncaged when the pitch angle is decreased to 20 ± 5 degrees and shall remain uncaged thereafter for all pitch angles.

The Centaur stabilization loop was mechanized to meet these specifications. Figure 6.5-1 is a descriptive block diagram of stabilization loop interdependency under vehicle turning rates. To the lower left of the figure is the fourth gimbal loop. It is seen that this is the only gimbal which is not gyro stabilized. Its function is to sense the second gimbal angular displacement, drive itself to maintain the second gimbal at 0° , and thus keep the second gimbal away from its stops. The rate integrating gyros control the position of the inner three gimbals.

An example of a pure vehicle yaw disturbance will be given to illustrate the stabilization system. To the upper left, of the figure a yaw input ($\dot{\psi}$) is imposed by the vehicle on the platform case. Assume that all platform gimbal angles are 0° for this example. Then, because of fourth and third gimbal geometry (rotational axes are orthogonal to axis of rate) the rate, $\dot{\beta}_1$, is simply about the second gimbal axis. Since the first gimbal is oriented at 0° the rate is sensed by the V gyro, which is along course (for the purpose of this example). The B1B resolver phases the gyro signals so that the second gimbal is restored by the amplifier along-course gyro rate information.

The fourth gimbal phasing switch (Figure 6.5-2) is necessary to control the direction in which the fourth gimbal must drive to restore the second gimbal to 0° . The phasing switch receives information from the third gimbal resolver (B5B) to accomplish this function. Specifically, if the third gimbal is $90^\circ \pm 89^\circ$, the fourth gimbal will drive in one direction. If the third gimbal is $270^\circ \pm 89^\circ$, the fourth gimbal will drive in the opposite direction.

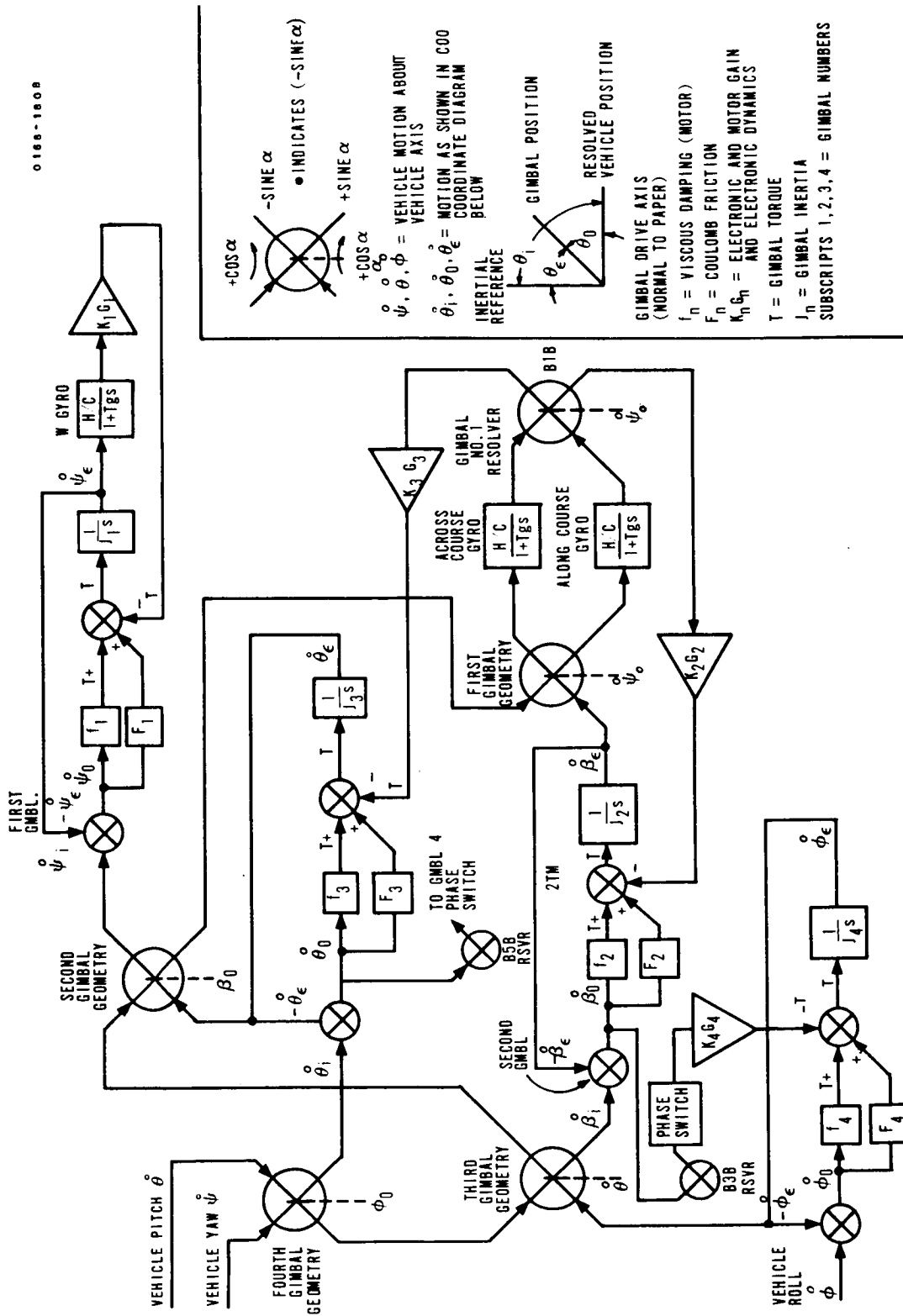


FIGURE 6.5-1. FUNCTIONAL DIAGRAM OF INERTIAL PLATFORM STABILIZATION LOOPS

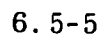


FIGURE 6.5-2. - FOURTH GIMBAL PHASING AND CAGE CIRCUITS

6.5.3. -1 System Design (1959). - The systems design effort on the original -1 system was primarily concerned with insuring that static and dynamic accuracies could be met. This involved analysis of the gain and rate compensation requirements of each loop, working along with the hardware designers. (Refer to Topic 2.11 for details of the electronics design.)

Tests devised to verify proper operation of the -1 stabilization loops included:

1. Servo loop gain - with the gimbals gyro-stabilized a precision torque was applied to the gimbal and the angular displacement measured.
2. Servo loop gain margin - the stabilization loops were closed and the gyro signal generator excitation was increased from 3.7 vrms to 5.3 vrms. The gimbals should show no oscillations in excess of 5 arc-seconds p-p, and slight gimbal disturbance torques should not cause sustained oscillations.
3. Servo loop threshold - each gimbal loop threshold was checked by slowly moving the platform case (mounted on a precision table) a few arc-seconds in one direction, and then the other, while optically monitoring a mirror on the stable element.
4. Stable element isolation - the platform was mounted on a gimballed fixture which was capable of imparting sinusoidal rates of 0.5 to 20 Hz at 5 to 50 milliradians to the platform. While monitoring the gyro's preamplifier output, each axis was checked for no greater than ± 40 arc-seconds movement while the case was disturbed sinusoidally ± 5 milliradians.
5. Angular velocity and acceleration - using the same test setup as for (4), the platform case was exposed to sinusoidal rates sufficient to reach an angular velocity of 16 deg/sec and an angular acceleration of 90 deg/sec. The reference (dynamic accuracy) must remain within ± 40 arc-seconds during these rates.
6. Gimbal flip - the first and fourth gimbal axes were oriented so they were coincident while the stabilization loops were closed. The test results indicated whether the flip was electrical (phase change) or mechanical (first and fourth gimbals counter-rotate 180°), depending upon second gimbal orientation.
7. Servo loop response - a 7.2 kHz error signal was injected at the input to the first section (A1 section) of the 7.2 kHz GCA, causing an angular gimbal offset. The error signal was removed and the time for oscillations to damp out was limited to 200 milliseconds.

8. Servo loop saturation recovery - the maximum time for the stabilization loop to recover from a fully saturated condition was 750 milliseconds. The loop was saturated by manually forcing the gimbal. The recovery time was determined from a recording of servo motor voltage. (The performance of the loop under these conditions was important when switching the platform from coarse alignment to the gyro stabilized mode.)

These tests were performed on a platform test station, but the platform electronics unit (which was intended to be shipped with the particular platform) was usually required to insure the meeting of all requirements.

6.5.4. Rate Network and Other -3 System Changes (Early 1962). - Loop analysis showed that the first configuration of the stabilization loop was unsatisfactory. Even after much adjustment, leading to successful testing, the loop could burst into oscillation at any time. A new rate network was designed, and loop gains were increased without jeopardizing loop margins.

The customer requirements for static and dynamic accuracies were increased to ± 15 arc-seconds and ± 60 arc-seconds, respectively. Also gimbal response recovery time was decreased to 150 ms.

A limiting network was added to the input of the first gimbal GCA to overcome loop saturation recovery problems. (Details are contained in Topic 2.11.)

At this time, the gimbal torque motors were changed in the platform (ref. Topic 2.5). The -1 system platforms contained motors with stainless steel housings, which weighed 1.2 pounds and possessed a torque rating of 10 oz-in. The newer motor had an aluminum case, weighed 0.75 pound, and was rated at 15 oz-in of torque. In addition to increasing torque capability, a significant weight reduction was achieved. The opposite end of each gimbal contains a resolver which has an aluminum case. In order to balance the gimbal against the older stainless steel torque motor, weight had to be added to the resolver end. When the motor weight was reduced by 0.45 pound, the balance weights on the gimbal were reduced a like amount.

6.5.5. Design of DC Amplifier or -3B Stabilization Loop (1962). - The problems of low gain, on the one hand, or low gain and phase margin on the other pointed up the inherent limitations of the stabilization loop design. A new design was begun, incorporating advanced techniques from

automatic control theory, and overcoming low signal level amplifier saturation. Some features of the new loop mechanization were:

1. Improved gain distribution among elements of the stabilization electronics.
2. Active rate-amplifier instead of passive network (contributed to 1.).
3. Differential voltage preamplifier.
4. Polarity switch instead of a 400 Hz demod.
5. Electronics would be packaged so that only electrical, not mechanical changes would be made in the PE. As stated in Topic 2.11, the new design was not incorporated because of funding limitations.

6.5.6. Phase I Product Improvements (1964-1965). - A number of recommendations were made at this time to analyze and optimize the gimbal servo loops - short of complete redesign. Some of the areas considered were:

1. First gimbal loop nulling before gyro stabilization. - The gyro gimbal was driven into its stops during coarse alignment of the platform from one orientation to the next. The gimbal stabilization loop was then closed with the gyro gimbal against its stops. The rate input to the gyro by closure of the platform loops in this condition could cause significant shifts in the gyro's flex lead restraint torque (component of gyro constant torque). The problem lay mainly with the first gimbal loop. The other gimbal loops, because of their dynamic characteristics, could not reach high enough angular rates to be significant. The proposed solution to the problem was to provide a gyro gimbal nulling loop that would be operative after coarse alignment and before gyro stabilization (fine) alignment. This was to be a simple rate loop that tied the signal generator back on its own torquer. Figure 6.5-3 is a block diagram of the solution which was proposed. This proposal was not implemented because of the high cost/effectiveness ratio of the solution. A later gyro modification was made to reduce the gimbal OA stop angles, which essentially solved this problem.
2. First gimbal loop study. - The original -3 loop analysis called for a gain between the platform gimbal (gyro 1A) and torque motor of 30 inch-ounces of torque for each milliradian of platform rotation. Subsequent to this, it was necessary to add diode limiters to the loop to enable the loop to recover from a saturated condition. These diodes reduced the gain at larger gimbal

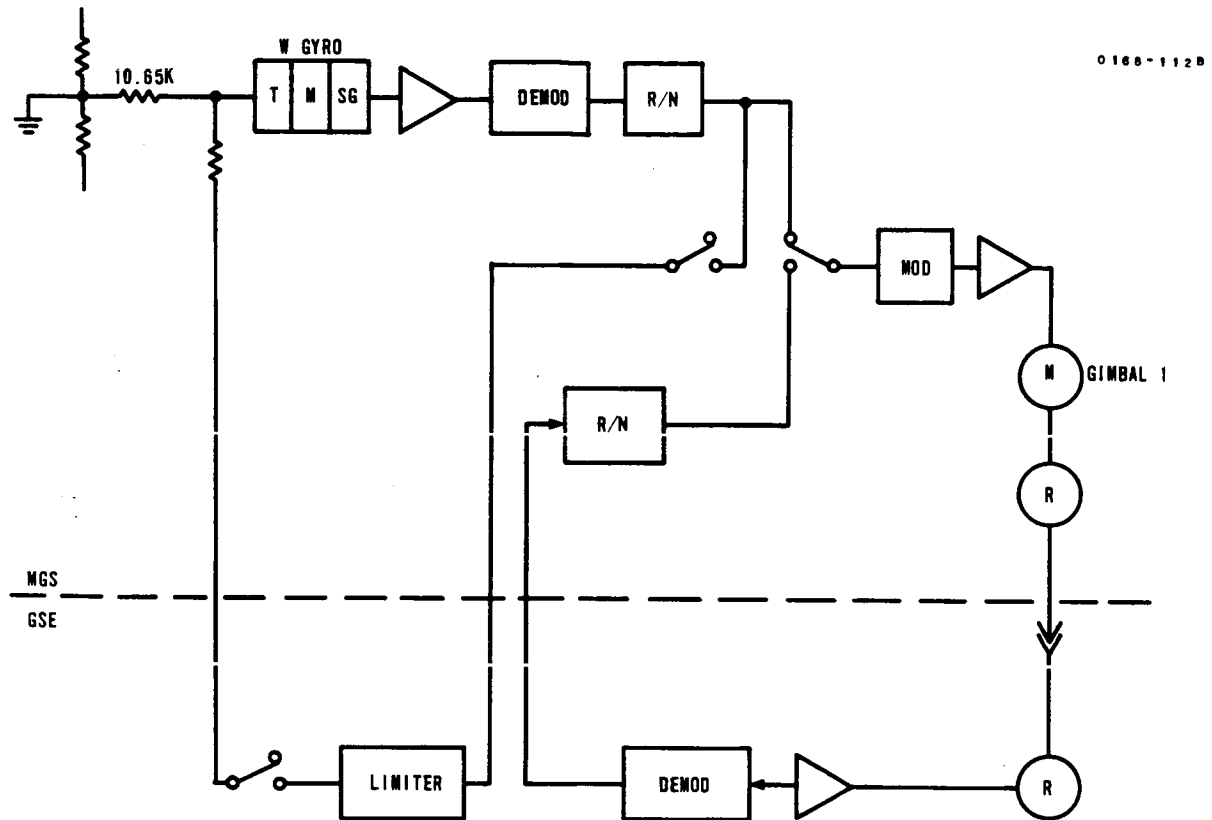


FIGURE 6.5-3. A METHOD FOR COARSE ALIGNMENT
LOOP MECHANIZATION

angles. Therefore, when the static gain was measured at large (but not abnormal) gimbal angles, the gain appeared low. A modification to the attenuation of the diode input network in the linear region was made to raise the gain so that gain at large angles was measured correctly. However, the calculated gain through the loops (ignoring the non-linear diodes) indicated inadequate gain margin on the basis of linear analysis. The gain was excessive only over a restricted portion of the dynamic swing. The gain was lowered at large angles by the diodes, and at small angles by the effect of friction. However, as described above, the existing gain was not determined by analysis and, therefore, the effects of variations in gain were not established. Linear analysis indicated that it might be possible for gain build-up (due to tolerances plus temperature variations) to drive the loop unstable. An analog computer study showed that the first gimbal loop gain could be reduced, and it was.

3. Third gimbal loop study. - This loop suffered from poor gain distribution within the loop. When saturation occurred before the rate network, all rate information was lost, making it possible for the loop to be unstable under these conditions. This saturation normally occurred in switching from coarse align to the stabilization mode. The only correct solution for this problem was to increase amplifier saturation levels. This involved almost complete redesign of the gimbal control amplifier. The approach used until then was to add non-linearities (diodes), which reduced the gain at specific points in the loop for large platform angles. These fixes were barely adequate; they allowed the loop to recover from saturation but not with a great deal of margin. The third gimbal loop, in particular, had a problem in this respect. Honeywell proposed a complete study of this loop, including non-linearities to define the conditions for which oscillation can occur, and means for prevention. The study revealed that no adjustments or minor loop changes could achieve any significant improvement in the loop. The best way to fix the problem would have been a new loop design.
4. Fourth gimbal loop study. - Honeywell recommended a study of the possible benefits of increased gain in the fourth gimbal caged mode, since the results of previous analysis indicated this is needed and that no detrimental effects would be noted. This study included an analog simulation of:
 - a. The second and fourth gimbal loops operating simultaneously.
 - b. The fourth gimbal loop in the caged mode.

- c. Rate table tests on the system with increased gain in the fourth gimbal caging loop.
- d. Vibration tests with increased gain in the fourth gimbal caging loop.

The study revealed no problems with the existing loop and gain distribution.

5. Checking Gimbal Loop Performance on the Pad. - Many questions were raised on the validity of the present step response test. This step response was originally envisioned as a quick test in addition to the frequency test run on the gimballed platform rate table. It was not practical to run the frequency test at ETR. Therefore, a means for improved gimbal response testing was investigated. The following changes could be incorporated in the current or future designs.
- a. The gimbal control amplifiers could be modified to include a means for putting a voltage step directly into the output amplifier. This inhibits sharp transients, (due to step changes through the rate network) from saturating the output section of the gimbal control amplifier and permits larger step voltages to be used. This would reduce the effect of non-linear friction on the responses and make them more predictable.
 - b. The monitor point in the loop could be changed from a point across the torque motor, to the output of the first demodulator. Monitoring would permit easy observation of platform motion, which defines how well the loop is performing. The voltage across the torque motor, due to variation in friction, is confusing and misleading.

At that point in the IGS program (mid-1964), the benefits to be derived from these changes did not warrant the expense of the hardware change.

6. Bang-Bang Output for GCA. - Honeywell proposed a non-linear output amplifier such that a small input error signal provided full output torque. Preliminary analysis indicated this could be controlled with minimum change to the compensation networks by using an integrated-rate feedback loop around the non-linear amplifier, similar to that used in the accelerometer loops. The advantages of such a loop were:
- a. Loop performance would be almost independent of friction. - In the existing loops static accuracy was a function of static

friction. If the friction doubles, then static accuracy was halved since the platform error must increase until enough voltage is generated across the torque motor to overcome the friction. With the bang-bang output stage, the platform error must only be sufficient to trigger the amplifier, providing full output to decrease the error to zero. A change in friction, due to flight environment, would result only in a small percentage gain decrease in the loop since the effective torque, T_e , is decreased by the increased frictional torque T_f . ($T_e = T - T_f$.) It would not cause any decrease in platform static accuracy.

- b. Decreased power requirements. - This type amplifier, if properly controlled, would require less power than linear amplifiers. The power dissipated in the power stage driving the torque motor would be practically eliminated. In addition, the power used to overcome friction would be drastically reduced, since the output would be either full on, or full off, so the energy used to overcome friction during the on time would be a small percentage of the energy available. With a linear amplifier, a small disturbance input results in a voltage level across the torque motor which just exceeds the voltage necessary to overcome friction. Therefore, most of the energy is dissipated as friction loss.

Honeywell proposed the bang-bang output stage as a possible solution to the gimbal friction problems, which frequently occurred with the existing platform design. The study included a brief extension of the analog studies described under the first and third gimbal loop studies (items 2 and 3 above).

This effort on the bang-bang loop was not authorized by NASA since it was felt that a linear loop could satisfy Centaur requirements.

6.5.7. Deletion of Rate Table Tests (March 1964). The two rate tests previously mentioned (stable element isolation and angular velocity and acceleration) were dropped at this time for two reasons:

- a. No operating platform had ever failed the tests.
- b. The dynamic accuracy about any axis of all platforms was well within the ± 60 arc-second specification.

6.5.8. Phase II Product Improvements (March 1966). - A number of MGS improvements were made under the Phase II program. The changes affecting the stabilization loops were:

- a. GG49D26 gyro - This gyro (refer to Topic 2.2) was implemented to reduce the effects of flex lead restraint torques and large OA stop angles.
- b. The gain of the first gimbal loop was reduced according to the recommendation of the earlier analysis.

6.5.9. Recurrence of Loop Saturation Problems (March 1967). - The presence of a certain type of GG49D26 gyro in the W gyro position caused non-linear oscillations of the first gimbal loop. The gyros which had gimbal stops greater than approximately ± 0.5 degree, were found to cause the oscillations because damping for large signals was insufficient. For an interim period, the W gyro was selected (for stop angles ≤ 0.4 degree) to circumvent the problem. However, limited gyro availability and a desire for a technically satisfactory solution led to an investigation of the whole loop.

The ensuing study revealed that the A2 section of the GCA was not recovering from a saturated condition fast enough to stop the gyro gimbal. A monitor of gyro gimbal position showed a limit cycle of approximately 16 cycles per second for the gyros with larger than $\sim \pm 0.5$ degree stops. A rate network modification was made (refer to Topic 2.11) which provided damping at large signal levels, and solved the problem.

While testing and analog computer simulations proved the desirability and effectiveness of the rate network change, a complete non-linear servo analysis was not performed. The non-linearities of the loop were such that good analytical models could not be established. The knowledge that was gained came from the empirically known conditions at the limits.

This saturation and phase margin problem would not have presented itself if the improved stabilization amplifier had been implemented when it was proposed in 1962.

6.5.10. The Improved Centaur GCE Design (1967). - The linear gimbal control mechanization proposed in 1962 was adequate for the needs of the present or improved Centaur system. That design has been adapted for use in the improved IMG, and has been designated as the GCE (gimbal

control electronics). The design goals for the first gimbal loop, which is a typical loop, are:

1. Open loop gain twice the present value. - This goal was established to allow procurement of rotary components (slip rings, resolvers, torque motors) with higher friction levels than are presently used. Component cost should thus be reduced.
2. Closed loop crossover between 40 and 200 Hz. - The natural frequency of the loop should be greater than 40 Hz to avoid normal flight rates and less than 200 Hz to prevent coincidence with platform isolator and structure resonances.
3. Amplifiers linear for maximum gyro displacement. - This goal is one dictated by good servo loop design practice. The problems present in the original Centaur design were a result of failure to make this a requirement.

The following block diagram (Figure 6.5-4) represents a typical GCE loop. The signal generator excitation frequency was raised from 7.2 kHz to 14.4 kHz so that the demodulator filter frequencies would not interfere with the loop response. There is no gimbal response test error input in the loop because sufficient margins will insure proper performance. Therefore, no marginal loop performance problems should be present.

Worst-case computer analysis is being performed on all loops and significant parameters to insure that component variation will not create performance degradation.

A comparison of expected IMG loop performance versus that of the -3 Centaur loop is made in Table 6.5-I.

Although the design goal of amplifier linearity for any gyro angle was not 100 percent realized, the increased damping, phase margin, and amplifier saturation levels are significantly improved.

6.5.11. Conclusions. - The problems encountered during Centaur gyro stabilization loop development were:

1. Insufficient damping.
2. Low gain and phase margins.
3. Low amplifier saturation levels, causing non-linear oscillations.

Much of the analysis performed was of the "catch up" variety, with major problems providing the stimulus. The primary lesson that was

0167-94A

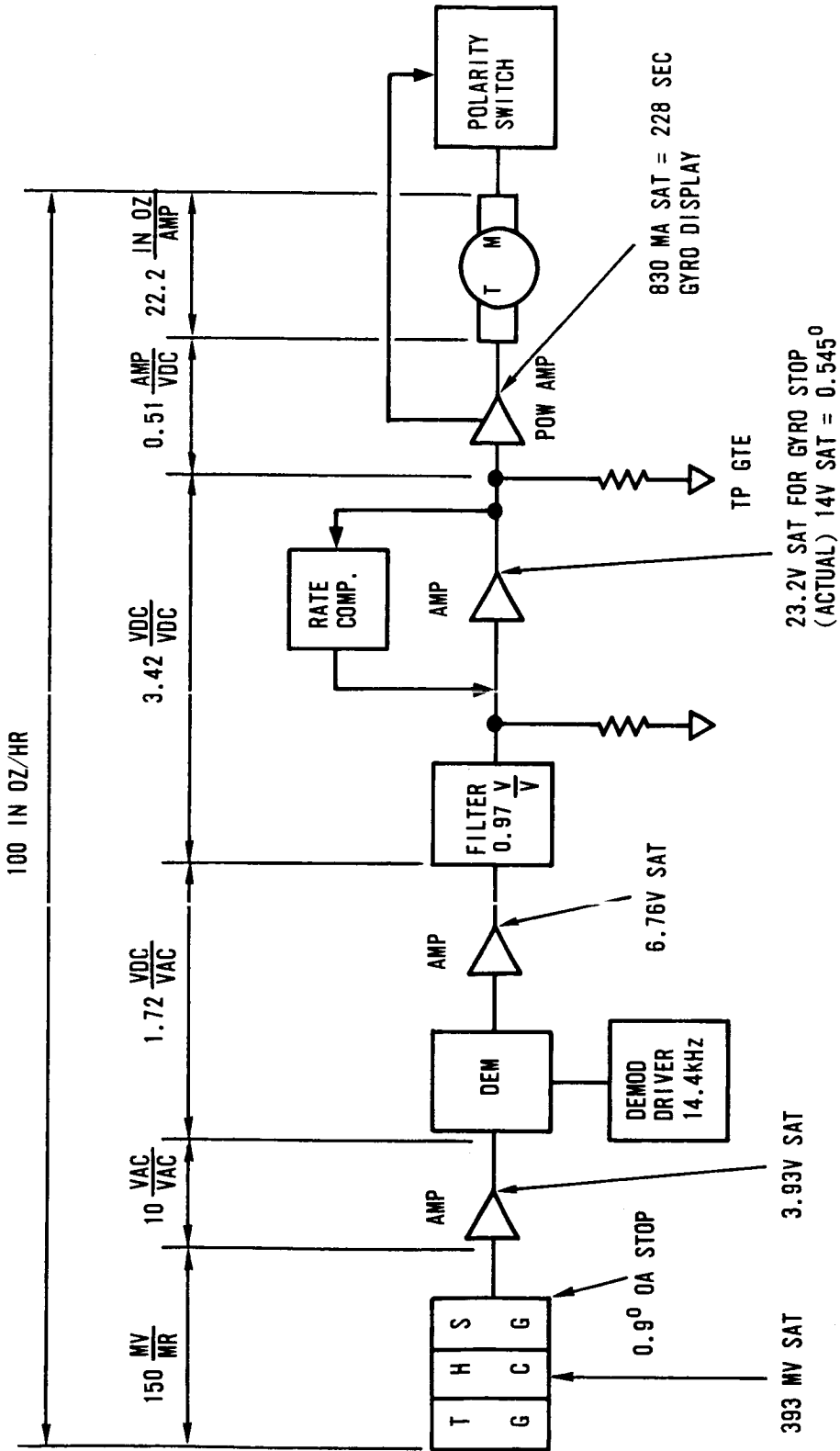


FIGURE 6.5-4. GCE BLOCK DIAGRAM

TABLE 6.5-I

COMPARISON OF -3 CENTAUR VERSUS
EXPECTED IMG LOOP PERFORMANCE

	-3 Centaur	Improved Centaur Linear Control Loop
Static Stiffness	51 $\frac{\text{in. oz}}{\text{m rad}}$	100 $\frac{\text{in. oz}}{\text{m rad}}$
Gain Margin	+6 db	+11.5 db
Phase Margin	+32 degrees	+41 degrees
Closed Loop Natural Frequency	94 $\frac{\text{cycles}}{\text{sec.}}$	132 $\frac{\text{cycles}}{\text{sec.}}$
Closed Loop Damping Ratio	0.35	0.48
Closed Loop Peaking at frequency	+5.8 db at 84 $\frac{\text{cycles}}{\text{sec.}}$	+3.0 db at 100 $\frac{\text{cycles}}{\text{sec.}}$
Platform Gimbal Dis- placement (arc-sec) per unit Disturbance Torque (in. oz) at zero frequency	4.04 $\frac{\text{arc-sec}}{\text{in. oz}}$	2.06 $\frac{\text{arc-sec}}{\text{in. oz}}$
Maximum Platform Gimbal Displacement (arc-sec) per unit Disturbance Torque (in. oz) at frequency	9.77 $\frac{\text{arc-sec}}{\text{in. oz}}$ at 4.8 $\frac{\text{cycles}}{\text{sec.}}$	4.12 $\frac{\text{arc-sec}}{\text{in. oz}}$ at 6 $\frac{\text{cycles}}{\text{sec.}}$

learned from the development experiences was that stabilization loop design should be guided by certain requirements. These external requirements should be much more detailed than the general procurement specification and should include:

1. Gain and phase margins.
2. Range of linear operation.
3. Loop performance under non-linear conditions.
4. Damping and other closed loop servo parameters.

If requirements such as these are established at the conceptual stages of design, most of the disadvantages of previous designs can be avoided. This planning philosophy was followed in improved Centaur, and a successful design was produced.

Topic 6. 6

Platform Coarse Alignment Loops

6. 6. 1. Summary. - The platform coarse alignment loop, while not a flight loop, is needed to position the platform into calibration and preflight orientations. The problems associated with this loop have been of the nuisance type, and they have caused many hours to be spent investigating supposed and unreal airborne hardware problems. The following problems have been encountered in this loop:

1. Initial design/development problems.
2. Gimbal spin inhibit circuit nuisance tripping.
3. Servo loop noise.

The lessons learned through experience with the coarse alignment loop have served as a basis for a much simplified IMG platform gimbal alignment technique.

6. 6. 2. Introduction. - In order to rapidly orient the platform's inertial sensors for calibration and flight, a means for externally controlling the gimbals is required. Two possible solutions to this which were considered were:

1. Apply high-rate torquing to the gyros, which in turn would cause the gimbal to move to the desired angle.
2. Slave the platform gimbal to an external reference, rather than the gyro; and set the reference to the desired angle.

Both of these methods are in general use for platform gimbal alignment. However, the former method was originally rejected for the Centaur IGS because it was thought that the GG49 gyro could only be torqued at the relatively slow rate of 41.55 degrees per hour without magnetizing the control field. Magnetization of the control field results in unwanted fixed torques in the gyro, if the pattern field is energized, as was the case at that time in the IGS. Hence method No. 2 was used for the IGS.

6. 6. 3. Original -1 and -3 IGS Design (1959-62). - The resolvers on each gimbal, which comprise the steering resolver chain, provide a convenient means of monitoring relative gimbal angles. If the steering chain is broken, each

resolver can be excited separately, and the individual resolver outputs can be used as feedback elements in a gimbal positioning servo loop. A four gimbal platform necessarily has a redundant gimbal. Therefore, only three gimbals need be oriented, and the remaining gimbal can be slaved to a reference. The second gimbal is the obvious choice for the slaved gimbal because it only has ± 15 degrees of freedom relative to the third gimbal. If it were not the slaved gimbal, a complicated technique would be required to angleshare the alignment capabilities between the inner roll and outer roll gimbals. Thus, the fourth (outer roll) gimbal was mechanized for 360 degrees alignment, and the second gimbal is caged upon its own resolver at 0° .

Other elements of the airborne equipment, which were used for the platform coarse alignment were the power amplifier (A2 section) of the gimbal control amplifier, and the gimbal torque motor.

The simplified block diagram in Figure 6.6-1 contains a differential resolver, amplifier-demodulator, and filter network, which are not a part of the airborne equipment. These loop elements are contained in a panel of the GSE designated as the Alignment Reference Unit (ARU). The differential resolver is gear-coupled to a drive motor, which is turned off, CW, or CCW by the operator. An angle scale is attached to the differential resolver shaft, and is visible through a window in the ARU. Thus, the operator slews the differential resolver with the motor until the desired angle is visible in the window. The platform gimbal follows the ARU resolver at a rate controlled by the resolver drive motor. Figure 6.6-2 is a detailed block diagram of a coarse alignment loop. Two drive motor speeds were provided, three degrees per second and 1.5 degrees per second. The higher rate is the maximum desired speed at which the single-degree-of-freedom gyro should precess into its stops. (Actually, the gyro gain multiplies this by six for an input about the gyro input axis.) The lower speed affords better operator accuracy near the desired alignment angle.

A coarse alignment loop, which would automatically align the gimbals to pre-selected angles, was considered as an alternative to the semi-automatic method described. However, the added complexity and cost of such an alignment loop was not compatible with the essentially manual test philosophy which prevailed at the time.

0168-137A

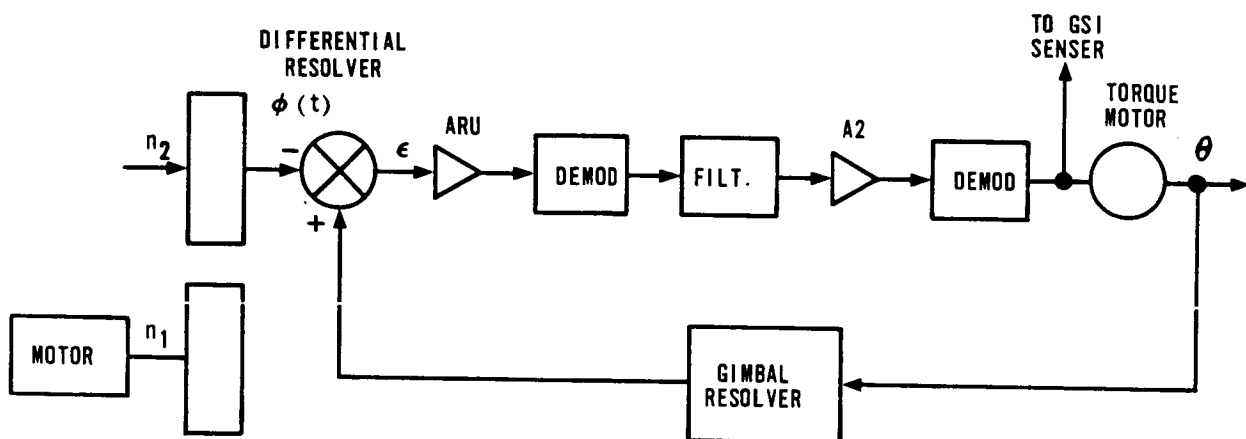


FIGURE 6.6-1. SIMPLIFIED COARSE ALIGNMENT LOOP

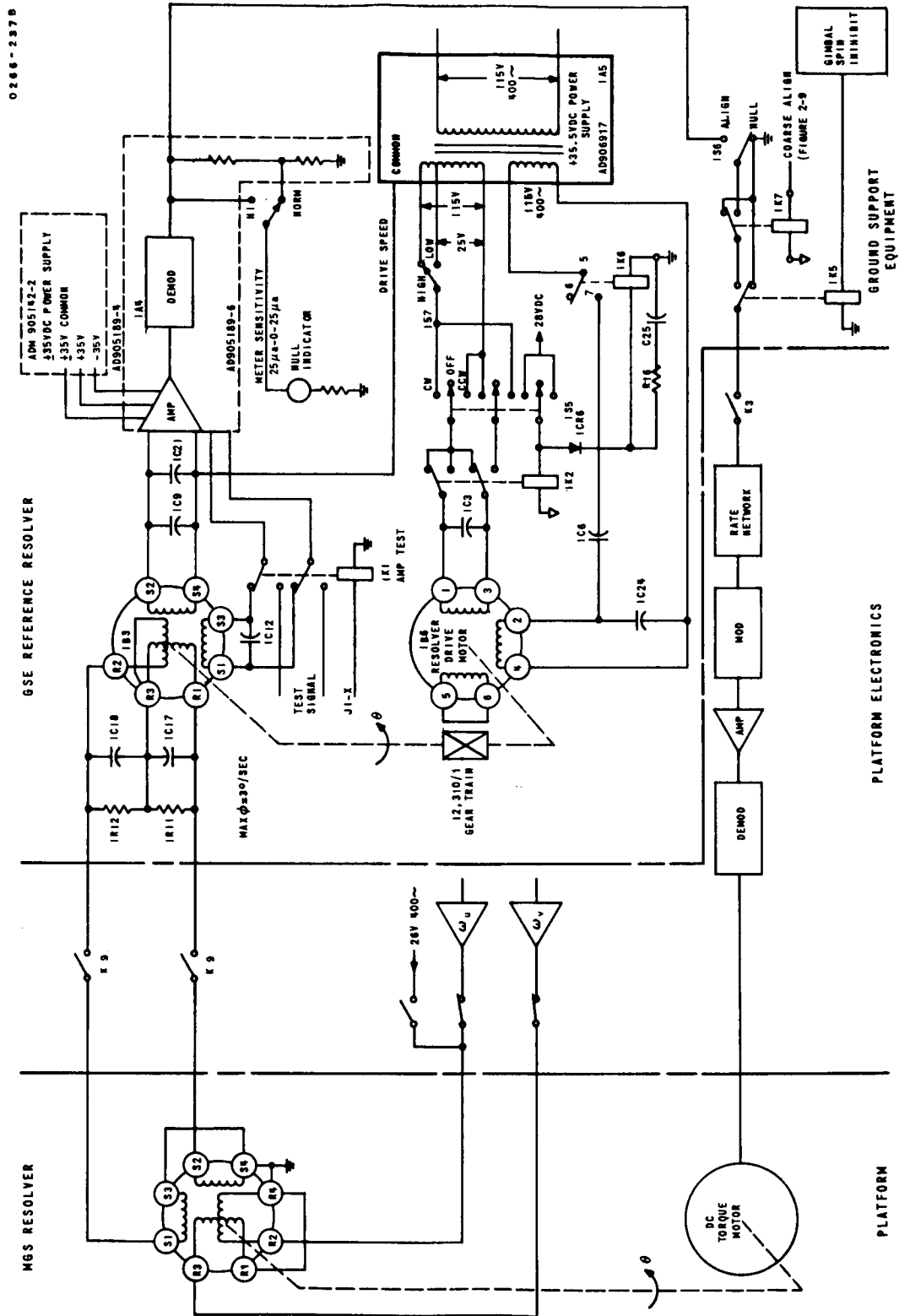


FIGURE 6.6-2. TYPICAL RESOLVER COARSE ALIGN LOOP

The major initial design problems with the coarse align loop were:

1. Classical servo loop non-linearities associated with the gear train in the ARU.
2. Gain changes for the ARU amplifier-demodulator were required to meet an accuracy design goal of $\pm 1^\circ$.

Both of these problems were overcome by straightforward linear and non-linear servo analysis.

6.6.4. Gimbal Spin Inhibit Modification (1962). - An operational problem existed in this alignment mechanization if θ and ϕ are not equal when the loop was closed. The magnitude of the error signal would cause rapid gimbal movement at an uncontrolled rate. This problem was particularly acute if θ and ϕ were improperly nulled 180° apart. If the rate was too high, the gyros could be damaged. Operational procedures require that the loop be nulled at the proper angle. But to overcome the hazard associated with this potential problem and other sources of uncontrolled gimbal rates, a protective sensing circuit was added to the ARU. This circuit was designated as the gimbal spin inhibit (GSI) circuit. Signal inputs to the gimbal 1, 3, and 4 torque motors are constantly monitored by this circuit. If any one or more of these inputs exceeds a preset voltage level for a period of approximately 250 milliseconds or longer, the condition is interpreted as a spinning platform gimbal and the inhibit device is activated.

The circuit detects both positive or negative dc torque motor drive voltages. The polarity inverter, which accepts only negative dc voltages, provides a positive voltage output which is acceptable to the emitter-follower. (See Figures 6.6-3 and 6.6-4.) Positive input voltages are coupled directly to the emitter-follower. The input impedance presented by this circuit to the gimbal servo signals is in excess of 45 k ohms. The output of the emitter-follower will rise to a positive voltage whenever a positive or negative voltage exists on any of the input lines. Therefore, the emitter-follower output represents, with some loss of amplitude, the absolute value of the input voltage.

The percentage of voltage coupled to the level detector is variable permitting the choice of a voltage reference. The reference element is a zener diode in the base lead of the level detector. Once the breakdown voltage of the zener has been exceeded, the level detector goes quickly to saturation, causing the voltage at the collector of this common emitter stage to fall to approximately zero volts. This in turn provides a path for saturating base current for the PNP relay driver stage, and relay K1 on

0166-72A

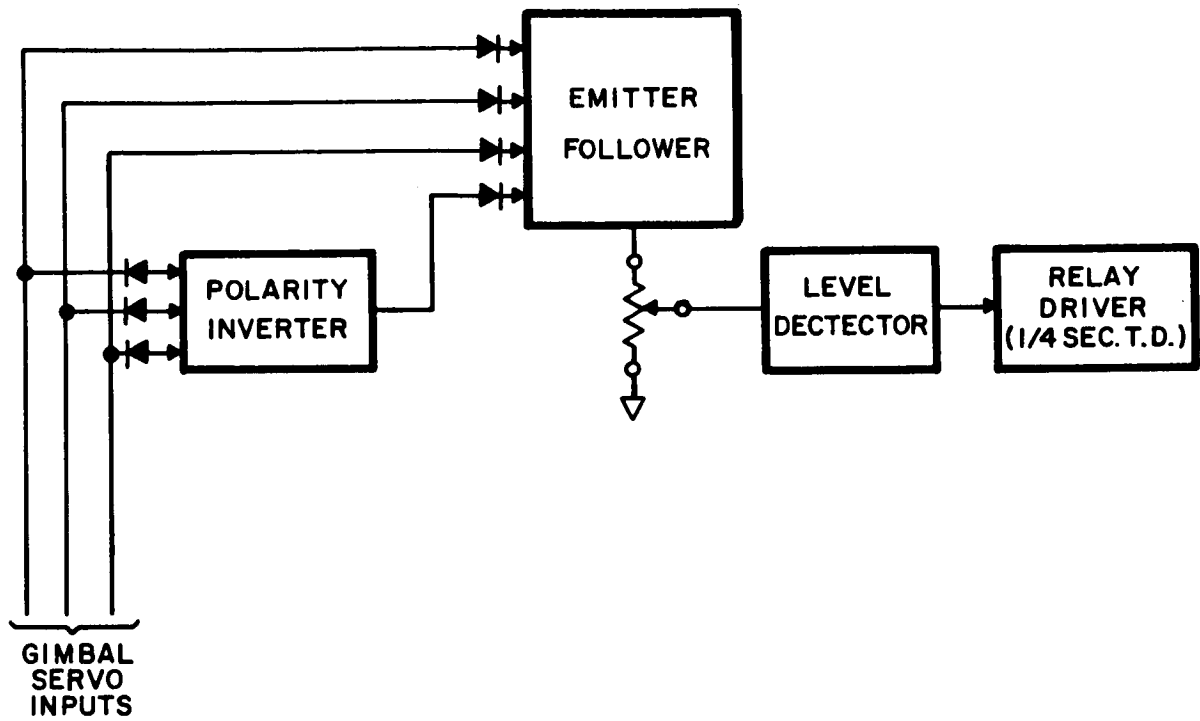


FIGURE 6.6-3. PLATFORM GIMBAL SPIN INHIBIT
PRINTED BOARD - BLOCK DIAGRAM

0165-2528

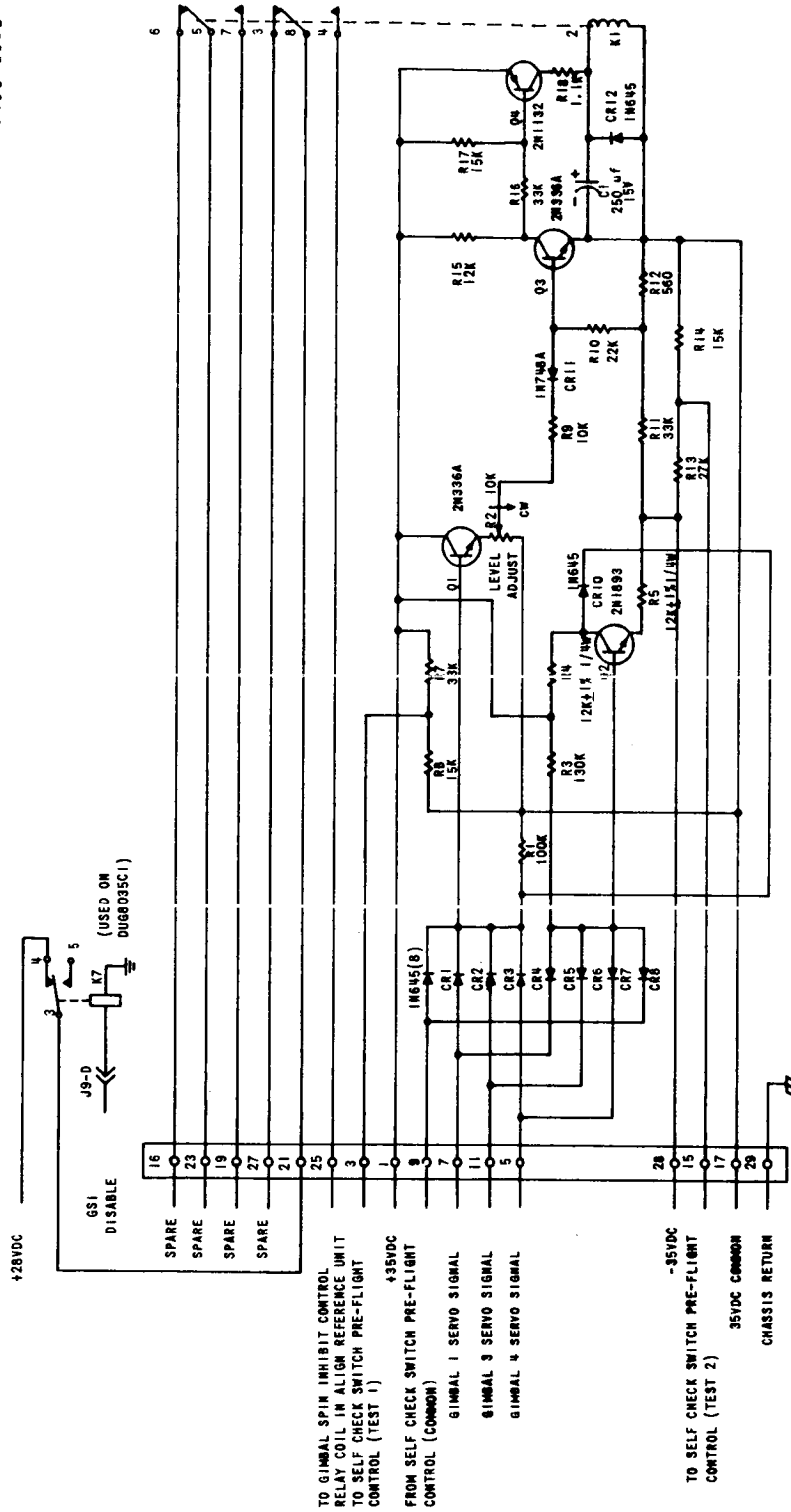


FIGURE 6.6-4. PLATFORM GIMBAL SPIN INHIBIT SCHEMATIC

the printed circuit board energizes. (An RC delay of approximately 250 milliseconds prevents the relay from energizing on short duration, high level inputs.)

The K1 relay closure results in closure and latching of control relay 1K5 in the alignment reference unit. The GIMBAL SPIN INHIBIT indicator on the MGS preflight control panel is illuminated and the guidance ready signal, if present, is removed. The actuation of relay 1K5 contacts opens the alignment signal paths from the GSE to the MGS gimbal servo loops. (See Figure 6.6-2.) After the cause of the gimbal spin condition has been eliminated, all circuits affected by the inhibiting action may be restored to their original condition by depressing the MODE SET and gimbal spin inhibit RESET switches located on the MGS preflight control panel.

6.6.5. Expansion of Platform Coarse Alignment Requirements (April, 1964). -

At this time a new requirement was imposed on the coarse alignment loop by field operational procedures. The Centaur miniature platform inter-gimbal clearances are rather tight. A field procedure was adopted whereby each gimbal was driven 360° or more while a strip chart recording of torque motor voltage was made. Gimbal hang-up or high friction could thus be checked without opening the platform. This test is performed at nearly every level of system testing, and as part of pre-launch preparations.

The effect of noise in the coarse align servo loop was not observed to degrade positioning accuracy. However, when these new test requirements were added, noise in the coarse alignment loop could cause a platform to be rejected or suspected. Marginal test results caused by noise would invariably imply a defective platform and result in extensive investigations. The noise was characterized by spikes (gearing backlash) and large amounts of 60 Hz power interference. Sometimes the voltage spikes were sufficient to trip the GSI protection circuit. Because of the tendency to use the coarse align signal incorrectly for an indicator of platform friction, the IMG is being designed to provide a more meaningful monitor signal.

6.6.6. Gimbal Spin Inhibit Redesign (June, 1965). -

To prevent this nuisance tripping of the GSI circuit the gimbal spin detection circuit was redesigned. Essentially, an integrator filter was added ahead of the emitter-follower stage (Reference Figure 6.6-5). A voltage which persists for a certain time period is interpreted as a gimbal spinning at 55 degrees/second, and the circuit is activated. Figure 6.6-6 depicts the resulting GSI circuit. This is similar to Figure 6.6-4, except for the input diode logic and time delay relay K1.

0 2 6 6 - 2 5 5 B

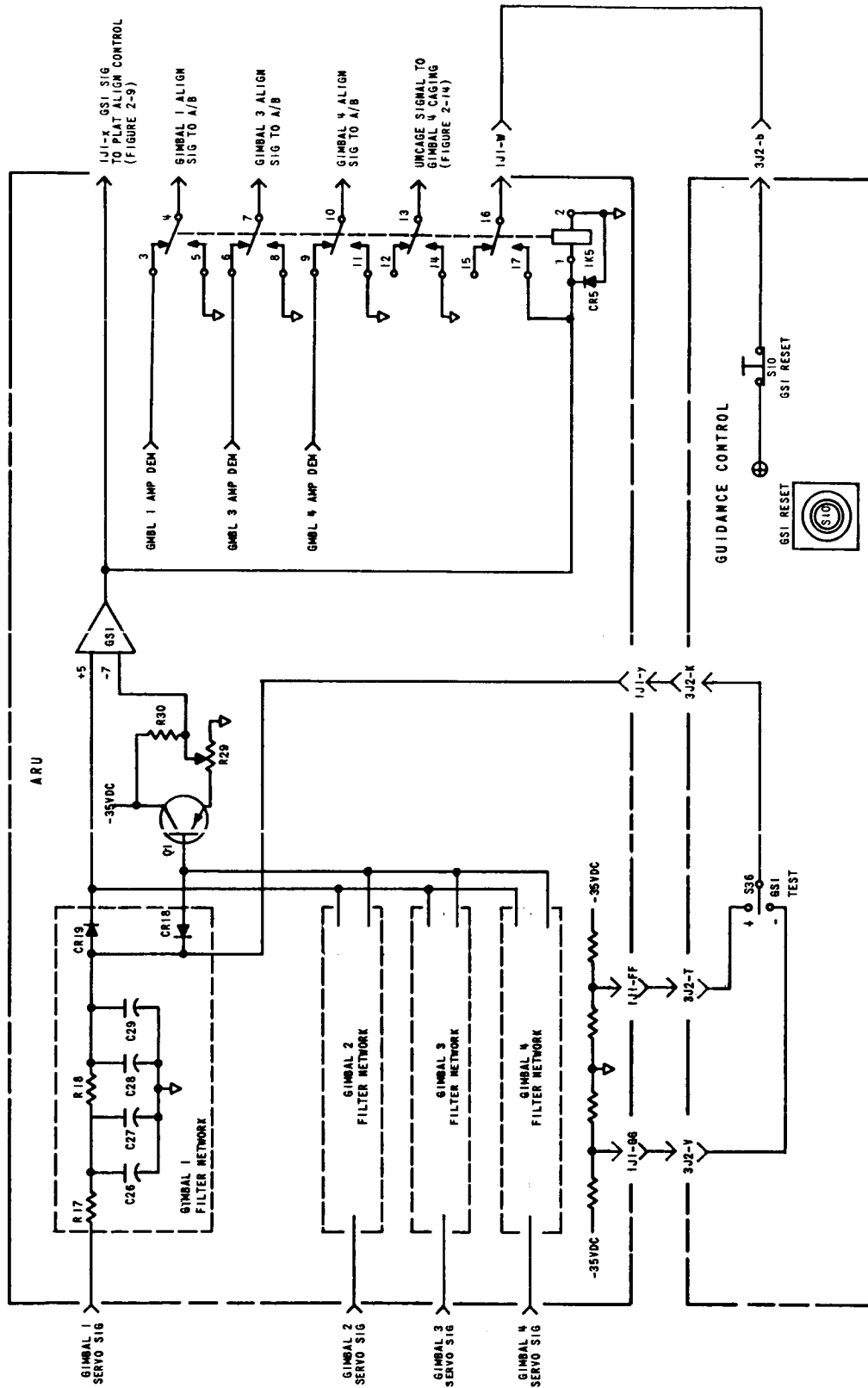


FIGURE 6.6-5. GIMBAL SPIN INHIBIT BLOCK DIAGRAM

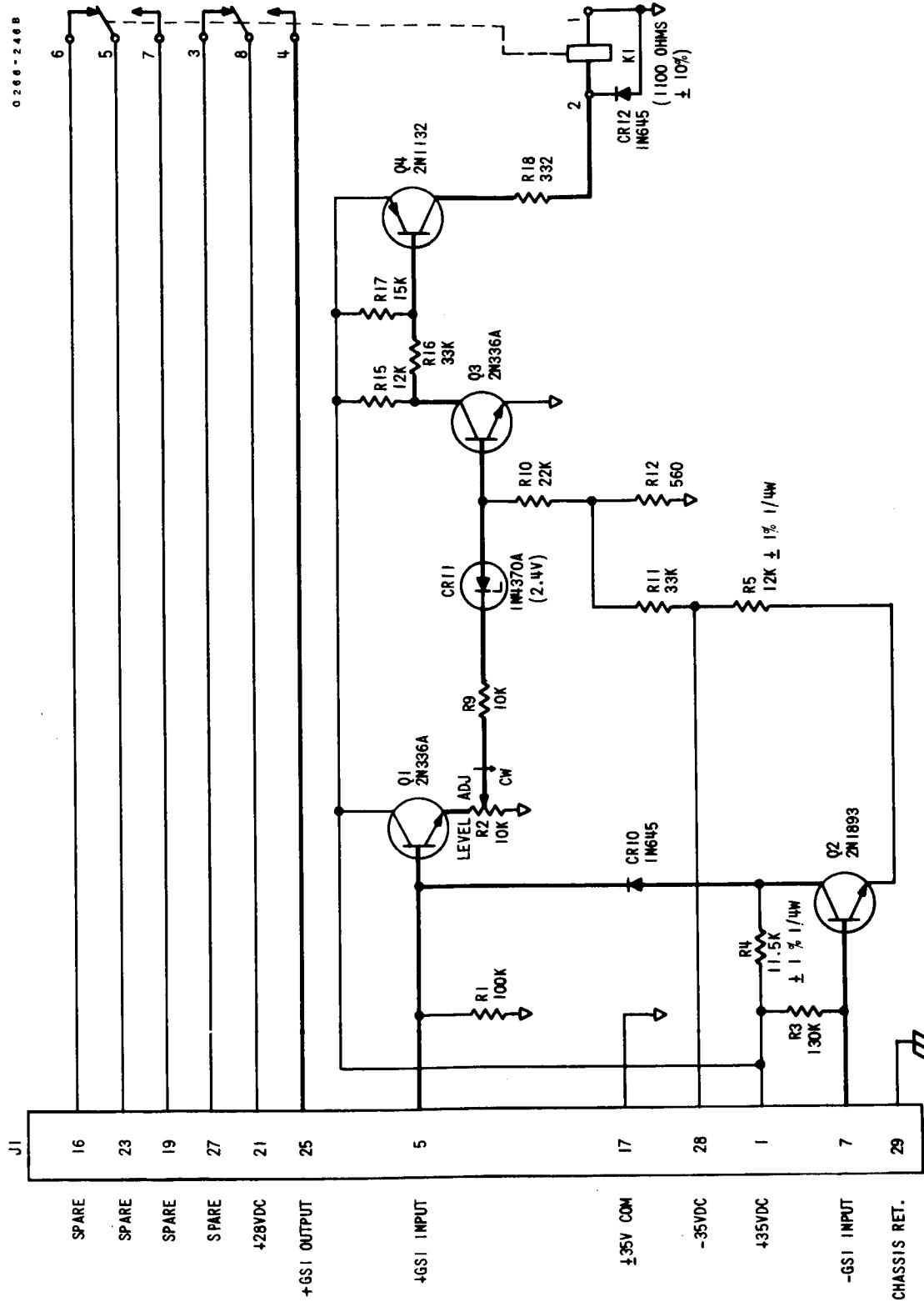


FIGURE 6. 6-6. GIMBAL SPIN INHIBIT SCHEMATIC

6. 6. 7. Present Status (1967). - The noise in the coarse alignment loops remains a problem when the loop is used to check gimbal clearance. A study of loop gain and phase margins showed that additional filtering within each loop would degrade accuracy and/or stability. Low-pass filtering of the servo motor voltages before they are recorded has proven to be a relatively inexpensive solution to the noise problem. Thus, the noise which was not a problem in the original design is still present today. But methods have been devised to circumvent the effect of the noise on present-day needs.

6. 6. 8. "Doing It Over Today - The IMG". - The original coarse alignment philosophy rejected the concept of torquing the gyro for gimbal reorientation because of residual magnetism. For the IMG, gimbal reorientation by high-rate gyro torquing was selected. To overcome the residual magnetism, a torquer degaussing scheme was considered. However, such a scheme adds complexity to the gyro torquing mechanization. Subsequent study showed that the residual magnetism does not cause gyro drift if both the gyro control and pattern torquing fields are opened. With the present operational concept of no in-flight torquing, drift from magnetism will be non-existent.

The improved Centaur IMG (Figure 6. 6-7) concept actually eliminates a "coarse" alignment loop; the gyro is always closed into the stabilization loop. The gyro torquing electronics (GTE) block diagram shows how rapid realignment of the platform is achieved. When 46 ma is applied to the gyro control field and 36 ma is applied to the pattern field, the gyro (and consequently the gimbal) will precess at 0.9 degrees per second. When realignment is complete, the control field current is dropped to 1 ma and the computer then provides gyro trim. This mechanization will provide accurate, automatic alignment. Also, the loop noise, which is presently caused by the GSE gear-train and resolver mechanization, will not be a problem.

6. 6. 9. Conclusions. - The difficulties encountered with the electro-mechanical, manual, coarse alignment loop have provided several good lessons for future designs. Although the original design goals of accuracy and loop stability were met, there was no provision for possible increased operational requirements upon the loop. In the improved Centaur design, GSE gears and resolvers were eliminated. Good overall alignment loop performance is now available for platform orientation and other test requirements.

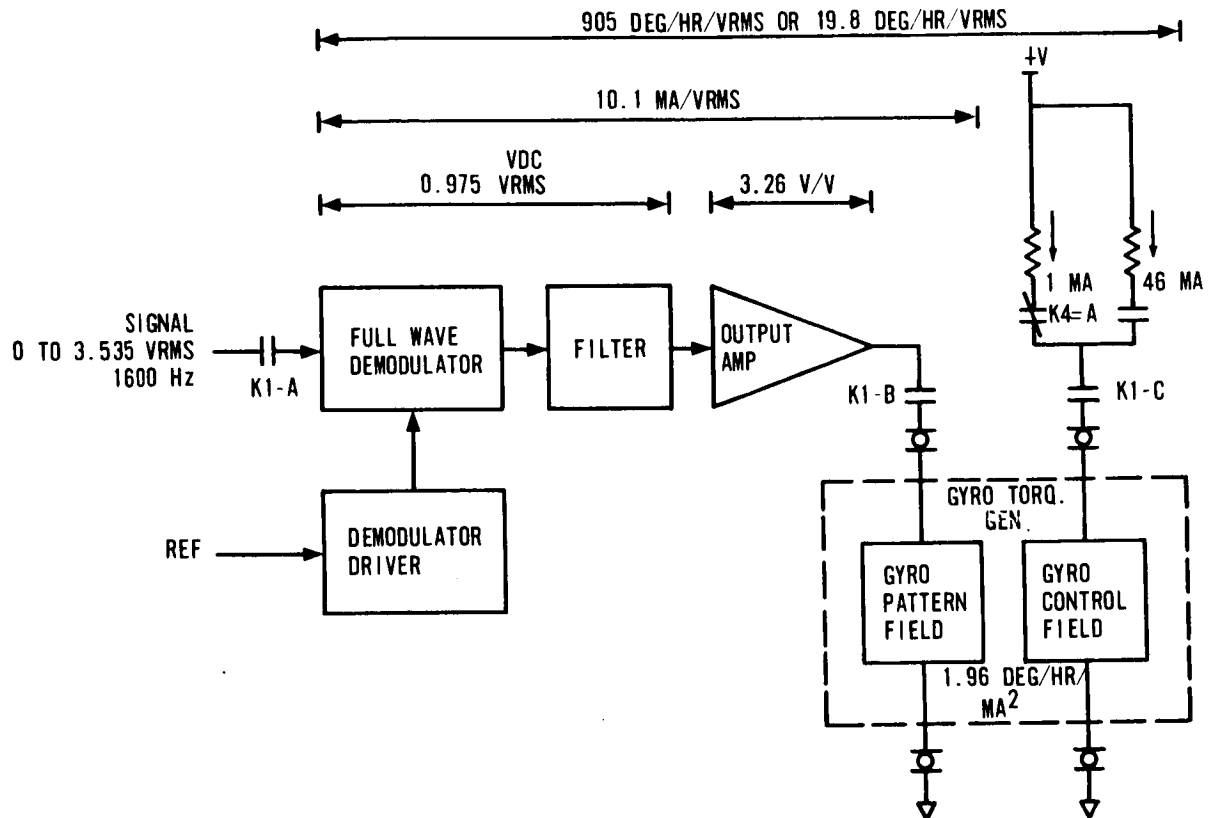


FIGURE 6. 6-7. GTE BLOCK DIAGRAM

Topic 6. 7

Steering Signal Coordinate Transformation

6. 7. 1. Introduction. - Steering signals are generated in the Computer to provide missile steering corrections for any differences in the pointing direction of the actual and the desired thrust vector. These steering signals are referenced to inertial space.

Vehicle coordinates change with respect to inertial coordinates as vehicle attitude changes. As the gimbals move about the stable element during vehicle maneuvers, the motion is sensed by the gimbal angle resolvers mounted between the gimbals and vehicle frame and converted to attitude information. Since the gimbals move relative to each other in complex trigonometric patterns, the resolvers are electrically interconnected into a "chain" to resolve the mechanical motions into accurate attitude information. In actual practice, the chain performs a dynamic matrix transformation used to transform a vector from the stable reference frame to the vehicle coordinate system. The Resolver description is in Topic 2. 4, while the Resolver Electronics is described in Topic 2. 12.

6. 7. 2. Discussion. -

6. 7. 2. 1. Coordinate Transformation. - An example of coordinate transformation is shown in Figure 6. 7-1. The vector R is shown in terms of the Up, Vp rectangular coordinate system. It is desired to express this vector in terms of the B, A rectangular coordinate system which is displaced from the Up, Vp coordinate system by some angle α_1 . The relationship between input and output for resolver B1A can be expressed by the following equations.

$$A = Up \cos \alpha_1 + Vp \sin \alpha_1$$

$$B = Vp \cos \alpha_1 - Up \sin \alpha_1$$

It should be noted from the example shown in Figure 6. 7-2 that a resolver can perform a coordinate transformation of two coordinates. The coordinates must be in the same plane as the angle about which they are resolved and the resultant output coordinates remain in the same plane.

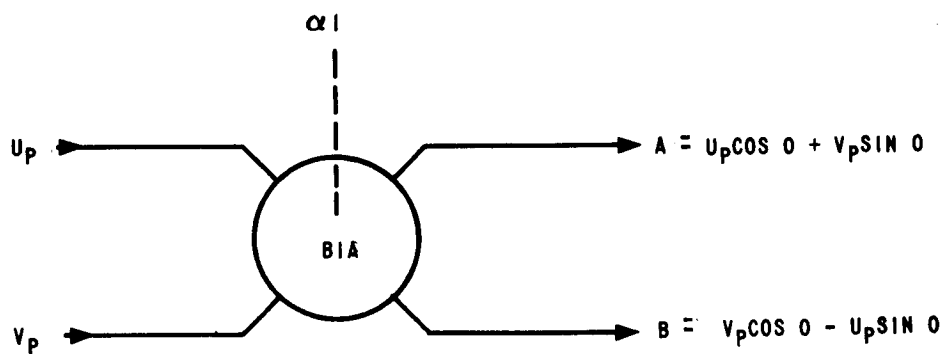
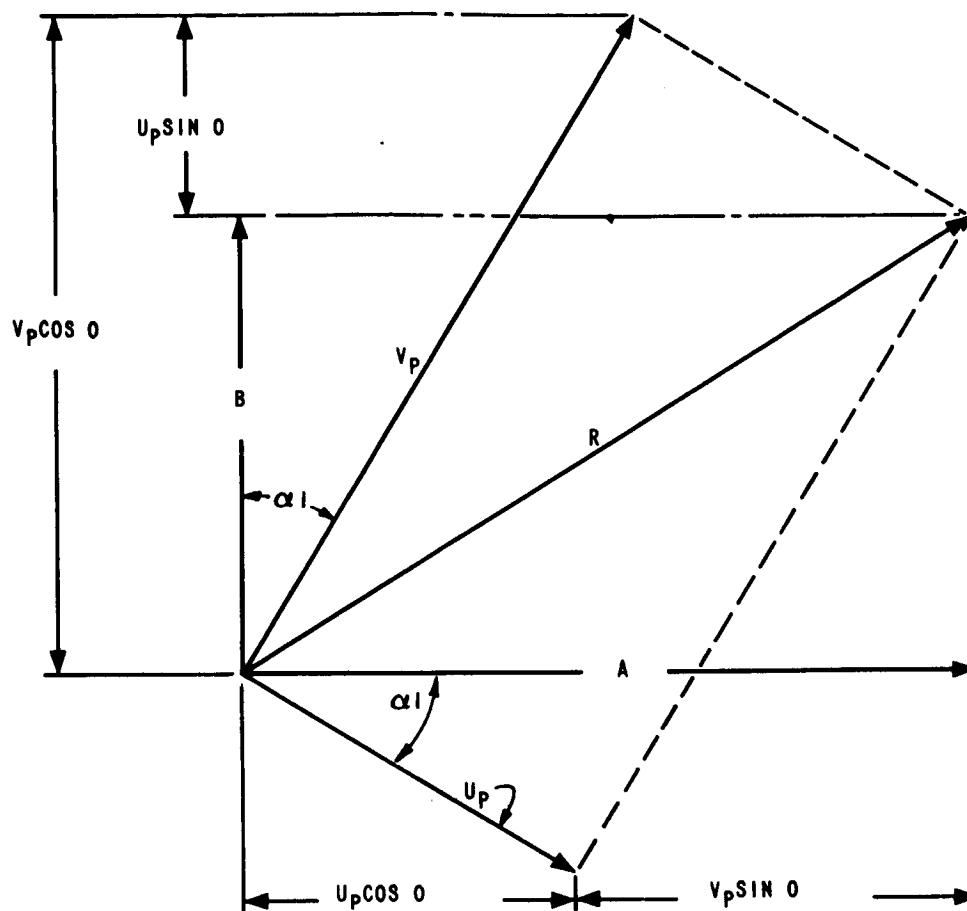
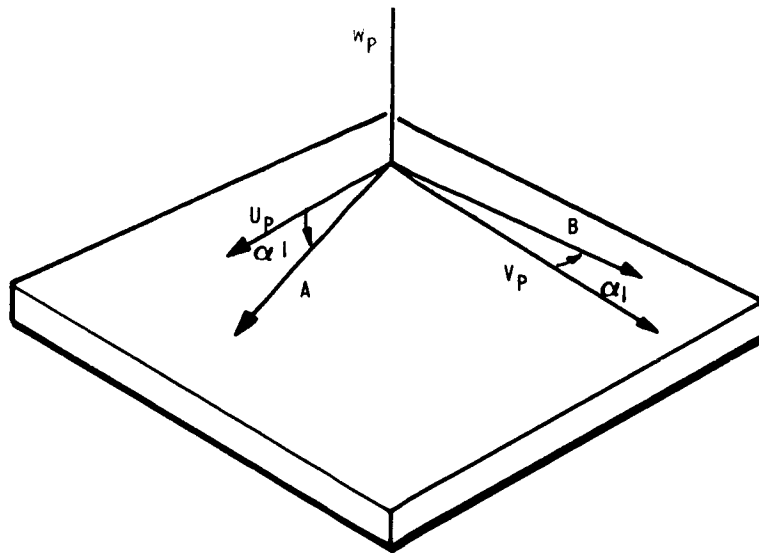
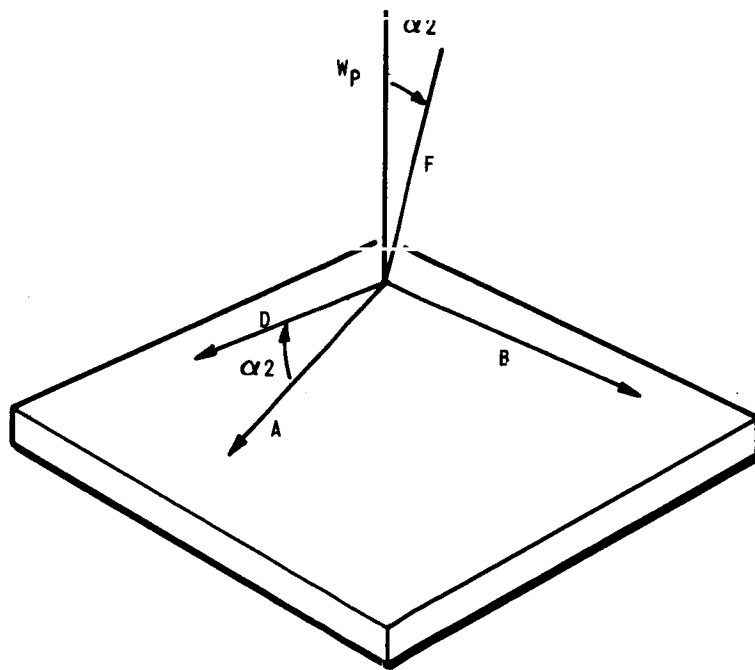


FIGURE 6.7-1. COORDINATE TRANSFORMATION



a. Transformation of coordinates U_p and V_p about an angle α_1



b. Transformation of coordinates W_p and A about an angle α_2

FIGURE 6.7-2. COORDINATE TRANSFORMATION ABOUT ANGLES α_1 AND α_2

Now consider a third coordinate, W_p , which is mutually perpendicular to coordinates U_p and V_p , (see Figure 6.7-2). The output coordinates A and B will also be mutually perpendicular to coordinate W . Therefore, the three form a valid coordinate system. Coordinates A and W are then applied as inputs to resolver B3A and the second coordinate transformation is performed about the angle α_2 as shown in Figure 6.7-2. This same procedure is repeated for the transformation of the effected coordinates about angles α_3 and α_4 . The resultant outputs X and Y have been modified for any differences in attitude between the vehicle and stable element and therefore can be used to steer the vehicle.

6.7.2.2. Derivation of Resolver Chain Output Equations. - Using the resolvers to derive the sine and cosine functions, it is possible to provide a coordinate transformation of any vector. A simplified schematic and signal flow graph of the resolver chain are shown in Figure 6.7-3. The graph may be referenced to the schematic by the intermediate points, A through J , which are labeled on both diagrams.

The following equations express the outputs as functions of inputs and the transformation angle as shown in Figure 6.7-3.

The attenuation value (K) for each resolver has been omitted and the gimbal angles α_1 through α_4 are shown by the number 1 through 4 for clarity in the equations.

$$\begin{aligned} A &= U \cos 1 + V \sin 1 \\ B &= V \cos 1 - U \sin 1 \\ C &= W \\ D &= A \cos 2 - C \sin 2 \\ E &= B \end{aligned}$$

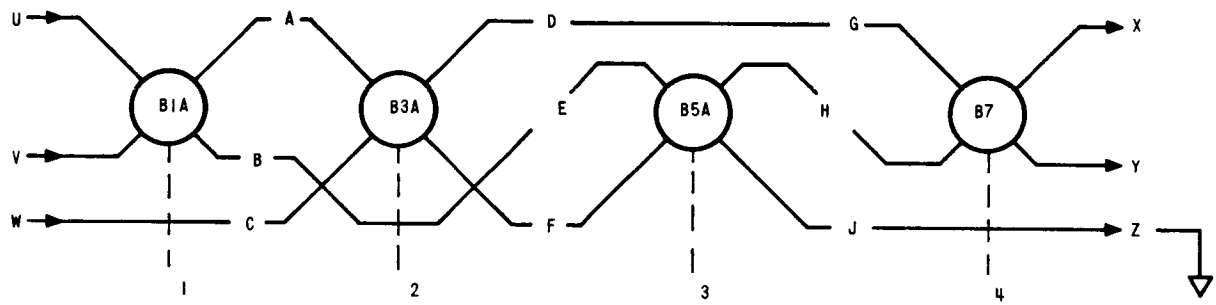
$$\begin{aligned} F &= C \cos 2 + A \sin 2 \\ G &= D \\ H &= E \cos 3 + F \sin 3 \\ J &= F \cos 3 - E \sin 3 \end{aligned}$$

$$\begin{aligned} X &= G \cos 4 + H \sin 4 \\ Y &= H \cos 4 - G \sin 4 \end{aligned}$$

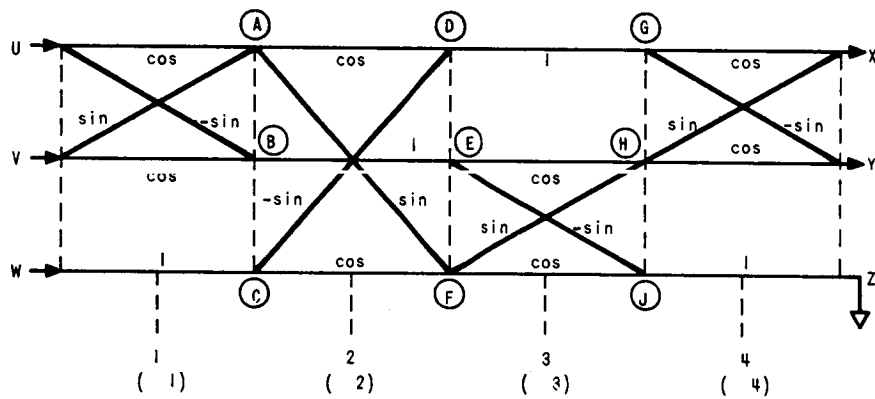
Expanding and collecting like terms results in the following output equations:

$$\begin{aligned} X &= U (\cos 1 \cos 2 \cos 4 - \sin 1 \cos 3 \sin 4 + \cos 1 \sin 2 \sin 3 \sin 4) \\ &\quad + V (\sin 1 \cos 2 \cos 4 + \cos 1 \cos 3 \sin 4 + \sin 1 \sin 2 \sin 3 \sin 4) \\ &\quad + W (\cos 2 \sin 3 \sin 4 - \sin 2 \cos 4) \end{aligned}$$

0665-2318



(a). RESOLVER CHAIN



(b). SIGNAL FLOW GRAPH

FIGURE 6.7-3. RESOLVER CHAIN SCHEMATIC AND SIGNAL FLOW GRAPH

As an example the coordinate transformation of the U term of the X output equation is illustrated in Figure 6.7-4. There are three paths from U to X through the signal flow graph. The first is a straight line across the top of the graph giving the term

$$U (\cos 1 \cos 2 \cos 4 + \dots)$$

(Note that this path is not resolved about α_3 and therefore does not contain an α_3 term.)

The second path yields

$$U (-\sin 1 \cos 3 \sin 4)$$

Again there is no α_2 term

and the third path yields

$$U (+\cos 1 \sin 2 \sin 3 \sin 4)$$

Adding the three terms we have

$$U (\cos 1 \cos 2 \cos 4 - \sin 1 \cos 3 \sin 4 + \cos 1 \sin 2 \sin 3 \sin 4).$$

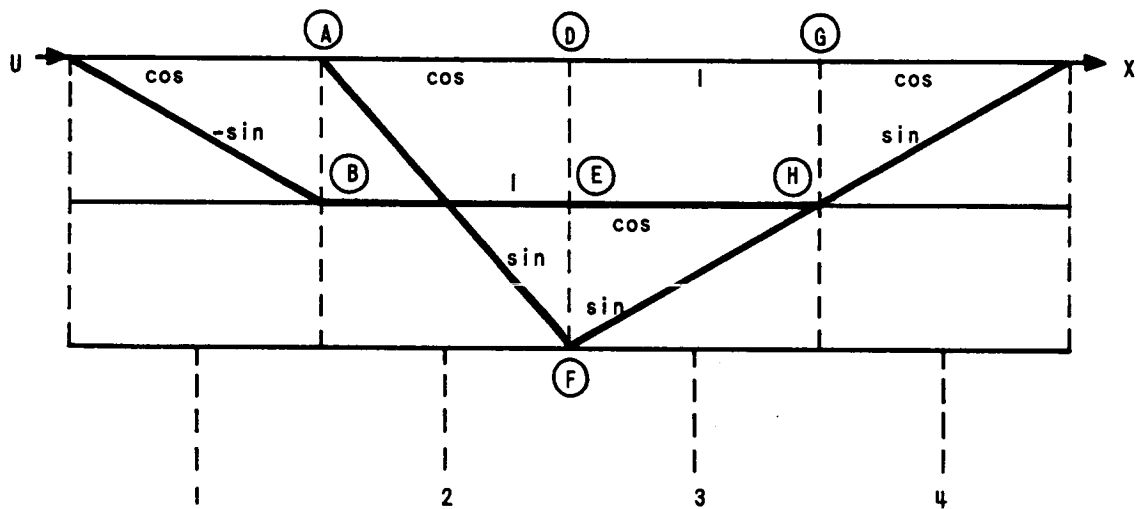
Repeating the operation for the V and W inputs results in the final output equation for X.

The final equations represent the analog signal which is fed to the missile autopilot to control steering.

6.7.2.3. Flight Performance. - Figure 6.7-5 is a simplified diagram of the Centaur control system illustrating the incorporation of the resolver chain. During normal flight operations the accelerometers sense linear accelerations and are rebalanced to their nulls with constant energy pulses. The computer counts pulses, referenced to inertial space, and computes velocity to-be-gained. This vector (\vec{V}_g), is also expressed in the inertial U, V, and W axes. Corrections to the vehicle trajectory are sent from the computer in the form of attitude steering signals.

The computer steering signals are generated as shown schematically in Figure 6.7-5. The steering Potentiometers are excited by 400 Hz, 27 Vrms signals. The potentiometers are center-tapped to ground to provide either zero or π phase reference. Servo controlled wipers are positioned by the computer in accordance with the requirements for attitude with respect to inertial coordinates.

0665-2668



(Paths of Signal Flow Graph Between U and X)

FIGURE 6.7-4. COORDINATE TRANSFORMATION
OF U INTO X

0668-2288

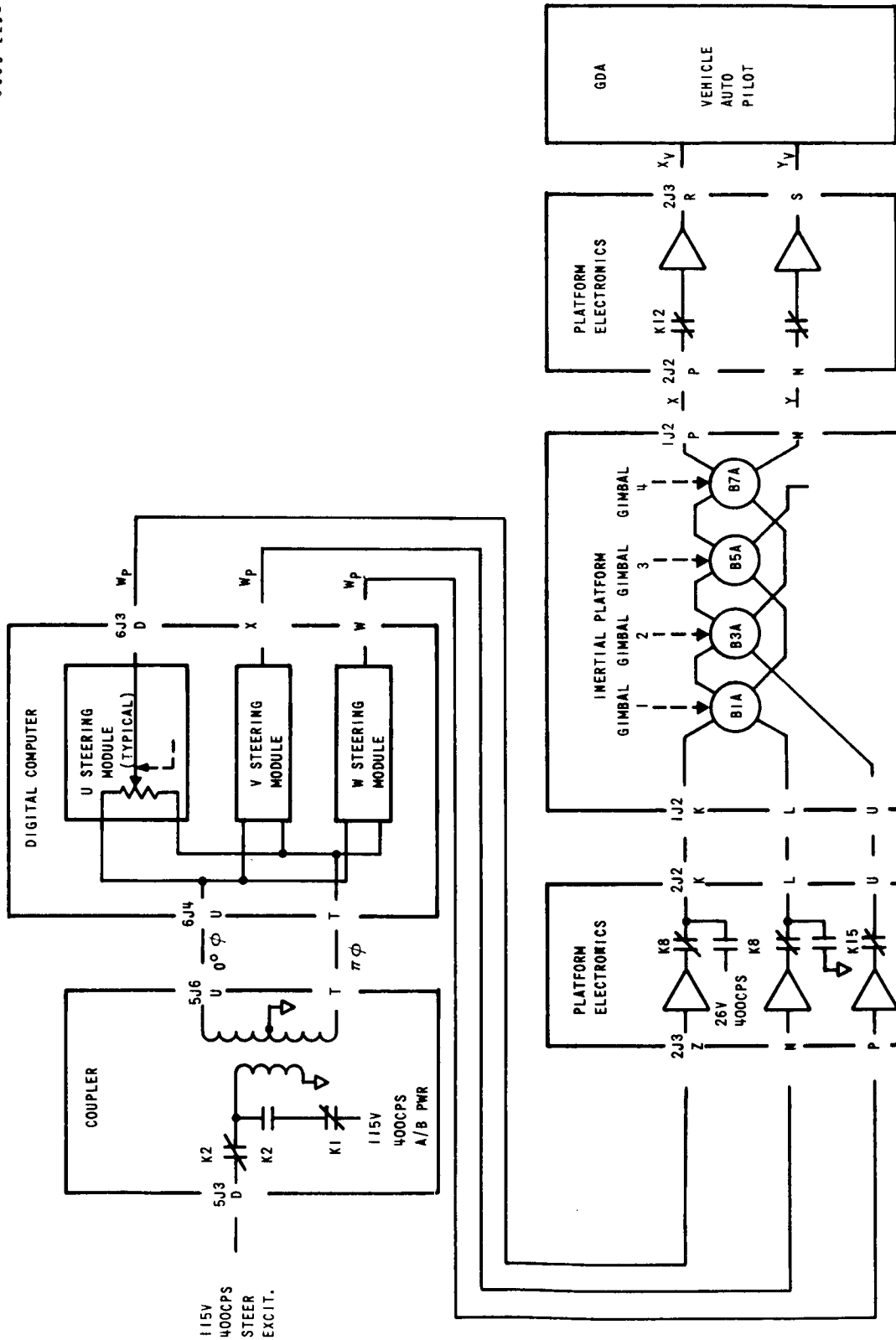


FIGURE 6.7-5. FUNCTION OF THE COORDINATE TRANSFORMATION RESOLVER CHAIN

These signals are inserted in the Up, Vp and Wp inputs, and transformed in the resolver chain to X and Y (pitch and yaw) channels of the autopilot.

The Z axis output is not brought out of the resolver chain, but is terminated in the platform electronics unit. The present Centaur mission and control systems require pitch and yaw steering information only. The resolver chain properly directs the X and Y signal outputs, regardless of roll attitude. The vehicle is roll rate stabilized, however, using a rate gyro in the autopilot.

Prior to termination of the orbital coast phase, the missile must be aligned in the direction required for the next powered phase, that is, along the velocity to-be-gained vector \vec{V}_g . The computer derives the desired attitude vector and inserts the proper voltages at the input to the resolver chain. As the X and Y outputs null out, the longitudinal axis of the missile is aligned in the V_g direction.

After spacecraft separation the Centaur vehicle is realigned approximately 180° from the vector \vec{V}_g . The maneuver is done to allow residual fuel blowdown to separate the Centaur vehicle from the spacecraft so that "lock on" will be to the proper star rather than the Centaur vehicle. Again the computer derives the desired attitude vector and inserts the proper voltages at the input to the resolver chain.

6.7.3. Conclusion. - The present IGS and IMG steering signal coordinate transformation mechanizations are adequate. Trade-off studies were performed, as part of the IMG development program on an alternate mechanization, wherein precision gimbal angle pickoffs were used to provide inputs to the Navigation Computer. The Computer would then perform the coordinate transformation function. Although performance and reliability might be upgraded in other gimballed systems, using computer coordinate transformation, the technique proved to be unfeasible for the IMG because of the Euler angle equations requirements under the high angular rates associated with gimbal flip conditions. These requirements exceeded the computational speed capability of all candidate, state of the art computers. Another detrimental factor for this approach was the relatively high cost of precision gimbal angle pickoffs.

The experience gained on Centaur has also pointed out several important lessons which should be applied to future IGS development programs. These lessons include:

1. The need for careful definition and evaluation of the specific resolver parameters, which are critical to the intended application.
2. Within the constraints of No. 1, attention should be paid to the early development of a resolver second source (this may imply standardizing subassemblies of the resolver, which must be traded off against the design constraints).
3. Special attention must be given to:
 - a. specification of resolver requirements.
 - b. evaluation and selection of vendors.
 - c. review and control of vendor designs, processes, inspection points, and test methods.
 - d. continuing configuration control once the design, processes, etc., are acceptable.
4. Mechanization of resolver chains, using active compensation techniques, is highly desirable for either two-axis or three-axis coordinate transformation.
5. The application of resolver chains can be expanded on future programs (as has been already done on Centaur and other existing programs) to include gyro drift calibrations, measurement of vehicle perturbations (such as twist during tanking on the launch pad), etc.

Topic 6.8

Automatic Self-Leveling

6.8.1. Summary. - Automatic self-leveling has remained essentially the same throughout the Centaur guidance program. There have been no significant problems encountered or changes made since the original mechanization. The IMG mechanization is also remaining the same as the original mechanization.

6.8.2. Functional Description. - The self-leveling mode is automatically controlled by the guidance computer. The computer processes velocity information from the level accelerometers to maintain gimbal attitude through zero torquing.

The platform is generally oriented with one axis vertical and two axes horizontal. The horizontal axes will usually be aligned along the north and east Earth axes. Thus, the gyro and accelerometer triads are oriented so that the input axes are along the azimuth, north and east axes. Azimuth alignment is covered in Topic 6.9.

The self-leveling loops are mechanized using the accelerometers to sense a component of gravity resulting from an off level condition. Incremental velocity from the accelerometer loop is fed to the airborne computer where corrective gyro torquing rates are developed and commanded through the gyro torquing potentiometer outputs from the computer. Through gyro precession, the corrective gyro torquing drives the appropriate gimbal servo(s) to correct the off level condition. The gyro output signals (north and east) are resolved through a heading coordinate resolver to drive the pitch and yaw gimbal servo loops. Figure 6.8-1 illustrates the level loop mechanization.

Centaur guidance utilizes automatic self-leveling during various portions of the calibration and final align modes. The level hold equations that are mechanized in the airborne computer provide a damped gyro torquing rate correction. The gyro torquing rate is updated each compute cycle (approximately one second). The level hold equations have remained the same throughout the Centaur IGS Program.

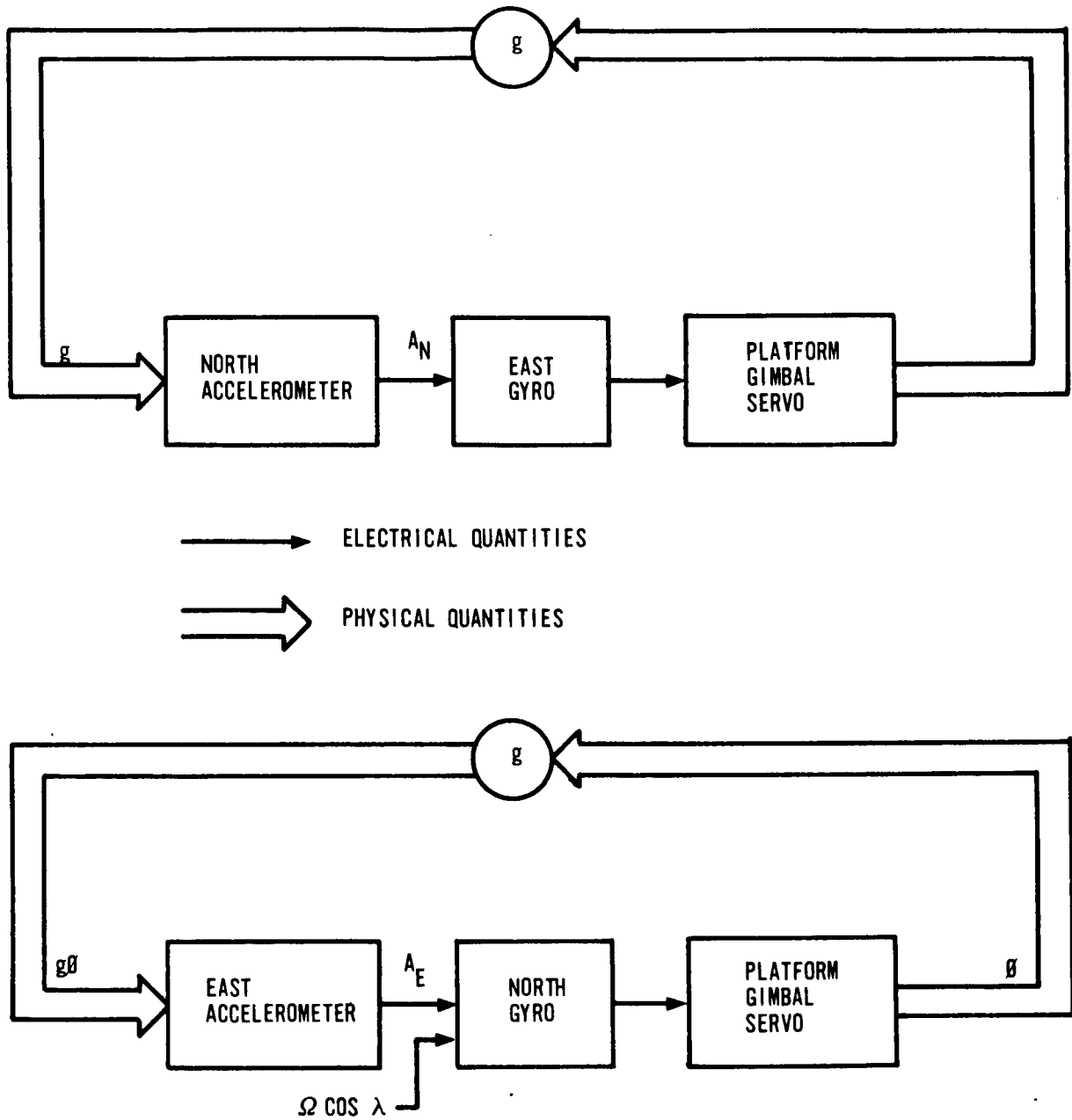


FIGURE 6.8-1. LEVEL LOOP DIAGRAM

The level gyro torquing equations are:

$$1. \quad W_N = W_d + W_{ER} + \Delta W_N \quad \text{North gyro}$$

$$2. \quad W_E = W_d + \Delta W_E \quad \text{East gyro}$$

where: W_N and W_E = the total torquing rates applied during level hold.

W_d = gyro drift compensation

W_{ER} = Earth's rate compensation

ΔW_N and ΔW_E = level hold corrective gyro torquing rates.

The corrective gyro torquing rate equations are:

$$\Delta W_{N_i} = K_1 V_{E_i} + K_2 V_{E_{i-1}} + K_3 \Delta W_{N_{i-1}}$$

$$\Delta W_{E_i} = K_1 V_{N_i} + K_2 V_{N_{i-1}} + K_3 \Delta W_{E_{i-1}}$$

where:

V_{N_i} and V_{E_i} = cumulative velocity since start of level hold through the latest compute cycle

$V_{N_{i-1}}$ and $V_{E_{i-1}}$ = above term less latest compute cycle ΔV 's

ΔW_{N_i} and ΔW_{E_i} = new value for level hold corrective torquing

$\Delta W_{N_{i-1}}$ and $\Delta W_{E_{i-1}}$ = last value of above term

$$K_1 = 2.01087 \text{ deg/hr/ft/sec}$$

$$K_2 = 2.00395 \text{ deg/hr/ft/sec}$$

$$K_3 = 0.966101 \text{ deg/hr.}$$

K₁, 2, 3 have remained the same throughout the Centaur IGS Program with the exception of changes necessitated by changes in compute cycle time.

6.8.3. Problems. - There have been no problems directly attributable to the mechanization of the automatic self-leveling loop. However, there have been problems associated with other more basic portions of the IGS that have adversely affected level loop operation. These problems involved the basic gyro-gimbal stabilization function and the accelerometer-velocity measurement function. The problems, their causes and solutions, are discussed in other sections of this report having to do with the basic function or functions. This discussion will be limited to a description of the type of problem and its effect on automatic self-leveling.

Accelerometer or accelerometer loop deadzone is an effect, which limits the ability of the accelerometer loop to sense small changes in acceleration when operating at or near a zero "g" input. This problem was seen with the GG116 accelerometer and with the early GG177 accelerometer digital electronics. Deadzone magnitudes of one-half to one arc-minute were often seen.

The characteristic of the level loop operation with deadzone present was to permit random wandering of the platform gimbal within the range of the deadzone. Adoption of the GG177 accelerometer eliminated the accelerometer as a significant source of deadzone error. Modification of the early Phase II PIP accelerometer loop electronics corrected the latest source of the level loop problem. This was the coupler pulse dropping incident which is covered in Topic 2.15.

Gimbal stabilization loop deadzone, if large enough, would create a similar effect on the self-leveling loop. This has never been a problem on the Centaur program and should it occur it would be due to a gross failure within the stabilization loop itself.

Gyro random drift can create a wandering of the level loop again similar to accelerometer loop deadzone provided the drift changes are faster than the time constant of the level loop. The magnitude of this effect is insignificant except where the gyro may be failing.

6.8.4. The IMG Design. - The IMG design is essentially the same as the present IGS automatic self-leveling design. The requirements of the IMG can be met with the present mechanization which has been successful throughout the evolution of Centaur guidance. In the future some consideration may be made toward optimizing the software portion of automatic

self-leveling since there is a lesser restriction on computer memory space with the IMG design.

6.8.5. Conclusions. - There have been no significant changes or problems in the self-leveling loop mechanization during the Centaur program, and the mechanization will continue in the IMG program, since it offers the basic advantages of using one set of accelerometers for level alignment and in-flight velocity measurement.

Topic 6.9

Final Azimuth Alignment

6.9.1. Summary. - Both self-contained gyrocompassing and ground based optics have been used during the program for final, or prelaunch, azimuth alignment of the platform. In this report, primary emphasis is placed on alignment by optics since comprehensive discussions of gyrocompassing techniques and limitations can be found in a number of published textbooks on inertial guidance.

Prior to the AC-4 launch in December 1964, gyrocompassing was used to accomplish final azimuth alignment of the platform at the ETR launch complex. This means provided sufficient alignment accuracy to meet flight test objectives up to that time. The GSE equipment to provide an optical azimuth alignment capability was operational in time for the AC-4 launch and has been used for final platform azimuth alignment for all subsequent Atlas/Centaur flights.

Azimuth alignment of the platform by optics provided an improvement in azimuth alignment accuracy of better than 10 to 1 over that achieved by gyrocompassing. This alignment improvement significantly improved the mission accuracy of the MGS; however, the dollar cost for the development and implementation of the optical alignment capability (that is, optical GSE) to achieve this improvement was also significant.

Problems encountered with final azimuth alignment were:

1. Gyrocompassing - The mechanization and implementation of gyrocompassing was accomplished with some significant problems. These were analyzed and solved on the -1 program. However, concurrent with the advent of the Surveyor mission requirement, an azimuth alignment requirement of 0.75 mr maximum misalignment was established as necessary for compatibility with the specified MGS mission accuracy requirements. This new alignment requirement was well beyond the gyrocompassing capability at that time (≈ 3 mr, one sigma); therefore, the combination of hardware configuration and redesign constraints, plus the prevailing alignment technique state of the art dictated a need for an optical alignment capability.

2. Optical Alignment - The optical azimuth mechanization and implementation was accomplished with few and only minor problems. An operational problem, which has occasionally been encountered during prelaunch operations, stems from vapor plumes during vehicle tanking. Under certain wind conditions, interference in the optical line of sight is created by drifting vapor plumes, causing intermittent alignment loop operation. While this problem is of the nuisance variety, it is significant from the "launch-on-time" aspect of vehicle launch operations; and, lock-out provisions have been made in the automatic countdown sequence logic to reduce the risk of a forced "hold" due to this cause. Although this problem has been successfully circumvented, it could be avoided in future applications by judicious location of propellant vent openings; or, if practical, the use of optical sight tubes.

The following discussions pertain primarily to the system design aspects of azimuth alignment and use. Hardware development is covered in Topic 5.4.

6.9.2. Introduction. - From the inception of the Centaur program until late 1963, customer specifications provided alternate MGS mission accuracy requirements, in terms of velocity error normal to the orbital plane, depending upon the platform azimuth alignment technique used (gyrocompassing or optical). For the 110-mile orbit mission, a velocity error of 71.0 ft/sec (one sigma) at final Centaur engine cutoff was acceptable for final azimuth alignment by gyrocompassing; or, for alignment by optics, the acceptable velocity error was a much smaller value of 7.0 ft/sec (one sigma). Even though the platform was configured with the necessary interfaces for azimuth alignment by optics during this period, the 15-30 arc-minute alignment accuracy by gyrocompassing was considered adequate for the missions at hand, and no funds were made available for the development of the necessary GSE to provide an optical azimuth alignment capability at the launch complex.

6.9.3. Gyrocompassing (Dash 1 to 1964). - Azimuth self-alignment by gyrocompassing is based on the principle that when the platform stable element is misaligned in azimuth the east gyro will sense a component of the Earth's rotational rate. Any sensed rate will result in a tilt out of level about the east axis and the generation of an output signal by the north accelerometer. By using this accelerometer signal as a control to torque the azimuth gyro, the stable element can be rotated in azimuth until no component of Earth's rotation is sensed by the east gyro.

Figure 6.9-1 shows a simplified block diagram of the self-leveling and gyrocompassing loops. Figure 6.9-2 shows the alignment of the inertial components for a 105 degree final azimuth alignment heading which is typical for launch from Complex 36A at ETR. Referring to Figure 6.9-1, the torquing of the gyros is controlled by the guidance computer according to the following equations:

$$(1) \quad W_E = U_g + W_{dE} + \Delta W_{dEi} \text{ (East gyro torque rate)}$$

$$(2) \quad W_N = V_g + W_{dN} + \Delta W_{dNi} \text{ (North gyro torque rate)}$$

$$(3) \quad W_A = W_g + W_{dA} + \Delta W_{dAi} \text{ (Azimuth gyro torque rate)}$$

U_g , V_g , and W_g are geodetic constants predetermined and stored in the computer, which specifically define the nominal launch azimuth. Referring to Figure 6.9-2, these constants can be determined to be as follows:

$$U_g = [\cos lt] [\sin B]$$

$$V_g = [\cos lt] [\cos B]$$

$$W_g = \Omega \sin lt$$

Where:

Ω is Earth's rotational rate

B = nominal launch azimuth, ψ , - 90 deg

lt = latitude

The W_{dE} , W_{dN} , and W_{dA} terms are the drift trim values required to compensate for the measured, or calibrated, gyro drift terms, that is--inherent constant torque and mass unbalance drift rates. The values of these terms are determined during gyro calibration and stored in the computer prior to final alignment.

The ΔW_d terms are the damping terms that torque the gyros in accordance with the instantaneous off-level information, provided by the level accelerometers. The ΔW_d terms are calculated by the guidance

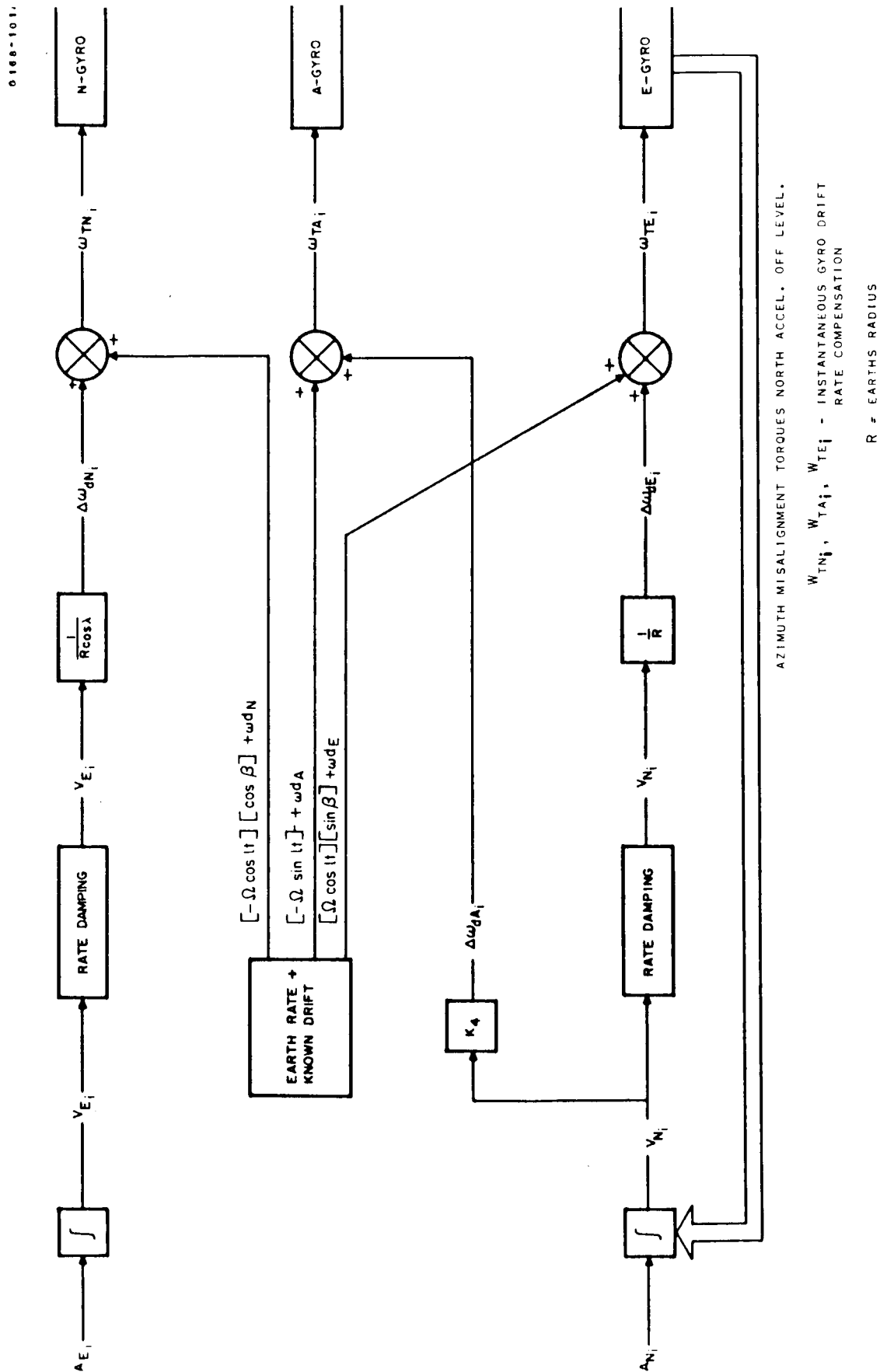


FIGURE 6.9-1. SELF-LEVELING GYROCOMPASSING LOOP, SIMPLIFIED BLOCK DIAGRAM

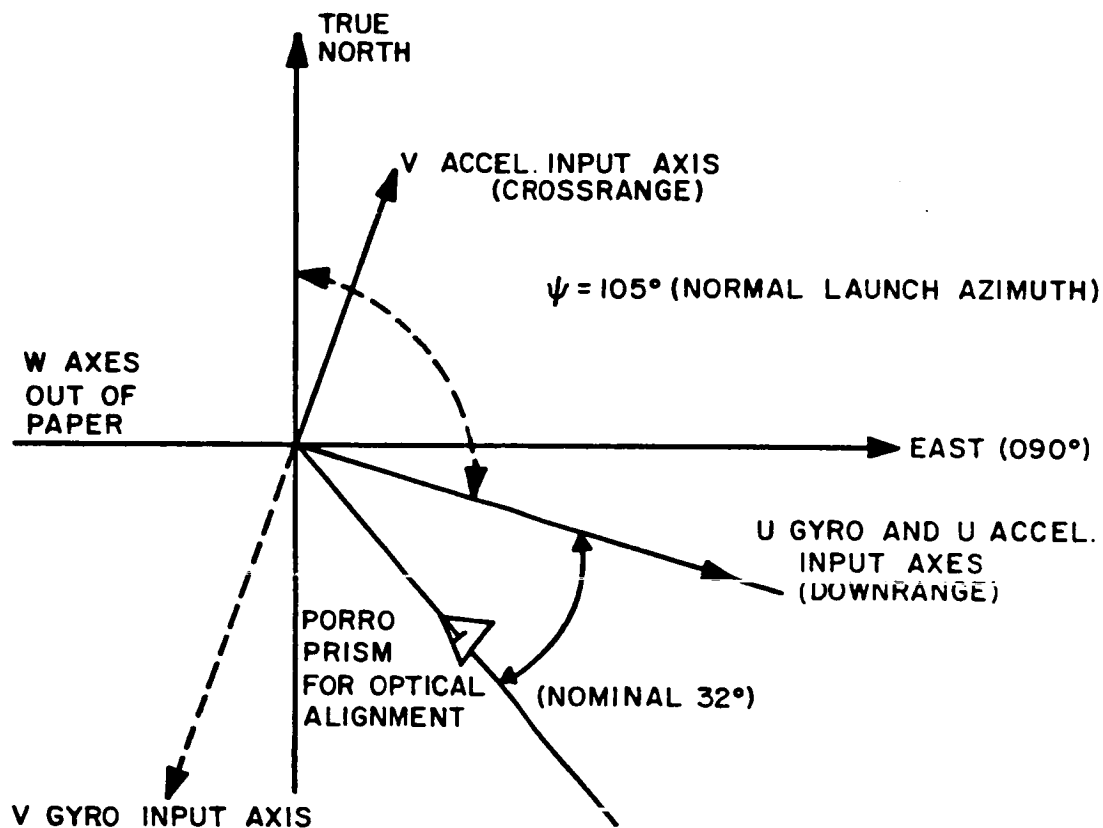


FIGURE 6.9-2. ALIGNMENT OF INERTIAL COMPONENTS IN LAUNCH CONFIGURATION

computer from the accelerometer incremental velocity outputs. Gain constants used in these computations are predetermined and stored in the computer memory.

The alignment accuracy of gyrocompassing is limited essentially by the untrimmed drift rate of the east gyro, since the azimuth alignment of the stable element is continually adjusted until any untrimmed drift rate is balanced by a component of Earth's rate. Theoretically, the alignment error will correspond with the random drift of the east gyro. In practice, however, errors or uncertainties in gyro drift calibration and in gyro torquing loop scale factor provide additional uncertainty factors in the untrimmed drift rate which results in corresponding errors in azimuth alignment. As mentioned previously, azimuth alignment accuracy by gyrocompassing was typically in the range of 15-30 arc-minutes.

6.9.4. Optical Azimuth Alignment (1963 to Present). - With the advent of the Surveyor mission and the more demanding azimuth alignment accuracy requirements, it was apparent that the azimuth alignment accuracy achievable by the conventional gyrocompassing implementation would not be adequate. In the second quarter of 1963, engineering studies were begun toward the definition, mechanization, and implementation of an optical azimuth alignment control system. Figure 6.9-3 provides a simplified block diagram of the Centaur optical azimuth alignment control system. The launch complex site geometry layout, which was a prime consideration in the establishment of the autotheodolite requirements, is shown in Figure 6.9-4. The alignment system consists of a long range autotheodolite with associated electronics, controls, and status displays. One optical and one electrical interface exist between the ground equipment and the IMU to provide a closed loop analog control of the azimuth orientation of the stable element. A Porro prism mounted on the inertial platform stable element provides the optical interface with the autotheodolite. The electrical interface is with the torquing loop of the azimuth gyro. The optical axis, or line of sight, of the ground based autotheodolite establishes the azimuth reference to which the stable element is aligned. After optical acquisition, any misalignment of the Porro prism to the reference azimuth is sensed by the optics and corrected by an appropriate torquing signal to the azimuth gyro. During azimuth alignment, the stable element is gyro stabilized and operated in a self-leveling mode. During prelaunch operations, the alignment system is remotely controlled from the blockhouse. The azimuth of the platform is controlled by the operator to effect prism capture. After prism capture, azimuth alignment is maintained automatically until the MGS flight mode is initiated. Controls and status displays are also provided in the optics shelter which permit calibration, alignment, and maintenance of the optics equipment independent of blockhouse activities.

0100-90A

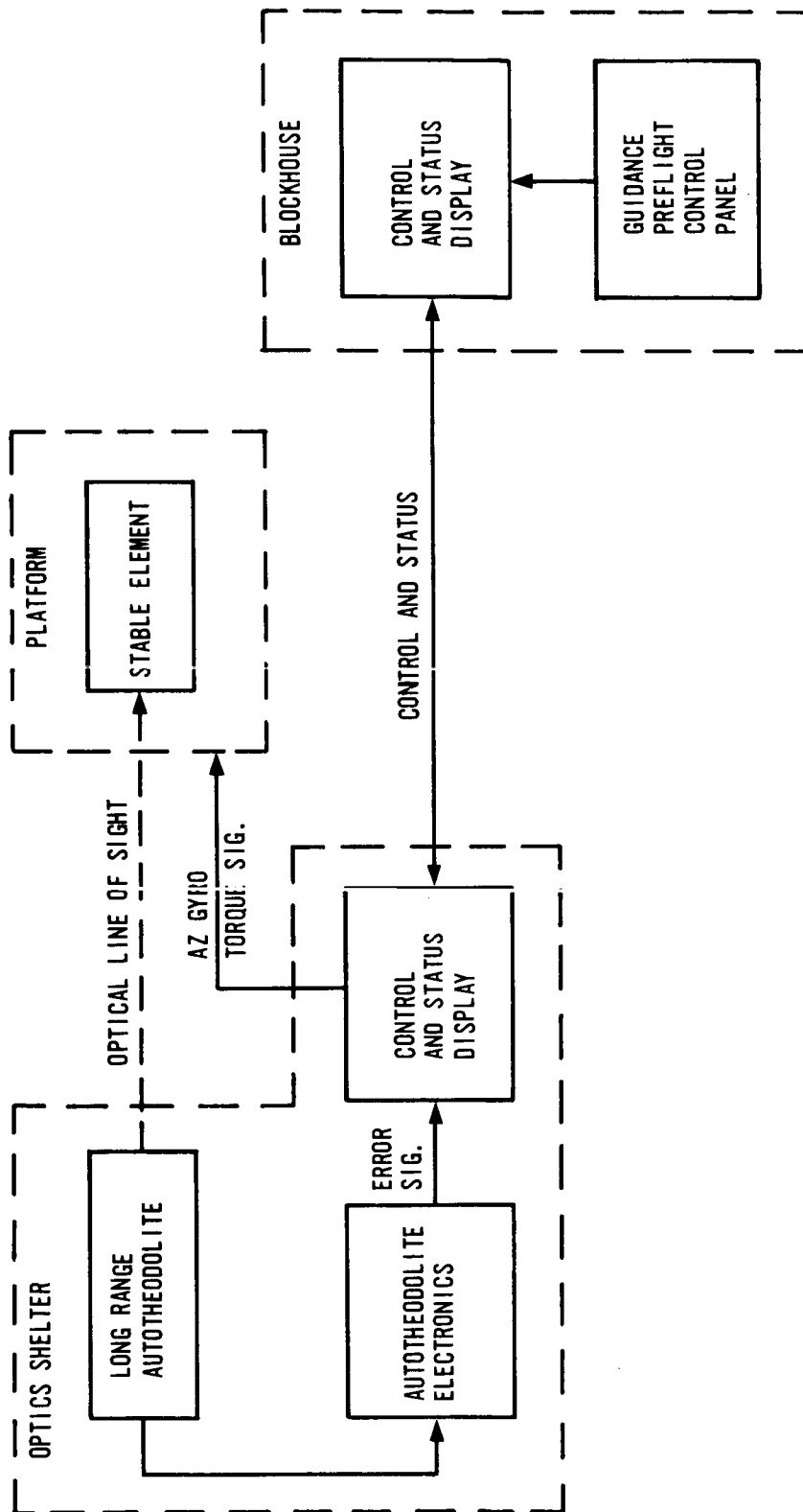


FIGURE 6.9-3. AZIMUTH ALIGNMENT CONTROL SYSTEM,
BLOCK DIAGRAM

NOTE: ALL DIMENSIONS ARE
NOMINAL AND ARE PRO-
VIDED FOR REFERENCE ONLY

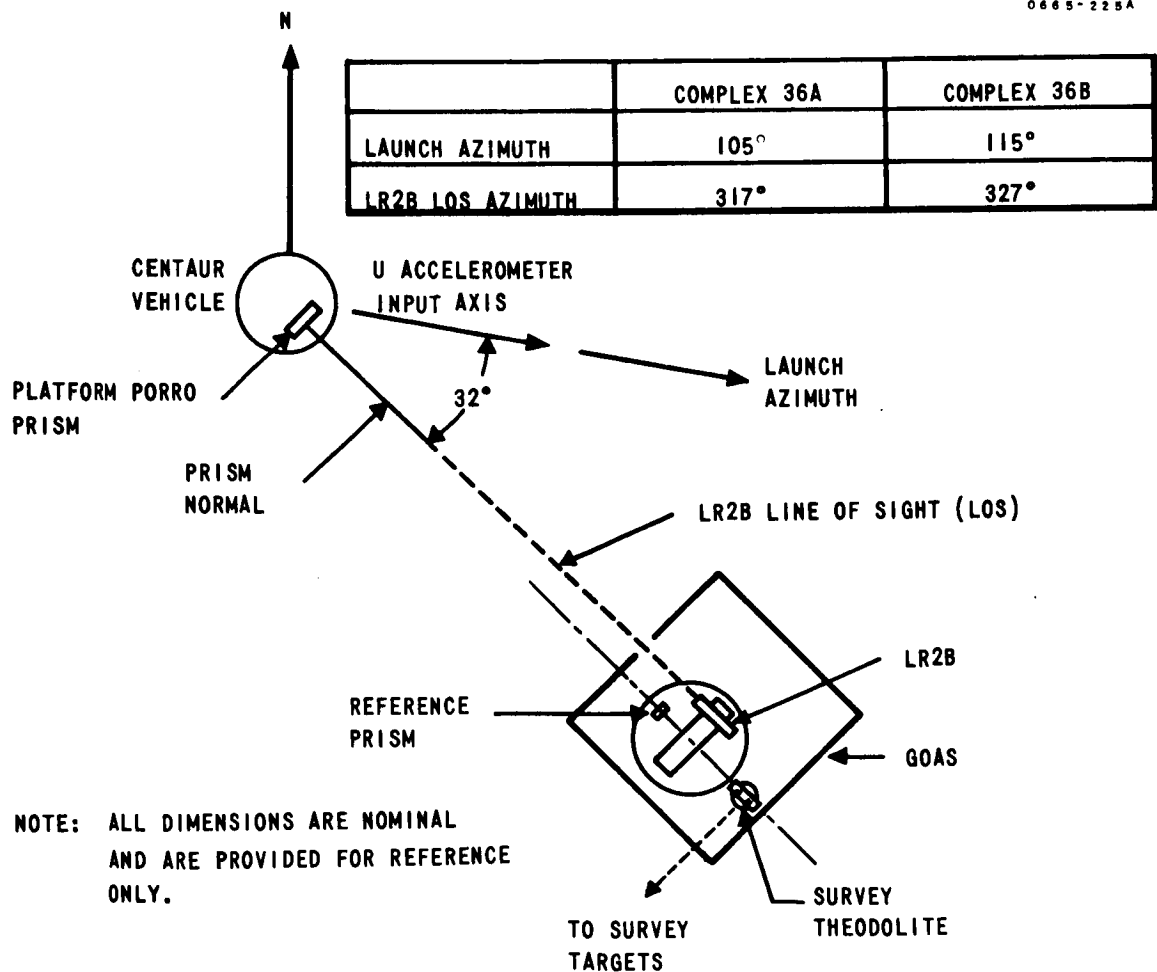
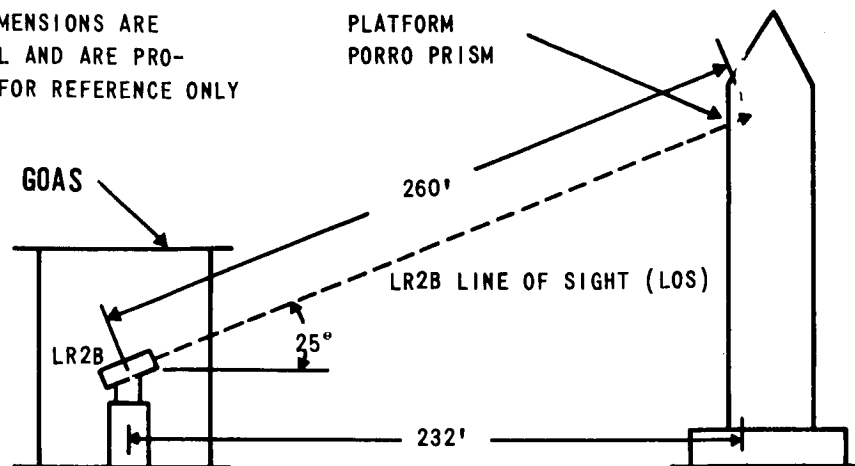


FIGURE 6.9-4. LAUNCH COMPLEX SITE LAYOUT

6.9.4.1. Considerations and Trade-offs. - Significant factors in the development of the optical alignment system are covered in the following paragraphs.

1. Autotheodolite Selection and Configuration - Because of schedule commitments, it was necessary to make an early selection of the autotheodolite to use in the alignment system so that long lead items could be ordered and any engineering effort required for interface adaptation could be started by the supplier. This was not an ideal situation as selection had to be based on preliminary requirements. However, establishment of firm requirements in a timely manner and close technical coordination with the supplier precluded any significant technical or schedule problems. In reality, several important requirements of the autotheodolite were firm before the final autotheodolite selection had to be made. These requirements, dictated by platform Porro prism size limitations (1 inch X 7/8 inch), the launch site geometry (see Figure 6.9-4) and vehicle sway characteristics were:
 1. Operating range: 250 to 300 feet
 2. Sway tracking: 12 inches (static)
5 inches peak to peak at 1 Hz (dynamic)
 3. Operation compatible with a 1 inch by 7/8 inch prism

Armed with these requirements and preliminary accuracy requirements, a survey of available units, either off-the-shelf or ready developed, was made. The selection field was quickly narrowed to two units-- the Davidson Model 985 which had been developed and used operationally for an earlier missile program; and, the Perkin-Elmer Model LR2A which had been developed for the Saturn program. The criteria for making the final selection were overall performance, modifications required, reliability, delivery, and cost. The primary objective in the selection was to produce a working, reliable optical alignment system capable of meeting all Centaur requirements and exhibiting good operating characteristics. Delivery was considered in the interest of minimizing impact on overall program scheduling. As there was little difference to consider in the estimated basic price of the two units, costs were considered to the extent of minimizing development dollars. In the final analysis, it was determined that in most

performance characteristics there was little difference between the two units, although certain modifications were required or desirable on both. One very critical area was revealed, however, that ultimately led to the selection of the Perkin-Elmer unit. This area was that of dynamic sway tracking capabilities of the two units. The Davidson 985 unit as designed could not meet the sway tracking requirements. To meet the requirements, modifications would have been required, and were considered major in nature. Further investigation also revealed that the advertised dynamic sway tracking capabilities in one specific application of the Davidson unit was at best marginal. The Perkin-Elmer LR2A unit, on the other hand, not only was capable of meeting the sway tracking requirements without modification, but employed an entirely different approach to the problem which enhanced performance and reliability while minimizing mechanical alignment and mounting pier stability problems. These performance advantages of the Perkin-Elmer unit, plus consideration of the natural cost and delivery risks associated with a major redesign of the Davidson unit, resulted in the selection of the Perkin-Elmer LR2A unit.

The Perkin-Elmer LR2A, as designed, provided a number of features, which were not necessary for the Centaur application. The 8 inch (aperture size) autocollimator was provisioned for remote monitoring by closed loop television. In addition, the azimuth and elevation alignment mechanisms were power driven to permit alignment from a remote location. In the interest of improved reliability by design simplification, these features were eliminated. Views of the simplified unit, designated as the LR2B, are shown in Figure 6.9-5. The base mount is a precision lath bed. The autocollimator can be translated manually, by a worm screw arrangement, across the base mount to accommodate vehicle static or long term sway, and to view the reference prism, which is provided for alignment of the autocollimator to the surveyed azimuth reference. Vehicle dynamic sway is simply accommodated by the autocollimator aperture size.

2. Alignment Accuracy and Error Sources - The alignment system is required to orient the inertial triad (specifically the down range U accelerometer) so that misalignment at launch does not exceed 0.75 milliradians 150 arc-seconds. This requirement excludes the effects of surveying errors and autotheodolite mounting pier instabilities, but includes the errors or uncertainties of all other

0166-78A

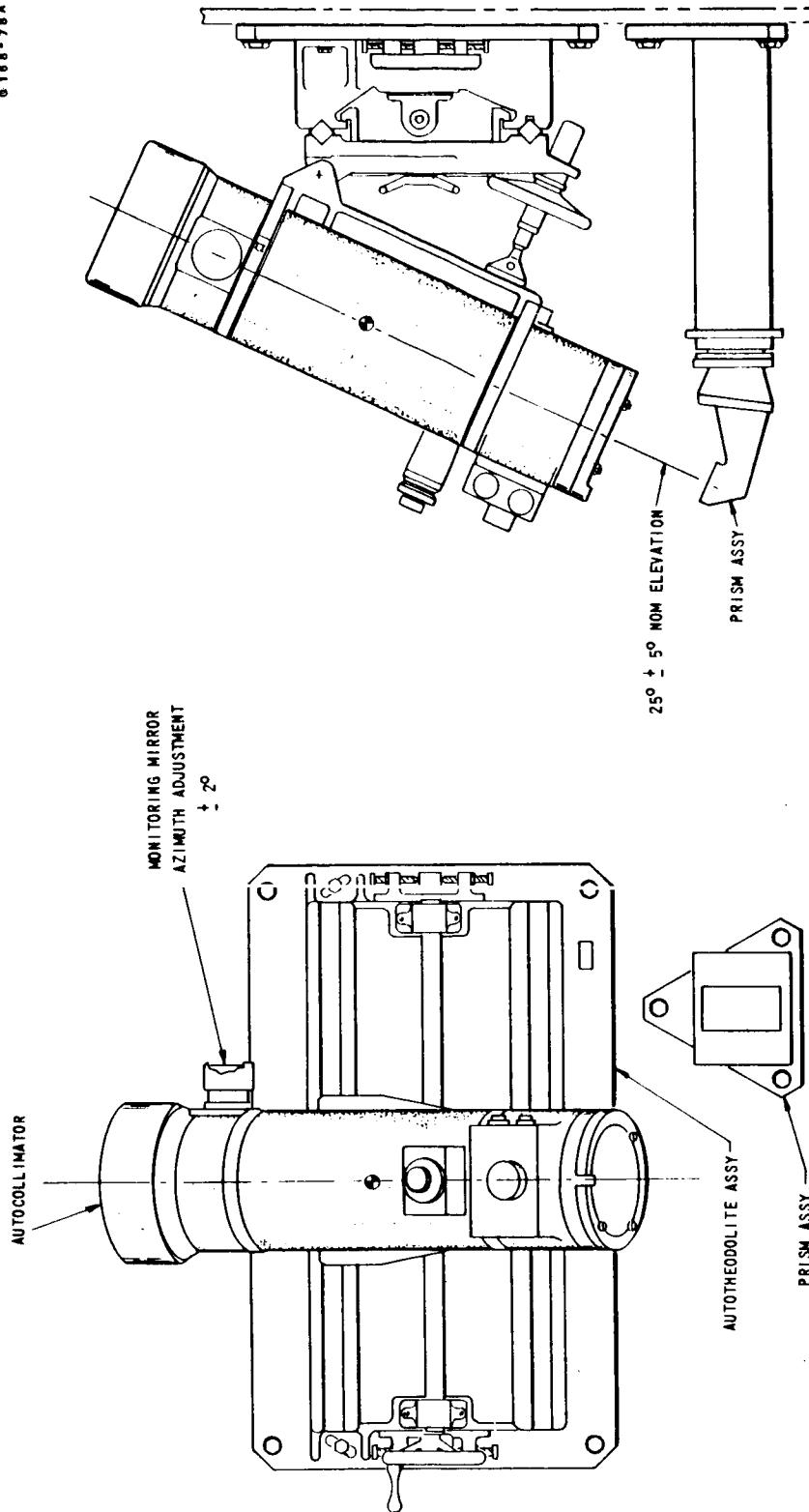


FIGURE 6.9-5. AUTOTHEODOLITE

effects such as platform Porro prism geometry errors, platform prism to accelerometer misalignment and stability, servo loop accuracy including the effects of optical noise (shimmer), autotheodolite errors, and vehicle sway.

Error sources contributing to alignment inaccuracy can be divided into four basic groups as follows:

- a. **Porro Prism Geometry Error.** - Uncertainties in azimuth alignment result from geometry errors introduced into the alignment system as a result of platform Porro prism misalignments. First, any deviation from the nominal alignment angle between the Porro prism normal and the U accelerometer input axis in the azimuth plane results in an equivalent azimuth alignment error. Secondly, an error of significance is cross-coupled into the azimuth plane as a result of deviation, or skew, of the prism apex from the horizontal, or level. The azimuth alignment error as a result of prism skew is the product of the skew angle and the sine of the sight line elevation angle. Two factors contribute to the level uncertainty of the prism apex: (1) alignment and mounting instability of the prism apex in the vertical plane; and (2) system self-level misalignment. Since nominal misalignments can be calibrated and appropriately compensated, it is the instability of prism alignment which is of prime importance.
- b. **Optical Line of Sight Misalignment.** - The optical line of sight from the alignment optics to the platform prism establishes the azimuth point of reference for alignment. Misalignments of the line of sight result from inaccuracies of the autotheodolite alignment mechanism (refer to Figure 6.9-5) and from azimuth deviations introduced by glass windows in the line of sight. Azimuth alignment errors are caused by mechanical shifts of the autocollimator when translated from the reference prism, after azimuth alignment, to the platform Porro prism. Shifts or rotations of the autocollimator occur as a result of inaccuracies in the translation mechanism, and occur both in the horizontal plane and the vertical plane. Rotation in the horizontal plane introduces errors directly into the alignment.

Rotation in the vertical plane cross-couples error into the azimuth plane because of the elevated line of sight. The resulting azimuth error being the product of the elevation angle of the line of sight and the sine of the angle through which the autocollimator is rotated. This aspect required careful attention during the design of the autotheodolite base mount, but no serious design or manufacturing problems were encountered. Although usually small, alignment deviations result from glass windows along the optical line of sight, windows in the platform top cover and in the optics shelter hatch had to be considered.

- c. Pointing Error. - The pointing error results from the inability of the optical control servo loop to align and hold the platform Porro prism precisely to the established line of sight. Essentially, the pointing error, or uncertainty, corresponds to the position accuracy of the servo loop.

In the loop, pointing errors result from autotheodolite null uncertainty, electrical bias or offset, and computer torquing potentiometer error in compensating for gyro drift. Optical noise introduced in the loop also affects the accuracy of aligning the platform prism to the established optical line of sight.

In budgeting this error during the alignment system development, an error of 5 arc-seconds was allocated to the servo loop positioning accuracy, excluding the effects of optical noise. This allowance was proven adequate during tests at ETR, even in the presence of $\pm 2\frac{1}{2}$ inches of vehicle sway.

Alignment errors resulting from the effects of optical noise, or shimmer, are of course dependent on atmospheric conditions. Under a variety of atmospheric conditions, that is, overcast, rain, bright and sunny, and rapid temperature changes-- maximum instantaneous errors of up to 8 arc-seconds due to shimmer were measured during validation testing at the ETR launch complex. Although this error probably could have been reduced by loop filtering optimization, no attempt was made as the error was well within the error budget.

- d. Gyro Torquing Potentiometer Reset Error. - During the MGS final align mode of operation, compensation for Earth's rate and calibrated gyro drift rate is provided for the azimuth gyro by the guidance computer via the gyro torquing potentiometer. While this drift compensation is not essential to the operation of the azimuth alignment system, it is provided to minimize azimuth drift in the event of inadvertent opening of the alignment control loop. The time required by the computer to properly reset the torquing potentiometer after initiation of the flight program results in a small error in azimuth alignment.
3. Control Loop Design and Analysis - Figure 6.9-6 is a simplified schematic of the optical alignment control loop. To verify adequate gain and phase margins for stability, the loop transfer function was programmed for nominal case servo loop analysis by computer. Verification of loop stability was also made using the root locus method. During integration and validation testing of the alignment system at ETR, it was determined that the operating margin of the autotheodolite during adverse atmospheric conditions, that is, rain, mist-- could be improved by increasing the nominal autotheodolite scale factor from 0.1/arc-second to 0.2/arc-second. This change was made (potentiometer adjustment is provided); however, at the same time, the gain of the operational amplifier, A1, was reduced by a factor of 2 in order to retain the same overall loop gain.

In the development of the control loop, alignment system operational aspects, that is, closed loop/manual control operation, and the GSE/MGS interface were important considerations. As extensive changes in the Perkin-Elmer LR2A autotheodolite electronics would have been necessary to interface directly with the MGS, the use of additional electronics in conjunction with the basic LR2A electronics design was studied. As a result, it was decided to incorporate buffer electronics, in the form of an operational amplifier, in the loop mechanization to provide the necessary gain, voltage and current levels. This approach minimized changes in the LR2A electronics design, and by precluding a direct interface of vendor designed and furnished equipment with the MGS, direct in-house control of the loop design was maintained. In addition, the operational amplifier facilitated implementation

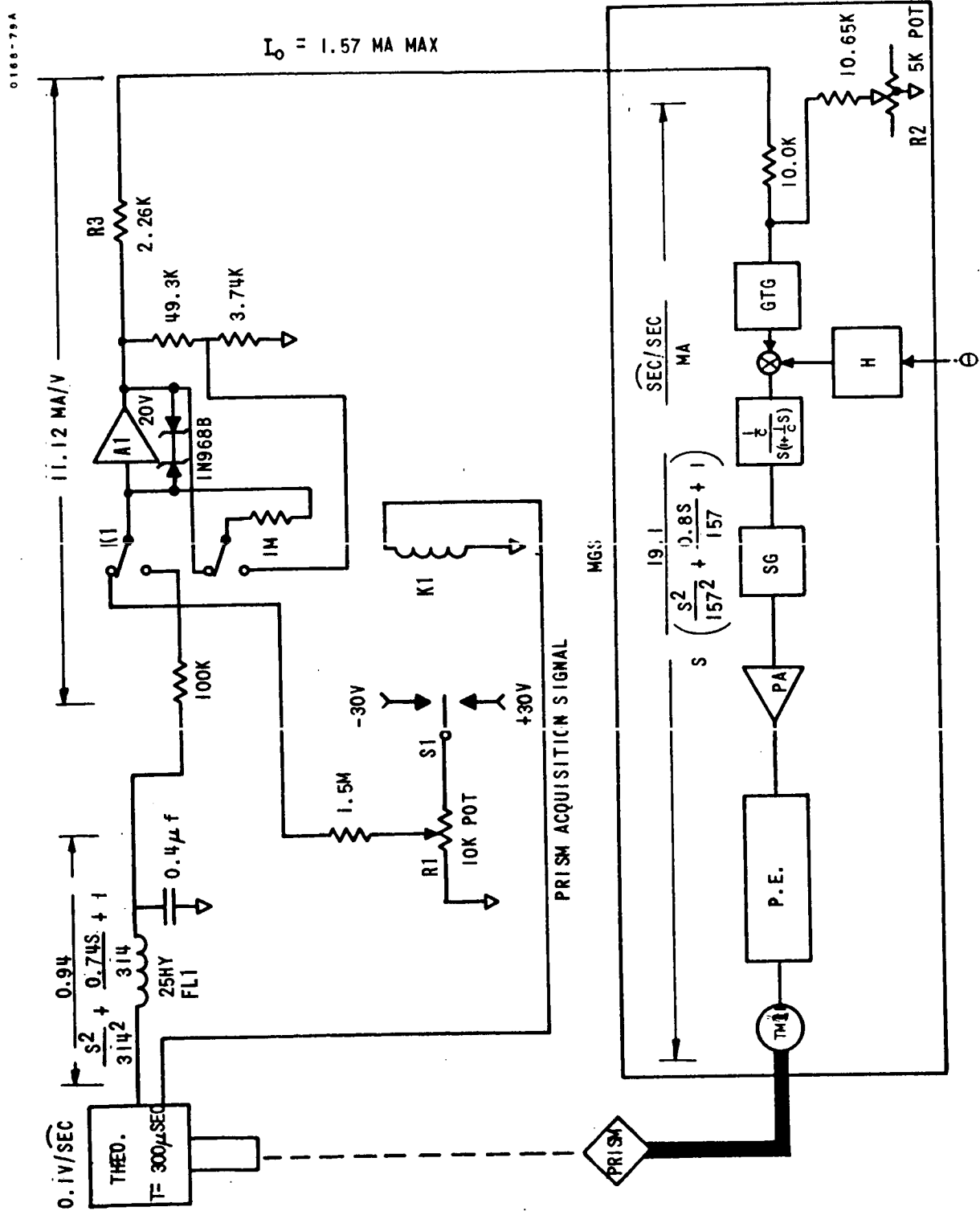


FIGURE 6.9-6. OPTICAL ALIGNMENT CONTROL LOOP

of control current limiting and dual operating modes (automatic/manual). Control current limiting is required to preclude gyro drift changes due to torque generator magnetic hysteresis effects. Referring to Figure 6.9-6, the back-to-back zener diodes across amplifier A1 in conjunction with R3 provide the necessary limiting action. The zener diodes also preclude excessive loop recovery time by preventing hard saturation of the amplifier.

Operational considerations required a manual control capability for initial capture, or acquisition, of the platform Porro prism. By control mode switching at the input of the operational amplifier, a constant source impedance was provided to the load with minimum parts and design effort.

The filter, FL1, shown in Figure 6.9-6 was provided primarily to smooth the unfiltered dc error output signal of the LR2A electronics.

A loop mechanization using discrete or digital control is a feasible alternative for an alignment system of this type and loops mechanized as such have been developed and successfully used at Honeywell in short range applications. However, limited guidance computer memory space and lack of spare input discrete channels precluded any serious consideration of a digital control loop for the Centaur application.

4. Platform Porro Prism Size - The relative small size of the platform prism (1 inch x 7/8 inch) coupled with the 265 feet optics operating range at the launch complex was considered to be a potential problem source and close attention was given to this aspect of the alignment system. The first and most obvious means of providing additional safety factor in this area was to increase the prism size. This could not be accomplished, however, because of limited mechanical clearances within the platform gimbal assembly. Since the LR2A unit was originally designed for compatibility with a 2 inch x 2 inch prism, analysis and tests were performed to ensure that autotheodolite performance would not be significantly degraded when operated with the smaller prism. The analysis and tests yielded positive results; however, as optical losses within the LR2A optics assembly could be reduced (≈ 7 percent) simply and at minimal cost by use of gold coated elements in lieu of aluminized or silver coated elements, this change was made to obtain an additional margin of safety.

5. Platform Prism Shading - In the launch orientation, the inertial platform is in a gimbal flip orientation and the redundant outer role gimbal is normally caged so that the platform pitch axis is coincident with the vehicle pitch axis. With this orientation, the inner role gimbal obscures, or shades, more than 50 percent of the Porro prism. It was possible, however, to provide full optical access to the platform prism by rotating, or offsetting, the platform gimbal assembly without interfering with the alignment or stabilization of the inertial element during final prelaunch IMU alignment. Two approaches were considered for offsetting the gimbal assembly as follows:

- (a) Provide in the airborne equipment a bias signal which could be introduced into the gimbal caging loop during optical alignment to provide the necessary gimbal offset.
- (b) Maintain Alignment Reference Unit (ARU) coarse alignment control during final alignment. The required offset to be provided by appropriate setting of the ARU reference resolver.

Both approaches were evaluated and determined to be workable; however, since modifications of the caging loop would have involved airborne hardware changes, it was decided to use the coarse alignment control approach as only GSE control logic and procedural changes were involved. During integration and validation testing at ETR, it was determined that the alignment system would operate without accuracy degradation with the prism shaded and the requirement for gimbal offsetting was deleted.

6. Optical Acquisition (Prism Capture) - In order to close the optical alignment control loop, the platform prism must first be aligned in azimuth so that the reflected collimated light beam is within the acquisition, or capture, angle of the autotheodolite. Both automatic and manual control approaches to accomplish initial acquisition were considered. From an operational standpoint, automatic acquisition is desirable as the operator is removed from the loop. An automatic mechanization using the guidance computer for control was determined feasible, and could have been implemented simply with software (computer program) changes only. Limited computer memory storage, however, ruled out this approach. Since the existing guidance GSE was basically manual, a relatively complex programmer would have

been required for automatic acquisition by GSE control. Therefore, acquisition by operator control was considered the best trade-off and manual control for acquisition was implemented. Acquisition by manual control has proven to be no problem; however, in line with the automatic checkout philosophy of the Computer Controlled Launch Set (CCLS), which is now operational at the launch complex, optical acquisition is now accomplished automatically.

6.9.4.2. Developmental Testing. - The primary purpose of the developmental testing was to verify the opto-electrical control loop stability and response, and to investigate and verify certain system operating concepts being considered. Since no long range autotheodolite was available for these tests, all testing was performed in the laboratory and with short range optics. A reasonable simulation of the proposed alignment system was achieved, and the test results established a high level of confidence in the operation and performance of the proposed mechanization and design.

6.9.4.3. Problems. - Problems encountered in the design, build and operational use of the optical azimuth alignment control system have been few. By far, the most significant problem stems from fuel boil-off vapor plumes. Under certain wind conditions, plumes from the vehicle tanking operation drift through the optical line of sight. The light beam path between the platform prism and the ground based optics is disrupted causing acquisition loss and intermittent control loop operation. This condition can lead to a countdown hold and possibly failure to launch on time. In extreme cases a launch delay could result.

As an optical sight tube is not practical and relocation of vent openings was determined unfeasible, the source of this problem has not been eliminated. The problem has been successfully circumvented, however, by allowing continuous acquisition loss to extend for a period of 90 seconds before forcing a countdown hold. This approach can result in less than optimum alignment accuracy because of untrimmed azimuth gyro drift; however, the error would be relatively small, and the slight guidance accuracy degradation is a good trade-off for the obtained reduced risk of a forced hold and possible launch abort.

Problems of lesser scope have been experienced with the optical GSE hardware. Those problems are discussed in Topic 5.4.

6.9.4.4. Doing It Over Today. - Today, with laser development advancing the state of the art of precision alignment, such devices would have to be considered in any alignment system requiring high accuracy.

For the Advanced IMG, the use of the existing azimuth alignment control system is planned with modifications only for interface compatibility.

6.9.5. Conclusions. - Gyrocompassing provides an economical means of accomplishing final azimuth alignment of an inertial guidance system. It can be implemented totally self-contained within the guidance system thereby eliminating any requirement for support equipment. The alignment accuracy achievable by gyrocompassing, however, is limited by the untrimmed drift rate of the east gyro. Therefore, for a given system, the alignment accuracy achievable is not only dependent on the east gyro random drift rate, but also on the ability to accurately measure and compensate for the inherent fixed drift rate of the gyro.

A significant improvement in final azimuth alignment accuracy can be achieved by use of ground based optics. This, of course, requires additional launch site GSE and facilities, that is, optics shelter, hence added costs. Also, a clear line of sight is basic to any optical measurement or control concept. Therefore, both the natural and the man-made environments at the launch complex are important factors in the consideration of optics for operational use.

Topic 6.10

Active Temperature Control Loops

6.10.1. Introduction. - Active temperature control loops in the platform perform the function of maintaining the inertial components at a predetermined operating temperature. Close control about the operating set point is mandatory in order to minimize errors introduced by changes in fluid damping (c) fluid density (ρ), and component-to-component temperature gradients. The present design and mechanization of the Temperature Control loops are such that for any power requirement called for by the gyros or accelerometers, within the proportional control range of the TCAs, (0.19 to 14 watts for the gyros and 0.22 to 17 watts for the accelerometers), the inertial components will be controlled to $+180^{\circ}\text{F} \pm 0.5^{\circ}\text{F}$, where $+180^{\circ}\text{F}$ is the operating temperature set point. Details of the TCA circuit design are given in Topic 2.8.

6.10.2. TCA Power Versus Platform Case Skin Temperature. - The power required of the TCA's to maintain the components at their operating temperature set point is inversely proportional to the platform case skin temperature (see Figure 6.10-2). The present interface specification for the MGS specifies that the system must provide satisfactory performance over a platform case skin temperature range of $+50^{\circ}\text{F}$ to $+120^{\circ}\text{F}$. Over this temperature range, the TCAs must provide proportional heat control of the gyros and accelerometers. On the launch pad the guidance compartment uses forced air conditioning to provide an air ambient such that the equipment case skin temperatures are maintained within specified operating limits. During lift-off and orbital flight, complete dependence is upon passive thermal control to maintain the case skin temperature within limits. Once out of the Earth's atmosphere, the primary external source of heat to the platform is from solar radiation. Typical case skin temperature changes from t_0 (lift-off) to 25 minutes after lift-off as shown by Figure 6.10-1.

6.10.3. Comparison of Thermal Lags. - The thermal time constant between the platform case and the inertial components has been determined to be approximately 20 minutes. That is, for a step change in case temperature (a physically unrealizable situation), approximately 20 minutes are required for the inertial component TCAs to reach 63 percent of their new steady state operating power level.

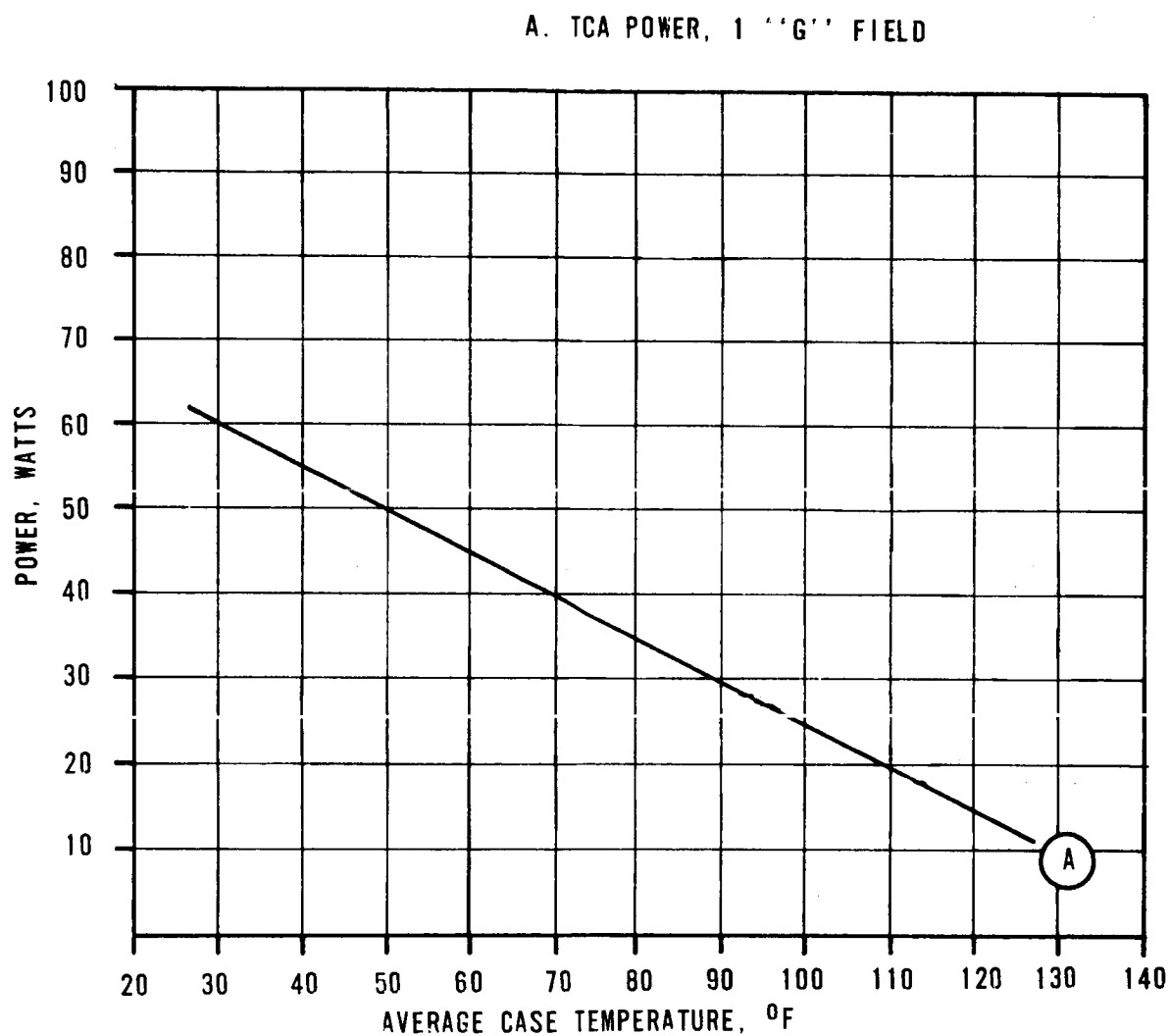


FIGURE 6.10-2. INERTIAL PLATFORM STEADY STATE POWER
AS A FUNCTION OF CASE TEMPERATURE

With the inertial components operating in a closed thermal loop, the thermal time constant of the temperature control loop was determined. A step input into the loop was initiated by increasing the sensor resistance 3 ohms (equivalent to $+2^{\circ}\text{F}$). The time required to reach 63 percent of the new steady state level was shown to be 100 seconds or less.

Considering the platform case skin to inertial component thermal lag and the nature of orbital cyclic solar loading, 40-minute exposure at 500 BTU/hr-ft² and 50-minute exposure at 65 BTU/hr-ft², it is seen that the thermal loop transient response requirements will be dictated by localized inertial component power requirements.

6.10.4. Temperature Control Loop Threshold. - Thermal interaction of the six inertial components while under the influence of changing case skin temperatures and heat paths (due to changes in relative gimbal angles) produce variations in individual component heater power requirements. The threshold of the TCA is such that for a change of 0.1 ohm or less in sensor resistance (equivalent to 0.07°F change), a nominal 3.3-volt change in output voltage to the component heater results. In addition to the low loop threshold, close thermal coupling between the heater and sensor results in a tight thermal control loop. Actual data indicates maximum deviation about the $+180^{\circ}\text{F}$ control point to be $\pm 0.2^{\circ}\text{F}$ or less.

6.10.5. Typical Heater - Sensor Thermal Lag. - Figure 6.10-3 illustrates a plot of the thermal lag between the heater and sensors for the DGG49 gyro as the heater voltage was varied ± 10 volts about the -24 volt DC midrange control point (see Figure 6.10-4) at the frequencies illustrated. Due to the heater-sensor configuration used on the present accelerometers (wrap on blanket type) even closer heater-sensor thermal coupling exists (reference Topic 2.3).

The temperature control loops that have resulted from the IMG studies are unchanged insofar as thermal control is concerned. Changes were incorporated in the TCA design primarily to reduce power line noise injection and radiated noise. These changes are being incorporated to improve the IMG performance with respect to Electromagnetic Compatibility requirements.

6.10.6 Summary and Conclusions. - The active thermal control loops in the platform are capable of providing adequate control such that under worst case transient conditions, the operating temperature of the inertial components will be under proportional control.

0160-123A

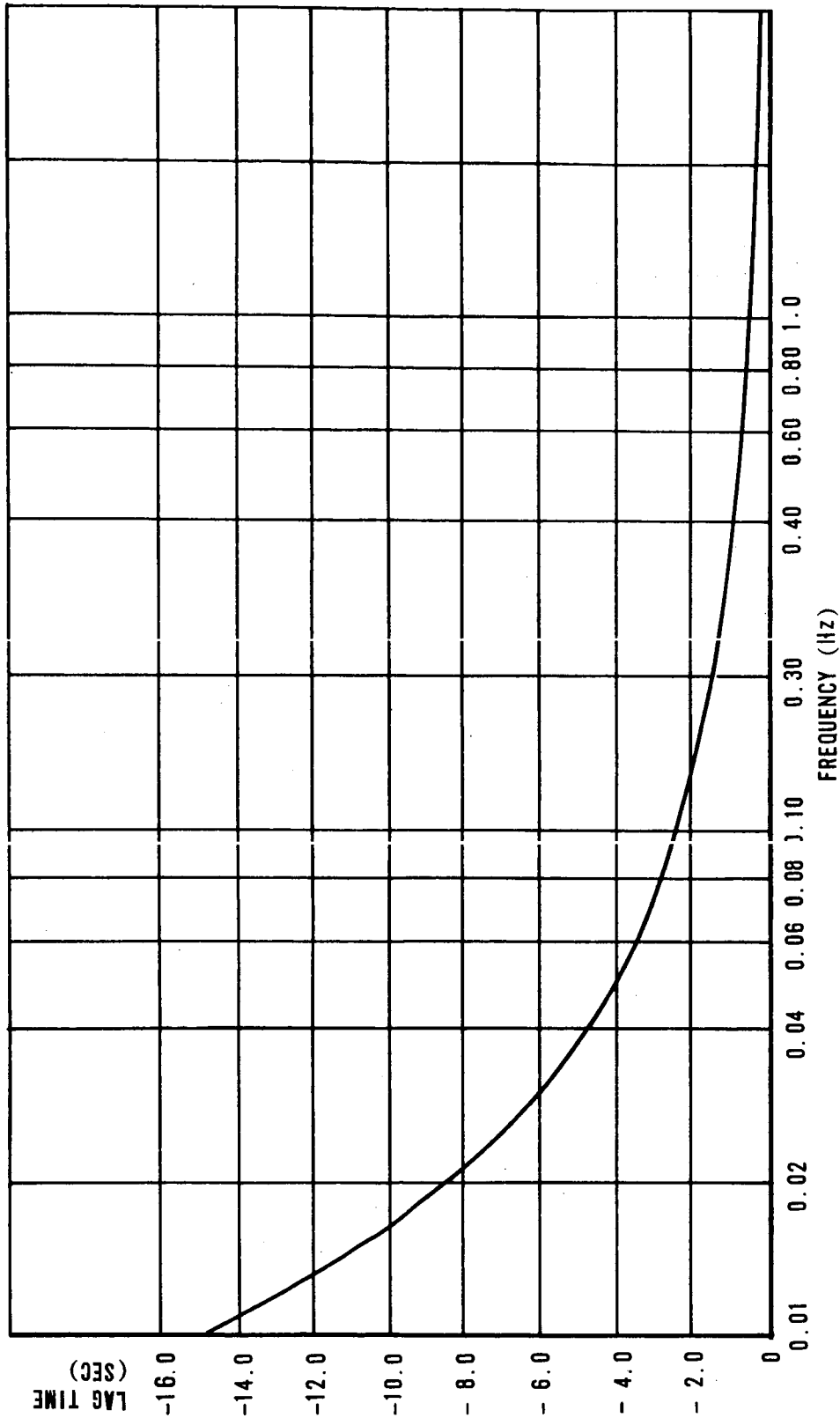


FIGURE 6.10-3. THERMAL LAG TIME BETWEEN HEATER AND SENSOR
TCA CONTROLLING AT 6 WATTS

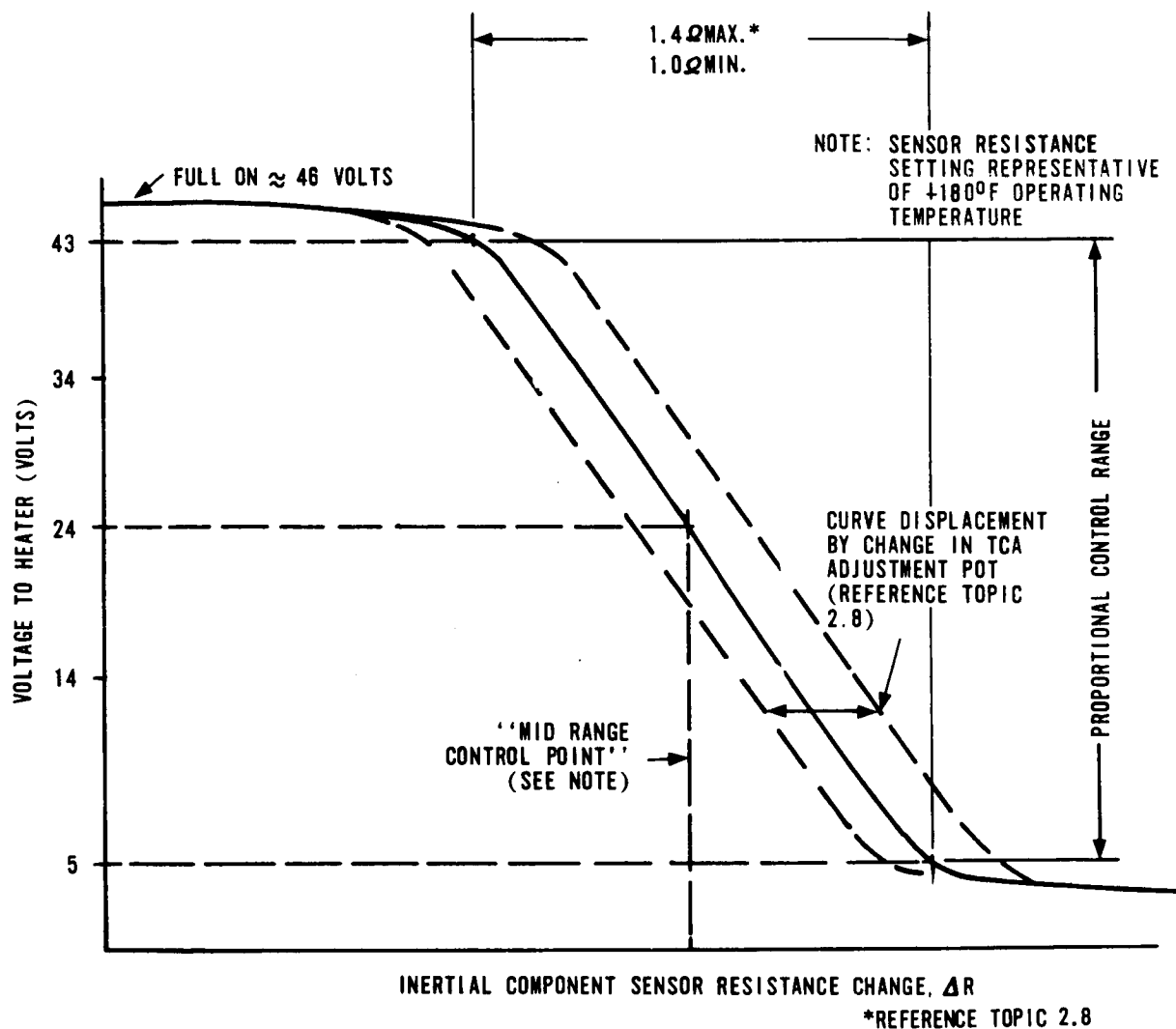


FIGURE 6.10-4. TEMPERATURE CONTROL AMPLIFIER OPERATIONAL CURVE

Deviations about the +180°F control point are nominally held to $\pm 0.2^\circ\text{F}$ or less as a result of the low loop threshold and the close thermal coupling of the heater-sensor configuration. Changes made to the TCA for the IMG studies were based primarily on noise considerations not on thermal control.

Topic 6.11

Gyro Torquing Mechanization

6.11.1. Introduction. - One of the primary functions of the Centaur Inertial Guidance System is to acquire and maintain an accurate attitude reference. This reference may be with respect to local vertical for purposes of calibration, or inertial space as is the case during flight. Once a desired orientation has been achieved, the ability of the system to maintain an attitude reference is directly related to the accuracy and stability of the gyros used to determine angular motion of the inertial element. Because each gyro is subject to unwanted forces which tend to turn it from its desired reference position, a method of compensating the predictable angular displacements is required if maximum accuracy is to be realized. One method is to physically compensate the unwanted forces by introducing an opposing torque at the gyro gimbal. The effectiveness of this method depends not only on the ability to determine the magnitude and direction of the undesired torques to be compensated, but the ability to develop the precise amount of opposing torque at the gyro gimbal, since any difference between the two will result in angular motion. A logical extension of this phenomenon is to use the gyro torquing capability for repositioning the inertial element. This approach has been used during fine alignment where only small angular corrections are required. Major repositioning efforts required during course alignment, however, have been traditionally accomplished by Platform gimbal torquing on the Centaur Program, since gyro torquing in excess of 40 deg/hr results in torquer hysteresis effects which adversely affect system performance and rates within this range are impractical.

6.11.2. General Gyro Torquing Mechanization Description. -

6.11.2.1. Computer Torquing. - Each digital computer torquing module provides an analog output from a 20-turn 10K potentiometer. The torquing potentiometer (Figure 6.11-1) is supplied with precision +22.2 volts dc and -22.2 volts dc from the coupler.

The computer calculates the required gyro torquing rates and compares it with the actual torquing rate in the error determining logic. Any difference generates an error signal which is sent to the error hold circuit which stores and maintains it as an input to the servo amplifier until a new signal

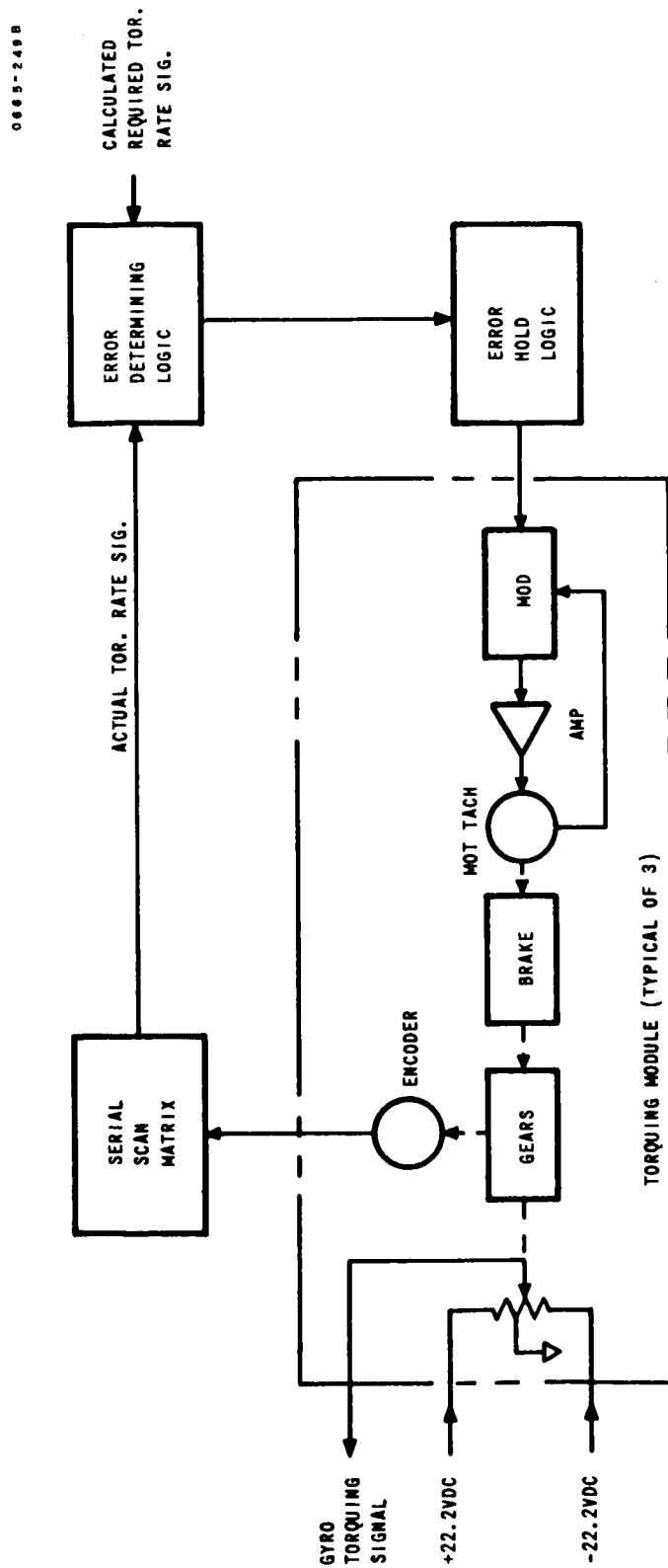


FIGURE 6.11-1. COMPUTER GYRO TORQUING

is received. The servo amplifier will cause the motor to drive in the direction to reduce the error. The motor positions the potentiometer and an encoder through a gear train. The encoder is an analog to digital converter whose output represents the actual torquing rate. The serial scan matrix converts this signal to serial form and routes it to the error determining logic where it is again compared with the required torquing rate.

This cycle continues until the actual torquing rate equals the required torquing rate. The error hold circuit will then receive a no error signal causing it to change the stored error signal and stop the motor. A brake holds the gear train in a fixed position during power transfer and inflight coast phases.

6.11.2.2. Optical Torquing. - A simplified block diagram of the optical torquing signal developed in the GSE is shown in Figure 6.11-2. The platform azimuth gimbal must first be positioned so that the collimated light beam from the autotheodolite is reflected back by the Porro prism within the field of view, acquisition range, of the autotheodolite. The reflected light beam causes the autotheodolite to generate an error signal. The magnitude of the error signal is proportional to the Porro prism deviation within a range of 15 arc-seconds on either side of null and constant above this range. The polarity of this signal indicates the direction of deviation. This signal is amplified and routed to the coupler where it is summed with the torquing signal from the computer. The summed signal is applied to the W gyro torquer. Torquing the gyro will generate an error signal from the signal generator which is amplified in the preamplifier and sent to the GCA. The resultant GCA output will be applied to the azimuth gimbal torque motor, driving it in the direction to reduce the autotheodolite error signal to null. When the error signal reaches null the optical torquing signal will be zero and the azimuth gimbal will be aligned to the desired angle.

6.11.3. In-Flight Gyro Torquing. - While the initial design of the Centaur Guidance System provided computer controlled in-flight gyro torquing for compensation of the constant drift and g-sensitive drift parameters, failure of six -3 torquing modules from August 1962 through October 1962, and eight dualsyn short failures through 10 September 1963 stimulated search for an alternate method of drift compensations. Since both AC-2 and AC-3 (flown on 27 November 1963 and 30 June 1964, respectively) were to be flown open-loop, it was decided that more useful information could be obtained from the guidance system by allowing the inertial element to drift at the uncompensated gyro drift rate rather than risk an in-flight torquing

0665-2388

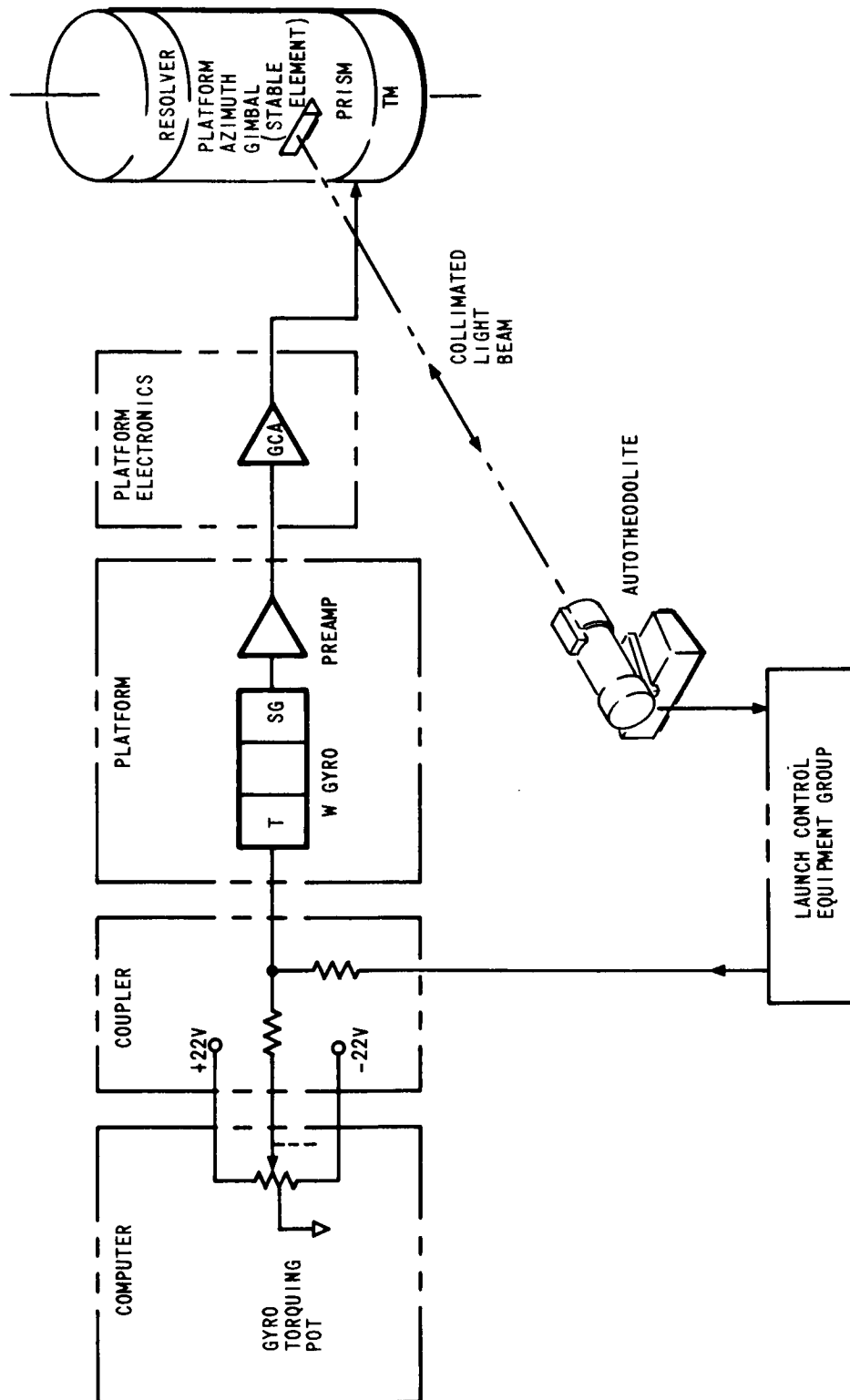


FIGURE 6.11-2. OPTICAL GYRO TORQUING LOOP

failure which would cause inertial reference to be lost. For this reason, a relay box was installed on the vehicle which would allow gyro torquing signals to be monitored via telemetry, but prevent them from reaching the gyros themselves.

Gyro torquing reliability was significantly improved through the mylar insulation between the torquer and signal generator of the gyro dualsyn, and in-flight torquing was successfully used for AC-4, 5, 6, and 8 covering the time period of 11 December 1964 through 8 April 1966. In the interim, however, an approach to the mathematical compensation of gyro drift had been developed by GD/C. With the attraction of greater reliability to be gained, it was decided to abandon in-flight torquing in lieu of mathematical compensation, and use the gyro torquing capability only for preflight fine alignment and drift compensation. The Improved Centaur System supports this philosophy, and relies on computer compensation for in-flight gyro drift.

6.11.4. Preflight Gyro Torquing. - As previously stated, preflight gyro torquing has traditionally been used only for fine alignment and drift compensation. Under computer control, leveling equations are solved to obtain the required torque rates to fine align the inertial element about two axes. On the early flights, gyrocompass equations were also used for azimuth alignment prior to launch, but for AC-4 and on, the analog gyro torquing signal has been obtained by summing the optical alignment output with the computer compensation values for azimuth alignment.

6.11.5. "Doing It Over Today" - The IMG. - The simplicity offered by a system with reorientation controlled totally by gyro torquing has had appeal throughout the Centaur Program.

Platform level tests were conducted using a "slew box" which repositioned the platform via gyro torquing to determine the effects of gimbal torquing on gyro parameters. Calibration performed using this technique demonstrated that improvements could be attained in the calibration of gyro parameters if platform reorientation were affected through gyro torquing. With this added incentive, a design effort was initiated to derive the benefits of a gyro torquing realignment scheme without paying the penalty of the residual torques (due to torquer hysteresis) resulting from the necessarily high torquing rates. The results of this successful design effort are presented in Topic 2.17, "Gyro Torquing Electronics". Of interest here is the shift in emphasis on realignment via gyro torquing from that of being detrimental to system accuracy to that of being beneficial to system accuracy. With no specific in-flight gyro torquing

requirements, methods were then investigated by which the mechanization could be simplified if in-flight torquing requirements were deleted. It was concluded that a significant hardware reduction could be realized by using three of the six D/A converters (required for three axis steering) for gyro torquing during preflight operations. Depending upon improved software capabilities brought about by the incorporation of a new computer and advanced analytical techniques, three D/A converters were shared in this manner, precluding in-flight gyro torquing.

6.11.5.1. Operational Implications. - Sharing the Digital Computer Unit (DCU) D/A converters for steering functions in-flight and both torquing and steering functions on the ground offers the advantages previously discussed but presents ground operational implications that must be considered in the checkout procedures.

1. The analog information for gyro torquing is tapped off the steering input lines just before the resolver chain. To prevent degrading the in-flight reliability, the steering function is never interrupted. Therefore, the signal for torquing does flow through the chain and out of the IMG. Similarly, the azimuth position vector for aligning the inertial reference is sent through the steering chain.

If it is undesirable that this information reach the autopilot, some means of interrupting this signal must be provided external to the IMG. This could conveniently be done in the DCU by software control for a digital autopilot interface or in the autopilot for an analog autopilot interface. Both operations were considered and it was determined that neither would present an operational or mechanization problem. It should be remembered that the present autopilot has the capability, through ground control of a relay, of accepting or rejecting the guidance steering outputs.

2. Ground checkout of three axis steering (two vectors of different frequencies) must be done with the inertial reference free drifting. When two precise steering vectors are required, gyro torquing must be discontinued and the platform allowed to drift. Of course, a single vector can be commanded while the platform is maintained stable by gyro torquing. This is sufficient to check the accuracy of the IMG.

This operation was considered and it was decided that it was no problem. Accuracy tests could be made with one frequency while the second frequency provided torquing information to hold the

position. Compatibility tests could be made with both frequencies used for position vectors and the inertial reference free drifting. This is in line with present test philosophy where certain integrated tests, including booster steering checkout, are made with the inertial reference drifting in an Earth Spin Test.

6.11.6. Conclusions. - The optimum gyro torquing mechanization is entirely dependent on the application or range of applications in which the system is desired to be used. The particular mechanization selected for the IMG is predicated on its use as a true inertial (i.e., space stabilized) guidance system. As such, in-flight gyro torquing is an option, but not a requirement. The sophistication which has been achieved in accommodating a drifting platform by coordinate transformations within the flight computer has made this a highly desirable approach. Not only is a cost savings realized in reduced hardware and associated testing, but system reliability is also enhanced. However, mathematical compensation is not practical for all applications. For example, a system using local vertical as a reference attitude must have the capability to compensate or counteract the 15-degree/hour gyro precession caused by the Earth's rotation. Although coordinate transformation of this rate poses no major problem, the task of interpreting the accelerometer outputs from this rotating platform is more complex.

Topic 6.12

Present MGS and GSE Mode Control

6.12.1. Introduction and Summary. - This topic is primarily descriptive in nature and is presented here to acquaint the reader with how the basic GSE/MGS functional interface is accomplished for system calibration and checkout. In the present IGS, the mode control is basically manual operating, requiring the operator to set a selector switch on the GSE to the desired mode. By present system checkout standards, this approach is antiquated, which is not surprising since it dates back to 1959. Problems on the Centaur Program occurred with this mechanization principally due to Mode Control Switch reliability deficiencies (reference Topics 5.2 and 6.18). Otherwise, the present mode control scheme has proven to be satisfactory for its intended purpose.

In the IMG design, the up-to-date concepts of fully-automated, computer controlled testing are being implemented. Hence, external mode control will be very simple and direct. Also, the flexibility of having the DDP-516 computer in the loop will facilitate the operation of special modes, or routines, such as a fault isolation mode, controlled by the computer logic.

6.12.2. IGS Mechanization. - Control of the MGS preflight modes of operation is accomplished primarily through use of a mode select switch on the ground support equipment. Other controls supplement the mode select switch in establishing the various test and operating modes. The positions and functions of the mode select switch are:

1. Off - Prime power is off in the MGS and GSE.
2. GSE Power On - Prime power is applied to the GSE, to the computer warm-up and standby lines, and fast heat may be applied to the platform.
3. MGS Power On - Prime power is applied to the MGS through control of a relay in the coupler (reference Topic 6.13).
4. Computer Test - Used in conjunction with the GSE computer control switches to perform the computer test program.
5. Align 1 through Align 6 - MGS calibration is performed.
6. Integrated Test - Computer and GSE discrete signals are monitored.

7. Final Align - After coarse alignment, the platform is slaved to the local vertical by the computer and azimuth alignment is accomplished by the optical alignment control group (reference Topic 6.9).
8. Flight - The MGS is switched from Earth reference to inertial reference via relay circuitry in the Platform Electronics.

The Platform Electronics contains the circuitry necessary to position the inertial platform gimbals and perform the switching required for the modes of operation. Fourteen relays controlled by the ground support equipment allow selection of the operating modes by switching inputs to the gimbal control amplifiers. The platform electronics circuitry has two basic modes of operation, the coarse align and the fine align mode.

In coarse align, the GSE positions the gimbals for calibration and preflight (coarse) alignment. In the fine align mode, the inertial platform is gyro stabilized, and gimbal orientation can be controlled by gyro torquing signals.

During MGS calibration, several measurements must be made, including accelerometer scale factor and bias, gyro drifts, and orthogonality. To make these measurements requires that the platform be positioned in six different orientations. The positioning is controlled by the mode select switch in the GSE and the GSE alignment reference unit through circuitry in the Platform Electronics. During the coarse align portion of each align mode, the platform gimbals are slewed to predetermined angles by the alignment reference unit. Each align position on the mode select switch generates a ten-bit binary code which is routed to the computer along ten lines.

The selected code is set into the computer by depressing a switch (mode set) at the GSE. The computer then enters into a programmed calibration routine dependent upon the mode code command (reference Topic 3.4).

The code lines to the computer are supplied with 35.5 volts dc. At one point in the Centaur Program (1964-1965 period), the use of 28 volts dc was considered for this function to simplify the GSE circuitry and eliminate the requirement for a 35.5 volt dc power supply. However, a worst case analysis indicated the computer would not operate with 28 volts dc at the launch complex because of the large voltage drop in the long lines from the GSE, and hence, the 35-volt dc capability was retained.

6.12.3. The Improved Centaur Design (IMG) Mode Control. - Two powered modes will be provided by the IMG mechanization; e.g., power sequencing mode (reference Topic 6.13), and operating mode. The operating mode will include submodes such as gimbal alignment, calibration, and flight. All modes will be entered and exited under computer commands on interface control lines.

Control of the IMG will be provided to move the platform gimbals at a fast rate for gimbal orientation, and at a slow rate during calibration to compensate for gimbal drifts due to gyro drift rate and/or Earth's rate. Discretes generated in the computer or GSE will control the IMG gyro torquing electronics based on information signals from the resolver chain and from the velocity measurement loop.

Topic 6.13

System Power Requirements and Distribution

6.13.1. Present Centaur MGS. -

6.13.1.1. MGS Prime Power Requirements. - The primary 115 volts, 400 Hz power for the present Centaur MGS is obtained from the Centaur vehicle static inverter. Prime 28 volt dc power originates either at ground support equipment (checkout mode) or the vehicle battery (flight mode). The prime power sources are routed to the coupler which contains the switching circuitry necessary to control power application to the MGS. A block diagram of the MGS power distribution is shown in Figure 6.13-1.

Power consumed by the MGS has varied over the years, because of designs and modifications to the system. The power dissipation specification requirements placed on the MGS at the beginning of the Centaur Program in 1959 (-1 system) were:

Boost Phase -

28 volts dc - 231 watts max.

115 volts ac - 337 watts max.

Coast Phase -

28 volts dc - 196 watts max.

115 volts ac - 192 watts max.

With the development of the -3 system in 1961-62, MGS power specification requirements were modified to comply with this design. The -3 design increased ac loads because of the use of 400 Hz to develop the platform TCA supply (40 volts dc initially - reference Topic 2.8) and redesign of the accelerometer rebalance circuits. The system power requirement was then (early 1961) specified as:

Boost Phase -

28 volts dc - 175 watts max.

115 volts ac - 377 watts max.

Coast Phase -

28 volts dc - 160 watts max.

115 volts ac - 213 watts max.

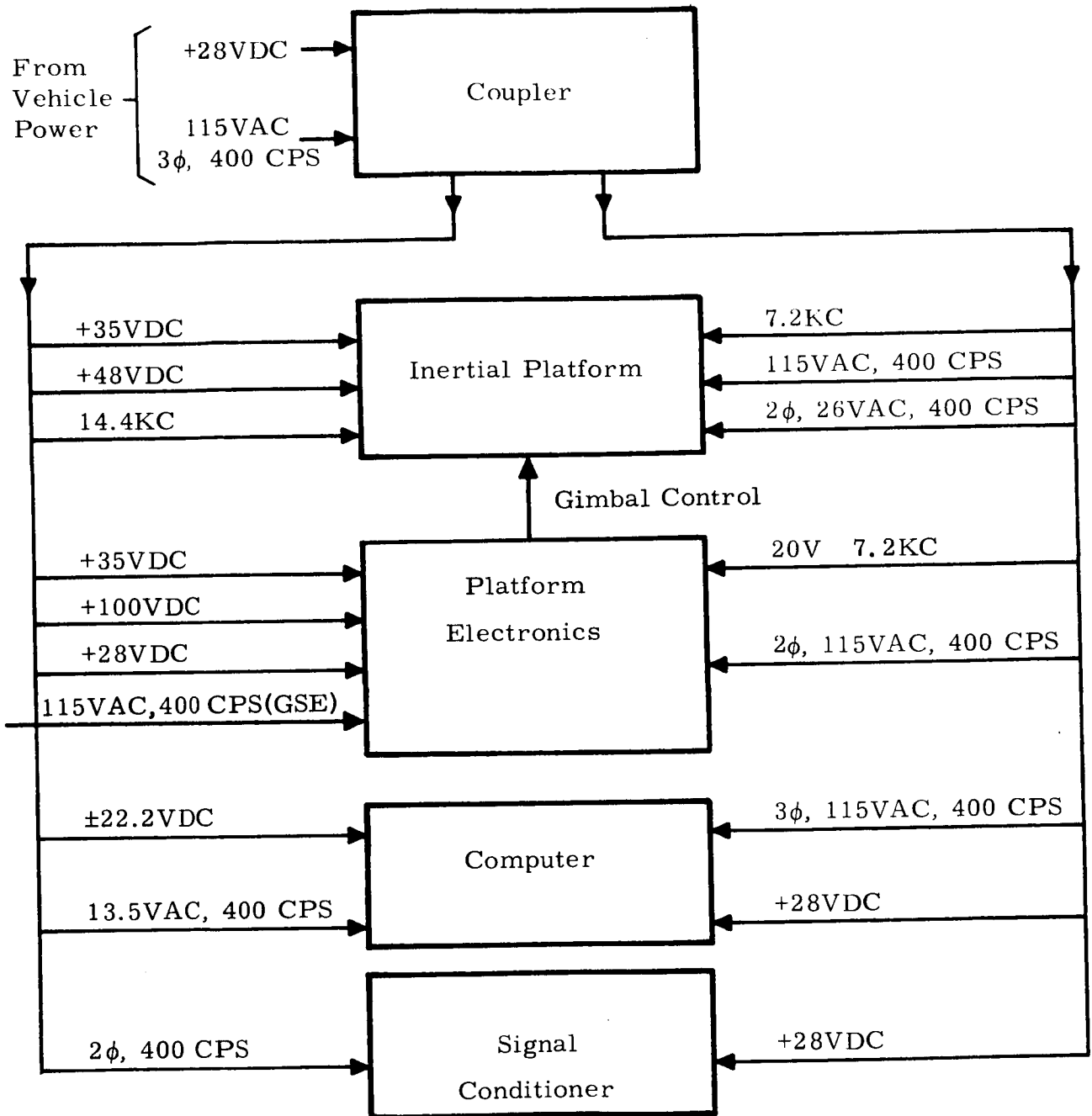


FIGURE 6.13-1. POWER DISTRIBUTION BLOCK DIAGRAM

In late 1961, an analysis of the power requirements for the -3 system was completed. Because of a lack of -3 system test data, the analysis was based on measured values obtained from -1 units and calculations of the effects of the -3 design changes. The values obtained from this effort indicated that the ac requirements were in excess of those specified for the system. The specifications were not changed at that time, however, pending results of -3 system testing.

Power measurements were performed on the -3 MGS during 1963 by both Honeywell and GD/C. In early 1964, the power specification was changed to reflect the following requirements:

Full Power Phase (Computer On) -
28 volts dc - 200 watts max.
115 volts ac - 470 watts max.

Computer Standby Phase -
28 volts dc - 170 watts max.
115 volts ac - 310 watts max.

Total power consumption characteristics of the present configuration MGS were obtained through tests conducted in 1965. Resulting profiles of 115 volts, 400 Hz power are given in Figures 6.13-2, 3 and 4. The figures include the measured real power, reactive power, and the calculated power factor for each mode of operation. Figure 6.13-5 gives the profile of the 28 volt dc current and power characteristics in the various modes of MGS operation.

Table 6.13-1 presents the average power values measured in calibration align modes 1 through 6, final align, and simulated flight. The power consumption characteristics of the present navigation computer (GPK-33) operating at the system level is presented in Table 6.13-2. Within the accuracy of the instrumentation, the total power consumed by the present MGS continues to meet the basic requirements established in 1964.

6.13.1.2. Power Switching and Interlock. - Primary ac power for the MGS is provided by the Centaur vehicle autopilot static inverter which supplied 115VAC, 400 Hz to the coupler. Either ground (GSE) or airborne (battery) 28VDC prime power is supplied to the coupler through the Centaur main power changeover switch in the autopilot. Application of the prime power to the MGS circuits is controlled by a four pole latching relay (set/reset) in the coupler (Relay K1, Figures 6.13-6 and 7). This relay applies three-phase 115 volt, 400 Hz power and 28 volt dc power to the MGS upon command from the GSE.

0169-120A

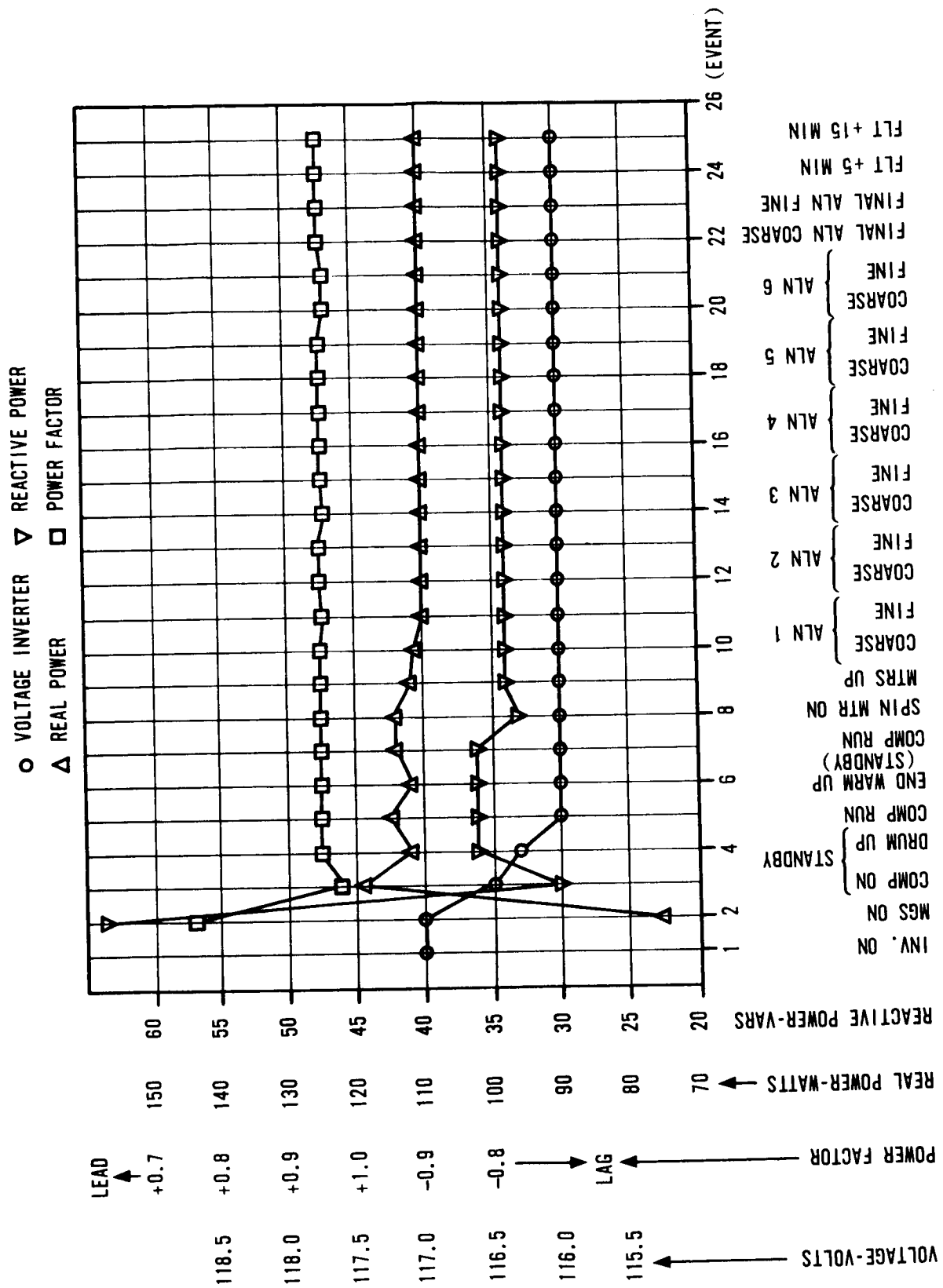


FIGURE 6.13-2. 400 HERTZ, PHASE A PRESENT CENTAUR MGS POWER CHARACTERISTICS

0100-126A

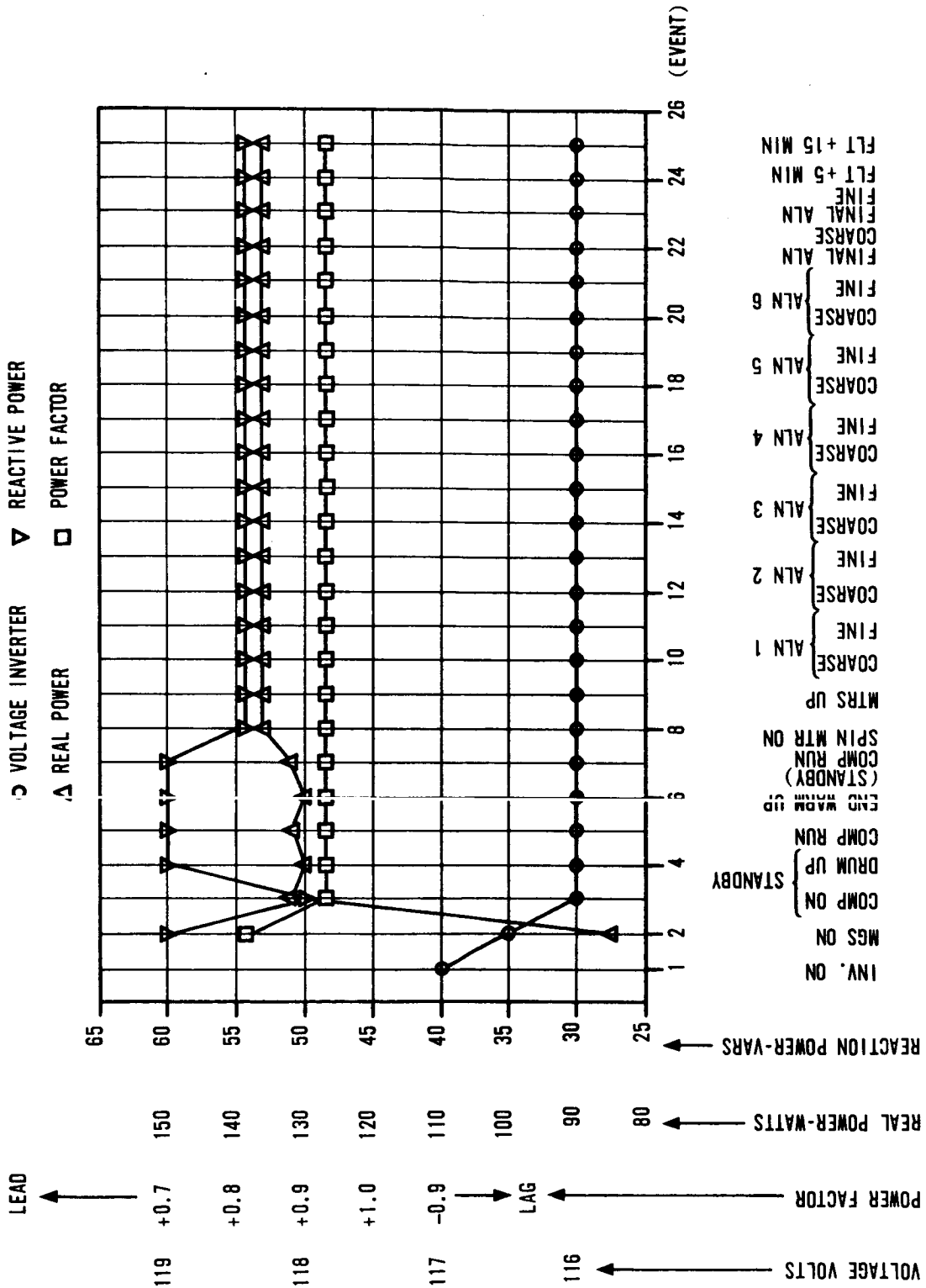


FIGURE 6.13-3. 400 HERTZ, PHASE B PRESENT CENTAUR MGS POWER CHARACTERISTICS

0166-138A

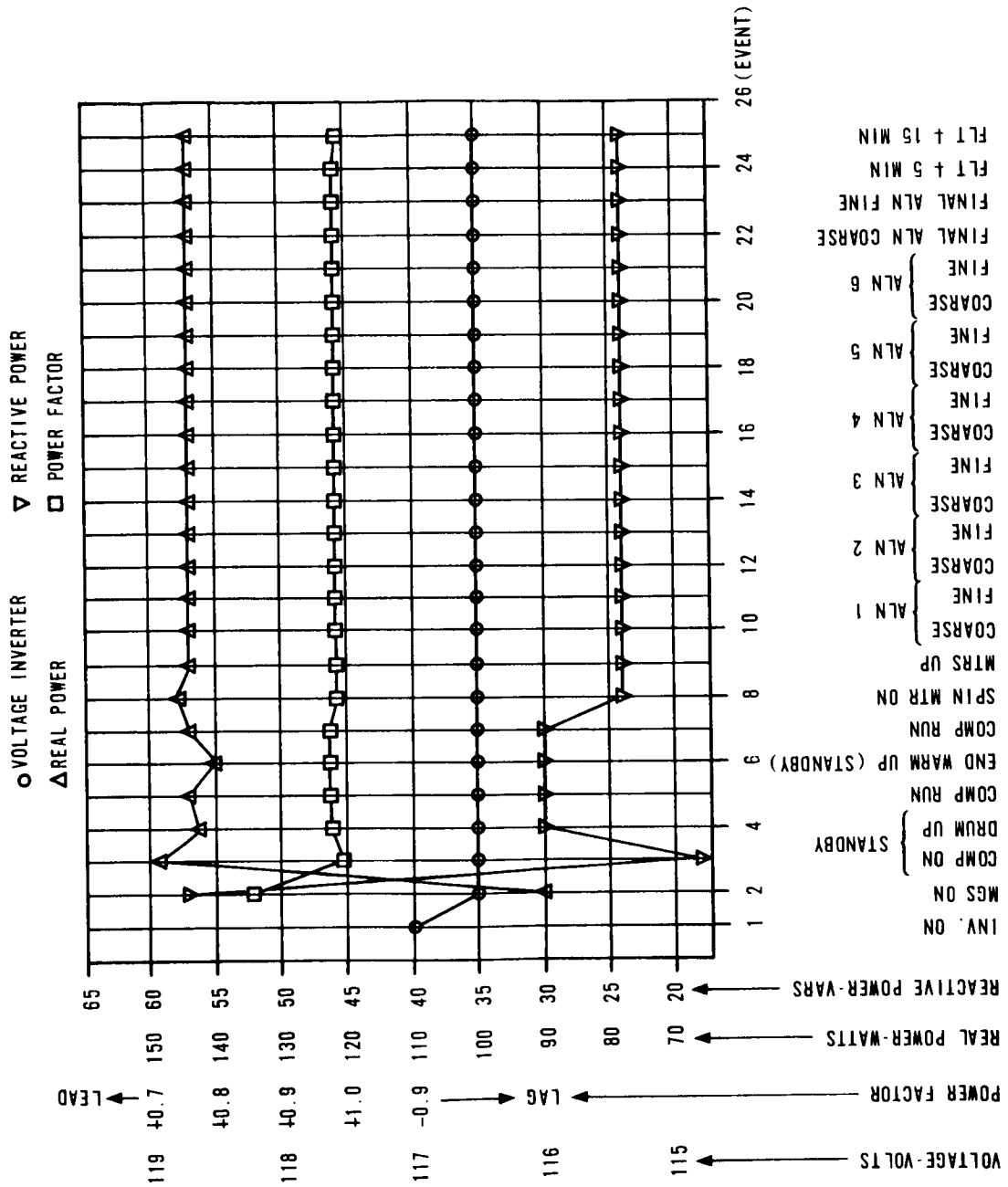


FIGURE 6.13-4. 400 HERTZ, PHASE C PRESENT CENTAUR
MGS POWER CHARACTERISTICS

0166-122A

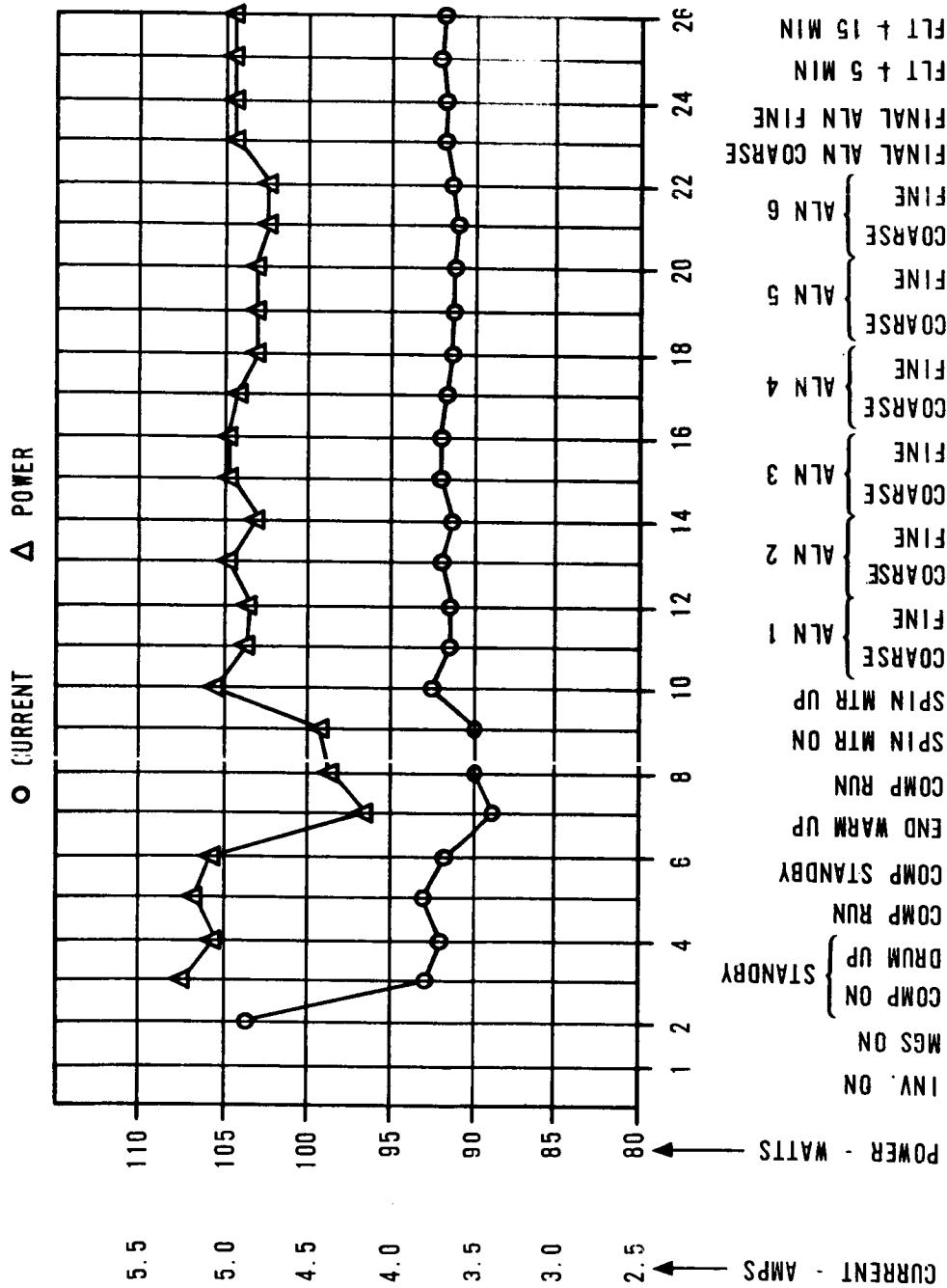


FIGURE 6.13-5. PRESENT CENTAUR MGS POWER CHARACTERISTICS 28 VDC

TABLE 6.13-I

PRESENT MGS AVERAGE POWER CHARACTERISTICS

	Phase A	Phase B	Phase C
Real Power (watts)	110	136	144
Reactive Power (VARs)	34	54	24
Power Factor	0.956	0.931	0.986
	lead	lead	lead
<p>Total Power (watts) = $\sum (\text{Real Power}) = 390$</p> <p>MGS Vector Power Factor = $\frac{\sum (\text{Real Power})}{\sqrt{(\sum \text{Real Power})^2 + (\sum \text{Reactive Power})^2}}$</p> <p>= 0.960 lead</p> <p>28 VDC Current (amps) = 3.66</p> <p>28 VDC Power (watts) = 103.61</p>			

TABLE 6.13-II

NAVIGATION COMPUTER (GPK-33) POWER CHARACTERISTICS

Phase (400 Hz)	Parameter	Computer Conditions	
		Standby	Run
Phase A	Reactive Power (VARs)	24.0	24.0
	Real Power (Watts)	54.0	60.0
	Power Factor	0.913 Lag	0.927 Lag
	Voltage (Volts)	115.5	115.5
Phase B	Reactive Power (VARs)	6.0	6.0
	Real Power (Watts)	52.5	60.0
	Power Factor	0.993 Lag	0.995 Lag
	Voltage (Volts)	116.0	116.0
Phase C	Reactive Power (VARs)	24.0	24.0
	Real Power (Watts)	62.3	67.5
	Power Factor	0.933 Lag	0.942 Lag
	Voltage (Volts)	116.0	116.0

28 VDC Characteristics

Current (Amps)	0.6	0.3
Power (Watts)	16.91	8.54

0566-410A

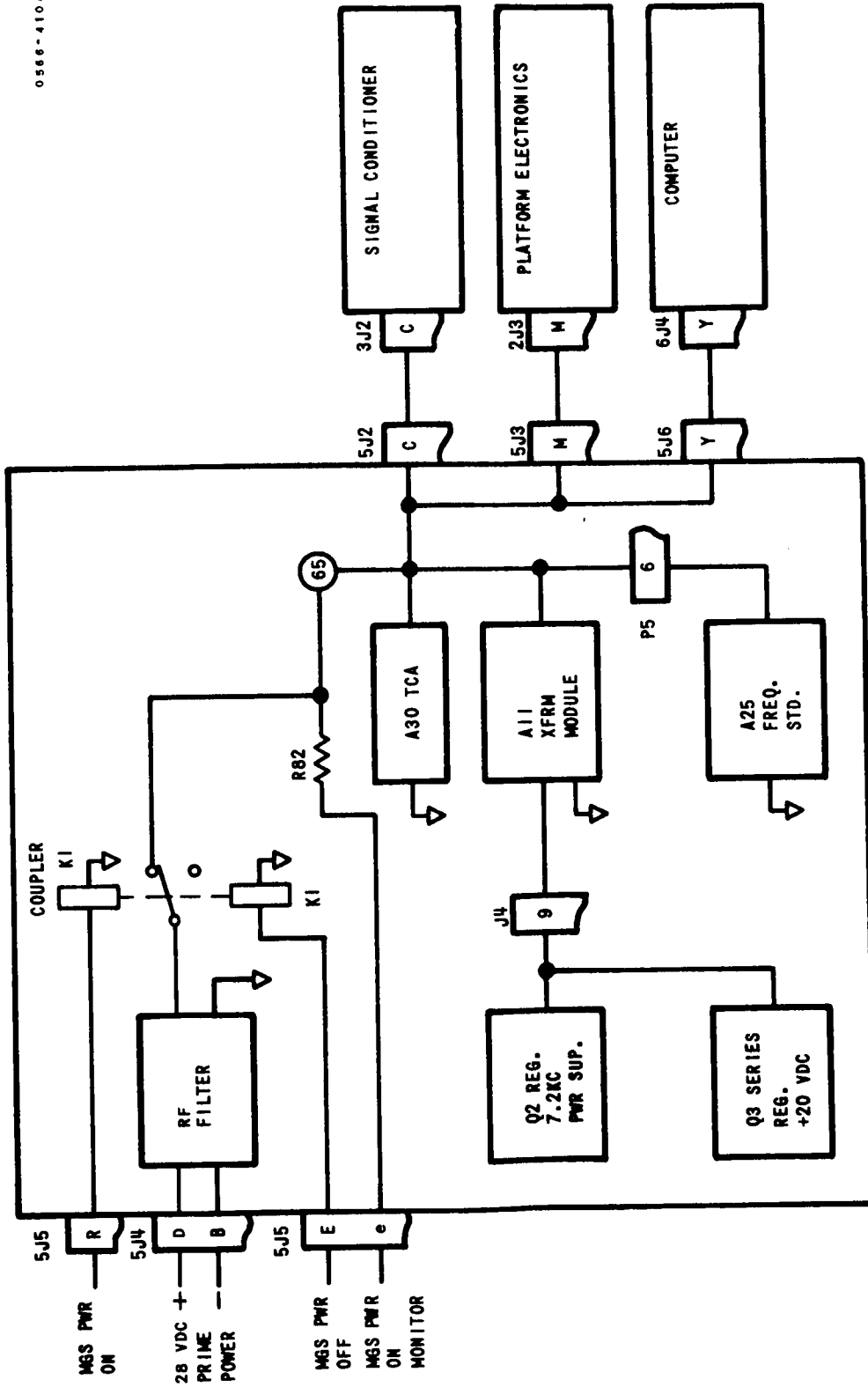


FIGURE 6.13-6. DC PRIME POWER DISTRIBUTION

0566-422C

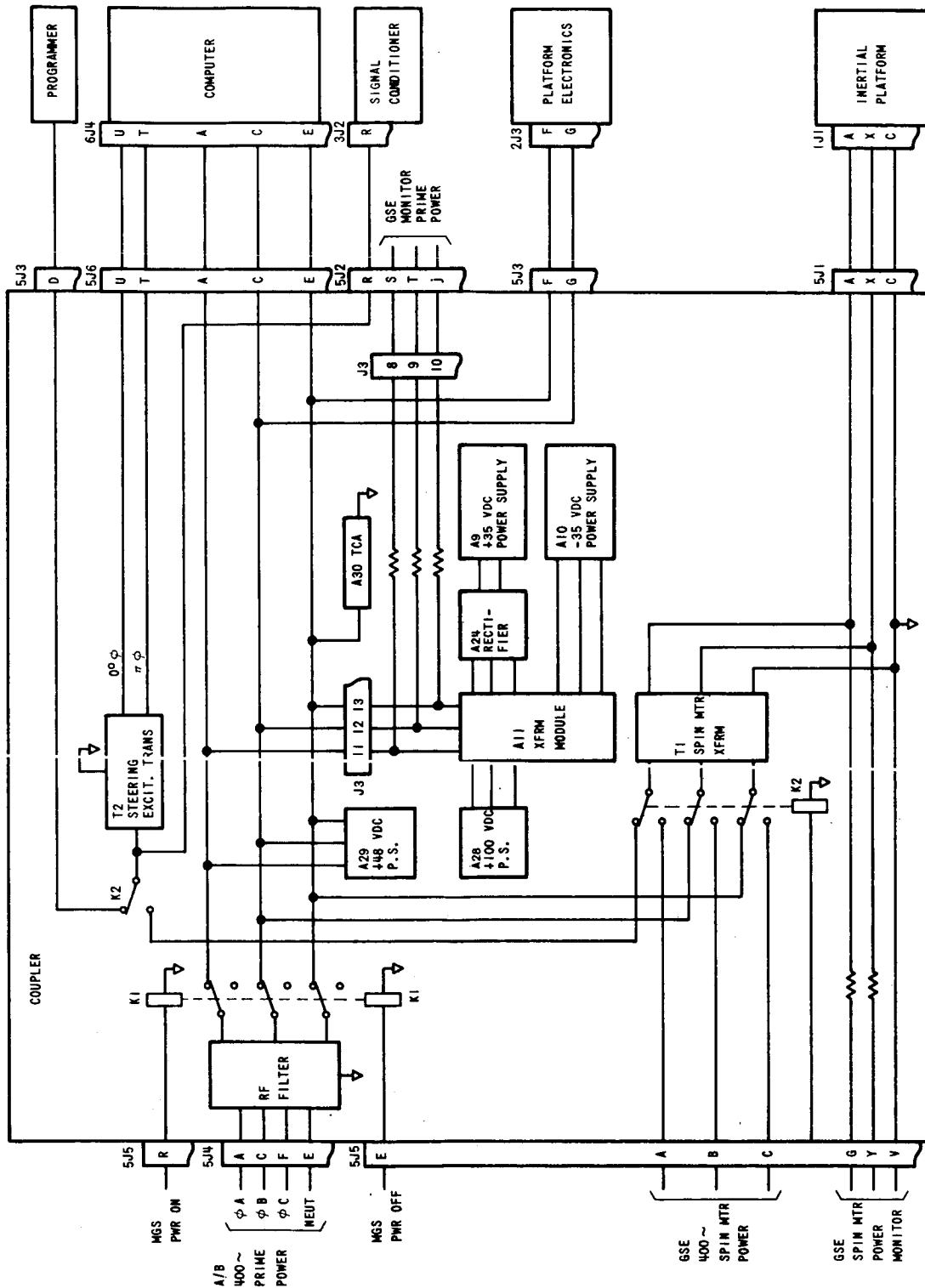


FIGURE 6.13-7. AC PRIME POWER DISTRIBUTION

Referring to Figure 6.13-7, relay K2 is used for switching the three-phase 115 volt, 400 Hz spin motor excitation to the spin motor transformer T1 and the excitation to the steering excitation transformer T2. This relay is controlled by a signal from ground support equipment. In the preflight mode of operation at the launch complex, the relay is energized and spin motor power is off. In the flight mode, the relay is de-energized and spin motor excitation is supplied from vehicle power, through relay K1.

The prime power switching logic in -1 and early -3 Centaur couplers was designed to apply power to the MGS circuits in the absence of a 28 VDC command signal from the GSE, thereby providing fail-safe operation during flight. However, it was found that the power control logic was such that inadvertent application of prime power to the MGS was possible during ground operations without proper sequencing by the GSE; i.e., positive control of prime power was needed. Several instances of uncontrolled application of MGS prime power were experienced during testing in the 1962-1964 period. The application of prime power to an MGS not under full GSE control caused the guidance system to be energized in the gyro stabilized mode without the required pre-operational warmup conditions being satisfied. Of concern were the possibilities of damaging effects to gyro flex leads and pivots caused by energizing the spin motors on a gyro which is not up to operating temperature, and also due to excessive rates. Energizing a "cold" gyro could cause excessive stress on and possible failure of flex leads and pivots due to the high viscosity of the gyro flotation fluid at temperatures below 160°F. When gyro spin motor excitation is removed; e.g., at system shutdown, the gyro gimbals tend to move against a stop. If the gyro spin motor excitation is subsequently applied before proper warmup, gyro gimbal movement could result while the flotation fluid was in a semi-fluid state, and permanent damage could be sustained by the flex leads. Further, with MGS power on (spin motors not excited and the gyro gimbals against a stop), the gyro signal generator develops a maximum output. The large gyro signal generator output signal could cause platform gimbal spins if the gimbal control amplifiers were energized, which could be of such magnitude to cause gyro failure by shearing of the pivots.

Even if the gyros were up to flotation temperature when MGS prime power was inadvertently applied, the gimbal stabilization loop would be unstable until the gyro spin motors were up to speed. Platform gimbal oscillations and high angular rates would result, causing possible damage to the gyro similar to that discussed above.

Physically related to positive control of MGS power was an interaction condition which existed between airborne and GSE +28VDC power. During MGS testing, the GSE +28VDC and the airborne 28VDC were electrically connected together under certain operational conditions. If a difference of potential existed between the two sources, a current would flow between the sources which could have resulted in unpredictable test results.

In 1965, positive control of MGS prime power was accomplished by the replacement of the then existing single coil, non-latching power control relay in the coupler with a two coil, bi-stable, magnetic relay. Inherent in this change was also the elimination of the airborne/GSE +28VDC power interaction problem.

An alternate solution to the positive power control problem was the generation of a new 28VDC signal which would be routed to and "ANDed" with the prime MGS 400 Hz power turn-on control logic. However, the replacement of the power control relay in the coupler was considered the best technical approach.

6.13.1.3. Secondary Power Supplies. - Diagrams of the distribution of the 28 volt dc and 115 volt, 400 Hz prime power are shown in Figures 6.13-6 and 7. A number of secondary power supplies are also required for the MGS. The function of the secondary supplies are listed below:

1. +35VDC Power Supply - Produces +35 volts ± 1 percent dc with load variations from 1.6 to 3 amperes for circuits in the coupler, platform, platform electronics and signal conditioner.
2. -35VDC Power Supply - Furnishes excitation to coupler amplifiers.
3. Combined Voltage Regulator (CVR), +22VDC and -22VDC - Supply 22 milliamperes of direct current to the gyro torquer potentiometers in the computer.
4. +20VDC Power Supply - Converts 28VDC vehicle power to a regulated 20VDC source to energize circuits in the coupler. Those circuits are the Isolated Power Supply (IPS), Precision Timing Generator (PTG), 14.4 kHz Demodulator Driver, delta V output, and the 14.4 kHz and 7.2 kHz supplies.
5. +100VDC Power Supply - Furnishes +100 volts non-regulated to the Platform Electronics unit for resolver chain input amplifier and phase switch excitation.
6. +48VDC Power Supply - Supplies heater current for the platform TCA's.
7. Isolated Power Supply - Provides fifteen isolated dc voltages to the master gate and the logic and level circuits.

8. Precision Voltage Reference (PVR) - Provides the three ARCS modules with a regulated voltage reference of 6.3 volts dc.
9. 14.4 kHz and 7.2 kHz Power Supply - Furnishes precise frequency outputs for the gyro signal generators, accelerometer signal generators, and the 14.4 kHz demodulator driver.

In -1 and early -3 Centaur systems using GG116 accelerometers, 400 Hz, and later 100 Hz, dither excitation was required to improve the accelerometer null uncertainty. This excitation source was located in the Platform Electronics (PE) and consisted of a 100 Hz oscillator which provided 1.35 volts rms to the platform accelerometers. This device was comprised of a single stage tuned collector oscillator and a transformer coupled, push-pull, common collector power amplifier. The positive feedback required for oscillation was obtained by capacitor and inductor coupling the oscillator's base and collector junctions.

With the incorporation in 1965 of the GG177 accelerometer in the Centaur platform, 100 Hz dither excitation was no longer required and was eliminated.

The Isolated Power Supply was also redesigned during the Phase II PIP program. This effort resulted from several problem areas involving overstressed transformers, efficiency, high noise source in the coupler, and the 11 volt dc output regulation requirement.

The above problem areas, along with the planned redesign of the 7.2 KC and 14.4 KC supply circuits (also distributed between the "Filter Module", and "Frequency Divider and Power Amplifiers board") resulted in the concept below:

1. Redesign the IPS DC/DC converter for better regulation and efficiency, and to eliminate overstressed components.
2. Relocate circuit components to minimize routing of high level signals. Package all 14.4 KC and 7.2 KC power supply circuits on the PC board and package the Frequency Standard and IPS circuits in the Filter Module.

Concept and Design Changes - Three different IPS circuit designs were completed during the course of the Phase II PIP program. They are discussed in chronological order.

1. First Design (Non-synchronous 15 KC Power Converter). - This was a standard DC/DC power converter similar to the original

- 4 KC converter. This converter operated at 15 KC and used LC rather than RC filter networks to achieve better regulation and efficiency.
2. Concept Change. - This change resulted from a desire to have the power converter operating frequency synchronized to eliminate "beat frequency effects", and system errors contributed to frequency shifts.
3. Second Design (Synchronous 14.4 KC Power Converter). - The second design consisted of power amplifying a 14.4 KC precision square wave signal from the PTG and converting it to dc.
4. Concept Change. - This change resulted from a potential problem involving the IPS with pulse dropping and deadzone. This problem was investigated and solved on Phase I PIP program and was attributed to IPS noise and transformer capacitance. This change in concept led to new transformer capacitance specifications, and an investigation into reducing the IPS noise on the system level.

An investigation was conducted to determine the noise levels and choose between two approaches. Both approaches used the Phase I PIP transformer rectifier and filter networks. One approach operated at 14.4 KC and the other at 1.8 KC.

Results of the system evaluation led to the selection of the 1.8 KC operated power converter design because of the reduced noise levels on the torquer current and ARCS output. The noise reduction is attributed to the fact that IPS switching occurs during dummy load time and, the use of slower switching speed power transistors.

During the Phase II PIP design and development, the worst case analysis of the AC Power Supply indicated that the circuit would meet its requirements under worst case conditions. However, a noise problem occurred in the 14.4 KC supply when the circuit was packaged on a printed circuit board. Noise was coupled into the 14.4 KC Regulator from the ground path, causing excessive noise on the 20 volt Power Supply. The problem was eliminated by adding a high frequency roll-off capacitor to the differential amplifier stage of the regulator, and a decoupling capacitor across the 20 volt supply on the board. This problem verifies the fact that circuits are not packaged on "paper" but on printed circuit boards or modules that have undefined capacitances and inductances. Worst case analysis therefore is not the end, but only the beginning of a good design.

6.13.2. The Improved Centaur IMG. -

6.13.2.1. IMG Primary Power. - The IMG will receive prime power for its operation from the vehicle 27.5 volt dc power source. The total power requirements for the IMG will be approximately 210 watts nominal.

6.13.2.2. IMG Power Control. - All IMG functions, with the exception of gyro spin motor power and stabilization loop power, become operative with the application of 27.5 volts dc nominal at the IMG power connector. The IMG will provide the necessary internal switching of the spin motor power and stabilization loop power, and selection of gyro torquing rates and polarities when commanded by control signals external to the IMG. The vehicle computer, with associated input/output equipment, will provide the necessary logic for sequencing the IMG power. After initial application of vehicle power to the IMG, sufficient time will be allowed for the inertial components to warm up before external control signals are permitted to energize the gyro spin motors or enable the stabilization loops. This will prevent possible gyro torques during the time that the gyro flotation fluid has a high viscosity and will also prevent the generation of platform gimbal drive signals by a gyro gimbal being offset from null.

When the gyros have reached proper operating temperature, gyro spin motor energization will be enabled, but the stabilization loops will remain disabled until the spin motors reach synchronous speed.

The requirements for the power sequencing function are:

1. Power control will be accomplished with latching relays.
2. The power control relays will be energized with 27.5VDC and energization may be either continuous or intermittent.
3. The power control function will be positively disabled for in-flight operation.
4. Gyro spin motor power will not be applied until the IMG has determined that the gyro temperature is satisfactory.
5. Gimbal Control Electronics (GCE) power will not be applied until at least 100 seconds have elapsed after application of spin motor power.
6. A single IMG OFF command will reset all power control relays to OFF.
7. The IMG will inhibit the IMG ON command unless spin motor and GCE control relays are OFF.

8. The IMG will inhibit the Spin Motor ON command, unless the IMG determined temperature condition is satisfied.
9. The IMG will inhibit the GCE ON command unless the Spin Motor ON condition is established.

The mechanization of the power sequencing function is accomplished by use of latching relays. The relay circuits are connected to provide the required interlocks within the IMG. Relay ON and OFF commands are generated by equipment external to the IMG. The time separation of the "ON" discretes is provided by the equipment that generates the commands.

The operation of the power sequencing function is illustrated in Figure 6.13-8.

The ON-OFF commands must be of sufficient duration, approximately 0.05 second, to insure IMG relay response. The OFF command at the start of the sequence provides additional assurance that all IMG relays are initially set to the OFF condition.

The IMG relay circuits are shown in Figure 6.13-9.

6.13.2.3. IMG Secondary Power. -

SEU DC Power Supply. - The dc power supply located in the SEU will provide the secondary power required for the IMG. In comparison with the present Centaur MGS, the number of different internal supply voltages required has been significantly reduced. The block diagram of Figure 6.13-10 shows the functional mechanization within the SEU. The final configuration of the dc power supply will be designed to provide attenuation of the power source ripple voltages and to absorb or store energy during the transient conditions, thus preventing these signals from affecting the dc supply output voltages.

The dc power supply mechanization is shown in block diagram form in Figure 6.13-11. Following the RF and AF filter circuits the input power is fed to a pre-regulator circuit operating from the prime power. The pre-regulator is followed by a dc-dc converter with additional Class A regulators for the precision dc voltages.

The pre-regulator 15V dc output is fed to the dc-dc converter which supplies outputs of 43V for the 35V dc Class A regulator, the plus and minus 15 volt supplies, the plus and minus 20 volt supply, and the 5V dc supply.

0168-97A

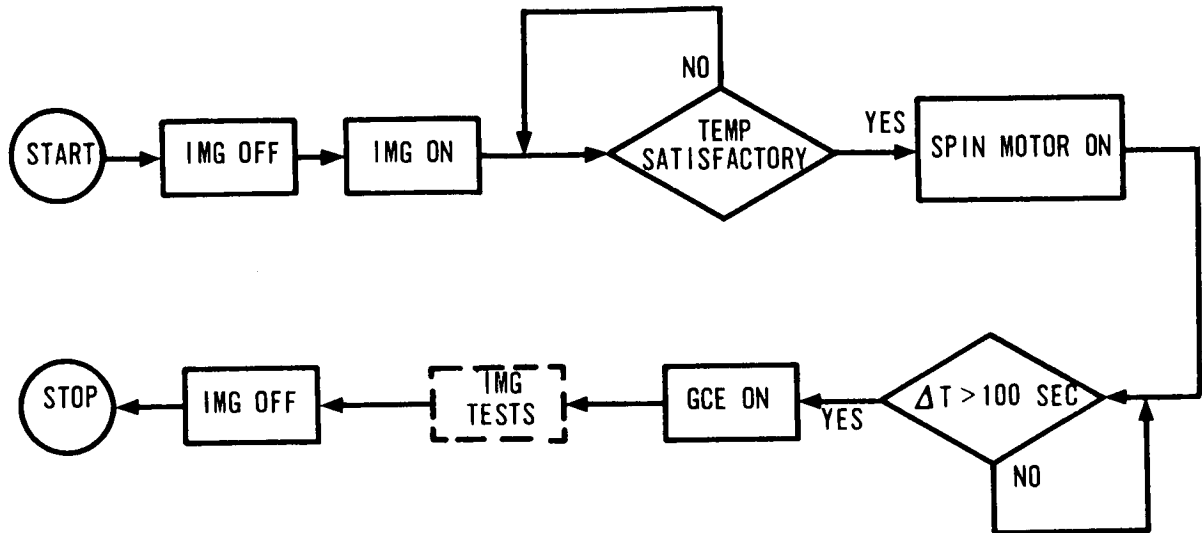


FIGURE 6.13-8. IMG POWER CONTROL

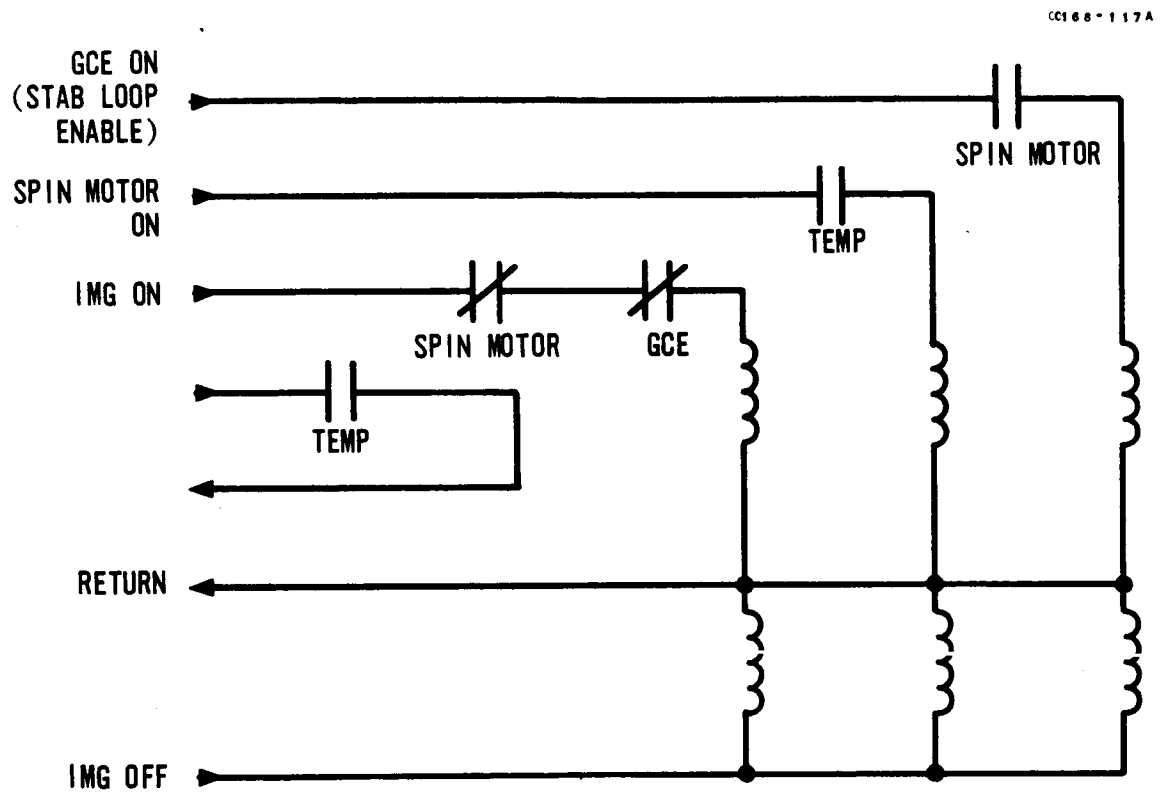


FIGURE 6.13-9. IMG POWER SEQUENCING RELAYS

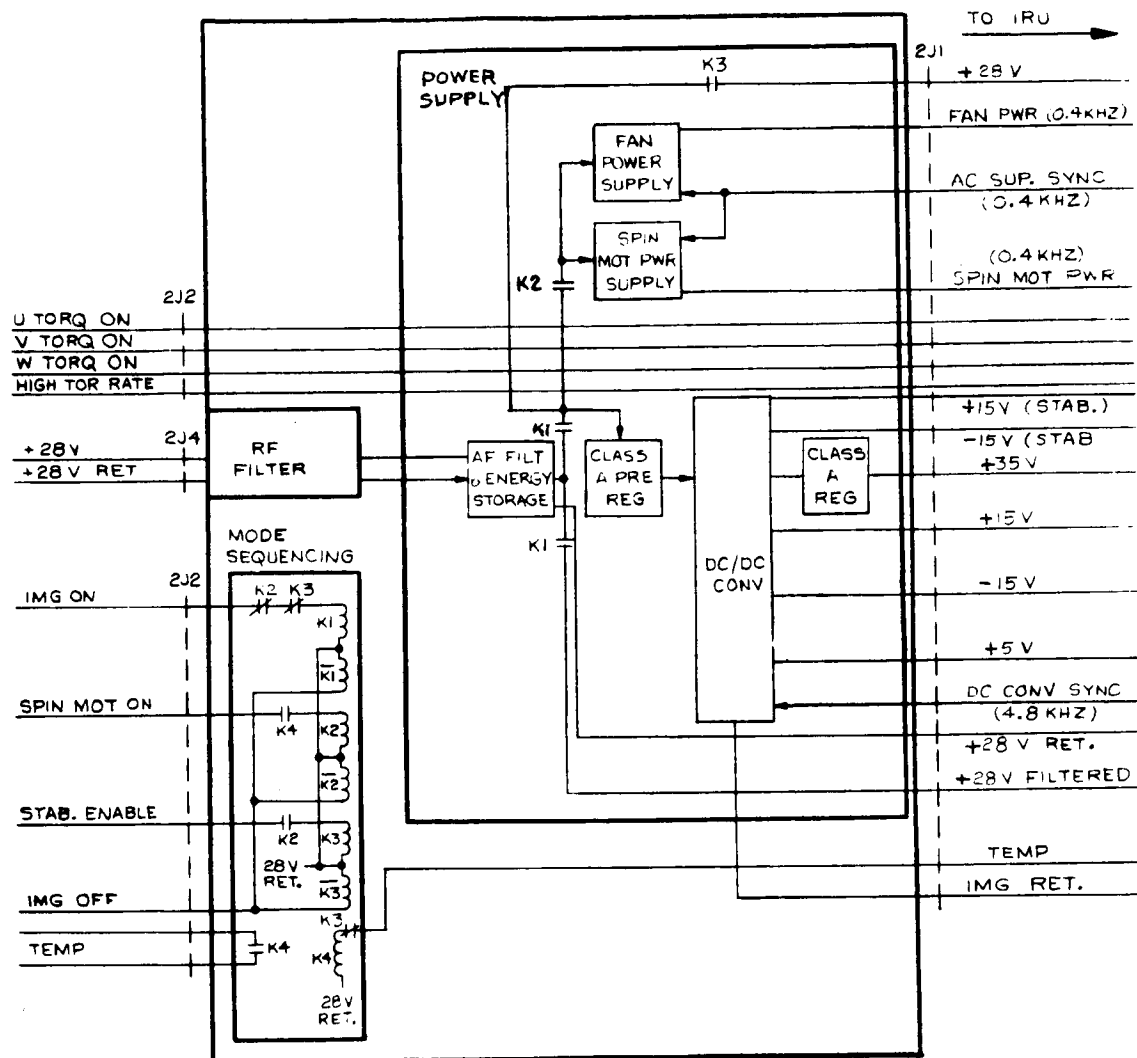


FIGURE 6.13-10. SEU FUNCTIONAL BLOCK DIAGRAM

0166-93A

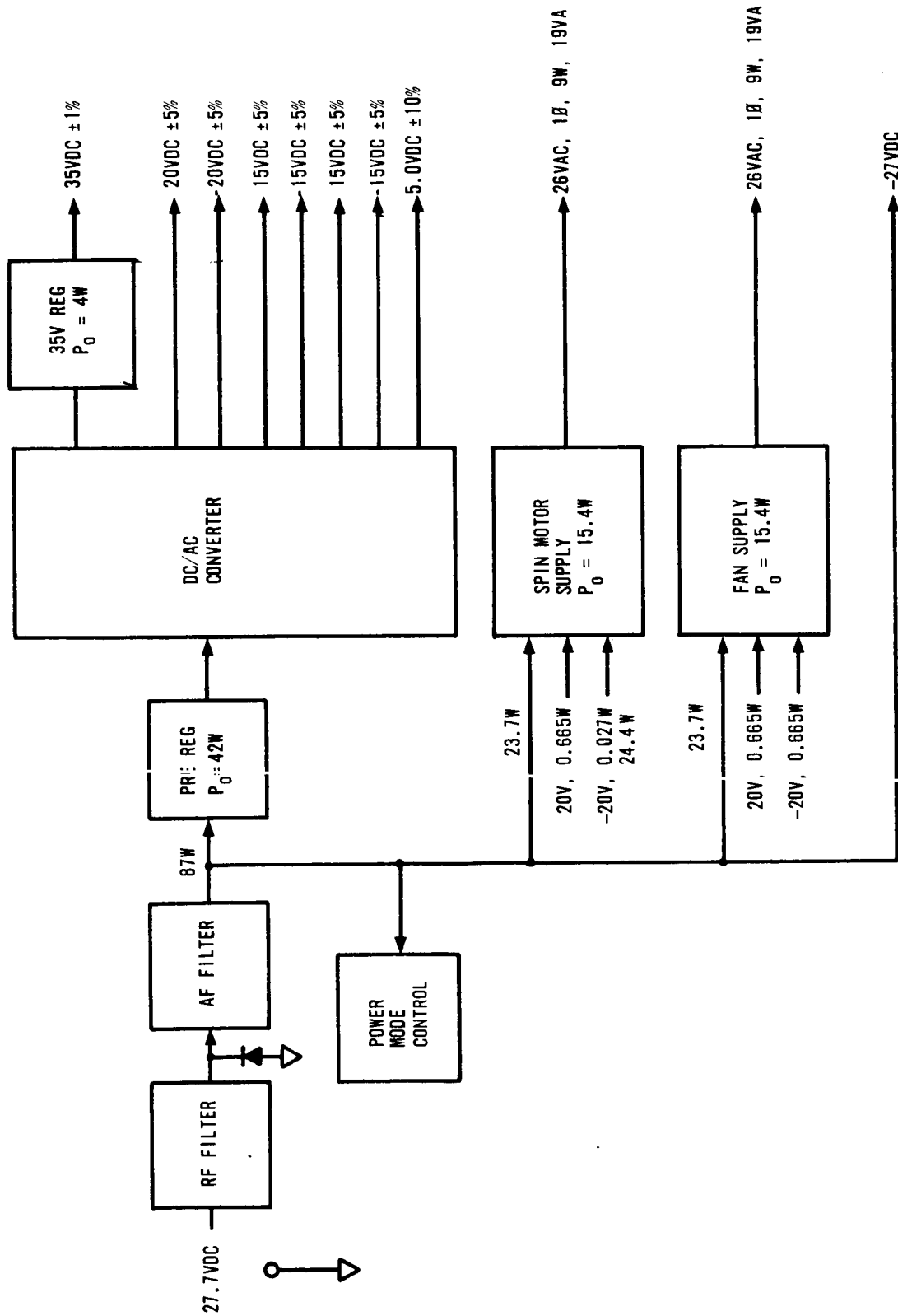


FIGURE 6.13-11. DC POWER SUPPLY MECHANIZATION PRELIMINARY

As seen in the block diagram, the 400 Hz ac voltages for the spin motor and fan supplies are converted from the prime power filtered output. Sinusoidal output waveforms are obtained by filtering the square wave outputs of the dc-ac switching converter and power amplifier.

The precision ac voltages required for the gyro, accelerometer, and resolver excitations are obtained from power amplifier and filter circuits. The excitation frequencies are provided by precision timing count-down circuits.

In the early stages of development of the dc power supply three basic dc to dc power converter approaches that could be used to obtain system dc voltages were considered. These three alternatives are described for reference in the following paragraphs along with the merits of each.

Alternate A: A pulse width controlled dc to dc converter operating from the 28 volt dc prime power, followed by Class A regulators in those cases where additional regulation is required. A block diagram is shown in Figure 6.13-12. This was the most efficient design, 79 to 87 percent, for total IMG power conversion, and would provide isolation of all outputs from the prime power. An objection to this approach was limited bandwidth which was constrained by the maximum operating frequency. The performance of this converter would require an operating frequency of approximately 10 kHz and a power line filter, designed to operate in conjunction with the converter, to attenuate the power line ripple above 300 Hz. This approach was rejected for the following reasons:

1. The design was more complex.
2. The approach had not been demonstrated for an operating frequency of 10 kHz. Switching losses would reduce efficiency and time delays would degrade the upper and lower line voltage operating limits of the converter.
3. The converter output voltage filters were more complex because of the pulse limits to which they must be designed. The noise on the output voltages would be larger than the other two converter approaches.

Alternate B: A dc to dc converter operating from 28 volts dc prime power, followed by four Class A regulators and one switching mode regulator. A block diagram is shown in Figure 6.13-13.

0168-73A

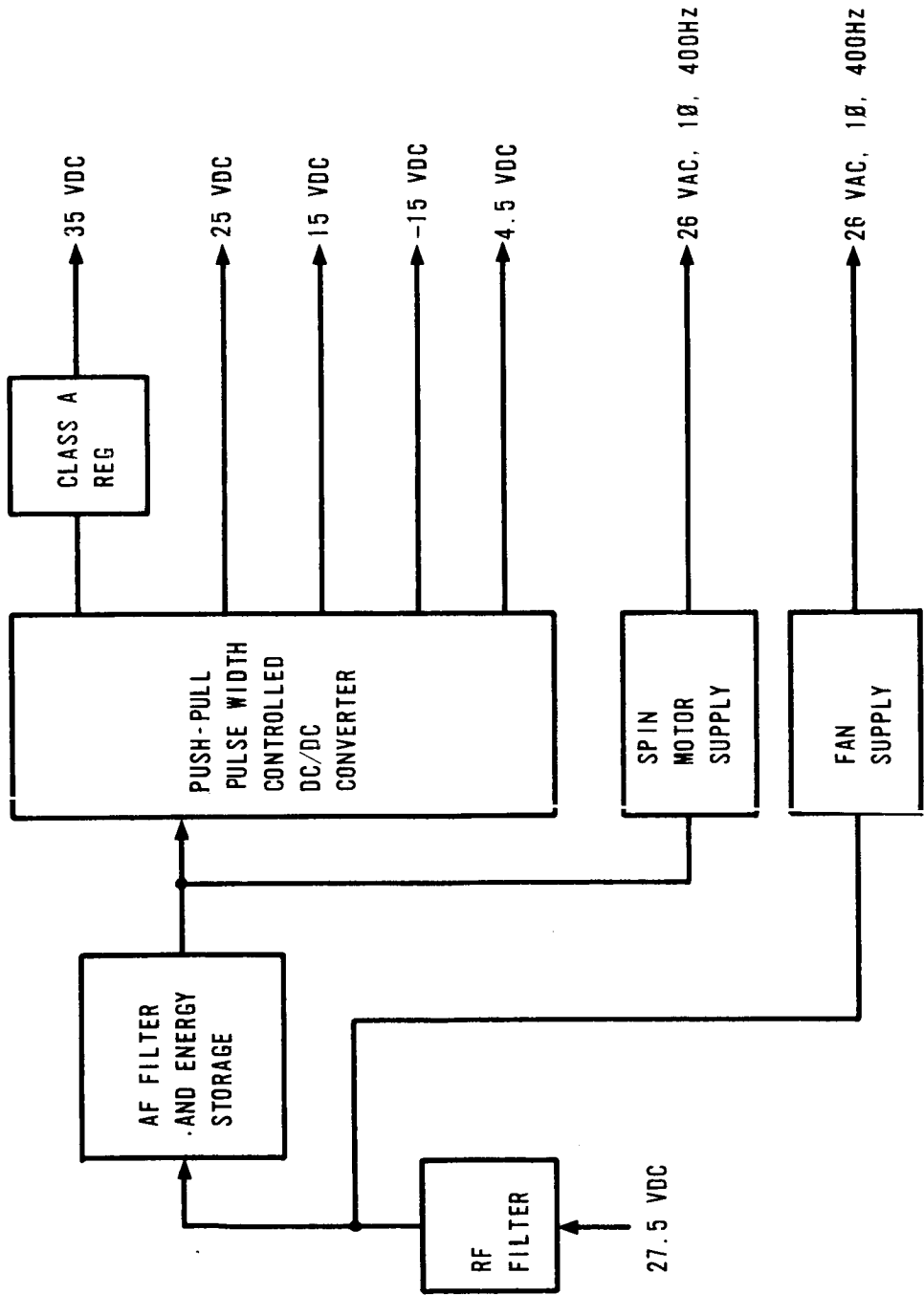


FIGURE 6.13-12. POWER SUPPLY BLOCK DIAGRAM - ALTERNATE A

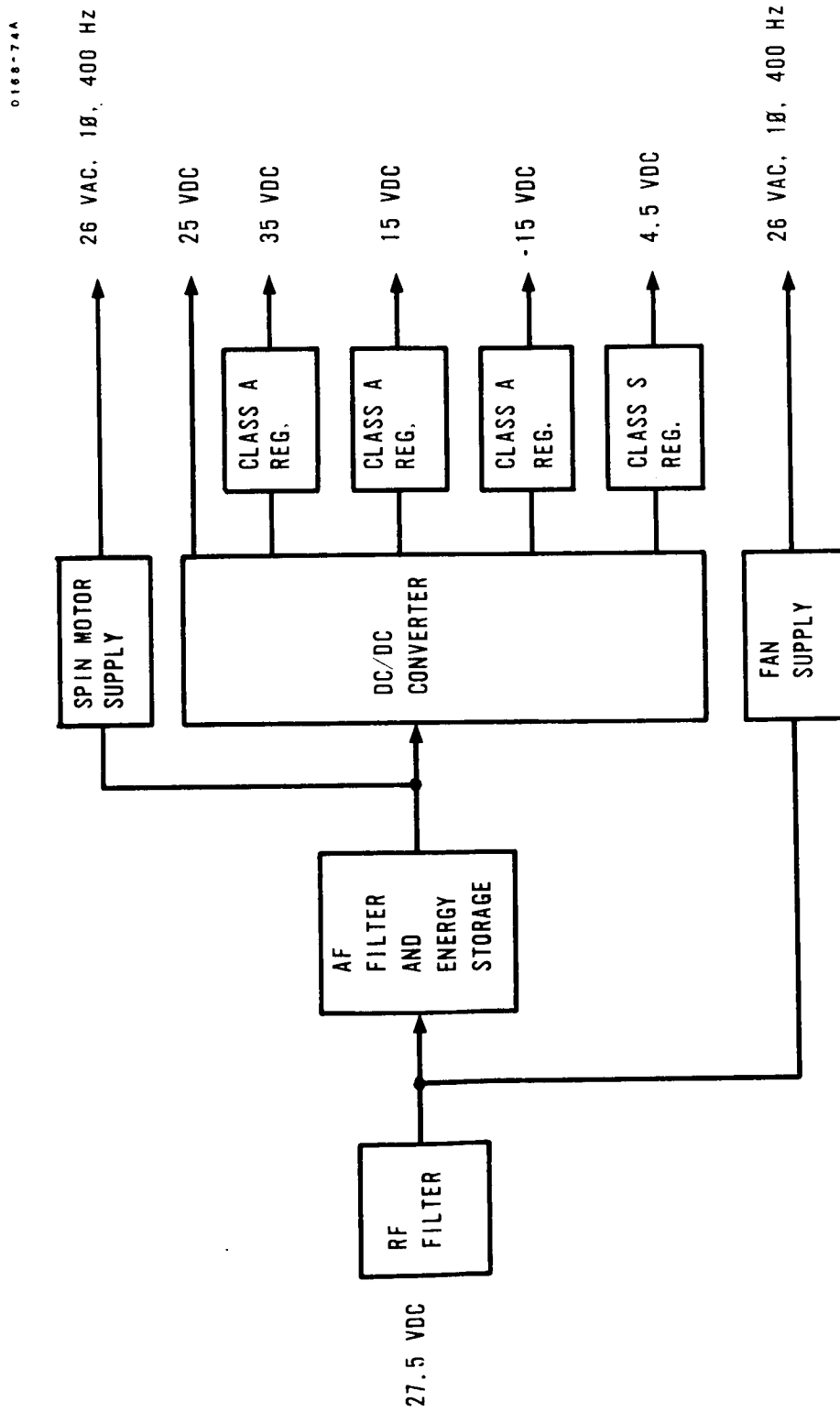


FIGURE 6.13-13. POWER SUPPLY BLOCK DIAGRAM - ALTERNATE B

The IMG power supply efficiency of this approach was comparable to Alternate C, which was approximately 65 percent. This approach offered the best regulation for all output voltages and provided isolation of all system voltages from prime power.

This approach was rejected because it required a regulator for each output voltage and large filters for energy storage during transients. This would have resulted in the power supply being more expensive and less reliable.

Alternate C: A pre-regulator operating from the 28 volts dc prime power, followed by a dc to dc converter, followed by Class A regulators in those cases where additional regulation is required. A block diagram is shown in Figure 6.13-14.

This was a conventional and straightforward approach to the power supply mechanization which minimized the amount of power conditioning and simplified the power supply design.

This concept has been used on several in-house programs and its performance has been satisfactorily demonstrated. This basic approach was favored over alternates A and B for the following reasons:

1. More economical and reliable because it was less complex and contained fewer circuits and components.
2. Demonstrated performance on other programs such as the Alert Computer and the "Prime" Inertial Guidance System.
3. There was no significant advantage to be gained in weight or volume from any one of the approaches considered.

SEU AC Supplies. - The ac supplies, spin motor power and fan power, use circuit concepts developed for the present IGS and SEU programs.

A number of spin motor supply excitations were considered. Several excitation approaches were used in an evaluation test to compare performance of the DGG49D gyro. The final selection is the single phase, sinusoidal supply excitation. Approaches that were considered are covered below:

1. Two Phase Square Wave Excitation - The gyro under test never reached synchronous speed.

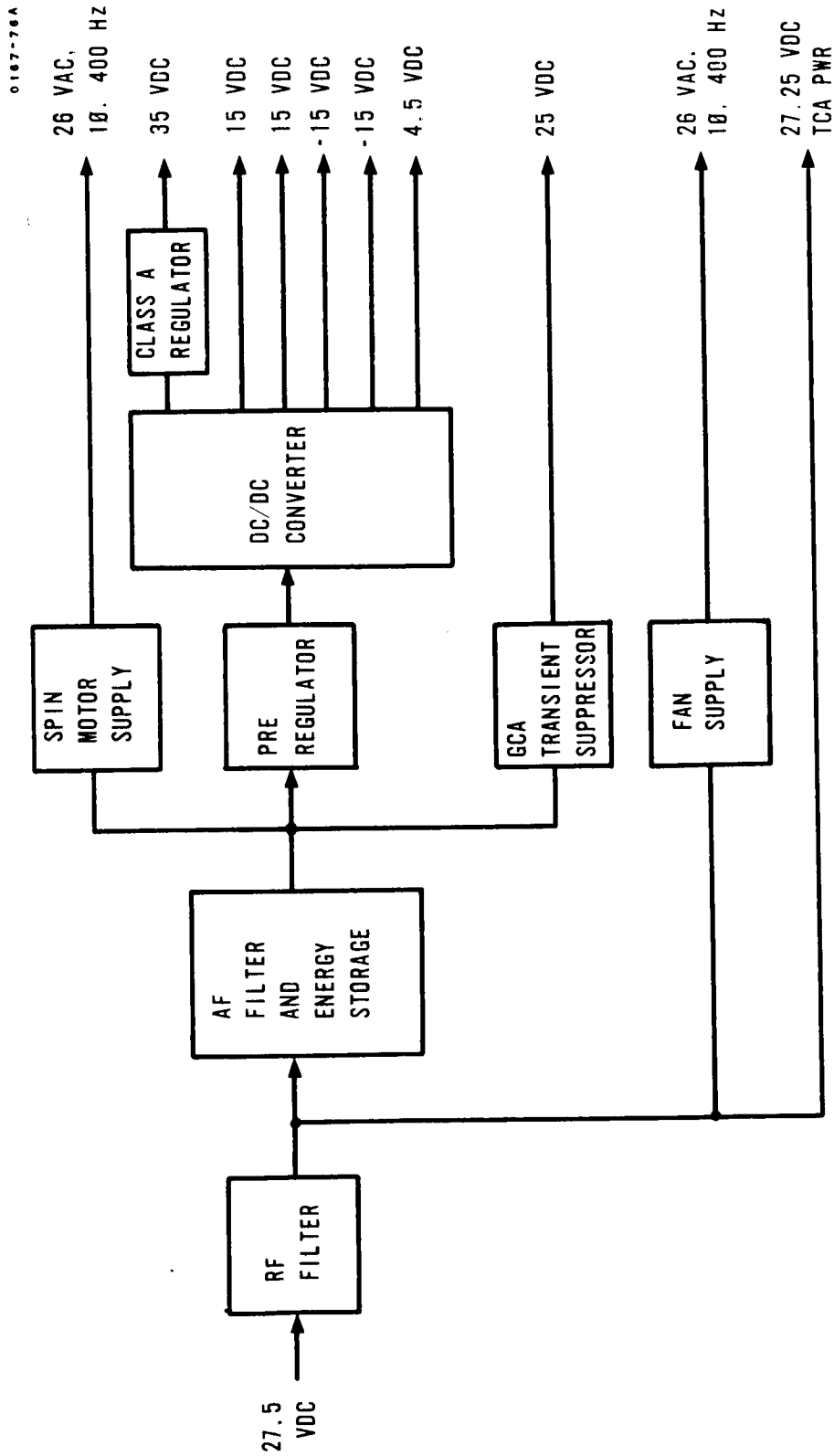


FIGURE 6.13-14. POWER SUPPLY BLOCK DIAGRAM - ALTERNATE C

2. Three Phase Quasi Square Wave Excitation - This approach has been used on the Dyna-Soar (X-20) and other in-house inertial guidance programs. Its performance was comparable to other excitation approaches. The disadvantage was that noise generated by the square wave coupled into the signal generator secondary.
3. Single Phase Sinusoidal Excitation - The performance of this excitation was satisfactory and comparable to other approaches. This approach resulted in the most economical and reliable power supply mechanization considered. The power supply mechanization required approximately 50 percent fewer components over the three phase quasi square wave supply. Noise was minimized by the use of sinusoidal waveform excitation.

The fan supply provides ac excitation to a fan located in the IRU. Only one fan supply mechanization was considered; e. g., a 400 Hz, sinewave, single phase supply comprised of a 400 Hz switching mode buffer and power amplifier, and filter. The bases for this mechanization were:

1. The supply was synchronized with the precision timing generator signal to minimize beat-frequency and random noise effects within the system.
2. A sinusoidal excitation was selected over a square wave to minimize noise coupling into sensitive system areas.
3. The noncritical application of the fan excitation allowed the use of straight 400 Hz power amplification, of the simplest form, to minimize circuitry and component count.

IRU Excitation Supplies. - The IRU excitation contains four power supplies used to provide ac excitation to various circuit functions located in the IRU. These supplies are described below:

1. Gyro Signal Excitation Supply - Provides a 14.4 kHz sinusoidal excitation to three parallel connected gyro signal primary windings, and a demodulator reference.
2. Accelerometer Excitation Supply - Provides a 57.6 kHz sinusoidal excitation to three parallel connected accelerometers.
3. Steering Reference Excitation Supplies - Two supplies providing 2.4 kHz and a 3.2 kHz sinusoidal excitation to the steering reference amplifiers.

The IRU power supply mechanization uses a standard circuit concept for all four applications. The circuit is taken from one developed for the present Centaur IGS and represents a low risk, simple, and economical approach.

There were three basic candidate mechanizations considered for use in the IRU. Tradeoff considerations are discussed below:

1. Regulated AC Supply - This design required approximately 50 percent more components over the other circuit mechanizations and was rejected from the standpoint of economy and reliability.
2. Power Amplifier and Low Pass (RC) Filter Supply - This circuit contained fewer components than the other two designs considered, but it required a controlled temperature environment such as was available on the platform stable element and the space limitations at this location was a prime reason for rejection of this design. Further, a disadvantage of this supply was that a dc component was contained in the waveform which was undesirable for the gyro excitation application.
3. Power Amplifier and Bandpass (LC) Filter Supply - This design was selected as the best alternative because of economy and reliability resulting from fewer circuit components at a slight sacrifice in performance. This selection was possible because of an allowable relaxation in excitation requirements, achieved partly by a relaxation in the error budget, and also by reducing load regulation tolerances by locating the supply in the same unit as the load. An approximate 50 percent reduction in components was achieved over the regulated ac supply mechanization.

6.13.2.4. Conclusions. - Experience gained during the -1 and -3 Centaur Programs has proved valuable during the IMG system power design and development. Significant power and weight savings have been realized through efficient power conversion, use of integrated circuits, and through simplification of design.

The utilization of a single 27.5VDC prime power source for the IMG has resulted in interface simplification over that for the present Centaur MGS, which requires both a 28VDC source and 115 volt, 400 Hz, 3 phase source. A potential noise source is also eliminated; e.g., since the 115 volt, 400 Hz power is presently generated from the three phase 400 Hz airborne inverter which also furnishes power to other systems, the MGS prime power ac input is vulnerable to any transients caused by these other systems. Although the IMG power supplies could be simplified further if

vehicle AC power were available, the tradeoff with other vehicle requirements has resulted in a decision to use the single 27.5VDC source.

The number of different secondary power sources required for IMG system operation has been significantly reduced. Circuit components have been kept to a minimum consistent with good design contributing to improved reliability. All IMG power supplies are located in one unit (SEU) providing isolation of noisy power supply circuits from circuits having high noise susceptibility which are located in the IRU. Further, circuitry associated with IMG secondary power is synchronized with critical timing signals within the IMG such that the effect of power supply noise being injected into critical signal paths is reduced.

Topic 6.14

IGS Electrical Interface and Grounding

6.14.1. Electrical Interface Control. - The need for control of the electrical interface within and between MGS units, MGS to GSE, and MGS to other vehicle subsystems was recognized early in the Centaur program. As such, interface drawings were prepared during the 1961-62 period by GD/C. These documents were a start in the right direction, but were incomplete in that control of the vehicle harness parameters and budgets for instrumentation loads were not covered. Further, since Honeywell generated the data contained on the drawings which were prepared and maintained by GD/C, excessive inter-company correspondence was necessary to coordinate the continual updating of information and timely drawing maintenance was difficult.

To alleviate these problems with interface control, Honeywell was authorized in 1966 to generate a new set of drawings for complete control of interfaces and interconnections applicable to integration of the MGS into the Centaur vehicle/launch complex configurations. Specifically, these Interface Control Drawings (ICD's) control:

1. Electrical and mechanical interfaces between MGS units and Centaur vehicle subsystems.
2. Electrical interfaces between the MGS and system level test and launch equipment.
3. The requirements for all cabling which connects to MGS units.

MGS signal monitoring is necessarily a factor in interface control. The philosophy of the signal monitoring scheme on the present system falls into two categories. First, the signals interfacing with the flight unit, i. e., signal conditioner, are isolated to the extent that a short would only cause a slight degradation in performance in a loop. In all cases this degradation will not adversely affect a flight. The second category is the flight unit-to-GSE interface. These signals are isolated to the extent that a short would not damage the circuits. After liftoff the short caused by a GSE problem would no longer exist, thus the system would resume normal operation.

This same philosophy is being adopted in the Centaur IMG Program.

6.14.2. Grounding/Return Interconnection. - During the course of the Centaur program, many problems have been encountered which were the result of improper grounding and shielding techniques, or "sneak" paths creating ground loops resulting in grounding problems. The present IGS hardware is a product of evolution. Since the original -1 IGS design, many contract change orders have directed modifications, or redesign in specific, limited areas. Tradeoffs in arriving at the hardware area and extent of the change have often resulted in compromises. Successive limited changes have, therefore, narrowed the choices of workable solutions in certain functional areas. In some cases, more optimum solutions may have been withheld when specific constraints on hardware redesign were established for a modification. Such methods are frequently justified as necessary in terms of technical risk, cost, and schedule. However, these methods made it difficult, and sometimes impossible, to maintain the integrity of the system grounding scheme with respect to the preferred grounding philosophy.

The initial grounding scheme for the IGS was less than optimum. Successive modifications led to more and more complexity in grounding interconnection, interaction, and interdependence. A point was reached when minor hardware grounding/return changes could produce subtle and unpredictable effects in widespread hardware areas. The dilemma can be traced to the undue complexity of the "return trees" and the relative difficulty in understanding which portions were absolutely necessary.

The interconnection of MGS returns and grounds is accomplished primarily in the Coupler. During the initial -3 MGS development in 1961-62, the Coupler design was reviewed and significant changes in the unit grounding configuration were incorporated. Circuit ground tie points were relocated to reduce to a minimum the conductive coupling resulting from currents in ground wires. The 400 Hz neutral in the Coupler was completely isolated from other Coupler circuit grounds and was referenced to chassis at vehicle power. Further the addition of a chassis stud in the Coupler provided a single tie point for shields which had previously been tied to the chassis at many points.

In the 1964-65 period, during the Phase II PIP redesign effort, the Coupler ground/return configuration was further improved along with other intra-unit wiring. Areas where mutual coupling of signals could occur, common power sources, common signal returns, chassis ground, and cabling were reviewed and modified where necessary. When theoretical analysis indicated that mutual coupling in a certain area might impose significant noise on critical signals, the units and interface were tested and evaluated.

During 1966, better understanding of the MGS "grounding" was made possible by the preparation of detailed grounding diagrams. These drawings provided individual prints for each MGS unit and for the vehicle harness. The overall layout presented matching interfaces of the separate prints to aid in the study of the complete "grounding" picture. The drawings greatly simplified the tracing of MGS return interconnections within the Centaur vehicle, and emphasized the need for being able to follow the airborne returns into the launch site cabling and GSE. An effort was initiated to further assure that the final airborne hardware configurations adhered to the known and specified interconnection/isolation criteria represented on the grounding diagrams. Within a separate MGS unit, the relatively simple interconnection of returns with a minimum of sneak paths permitted straightforward specifications (zero or infinity) for applicable resistance measurements.

However, the vehicle harness interconnection of the MGS units provided a complex interconnection of returns, between which many sneak paths existed due to individual loads from one supply line utilizing different returns. The applicable checks of the MGS/Vehicle installation were, therefore, relegated to the determination of only gross discrepancies. The sneak paths were analyzed as a possible minimum shunt resistance of 27 ohms between "isolated" returns. The sneak paths contained non-linear elements which caused resistance measurements to be affected by the voltage and/or polarity of instrumentation. This resistance effectively appeared across the points where the isolation check was to be made. The result was that near-short circuit discrepancies were all that could be detected.

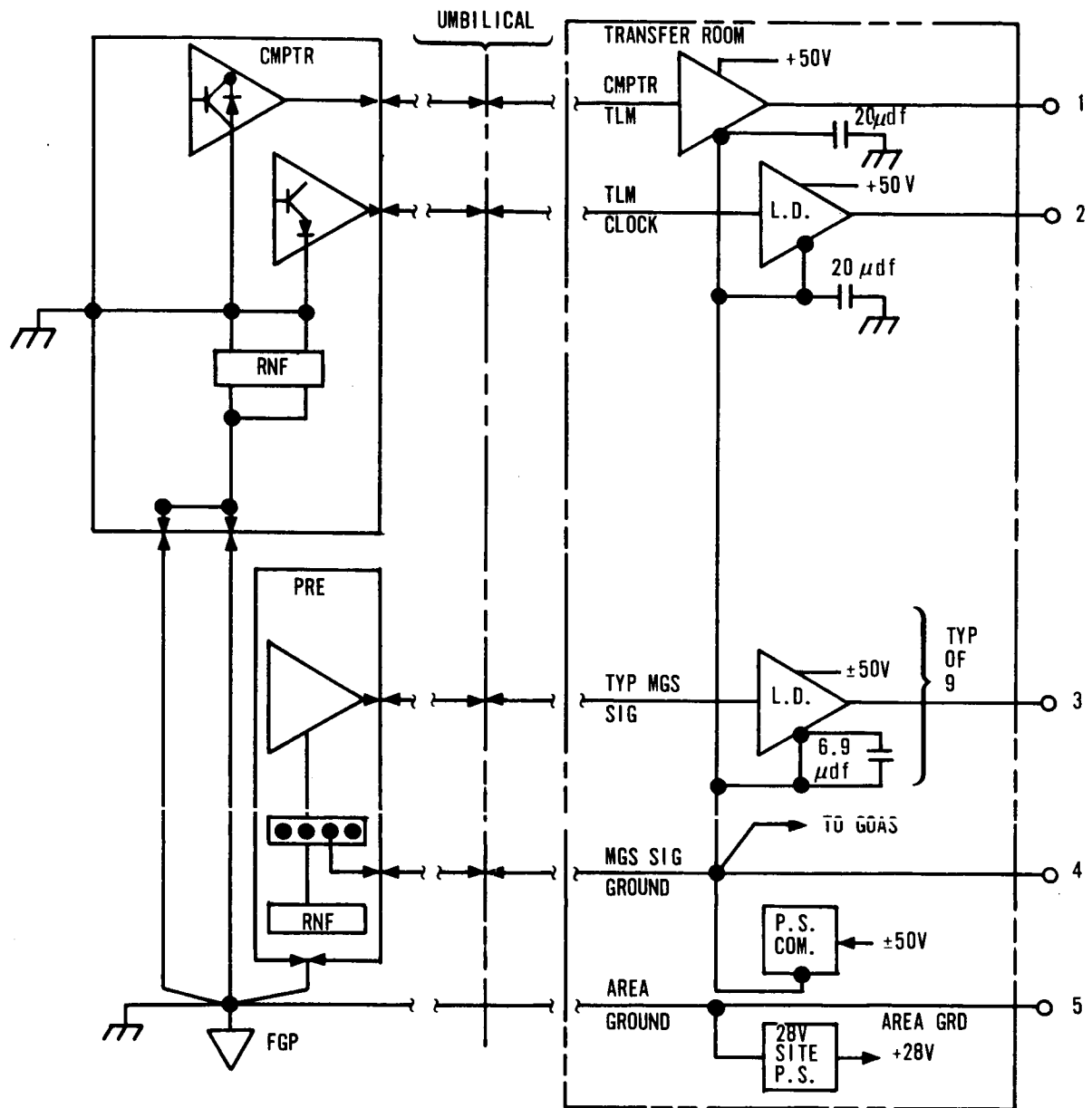
Further, the grounding diagrams for MGS units were utilized as a check against the Unit Acceptance Test (UAT) specifications for the guarantee of applicable continuity and isolation. In order to be meaningful, the associated resistance checks (particularly isolation) were made after the unit was fully assembled and pressurized.

6.14.3. Grounding/Return Problems. - The following paragraphs describe in detail some of the major problems encountered with grounds and/or signal returns in the Centaur IGS. The examples serve to illustrate the type of grounding and return problems which can be encountered in a guidance system, and are intended to stress the importance of maintaining grounding/return integrity during initial design and throughout the development or modification phases.

6.14.3.1. Computer to RL&R Communication. - The transmission of the CMPTR TLM and TLM CLOCK signals from the Computer to the Remote Load and Read Test Set (RL&R) has a considerable history of problems and interim fixes. The intended Honeywell philosophy regarding "ground loops", isolation of returns, return references, common impedances, shielding application, shielding termination and line filtering were compromised.

The problem was associated with several factors, which are listed below and depicted in Figure 6.14-1:

1. The Computer TLM and TLM CLOCK signals were referenced to Computer Chassis (Airframe) at the point of origin.
2. The only applicable airborne reference available for line drivers in the transfer room was MGS SIGNAL GROUND. Hence, all eleven drivers shared a common return. The eleven line drivers in the Transfer Room also shared common power supplies. The Computer TLM and TLM CLOCK channels operated from +50V dc (zener regulated to $\pm 30V$). The nine other channels operated from $\pm 50V$ dc. One $\pm 50V$ supply was utilized, another cause of common reference for the eleven drivers.
3. MGS SIGNAL GROUND reference for the Computer TLM and TLM CLOCK inputs to the line drivers placed the following voltage drops in series with these inputs:
 - The MGS SIGNAL GROUND lead from Transfer Room to Coupler carrying all eleven line driver input return currents and other applicable site and GSE return currents.
 - The series impedance of the Coupler RNF section in the 28VDC RETURN path carrying dc power return currents.
 - MGS 28 VDC RETURN lead from the Coupler to FGP, carrying dc power return currents.
 - The Airframe, from vehicle forward ground plate (FGP) to Computer chassis (in parallel with two conductors from FGP to the Computer carrying undefined currents).
4. The Computer TLM and TLM CLOCK signal return currents flowing through the MGS SIGNAL GROUND (TB2 in the Coupler) to FGP path caused undesirable digital noise modulation between



 DENOTES CHASSIS TIE POINT IN UNIT SHOWN

FIGURE 6.14-1. COMPUTER TO RL&R
SIGNAL COMMUNICATION LINK
(Sheet 1 of 2)

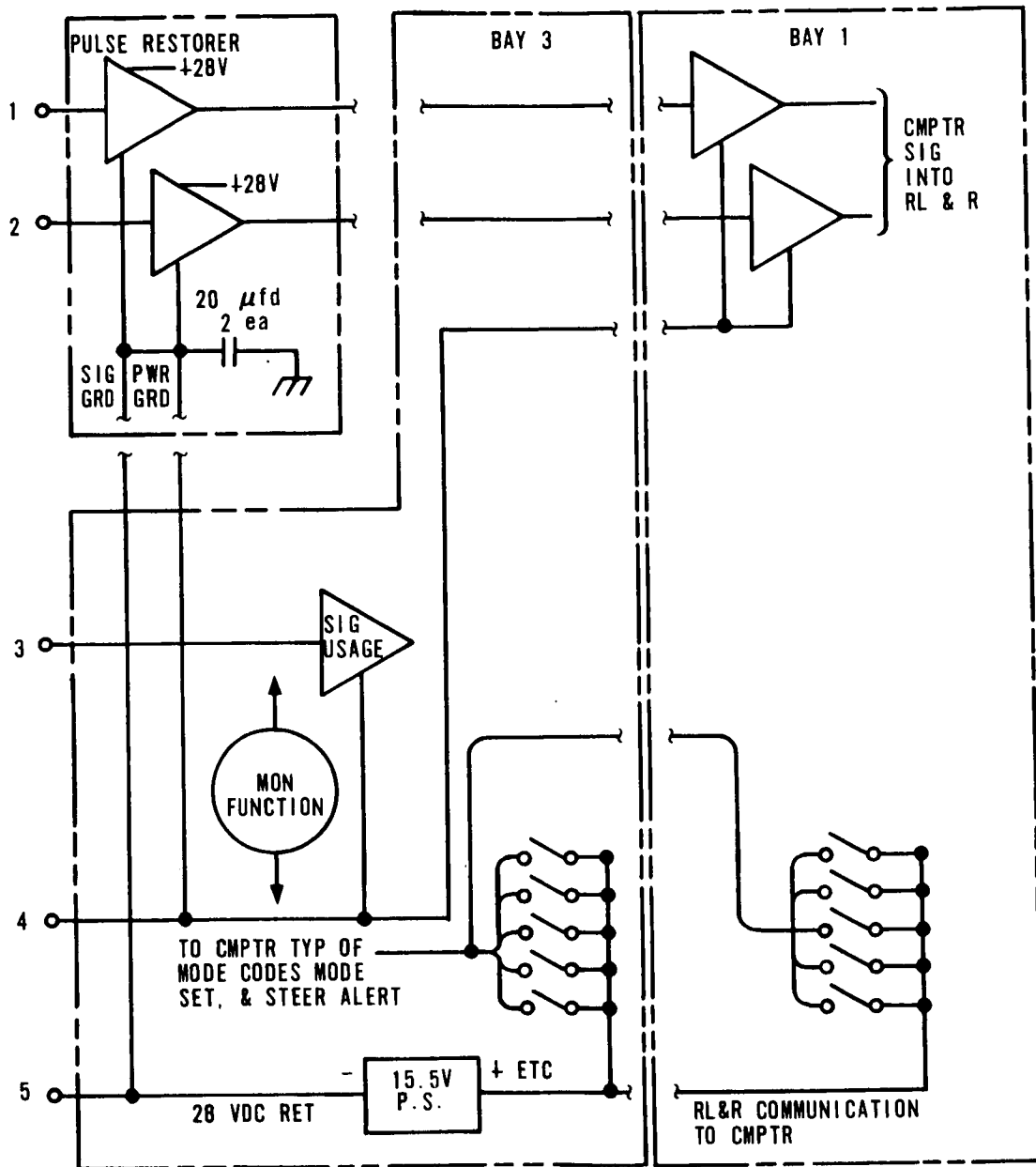


FIGURE 6.14-1. COMPUTER TO RL&R
SIGNAL COMMUNICATION LINK
(Sheet 2 of 2)

those two points prior to umbilical eject. (NOTE: Special current monitoring provisions in this return path during AC-7 Guidance-Autopilot tests showed digital noise currents until umbilical eject.) This digital noise, therefore, appears in series with all TLM system inputs from the MGS.

5. The relatively low input impedance of blockhouse Pulse Restorers in the Computer TLM and TLM CLOCK channels caused heavy signal currents to flow in the loop between these units and the aforementioned line drivers. The MGS SIGNAL GROUND lead being used as the single return path for these signal currents caused a large voltage drop to exist on a portion of the MGS SIGNAL GROUND line to the GSE. As a result, the effective digital noise on the other MGS-to-GSE signals referenced to MGS SIGNAL GROUND prevented normal GSE operation in this configuration. Also, the blockhouse Pulse Restorers were designed to be powered by +28 VDC. The circuitry is direct coupled, making Signal return and Power return common within the unit. The +28V dc Site Power was utilized resulting in referencing the Composite Pulse Restorer Return to Blockhouse 28V Return (or AREA GROUND).
6. The ac noise level between MGS SIGNAL GROUND (the line driver signal reference) and AREA GROUND (the Pulse Restorer reference) precluded proper operation of these units without also referencing the Pulse Restorers to MGS SIGNAL GROUND. This perpetrated a "ground loop" by interconnecting MGS SIGNAL GROUND to AREA GROUND, although they were already common at the one intended airborne point, the FGP.
7. The site "ground loop" caused a change in MGS airborne dc power return currents at umbilical eject. The associated umbilical line ejection, therefore, interrupted a current. In addition, the TLM offset of MGS signals was a function of current in the MGS 28V RETURN line and, therefore, changed at umbilical eject. Further, the site "ground loop" short circuited the RNF section in the MGS prime power interface 28V dc RETURN line to the FGP. This compromised the intended line filtering protection until umbilical eject.
8. The Honeywell GSE is intended to monitor and utilize signals with respect to the applicable airborne returns. MGS SIGNAL GROUND and other airborne returns are, therefore, intended to be brought

to the GSE as isolated, low current returns with current flow due only to IGS functions. The compromise of this aspect by the site "ground loop" caused offsets and anomalies in the associated effective inputs to the GSE. The offsets and anomalies were functions of Launch Complex phenomena that should have been entirely independent. This caused a known signal level at the MGS to produce different GSE "readings" from pad 36A to 36B, from Vehicle to Vehicle and as a function of complex activity.

The grounding problem was corrected by referencing the signal channels for Computer TLM and TLM CLOCK to area ground. This was accomplished by (1) providing a separate 50 volt power source for the associated isolation amplifier in the transfer room, and (2) providing 28 volt site power as the excitation source for the two associated pulse restorers in the blockhouse.

6.14.3.2. 400 Cycle Neutral Isolation in Computer. - The NAV Computer ac prime power return is common to the Computer chassis as is the Computer dc prime power returns and loads on both the ac and dc sources. In addition, some direct coupled Computer signal circuitry utilizes the prime 28V dc source. Hence, all associated signal returns are referenced to Computer chassis. This configuration still exists in the present Centaur MGS.

Several undesirable points of this situation are:

- a. The intermixing of Computer ac and dc power return currents in an impedance common with Computer signal returns unnecessarily compromises the signal-to-noise ratio.
- b. The intermixing of these same currents with undefined airframe currents allows common mode noise coupling between all computer returns.
- c. Return of the Computer ac load currents via airframe are an exception rather than the rule on the Centaur vehicle. The deletion of power currents, particularly ac currents, from airframe is very desirable in order to approach an equipotential airframe reference. With iZ drops in the airframe, the task of providing adequate shield references is made more difficult. The importance of this item is illustrated by the mandatory prevention of airframe power currents on some programs.

At one time in the -3 MGS, the Computer 400 Hz neutral was routed directly from the coupler to the computer, creating a ground loop through

the airframe via the computer chassis. This compromised the associated MGS conducted interference suppression provisions at the prime power interface. The ground loop was eliminated by routing the computer 400 Hz neutral directly from the computer to the vehicle ground plate. However, the isolation of 400 Hz neutral from computer chassis would still be desirable. This would then make possible the same conducted interference considerations for the computer NEUTRAL as is presently provided on the three phase lines. The phase lines are presently routed through the coupler and the associated RNF sections (and relay contacts) therein. Whatever the routing for phase lines, considerable advantage results from similar routing for Neutral. Since the routing for phase lines cannot be changed (for practical reasons), it would be desirable to route the computer NEUTRAL through the coupler also. The advantages of this provision would be:

1. Common routing of the neutral with the phase lines would result in a "quad". This would provide considerable improvement in vehicle harness between FGP and coupler, FGP and computer, and coupler and computer.
2. The lesser protection against conducted interference on the computer NEUTRAL line (due to not being routed through coupler filter section) results in a reduction of the effective protection on the three phase lines in the coupler. Consider the computer RNF schematic of Figure 6.14-2. The Neutral line is seen to be bypassed to each of the phase lines with the capacitive filter elements. A noise injection in series with the computer NEUTRAL line would, therefore, couple into the phase lines and be conducted back into the coupler. This situation would be eliminated by the subject re-routing whereas:
 - The effective conducted interference protection would be commensurate on all four ac power lines for both the computer and the remainder of the MGS.
 - The commonality of neutral in coupler and computer would alleviate the possibility of a noise injection in series with one and not the other.
 - The associated shielding and magnetic field cancellation within the vehicle harness would be greatly improved.

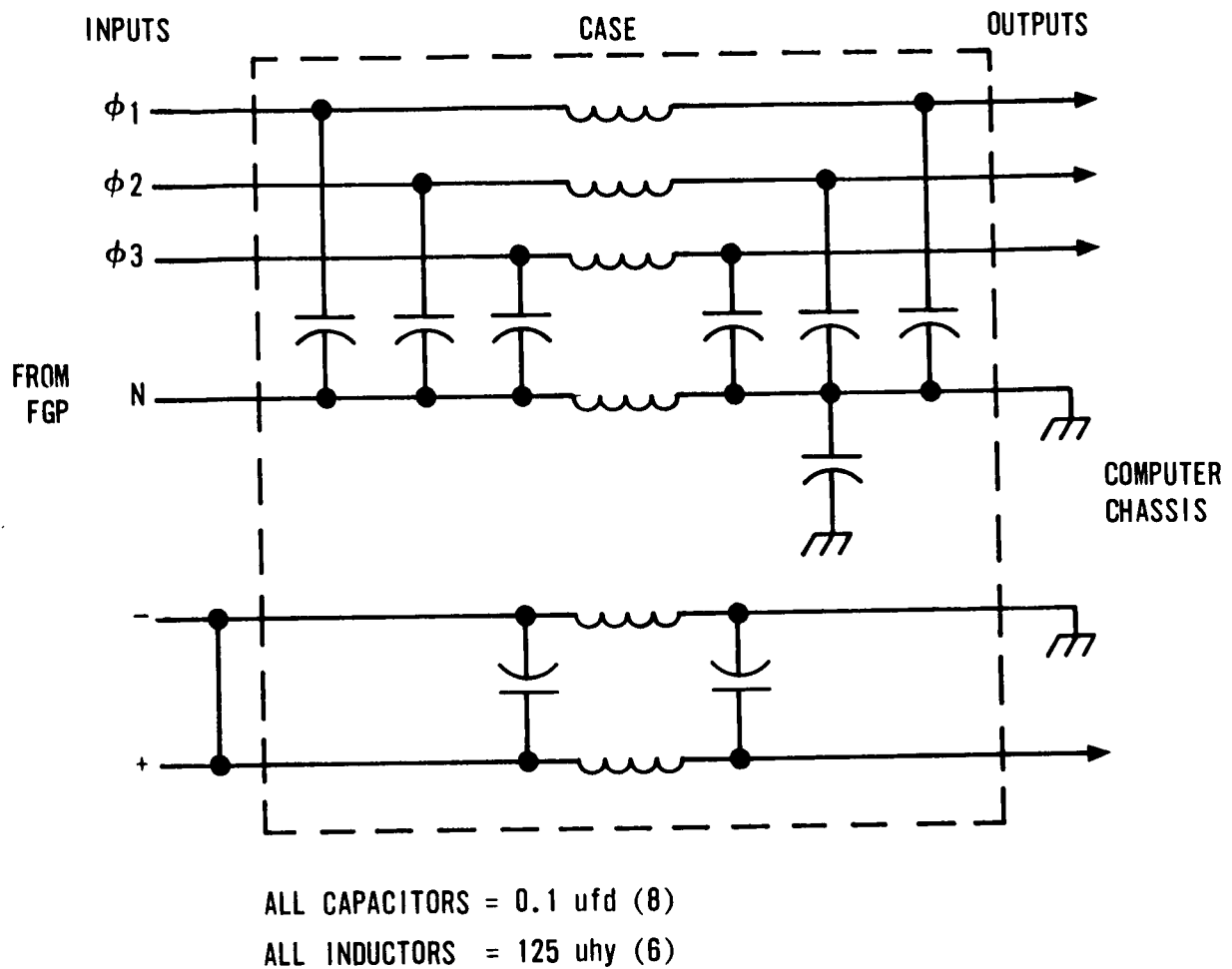


FIGURE 6.14-2. COMPUTER RADIO NOISE FILTER SCHEMATIC

6.14.3.3. Resolver Common Lines to GSE. - Another area of current concern is that the interconnection of the four RESOLVER COMMON lines at the airborne end and by pairs at the GSE end does not take full advantage of the existing cabling considerations of (1) four separate returns or (2) twisted pairs. See Figure 6.14-3 for a sketch of the subject returns from end to end. This area was a suspected cause of several unresolved anomalies of gimbal excursions or drive during coarse align at the launch complex in 1965-66.

With existing component limitations precluding complete isolation at either end, any method of providing more than one return lead per resolver channel will be an extravagance. The same limitations make providing any less than one return lead per channel a compromise.

The existing component limitations are:

- a. In the platform, the associated returns are separate at the resolvers but are interconnected due to slip-ring limitations. One unique resolver common line exists between the platform and platform electronics (PE). The resolver common is interconnected to +35V return (and hence MGS signal ground in the PE). The PE routes the associated G1 and G3 resolver Hi lines through switches and then to the GSE for the coarse align function. The equivalent G4 coarse align signals are, in addition, routed through band-pass amplifiers in the PE which are referenced to resolver common (also +35V return and MGS signal ground). The resolver common is not switched and fans out to four lines from the PE. The four resolver lines between PE and GSE are in four separate twisted pairs through site cabling. These pairs are associated only with G1 and G3 coarse align signals.

The "airborne end" limitations affecting coarse align return isolation are therefore in the platform exclusively from G1 and G3 and in the platform and PE for G4. The effect is that, at the airborne end, all resolver returns must be interconnected.

- b. In the GSE, the resolvers utilized for coarse align (in the ARU) have both stator winding returns interconnected internal to the component. The effect is that, at the GSE end, the two signals associated with each gimbal resolver must share a common reference.

0160-92A

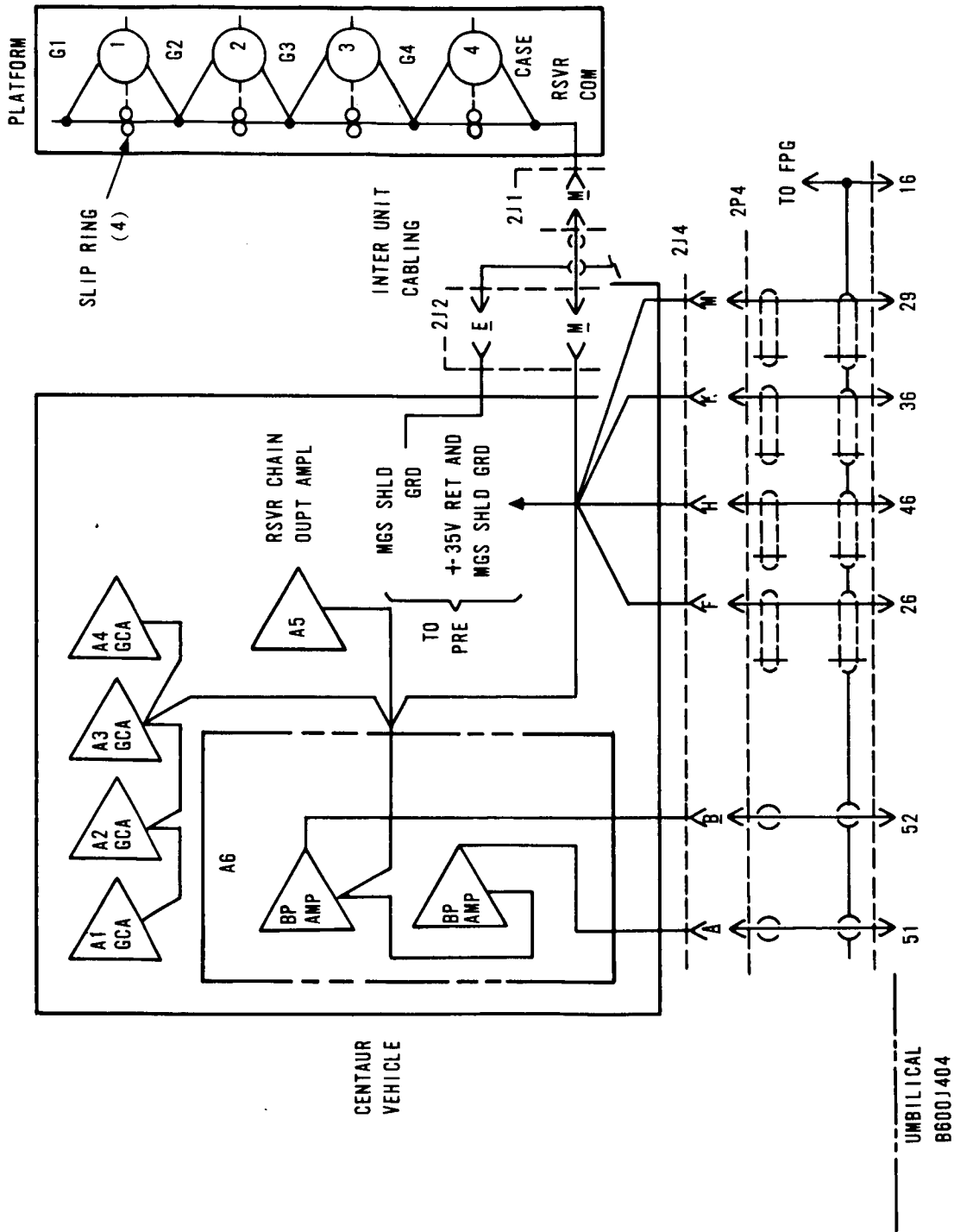


FIGURE 6.14-3. RESOLVER COMMON INTERCONNECTION
FROM PLATFORM TO ARU (Sheet 1 of 2)

0168-89A

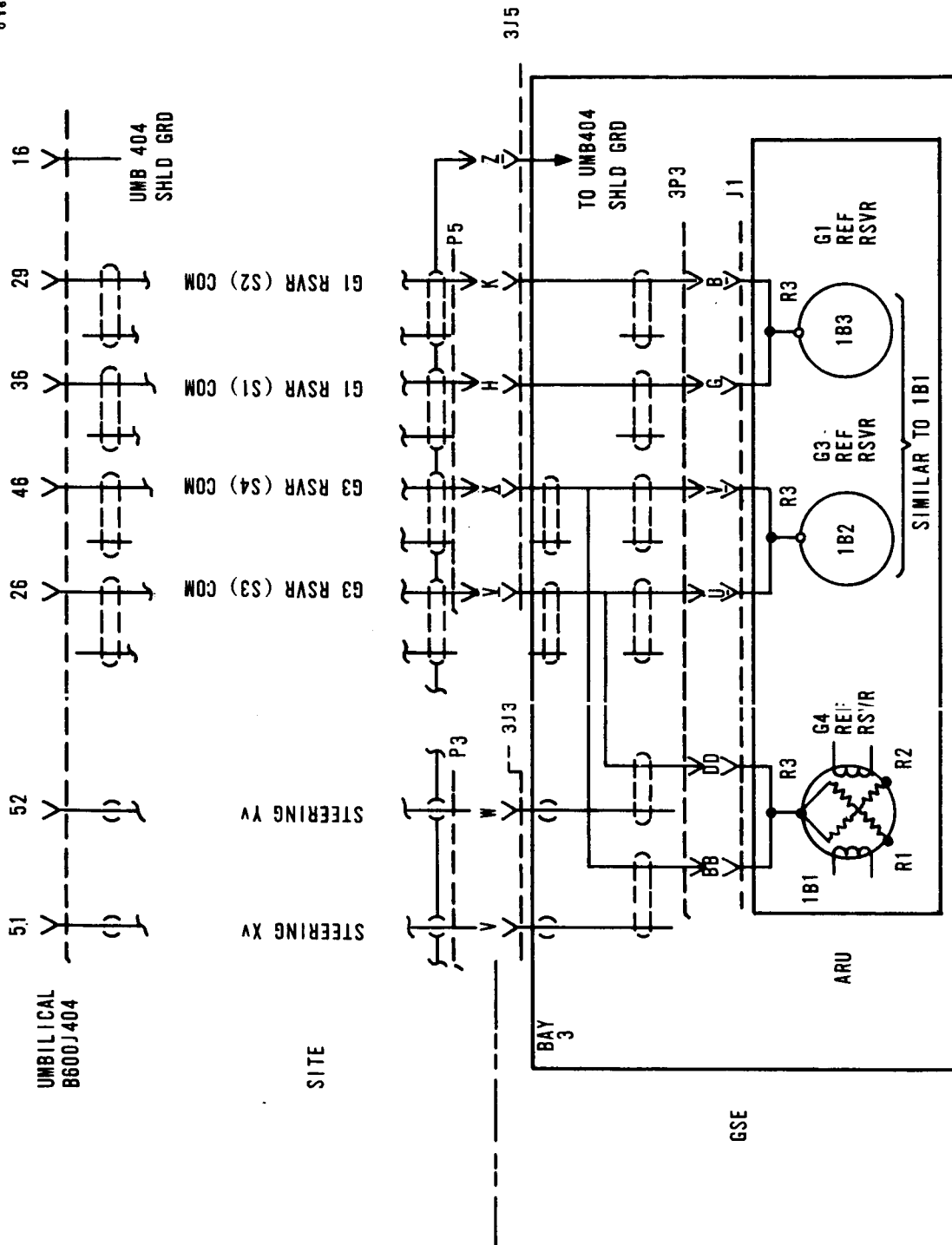


FIGURE 6.14-3. RESOLVER COMMON INTERCONNECTION FROM PLATFORM TO ARU (Sheet 2 of 2)

The optimum solution to the situation appears to be isolation of the GSE resolver windings and provision of 6 twisted pairs that have returns interconnected only in the airborne hardware. This eliminates the associated ground loops entirely. This approach is also the most costly and, therefore, tradeoffs must be considered.

The next most advantageous solution appears to be isolation by resolver channels, e. g., the three (G1, G3, and G4) returns individually isolated. If the use of twisted pairs is continued, this will require that the two individually shielded lines presently in use for Steering Monitor Xv and Yv (also serving as the G4 coarse align signal) be replaced by twisted pairs from end to end. This isolates effective ground loops to individual resolver channels. This approach is also costly, requiring vehicle and site cabling modifications as well as GSE wiring changes. The airborne end may share a common PE connector pin for the resolver channels.

An extension of the previous approach would be to effect isolation by resolver channels and utilize twisted triads for each. An investigation of crosstalk limitations would be required to determine the necessity for individually shielding the Hi lines within the triad or if an overall shield will suffice.

An important factor in considering leaving the status quo is the relative gains of the coarse align loops with respect to the noise immunity provisions. Whereas G4 is the highest gain coarse align loop, the G4 and G3 reference resolvers (GSE) share returns. G1 and G3 coarse align loop gains are nearly the same, yet G1 has better noise immunity with respect to return impedances.

6.14.3.4. Delta V Return Loop. - The delta V Return between Signal Conditioner and Coupler presently causes a "ground loop". A sketch of the associated wiring is presented in Figure 6.14-4. In the past, this circuit area (signal conditioner) has experienced noise problems or "false triggering" in isolated instances. Associated switching noise also exists on the other signal conditioner channels that share the same return(s). These two phenomena are, at least in part, a result of the subject return loop. The logical solution is to isolate the so-called "delta V Return" at the Coupler end. This is readily done by collectively isolating the six transformer secondaries that are associated with the signal conditioner (reference Figure 6.14-4).

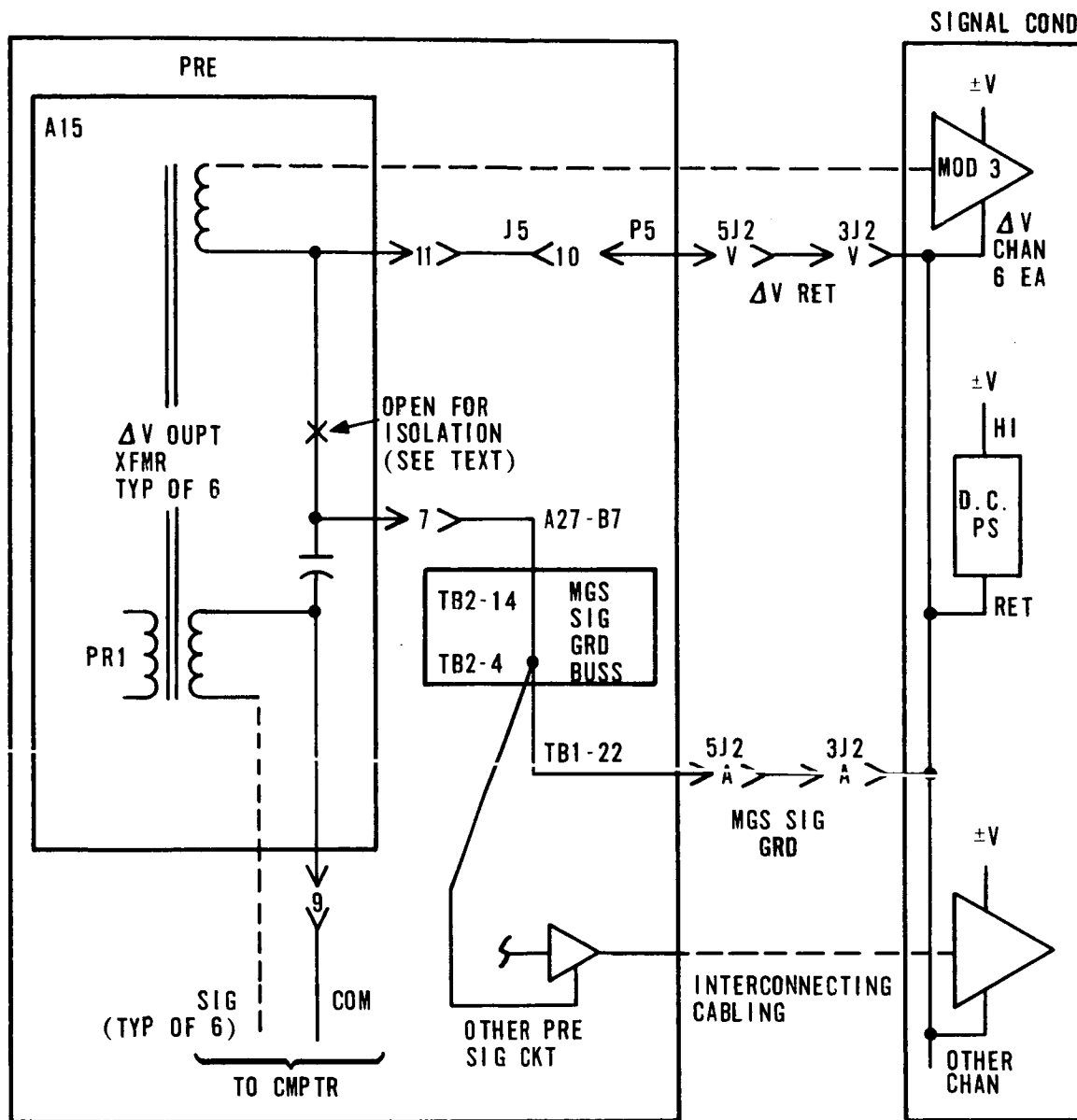


FIGURE 6.14-4. DELTA V COMPATIBILITY AND AN ASSOCIATED GROUND LOOP

The solution would fully isolate the return currents associated with signal conditioned delta V pulses to the Delta V Return lead, providing the following advantages:

- a. The Delta V pulse signal inputs to the SC would not have the present noise injection due to common impedance with other signal inputs to SC.
- b. All SC input pulse return currents would be deleted from the return associated with nonpulse signals within the SC.

The subject "ground loop" is inter-related with several past problem causes and solutions. The problems have been in the compatibility of SC and computer delta V circuitry that share a common transformer source in the Coupler. Crosstalk between the two signal paths has been detrimental due to:

1. Insufficient noise immunity in the applicable SC channels.
2. Improper signal termination in the computer resulting in a delayed signal reflection of appreciable magnitude.
3. Mutual coupling between the two signal windings on a common transformer in the Coupler.

The interim solutions to related past problems have been limited to the Coupler delta V output module, which is the source of the signals. Such solutions have not been effective in fully eliminating the compatibility problem. The present degree of compatibility is apparently somewhat dependent on the subject "ground loop". This is a case where two (or more) "wrongs" may be resulting in a "right". The right, however, is with respect to the specific problem area; whereas the "ground loop" (a wrong) has detrimental effects that are widespread.

The history of this grounding problem indicates that two factors have resulted in the associated grounding compromises; e. g., (1) grounding considerations have received low priority in trade-off studies, and (2) the limited hardware area in which a fix was permissible did not include two major causes of the problem. The rectification of the "grounding compromises" require consideration of the total problem.

6.14.3.5. Line Filtering Applied to MGS Signal Ground. - The "line" filtering presently applied to MGS SIGNAL GROUND at two places external to Honeywell hardware is in conflict with the Honeywell concepts of:

1. Line filtering.
2. AC and dc isolation of returns.
3. Sharing of common return for many signals.

Undesirable shunt capacitance "line" filters exist in some Transfer Room line drivers and in the Limit Cycle Monitor (LCM) panel in the Blockhouse at the launch complex.

Each of these applications utilize the filtering to the possible advantage of the local circuitry without regard to the undesirable effects upon other signal usage sharing that particular return. The possible advantage to local circuitry is in placing the local signal return at a lower noise potential with respect to the chassis or enclosure (shielding medium). The disadvantage is to the same circuitry and to other critical circuitry that would at best utilize a return of the same isolation, noise level, and hence, filtering as for the signal Hi.

The high capacity component values utilized in the subject filters oppose the usual concept of "line" filtering. The values indicate the use of bypass capacitors which exhibit self-resonance at low RF frequencies. They typically are ineffective to frequencies above resonance. The usual low pass line filter characteristic is not present.

The use of polarized capacitors in several of the subject locations is a serious shortcoming. There is no specification, control or guarantee of a specific polarity or magnitude of the potential between MGS SIGNAL GROUND and chassis (or area ground) at any of the locations. The polarized capacitors may, therefore, be acting as diodes, thereby further compromising the intended dc isolation of MGS SIGNAL GROUND. More important, is the fact that the polarity may change with the installation (pad, vehicle, etc.) or the operation thereof. One of the more significant operations that most certainly affects the potential at any of the subject locations is vehicle power changeover. The AC-7 data indicates a switching of approximately 68 amperes dc at that time. The associated change in IR drops in site return wiring may be sufficient to cause a radical change in the equivalent circuit for the subject filters. This phenomena may be partially responsible for past anomalies noted at power changeover.

The dc isolation of MGS Signal Ground is violated by the physical resistors in the LCM. In addition, the leakage current of such a grand total capacity is, in effect, a significantly low resistance.

The Honeywell GSE utilizes MGS Signal Ground as a common return for some monitoring functions, and for some operational signals. The associated signals have both ac and dc characteristics. For the ac characteristics, the return should be at the same relative noise level as the signal Hi. Balanced line filtering or signal filtering are the only ways to

accomplish this. The need for heavily bypassing a signal return to chassis implies that less noise is present between signal Hi and chassis than between signal Hi and the signal return. For ac signal characteristics, this means that the use of a separate, heavily bypassed signal return is superfluous.

For the dc characteristics, the return IR drop must be kept negligible with regard to accuracy or usability of the most critical dc signal characteristic. Where selection of monitoring functions or signal usage can be made, a minimization of associated return currents can be effected during critical operations. Permanent monitors, and signal/line filters that are hardwired cause continuous return currents that can present serious limitations to utilization of ac or dc signal characteristics. The ability to delete the requirement of dc isolation of such a return implies that a smaller, or a better defined IR drop is present on some other local return. For dc signal characteristics, this means the use of a separate non-isolated signal return is superfluous.

In summary, either the subject filtering or the associated separate return is not needed in those circuit areas. The sharing of the return with other critical signal functions is the limiting factor.

6.14.3.6. Interdependence of MGS Signal Ground and MGS 28 V Return. - Some MGS electronic signal circuitry utilizes 28V dc prime power. Without isolation, this circuitry must share a common signal reference with essentially all other MGS circuitry. This has resulted in MGS Signal Ground being interconnected to the dc prime power source via the 28V dc Return. The associated vehicle dc prime power source is "single point" connected to the Vehicle airframe at the Forward Ground Plate (FGP).

Although an extension of this "single point" return interconnection criteria is not utilized by some airborne systems or hardware, it is a necessity for the MGS. This stems from the series of evolutionary restrictions that cause the interconnection of critical signal returns with prime power and vehicle airframe at a point remote from the MGS.

Both the high and low sides of ac and dc prime power should, therefore, be treated as "Hot" lines. MGS signal returns should also be treated as "Hot" lines within the MGS and GSE. This criteria is intended to be imposed on any site or test configuration cabling and at any interfacing system.

Although not presently practical, it would be a great advantage to the MGS to be able to reference the critical signal returns, in fact, all signal returns, to a local "single point" on the airframe. The location of the point should be in the area of the most critical signal circuitry referenced to (or interconnected by) that return "tree". The main advantage is a vast improvement in shielding effectiveness when enclosures and structure are at essentially the same noise level as the signal return. This also implies greater shielded effectiveness of conductor shields by making practical the termination to chassis and possibly the termination at both ends. The impracticality of implementing such a change lies in the present great interdependence of signal references and dc prime power return.

One problem encountered in the -3 and Phase II PIP systems which was caused by the interaction of MGS Signal Ground and MGS 28 volt return (signal reference sharing) concerned certain MGS telemetry output signals. Demodulated ac signals to telemetry are biased at 2.5 volts (which represents a zero signal output) and provides a means of determining signal polarity. Upon installation of the MGS on the vehicle, an offset from the original 2.5 volt bias point was noted; e. g., 2.5 volts no longer represented zero signal output. Hence, this offset gave an indication of an apparent signal output when in fact no signal was present.

6.14.4. Honeywell Grounding Philosophy. - In general, the prime considerations of the Honeywell grounding philosophy are:

1. The flight configuration is the ultimate proof of compatibility and performance of the MGS.
2. The launch complex and other test configurations should not be more restrictive on airborne hardware design than the flight configuration.
3. Other test configurations should duplicate or simulate the launch configuration insofar as the necessary (or existing) hardware permits.

Therefore, for each pertinent aspect, the concern should be first for the vehicle installation, second for the launch configuration, and third, for other test configurations. This grounding philosophy was phased into the later stages of IGS development, but it is being designed in "from the start" for the IMG.

The grounding, bonding, shielding, filtering, return interconnection and related design aspects are covered in detail in the following paragraphs.

6.14.4.1. Single Point Return Interconnection. - Honeywell subscribes to the "single point" philosophy of return interconnection. This is considered to be the most applicable method of maintaining return paths, currents, noise levels and impedances that are definable in terms of specific MGS (or IGS) parameters and not those of other systems. This is a basic method of maintaining the necessary integrity of complex "ground trees" that interconnect many critical signal areas. Integrity is necessary in terms of performance parameters which may be degraded by extraneous noise or common mode currents.

The intent of single-point interconnection is: (1) to be able to define a unique return path from load to source and (2) to define the common impedances and current flow therein caused by other loads and sources that must be interconnected.

6.14.4.2. Return References. - A unique return path (reference) for a given current from load to source should be established. Where several sources must share a common reference, the mixing of return currents should be prevented (or minimized) beyond the "single point" of interconnection. This is of particular importance for system interface returns, of which prime power returns are the most critical. Prime power returns (all power lines) always have unique interference control goals or requirements which are specified on a per-line test basis. The intermixing of power return currents would unnecessarily extend the conducted interference and susceptibility problems into hardware areas that should be independent. Signal returns have many of the same basic problems.

The Centaur vehicle "single point" interconnection of airframe, ac return and dc return associated with the MGS is the forward ground plate (FGP) which is external to the MGS. This requires separate MGS return lines to establish the unique return paths. All incoming power lines that are "ungrounded" within the MGS are subject to the applicable interference control goals or requirements. The result is, radio noise filter (RNF) sections are necessary on the ac and dc return lines (as well as all other power lines). This aspect places series impedances in each line. Considering the reference of a load (or monitor function) to the wrong power return branch, the iZ drop of one or both RNF sections may appear in series. A necessity for the one purpose therefore becomes a detriment to those signals referenced to the wrong return.

Once the unique return path is established, adjacent routing of the signal H_i and return can significantly decrease undesired electrostatic and particularly electromagnetic coupling. This promotes (or makes

practical) the twisting of the Hi and return lines for a given signal or power distribution. The full advantage of twisting (to reduce coupled energy to and/or from the lines) cannot be gained unless the net current in the twisted conductors is zero. The practice of twisting a group of lines with a shared common conductor is an extension of this concept. This may eliminate the need for shielding the subject leads. If needed, however, an overall shield on the twisted pair or group may suffice and result in considerable savings in weight and ease of build. For a group of leads, "crosstalk" may be a problem limiting the simple overall shielding approach, and individual shields are necessary. The twisting of a group of individually shielded leads is still practical provided the individual shields are not terminated at both ends (forming a loop via shield return outside the twisted group).

6.14.4.3. Ground Loops. - Inherent in the application of the "single point" return interconnection scheme is the prevention of ground loops. The intent is to prevent multiple return paths for a specific return current. One deleterious effect due to multiple paths is related to the magnitude of current flow, the area of the loop and the degree of coupling to other lines or circuits. The loop acts as a one turn transformer winding that can inductively couple energy to and/or from itself. Therefore, when the need for more "copper" dictates the use of two return lines, certain precautions must be taken to avoid an effective ground loop. The lines should be identical in origination point, destination point, routing, length, wire type, should be twisted together, and appear on adjacent connector pins.

A second harmful effect of ground loops is the complication of common impedances (and currents therein) shared with other circuits, assemblies, or systems. This results in interaction of otherwise independent functions, and presents a situation that defies analysis for a complex "ground tree" containing many time dependent return currents. A problem associated with such a situation may be very difficult or impossible to reproduce by controlled testing.

Shield terminations are a prevalent source of ground loops. In general, the full RF range of shielded effectiveness necessary for interference control to a typical specification requires conductor shield termination at both ends. For the same reason, termination must be of short "electrical length" to the reference ground plane (airframe, enclosure, chassis, etc.). Short "electrical length" in the KMc range is, by rule of thumb, less than three inches. Where such termination (both ends to chassis) is practical in terms of the enclosed signal, certain precautions must be imposed to

avoid an effective ground loop. This can be done by dressing the conductors close to structure and not threading susceptible or interfering signal leads through the loop formed by the shield and airframe. Actually, the interconnection of two points of structure by a shield (or conductor) is no more of a ground loop than is the several structural paths between two points. The same considerations of "loop" current, area and degrees of coupling apply as previously explained.

The termination of both ends of a shield to other than chassis is not desirable. Such termination implies a conductor between the two ends. The futility of terminating the far end of a shield via a conductor that approaches the "electrical length" of the shield can be readily understood.

6.14.4.4. Bonding. - The bonding of equipment has the following purposes:

1. Protect personnel from shock hazard.
2. Prevent the development of RF potentials.
3. Provide fault-current return paths.
4. Prevent the accumulation of static charge.
5. Provide the RF conductivity necessary to maintain the required shielded effectiveness.

Bonding of all major internal and all external metal parts of enclosures together and to the airframe (or area ground) should be provided. The metal structural parts of all enclosures should be bonded together by contact surfaces of sufficient conductivity, area, and contact pressure.

Enclosures to Structure. - The bonding of enclosures to structure is best accomplished by a strap between two specially designed bonding areas. The reasons behind the choice of a strap over utilization of the mounting surface(s) are:

1. Three of the five (or six) MGS units are vibration isolated, making some type of jumper necessary.
2. The Vehicle Airframe carries signal and power return currents which would be precluded from flowing through the MGS enclosures by single point bonding.
3. It is difficult to guarantee smooth and clean mounting surfaces at time of installation. They cannot be inspected or cleaned with the equipment installed.
4. Mounting surfaces tend to shift or creep during shock, vibration, or temperature change.

The desired enclosure bonding provisions should be: (based on MIL-B-5087)

1. Provide clean conductive bonding surfaces.
2. The surfaces shall be independent of hold-down or structural integrity provisions.
3. The location of the surfaces shall be chosen so as to minimize bonding strap length (and provide for sufficient flexibility on isolated units).
4. The strap length-to-width ratio shall not exceed 5 to 1.
5. The strap shall be solid copper (plated if necessary) and a minimum of 0.025 inch thick.
6. The bonding surface area at either end shall be the strap width squared as a minimum.
7. The strap end fastener hardware and installation (cleaning and torquing) procedures shall be specified in the applicable document.
8. The strap and hardware shall apply sufficient and uniform pressure over the entire bonding surface.

Enclosure to Enclosure. - Of particular interest is the RF conductivity between MGS enclosures and from each MGS enclosure to the homogeneous vehicle structure. Means of specification for applicable parameters are desirable. The areas of concern are: (1) the mounting shelf conductivity and (2) the bonding of vehicle structural components in series (such as Platform mounting ring).

External "Skin". - The necessity for bonding between the external parts making up the "skin" of an enclosure is governed by the requirement for "case shielding". This requirement necessitates a continuous bond along all "skin" seams and joints. This aspect is covered in a separate paragraph under that title.

Internal Parts. - The bonding together of internal structural metal parts of unit enclosures is best accomplished by conductive mating surfaces. This requires the removal of any non-conductive finish such as paint or anodize. Where surface protection is an overriding factor, spot facing under fasteners in combination with wire jumpers or straps can provide effective continuity. A requirement for bonding to establish a shielded compartment within the enclosure would be handled the same as for "case shielding".

6.14.4.5. Shielding. - The basic philosophy of shielding application is to reduce the emanations from "noise" sources and to raise the susceptibility thresholds of critical areas, thereby effecting compatibility. Shielding will be considered in two categories: (1) case shielding as supplied by unit (or assembly) enclosures, and (2) conductor shielding as provided by sheaths enclosing one or more conductors.

The purpose of shielding is to suitably reduce the transfer of radiated electromagnetic energy to or from the enclosed assembly or conductor(s). Tests and control of radiated interference and susceptibility are based on signal reception and generation with respect to a "ground plane". This ground plane represents the vehicle airframe to which the hardware unit enclosures are bonded. The test requirements are a reasonable simulation of the actual radiation environment on the vehicle, and hence the control measures must be applicable. Therefore, any shielded effectiveness to prevent the transfer of such radiated energy must be with respect to the same reference, vehicle airframe.

The amount of shielding should be minimized by use only where necessary to provide a safe margin of compatibility with a reasonable external environment and the adjacent internal signals or circuits and their interference/susceptibility characteristics.

Reducing the amount of required shielding should be a goal. Several means of accomplishing this goal are listed below:

1. Minimize the level (amplitude and/or power) of the required signal characteristics for interference reduction purposes.
2. Reduce or eliminate the non-required or extraneous signal characteristics for interference reduction purposes.
3. Lower the impedance levels of signal lines for improved susceptibility thresholds.
4. Minimize the fan-out or distribution of signal lines having critical interference and/or susceptibility characteristics. Therefore, attempt to limit critical lines to within one unit and minimize the number of interface signals.
5. Provide common-mode noise rejection, where applicable, to prevent critical shielding problems. Utilize balanced signal lines and/or twisted pairs for critical signals.

6. By layout planning, take advantage of spatial separation for potentially incompatible signals, circuits or assemblies. Establish routing and lead dressing criteria to reduce the variance in "crosstalk" coupling characteristics from one system to the next.
7. Replace several shields with one overall cable (or group) shield where the application is for compatibility with the external environment rather than for the reduction of crosstalk within the cable.
8. Take advantage of shielding that can be provided by structure rather than complicated or rigidly controlled conductor shields. Utilize structure, unit enclosures, channels, assembly cases, or compartments for this purpose.

Case Shielding. - From the standpoint of the enclosed hardware, the enclosure protects against susceptibility to radiation from external sources and prevents radiation of interference to external hardware. As previously noted, this dictates that the enclosure(s) be RF tight and bonded with a low RF impedance to the reference point for the RF energy; i. e., the airframe.

In general, the required case shielding is provided by the proper material/thickness combination to supply an inherent shielded effectiveness (of penetrative plus reflective losses) over the frequency range of interest. The inherent shielded effectiveness is realized only if no discontinuities (leakage) exist in the case. Seams, joints, access holes, ventilation openings, etc., tend to reduce the shielded effectiveness of a practical enclosure. Therefore, maintaining the required shielded effectiveness necessitates sufficient electrical continuity along all seams or joints and reduction of effective size of holes, openings, or length of poor (or no) contact along seams.

The unit enclosures shall provide a shielded effectiveness that is sufficient to reduce the applicable transfer of radiated electromagnetic energy and thereby provide compatibility with that aspect of the environment. As a goal, 80 db of shielded effectiveness should be provided over the range of 150 kHz to 1g Hz.

In practice, the above goal means a minimum enclosure "skin" thickness for aluminum, magnesium, or stainless steel of 0.08, 0.10, or 0.014 inch, respectively. The size and number of uncovered (unshielded) openings should be minimized with the largest cross dimension 0.5 inch maximum. Minimizing the discontinuities at seams, joints or access

plates can be accomplished with welding, appropriate screw or rivet spacing, sufficient overlap and/or conductive mesh gasketing. The shielded effectiveness of ventilation or optical access holes can be assured by proper use of honeycomb (waveguide tubes) conductive glass or wire screening.

Conductive Shields. - From the standpoint of the enclosed signal(s), the conductor shields prevent crosstalk, protect against susceptibility to radiation from external sources and prevent radiation of interference to external hardware. As previously noted, the optimum shield termination for the RF spectrum is to the referenced point for the RF energy; i. e., the airframe.

In general, applicable conductor shielding practices involve the use of braided sheaths. These sheaths generally provide 90 to 95 percent area coverage and are conductive but non-ferrous. As such, the inherent maximum shielded effectiveness is:

1. Limited by area coverage consideration.
2. Applicable to electrostatic fields rather than magnetic fields.
3. Varies with frequency in that low frequencies are generally associated with low impedance fields which are predominantly magnetic, high frequencies are generally associated with high impedance fields which are predominantly electrostatic.
4. Dependent on the segmented lengths of the shielded conductor.
5. Dependent on termination criteria for each shield segment; i. e., at one or both ends, and the worst case "electrical length" from any point thereon to the equipotential surface.
6. A realizable maximum of 50 to 55 db (for a single layer) at 150 Hz, reducing to zero at some higher frequency determined by segment length and termination criteria.

Shield Currents. - In no instance, is line shielding intended to carry current below 150 kHz. This does not preclude the use of shielding on either ac or dc power circuits where necessary to control radiated energy transfer.

Shield Isolation. - Each line shield, group shield, or overall cable shield is intended to be insulated from all other cable shields except at the end point or points where termination is specified.

Shield Termination. - A rule of thumb is that RF sensitive signal (intentional signal frequency spectrum above 150 kHz) shields require termination at both ends, and AF sensitive signal (intentional signal frequency spectrum below 150 kHz) shields require termination at only one end. This is based on the degrading effect of the shielding medium on the enclosed signal. It happens that these criteria are optimum to reduce radiated energy transfer (to and from) an enclosed RF lead but are a serious compromise for AF leads. Since interference control aspects include effective limitations on allowable radiated (and conducted) energy transfer to and from an equipment both above and below 150 kHz, an incompatibility exists with such shielding techniques.

The "one and only" termination for AF signal shields is usually necessary due to the detrimental effect of shield currents if termination were made at both ends. The shield currents may be a result of the difference in potential between the two points of termination and induced magnetic flux linking the loop formed by shield and return between ends.

The detrimental effect is usually evidenced by the coupling of AF noise currents onto the inner conductor. The noise, in most cases, falls within the signal frequency spectrum.

Application. - The application of a shield on a conductor must first consider the enclosed signal to shield compatibility and second the compatibility of the shielded signal to external environment. Therefore, an AF sensitive signal may require shield termination at only one end for signal to shield compatibility but requires additional reduction of radiated energy transfer to be compatible with the external environment. A prevalent example of this situation is for square wave or pulse signals where the repetition rate is in the AF range and the required waveshape characteristics (rise and fall times) contain spectrum components well into the RF range. The associated circuitry must, therefore, have response spanning portions of the AF and RF ranges. The complete solution to such a compatibility problem is to specify two layers of separate and isolated shields on the applicable conductors. The inner shield (for AF compatibility) should be terminated only at one end to a return of sufficiently low noise with respect to the enclosed signal reference. The outer shield (for RF compatibility) should be terminated at both ends to chassis, enclosure, airframe or area ground. This is where the "shielded system" (see later paragraph) approach pays off in the reduction of complicated shield requirements.

Termination Practices. - Conductor shield termination practices shall be limited by the following criteria:

1. Specify a given shield segment termination to maximize the reduction of electromagnetic radiation consistent with the limitations on enclosed signal degradation by extraneous noise coupling due to shield currents or via conductor-to-shield capacitance. That is, wherever possible, specify:
 - Termination of both ends of each segment of shield.
 - Terminate shortly and directly to enclosure (chassis). As a goal, less than three inches in length.
2. Whenever the critical nature of the enclosed signal precludes the above, specify:
 - Termination of only one end where detrimental shield current flow would be caused by the difference in potential of the two termination points, or by magnetic flux changes linking the associated shield/return loop.
 - Termination to a return of sufficiently low noise with respect to the enclosed signal reference. Minimize the "electrical length" of the return point with respect to the enclosure (chassis).
3. Whenever the criteria of (2) above provides insufficient reduction of radiated energy transfer, an additional shield is required. Then, a second shield, outside of the first and electrically isolated therefrom, shall be specified. Termination of this shield shall be in accordance with (1) above.
4. Conductor shields should carry no signal or power return currents. Conversely, the two ends of a shield should not be terminated to points between which signal or power currents flow. For this purpose, enclosures, chassis and/or airframe are considered an equipotential surface.

NOTE: One exception which should permit current flow in the shield would be a coaxial transmission line properly driven and loaded by the characteristic impedance.

Overall Cable Shields. - A special case of conductor shields is a shield enclosing a complete cable. In the "shielded system" concept (see later paragraph), an overall cable shield may be the practical way to extend the shielded effectiveness from one unit enclosure to another. This is of particular advantage as a replacement for many individual shields whose major purpose would be to provide compatibility with the external environment rather than crosstalk within the cable. In such case, one overall shield may replace many separate ones resulting in a reduction of weight, volume, and wiring complexity. The overall shield may also eliminate the need for suppression of all or part of the extraneous waveform characteristics of the associated signals.

A practical advantage of overall cable shields is that special RF tight end termination hardware is available. Proper usage of such hardware can provide a shielded effectiveness that could only be duplicated (on an individual conductor shield basis) by all coaxial connector pins or equivalent separate (BNC type) connectors. The lengths of unshielded conduction, and associated leakage at shield termination, are thereby eliminated.

The aforementioned cable sheath termination hardware attaches to the cable end connector and provides contact with the braid around the complete circumference. Sheath termination is, therefore, to the enclosure via the mating contact of connector shells.

NOTE: An overall shield must be provided with an insulating jacket to prevent inadvertent or intermittent contact with metal objects and/or structure. Also, where a two-layer shield is specified, the advantage of additional reflective losses may be gained by insulating the two layers except at the ends.

Current Flow in Shields and Enclosures. - No power or signal return currents should flow in conductor shields on conductors nor in enclosures, chassis, airframe or structure. Shielding or structure should carry only shielding currents.

A special case of the above is present for coaxial cables, carrying RF signals (above 150 kHz). The coax may then be driven and terminated by the characteristic impedance and thereby the outside conductor or shield becomes the return. In this case, connecting the return to airframe or area ground at both ends is an accepted practice. The maximum practical distances between such references for the return/shield is dependent on the enclosed signal frequency, the standing wave ratio, and the critical nature of the environment.

RF filters are a special case where shunt filter currents are caused to flow via enclosures and structure back to the source of the filtered energy. RF filters, properly applied, provide an insertion loss with respect to the enclosure or "barrier" through which the filtered line must pass. This is because all incident RF energy is assumed to be referenced to the "ground plane", of which the enclosure becomes a part through bonding. The RF susceptibility test methods utilize the assumed reference criteria. Therefore, for ac lines, a reactive power frequency filter return current will be caused to flow in the enclosure if the return is also referenced to the "ground plane". For three phase balanced lines (and balanced filter), this effective current cancels out. In any case, the subject current is small or may be sufficiently limited by filter design.

6.14.4.6. Filtering. - Filtering will be considered in two categories: (1) Signal filtering as applied from hi to low of the lines across which the signal appears and; (2) Line filtering as applied from the line to chassis or enclosure.

Signal Filtering. - The filtering of a signal or power voltage, to limit or shape the desired amplitude/frequency characteristics of energy transfer from source to load (or vice versa) will be referred to as Signal Filtering. Signal filtering should be applied from Hi to Lo of the lines across which the signal or power voltage appears. In practice, series impedances are placed in the Hi and/or Lo lines and shunt impedances are placed from Hi to Lo. Typical examples of signal filtering are rate networks and ripple filters.

Line Filtering. - The filtering of any conductor (signal, power, or even spare) to reduce the conducted RF "noise" to or from the point of application will be referred to as Line Filtering. The conducted RF "noise" is an undesired or unnecessary characteristic of the waveshape appearing on the conductor and may be caused by signal generation, load characteristics or extraneous coupling. Line filtering should be applied from the conductor to the chassis or enclosure. In practice, series impedance are placed in the conductor path and shunt impedances are placed from the conductor to chassis or enclosure. Typical examples of line filtering are the individual interface power line filter sections on each MGS power interface line.

NOTE: For signal or power voltages referenced to the enclosure, Signal and Line Filtering would take the same form and overlap in functions.

Filter/Application. - All interface lines except those to be interconnected with site returns should be treated as "Hot" lines with load limitations as applicable only between Hi and Lo. Sufficient consideration of the load/filtering currents in a common return is necessary for compatibility of the most critical aspect of each signal sharing that return.

6.14.4.7. "Shielded System". - The "Shielded System" concept of radiated interference control of the MGS as installed on vehicle applies control measures to the system as a whole rather than to the many separate sources therein. The application of this concept therefore minimizes the control measures required to achieve compatibility goals with an inherently "noisy" system containing numerous digital and pulse signals. It is of particular advantage where the signal characteristics required for system performance result in radiated levels above typical specification limits. In such cases, an interference producing signal must be contained (shielded) rather than suppressed (filtered). The existence of numerous signals of this type make containing them at the system level more economical.

NOTE: This does not negate the useful idea of "suppressing at the source". Where outstanding interference sources exist, they should be suppressed to the average levels within the "Shielded System".

The radiated energy levels inside most digital equipment are well above the radiated susceptibility test levels of specs such as MIL-I-26600 or MIL-I-6181. This makes the EMC aspects unique in two respects; (1) solving the internal compatibility also solves radiated susceptibility, and (2) shielding to solve the radiated interference problem is the limiting factor with regard to the external environment.

The hardware aspects of this concept generally are:

1. Provide system enclosures that are of sufficient shielded effectiveness to reduce the applicable radiated interference below acceptable limits.
2. Cabling that interconnects system units requires shielding on a per-conductor and/or overall cable basis. This should provide sufficient shielded effectiveness to reduce the applicable radiated interference below acceptable limits. (Note: Assuming that both units interconnected by a cable are "noisy", suppression components at both ends of a non-interference producing signal line would be required to replace shielding thereon.)

3. Power interface lines must be sufficiently filtered to reduce the applicable radiated interference below acceptable limits. No shielding is allowed on these lines when demonstrating compliance to the limits. (Note: This aspect would be the same regardless of the "shielded system" approach. This same filtering also does the job of conducted RF interference suppression.)
 4. Signal interface lines must have a combination of suppression and/or shielding to reduce the applicable radiated interference below acceptable limits. When interference producing signals must be routed between two systems along with non-interference producing signals (defined by required signal characteristics), the advantage of shielding over suppression are evident.
- 6.14.5. Conclusions. - The interface and grounding philosophy must be established at the beginning of a design/development program. The experience of the IGS development was an excellent lesson in this regard.

Implementation of the philosophy, developed during the IGS program resulted in more effective electrical noise control within the IGS and its interfaces. Since the grounding and return interconnection philosophy evolved after the initial design of the IGS, it was necessarily a compromise approach to electromagnetic interference control. However, the basic philosophy should be even more effective in future IGS and vehicle designs since it can be applied at the inception of the program and used as a standard for evaluating any IGS/vehicle interface parameters or design changes.

Topic 6.15

IGS Mechanical Design

6.15.1. Introduction and Summary. - This topic emphasizes the system design factors associated with the MGS mechanical interface. More specifically, the MGS mechanical interface, as affected by environmental inputs, will be discussed. For more detail, on individual unit considerations and problems, the reader is directed to Topics 2.9, 2.14, 2.20 and 3.6.

The primary environmental inputs under consideration are:

1. Vibration
2. Shock
3. Thermal
4. Linear acceleration
5. Atmospheric pressure
6. Humidity
7. Adverse atmospheric environment in any probable combination (salt, smoke, liquid oxygen boil off, etc.)
8. Radiation exposure.

When taking into account each of the environmental inputs and the resulting constraints imposed upon the hardware design, an appreciation is achieved for the necessity of realistically relating specification requirements with the operational environment.

6.15.2 Vibration. - Operational vibration requirements for the MGS have been defined in terms of simultaneously applied random and sinusoidal inputs. Comparison of specification vibration levels with actual inflight data indicates that over-specification exists in the area of vibration. From a hardware design standpoint, a margin of safety must be built into a design, to assure performance with any specified input. Specifying beyond a reasonable margin of safety can be costly, and it may require trade-offs in the hardware design that otherwise would not be required. Although the Centaur vibration environment is still somewhat "over-specified", the degree of over-specification is not severe (from a cost effectiveness standpoint). During the course of the program, however, Honeywell, the vehicle contractor, and NASA have teetered on the brink of expensive over-specification. At one time, emphasis was placed on sinusoidal inputs at double the levels in the present specification. This resulted in some unnecessary

test work and almost became a major design impact before the specification was revised to more realistic levels. Centaur is not unique in this regard. Most major guidance system designs have encountered it. On future programs, it would be wise, from a cost effectiveness standpoint, to very carefully consider the specified vibration environment and obtain the desired safety margin by considering the total system (vehicle and its internal mounting structures, IGS mounting techniques, vibration sources throughout the vehicle, plus attenuation, damping, and related factors in transmitting vibrations from the sources to the IGS equipment).

6.15.3. Shock. - Closely associated with the vibrational input is shock. Shock, as specified for operational and qualification environments, is an important consideration in the MGS-to-vehicle interface. In the present Centaur MGS, shock and vibration attenuation is achieved through the use of isolators on several of the units. The mounting adapter shelf, to which the MGS is attached in the vehicle, is subjected to high frequency shock in the order of 100 to 200 g's with shock frequencies covering the range from 30 to 1800 Hz. Through judicious selection of shock isolators, the frequency spectrum that is predominant during shock input is highly attenuated. Resonance of the isolators is below 100 Hz, with sharp attenuation for higher frequencies. The Computer, the Coupler, and the Platform are isolator mounted. The Signal Conditioner and Platform Electronics, due to their physical size, weight, and structural damping characteristics, are capable of being hard mounted without approaching structural design limits. The improved IMG features hard mounting at the Center of Gravity for the Inertial Reference Unit (IRU), which has its own internal vibration isolation system. Through the use of internal ring isolators, sprung weight is reduced and hard mounting at the Center of Gravity is made possible. Operation of the elastomer isolation system in an inert, temperature-controlled environment is conducive to longer life for the isolators. Through hard mounting, sway space is eliminated, an important factor where space is at a premium.

In choosing an isolator, factors such as deflection linearity due to linear acceleration loading, returnability or hysteresis, transmissibility versus frequency, temperature effects and others, must be considered and weighed accordingly. As mentioned later, thermal conductance through the isolator mounts, used on the -1 and -3 Centaur hardware, was also a factor. For sustained linear acceleration, a prime concern with isolator mounted equipment is that the isolators do not "bottom" out.

6.15.4. Atmospheric Pressure. - The effect of pressure upon the MGS interface was discussed under platform unit packaging (reference Topic 2.9). The effect of pressure, or the lack thereof (vacuum), upon thermal conductance was considered from several aspects. Thermal conductance

through a gas media is independent of pressure until pressure is reduced to the point where the mean free path of the gas molecules approaches the conductance path between the heat sink and heat source. Considering the MGS-Vehicle interface, the effect of reduced pressure upon thermal conductance is negligible. Acoustic (pressure modulation) effects have also been considered, but for all practical purposes, the acoustic environment has little or no effect upon the MGS interface.

6.15.5. Adverse Atmospheric Environments. - Closely related with the atmospheric pressure requirement, insofar as design interface considerations are concerned, are requirements imposed by humidity and adverse atmospheric conditions. Design interface considerations, which take these into account, include surface finish and material studies (bonding, resistance to corrosive elements, thermal properties, etc.), and dielectric studies (breakdown of dielectric under negative pressure, in combination with humidity), particularly in the areas of cable connector plugs and interconnect harnesses.

Operation of the MGS under positive internal pressure serves the purpose of providing a clean, inert operating atmosphere. Consideration of the thermal properties exhibited by various fill gases is a significant factor in the proper gas selection. By operating under positive pressure, contaminated air is prevented from entering the equipment.

Consideration for operating the MGS in an explosive atmosphere prompted the use of hermetically sealed components. To further impede the chance of arcing during mode sequencing or switching, nitrogen has been included in the gas mixture.

6.15.6. Radiation. - For the Centaur missions, the MGS radiation environment specification was based upon the measured Van Allen belt plus the artificial belt created by the Starfish project. The specified electron radiation levels imposed no real constraints upon the MGS design. The design of guidance sets for other types of missions should, however, take into consideration the radiation environment to be encountered and IGS design constraints imposed accordingly. The type of radiation and the time-accumulative dosage are factors to be considered. This area is one deserving of greater attention on future programs.

6.15.7. Thermal Environment. - Perhaps the environment that presented as much concern as any other on Centaur, insofar as MGS-vehicle interface is concerned, was the thermal environmental exposure.

The MGS is designed to operate and perform with the guidance compartment ambient controlled, such that the average unit skin temperatures are maintained within specified limits. Initial specifications for the -1 program specified one case temperature limit for all IGS units. Due to problems encountered in maintaining all unit skin temperatures at one set of limits, later specifications (-3 and on) called out a case temperature limit for the platform and another for the other "boxes" making up the MGS. The following represents the case skin temperature specification evolution:

Original (-1):

	<u>Launch*</u>	<u>Flight*</u>
MGS	+30°F to +120°F	+30°F to +120°F

Present (-3 and On):

	<u>Launch*</u>	<u>Flight*</u>
Platform	+50°F to +120°F	+50°F to +120°F
All Other Units	+40°F to +130°F	+30°F to +130°F

*To be interpreted as average skin temperatures.

Problems were evidenced in the past during vehicle tanking operations (filling cryogenic tanks). The problem exhibited itself as a sudden temperature drop in the guidance compartment of the vehicle. This was attributed to the close proximity of the cryogenic fuel tanks to the MGS. Inability to maintain minimum skin temperature requirements resulted. To circumvent this situation, the guidance compartment air conditioning temperature was raised approximately 10°F during "tanking". In addition, foil covered foam type insulation was added to the bulkhead between the cryogenic tanks and the MGS Adapter mounting shelf, thus providing additional thermal isolation. It is noteworthy that the launch pad, pre-launch guidance compartment temperature control is a manual operation, that is, no active temperature control loop exists. From T₀ (launch) on through orbital flight, no active temperature control exists aboard the vehicle either. Passive thermal control to maintain case skin temperatures within specified limits thus must be relied upon from launch through orbital flight. (Reference Topic 6.10.)

Passive thermal control is achieved primarily through the judicious selection of the surface finish for the MGS Units. The initial surface finish of the units (-1 and early -3 Centaur) was electroplated gold over the base metal. This was later changed, and the following surface finishes now exist for the present hardware:

<u>Unit</u>	<u>Finish</u>
Signal Conditioner	Gold plate
Platform Elect.	White polyurethane enamel
Coupler	White polyurethane enamel
Platform	White polyurethane enamel
Computer	White polyurethane enamel

Primary requirements for selection of the surface finish were dictated by the thermal load (solar exposure) experienced by the MGS during orbital flight. During orbital flight, the primary mode of heat transfer between the MGS and its immediate and extended surrounding is through radiation, and hence, emphasis was placed upon surface finishes which provided the desired absorbtivity/emissivity (α/ϵ) ratio (reference Topics 6.10 and 2.10). Surface finishes for the MGS units are considered a major interface point. This interface was originally controlled by the vehicle contractor (GD/C), but is now mutually defined by NASA, GD/C and Honeywell.

6.15.8. MGS Mounting. - One other interface which deserves brief mention is the type of mounting used between the MGS and the mounting adapter shelf on the vehicle. The interface between the MGS and the vehicle mounting shelf utilizes both the hard mount (units mounted directly to adapter plate) and "soft mount" (isolators used for purposes of shock and vibration isolation; reference Topic 6.15) techniques. The primary consideration is shock and vibration isolation for the units mounted on isolators. However, thermal resistance of the isolators was also considered. The mode of isolator heat transfer (conduction) was found to be negligible. Altitude (and in turn pressure) effects upon the overall conductive heat transfer were considered in the study.

6.15.9. Conclusions. - To summarize, complete specification of all probable environments, including the nature of the environment, the level and time duration, is essential. In order to realize hardware compatibility with environmental requirements, there must be full appreciation of the effects of these environments, and how they are reflected into the hardware design requirements. "Over-specification" of requirement should be avoided if at all possible, since undesirable trade-offs, requiring

design compromises in other areas and high costs, may result. Established design safety margins should be established for the hardware and the specified environmental inputs. Once these margins are defined, the IGS designer must be careful to avoid "over-designing" whenever possible. With the present availability of good computer math models, they should be used extensively and early in the design phase to define realistic IGS requirements. The simulations can in turn assist the IGS designer in arriving at well-balanced and effective hardware packaging and mounting designs. Centaur experience has shown that specifying MGS thermal environmental requirements in terms of unit skin temperature alone is an indirect and incomplete approach. The specifying of an ambient thermal environment, including volume and temperature of air flow (if forced convection is used), type and amount of solar loading, and mounting surface temperatures would be more definitive. This approach has special merit when applied to units having active internal temperature control and is being implemented by GD/C, Honeywell and NASA LeRC in specifying the thermal environment for the IMG.

Topic 6.16

System Operational Requirements and Techniques

6.16.1. Introduction. - This topic is concerned with the evolution and establishment of maintenance and operational requirements.

Included in this guidance system operational discussion are:

1. Alignment of the platform
2. Calibration of inertial components
3. Performance versus storage requirements
4. Testing philosophy
5. Maintenance.

Conclusions, as warranted, are provided at the end of each discussion.

6.16.2. Platform Alignment Techniques. -

6.16.2.1. Alignment of the Present IGS. - The guidance platform must be erected and aligned prior to calibration or flight. To accomplish alignment, the platform gimbals are first set to within ± 2 degrees of a desired orientation by the ground support equipment. (Refer to Topic 6.6 on Platform Coarse Align Loops.) The gimbals are then switched from a ground control mode to a gyro control mode which is termed "fine align".

The guidance computer supplies corrective torquing to the gyros to maintain the platform referenced to local vertical during most ground testing (refer to Topic 6.8). The azimuth alignment prior to launch is accomplished optically, via a porro prism mounted on the inner gimbal, viewed through a window in the platform. Early in the Centaur program, gyrocompassing was employed as an azimuth alignment technique, but mission accuracy requirements have precluded its use for prelaunch alignment since 1962. For laboratory and factory azimuth alignment, the azimuth gyro position is established by the appropriate resolver to within ± 2 degrees.

6.16.2.2. Alignment of the IMG. - No major alignment problems have occurred on the Centaur IGS program in relation to the basic alignment philosophy (some level hold, hardware-related, problems were of major concern). Therefore, Improved Centaur had no pre-existing problems to overcome. The only alignment problem presented for solution to the IMG designers was one resulting from a non-precision torquing capability. If a gyro, with its IA vertical, were torqued open loop with Earth's rate and best known gyro compensation, large drift errors could result. The residual drift of the gyro, caused by the high torquing currents from platform reorientation, could cause a degree per hour or more drift. For this reason, a gimbal resolver will be used as an error detector for closed loop, vertical gyro torquing in the IMG.

6.16.3. Calibration and Test Philosophy. -

6.16.3.1. IGS Calibration. - The calibration of gyro and accelerometer parameters provides not only an error model for compensation purposes, but repeated calibrations (back-to-back or over a period of time) give an indication of basic inertial component stability. Predictions about future performance capability can thus be made.

The original Centaur inertial component calibration philosophy was framed within the following requirements:

1. Accelerometer bias, scale factor, gyro constant torque and gyro mass unbalance along the input axis (MUIA) would be calibrated 6 to 10 hours before launch.
2. Accelerometer triad alignment and gyro mass unbalance along the spin axis (MUSA) would be calibrated optically in the hangar lab within 14 days of launch.

To assure that all flight guidance systems would meet these requirements, the Honeywell factory acceptance test was designed to simulate a launch countdown schedule. Figure 6.16-1 represents the tests that were performed. Calibrations #1 and #2 simulated ETR Lab back-to-back calibrations. The cooldown between calibrations #2 and #3 simulated the time during which the guidance system was removed from the lab and installed on the vehicle. Calibration #3 simulated the pre-launch calibration, followed by in-flight vibrations. Calibrations #4 and #5 were to simulate in-flight performance checks at the start and end of the flight. The Δ 's noted in the table were parameter shifts used to assess midcourse correction requirements.

0160-129A

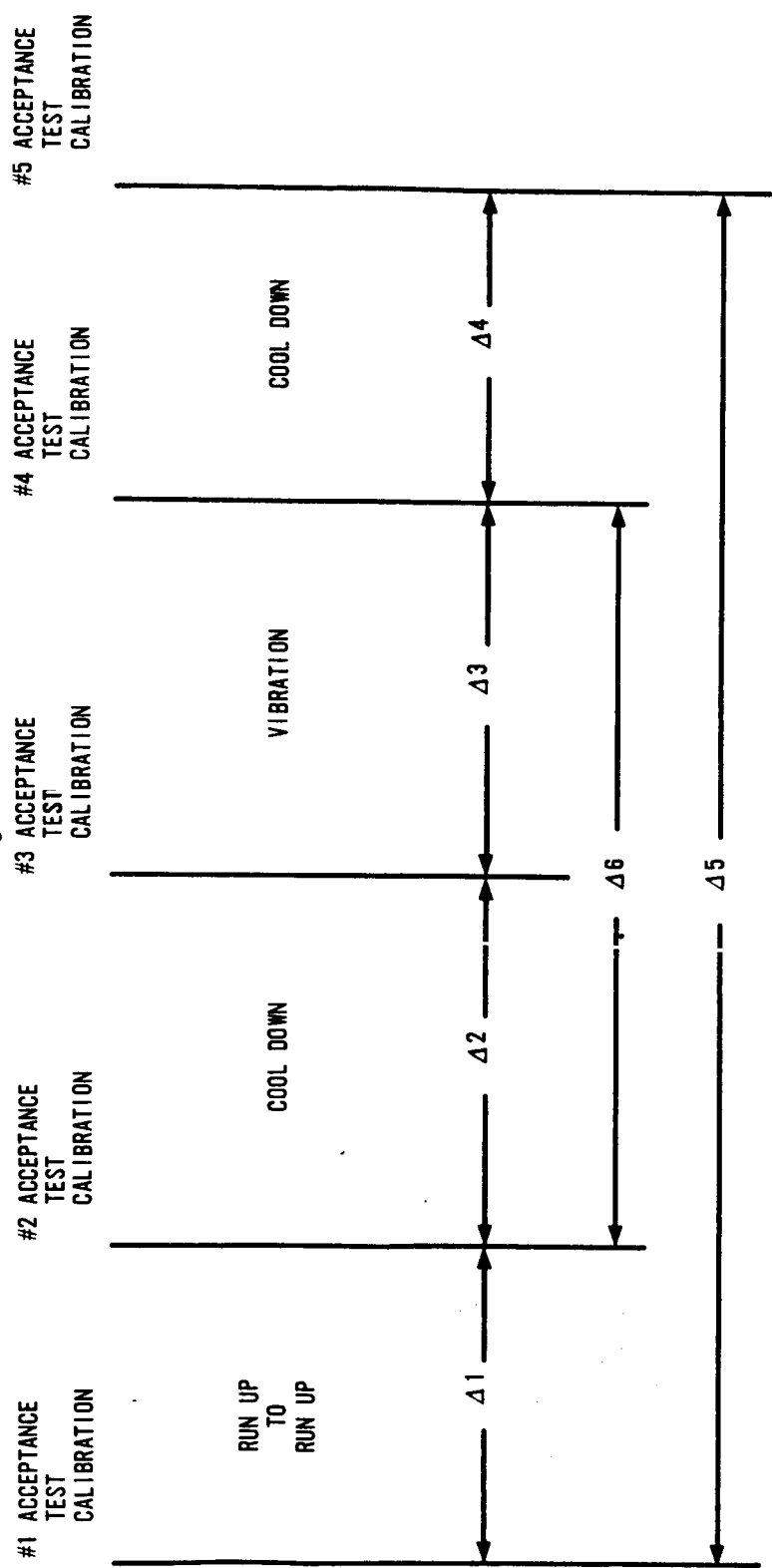


FIGURE 6.16-1. ACCEPTANCE TEST SCHEDULE AND PARAMETER SHIFT NOMENCLATURE

6.16.3.2. -1 and -3 System Calibration. - The guidance computer, with its preflight program, controls the attitude of the platform so the inertial components can be calibrated. The mission sensitivity of the parameters, and their interdependency in the calibration, determine the order of parameter calibrations. Table 16.6-I lists the order of IGS parameter calibration in use until May, 1966. Originally, the system calibration was followed by a drift verification (with the gyros trimmed to the latest calibrated values) in integrated test modes 1-3. When these modes were developed, the contributions of errors from gyro torquing scale factor and SVT effects, which often caused as much or more error than was present from the calibration and gyro instability, were not fully defined.

6.16.3.3. Calibration-Recalibration Technique (July 1965). - The relatively large gyro drift verification values observed with the early calibration technique led to a "calibrate/recalibrate" philosophy. The gyro term was calibrated in the usual orientation and sequence, but before reorientation for the next calibration mode, a second calibration would be run. The benefit of this back-to-back calibration was a minimization of errors other than gyro instability. The reason that this method was not effective did not become apparent until December, 1965, when gyro SVT effects were identified (refer to Topic 2.2).

With the increased number of data points, caused by this back-to-back calibration technique, the number of acceptance test calibration runs was reduced to three (refer to Figure 6.16-2). Coincident with this calibration philosophy, there was a deletion of vibration during system acceptance tests. The vibration test was performed, prior to system testing, during each unit acceptance test. This change reduced the system acceptance test scope basically to checks of gyro and accelerometer performance across a cooldown or without cooldown.

6.16.3.4. Universal Ground Tape (UGT) Calibration (March 1966). - The platform orientations used for the earlier calibration methods caused the accelerometer parameters to be based upon data which was spread out in time. For instance, the most mission-sensitive accelerometer, the U (downrange) accelerometer was calibrated on the basis of data from Align Mode 2 and Align Mode 6. These two align modes could be 4 hours or more apart. The device, or its loop electronics, could change characteristics slightly in the interval, and an optimum bias and scale factor calibration would be unobtainable.

The UGT calibration technique employed orientations such that each accelerometer was oriented IA up immediately preceding or following a

TABLE 6.16-I. ALIGN MODE SUMMARY

Align 1:	(a) Compute U Gyro g-insensitive drift (d_{10}) (b) Read W Accelerometer up
Align 2:	(a) Compute W gyro g-insensitive drift (d_{16}) (b) Read U Accelerometer down (c)* Measure azimuth drift for U gyro MUSRA calculation (d_{12})
Align 3:	(a) Compute V gyro g-insensitive drift (d_{13}) (b) Read W Accelerometer down (c)* Measure azimuth drift for W gyro MUSRA calculation (d_{18})
Align 4:	(a) Compute W gyro non-g and MUIA drift (d_{16} and d_{17}) (b) Read V accelerometer down (c)* Measure azimuth drift for V gyro MUSRA calculation (d_{15})
Align 5:	(a) Compute U gyro non-g and MUIA drift (d_{10} - d_{11}) (b) Read V accelerometer up
Align 6:	(a) Compute V gyro non-g and MUIA drift (d_{13} and d_{14}) (b) Read U accelerometer up
Solve:	(a) Solve for MUIA (d_{11} , d_{14} , d_{17}), (b) Accelerometer Scale Factor (d_1 , d_2 , d_3) and (c) Accelerometer Bias (d_7 , d_8 , d_9) terms
Test Align 1:	(a) Orient for Integrated Test 1 (b) Check all accelerometers
Int. Test 1:*	Verification of Drift Trim (a) About North Axis: $W_{CT} + W_{IA}$ (b) About East Axis: $U_{CT} + U_{IA}$ (c) About Azimuth Axis: $V_{CT} + V_{SRA}$
Test Align 2:	(a) Orient for Integrated Test 2 (b) Check all accelerometers
Int. Test 2:*	Verification of Drift Trim (a) About north axis: W_{CT} (b) About east axis: $V_{CT} + V_{IA}$ (c) About Azimuth axis: $U_{CT} - U_{SRA}$
Test Align 3:	(a) Orient for Integrated Test 3 (b) Check all accelerometers
Int. Test 3:*	Verification of Drift Trim (a) About north axis: U_{CT} (b) About east axis: V_{CT} (c) About azimuth axis: $W_{CT} - W_{SRA}$
Final Align:	Orient for Flight (U down range, W vertical)
Flight:	Space Stabilized, solve in flight equations

* Optical Measurements

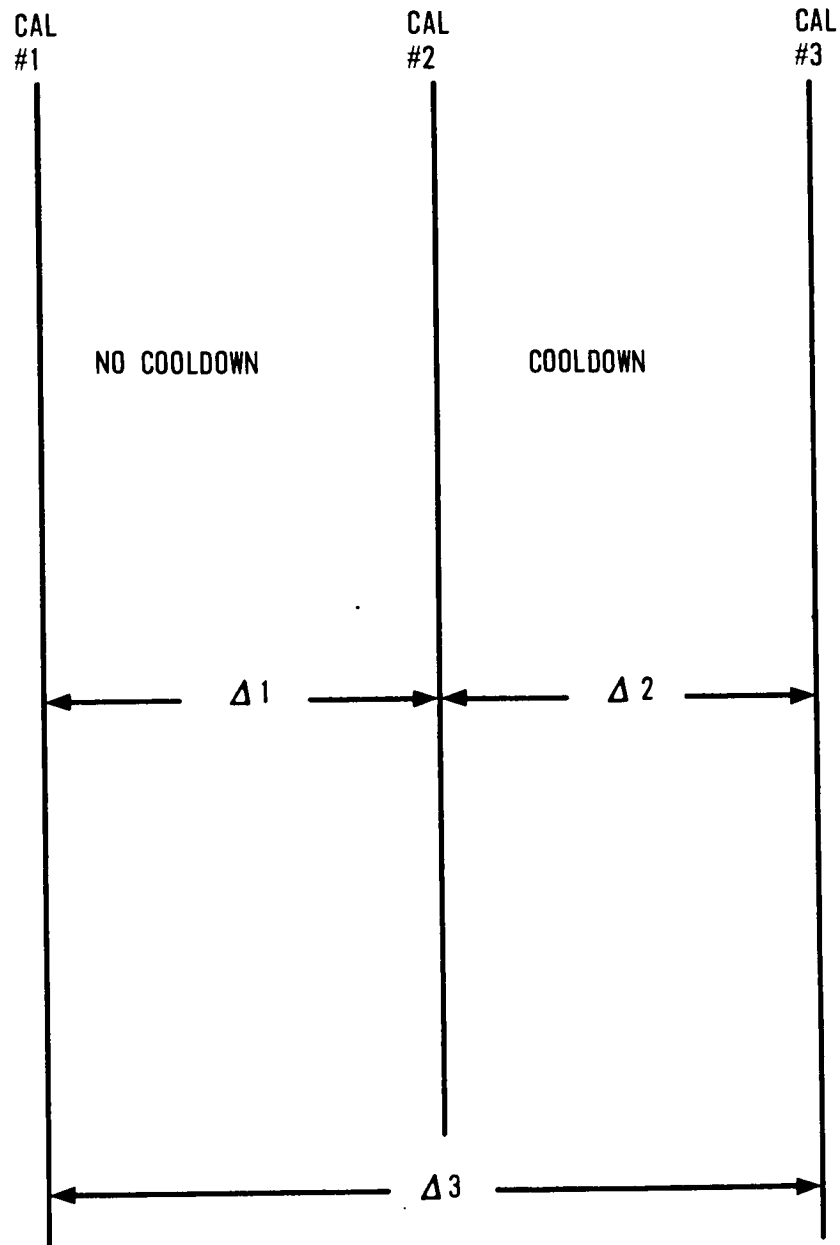


FIGURE 6.16-2. ACCEPTANCE TEST SCHEDULE WITH
CALIBRATION - RECALIBRATION PHILOSOPHY

mode where it was IA down. This minimized the time across which the calibration was made. In addition, the sequence of calibration was changed so that the most mission-sensitive accelerometer was calibrated last, preceded by the second most mission-sensitive accelerometer, and so on.

The rearrangement of platform orientations, caused by this change, had an effect upon the gyro calibration. The constant torque terms could not be calibrated before the MUIA terms in all cases, as had been the rule with previous calibration methods. However, the guidance computer program was rewritten to compensate for this difference, with no loss of overall accuracy. Table 6.16-II shows a matrix of: 1) align modes; 2) north, east, and azimuth gyro torquing; and 3) the sequence of parameter calculation. In addition to the above changes, the UGT program included a method for calibrating accelerometer triad (rho angle) misalignment angles without optics. Previously, the measurement of the angle between the input axes of any two accelerometers required two accelerometer measurements of levelness, two optical measurements via autocollimator, and a multi-step manual calculation. The error sources associated with that method were many and chronically present. The advantage gained from automatic rho angle calibration was a reduction in the calibration uncertainty from approximately $\pm 200 \mu$ rad to approximately $\pm 50 \mu$ rad (three sigma).

6.16.3.5. Non-Optical MUSA Calibration Techniques. - In recent years, several attempts have been made at revising the gyro MUSA calibration to eliminate the use of manual optical techniques. Although the optical method is sufficiently accurate, it is very subject to subtle mistakes by engineers and technicians. Such mistakes have caused extensive trouble-shooting and concern for gyros' performance capabilities, and at a minimum, have required otherwise unnecessary retesting and calibrations.

In the spring of 1967, a break-through was achieved when it was proven that azimuth resolver readout precision could be good enough to permit manual MUSA calibration without the use of optics. A special advantage of this technique was that it could be used on the launch pad, thus overcoming another major limitation of the optical technique and averting the need for a 60-day performance requirement on gyro MUSA stability (covered in a later paragraph, 6.16.4.3). The manual technique still possessed the risk of operator errors, but the providing of an analog tape record of the calibration, as well as self-checks in setting up the equipment, minimized this risk. The manual, non-optical technique was proven out at ETR, on AC-11 vehicle, in June, 1967. However, with the subsequent shift to use of CCLS (see Topic 5.2) at ETR, this non-optical technique has not been implemented, since it reverts to the use of a manual technique.

TABLE 6.16-II. COMPENSATION PARAMETERS

0160-142A

FUNCTION	EARTH RATE PLUS DRIFT RATE COMPENSATION			COMPUTER PROGRAM DETERMINED
	WDNO	WDEO	WDAO	
ALIGN MODE 1	$d_{16} + d_{17} g + \Omega \cos \lambda$	$d_{10} + d_{11} g$	$d_{13} + d_{15} g + \Omega \sin \lambda$	d_2, d_8
ALIGN MODE 2	$d_{10} - d_{11} g + \Omega \cos \lambda$	$d_{16} - d_{17} g$	$d_{13} - d_{15} g - \Omega \sin \lambda$	
ALIGN MODE 3	$d_{10} + \Omega \cos \lambda$	d_{13}	$d_{16} + d_{18} g + \Omega \sin \lambda$	d_{10}, d_{11}
ALIGN MODE 4	$d_{13} + \Omega \cos \lambda$	d_{10}	$d_{16} - d_{18} g - \Omega \sin \lambda$	d_9, d_3, d_{13}, d_{15}
ALIGN MODE 5	$d_{13} + d_{14} g + \Omega \cos \lambda$	d_{16}	$d_{10} - d_{12} g - \Omega \sin \lambda$	d_{14}
ALIGN MODE 6	$d_{16} + \Omega \cos \lambda$	$d_{13} - d_{14} g$	$d_{10} + d_{12} g + \Omega \sin \lambda$	$d_1, d_7, d_{16}, d_{17}, d_{18}, d_{12}$
ALIGN MODE 7	$d_{16} + d_{17} (0.707^{\circ}) g + \Omega \cos \lambda$	$d_{10} + d_{11} (0.707^{\circ}) g - d_{12} (0.707^{\circ}) g - (0.707^{\circ}) \Omega \sin \lambda$	$d_{13} + d_{14} (0.707^{\circ}) g + d_{15} (0.707^{\circ}) g + (0.707^{\circ}) \Omega \sin \lambda$	d_4
ALIGN MODE 8	$d_{13} + d_{14} (0.707^{\circ}) g - \Omega \cos \lambda$	$d_{16} - d_{18} (0.707^{\circ}) g - (0.707^{\circ}) \Omega \sin \lambda$	$d_{10} - d_{12} (0.707^{\circ}) g - (0.707^{\circ}) \Omega \sin \lambda$	d_5
ALIGN MODE 9	$d_{10} + d_{11} (0.707^{\circ}) g + \Omega \cos \lambda$	$d_{13} + d_{15} (0.707^{\circ}) g + (0.707^{\circ}) \Omega \sin \lambda$	$d_{16} + d_{17} (0.707^{\circ}) g - d_{18} (0.707^{\circ}) g - (0.707^{\circ}) \Omega \sin \lambda$	d_6
FINAL ALIGN	$d_{13} + \Omega \cos \lambda \cos \beta$	$d_{10} + \Omega \cos \lambda \sin \beta$	$d_{16} - d_{18} g - \Omega \sin \lambda$	

Another non-optical MUSA technique received attention (by GD/C for the IGS and by Honeywell for the IMG) during 1967. This technique, which has the advantage of being fully automatic, is in effect a "reverse gyro-compassing". Its major drawback is the amplified sensitivity to east gyro drift uncertainties. Although the technique was not perfected for use with the IGS, the future prognosis for it is good, especially if statistical filtering techniques can be used to reduce the effects of the unwanted instabilities. As noted in the following sub-topic, Honeywell is pursuing this technique for use with the IMG.

6.16.3.6. Calibration of the IMG. - Calibration requirements and techniques for the IMG are now being fully developed. The key feature of the IMG calibration is that all gimbal reorientations and parameter measurements are computer-controlled. A plethora of human operator errors in the past proved the need for a computer-controlled, automatic calibration scheme. Although past calibration methods involved the use of the guidance computer for calculations and gyro torquing, the operator was heavily involved in the operation. Much engineering effort was expended in "detective work" associated with operator errors. This was necessary in order to indict or exonerate the hardware when a question between hardware failure and operator error was present. To achieve the goal of fully automatic calibration, the development of an automatic, non-optical gyro MUSA measurement technique must be accomplished. Such a method has been proven feasible, and is now being evaluated for its total calibration accuracy.

6.16.4. Performance Versus Storage Requirements. -

6.16.4.1. Initial -3 IGS Requirements. - The Centaur -3 guidance system was required by specification to perform across storage as follows (for initial Surveyor missions):

1. Drift due to acceleration about gyro spin axes shall not exceed the following, within two weeks of launch:

U gyro - 0.63 deg/hr/g
 V gyro - 0.63 deg/hr/g
 W gyro - 1.20 deg/hr/g

2. When stored inside a building, the guidance system should perform without impairment under the following conditions:
 - i. Starting at 70°F ambient, with air movement due only to convection, the air temperature may be lowered to 30°F for eight hours.
 - ii. Starting at 70°F ambient, with air movement due only to convection, the air temperature may be raised to 120°F for six hours.
3. The guidance set shall perform as specified when exposed to any probable combination of rain, fog, smoke, wind, ozone, sand, dust, and salt spray after or during storage.
4. Assuming hangar lab calibration within two weeks of launch, the following triad angular alignment stability should be maintained:

U to V accelerometer input axes 0.45 mrad
 V to W accelerometer input axes 0.75 mrad
 V to W accelerometer input axes 1.50 mrad

6.16.4.2. Increased Long Term Stability of MUSA and Rho Angle Terms (July 1965). - A review of long term stability of MUSA and rho terms led to an extension of storage requirements for these terms to 45 days. A correlation study showed that the same performance could be expected up to 45 days, as had been expected within 14 days. The effectivity of this requirement was AC-6 (launched 11 August 1965) and on.

6.16.4.3. Most Recent Requirements for Stability Across Storage of MUSA, Rho Angles, and Porro Prism Angle (January, 1967). - The long term stability of gyro MUSA, accelerometer triad orthogonality, and porro-prism angle was extended to 60 days on the basis of experience and operational lead times at ETR. The advantage of the longer requirement was that any delays in the launch sequence would be less likely to necessitate removal of the MGS from the vehicle and recalibration of these terms in the laboratory.

Storage requirements for Centaur guidance hardware have essentially been geared to operational needs at ETR. The guidance system has never been required to perform at a certain level after an indefinite storage (6-12 months, or more). Calibration of inertial components has been, and will continue to be, a necessary step in the preparation of a guidance system for use after storage.

6.16.5 Operational Test Philosophy and Control. - The original -1 and -3 guidance operational test philosophy was established in the early days of the program primarily by the customer. The guidance systems were briefly tested in the Honeywell factory, and shipped to the vehicle assembly plant in San Diego. Guidance personnel operated the equipment for post-shipment tests and other tests prior to installation on the vehicle in the factory. Once installed on the vehicle, vehicle contractor personnel defined and performed the testing. If a failure occurred, the MGS was removed to the guidance lab for diagnosis and repair. The test procedures used by the vehicle contractor were generated and maintained at that facility. Also, the guidance computer preflight program was under vehicle contractor control.

Once the vehicle tests were completed, the vehicle and guidance system were shipped to ETR. There, vehicle personnel operated the guidance system, and guidance personnel provided field engineering support. The guidance system operational procedures for the ETR laboratory and the launch pad were written by resident ETR personnel. This operational philosophy has been essentially unchanged to this day, except that joint working groups of vehicle, guidance and NASA engineers now jointly establish the basic operational test requirements. Guidance contractor contributions are also made through detailed acceptance test procedures, participation in technical coordination meetings, and review of the vehicle systems Unified Test Plan (UTP). Each of these contributions will be explained further:

1. Test Procedures - The Honeywell-written and customer-approved acceptance test procedures provide a model procedure for operation of the guidance system in the field. However, because of slight laboratory test equipment differences from site to site, each major test location publishes its own test procedures. The field sites draw heavily from the guidance factory test procedures.
2. Technical Coordination Meetings - When differences in operational techniques arise, the subject becomes an agenda item for a technical coordination meeting (in years past, special working groups met to define requirements and approve techniques). All parties present their views, and NASA-LeRC assigns the action to implement, or to perform further analysis on the most favorable approach.

3. Unified Test Plan - The vehicle contractor maintains an overall (total vehicle systems) test plan and requirements document. The guidance contractor receives review copies of the UTP and forwards recommended changes to NASA-LeRC. If NASA-LeRC concurs, a technical directive is sent to the vehicle contractor to accomplish the change in the UTP.

Although the present approach has been effective, there have been some efforts to more closely standardize the operational procedures. In 1964, an effort was made to bring the various test site procedures together in one document, still allowing for site-to-site test equipment differences. The effort was begun because there was a belief that calibration and operational data were lacking continuity among the several test sites. For instance, MUSA measurements at one location were made during a calibration mode, but they were measured after the calibration mode at another location. There was concern that undefined factors could influence the data obtained by the two different methods.

A series of discussions among representatives of all test sites resulted in a decision not to produce a single test procedure document. Instead, the flexibility of local operational procedure control was maintained. The overall coordination of operational procedures has since been effectively accomplished via working groups composed of individual site representatives (Vehicle Contractor, IGS Contractor, and NASA engineers).

6.16.5.1. Conclusions. - A more accurate measure of guidance system performance could be obtained during development phases if operational philosophy is made consistent at all sites. The early Centaur operational philosophy was less than ideal in this regard, because a separate operational philosophy existed at each test site. If a uniform policy is formulated and followed, the overall measure of guidance system performance will also become more reliable and efficient. In fact, the total amount of testing from manufacture to launch of a guidance system could be optimized if a unified operational philosophy is adopted. There would be fewer tests repeated because of site-to-site procedures and data differences.

The source of such operational philosophy should be a working group, comprised of representatives of the IGS Contractor, the Vehicle Contractor, field site personnel, and the Contracting Agency. If each representative has a working knowledge of the operational constraints at his site, then it will be possible to minimize delays in resolution of operational testing philosophy and problems.

6.16.6. Maintenance Philosophy and Requirements. -

6.16.6.1. MGS Maintenance Philosophy for -1 and -3 IGS Hardware. -

The early Centaur maintenance philosophy was not, as far as can be determined, a formal documented set of requirements. There was general agreement to keep a platform, platform electronics, and coupler together to minimize coupler tuning and to avoid gyro stabilization loop problems. Also, as a rule there was to be no platform rework outside of Honeywell's cleanroom facilities. Any subassembly, other than those in the platform, could be field replaced if there was not extensive soldering and rewiring involved. On one occasion, a plug-in ARCS board was replaced in a Coupler (while installed on a vehicle) only a few days before launch. Operation and maintenance manuals were provided to field personnel through the field service organization. These manuals described the approved methods for servicing all guidance and related equipment in the field, but they did not establish the overall maintenance requirements.

6.16.6.2. AC-7/AC-8 Maintenance Philosophy (October, 1965). - Special thermal ramp tests of couplers were found to be very effective in screening out potential accelerometer rebalance electronics and power supply failures. Hence, all couplers were required to pass such a test before becoming certified. The thermal ramp requirement posed a field problem: If couplers require such a test, how can a subassembly be properly replaced in the field?

A formal maintenance philosophy document was prepared (effectivity AC-7/AC-8) to explicitly list the field-replaceable subassemblies and defined the appropriate re-certification tests. In the coupler, seven out of 16 plug-in modules could not be replaced without performing the thermal test. The resolver chain electronics buffer amplifiers were the only subassemblies which could be replaced in the PE. The stabilization loop electronics required threshold gain and balancing adjustments on a factory test station. The only unit level test stations designated for field locations were the signal conditioner and computer test station. Consequently, any computer card or signal conditioner module could be replaced in the field with a certified spare part, and the unit could be re-certified at the site.

The tests to be performed on any subassembly used as a field spare were also defined in the AC-7/AC-8 maintenance philosophy document. These tests usually required vibration in an actual or simulated unit of the MGS, plus complete pre-and-post-vibration functional checks.

6.16.6.3. Phase II PIP Maintenance Philosophy (June 1966). - With the performance and operational improvements brought about through the Phase II PIP changes, the coupler thermal test was required for screening fewer subassemblies. The number of non field-replaceable subassemblies dropped from seven to three. Again, in November, 1966, another coupler subassembly was added to the field-replaceable list.

6.16.6.4. IMG Maintenance Philosophy. - The IMG maintenance philosophy will be very simple because of the basic two-box design. With most of the electronics contained physically in the same assembly (IRU) with the inertial reference, maintenance of the IRU will need to be done in the Honeywell factory. It is conceivable that the power supplies in the SEU will be field replaceable although no firm groundrule has been set. There has been a determined effort to provide external monitor points for all SEU supplies, so that fault isolation can be accomplished without opening the unit.

6.16.6.5. Maintenance Philosophy Conclusions. - Centaur experiences have provided a valuable lesson in defining and implementing a workable maintenance philosophy. In retrospect, the equipment design is the basis for any maintenance philosophy. If the design includes planning for maintenance, then the task becomes much simpler to implement. Even if maintenance is given low priority in the design, a formal, documented set of requirements will assist in getting the hardware repaired with fewer delays. Finally, once a maintenance requirement document is established, it must periodically be reviewed and revised so that it is viable and does not impose outdated or inadequate requirements.

Topic 6.17

IGS Testing

6.17.1. Introduction. - This section of the report will deal with a discussion of the definition and evolution of test requirements and philosophies through the various phases of the Centaur Guidance development program. Throughout the program there has been a trend toward increased sophistication and effectiveness of testing. This was necessitated by the many and varied problems encountered in the early phases of the program. Also, desire on the part of both the customers (GDC, early program and NASA, present program) and Honeywell for increased IGS reliability and performance contributed greatly to this trend.

Early Centaur guidance was plagued by problems. Breadboard and module testing was generally performed to check out basic circuit operation without regard to marginal conditions (power, signal, temperature, etc.) or final circuit layout. As a result, many circuits, which operated properly under ideal conditions, failed to perform their functions when operated within complete IGS units under less than ideal conditions. The fact that many circuit designs lacked thorough worst case analysis aggravated this situation. In an attempt to solve the problems that existed and to prove out redesigned circuits to more realistic conditions, the breadboard and module design and test philosophy has evolved to the present use of computed-aided worst case design analysis, verified by worst case testing.

Diagnosis of the problems encountered during early unit level and system level testing was aggravated by the inadequate module testing. It was the rule, rather than the exception, for multiple problems to be present at one time, with many of the more subtle problems being masked and therefore remaining undiscovered throughout the early phases of testing. This made efficient troubleshooting very difficult.

The basic phases of IGS development have been (reference Topic 1.1):

1. -1 system design
2. -3 system design
3. Phase I PIP system design
4. GG177/ Dual Resolver Retrofit

5. Phase II PIP system design
6. Advanced IMG development.

with many intermediate redesigns of individual circuits.

IGS testing has consisted of several phases of informal and formal design test programs, such as "Design Evaluation Test", "Design Proof Test", "Test and Evaluation Program" in addition to: the breadboard and module evaluation testing of each design, engineering and production prototype testing, and production acceptance testing. The following sections will take each of the Centaur IGS test phases and discuss the test philosophies involved.

6.17.2 Engineering Evaluation Testing. -

6.17.2.1. Summary. - Engineering evaluation testing is an essential part of the design process. It encompasses testing at all levels of design effort, ranging from verification of component characteristics and individual circuit operation, through complete system operation within a variety of environmental conditions.

The history of Centaur IGS engineering evaluation testing has evolved from individual, designer specified test requirements through program management/customer planned and specified test programs and requirements. This was the result of the lessons learned from the many problems encountered early in the program.

The approach here will be to discuss the basic test requirements or philosophies followed in all phases of testing through the various phases of Centaur IGS development.

6.17.2.2. -1 Centaur IGS (1959-62). - This design of the Centaur IGS was built and tested without the benefit of strict, program formulated, test requirements and philosophies. Although a qualification program was planned, it was never funded and hence not performed. Breadboard and module tests were performed to requirements formulated by the designers. The inclusion of tests under marginal power, signal, and environmental conditions was primarily at the discretion of the individual designers. Breadboard layouts seldom simulated the actual circuit layouts, even on critical circuits where noise coupling, stray capacitance, etc., could be troublesome. Module tests were usually performed under fairly ideal conditions; that is, individual power supplies, nominal input signals, nominal power supply voltages, and non-exact loads (poor simulation of

load impedance with little attention to the reactive load components). Often circuit designs were released without test data showing successful operation, when interconnected with the actual input and output circuitry.

A multitude of problems resulted from the above deficiencies in testing. Unit level testing was the first place where the individual circuit boards were brought together. Problems were encountered, many of which could have been avoided had the above described deficiencies in breadboard and module testing not existed.

Unit level testing (platform, pulse rebalance electronics, etc.) consisted basically of engineering specification testing, again with little attention to operation under marginal conditions. Even under optimum laboratory conditions, a large variety of problems were encountered. This caused serious delays in the test cycle. Environmental testing, where performed, was completed with difficulty and often with marginal success. As mentioned earlier no formal qualification program, at unit or system level, was funded or performed.

System level test experience was similar to unit level test experience. Multiple problems, schedule delays, less than optimum, last minute, design fixes all plagued the early -1 program. System test requirements at Honeywell for this first design of Centaur IGS were largely for checkout under laboratory conditions. Environmental tests, where performed, were largely a matter of problems encountered, with attendant fixes in an attempt to complete the tests.

The -1 system was in retrospect a system of marginal individual circuit performance, which caused extreme difficulty in successful completion of unit and system level testing. This led to recognition of the need for extensive redesign of many circuits with increased attention to unit and system design engineering in the areas of loop and error analysis, grounding, interconnect wire routing, and mechanical structures.

Another major contributor to inadequate -1 system testing was the lack of an engineering testbed system at Honeywell. The investigative tests that were run, had to be performed with deliverable equipment.

6.17.2.3. -3 Centaur IGS (1961-1965). - The -3 Centaur IGS design was a considerable improvement over the original -1 design. Test requirements and philosophies became much better defined, particularly at unit and system levels.

Breadboard and module level test requirements remained largely under the control of the individual designers. In most cases, the designers recognized the need for more extensive evaluation testing of their designs. As a rule, this was still inadequate in at least one of the following areas: vibration and thermal test requirements, proper simulation of input and output circuit signals and impedances, marginal power supply voltage tests, and marginal input signal tests.

Unit level testing again consisted essentially of Engineering Specification testing with selected environmental tests. Specifications did show improvement in detail test requirements.

Basic system level testing showed considerable improvement in specification of test requirements. Having recognized the need for more extensive system evaluation testing, Honeywell had proposed allocation of two systems as "Engineering Testbed Systems". The first of these systems began operation in August, 1962. Some of the early tests or investigations performed after the initial debugging and acceptance tests were:

1. Accelerometer loop noise investigation.
2. Accelerometer loop design investigation.
3. Limited thermal map of the coupler.

The nature of these tests were, in the most part, problem investigations or efforts to gain additional insight into the system operation.

Recognizing the vital role that test information plays in the design process Honeywell proposed (late 1962) a formal test program, initially called the "Flight Certification Test Program" and later called the "Test and Evaluation" (T&E) program.

The objectives of the T&E program were to perform a comprehensive test program leading toward a thorough ground evaluation of the Centaur IGS. The program was performed including continuation of the engineering evaluation tests on the testbed systems, system grounding tests, accelerometer rebalance loop evaluation in the system, evaluation of spin motor reaction torque gyro drift compensation techniques, plus thermal and magnetic shielding tests. Further testing under laboratory conditions was performed consisting of a series of confidence tests, calibration tests and accuracy measurement tests. These tests put time on the systems and accumulated system calibration data for purposes of inertial component stability studies.

Additional tests performed at the Honeywell facility under this program were environmental in nature. They consisted primarily of temperature, altitude, acceleration, shock, and vibration tests. Environmental testing was performed to nominal or expected environment levels, to worst case or qualification test levels, and were planned for overstress levels.

During the T&E program at Honeywell, additional "Design Proof Tests" were being performed by GD/C at their facility in San Diego, using a testbed system provided to them for that purpose. These tests included overstress environmental tests.

The T&E environmental tests on the -3 system disclosed fundamental weaknesses in the internal coupler mounting structure and in the stability of the accelerometer loops while operated within a range of temperatures. Test data and operating time accumulated on -3 systems was fairly extensive by this time. From this data, it could be seen that system reliability was insufficient and that the design still contained some fundamental weaknesses. This brought about a series of product improvement plans (PIP) which were proposed to NASA.

6.17.2.4. Phase I PIP. - In February, 1964, Honeywell submitted a proposal, "Product Improvement Program". This program later known as "Phase I PIP" was begun in mid-1964. The objective of Phase I PIP was primarily to accomplish improvements in system performance in line with the Surveyor mission requirements. Test philosophies by this time in the Centaur IGS program reflected the need for strong, management-specified requirements. As a result, system design and test had become much more sophisticated.

Breadboard and module test became more detailed, covering the areas of environmental testing, closer attention to simulation of input and output circuit characteristics, and marginal signal and power test requirements.

The Phase I PIP redesign accomplished its objectives except for a continuing problem with the accelerometer rebalance current supply. System performance showed considerable improvement. System operation had now become good enough that problems which had previously been masked by other, more severe, problems and by operational conditions, were uncovered.

While the Phase I PIP retrofit was being performed, centrifuge tests were being performed on the GG116 accelerometer. These tests were instrumental in demonstration of fundamental weaknesses in the accelerometer. Prior to this time, little test information was available on the precise

operation of digital accelerometer loops under high acceleration inputs. This series of tests were a significant milestone in Centaur testing. They showed the value and need for demonstration of major IGS loop operation under closely simulated operational conditions. This type of testing is costly, but major deficiencies may remain undiscovered without testing of this nature.

Centrifuge tests were also performed to evaluate the GG177 under high acceleration inputs. The tests confirmed that the GG177 was far superior to the GG116.

This resulted in the GG177/dual resolver retrofit. The dual resolver portion of this retrofit was to provide additional guidance control capability. The GG177/dual resolver retrofit began in mid-1964.

The GG177 retrofit became intermeshed with the Phase I PIP redesign. Thus, many design improvements were being incorporated into the Centaur IGS in a short time. Anticipating that technical problems would arise during the period of change, and recognizing that the problems had to be solved in a timely manner, test philosophy continued to change, with emphasis on more detailed design evaluation testing at all levels of test.

Board and module level testing requirement remained, as in -3 Centaur detailed, but still under individual designer control.

An engineering system was modified and allocated for GG177/Phase I PIP prototype testing. The objective was a quick verification of the new configuration systems' operation under extreme temperature and vibration environments. This would permit correction of any gross problems in a timely manner. In addition, the prototype system tests resulted in recommendations which aided in the efficient completion of the formal "Design Evaluation Tests" (DET).

The objective of the Design Evaluation Tests was to determine that the GG177/Phase I PIP configuration MGS would operate satisfactorily within the environmental and performance requirements of the GD/C 55-04040, Revision F, specification. The tests performed were: Laboratory stability and reliability tests, thermal tests, vibration tests and Electromagnetic compatibility tests. These tests successfully qualified the design for Atlas Centaur flights.

6.17.2.5. Phase II PIP. - Fall, 1965, saw the go ahead for the Phase II PIP program. This program was to complete the changes, recognized as desirable, at the time of the Phase I PIP proposal and to correct the

ARCS deficiency remaining from Phase I PIP. Further it was to correct problems which were discovered after the Phase I PIP improvements.

The Phase II PIP proposal was for an integrated program containing all of the essential elements of a thorough development program. For the first time in the Centaur IGS development program, worst case circuit analysis and the associated worst case module testing became a program requirement. Prototype boards were built and tested. These tests served to verify adequacy of the designs at the earliest possible time in the design cycle.

Two prototypes of each board were built and tested. One set, then became part of the prototype coupler, while the other set was retained by Design Engineering for use as test assemblies.

The prototype board tests included:

1. ES test
2. Turn-on test
3. Twelve-hour stability test
4. Thermal cycling test, operating and non-operating
5. Load variation test
6. Line voltage variation test
7. Noise test
8. Shock test
9. Vibration test.

These tests constituted final validation of the electrical and mechanical circuit designs. They served to give maximum confidence in circuit operation prior to moving to the next higher level series of tests.

Prototype coupler tests were performed, using one set of the above thoroughly tested boards. The objective of the prototype coupler tests was to verify that the coupler would operate within specification as a separate unit. Prototype coupler tests consisted of Engineering Specification tests, thermal tests, and vibration tests.

Upon completion of the prototype coupler testing the prototype coupler was incorporated into a system (Phase II PIP configuration) and subjected to a series of Design Evaluation Tests (DET). These tests were a repeat of the necessary portions of the GG177/Phase I PIP DET. The objectives were to further evaluate the performance of the Phase II PIP coupler modifications and finally to evaluate the performance of the Phase II PIP Centaur MGS.

6.17.2.6. The Advanced IMG - "Doing It Over Again". - IMG test planning includes strict test requirements and philosophies dictated by technical management at Honeywell and NASA-LeRC. This resulted from the many lessons learned during the earlier IGS development cycles.

IMG test philosophy requires the following tests to be performed on engineering prototype units:

1. Board ES tests
2. Board DET
3. Unit ES
4. Unit DET
5. System ES
6. System DET.

An early production system will undergo formal qualification testing.

6.17.2.7. Conclusions. - Development of an inertial guidance system is an extremely complex process. This is further complicated by the fact that the state of the art is usually being pushed to its limit by the system requirements.

Testing plays an essential part in all stages of the design process. Lack of adequate test requirements and philosophies preclude timely detection of possible deficiencies; which, if not detected and corrected in a timely manner, become more and more serious as the development progresses. Problems not corrected at board level create increasingly serious problems at unit and system level. This makes the test programs more difficult or impossible to complete. The end result is a series of redesign efforts of greater magnitude than should normally be expected. The impact upon cost and schedule become significant.

Every effort should be made to correct design problems at the earliest possible point in the design process.

The present day success enjoyed by Centaur guidance could not have been achieved without the many comprehensive test programs performed during the latter stages of development. On future programs, effort should be made to simulate all aspects of operational requirements and conditions in order to provide the maximum assurance of meeting operational requirements.

6.17.3. Production Testing. -

6.17.3.1. Introduction. - Honeywell production test philosophy is based upon the following principles:

1. Tests are performed by Production personnel.
2. Process test content is controlled by the Engineering Specification (ES), which combines the requirements of the designer and the production engineer.
3. Acceptance test content is controlled by design engineering implementation of contractual requirements via released engineering documents.
4. Quality control participation in tests is limited to surveillance of tests and certification of test results. (An exception is the role of quality inspection related to purchase parts. In this case, quality personnel perform the testing and data reporting.)

There are two fundamental types of tests performed by Production:

1. Process (ES) tests of manufactured subassemblies and assemblies. These include tests of assemblies up to and including the MGS.
2. Acceptance tests of completed units or the total MGS. Such tests are used to demonstrate ability to meet contractual requirements, and are followed by selloff to the customer.

6.17.3.2. -1 Through Phase I PIP Process Testing. - The early philosophy for process testing of modules and subassemblies was simple adherence to the ES tests prescribed by the designer. There were some production prototype tests on a few of the more critical subassemblies, but not as a part of an overall test program. Often, the failure to meet an ES requirement was simply corrected by rework or adjustment of the subassembly.

As has been stated previously, the process test conditions were mostly ideal, and passage of the ES test did not always guarantee operation at the next assembly level.

A major obstacle in the processing of modules, and printed circuit board assemblies was the potting and conformal coating requirement. The curing of these coatings would affect some components in critical assemblies. Therefore, the ES test was run before and after potting.

Because of the lack of worst case design, the process testing could be multi-iterative on some subassemblies-- repeating and reworking until the subassembly was passed. Also, the lack of optimum design forced the specifications to be set at the lowest possible levels to maintain reasonable yield rates. As a result, the level-to-level specifications were often identical, with no allowance for funneling or tapering of the

requirements. It is an obviously undesirable situation to require equal operation and performance of a subassembly at both the subassembly and the higher assembly levels of test. Under this philosophy, a marginal failure of a subassembly at, for instance, coupler level is much more costly to find and correct than if the marginal failure had been screened out at a lower level. In summary, the non-optimized design and lack of authorized qualification testing forced most process test specifications to be uniform at all levels of assembly.

In order to supply spare subassemblies to the field for maintenance purposes, process testing was modified. Flight certification of subassemblies was accomplished by ES testing and some environmental (vibration, thermal) tests.

Production process test philosophy remained essentially unchanged for subassemblies and MGS units until engineering qualification testing and worst case design became fact with the Phase II PIP retrofit.

The unit level process tests were much like the subassembly process tests of this period, because the units were assembled from modules and subassemblies which were not of optimum design. That is, a large portion of the ES testing simply was concerned with displaying operational capability before entering system tests.

A significant advancement in coupler unit level tests was brought about by thermal testing. The previous engineering tests had shown that extremes in operating temperature would force potential failures to manifest themselves early in testing. The coupler was cold-soaked at 30°F case temperature and then the temperature was raised at a rate of 1°F/minute to 130°F. (These temperatures are the design operating limits for the coupler.) Initially, a major number of coupler subassemblies required this test (while assembled into the coupler). However, in Phase II process testing (discussion following), the number of subassemblies requiring thermal testing was greatly reduced. It should be strongly emphasized that thermal testing was a major factor in obtaining both failure experience data and acceptable coupler subassemblies. This test provided the designers with information for improving certain subassemblies, as well as providing a process test for Phases I and II hardware. Units other than the coupler were shown by engineering tests not to require thermal process testing.

6.17.3.3 Phase II PIP Process Testing. - The worst case analysis, which was a mark of the Phase II PIP design, greatly improved the production process test picture. The engineering development and prototype tests yielded a coupler design which was much more producible. Also, production prototype tests were devised for each lot of subassemblies. The first three, a middle, and a last subassembly were selected for expanded qualification tests to prove uniformity in the build process.

The flow of process (ES) testing for each Honeywell-manufactured unit of the MGS is shown in Figures 6.17-1 through 6.17-4. Wherever possible, efforts were made to funnel the specifications of parameters. That is, where sufficient margin existed, the lowest assembly level process test had the tightest specification. The last process test then had the loosest specification to meet the overall system requirement.

6.17.3.4. Production Testing for the IMG. - The results of the Phase II PIP design and test program serve as a model for IMG design and process testing. Following engineering development, design proof tests, and qualification tests the module/subassembly design will be released to production. As production of the module/subassembly begins, a series of sample tests will be run to proof the production process. The production prototype proof test content will be excerpted from the engineering design proof test plan. ES testing will be preformed 100 percent on modules and subassemblies.

6.17.3.5. Acceptance Testing. - For the present IGS there are two levels of acceptance testing performed-- unit and system level.

Unit Level. - Acceptance testing of units of the MGS was implemented in 1965. Up until this time, test philosophy dictated that the MGS acceptance test was the only vehicle for delivery of hardware.

For a period prior to 1965, much test time was put in a MGS before the total performance was acceptable. Systems tests could include 20 to 30 calibrations, component replacements and two or three vibrations of some of the units, before all performance requirements could be met. The implementation of a Unit Acceptance Test (UAT) philosophy was sought for several reasons:

- a. If units perform well enough to be accepted, they should be able to complete MGS system acceptance tests within a minimum of operating time.
- b. Accepted units could be used for maintenance support of systems in the field.
- c. Lower echelon testing is a less expensive means of finding the many problems which had been occupying system test equipment and personnel for extensive periods of time.

The unit acceptance test philosophy provided for vibration of each device while continuously recording critical signals. There was a significant advantage to this approach because a larger total number of functions could be monitored at unit level than could be monitored under system vibration conditions. Each unit vibration was preceded and followed by a set of operational tests. In the case of the platform, inertial component calibrations were also performed before and after the vibration test.

The unit acceptance test philosophy has proved to be satisfactory in all respects except one. The test stations which simulate the MGS interface for each unit must be equivalent or better than the actual airborne hardware. If this is not true, the test results cannot represent the best capabilities of the unit under test, but rather the worst capability of the test station. For a period of time, the platform test station pulse rebalance electronics simulator could not meet the standards of an actual coupler, and platform unit acceptance testing was stopped. A substitute unit acceptance test had to be devised until portions of the platform unit acceptance test station could be improved. The substitute UAT required actual system operation for performing the inertial component calibration portions of UAT. This, of course, was essentially a reversion to the conditions which were precursors of the UAT test philosophy. In retrospect, this problem could have been avoided if the test station design had been better controlled.

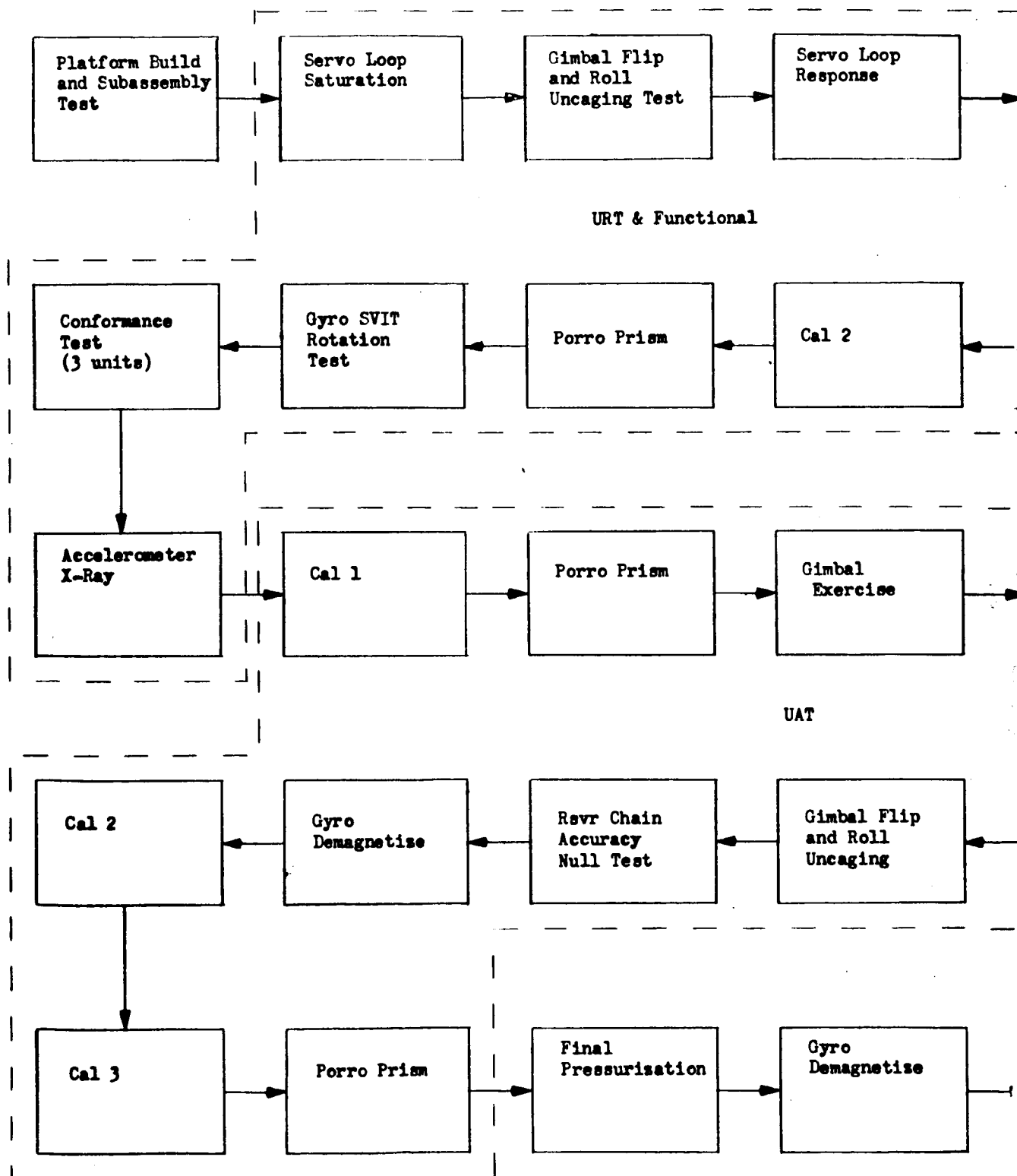
As a result of the UAT philosophy, and the improved Phase II PIP design, system testing can now be completed in a reasonable length of time without multiple failures. Consequently, the systems being shipped have experienced fewer unnecessary operating hours. Although very few IMU devices have been shipped to the field following UAT, the capability is still provided by this test philosophy to maintain signal conditioner and platform electronics for field support. (Generally, platforms and couplers are not shipped as individual units because each Coupler/Platform combination must be individually tuned and performance data history should be maintained.)

Navigation computer unit acceptance tests have included, among several types of testing, a marginal test. Marginal testing of digital equipment is useful for assuring proper operation under varying power supply conditions. (Refer to Topic 5.3.6 for a discussion of this test.) The initial difficulty with implementation of marginal testing was that the conditions of the marginal test were unrealistic. Instead of testing to the specification limits or to the design limits of the hardware, the test conditions were actually outside the designed circuit capability. In 1966, the conditions and limits for marginal test were made compatible with the design requirements and the test has become standard, not only as an acceptance test, but it has become a field test as well.

Flow diagrams of unit acceptance tests performed in production are contained in Figures 6.17-1 through 6.17-5.

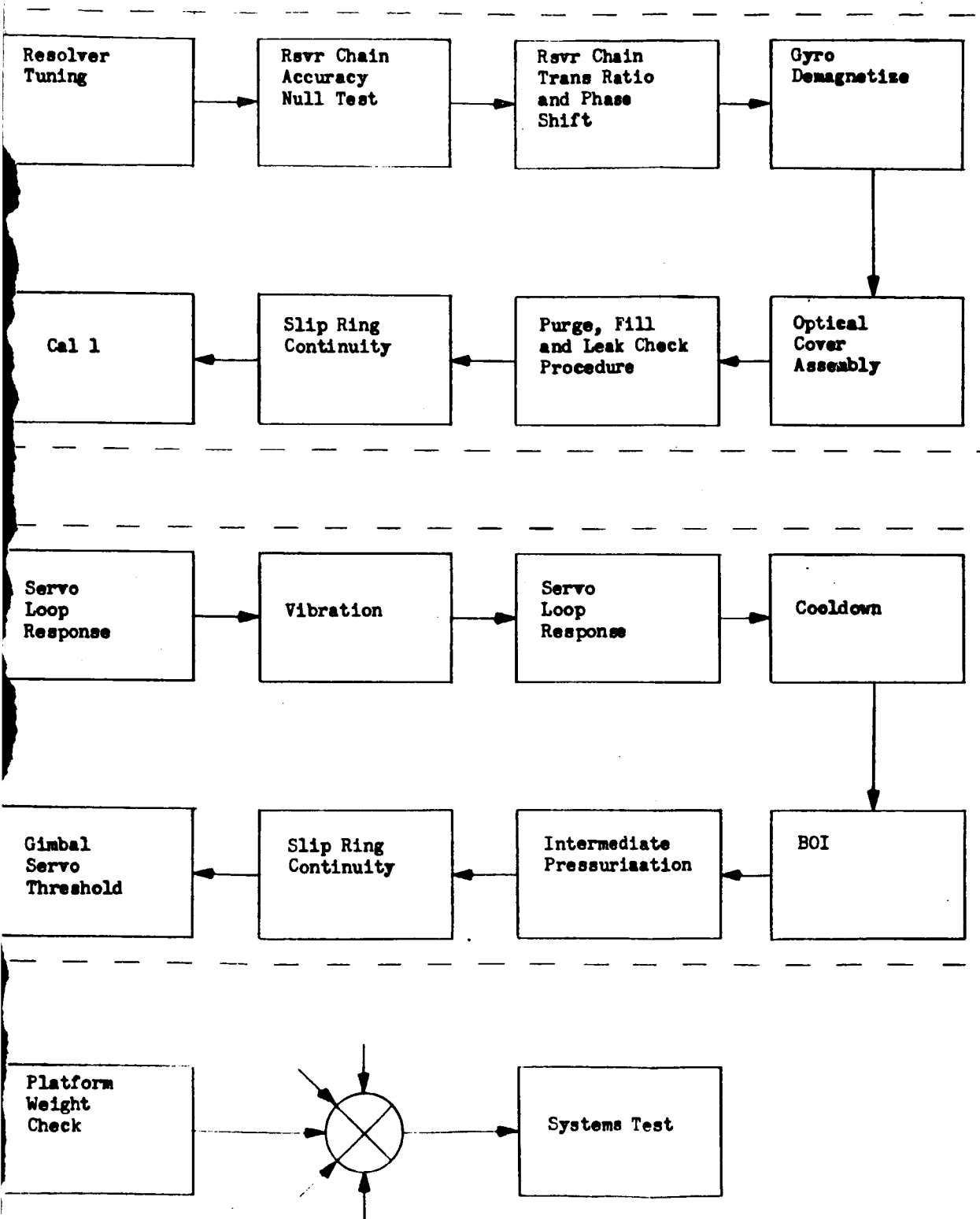
System Level. - The first (-1) Centaur guidance systems shipped to the vehicle contractor were not acceptance tested at Honeywell.

Pre-shipment tests ("OK-to-ship" tests) were performed by Design and Evaluation (Test department) engineering personnel, and not by the Production department. The discussion of disadvantages of acceptance testing outside of the Honeywell facility is presented in Topic 6.17.5.



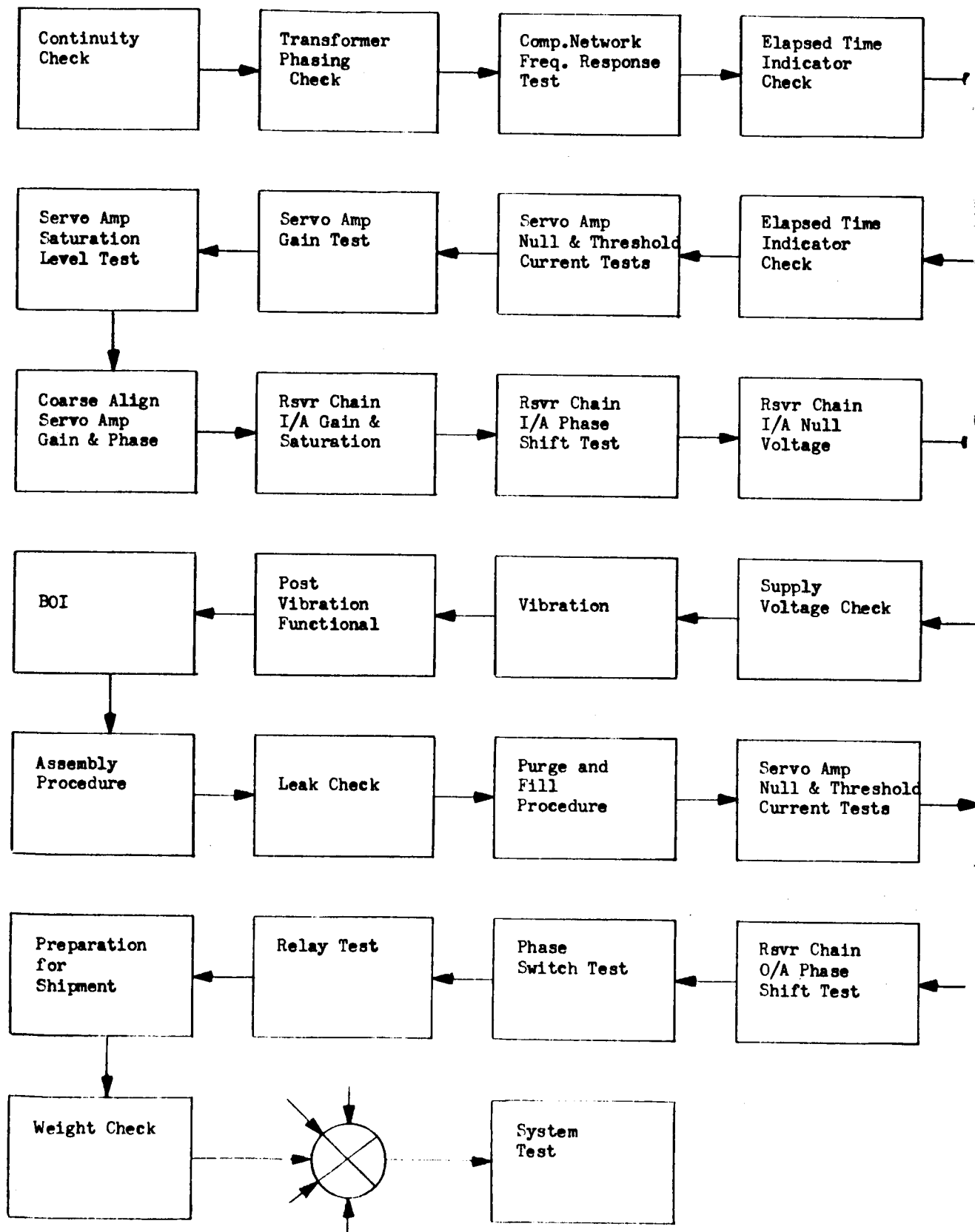
6-17-13

FOLDOUT FRAME

FIGURE 6.17-1. PLATFORM DETAIL
TEST FLOW (REV A)

FOLDOUT FRAME

~~0-17-10~~
6.17-14



6-17-15

FOLDOUT FRAME

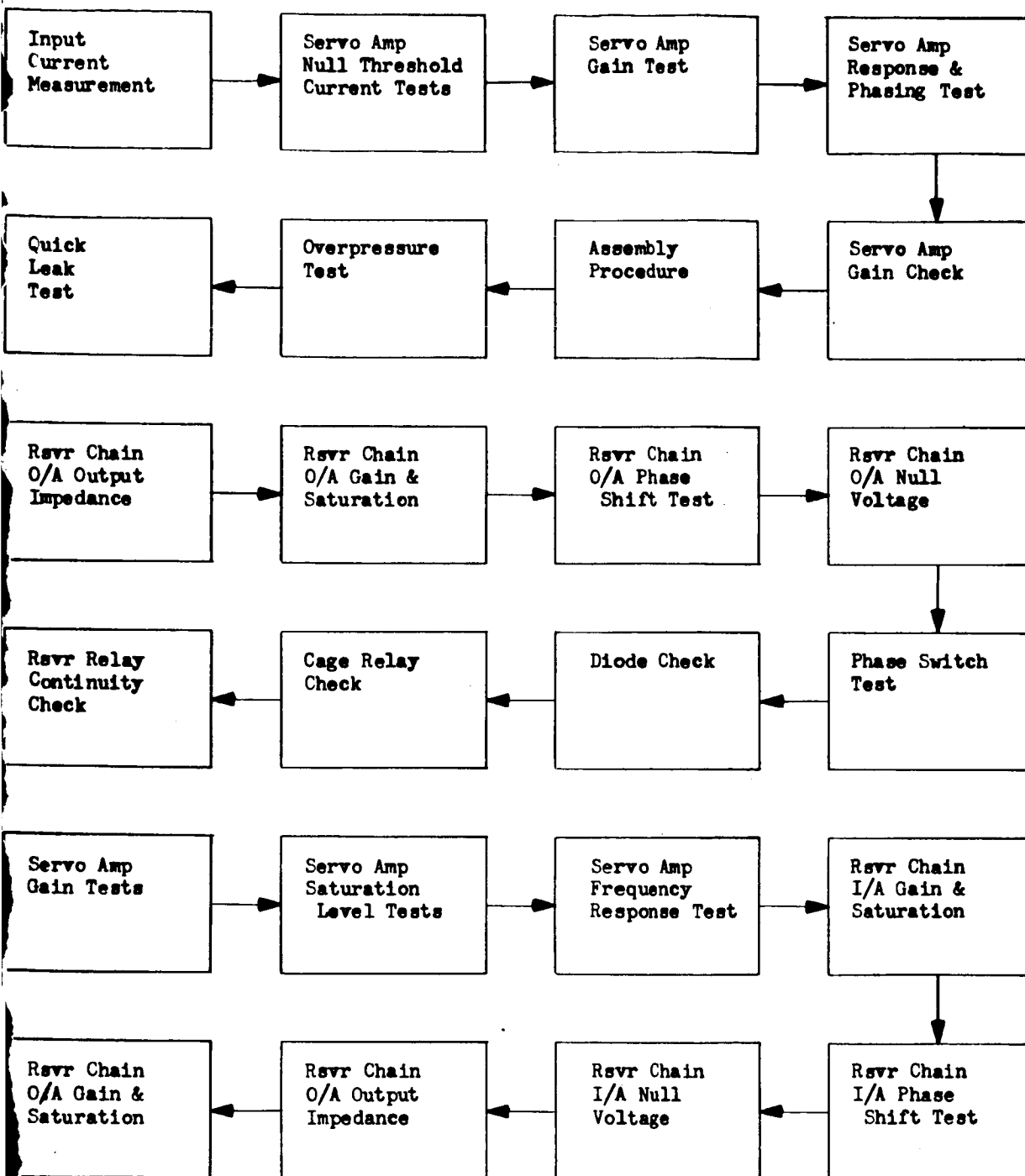
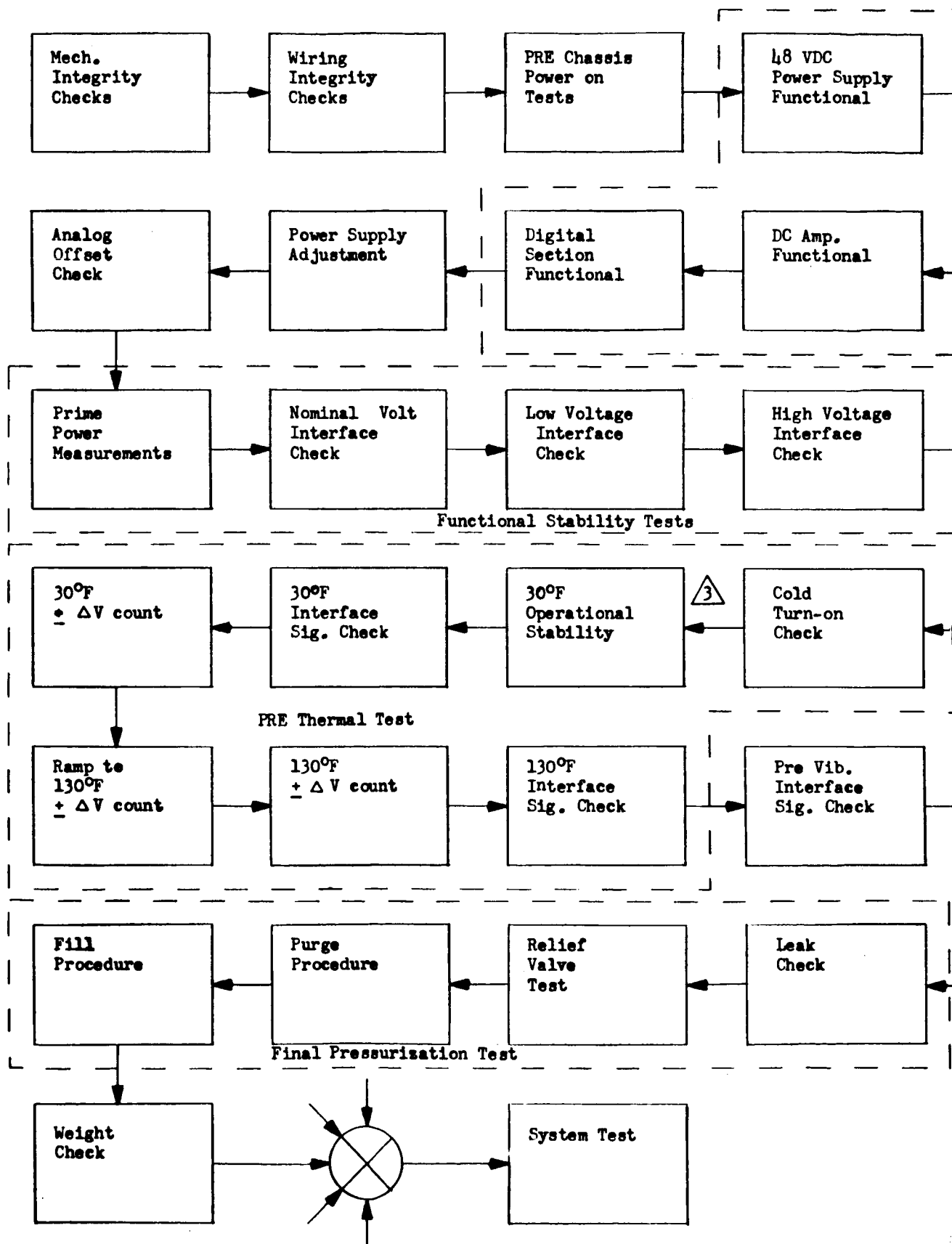


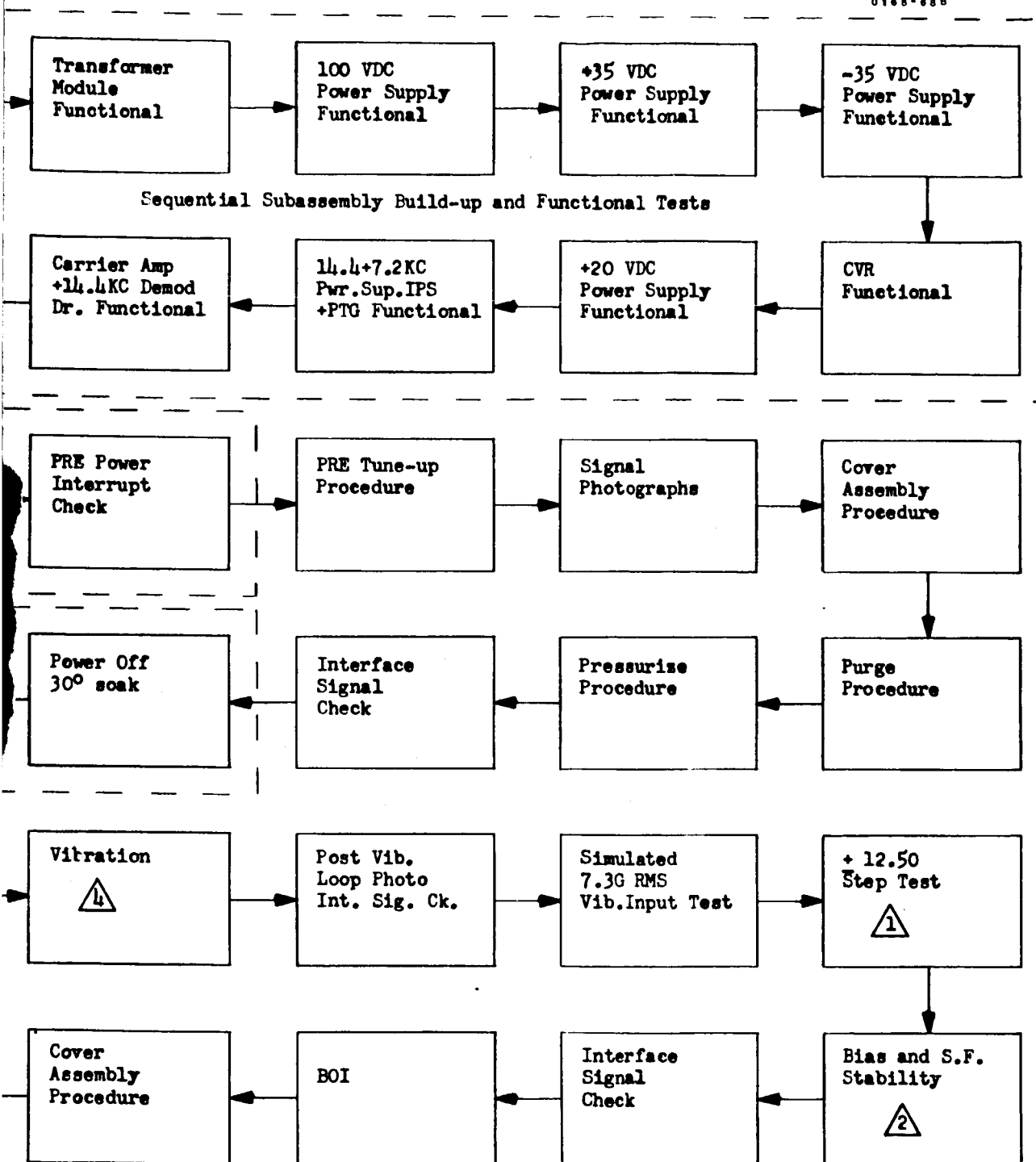
FIGURE 6.17-2. PLATFORM
ELECTRONICS DETAIL TEST FLOW



6-17-17

FOLDOUT FRAME

0166-688



1 Based on testing several GG177 coupler for transient response to $\pm 12.5g$ inputs to accumulate data before incorporating this test.

2 S.F. and Bias Stability; (minimum of 8 sets over 6 hrs.) Record $\pm 22.2VDC$ and GPFS.

3 Three loops simultaneously with three accel. block.
 4 Monitor ARCS Sensing Resistor Voltage during vibration.

FIGURE 6.17-3. PRE DETAILED TEST FLOW

FOLDOUT FRAME

~~6.17-17~~
 6.17-18

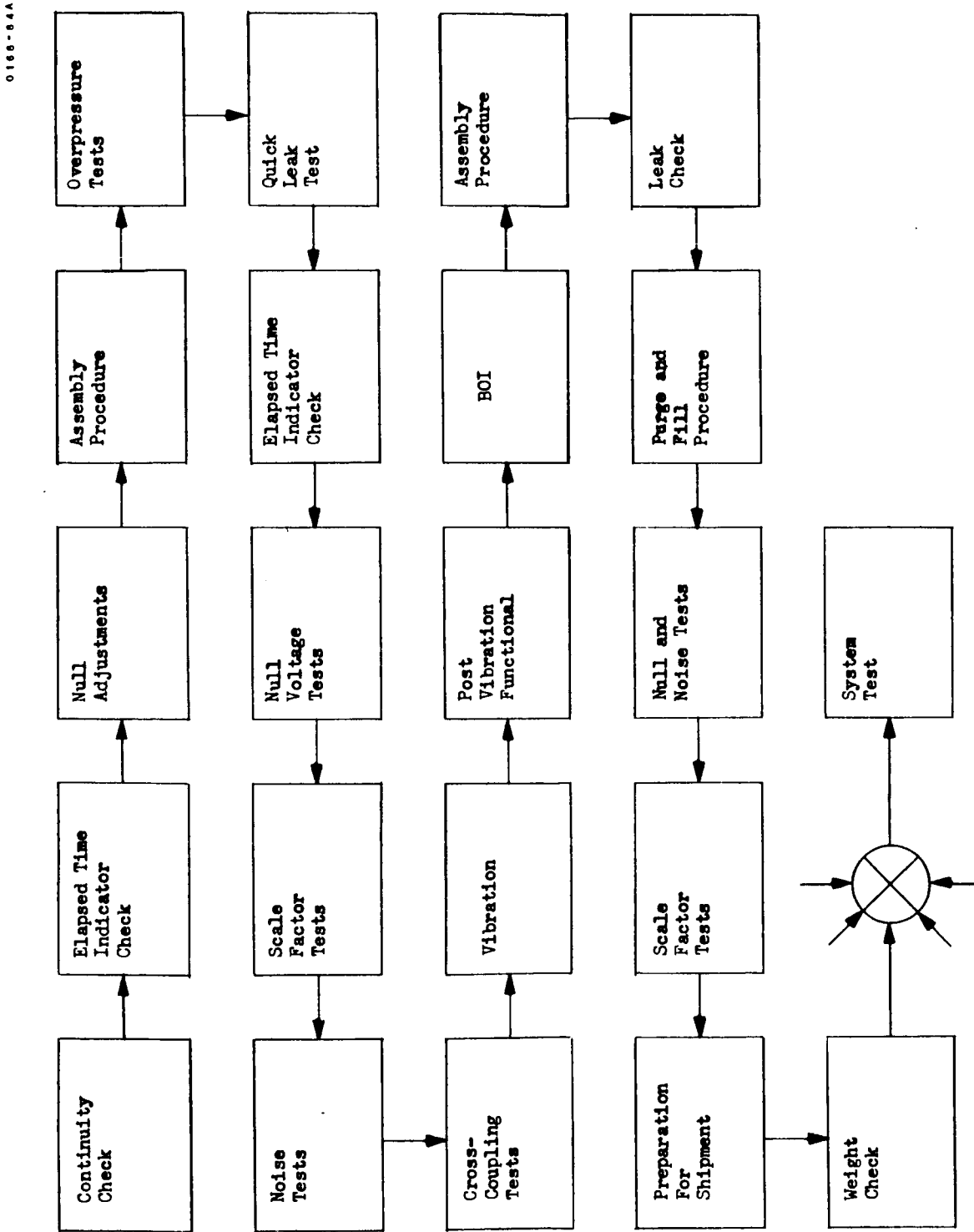


FIGURE 6.17-4. SIGNAL CONDITIONER DETAILED TEST FLOW

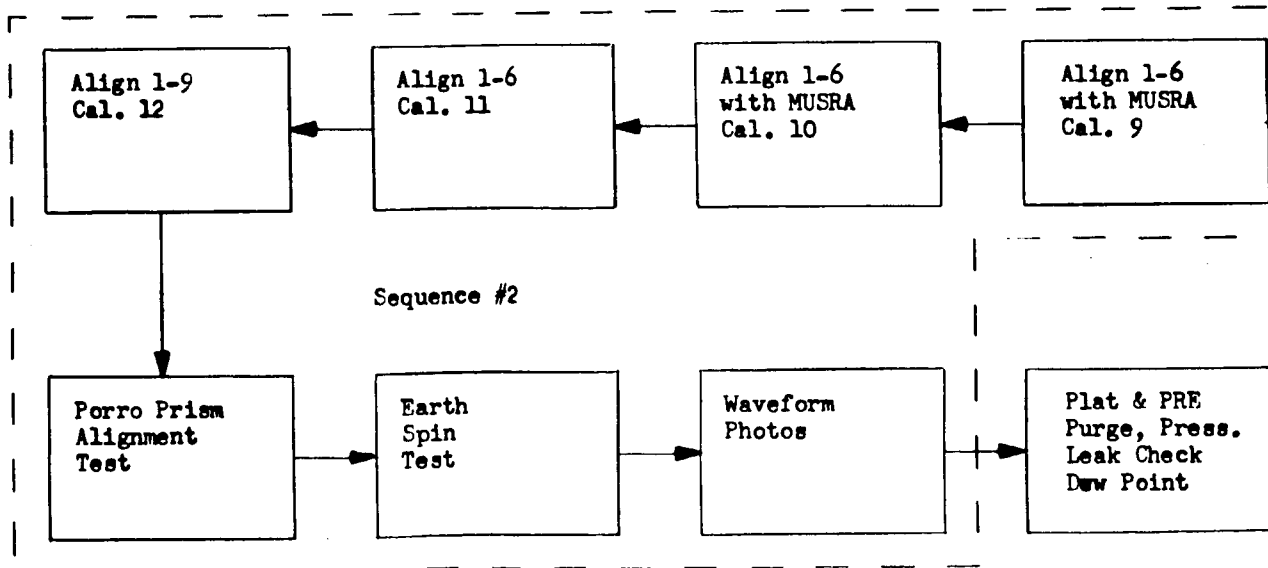
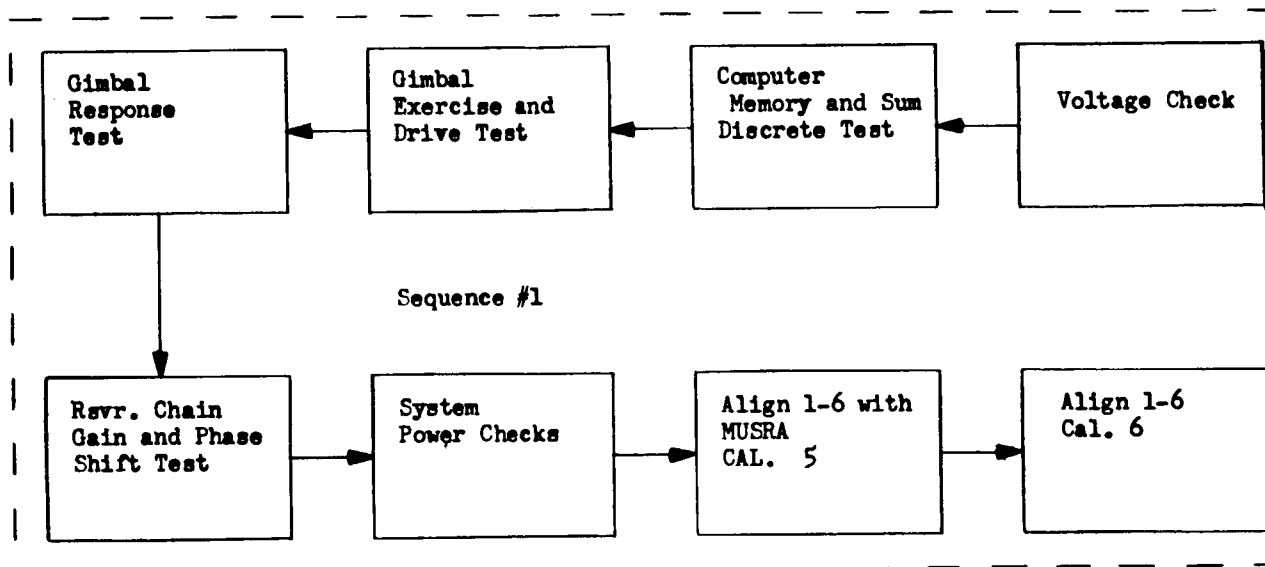
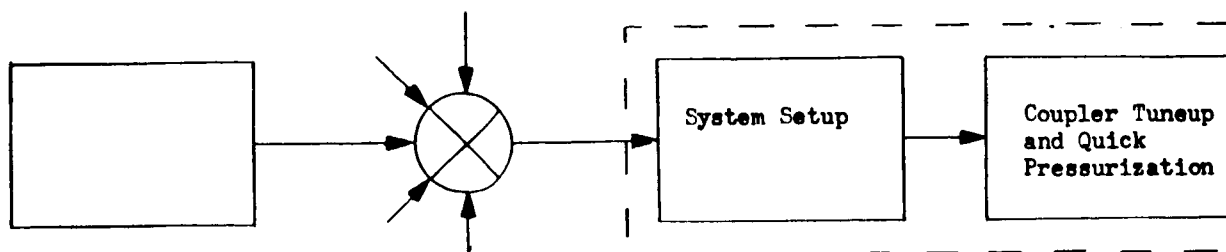
System Acceptance Tests (SAT) became a final production test in 1963 with the -3 Centaur system. The tests performed prerequisite to actual commencement of the SAT were intended to demonstrate a capability to enter SAT. Hence, they became known as "Confidence Tests". Often, confidence was gained only after many MGS calibrations and operational tests.

The SAT in 1963 was a marathon test. There were five calibrations of all system d values, two Earth spin tests, three-axis vibration of all units except the computer, and two cooldowns. With no problems at all, the elapsed time for the test was approximately 105 hours. However, there were problems, and most guidance systems took longer to complete SAT. When the logistics situation became acute prior to one launch, the customer temporarily agreed to a shorter SAT. This greatly aided the guidance system logistics, and the SAT was permanently shortened. The lesson was gained from this experience that acceptance tests can be so long that a point of diminishing value is reached.

The next major improvement in system acceptance testing was the deletion of vibration in the summer of 1965. This change occurred when UAT began. The SAT sequence was reduced by approximately 20 hours, and the need for a post-vibration calibration was eliminated. At this point, the SAT required approximately 40 hours from start to finish, and the probability of success was much improved.

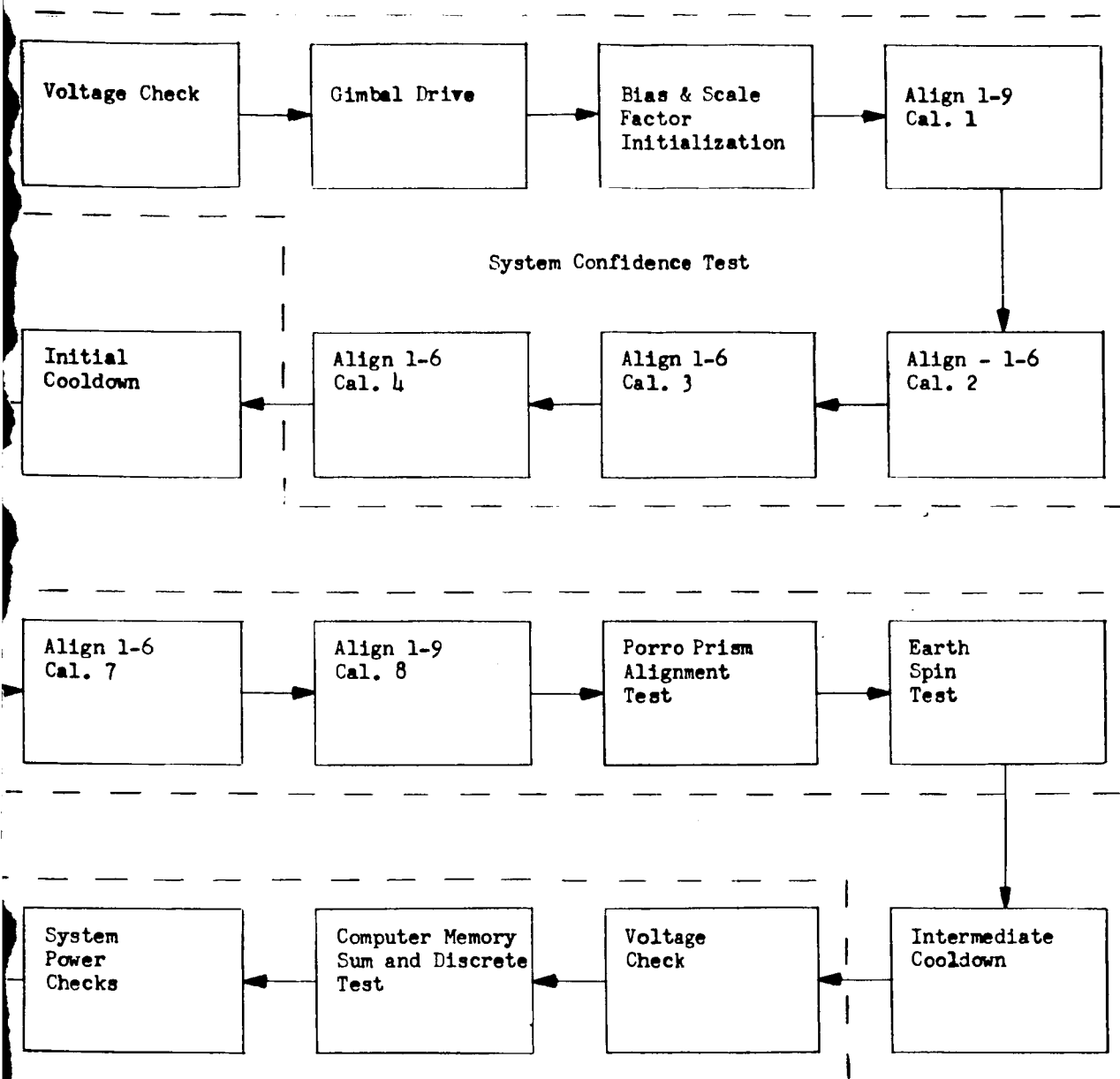
In the spring of 1966 the System Acceptance Test requirements were amended to allow an optional coupler or platform vibration. This occurred concurrently with the UAT test station problems discussed previously. If a UAT station was not operable for calibration of the platform, or if scheduling requirements warranted it, the limited system level vibration option could be exercised.

ADD-6 test requirements altered the form of the acceptance test considerably. NASA-LeRC wanted to have added inertial component calibration points without a reversion to the earlier test marathons. Thus, the acceptance test took the form of two test sequences separated by a single system cooldown. Each sequence contains four calibrations back to back without intervening tests. Three of these calibrations are called "quick six" or "short cal" because the full nine align modes are not run (the accelerometer orthogonality is not calibrated). The quick six calibration requires approximately three hours, so the total SAT length is not unreasonable. A larger data sample is thus obtained, upon which a better statistical estimate of performance can be made. Figure 6.17-5 is the



6-17-21

FOLDOUT FRAME



- Note: 1. Align 1-9 includes MUSRA.
 2. Cooldown is 6 hours or 3 hours with forced air.
 3. Ref. R-ED 21110, Rev. G

Ship

FIGURE 6.17-5. SYSTEM
 CONFIDENCE AND SAT TEST
 (REV A)

the flow diagram for the present SAT. The acceptance test is preceded by a limited number of calibrations (specified by ES) to prove the suitability of the hardware for acceptance testing.

Design Engineering Support of Production Testing. - In the early stages of design for production there must be effective communication between the designer and the production engineer. The technical problems present in early Centaur development required continued production support by unit and system design engineers, well beyond the initial stages.

In late 1964, a task team of system and unit design engineers and production engineers was formed to accomplish all fault isolation and testing of new build and returned -3 Centaur guidance systems. A key feature of this group's charter was the physical location of design, evaluation, and production engineering in the area where the build and test activity occurred. The grouping of all systems test equipment and systems test personnel into one organization and location afforded optimum use of test equipment and personnel. The worth of this type of testing organization had been demonstrated on another Honeywell system program, and the -3 Centaur system test situation required effective action. The group was identified as the Systems Evaluation and Test (E&T) group.

The responsibilities of this group were:

1. Analysis of unit level data to assure that no unit reached system tests unless it was fully qualified.
2. Scheduling and performance of all system testing-- both ES and acceptance testing.
3. Analysis of all system test data to insure that every characteristic was nominal, and that the system was completely flightworthy.
4. Investigate and develop solutions for problems which occur during systems tests.
5. For guidance systems returned from the field (RGs), develop fault isolation plans, and execute them.
6. Establish rework and retest plans to requalify RGs for flight.
7. Maintain control of unit and acceptance test philosophy and test procedures.
8. Provide designer-production joint solutions to process and build problems encountered.

The efforts of this group continued for over a year, and results were better than hoped for. Guidance systems were tested, shipped, and remained in the field as never before. The production engineers gained more insight into fault isolation and analysis and design engineers gained an appreciation for the types of problems encountered in production.

6.17.3.6. Conclusions. - The funneling of specifications for process tests between assembly levels should be a goal in both the hardware design and in the establishment of specifications. Many of the early Centaur problems could have been avoided if this precept had been held.

Thermal process testing of couplers was found to be not only an effective screening test, but also provided design deficiency data to the designers. This, in turn, was used to improve the subassembly designs, and to monitor build process proficiency.

Marginal testing of the digital navigation computer has been an effective means in establishing a high level of confidence in computer operation by verifying proper operation under non-nominal conditions of prime power and B+ voltage variations. Furthermore, computer testing under marginal voltage conditions has proven to be a useful technique in fault isolation, particularly in isolating malfunctions which occur intermittently under nominal operating conditions. In future planning for marginal testing, the hardware design limits should be well defined, and the test conditions should not exceed these limits.

Worst-case design and successful production process tests go hand-in-hand. The only real progress in production test results came after the designs were optimized. The alternative was found to result in a seemingly endless process of ES test, repair and ES test again, in order to yield any product.

Acceptance tests, too, benefited from the improvements brought by the redesign and engineering evaluation programs. The acceptance testing of units (of the MGS) proved to be a good prerequisite to system acceptance tests. The unit which has passed the lower level acceptance tests was found to have a much greater probability of completing system tests without problems. The UAT philosophy also provided a means of supporting systems in the field with certified spares. System acceptance tests should be planned to minimize the testing time. Once the testing has established the integrity of a system additional testing becomes of little value. At the time when production testing problems were critical, Honeywell found a joint production-engineering evaluation and test team was a most effective solution. The close working relationships between design and production developed timely and effective answers to problems.

6.17.4. Test Equipment Certification. - This section will discuss the concepts involved in test equipment accuracy requirements and certification policies and procedures which assure that the test equipment requirements will be met.

6.17.4.1 Test Equipment Accuracy Requirements. - Testing is performed to determine that the MGS and the circuits comprising the MGS meet design

requirements. In order to efficiently determine this, the test equipment used must have the capability of measuring parameters to accuracies and stabilities greater than the basic MGS requirements.

Ideally, test equipment accuracy should be such that the measurement error is insignificant compared to the MGS circuit stability requirements. Many MGS circuit requirements are very tight, therefore, trade-offs are often necessary due to the high costs involved when purchasing high accuracy instruments. Often, instruments having sufficient accuracy to make the measurement accuracy insignificant are unavailable.

The Centaur MGS test equipment accuracy philosophy is that, where possible, the test equipment should be capable of making measurements with a 10:1 ratio between instrumentation errors and MGS circuit requirements. Where strict MGS requirements are such that test equipment is not available or cannot be built within reasonable cost, a compromise to the 10:1 ratio is made, with a 3:1 ratio becoming acceptable.

6.17.4.2. Factory Test Equipment. - Factory Test Equipment (FTE) policies and procedures should provide a full spectrum of controls to assure that the test equipment is and remains capable of performing its required function(s).

Commercial test equipment is purchased based upon the manufacturers published specifications. Periodic preventive maintenance and certification is performed to assure that the equipment continually meets requirements. The maintenance and certification requirements for Centaur FTE have steadily improved to the present close controls which now exist over all phases of maintenance and certification.

Test equipment unique to guidance testing or unobtainable commercially is designed and built at Honeywell. The philosophy used to determine that a unit of test equipment meets the requirements for MGS test is similar to the design, build, test, and certification requirements for airborne hardware. The standards used are less strict than for airborne equipment since operational, environmental, maintenance, and reliability requirements are different, but they must be effective, nevertheless, if MGS and unit test requirements are to be met.

6.17.5. Post Shipment Ground Testing. - Centaur guidance testing performed after shipment from the Honeywell facility has undergone significant changes.

Abbreviated test sequence flow charts are shown in Figures 6.17-6, 6.17-7, and 6.17-8. These flow charts illustrate the major phases of testing at GD/C, San Diego and at ETR.

6.17.5.1. -1 MGS Post Shipment Testing (Figure 6.17-6). - System tests prior to shipment consisted of performance and functional testing under laboratory conditions. These tests were classified as "OK to ship tests". Upon arrival at GD/C, San Diego, the system underwent acceptance testing. The acceptance testing consisted of a series of performance and functional tests, vibration testing of all units except the computer, and another series of performance and functional tests. Computer vibration was performed at the Kearfott facility.

The acceptance testing subjected the MGS to more stringent tests than the "OK to ship tests". This created many problems. Failures requiring return of the MGS to Honeywell frequently occurred. This significantly lengthened the rework time and increased the cost of keeping systems in the field.

At that time the ETR test sequence was poorly defined, based upon today's standards. Launch day confidence was therefore limited both by lack of confidence in testing and by the marginal reliability of the system (Topic 6.17.2.2).

6.17.5.2. -3 MGS Post Shipment Testing (Figure 6.17-7). - Early in the -3 MGS phase of the program and prior to shipment of any -3 systems, agreement was reached (February 1963) to perform MGS acceptance testing with vibration at the Honeywell facility. Again the computer was vibrated during its acceptance test at the Kearfott facility. This was a major milestone in the development of MGS test philosophy.

Later in 1963, steps were taken to make firm definition of test requirements and philosophy for all guidance testing. The major decisions were:

1. To develop uniform requirements for guidance testing at all sites. At this time Honeywell had been working on "MGS Operational Procedures" in an attempt to better define MGS testing in a manner that was applicable to all sites. GD/C began work on a "Unified Test Plan (UTP)" document for the entire Centaur Vehicle including a section for the MGS. The UTP was to define the detail test requirements for all vehicle systems.
2. A groundrule that platforms and couplers, once married during acceptance testing should remain together through all field operations.
3. The establishment of the "Operation Working Group" with members from each contractor and government agency involved. The charter of the group was for formulation of standardized test procedures.

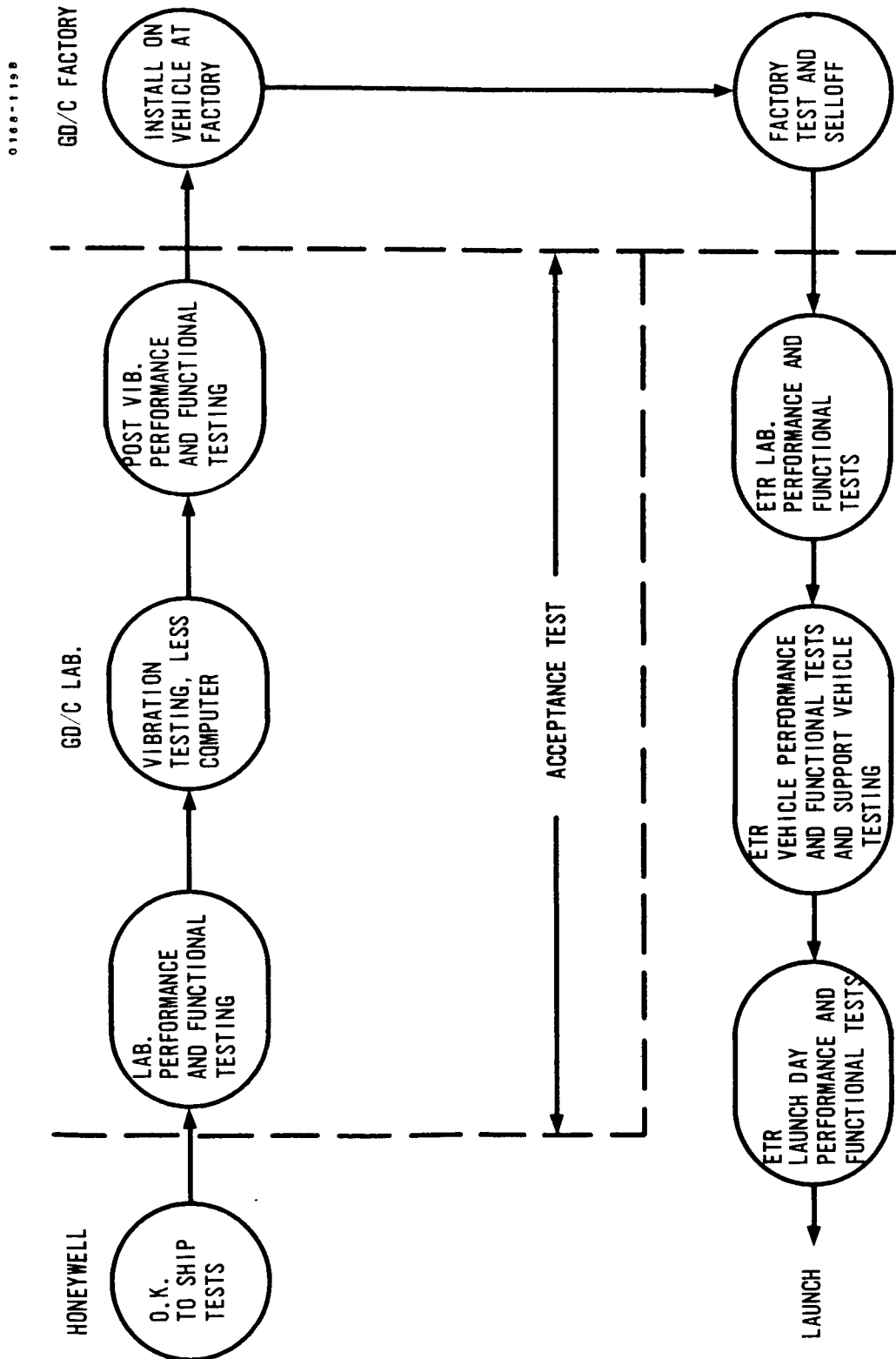


FIGURE 6.17-6. -1 MGS POST SHIPMENT TESTING (1959-1962)

0100-124A

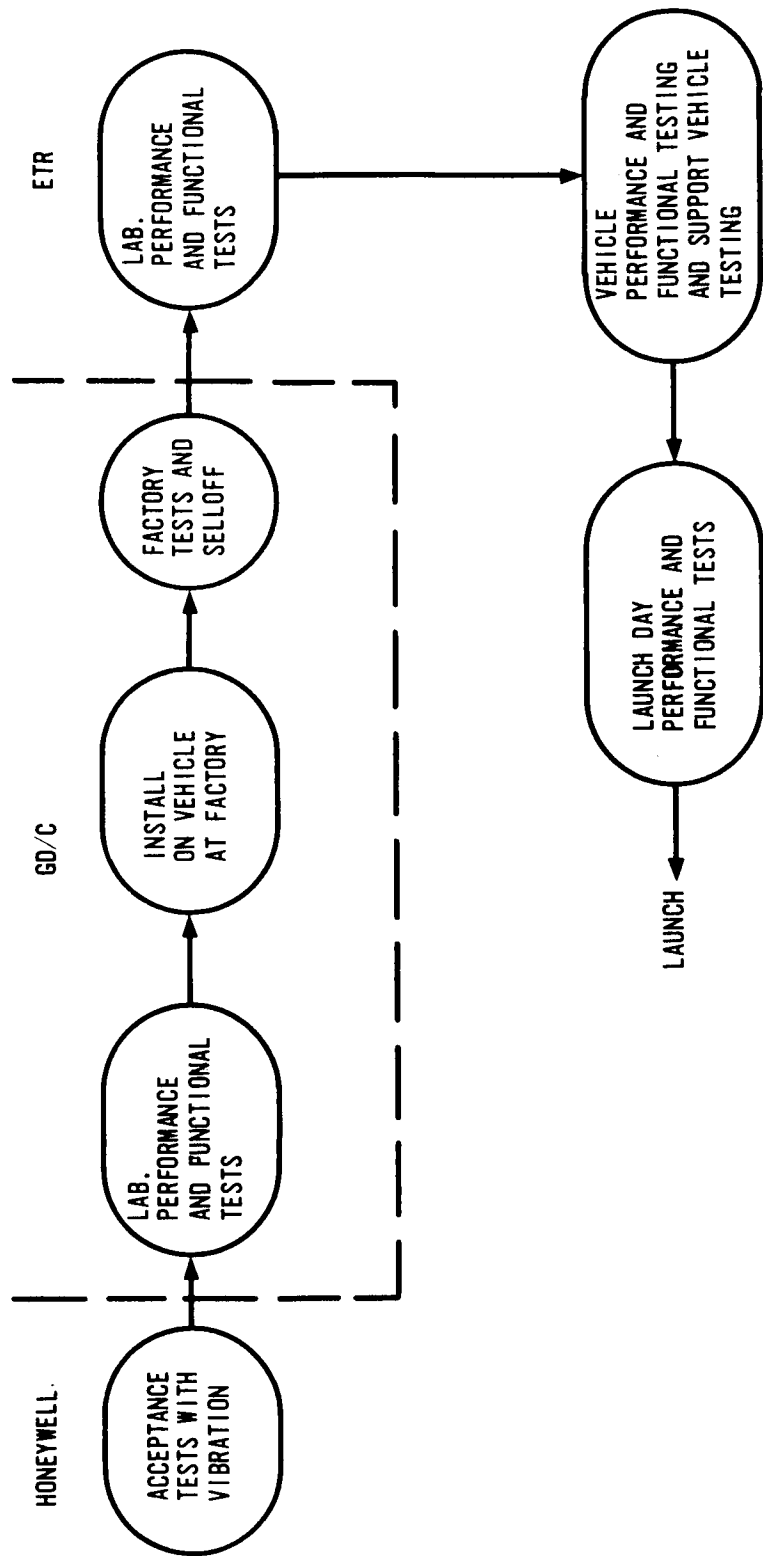


FIGURE 6.17-7. -3 MGS POST SHIPMENT TESTING (1961-1965)

The objective of this group was never fully realized. Standardized operational procedures have never been agreed upon for use at all field sites. The UTP has become a fully approved, standardized test requirements document but lacks the procedure detail.

Apparently the major reason for the lack of standardized operational procedures is that differences in test equipment at the various sites developed throughout the program. These, combined with differences in philosophy, between contractors prevented clear definition of standardized procedures.

6.17.6. Phase II PIP MGS Post Shipment Testing (Figure 6.17-8). - From the time of the -3 MGS to the present day, test requirements and philosophy continued to become better defined. The major change in test sequence has been the establishment of the CSTS "Combined System Test Stand" facility at GD/C, San Diego in 1965. This facility has since been deactivated (late 1967).

6.17.7. Conclusions. - The most severe MGS testing should take place at the manufacturing facility, where repairs are most efficient.

Comprehensive test philosophies should be agreed upon early in the development program. The requirements should be well defined and sufficiently detailed to provide assurance that MGS performance and reliability requirements will be met. Detail requirements can probably best be made by guidance contractor preparation with review by a working group composed of the representatives from each agency and contractor who are most familiar with the detailed testing.

6.17.8. Flight Test Program. - In addition to many phases of ground testing, Centaur guidance has undergone extensive flight testing associated with both the Atlas piggyback flight and eight Atlas-Centaur development flights. The guidance role during the flight tests began with open loop guidance evaluation and ended with guidance performing its full intended function.

At this point reference can be made to the historical summary of the Centaur Program contained in Topic 1.1. A brief recap of Centaur flight history is presented there.

6.17.8.1. Flight Summary. - This topic will present a more detailed discussion of the objectives and results of each flight test followed by a

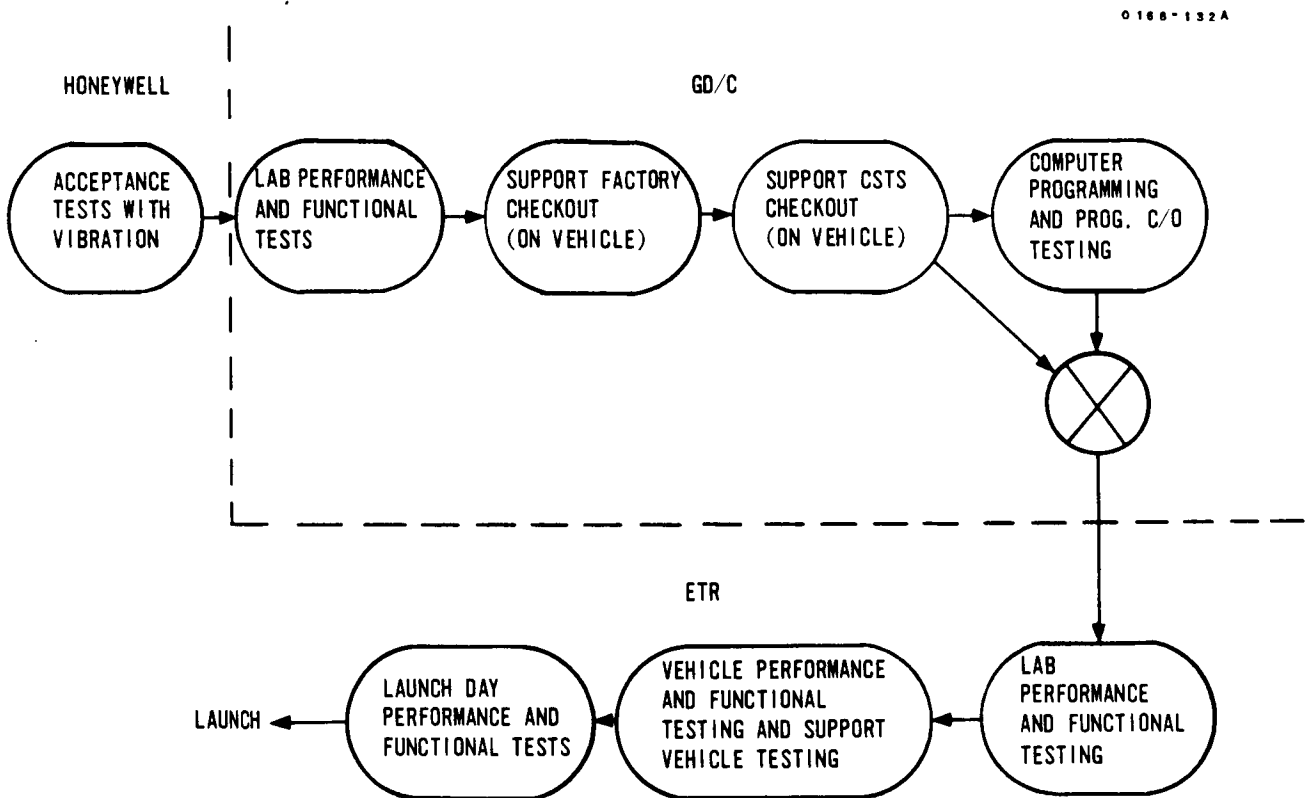


FIGURE 6.17-8. PRESENT DAY PHASE II PIP
POST SHIPMENT TESTING (1965-1967)

critique and recommendation. Since guidance evaluation is a continuous function, and as such was performed on all missions, information on the operational flights is included.

6.17.8.2. Piggyback (Centaur MGS 4 installed in Scientific Passenger Pod #7 which was attached to Atlas missile 25E) 2 October 1961.

Vehicle Objectives. - To provide a simulated Centaur flight environment in which the MGS could be operated and evaluated.

Guidance Function. - To operate in an open loop flight mode and provide signals indicative of MGS performance for telemetering.

Vehicle Results. - The desired flight environment and trajectory were achieved. Vibration measurements showed the Inertial Platform was subjected to 11.5 g rms maximum and up to 0.36 g^2 /cps with a predominant frequency of 1400 cps. The trajectory was that of an R&D test for a military re-entry payload. Atlas thrust terminated at about 300 seconds after liftoff. Thermal data showed about 20°F skin temperature increase for the MGS units during flight. About 1200 seconds of flight data were obtained before loss of telemetry.

Guidance Results. - Voltage transients at umbilical ejection caused the MGS Digital Computer to go into a Standby condition. Launch was accomplished with this condition which is a non-computational mode, therefore, no useful inflight Computer digital data were obtained. With only analog data a detailed, quantitative post flight evaluation was not possible. Data from accelerometer loops and gimbal stabilization loops indicated good stability and satisfactory performance throughout the flight. The steering signal inputs to the coordinate transformation chain were fixed values during flight. The steering output signals from the Platform showed the vehicle tumbling after payload separation from the Atlas. Rates up to 10 degrees per second were indicated. From the available data the MGS functional performance was entirely satisfactory.

6.17.8.3. AC-1, MGS 3, 8 May 1962. -

Vehicle Objectives. - To launch the Atlas/Centaur vehicle into a ballistic trajectory with a maximum altitude of 274 nautical miles and a range of 1059 nautical miles. The flight was to also demonstrate the structural integrity of the Atlas/Centaur vehicle, demonstrate the comparability of the Atlas and Centaur stages, evaluate the performance of the hydrogen fueled Centaur engines during second stage powered flight, and show restart capability in space.

Guidance Function. - To provide a stable attitude reference and generate appropriate steering signals and discretes to steer the Centaur vehicle into the planned ballistic trajectory. During the free-fall phase, the guidance computer equations were to be used to reorient the vehicle along the inertial W axis, and then steer the vehicle as it was fired in an almost vertical direction toward the Earth.

Guidance Results. - During prelaunch, difficulties were encountered when the electrical power was switched from external to internal vehicle power. This problem prevented the use of level hold immediately prior to launch, and the system was launched from coarse align with 3 degrees of misalignment. Less than perfect operation of the accelerometer loops was indicated during flight, but premature flight termination prevented a thorough analysis of the problem. Analysis might have been more complete if the telemetry channels had been of greater bandwidth.

6.17.8.4. AC-2, MGS 13, 27 November 1963. -

Flight Objectives. - To demonstrate the structural integrity of the Atlas-Centaur combination, the Atlas-Centaur separation system and the capability of the Centaur vehicle to operate in flight. Also, to demonstrate the capability of on-board systems to operate in the flight environment. Planned trajectory was direct ascent into elliptical orbit of approximately 340 n.m. perigee and 1000 n.m. apogee.

Guidance Functions. - To provide attitude reference and transformation of auto-pilot programmed steering vectors into vehicle co-ordinates. To operate in a flight mode and compute actual flight trajectory and generate steering signals, not to be used for controlling the vehicle, but to be telemetered to the ground for evaluation.

Guidance Results. - Attitude reference stability and steering vector transformation accuracy were excellent on the basis of telemetered data. The data indicated that the open loop trajectory computations were within the specified accuracy requirements.

6.17.8.5. AC-3, MGS 14, 30 June 1964. -

Flight Objectives. - To further qualify the Atlas-Centaur and all on-board systems for operational flight and to verify the integrity of a new nose fairing and insulation panel design. Planned trajectory was the same as for AC-2. This launch had been previously aborted due to W accelerometer bias and scale factor shifts in MGS 16 as indicated by the prelaunch MGS calibration. MGS 16 was replaced by MGS 14.

Guidance Functions. - To provide attitude reference and transformation of autopilot programmed steering vectors into vehicle coordinates. To operate in a flight mode and compute actual flight trajectory and generate steering signals, not to be used for controlling the vehicle, but to be telemetered to the ground for evaluation.

Guidance Results. - During the normal portion of the flight, the guidance system performed without anomaly although there was evidence of a pre-flight misalignment. Also, the MGS Computer experienced excessive shock due to impact of fragmented sections of the nose fairings at nose fairing jettison. This vehicle malfunction caused the MGS Computer to temporarily perform improper calculations. Attitude reference was maintained during the buildup of extreme angular rates caused by loss of hydraulic pressure in one engine actuator system. Several gimbal flips were successfully completed during the high rates although reference may have been lost during a gimbal flip when gimbal 2 apparently hit its stops.

6.17.8.6. AC-4, MGS 24, 11 December 1964. -

Flight Objectives. - To provide an instrumented test flight for verification of the Atlas-Centaur vehicle and all on-board systems. These items were of particular significance:

- a. This was a one-burn with a post-mission coast phase and second-burn experiment. That is, the Centaur engine was to be shut down and restarted in flight.
- b. This was the first flight in which the MGS was to be operated closed loop: i. e., to actually control the vehicle.
- c. This was the first flight of the improved nose fairing and insulation panel jettison system.

Guidance Function. - Compute the flight trajectory and issue steering signals for use in controlling the vehicle flight path. Issue Centaur engine cut-off signals based on missile thrust velocity for both Centaur powered phases.

Guidance Results. - The MGS guided the vehicle into an accurate circular orbit at the conclusion of Centaur first-burn. Vehicle coast phase problems created high reaction forces and vehicle tumbling. The guidance platform eventually tumbled once the vehicle rates became too violent.

6.17.8.7. AC-5, MGS 26, 2 March 1965. -

Flight Objectives. - To provide an instrumented test flight for verification of the capability to lift a Surveyor into an actual lunar transfer orbit to achieve spacecraft separation and to demonstrate the variable launch azimuth capability.

A dummy Surveyor was used and JPL DSIF tracking was provided.

Guidance Functions. - To compute flight trajectory and to generate signals for use in controlling the vehicle to a direct ascent lunar transfer. Also to provide steering signals for the reorient and retro maneuvers after the powered phase of flight which results in wide separation of the Centaur and Surveyor vehicles.

Guidance Results. - The flight was terminated essentially at lift-off and was too short to allow any significant guidance data to be obtained.

6.17.8.8. AC-6, MGS 27, 11 August 1965. -

Vehicle Objectives. - To demonstrate a variable launch azimuth capability, fly a direct ascent trajectory steered by an inertial guidance system and place a Surveyor payload model into a simulated lunar transfer orbit to impact the moon's surface. The vehicle launch time was intentionally biased to prevent an actual lunar impact.

Guidance Function. - To steer the Centaur vehicle and Surveyor spacecraft to injection into a simulated lunar trajectory. The system also was to provide engine cutoff discrettes to command the proper injection velocity. After spacecraft separation from the vehicle, the MGS was to reorient the Centaur vehicle for the retro thrusting maneuver.

Guidance Results. - This flight allowed the Atlas/Centaur missile and its systems to be declared operational for future direct ascent missions with a Surveyor Spacecraft. All Guidance System objectives were achieved to well within expected limits. This flight was the first time that an all inertial system guided a vehicle into deep space. Analysis of tracking data showed that if this had been an actual lunar mission, impact would have occurred on the edge of the crater Copernicus with no midcourse trajectory corrections. The programmed "pseudo" target location was 240 nautical miles from the simulated impact point. The guidance mid-course correction requirement was 6.6 meters per second.

6.17.8.9. AC-8, MGS 30, 7 April 1966. -

Flight Objectives. - To demonstrate the capability of the Atlas-Centaur vehicle to perform a two-burn mission, to demonstrate the performance of the improved guidance system (using GG177 accelerometers), and to place a Surveyor payload model into a highly elliptical simulated lunar transfer orbit. As with the AC-6 flight, the vehicle launch time was intentionally biased to prevent an actual lunar impact. The nominal two-burn mission consisted of the Atlas engines and first burn of the Centaur engines boosting the Centaur vehicle and spacecraft payload into a 90 nm near circular orbit around the Earth. After coasting in orbit for 25 minutes, the Centaur engines were to reignite and be steered by the MGS into a highly elliptical lunar transfer orbit.

Guidance Function. - To provide proper steering and discrete signals to the Atlas and Centaur flight control systems during the closed-loop, two-burn mission to inject the Surveyor model into the lunar transfer trajectory. After spacecraft separation the MGS was to steer the Centaur vehicle into the proper reorientation attitude for retro thrusting. The retro thrusting was performed so that on future operational missions the Centaur vehicle would be separated from the spacecraft a sufficient distance to preclude the Surveyor sun tracker from locking on to the vehicle rather than on to the Sun.

The MGS provided the following Primary Discretes:

1. BECO (Atlas Booster Engine Cut Off)
2. 1st MECO (Centaur First Main Engine Cut Off)
3. SET/VECO (Start "B" Timer/Vernier Engine Cut Off)
4. 2nd MECO (Centaur Second Main Engine Cut Off).

The MGS provided steering signals during the following phases:

1. Atlas Sustainer Thrust Phase
2. First Centaur Thrust Phase
3. Centaur Coast Phase
4. Second Centaur Thrust Phase
5. Centaur Reorient, Retromaneuver, and Post-Retromaneuver Phases.

Guidance Results. - The guidance system performed well within expected limits. Had this been an operational flight, a 5.3 meters/second midcourse correction would have been required to compensate for guidance hardware errors. Due to the failure of the Centaur to achieve a successful

second burn (attributed to an H_2O_2 system leak), the guidance equations and steering accuracy for the second burn could not be evaluated.

6.17.8.10. AC-10/Surveyor A, MGS 12B, 30 May 1966. -

Flight Objectives. - Using a direct ascent trajectory with a variable launch azimuth, the Atlas/Centaur vehicle was to place a Surveyor Spacecraft (SC-1) into a lunar transfer orbit so that the spacecraft could soft-land on the Moon's surface.

Guidance Function. - As this was an operational flight, the MGS was required to guide the vehicle and spacecraft to injection into a lunar transfer orbit. After spacecraft separation, the guidance system was to command the reorientation of the Centaur vehicle for the retromaneuver. During the flight, the MGS issues the following discretes:

1. BECO (Booster Engine Cut-Off)
2. MECO (Main Engine Cut-Off)
3. SECO/VECO backup (issued when -0.7 g acceleration sensed, indicating fuel depletion).

The MGS provides vehicle steering during the following phases:

1. Atlas Sustainer Thrust Phase
2. Centaur Thrust Phase
3. Centaur Reorient and Retromaneuver.

Guidance Results. Guidance system operation was good throughout the flight. The lunar orbital injection was so near optimum that the Mid-course Velocity Correction requirement was only 3.8 meters/second. Of this amount, only 1.6 m/sec was attributable to guidance.

6.17.8.11. AC-7/Surveyor B, MGS 16B, 20 September 1966. -

Mission. - Using a direct-ascent from 36A, the AC-10 vehicle was to inject Surveyor B into a translunar orbit. Touchdown was to be 0.67 deg/W long, 0.9 deg/N lat in the Sinus Medii.

Guidance Function. - The MGS was to provide measurements and corrections to inject the spacecraft into the lunar transfer orbit. Following

separation, a Centaur reorientation and deceleration would be commanded by the guidance computer. Flight discrete commands to be issued were BECO, SECO backup, and MECO. Steering phases were:

- a. Atlas Sustainer Burn
- b. Centaur Thrust
- c. Centaur Reorient.

Guidance Results. - The precision of orbital injection produced a lunar target miss of 87.4 nautical miles without mid-course correction. The correction requirements at midcourse (20.5 hours) were 1.16 m/sec. (miss only) and 1.20 m/sec (miss plus time).

6.17.8.12. - AC-9, MGS 18D, 26 October 1966. -

Flight Objectives. - The AC-9 vehicle was the final planned developmental flight vehicle. Objectives included demonstration of two-burn Centaur operation, flight testing of the improved (Phase II PIP) missile guidance set, demonstration of launch-on-time capability, utilization of guidance-augmented steering programs during the boost phase, and injection of a Surveyor mass model into a translunar orbit.

Guidance Function. - During the boost phase, guidance provided delta pitch and yaw commands from the computer (based upon pre-launch winds aloft measurements). The in-flight discrettes required were BECO, SECO backup, and MECO (twice). Steering phases were the same as for previous flights, except that booster steering augmentation was used.

Guidance Results. - The miss only 20-hour MCR for the flight was determined to be 6.5 meters/sec. Of this total, software and engine decay impulse contributed the major portions. Hardware MCR contribution was 1.4 meters/sec. The JPL miss distance before correction was calculated to be 629 nautical miles. This flight resulted in Atlas/Centaur becoming operational for two-burn flight.

6.17.8.13. AC-12/Surveyor C, MGS 31A, 17 April 1967. -

Mission. - This mission was the third attempt to place a SURVEYOR spacecraft into a lunar impact trajectory, softland the spacecraft on the lunar surface, and take close-up photographs of the area. A secondary objective was to accomplish the mission utilizing the operational two-burn capability of the CENTAUR vehicle.

Guidance Function. - The MGS was to provide steering, inertial measurements of velocity and displacement, and in-flight discrete commands required to attain a parking orbit. The parking orbit is followed by a coast phase, spacecraft injection into a translunar orbit, and Centaur retromaneuver-- all dependent upon the guidance system.

Guidance Results. - Guidance accurately detected the low Centaur thrust and adjusted the MECO command properly. The 20-hour midcourse requirement to land on the original target was 4.19 meters/sec. (The target was changed in flight because of a fuel burn-off requirement for SURVEYOR.) The miss distance on the Moon without midcourse correction was 250 nautical miles.

6.17.8.14. AC-11/Surveyor D, MGS 23D, 14 July 1967. -

Mission. - This mission was the fourth attempt to place a SURVEYOR into a lunar rendezvous orbit, softland the spacecraft on the lunar surface and acquire surface and soil information. This was the final of three SURVEYOR missions using the Centaur as a single burn vehicle. Future missions will utilize CENTAUR's restart capability from a low Earth orbit.

Guidance Function. - The guidance system was to provide steering augmentation during boost and full steering during sustainer, Centaur burn, and retromaneuver phases. In addition, inertial measurements and in-flight discrete commands were to be executed.

Guidance Results. - Guidance performed well within expected limits, resulting in a 20-hour MCR of 1.21 meters/sec for miss only. The uncorrected lunar impact point (without midcourse correction) was estimated by JPL to be 94 nautical miles from the target point in the Sinus Medii.

6.17.8.15. AC-13 Surveyor E, MGS 22C, 8 September 1967. -

Flight Objective. - This was the second Surveyor mission to utilize the Centaur two-burn capability in placing a Surveyor spacecraft into a lunar transfer orbit.

Guidance Function. - The MGS was to provide booster steering augmentation and full steering during Atlas-Sustainer and Centaur flight phases. This included inertial measurements of velocity and displacement, and in-flight discrete commands required to attain a parking orbit. The parking orbit was followed by a coast phase, spacecraft injection into a translunar orbit, and Centaur retromaneuver-- all dependent upon the guidance system.

Guidance Results. - The lunar impact point, before a mid-course correction, would have been 47 kilometers from the target. The required a 0.55 meters per second 20-hour mid-course correction (miss only). The miss plus time of flight MCR requirement was 1.21 meters per second.

6.17.8.16. AC-14/Surveyor F, MGS21B, 7 November 1967. -

Flight Objective and Guidance Function. - This flight, the third two-burn Atlas-Centaur-Surveyor launch, had the same flight objective and guidance requirements as AC-13/Surveyor E.

Guidance Results. - The 20-hour midcourse correction requirements were 1.18 meters/second (miss only) and 1.25 meters/second (miss plus time of flight).

6.17.8.17. Recap of Test Conditions for Development Flights. -

Piggyback, AC-1, AC-2, and AC-3. - These test flights were performed with guidance operating open loop. This was a requirement for the earliest flights in order not to jeopardize the entire mission. Guidance performance was evaluated through telemetry of MGS signals and guidance related vehicle signals, temperatures, vibration levels, etc. The temperature and vibration levels were important in order to determine what the flight environment actually was.

AC-4. - This and later test flights were operated with the MGS performing closed loop guidance. This flight was the last test flight utilizing only the original signal conditioner. Reference Topic 2.13.

AC-5, AC-6, AC-8, AC-9. - These test flights were all guidance closed loop flights. An additional Signal Conditioner unit (Auxiliary SC) was used for additional signal monitoring. AC-8 resulted in Atlas Centaur being declared operational for single burn missions. AC-9 resulted in Atlas/Centaur being declared operational for two-burn flights.

6.17.8.18. Conclusions. - Important points to consider in guidance development flight tests are:

Complete and accurate data must be obtained on all facets of MGS operation throughout the flight. Telemetry must have sufficient bandwidth for detail analysis of the data.

The MGS environment must be amply instrumented for confirmation of missile design information. Once the environment is thoroughly known, monitoring could be reduced to checks of representative points.

Early flight testing of developmental guidance system should be performed with guidance operating open loop, i.e., missile control should not be dependent upon unproven guidance hardware.

Once confidence is obtained through open loop guidance flight tests, closed loop performance demonstration tests are essential. Depending upon the program, these tests may be performed with or without payloads.

Flight testing can only be effective if positive design action for problem correction is taken.

Upon assumption of operational flights, data monitoring can be limited to that which is essential for flight evaluation and reasonable failure analysis.

The piggyback flight utilizing a vehicle that was being launched for other purposes was a good inexpensive, and early method of obtaining guidance flight evaluation data. Another method that might be considered, having similar advantages, would be the use of a smaller, less expensive guidance evaluation missile. This would provide design feed-back information at an earlier time than otherwise possible.

Topic 6. 18

Design - Reliability Approach

Introduction. - The money and effort invested in the design of complex electro-mechanical equipment, such as the IGS, must be justified by the performance and reliability requirements specified for the equipment. Once the requirements and resources are defined, there must then be assurance that these requirements will be met.

The Centaur IGS mission requirements are such that considerable emphasis must be placed on obtaining reliable system performance. At the beginning of the Centaur Program some of the mechanization concepts were relatively new and unproven. The task to develop them into reliable hardware was underestimated. In the years that followed, there developed a more comprehensive and well planned approach to the IGS development. Today, there is greater depth of knowledge and experience available to much more accurately define the investment necessary to meet the IGS requirements, and the disciplines which must be applied to insure they are met.

This topic deals with the reliability and design techniques applied during the four stages in the design and development of the Honeywell IGS for Centaur. The most significant point emerging from the treatment of this topic is that reliable equipment can be best obtained from the marriage of reliability and design engineering techniques and disciplines, -- starting in the early design stages, and carry through the design evaluation, production and operational phases of IGS development.

6. 18. 1. Parts Derating and Component Application. - Proper application of electronic components requires that their electrical ratings and characteristic parameter variations be satisfactorily accounted for in the design process. Experience throughout the industry indicates, and data verifies, that the designer must anticipate component parameter variations during the expected useful life of the component. These parameter changes must be accounted for in designing a circuit, so that under "worst-case" parameter variations the circuit will perform within specification limits. To enhance reliability, the designer must also de-rate component characteristics in accordance with data relating failure rate and stress levels.

6.18.1.1. Summary. - During the initial build phase of the -3 MGS the first Centaur IGS Reliability Program was implemented. This program included the task of "Improvement Studies", which required an analysis of the direct substitution of "High Reliability" parts (used in other Government funded programs) into the Centaur MGS. A Centaur preferred parts list was established through this study.

Component application reviews were conducted where overstress conditions were indicated by the stress analysis findings. Until 1965, stress analysis was limited to redesign areas and/or specific problem areas. In 1965 a complete, detailed stress analysis was performed on all electrical circuits in the Centaur MGS, including the vehicleborne computer. As a result, several part applications were improved by replacement or redesign to provide a greater margin of safety.

As part of the detailed stress analysis task, a component rating and parameter variation policy was established in 1965. The implementing of this policy ensured consistency of design and provided greater reliability.

Directly Replaceable Hi-Reliability Parts. - A review of all electrical parts used in the Centaur MGS and Direct Mission Support GSE was begun in June 1962. This task was initially assigned by GD/C to Honeywell, to update and improve the reliability of the equipment through the use of more reliable parts. From this review, all part types were catalogued into three major groups.

6.18.1.2. Group I. - The first group was composed of MGS and GSE parts, which could be directly replaced by parts listed in the Honeywell Approved Parts Manual, GD/C Standard Parts Manual and Military Standard Parts lists. Parts with adequate test data per the Interagency Data Exchange Program (IDEP), the Qualified Parts List (QPL) and MSFC M-ASTR-TSR-PPL-1 were also placed in this group. A total of 155 part types were in this category.

Semiconductors were of primary concern. Other part substitutions were to be implemented during any future redesign and modification and during the Phase I and II Product Improvement Programs (1964-1966). However, some difficulty arose in actually substituting the semiconductor preferred parts into the hardware. The parts were interchangeable, according to the parameters specified, but the possible variations in the unspecified parameters presented a risk. The affected drawings would

all have to be revised. The availability of most of the preferred parts was poor and procurement lead times were long. Existing stock would have to be scrapped.

After careful consideration of the circumstances, it was jointly decided by Honeywell, GD/C and NASA that an interchangeability list must be formulated for the MGS to provide a smooth transition from existing parts to the preferred parts. This approach allowed semiconductor substitution as the preferred parts became available but without expensive drawing changes and impact to the hardware build schedules.

6.18.1.3. Group II. - A second group of parts was defined for parts which could be replaced with high reliability parts through redesign or modification. The substitution of these parts was also to be implemented during any future redesign and modification and during the Product Improvement Programs.

6.18.1.4. Group III. - The third group of parts was composed of components which either could not be qualified for use on Centaur or for which there were no direct or indirect High Reliability part replacements. An extensive parts qualification program for these parts was proposed in 1963. The program also included the parts to replace those that were unsuitable. A total of 55 part types were to be qualified. An evaluation of the costs associated with the qualification tests indicated that the costs were extremely high. GD/C, Honeywell and NASA decided that the need for qualified parts did not justify the cost of the qualification program. Therefore, the program was not implemented.

6.18.1.5. Electrical Stress Analysis. - As part of the initial Reliability Program, all new or redesign efforts were subjected to electrical stress analysis. But it was not until 1965 that a detailed stress analysis was made of all circuits in the MGS. The primary objective of the stress analysis effort was to evaluate the component applications.

The Platform, Platform Electronics, Signal Conditioner and Navigation Computer stress analyses indicated that these units were free of reliability risk areas due to high stress conditions. However, the Coupler stress analysis revealed thirty-three part applications that presented reliability risk areas. For example, a solid tantalum capacitor used in the DC Amplifiers was calculated to be operating with a derated stress ratio of 1.58; the maximum allowable ratio being 1.0.

Ten of the identified risk areas were corrected immediately by redesign or part replacement through a retrofit program. The remaining component application risk areas were corrected during Phase I and Phase II of the Product Improvement Programs (PIP).

6.18.1.6. Component Rating and Parameter Variation. - During the course of the stress analysis performed on all circuits in the Centaur Guidance system in 1965, a standard policy for component rating and parameter variation was established by Honeywell for each specific component type (for example, silicon diodes and zener diodes were each given individual rating and variation standards). This policy was documented in Honeywell document R-ED 22036, and provided a means of accounting for the component parameter changes, so that under "worst case" parameter variations, the circuit would perform within specified limits.

The "end-of-life" environmental variations included those due to: long term storage; long term operation; thermal shock (including soldering and welding); mechanical shock; vibration and acceleration; atmospheric pressure and salt atmosphere. For example, capacitor variations were considered for the following parameters: capacitance value, ripple current, temperature coefficient of capacitor, leakage current, and surge voltage. Derating curves were drawn, defining the maximum allowable stress ratio for an ambient or case temperature from +25°C to +125°C.

This policy has been used since 1965 for all Centaur MGS redesign and new design work. Modifications to this policy are being made as more information and data becomes available.

6.18.1.7. Plans for Improved Centaur. - For Improved Centaur, stress analysis techniques are being applied by Reliability Engineering on all electrical parts in accordance with MIL-HDBK-217A. Part failure rates are being calculated, using the maximum stress levels and the maximum anticipated temperature for each component. The derating policy used for the Centaur IGS has been reviewed for adequacy and completeness. Revisions were made in light of the most recent data available. A change was made in resistor derating to include a case temperature derating which permits a more accurate determination of actual part stresses.

Maximum usage of "standard" preferred parts is an established program goal. In addition to offering cost benefits, component standardization greatly reduces the circuit analysis task being performed during the design/development phase of the program. To achieve this standardization, each Design Engineer has been furnished with a list of preferred

parts in the early stages of circuit design. This preferred parts list reflected the reliability requirements of the program as much as possible without placing unrealistic restrictions on the Designer. Unrealistic design restrictions would defeat the purpose of a preferred parts list, which is to meet the design requirements, using reliable parts and a minimum number of part types.

6.18.1.8. Conclusions. - A motto often used by present-day Centaur designers is "Homework before Hardware". This is a motto which can be applied to all production line or complex equipment. Once a design gets into the production stage, considerations such as the cost of making new drawings, the time lost in rework or delay, and the scrapping of costly materials often take precedence over reliability improvements. Therefore, by placing the proper emphasis on parts derating and component applications during the design of the hardware, reliability is enhanced and the production cost factors are held to a minimum.

6.18.2. Worst Case Versus Nominal Circuit Analysis. - This topic details the Design/Reliability approach used on worst case versus nominal circuit analysis techniques, including design centering and computer aided analyses. It begins with the -1 IGS and concludes with techniques that are being used today on the IMG design.

6.18.2.1. Background. - There was very little worst-case analysis performed on the -1 Centaur IGS. The worst-case circuit analysis that was performed was usually for redesign utilizing a more conservative design philosophy than in the original, nominal design. At this time, there were no computer-aided techniques such as are available today. There were a few attempts to utilize an analog Pace computer to simulate portions of some IGS control loops. The results of these attempts were inconclusive, since the math model could not be simulated correctly.

There was no formal worst case circuit analysis performed on -3 Centaur, until the Phase II PIP design phase. Both -3 and Phase I PIP utilized design-centering techniques, based upon actual test results. In fact, test results were the sole basis for worst-case analysis until Phase II PIP.

6.18.2.2. First Use of Worst-Case Analysis. - The Phase II PIP system was the first Centaur IGS design to fully utilize worst-case circuit design. This approach was used on the circuits redesigned for Phase II PIP. A worst case circuit analysis was also performed on some non-Phase II

designed circuitry. The approach used for Phase II redesign was:

1. Concept. - Upon receipt of the circuit specification, the concept was developed into a block diagrammed circuit.
2. Nominal Analysis. - After a block diagram of the circuit had been developed, each functional area of the block diagram was determined. These requirements covered the electrical performance as well as the interface requirements.
3. Nominal Circuit Design. - After the electrical performance characteristics, for each of the individual blocks of the sub-assembly block diagram, were determined, the actual circuit design was begun. The circuit design equations were derived; component values and power ratings were defined to meet design goals.
4. Breadboard Test. - Each breadboard was subjected to tests that determined that the specifications were met.
5. Parts Study and Selection. - After the circuit design calculations and breadboard test dates were obtained, the electrical design was reviewed to determine packaging requirements. High reliability parts were incorporated in all possible applications.
6. Engineering Specifications. - An engineering specification was written for each board assembly that established minimum performance requirements.
7. Equivalent Circuits. - Equivalent circuits were derived for transistors and diodes for ac, dc, and transient analyses. These equivalent circuit models were then employed throughout the Phase II PIP worst case analysis effort.
8. Worst Case Circuit Analysis (WCCA). - WCCA was performed on coupler circuitry to determine worst-case circuit performance under the worst-case parameter variations defined by the Honeywell Centaur derating policy. The analyses include dc, ac, and transient cases. When all equivalent circuits had been determined, the complete circuit was ready to be transformed into computer language. A nominal circuit requires approximately 15 dc analyses, eight ac analyses, and eight transient analyses. A

survey was made to find computer programs that were capable of accommodating the analysis requirements and also readily available to the circuit designer. Those selected were ECAP and NET-1.

6.18.2.3. ECAP Techniques. - The Electronic Circuit Analysis Program (known as ECAP) is an integrated system of programs which can be used by the electrical engineer in the design and analysis of electronic circuits. The system of programs can produce dc, ac and/or transient analysis of electrical networks from a description of the connections of the network (the circuit topology), a list of corresponding circuit element values, a selection of the type of analysis desired, description of the circuit excitation, and a list of the output desired. The engineer requires neither a knowledge of the internal construction of the system of programs, nor computer programming techniques to use ECAP effectively.

ECAP recognizes a set of standard electrical circuit elements. Any electrical network, that can be constructed from any or all of the different elements in the set, can be analyzed by ECAP. There is almost no limit to the number of ways the circuit elements can be arranged in the network. The set of standard circuit elements does not include electronic components, but in many cases, these components are easily simulated by means of equivalent circuits constructed of standard elements.

ECAP can handle electrical networks that contain as many as twenty nodes and sixty branches and is very easy to use. The only requirement for special knowledge is that the user be acquainted with the methods of communication with ECAP. These include:

1. The technique of describing a circuit to the program.
2. The specification of the type of analysis desired.
3. The interpretation of the results.

The problem of communicating with ECAP is particularly simple for the electrical engineer because the necessary input for ECAP, as well as its output, are expressed in the language of the electrical engineer. Once the input for ECAP is prepared, the statements are then punched on cards for entry into the data processing system. ECAP interprets the input statement, determines the network topology, generates the network equations, performs the desired analysis and produces the specified output in tabular form.

ECAP is designed for use primarily as an electronic circuit simulator, although it can be also applied effectively to the analysis of many other physical systems for which there exist corresponding electrical network analogs. ECAP allows the circuit designer to economically and efficiently examine the performance of a circuit during the various stages of its design by using a computer rather than a breadboard. In this way, a designer can rapidly determine the variations in circuit response that correspond to changes in circuit parameters. Early studies can be made of circuits that contain costly components, which may be difficult to obtain. Destructive excitation can be applied to the circuit with no fear of destroying expensive electronic circuit elements. Worst-case combinations which are difficult or practically impossible to realize in the laboratory can be examined. Measurements that may be difficult to make and time consuming to instrument can be made quite simply on the computer. Circuit connections can be changed rapidly. In many cases, ECAP can leave the designer with a clearer insight into the operation of the circuit than could be obtained with a breadboard study, and often at considerably less cost.

In the past, reliability estimates for electronic circuitry have been based upon statistical failure rate data on individual components. That is, an indication of the reliability of the circuit was obtained by relating electrical and thermal stresses placed upon the individual parts to data obtained from the past performance of similar components used in other systems. In this way, the estimate of the circuitry reliability is based upon the catastrophic failure rate of the individual components. On the other hand, it is assumed that the circuit components remain within the tolerance limits. However, in the same way that highly reliable parts cannot be expected to perform effectively in marginally designed circuits, the normal variations in components can also result in the unsatisfactory performance when hardware reaches the production phase, if the design was based only upon nominal part values. Out-of-tolerance circuit operation can also result from component variation with environmental changes, electrical stresses, and aging. The relationship between individual component tolerances and the overall performance of a circuit is often complex. For example, to restrict an output variable of a given circuit to a one percent variation of its nominal value, some circuit components may have to have an 0.1 percent tolerance or even an 0.01 percent tolerance. Others can be as high as 10 percent. Again, ECAP can be used as an aid in the determination of the necessary component tolerances to achieve a desired level of overall circuit performance.

The dc analysis ECAP program provides the user with a steady-state solution of linear networks (in terms of voltages, currents, and power losses). The Program uses partial derivatives and sensitivity coefficients

of network voltages with respect to the input parameters. The analysis is performed on both a worst case and a standard deviation basis, in terms of the sensitivity coefficients. The analysis requires the entry of parameter tolerances as input data. An automatic parameter modification capability has also been built into the dc analysis program to facilitate the input parameter variation.

The ac analysis ECAP program provides the user with the time-independent solution of voltages, currents, and power losses of linear electrical networks subjected to sine wave excitation at a fixed frequency. The ac analysis program also has provision for the automatic modification of parameters. Of particular interest is the automatic modification of the frequency (using logarithmic increments) to provide a frequency response analysis of the circuit.

The transient analysis ECAP program provides the user with the time response (voltages and currents), of an electrical network, subjected to user-specified driving functions. The outstanding feature of the transient analysis program is its capacity to handle problems characterized by the presence of non-linearities. This is accomplished by automatically switching branch parameter values as a function of circuit voltages and currents. To perform this task, switches are defined as part of the input data to the program.

All of the ECAP programs are written entirely in FORTRAN II-D. Consequently, the user can easily modify the program to include new features or change existing features as desired.

6.18.2.4.NET-1 Techniques. - NET-1 is a digital computer program which simulates the dc steady-state behavior and the transient behavior of a large class of electrical circuits which may contain passive and solid state components.

A circuit described to NET for analysis may include the following elements, connected in any manner, so long as the connections remain fixed: junction transistors, junction diodes, signal sources, fixed voltage sources, fixed value resistors, capacitors, inductors, and mutual inductive couplings. NET simulates the circuit behavior and describes it through printed summaries. Special capabilities of NET include:

1. Transformers may be represented by suitable combination of resistors, capacitors, inductors and mutual inductive coupling.

2. Zener diodes may be represented by an appropriate combination of junction diodes and voltages sources.
3. Switches may be simulated by the specification of initial and final conditions.
4. Negative values of resistance, capacitance, and inductance may be used in the construction of physically unrealizable circuits, which have interesting properties.
5. Many non-electrical physical problems have network analogies, some of which are not physically realizable. NET can perform calculations for many of these analogies.

The greatest virtue of the NET program is the ability to determine variations of circuit response due to changes in circuit parameters. For instance, it is possible to change junction capacitance, semiconductor bulk resistance, or leakage currents in a transistor or diode, and thus observe very accurately the effect of the change on the entire circuit. NET is also of value in optimizing designs, involving very costly components or components which are difficult to obtain. Destructive transient phenomena may be studied with no fear of destroying expensive transistors. Worst case combinations, which were frequently impossible to realize in the laboratory, may be achieved, as was the case with ECAP. Measurements which may be difficult to make on real circuits become quite simple. Since there is no interaction of measuring instruments with the circuit, the problems associated with instrumentation disappear. In many cases, NET will give the designer a clearer insight in the operation of the circuit than could be obtained from a breadboard or "slide rule" study.

Application of Worst-Case Analysis. - To facilitate the use of the program by engineers unfamiliar with digital computers, a number of features were added, including an input description, which employs conventional engineering terminology, automatic detection of circuit description errors wherever possible, and use of a library containing a list of parameters for each transistor and diode known to NET. New circuit elements for NET include diodes, mutual inductive coupling, multiple signal sources of five different basic waveforms and series sources. The transistor model has been extended to include operation in the saturation and active inverted modes. Cutoff currents and some temperature effects are included for both transistors and diodes. The program has been expanded to increase

the amount of information which the user can gain from a NET analysis. The additional information includes:

1. Checking of maximum ratings for transistors and diodes under conditions of power supply failure;
2. Ability to perform several steady-state analyses, for different values of applied voltages, during one NET run;
3. Calculation of power supply current drain and total circuit dissipation;
4. The ability to specify initial values of voltages, currents, and time in the transient analysis.

New programming techniques include:

1. Improvements in the Newton-Raphson iteration process and its convergence test;
2. Automatic compilation of the circuit transient code for solving the simultaneous differential and algebraic equations;
3. Automatic storage organization for matrices and other blocks of information to facilitate the analysis of large circuits; and
4. An algorithm for maximum coupling of the dependent variables for the differential equations during integration.

6.18.2.5. Worst-Case Analysis for the IMG. - The Centaur IMG design is utilizing worst-case circuit design for all circuits. Computer-aided circuit analysis programs (ECAP and NET-1) are being used to supplement hand calculations in order to predict and verify circuit performance in the detailed circuit design phase.

Component parameter variations and limits used in the calculations are, for the most part, consistent with the limits defined in the Honeywell Component Derating Policy. However, in order to allow some circuit designs to be practicable, even possible in some instances, three degrees of parameter variations and limits are employed. They are:

1. Conservative Worst Case Parameter Limits: This situation considers all component parameters at their worst case limit without regard to expected temperature or any other modifying criteria. This approach is the most economical to analyze since one computer run will normally suffice. From a performance standpoint, it is also the most conservative circuit.

2. **Correlated Parameter Limits:** This is a true worst case situation, but utilizes sets of circuit and temperature parameters that normally are consistent with each other, particularly in the area of semiconductor characteristics with regard to temperature. This technique requires more computer time than No. 1, but reduces the chance of overdesign.
3. **Interdependent Parameter Limits:** Past experience has demonstrated, some designs will arise where performance requirements dictate some parameter interdependence, such as tracking temperature and individual temperature coefficients (V_{BE} 's, etc.) throughout a circuit. The designer attempts to avoid such situations, but when it is deemed necessary, special controls and limits are employed to assure that the circuit will perform as required.

While ECAP and NET-1 are adequate to perform the intended analysis, other such programs and numerous subroutines are being investigated for whatever advantageous use can be made of them in specialized areas, or to support the two major programs (ECAP and NET).

6.18.2.6. **Conclusions.** - The Design/Reliability approach on the Centaur program to worst-case circuit analysis, including design-centering and computer-aided techniques, has evolved from no formal analysis in the -1 design, to a full blown computerized analysis for Phase II PIP and IMG. The advantages of this approach have been realized through improved flight performance of Phase II PIP systems. This approach to circuit analysis has greatly reduced the occurrence of marginal designs which were quite prevalent in past Centaur circuits. A new program should take the same approach as that being used in the IMG, that is, this technique is being used throughout the development phases, from the initial paper-design, through destructive testing. The advantages obtained from this approach are:

1. Optimum circuitry.
2. Reliable, conservative circuitry.
3. Rational, defensible test circuits.
4. A thorough understanding of the influence of each parameter in circuit performance.
5. A well-defined basis for design reviews.

6.18.3. The Role of Formal Failure Reporting and Analysis. - As in most organizations involved in the production and support of complex electrical and mechanical equipment, the feedback of problem areas to the designers at Honeywell is through a discrepancy or failure reporting system. This system, together with a formal failure analysis program, provides the means for a minimum response time between the development of a problem area and the implementation of effective corrective action.

6.18.3.1. Summary. - The formal failure reporting and analysis system on Centaur has evolved from a state of non-existence during early Centaur development to the present highly sophisticated reporting and analysis system. Through initiative and perseverance early in the -3 Centaur Program, GD/C, Honeywell and NASA built the foundation for the current procedures in spite of funding limitations. The failure reporting and analysis system strives for the earliest possible detection of problem areas, together with the implementation of corrective action, before MGS equipment reaches the field. This method of failure reporting and analysis has proven successful and has contributed greatly to the reliability growth of the Centaur Missile Guidance System (see Figure 6.18-1 for MTBF growth curve).

6.18.3.2. Discussion. - The establishment of a failure reporting and analysis program on Centaur was delayed during the early stages due to funding limitations. Honeywell and Librascope (computer manufacturer) presented several proposals to General Dynamics/Astronautics, Marshall Space Flight Center and NASA LeRC prior to the initial go-ahead for a funded Reliability Program which included a limited failure reporting and analysis effort. Prior to the go-ahead in June 1962, a Honeywell funded failure reporting effort did exist at the system level. During this period over 1,400 failure and malfunction reports were processed. From these reports, the replacement rates on assemblies and parts were established. Abnormal replacement rates helped designate areas requiring corrective action. As the result of a general Honeywell evaluation of these problem areas, the following recommendations were made to General Dynamics/Astronautics:

1. A formal parts application **review** and reliability stress analysis should be performed to identify and assess part weaknesses and marginal stress levels.
2. Design proofing tests should be accomplished to evaluate existing designs and proposed improvements.

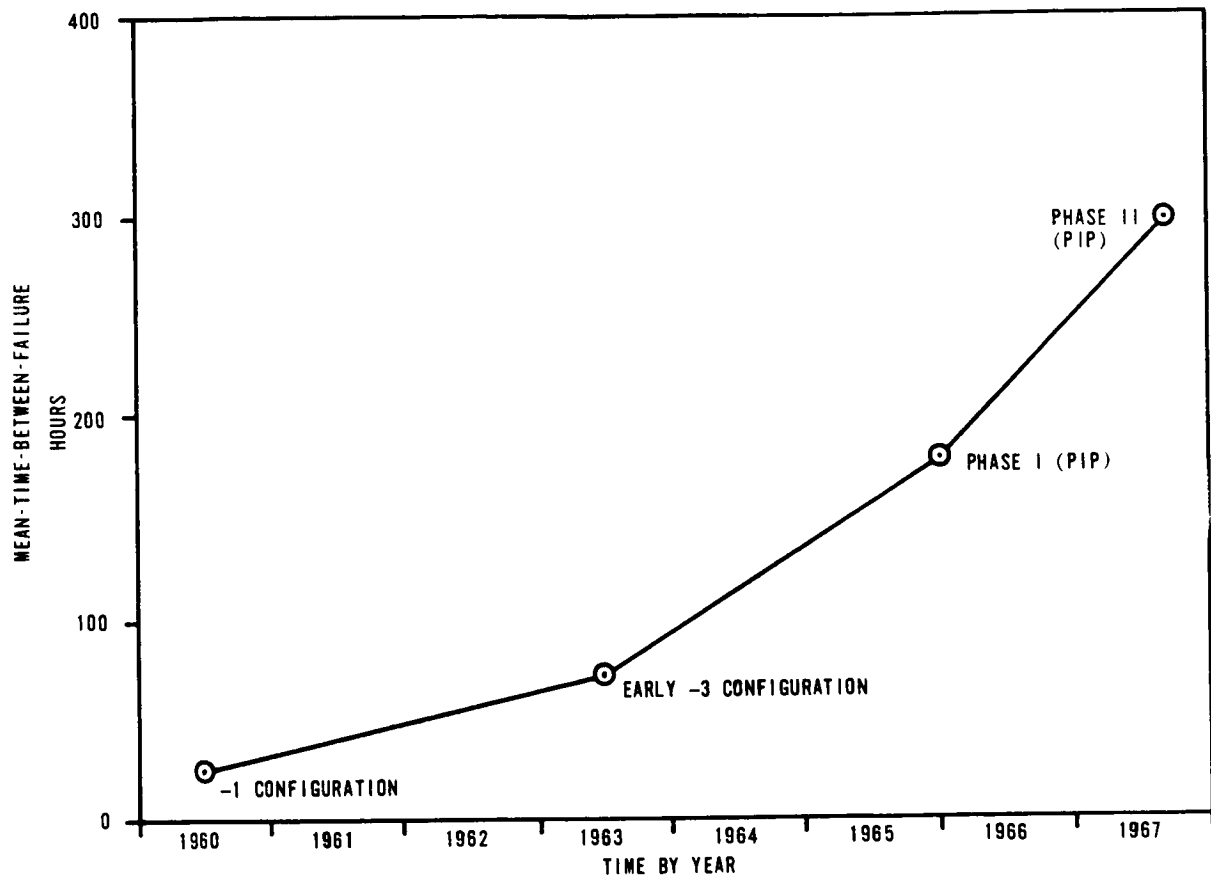


FIGURE 6.18-1. CENTAUR RELIABILITY GROWTH CURVE

3. Operating stability and reliability assurance tests should be performed to quantitatively determine the reliability and performance accuracy under controlled conditions.
4. Rocket sled tests were recommended to assess accelerometer loop capabilities and general system operation under high linear accelerations.

Subsequently, all of these recommendations were accomplished and have contributed greatly to the reliable guidance system Honeywell manufactures today.

The role of failure reporting and analysis was expanded with the contract Go-Ahead for the Reliability Program in June 1962. The Discrepancy Report had replaced the Failure Report in early 1962 and was being used at all levels of manufacturing and testing. Copies of all Discrepancy Reports were kept on file to aid the new task of formal failure analysis.

The task of formal failure analysis required a staff of Reliability Engineers and Engineering Aides. These people were obtained and assigned specifically to the Centaur Program. Also, in November 1963, a special laboratory for detailed failure analysis was established to provide a more effective reliability effort. Because of funding limitations, the formal analysis efforts were restricted to the system level failures until early 1965, when the contract was expanded to include formal failure analysis at the subsystem level.

The provisions for expanding formal failure analysis activity to the subsystem level was a significant step towards early detection and correction of problem areas. The cause of the failures at the subsystem level could now be better determined and corrective action taken to prevent failures during critical field operations and flight activity.

Since the establishment of a failure reporting and analysis program on Centaur, a great many hardware design changes and improvements have been formulated through the failure analysis activity. Some typical examples are listed below:

1. A failure pattern developed in the DGG49D15 Gyros, which were used in the early -3 Centaur Platforms. The failure mechanism was defined as an insulation breakdown (electrical short) between the associated windings internal to the dualsyn assembly. Failures of this type were considered "critical" and could cause a catastrophic mission failure.

Of several alternative solutions (reference Topic 2.2), the most practical was the use of 0.001 inch mylar insulating strips, which were inserted between all adjacent skeins during assembly of new and rebuilt gyros. As an interim measure, the gyros without mylar insulation were subjected to an insulation resistance check, which became familiarly known as the "Zap Test". This interim measure provided some additional safety margin, but the real cure was to replace all gyros without the mylar insulation, as the mylar insulated gyros became available. The incorporation of the mylar insulation has proven to be 100 percent effective against dualsyn failures due to skein to skein shorts.

2. Formal failure analyses were performed on four failed frequency standards used in the computer. The frequency standards were found to have poor crystal mounting and bonding. Failure of the frequency standard during flight could cause a catastrophic mission failure.

The vendor redesigned the crystal mounting by providing a hot etched surface to improve the crystal-to-crystal mount bonding. Also, Ecco Foam potting was applied to the binary sections to improve mechanical stability. The mounting technique used in the latest models (currently in all flight computers) was improved further by orienting the crystal with a 5 degree rotation. This rotation provides a more reliable bond between the etched crystal surface and the crystal mounting structure.

3. The signal conditioner module No. 1 experienced a high failure rate in late 1963 and early 1964 due to transistor failures. A failure in the signal conditioner would not cause a catastrophic mission failure, but it could result in the loss of important telemetry data.

The failures were found to be the result of negative transients on the 28 volt line, due to power switching. The 2.5 volt bias for the transistors which was obtained from the 28 volt line is now obtained from the voltage regulator in the signal conditioner. Thus, 28 volt line transients are prevented from reaching the transistors.

4. Through failure analysis, it was determined that mechanical overstress of the gyro header wiring can occur during installation and removal of the top dust cover. This overstress was the

primary cause for the broken head wire experienced at ETR during Day 2 Tests for AC-9. The failure of the wire during flight could have degraded the flight performance.

Improved header wiring was incorporated on all gyros shipped from the gyro manufacturer after 1 March 1967. This improvement consisted of wire rerouting, together with the use of a soft polyurethane potting.

In addition to the above specific examples, the Phase I and Phase II Product Improvement Programs eliminated many problem areas which had been identified earlier through failure analysis. Also, through failure analysis, the need for several direct part substitutions has been identified and new parts incorporated to improve part application or part reliability. Improvements in the hardware have also resulted from the use of higher quality workmanship standards, the need for which was a result of failure analysis findings.

6.18.3.3. Plans for Improved IMG Program. - During the engineering prototype assembly and test phase, discrepancy reports will be issued against all malfunctions and discrepancies. A record of each report will be maintained in the Honeywell Reliability Group to aid failure analysis.

Failure analysis activity will be applied to those failures that occur during the module unit and system tests to determine the cause of failure. Corrective action will be taken as necessary to prevent further failures and at the same time improve the reliability of the system.

During the production phase, discrepancy reports will be generated on all part, unit, assembly or system discrepancies occurring from the receiving inspection of components through final acceptance tests and field operations. Discrepancies occurring prior to Acceptance Test will be subject to informal failure analysis as necessary to provide an early warning of generic failure mechanisms or loss of process control.

During and following acceptance tests, all failures will be subjected to formal failure analysis. The appropriate corrective action for these failures will be formulated and implemented as required. Follow up will be performed to assure the effectiveness of the corrective action.

6.18.3.4. Conclusions. - The failure reporting and analysis effort was at a minimum during the early development of the Centaur Guidance System, due to funding limitations. Since then, more and more emphasis has been

placed on the early detection and correction of costly problem areas. The Improved Centaur Guidance Program is taking advantage of this increased emphasis. This approach should prove, in the long run, to be more economical by providing a more reliable guidance system throughout the production and operational phases of the program. For any new programs, the early application of a failure reporting and analysis is strongly recommended.

6.18.4. In-Line Failure Diagnosis. -

6.18.4.1. Summary. - As a contrast to formal failure analysis which ends with a formal "Failure Analysis Report", in-line failure diagnosis is performed in a more timely manner to provide immediate design feedback information. This process is essential for quick design action and for production efficiency-- that is, "keep the hardware moving".

6.18.4.2. Description of Technique. - In-line failure diagnosis begins with design engineering coverage of troubleshooting. Once the failure is isolated to a specific circuit an evaluation of the design significance is made. The circuit designer is often called in at this point to work as part of a Production Engineering, Systems Design Engineering, Reliability Engineering and Circuit Design Engineering team. This team proceeds with an informal failure diagnosis through test and analysis to determine the design significance of the failure and to recommend corrective action. Further team action will provide an evaluation of the "fix" when applied to the hardware. Depending upon the specific problem, the "fix" may first be tried out in test bed hardware. In some cases production will assume the risk by performing the modifications/repair and the evaluation in production hardware. All of the above action is performed on a rush basis to prevent excessive production delay.

An effective aid to the failure diagnosis portion of the above activities is an established test and analysis laboratory which is equipped (manpower and sophisticated test equipment) to isolate the failure to discrete components and to the exact causes within the failed components.

Use of these concepts of in-line failure diagnosis, team action and a failure diagnosis laboratory has proven useful in maintaining the ability to react to Centaur Program demands for timely recovery from problems which might affect overall program needs.

6. 18. 5. Mission Significance and Probability. -

6. 18. 5. 1. Introduction. - At times problems or indications of problems occur within a guidance system to a degree that might have a significant effect upon the success of a specific mission. An assessment of the mission significance of the errors caused by the problem and the probability of a more significant problem occurring can be made. When favorable, this assessment can result in demonstration of flightworthiness of a system for the intended mission thereby eliminating unnecessary rework and the attendant cost and possible mission delay.

6. 18. 5. 2. Mission Significance. - When a performance degradation type problem occurs within an MGS, an assessment of the mission significance is made. An example of this type of problem might be a W gyro parameter shift in an MGS slated for a Surveyor mission.

The assessment is made by calculating the partial midcourse correction requirement (MCR) for that parameter using a shift of the magnitude experienced combined with the mission sensitivity to shifts in that particular parameter. This provides a finite, quantitative assessment of the effect upon the mission by the actual problem.

Before a rationale of this type can be accepted, an additional assessment of the probability and effect of further degradation of the parameter in question must be made. This is done through knowledge of the failure modes experienced in different parameters. For example-- a gyro will sometimes experience a worsening of its performance with no indication of impending failure. Complete failure, when preceded by performance degradation, is typically a process requiring many hours of operation. Therefore, failure over the expected lifetime of the component is often extremely unlikely.

6. 18. 6. "Expect the Unexpected" - Major Reliability Risks. - When problems are experienced within a system it is important when assessing the cause to not accept the obvious answer too readily. It is important to take a critical attitude, looking beyond the obvious answers for possibly more subtle actual causes. The proper application of this attitude can prevent many blunders. Problems which might otherwise remain undiscovered for long periods can then be corrected early in the program minimizing their effect on the program.

6.18.7. Reliability. -

6.18.7.1. System GSE Reliability. - The need for reliability in Ground Support Equipment (GSE) is almost as great as the need for reliability in guidance systems. In many cases, the success of the MGS is dependent upon the GSE. During acceptance tests and other laboratory or vehicle tests prior to launch day, the GSE must perform its function properly to assure the adequate checkout of the MGS. However, the most critical period of operation for the GSE is during launch day operations.

Centaur GSE reliability goals were assigned for each major GSE configuration. These goals were derived from the success probabilities required during the launch day operations and from the inherent complexity of the equipment. Table 6.18-I presents the various configurations and estimated complexities together with their reliability goals and measurements.

TABLE 6.18-I.

CONFIGURATION COMPLEXITY AND RELIABILITY

GSE Configuration	Complexity* (Parts Count)	Reliability* Goal (MTBF)	Reliability Measurement (MTBF)
-1	887 est.	200 hours	---
Early -3 with RL&R	4,887 est.	200 hours	716 hours
Late -3 with RL&R	4,887 est.	500 hours	1,957 hours
Improved Centaur	6,208 est.	1,600 hours	?

* Does not include mechanical devices such as teletype printer, tape punch, etc.

A significant improvement in the measured MTBF is shown for the Late -3 configuration over the Early -3 configuration. Some of this improvement is due to the experience obtained in operating and handling the equipment, but the majority of improvement was obtained through the specific design changes and component improvements that have been made in the GSE in the past six years. The more subtle problem areas have required detailed failure analysis to define the failure causes. Typical examples of this type were:

1. Intermittent operation of the Hangar Align Switch was experienced on Preflight Control Panels at Honeywell, GD/C, and ETR. A malfunction of this nature could result in a 30-minute launch delay if it occurred during launch day operations.

An analysis of the intermittent switches revealed the cause of failure to be the accumulation on the contacts of epoxy picked up by the wiper while passing over the epoxy board.

The switch vendor was notified and the problem reviewed. The vendor supplied modified switch wafers to Honeywell for evaluation. The use of the modified switches was not an effective solution to this problem. (Refer to Subject 5.2.4. for further details concerning the switch modification.)

2. During field test operations in 1964, two defective 3K52 relays were experienced (one at NASA LeRC and one at GD/C, San Diego). The failure of this relay during launch day operations could have resulted in a 45-minute launch schedule delay.

Indications of the failure mode were obtained through an analysis of the circuit application. It was determined that relay 3K52 receives a reorient pulse every six-tenths of a second. Since 3K52 relay has an expected operation life of 100,000 operations, the life was being exceeded after 17 hours. The circuitry was subsequently modified to remove the relay and provide fully solid-state operation.

For the IMG-GSE solid state switching circuits are being used for high frequency switching. This improves the performance of the switching function and provides greater reliability by reducing the mechanical operations.

3. During Honeywell tests of Preflight Control H-1 in November 1964, following its modification to a B2 configuration, the Coarse Align Lamp failed to light when switching from Final Align Gyrocompass to Final Align Optics. The failure was traced to relay K6, which failed to de-energize. The failure of relay K6 to de-energize was attributed to the B2 configuration, which was a modification of Preflight Control Panels for Final Align Optics Verification. During switching from Final Align Gyrocompass to Final Align Optics, the circuit was supposed to reset through relay K6. Therefore, it was necessary for the relay drop-out time to be less than the manual switching time.

To obtain proper relay drop-out time, and at the same time keep the transient voltage to a tolerable level, a zener diode was placed in series with the relay arc suppression diode 3CR30.

4. A total of 32 failures were experienced on Heinemann Relays in the 1961-65 period. Replacement of these relays was implemented in 1965. The problems associated with the replacement of these relays are discussed in Subject 5.2.4. of this report. Although satisfactory performance has been achieved with the replacement relay (Agastat), the use of solid state devices is recommended in new GSE designs.

6.18.7.2. Plans for Improved Centaur GSE. - The GSE for the Improved Centaur System will be much more sophisticated than that currently used. Computerization is being used to replace many of the manual operations. However, to be most effective, this computerization requires the application of reliable parts plus sound design and reliability disciplines.

Parts, circuits and subcontracted devices are being selected on the basis of design suitability, using existing proven hardware where possible. These devices include the Honeywell 516 Computer, with its wide usage of integrated circuits. Electro-mechanical devices such as relays, servo motors and gear trains have been reduced to a minimum.

Sound design and reliability disciplines are necessary and are being applied during the design of the IMG-GSE. The designers derating policy has been revised to include the most recent data available. Stress analysis techniques are being used on all electrical parts in accordance with MIL-HDBK-217A, dated 1 December 1965. The Honeywell Reliability Engineering Handbook, and Honeywell Component Rating and Parameter Variation Practice is being used by the Design and Reliability engineers as a guide, specifically for parts selection, derating and stress analysis.

6.18.7.3. Conclusions. - Reliability becomes a real asset when it is designed into the equipment during the early design stages. Equipment that is initially "short-changed" reliability-wise almost inevitably suffers in down time and expensive changes later on. Reliability that is "added-on" after designs become hardware is difficult, costly, and not always effective. The most important lesson in reliability to be learned from Honeywell's experience with added-on and designed-in reliability on Centaur is that the GSE is as important to the success of a guidance system as the guidance system itself. Therefore, in the design of any new system, the GSE should receive just as much emphasis on the reliability design aspects, right from the beginning.

Topic 6.19

Specifications and Standards

6.19.1. Introduction. - Specifications serve the primary function of providing specific guidelines for the design, selection, processing, packaging, fabrication, or evaluation of materials or equipment. In the design and development of complex equipment such as the Centaur IGS, many such guidelines are required. Various agencies, both Military and civilian have in the past been responsible for the generation of specifications which are applicable, in part or in total, to the design, build, and test of IGS hardware. In order to enhance the success probability of a particular design in meeting its objectives, with a minimum amount of risk, and at minimum expenditures, many such specifications are imposed upon the design. If not carefully considered, they can sometimes hurt, rather than help the final hardware design.

This discussion will present, from a guidance manufacturer's point of view, a discussion of several key factors to consider in interpreting and applying specifications. In addition, hardware configuration control through specifications will be discussed.

6.19.2. Interpretation of Specifications. - For the subject under study, all applicable specifications are called out in the Work Statement under the System Specification Section.

Initial interpretation of specifications begin at the agency responsible for issuing a Request For Proposal (RFP). Prior to the release of a Work Statement, all means should be exercised to determine that those specifications applicable to the Program are called out. If only a section or portion of a particular specification applies, then this should be so noted in the appropriate section. Adverse effects upon cost and unnecessary design complexity or tradeoffs might otherwise result.

An equal responsibility for specification interpretation lies within the contractor responding to the RFP. A thorough study should be made as to the applicability of the referenced specifications, and the capability to comply with same. Additionally, those changes required in internal processes, facilities, and procedures, in order to fulfill the commitments of the specifications, should be considered. All questions regarding the

interpretation of the specifications should be discussed between the agency issuing the RFP and the contractor answering it. When a mutual understanding is arrived at, all negotiated and approved deviations to the applicable specification should be documented and made a part of the controlling contract specification.

6.19.3. Application of Specifications. - The extent to which any referenced specification shall apply must be delineated in the controlling document. A general statement to the effect that unless otherwise noted, "All documents referenced herein shall form a part of this specification to the extent stated herein", is commonly used. This means that if a document is listed in the controlling document under an "Applicable Documents" paragraph, then that document or portions thereof shall apply, only if referenced elsewhere in the controlling document. Failure to incorporate such a statement will eventually lead to costly problems, due to misinterpretations.

Throughout the evolution of Military Specifications, several revisions have resulted in some instances. Unless otherwise noted, previous revisions are not obsoleted by later revisions. There are instances where a mere change in the revision letter of a given specification could result in a drastic cost increase if implemented without proper evaluation. It is, therefore, very important to specify by revision date, revision letter, or some appropriate note, the particular version of the specification that is to be applied. It is equally important to understand the basic differences between the various revisions of the specifications. Taking exception to the use of a particular revision should be exercised if a program cost advantage can be realized without any sacrifice to the overall design integrity. Here, the contractor has an obligation to the Government, as well as his own management.

Although there are many reasons for having specifications, perhaps one of the more important aspects realized is the least appreciated: the design and development of a missile guidance system is a complex task, requiring design considerations which cover a multitude of specialized fields. It is beyond the capability of most designers to be proficient in every one of these fields. It is at this point where specifications provide useful guidelines for the designer, and hence should be looked upon by him as a design aid, rather than just another design constraint. This positive outlook toward specifications is often difficult to instill in some designers. However, it is an important aspect and should be emphasized.

6.19.4. Design and Hardware Configuration Control. - Control of design and hardware configuration becomes an ever-increasing necessity as space and defense programs grow in size. Complex systems require, in most cases, several contractors, all making equipment, which when integrated must satisfactorily perform the tasks defined. By imposing Military Specifications and Standards, secondary controls are inherently invoked upon the design and hardware configuration. The degree to which direct primary design and configuration control should be imposed could vary, depending upon whether the hardware is in the Research and Development (R&D) stage or ready for release to Production as a fully qualified product. Another factor to consider in implementing configuration control is cost. Full implementation of some Military and Civilian Agency configuration control programs is costly. Where the system is extremely complex or man-rated, the cost may be justified. Even in the case of unmanned space exploration missions, there may be justification for full configuration control. However, there are applications where partial configuration control may suffice without sacrifice of performance. An open mind should be used in assessing these possibilities.

Configuration control procedures should not be construed as functional design constraint procedures. Freedom of design within limits is a necessity. Configuration control should serve the primary function of assuring that each significant design change is separated and identified from each and every other significant change. Documentation and marking of the equipment so as to identify a particular change is part of this task.

6.19.5. Conclusions. - Specifications should be interpreted as design aids, not just as design "watchdogs". The quality of a particular design is built-in, not tested in. Specifications properly referenced, interpreted, and applied are a necessary part of any high quality design. Deviations from, or waivering of any part of a given specification, can only be justified when the full implications of such are fully understood and appreciated. On the other hand, improper or unnecessary referencing of "standard" specifications, regardless of their nature, can be costly and actually degrade, rather than aid a good design.

Design and configuration control serves a necessary function. The degree of configuration control implemented should be predicated upon the particular needs of the program. Full and arbitrary implementation of configuration control programs can be costly and possibly unjustified. The complexity of the program and the type of program are prime factors to be considered in setting up a configuration control plan.